Comparative bone histology of the turtle shell (carapace and plastron): implications for turtle systematics, functional morphology and turtle origins

Dissertation

zur

Erlangung des Doktorgrades (Dr. rer. nat.)

der

Mathematisch-Naturwissenschaftlichen Fakultät

der

Rheinischen Friedrich-Wilhelms-Universität zu Bonn

Vorgelegt von

Dipl. Geol. Torsten Michael Scheyer

aus

Mannheim-Neckarau

Bonn, 2007

Angefertigt mit Genehmigung der Mathematisch-Naturwissenschaftlichen Fakultät der
Rheinischen Friedrich-Wilhelms-Universität Bonn

1 Referent: PD Dr. P. Martin Sander
2 Referent: Prof. Dr. Thomas Martin

Tag der Promotion: **14. August 2007**

Diese Dissertation ist 2007 auf dem Hochschulschriftenserver der ULB Bonn
http://hss.ulb.uni-bonn.de/diss_online elektronisch publiziert.

Rheinische Friedrich-Wilhelms-Universität
Institut für Paläontologie
Nussallee 8
53115 Bonn
Dipl.-Geol. Torsten M. Scheyer

Bonn, Januar 2007

Erklärung

Hiermit erkläre ich an Eides statt, dass ich für meine Promotion keine anderen als die angegebenen Hilfsmittel benutzt habe, und dass die inhaltlich und wörtlich aus anderen Werken entnommenen Stellen und Zitate als solche gekennzeichnet sind.

Torsten Scheyer

Zusammenfassung—Die Knochenhistologie von Schildkrötenpanzern liefert wertvolle Ergebnisse zur Osteoderm- und Panzergenese, zur Rekonstruktion von fossilen Weichgeweben, zu phylogenetischen Hypothesen und zu funktionellen Aspekten des Schildkrötenpanzers, wobei Carapax und das Plastron generell ähnliche Ergebnisse zeigen. Neben intrinsischen, physiologischen Faktoren wird die Mikrostruktur des Panzerknochens von einem Mosaik phylogenetischer and funktionaler Faktoren beeinflusst. Das Verhältnis beider Einflüsse variiert sehr stark unter den Schildkrötengroßgruppen. Nur wenn funktionelle Aspekte nur schwach ausgeprägt sind, können phylogenetische Signale abgeleitet werden. Die Knochenhistologie kann demnach zur Überprüfung bestehender (morphologischer, molekularer oder serologischer) Verwandtschaftshypothesen genutzt werden.

Gruppen, die gut definierte Knochenmikrostrukturen aufweisen, sind die Bothremydidae, Pleurosternidae, Chelydridae, Plesiochelyidae und Thalassemydidae, Dermochelyidae, Dermatemydidae, Carettochelyidae, und Trionychidae. Weiterhin kann die systematische Position unsicher zugeordneter Taxa (z.B. aff. *Platychelys* sp., *Platysternon megacephalum*), sowie unzureichend bekanntes Materials bestimmt werden. Aff. *Platychelys* sp. sowie der Kirtlington Histomorph I werden beide den Pleurosternidae zugeordnet. Die Zuordnung des Histomorph I führt zu einer Ausdehnung des Fossilberichts der Pleurosternidae in den Mittleren Jura hinein. *P. megacephalum* zeigt einige histologische Gemeinsamkeiten mit den Chelydridae, was wiederum eine Unterstützung älterer morphologischer Hypothesen darstellt. In den restlichen Großgruppen ist kein klares phylogenetisches Signal vorhanden, oder es kommt zu einer Überprägung des Signals durch funktionelle Faktoren.

Die Anpassung der Knochenmikrostruktur des Panzers an das aquatische Milieu gehört zu den stärksten funktionellen Faktoren. Hierdurch konnte eine Gruppierung aller untersuchten Schildkröten in vier Kategorien (I „terrestrischer Lebensraum“ bis IV „extremste Anpassung an das aquatische/marine Milieu) bezüglich ihrer Ökologie/Palökologie vorgenommen werden. Vergleiche der ältesten Vertreter der Schildkröten mit rezenten ‚aquatischen’ und ‚terrestrischen’ Vertretern belegen unabhängig die terrestrische Palökologie der basalen Testudinata.

Die Knochenpanzermikrostrukturen wurden weiterhin zur Klärung des Ursprungs der Schildkröten genutzt. Basierend auf dem Vergleich von basalen Schildkröten und verschiedenen Außengruppenvertretern, welche Pareiasaurier, Placodontier, Mammalier, Archosauromorphe und Lepidosaurier beinhalteten, wird ein Ursprung innerhalb der Diapsida mit naher Verwandtschaft zu Archosauriern hypothetisiert. Für den Panzer der Placodontier wird weiterhin ein, in Osteodermen bisher unbekanntes knorpeliges Gewebe (´postkranialer faserknorpelhaltiger Knochen´), sowie ein generelles Modell der Osteogenese vorgestellt.

Abstract—The bone histology of the turtle shell is valuable for addressing osteoderm and shell formation, reconstruction of fossil integumentary soft-tissue structures, phylogenetic hypotheses and functional aspects of the turtle shell, with both carapace and plastron showing similar results. Besides intrinsic physiological factors, the shell bones are proposed to be influenced by a mosaic of phylogenetic and functional factors influencing the microstructural properties. The ratio between phylogenetic and functional constraints is highly variable among the major turtle groups, and only where functional aspects are less dominant, phylogenetic signals can be deduced from the bone histology. The bone histology can thus be used to verify existing intra-specific phylogenetic (e.g., morphological, molecular and serologic) hypotheses among turtles.

Groups that are well defined by bone histological characters are Bothremydidae, Pleurosternidae, Chelydridae, Plesiochelyidae and Thalassemydidae, Dermochelyidae, Dermatemydidae, Carettochelyidae and Trionychidae. Furthermore, the systematic position of uncertainly assigned taxa (e.g., aff. *Platychelys* sp., *Platysternon megacephalum*) and poorly known shell material (e.g., Kirtlington turtles) could be assessed. Aff. *Platychelys* sp., as well as Kirtlington histomorph I are both assigned to Pleurosternidae herein. Assignment of the latter taxon would indicate that the fossil record of Pleurosternidae has to be extended back into the Middle Jurassic. *P. megacephalum* was found to share some histological features with Chelydridae, thus supporting prior morphological hypothesis. In the other major turtle groups, the bone histology does not show clear phylogenetic signals or functional factors override existing phylogenetic signals respectively.

One functional aspect that profoundly influences turtle shell bone microstructures is the adaptation to an aquatic habitat and life-style. In this respect, all turtles were grouped into four categories (I “terrestrial environment” to IV “extreme adaptation to aquatic/marine environments”), based on their ecology/palaeoecology. Comparison of the oldest known turtles with recent ‘aquatic’ and ‘terrestrial’ turtles independently revealed a terrestrial palaeoecology for the basal Testudinata. Shell bone microstructures can further elucidate the origin of turtles. Based on the comparison of basal turtles and several outgroup taxa including osteoderm-bearing pareiasaurs, mammals, placodonts, archosauromorphs and lepidosaurs, the origin of turtles is hypothesised to lie within Diapsida, with close relationships to archosaurs. In the case of placodont armour, a unique bone tissue (here termed ´postcranial fibro-cartilaginous bone`) is described and a general model of osteogenesis is proposed.

Contents

1. Introduction

1.1 General introduction

Turtles are long since subject of scientific interest because of their highly unusual body bauplan. However, a comparative histological analysis of the main feature of the turtle, its shell, has never been conducted. In the last decades, bone histology emerged as an invaluable tool to analyse the biology of fossil vertebrates. Physiological, functional, and systematic questions were approached using this powerful scientific tool. This study was conducted to elucidate how bone histology can be applied to questions about the formation and origin of the turtle shell, its function and its systematic value for turtle interrelationships.

1.2 Morphology and anatomy of the turtle shell

The turtle shell (Figure 1) consists of a domed, dorsal carapace and a rather flat, ventral plastron (e.g., Młynarski, 1969, Zangerl, 1969). Generally, the carapace consists of eight neurals, eight costals, twenty-two peripherals (eleven on each side), a nuchal, one or two suprapygals and a pygal plate. From anterior to posterior, the plastron is organised into the paired epiplastra, a single entoplastron, two hyo-, two hypo- and two xiphiplastra. The elements of the plastron are usually thought to be associated with the clavicles (epiplastron), the interclavicle (entoplastron) and three to five paired bones, possibly from the gastral skeleton, of basal reptilians (e.g., Zangerl, 1939, 1969; Cherepanov, 1984; Gaffney and Meylan, 1988; Cherepanov, 1997). Basal turtles may retain also a pair of mesoplastra between the hyo- and hypoplastra, as well as a number of additional elements in the carapace (Zangerl, 1969). The marginal surfaces of adjacent shell elements are usually dominated by bony protrusions that interlock with the next shell element. This causes a characteristic suture between the shell elements, leading to a pattern that is of high taxonomic relevance (e.g., Zangerl, 1969). General descriptions of the shell morphology can be found, for example, in Zangerl (1939, 1969), Carroll (1988, 1993), Benton (2005) and Rieppel (2001).

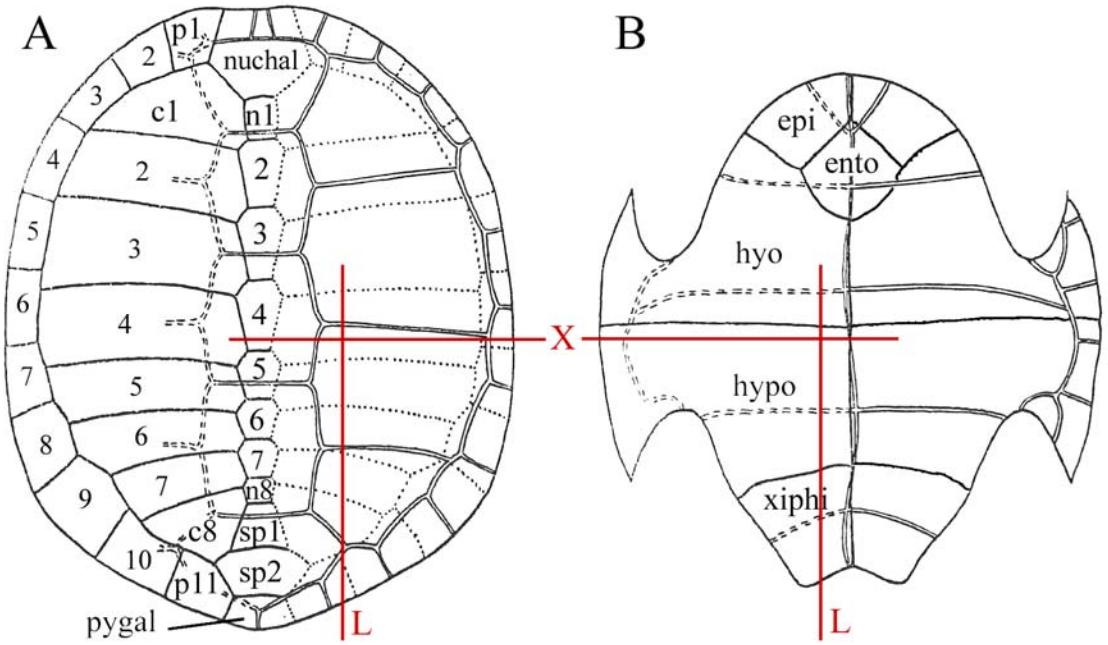

Figure 1: General schematic external view of A) carapace and B) plastron of a modern turtle shell modified after Zangerl (1969). Shield boundaries (double lines) are removed on the left hand side of each drawing to show bone boundaries (single full and stipled lines). n: neural; c: costal; p: peripheral; sp: suprapygal; lines marked with X and L: orientation of major transverse (X-section) and longitudinal (L-section) planes of sectioning

With the exception of Trionychidae, *Carettochelys insculpta* and *Dermochelys coriacea*, the shell bones of all extant turtles are covered by epidermal keratin shields/scutes. The bone sutures and the shield boundaries generally do not overlap. This composite structure of bones and overlying shields is generally interpreted to fulfil some kind of armour function (Zangerl, 1969). Similarly to the characteristic bone sutures, the shield/scute impressions, called sulci, are of high taxonomic value. In the three taxa that do not show keratin shields, the bones are covered with a thick leathery integument instead.

Both shell halves are usually connected by a lateral bony bridge, consisting of the dorsal peripherals of the bridge region and the dorsolateral processes of the hyo- and hypoplastron. In some taxa, e.g., in the Southeast Asian box turtles (*Cuora* spp., Bataguridae) or the New World box turtles (*Terrapene* spp., Emydidae), the reduction of the bridge into a loose joint allows the kinetic closure of the shell by pulling up the anterior and posterior plastral lobes.

The development of kinetic hinge systems in the shell is very common. It can further be found within pelomedusid, kinosternid and in testudinid turtles (Zangerl, 1969).

Among Testudinidae, the hinge-back tortoises (*Kinixys* spp.) have developed one of the most aberrant hinge systems. Instead of movable plastral lobes, a hinge has developed within the carapace through which the posterior part can be dorsoventrally raised and lowered. Other turtle taxa, including the Trionychidae and the Chelydridae, reduce the bridge until the ventral and dorsal armour elements are connect only by bony protrusions and soft connective tissue.

In several turtle lineages, the adult shells show a reduced number of bony elements as well as the retainment of large fontanelles between the shell bones. Otherwise, large fontanelles are characteristic for juvenile turtles, and they are usually closed during ontogeny (e.g., Zangerl, 1969). However, some shell variation has to be treated with caution for taxonomic purpose. In modern turtles, the shell morphology can be highly plastic due to exogenic factors (e.g., basking periods), malnutrition and pathologies (e.g., Frye, 1991, Sinn, 2004).

In cheloniid turtles, large fontanelles are retained between the costals and the peripherals of the carapace, as well as in the plastron. In trionychid turtles, the complete set of peripherals is reduced (with the exception of the posterior peripheral bones in *Lissemys punctata*, see 4.3.24) with the free rib ends being embedded in the marginal soft dermal rim. In Dermochelyidae, the primary (thecal) shell bones are almost completely reduced and a secondary (epithecal) mosaic armour of numerous small polygonal bony platelets developed (e.g., Zangerl, 1939; see Fig. 2).

For Trionychidae, Kordikova (2000, 2002) noted that many morphological differences of the turtle shell may be explained by the occurrence of heterochronic effects, especially of paedomorphosis. The delay or acceleration of certain shell elements compared to others leads to the loss of shell elements or the preservation of fontanelles in adult individuals (Kordikova, 2000).

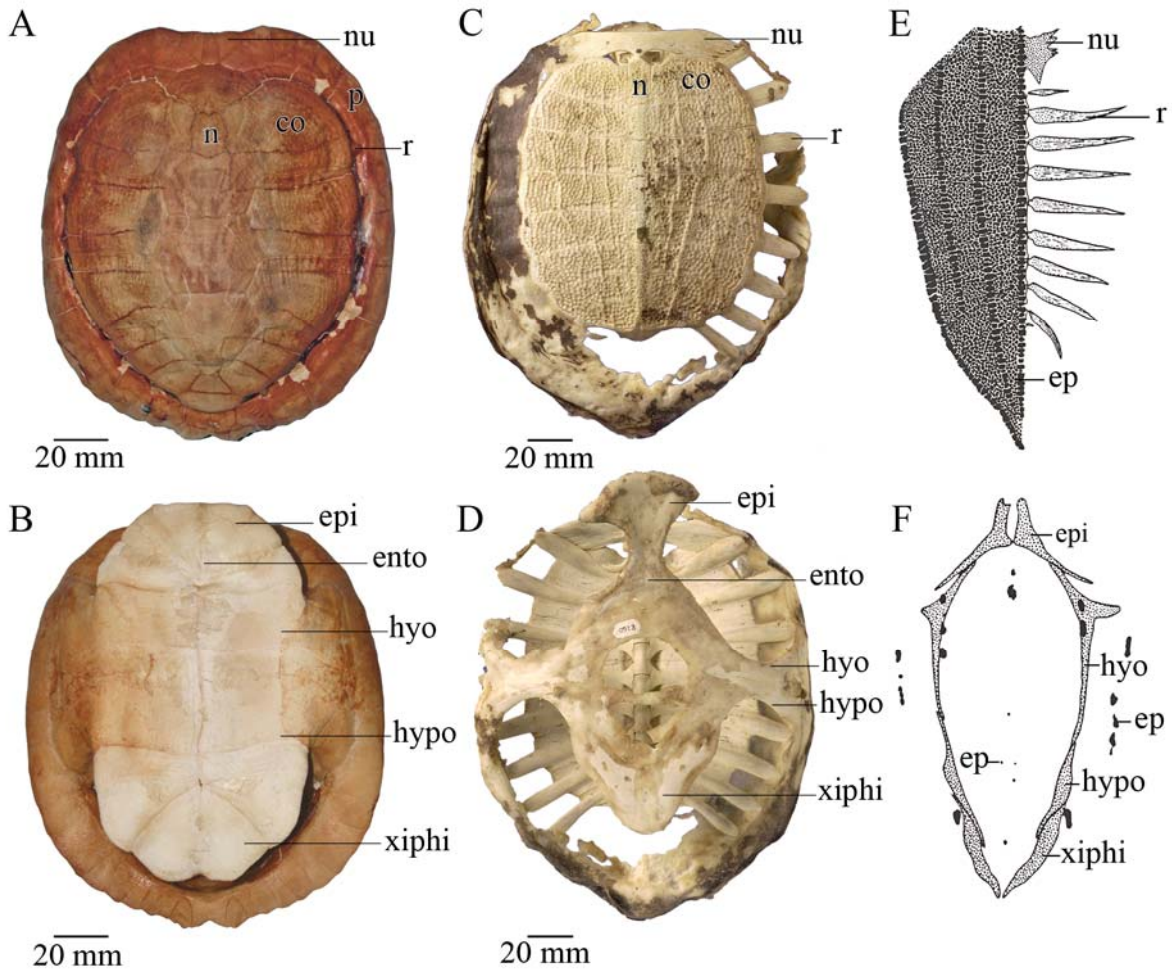

Figure 2: Comparison of turtles shells that show different stages of ossification. A) Carapace, B) plastron, connected by a bony bridge, of an almost completely ossified turtle shell (*Trachemys scipta;* IPB R590). C) Carapace and D) plastron of the reduced shell of a trionychid turtle (*Trionyx triunguis*, IPB R260). Peripherals and a bony bridge are not developed. Schematic drawing of E) the carapace and F) the plastron of *Dermochelys coriacea* (modified after Zangerl, 1939; not to scale). In E), the right side of the secondary (epithecal) armour, consisting of numerous small polygonal platelets and seven larger carapacial platelet ridges, is removed. Below the epithecal armour, the ribs and the only thecal remnant, the nuchal, is seen. In F), the thecal elements are still present (except the epiplastron) as thin bony rods and five plastral ridges are indicated through scattered platelets. co=costal; ep=epithecal ossification; epi=epiplastron; hyo=hyoplastron; hypo=hypoplastron; n=neural; nu=nuchal; p=peripheral; r=rib; xiphi=xiphiplastron.

1.3 Aims of the study

1.3.1 Implications for turtle systematics

Taxomomic studies of fossil and recent turtles usually focussed only on the osteological analysis of cranial and postcranial material. *But is the turtle shell microstructure (carapace and plastron) also of systematic value? Can taxa of uncertain systematic status be assigned to existing genera or more inclusive taxa, based on their shell histology?*—The first comparative approaches on bone histological sampling of turtle shells (e.g., Zangerl, 1969; Moss, 1969), already yielded interesting similarities and variation of the microstructures among turtle taxa. Those studies, however, focussed only on a few well known and easily available extant species. Easily recognised differences were found for example between tortoises and sea turtles (i.e., due to the reduction of internal cortical bone in sea turtles).

To address these questions, two composite phylogenetic trees were compiled to serve as working hypotheses for the turtle relationships. The first tree (Fig. 3) shows the interrelationship of the major groups of Testudinata. In the second tree (Fig. 4), all sampled turtle taxa are incorporated. The first tree is mainly based on published results of Gaffney and Meylan (1988), Meylan and Gaffney (1989), Rougier et al. (1995), Gaffney (1996), Hirayama (1998), Sukhanov (2006) and Joyce (2007). The second tree is based on many more individual data sets that were incorporated also in the morphological description of Testudinata (chapter 4). On this basis, the shell bone microstructures will be discussed and interpreted for each taxon and group. The existing hypotheses were tested and evaluated in the light of the new data presented in the current study. Special interest was paid to turtle taxa of uncertain phylogenetic position. Please note that there occur differences in nomenclature of turtle taxa between authors that follow the ICZN and those that follow the PhyloCode (*sensu* Joyce et al., 2004). A comparison of both systems is found in Danilov (2005:table 32).

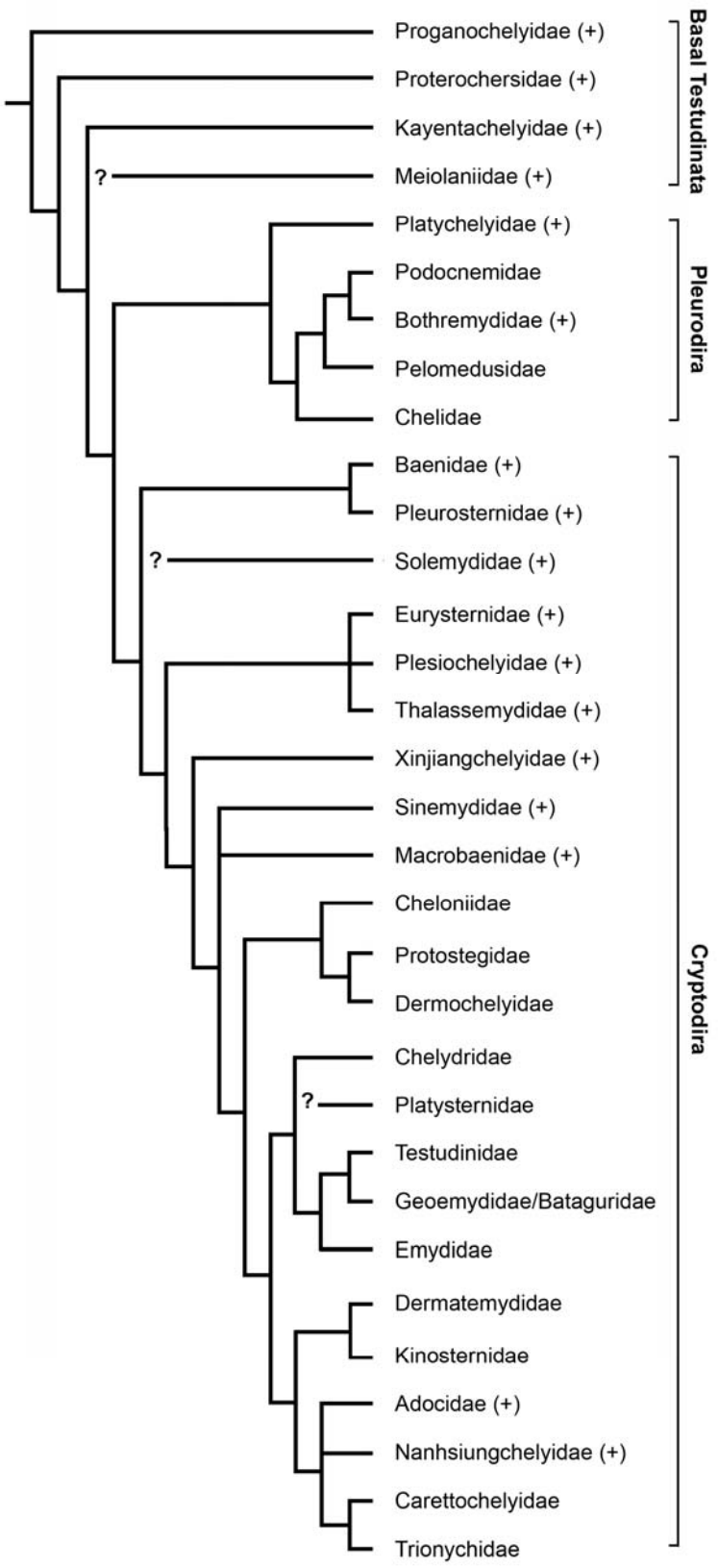

Figure 3: Phylogenetic working hypothesis of the major groups of Testudinata. Fossil taxa are marked by a cross. For source of data see text.

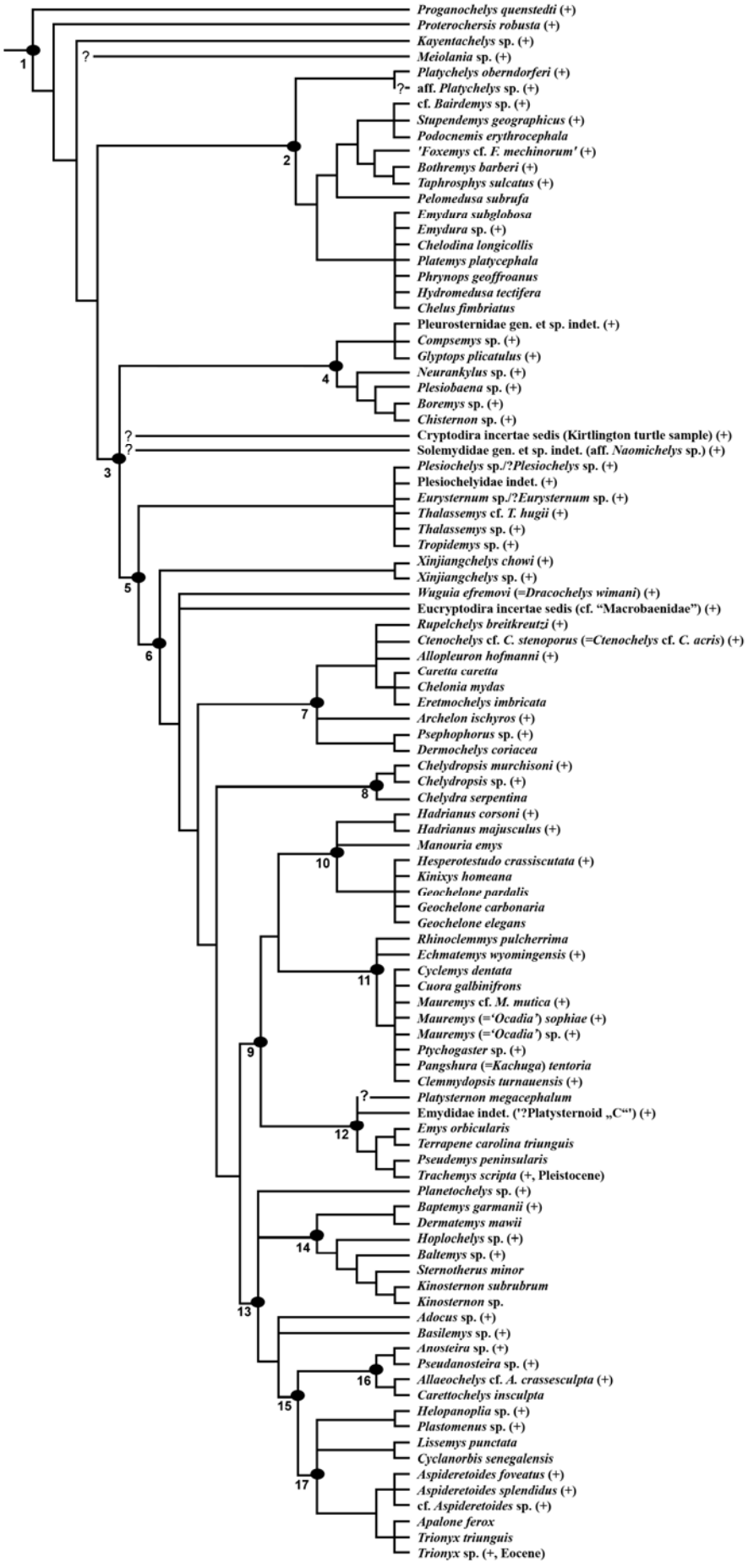
Proganochelys quenstedti (+)
Proterochersis robusta (+)
Kayentachelys sp. (+)
Meiolania sp. (+)
Platychelys oberndorferi (+)
aff. Platychelys sp. (+)
cf. Bairdemys sp. (+)
Stupendemys geographicus (+)
Podocnemis erythrocephala
'Foxemys cf. F. mechinorum' (+)
Bothremys barberi (+)
Taphrosphys sulcatus (+)
Pelomedusa subrufa
Emydura subglobosa
Emydura sp. (+)
Chelodina longicollis
Platemys platycephala
Phrynops geoffroanus
Hydromedusa tectifera
Chelus fimbriatus
Pleurosternidae gen. et sp. indet. (+)
Compsemys sp. (+)
Glyptops plicatulus (+)
Neurankylus sp. (+)
Plesiobaena sp. (+)
Boremys sp. (+)
Chisternon sp. (+)
Cryptodira incertae sedis (Kirtlington turtle sample) (+)
Solemydidae gen. et sp. indet. (aff. Naomichelys sp.) (+)
Plesiochelys sp./?Plesiochelys sp. (+)
Plesiochelyidae indet. (+)
Eurysternum sp./?Eurysternum sp. (+)
Thalassemys cf. T. hugii (+)
Thalassemys sp. (+)
Tropidemys sp. (+)
Xinjiangchelys chowi (+)
Xinjiangchelys sp. (+)
Wuguia efremovi (=Dracochelys wimani) (+)
Eucryptodira incertae sedis (cf. "Macrobaenidae") (+)
Rupelchelys breitkreutzi (+)
Ctenochelys cf. C. stenoporus (=Ctenochelys cf. C. acris) (+)
Allopleuron hofmanni (+)
Caretta caretta
Chelonia mydas
Eretmochelys imbricata
Archelon ischyros (+)
Psephophorus sp. (+)
Dermochelys coriacea
Chelydropsis murchisoni (+)
Chelydropsis sp. (+)
Chelydra serpentina
Hadrianus corsoni (+)
Hadrianus majusculus (+)
Manouria emys
Hesperotestudo crassiscutata (+)
Kinixys homeana
Geochelone pardalis
Geochelone carbonaria
Geochelone elegans
Rhinoclemmys pulcherrima
Echmatemys wyomingensis (+)
Cyclemys dentata
Cuora galbinifrons
Mauremys cf. M. mutica (+)
Mauremys (='Ocadia') sophiae (+)
Mauremys (='Ocadia') sp. (+)
Ptychogaster sp. (+)
Pangshura (=Kachuga) tentoria
Clemmydopsis turnauensis (+)
Platysternon megacephalum
Emydidae indet. ('?Platysternoid „C"') (+)
Emys orbicularis
Terrapene carolina triunguis
Pseudemys peninsularis
Trachemys scripta (+, Pleistocene)
Planetochelys sp. (+)
Baptemys garmanii (+)
Dermatemys mawii
Hoplochelys sp. (+)
Baltemys sp. (+)
Sternotherus minor
Kinosternon subrubrum
Kinosternon sp.
Adocus sp. (+)
Basilemys sp. (+)
Anosteira sp. (+)
Pseudanosteira sp. (+)
Allaeochelys cf. A. crassesculpta (+)
Carettochelys insculpta
Helopanoplia sp. (+)
Plastomenus sp. (+)
Lissemys punctata
Cyclanorbis senegalensis
Aspideretoides foveatus (+)
Aspideretoides splendidus (+)
cf. Aspideretoides sp. (+)
Apalone ferox
Trionyx triunguis
Trionyx sp. (+, Eocene)
1
2
3
4
5
6
7
8
9
10
11
12
13
14
15
16
17
?
?
?
?

Figure 4: Phylogentic working hypothesis of all sampled taxa of Testudinata. For source of data see text. Fossil taxa are marked by a cross. Taxa of uncertain phylogenetic position are marked with a question mark. 1=Testudinata; 2=Pleurodira; 3=Cryptodira; 4=Paracryptodira; 5=Eucryptodira; 6=; 7=Chelonioidea; 8=Chelydridae; 9=Testudinoidea; 10=Testudinidae; 11=Geoemydidae/Bataguridae; 12=Emydidae; 13=Trionychoidea; 14=Kinosternoidea; 15=Trionychia;16=Carettochelyidae; 17=Trionychidae

1.3.2 Implications for turtle shell functional morphology

The turtle shell is generally seen as armour, an adaptation against predation (see Burke, 1989a; Zangerl, 1969). *Are there microstructural adaptations to strengthen the shell? Are form and functional constraints that influence the bones strongly enough to override potential phylogenetic signals?*—Structural strengthening, e.g., through the development of plywood patterns, has been discussed for a wide variety of skeletal hard tissues among animals (e.g., Märkel and Gorny, 1973; Giraud et al., 1978; Pfretzschner, 1986, 1994; Kamat et al., 2000; Ricqlès et al., 2001; Scheyer and Sander, 2004). The strengthening structures are usually interpreted as being optimised against effecting stresses. Besides an armour function, the turtle shell serves as a support for the vertebral column within the carrying system and as attachment area for connective soft-tissues (e.g., breathing musculature). All these functions are hypothesised herein to influence the outer morphology of the shell bones as well as the internal bone microstructures. In the current study, the functionality of the turtle shell elements is analysed in context with the epidermal keratinous shields, whose borders do not overlap with the sutures of the underlying shell bones where appropriate.

Body size is a fundamental variable correlated with a large variety of aspects of the life history and anatomy of organisms, including bone structure (e.g., Klingenberg 1998; Liem et al. 2001). *Are there functional differences in the turtle shell related to the size of the turtle?*—The structure of the turtle shell bone is also likely to be determined by size and constrained by phylogenetic history. Bone histology can be influenced by size- and age-related factors, as discussed by Hailey and Lambert (2002) in a study of phenotypic and genetic differences in the growth of giant Afrotropical tortoises. In this context, the study of species at the end of the size spectrum variation is of special interest (i.e. small sized pelomedusoid turtles compared to giant *Stupendemys geographicus*).

In the case of the marine Dermochelyidae, secondary (epithecal) armour developed after an initial, almost complete reduction of the ancestral primary (thecal) shell. *Are there differences between the primary and secondary turtle armour?*—It is to be assessed if the smaller, secondary armour platelets are derived in their microstructure (optimised against stresses?), while at the same time providing higher mobility in the water.

Shell kinesis appears in several turtle lineages. *What evidence can be found for shell kinesis on the microscopical level?*—If shell kinesis is present in a turtle taxon, it proposedly alters the appearance of the normal sutured bone elements. Consequently, as these taxa adapt to the kinetic strains by remodelling their shell elements, the bone microstructure should also be affected. Muscle- or tendinous attachments of bones within hinges might be recognised in the form of specifically orientated collagen fibres (Sharpey's fibres) in the bone. The variation in the sutural contact of the bone as well as the presence of the Sharpey's fibres can be an indicator for functional constraints acting on the turtle shell.

1.3.3 Implications for turtle origins

Turtles are unique among all living reptiles in having an anapsid skull, a body encased in a rigid shell and limb girdles that are shifted into the rib cage (Zangerl, 1969). *Proganochelys quenstedti*, the basal-most turtle, and *Proterochersis robusta*, the oldest known turtle, already display such a bauplan, thus aggravating the reconstruction of turtle origins (Gaffney, 1990). While morphological hypotheses interpret turtles either as the last descendants of 'anapsid' parareptiles related to small procolophonids (Laurin and Reisz, 1995) or large herbivorous Permian pareiasaurs (Gregory, 1946; Lee, 1993, 1996, 1997, 2001), or as diapsid reptiles close to sauropterygians (Rieppel and deBraga, 1996; deBraga and Rieppel, 1997; Rieppel and Reisz, 1999) or lepidosaurs (e.g., Müller, 2003; Hill, 2005), recent molecular studies favour a turtle-archosaur relationship (e.g., Kumazawa and Nishida, 1999; Rest et al., 2003; Iwabe et al., 2004). While morphological hypotheses rely on the presence of extensive dermal armour in fossil and living groups for comparison (e.g., Lee, 1997; deBraga and Rieppel, 1997), embryological studies propose the turtle body plan to be a neomorphic structure (e.g., Burke, 1989b, 1991; Loredo et al., 2001; Gilbert et al., 2001; Kuraku et al., 2005). Increasing evidence of the current molecular studies results in the necessity to test the newly proposed

turtle-archosaur relationship against the older, mainly morphology-based hypotheses that turtles represent the last descendants of the parareptilian lineage.

Up to date, the origin of turtles is still hotly debated (Fig. 5). *In this respect, can the comparison of histological features of turtle and outgroup taxa provide evidence for common ancestors?*—A preliminary comparative approach that uses amniote osteoderm and turtle shell bone histological data is attempted to elucidate the origin of turtles. The sampling includes armour elements from taxa that are discussed as potential outgroups to the Testudinata. Similarities of the micro-structural arrangement of the armour elements may provide strong evidence for, or against, proposed sistergroup relationships.

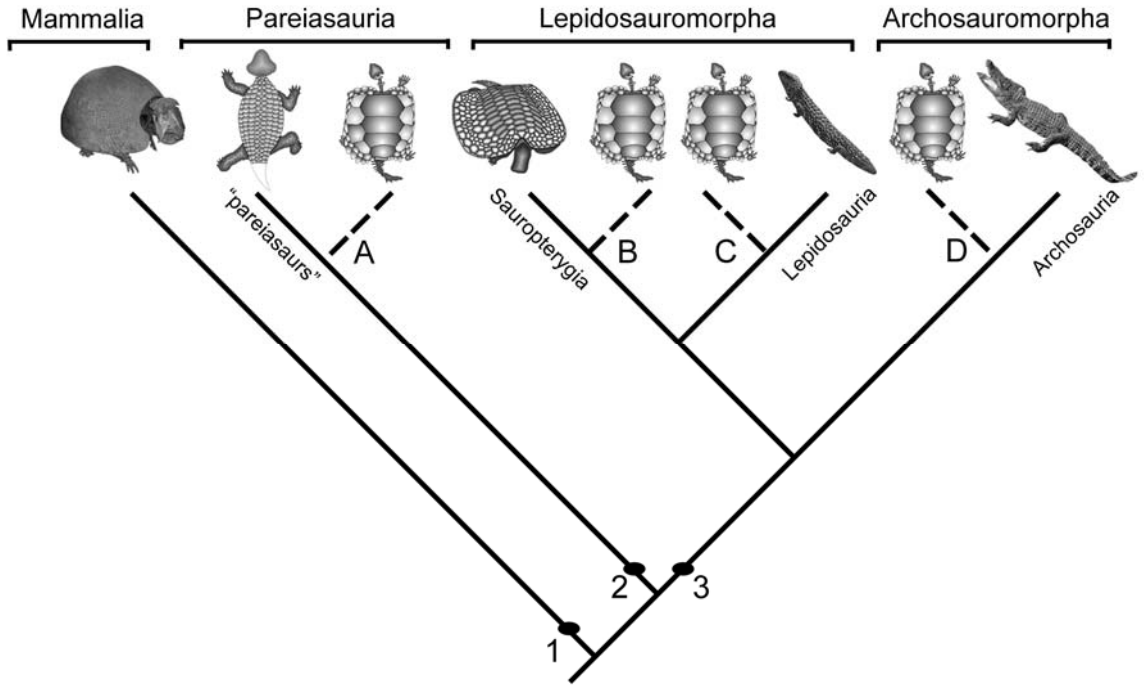

Figure 5: Proposed positions of turtles among amniotes that are to be tested by bone histological comparison of turtle shell bones and dermal skeletal elements of outgroup taxa. Hypothesis A) turtles are parareptiles and deeply nested within pareiasaurs; hypothesis B) turtles are derived diapsids most closely related to sauropterygians; hypothesis C) turtles are derived diapsids most closely related to lepidosaurs; hypothesis D) turtles are derived diapsids most closely related to archosaurs. For source of data on phylogenetic hypotheses of turtles see text. 1= Synapsida; 2= Parareptilia; 3= Diapsida

1.3.4 Implications for the ecology of turtles

During the Early Carboniferous, early tetrapods left the water to become the first terrestrial animals. They retained an amphibious life-style spending time on land and in water. With the evolution of the amnion egg, the Amniota were able to leave the aquatic habitat permanently. Since then, several groups of tetrapods, however, reversed their ecology and secondarily went back into the water (e.g., Seymour, 1982; Ricqlès and Buffrénil, 2001). In some cases, this secondary adaptation is so strong that the animals cannot leave the water anymore. Modern amphibians (e.g., Anura), modern crocodilians and also seals and sea lions (Pinnipedia) still have an amphibious life-style. The whales (Cetacea) or the dugong (Sirenia), on the other hand, are so strongly adapted that they could not live on land anymore. In the case of sea turtles, the adaptation is not complete because, being oviparous animals, they still have to visit their terrestrial nesting sites for egg deposition (Musick, 1999; Godley et al., 2002; Hays et al., 2003). Other marine animals like whales, dolphins and sirenians are viviparous and they do not leave the water at all. Besides those recent groups of animals, several fossil lineages among vertebrates are known that purely lived in a marine environment, including for example the mosasaurs (e.g., Caldwell and Lee, 2001) or the ichthyosaurs (e.g., Motani, 2005). Similar to modern whales and dolphins, their bodies were optimised for fast and agile swimming that did not allow movement on land anymore.

According to its preferred habitat, the vertebrate body plan begins to adapt over time. For example, many terrestrial animals are characterised by stout limbs necessary for movement on land. The bone histology of those limbs, particularly of the long bones, shows a stress-optimised build. Heavy bone tissue like cortical bone is used sparingly in a tube-like structure, while the bone interior comprises either a medullary cavity or, towards the epiphyseal ends of the bone, less heavy cancellous bone tissue (e.g., Castanet, 1985; Castanet et al., 1993). The network of bone trabeculae in the cancellous tissue is subject to continuous remodelling processes during growth (e.g., Francillon-Vieillot et al. 1990). Animals that retain an amphibious life-style may show a mixture of terrestrial and aquatic characteristics in bone histology (e.g., Esteban, 1990). In marine animals, adaptive changes in bone remodelling follows two general trends, first an increase in bone mass and second a decrease in bone mass (see Ricqlès, 1989; Ricqlès and Buffrénil, 2001 for overview). In the first case, bone can become more compact to counter buoyancy and to enable a hydrostatic stabilisation. These processes acting on the bone tissue are known as non-pathological pachyostosis and

osteosclerosis. This can be seen for example in the compact ribs of the sirenian *Dugong dugon* (Buffrénil and Schoevaert, 1988) that lives in a near-shore environment. Parts of the long bones of fossil pachypleurosaurs are composed of calcified cartilage, thus also increasing bone mass (e.g., Ricqlès, 1989; Ricqlès and Buffrénil, 2001). Second, a reversal from the compact condition to a well vascularised, spongy condition is observed, as compact bone layers show increasing amounts of primary osteons and vascular canals (e.g., Esteban, 1990). Consequently, the most advanced modification of bone histology is reached usually in pelagic marine taxa, e.g., *Dermochelys coriacea* (e.g., Rhodin et al., 1981). The compact and cancellous parts of the bone are no longer distinguishable from each other and a rather homogeneous spongy bone tissue is developed. The strong vascularisation of the bone may hint at fast growth and bone deposition. A medullary cavity is not developed. Furthermore, such a bone tissue characterises fast and agile swimmers. Examples for this stage are found for example among the dolphins (Buffrénil and Schoevaert, 1988), the fossil ichthyosaurs (Buffrénil et al., 1987; Buffrénil and Mazin, 1990) and the fossil mosasaurs (Sheldon, 1997).

During their evolutionary history, turtles show a wide range of adaptations, covering fully terrestrial to fully aquatic habitats. Today, only one group of turtles, the tortoises (Testudinidae), is completely terrestrial. All other crown-group turtles are either mainly aquatic or amphibious. As shown quantitatively by Joyce and Gauthier (2004), the turtle's adaptation to a life in water versus a purely terrestrial life may be expressed in the outer morphology of its limbs. While short and stout limbs seem to be more related to a terrestrial environment, longer and slender limbs are more characteristic for aquatic environs, with marine turtles showing the strongest adaptations in the development of flippers. The pig-nosed turtle *Carettochelys insculpta* constitutes an exception in present time, because, while sporting front flippers, it is not a marine turtle but lives in large freshwater river systems. Furthermore, due to the work of Joyce and Gauthier (2004), it is now possible to analyse fossil turtle palaeoecology independently of the sedimentary facies they are found in, by calculating size and length ratios of their limb bones. Still, well preserved limb material is a prerequisite for these studies, as well as a close comparison to extant turtles. Importantly, the authors concluded that the most basal turtles had a predominantly terrestrial life-style. The adaptation to the aquatic medium apparently occurred somewhere on the stem line before the turtles split into the two branches of the side-necked turtles (Pleurodira) and the hide-necked turtles (Cryptodira). While it is not unusual for vertebrates to secondarily return to the water

(e.g., the Cetacea, the Pinnipedia and the Sirenia) as described above, it is highly unusual for such a group to reverse ecology again to a terrestrial lifestyle.

Not only the outer shape of bones, but also the bone microstructures are influenced by the habitat that the animal lives in. *Can the ecology/palaeoecology of turtles be inferred by bone histology in this respect? What is the plesiomorphic palaeoecology for turtles?*—Although these questions are greatly dependent on functional aspects and phylogenetic constraints, they gained more and more importance as my study progressed. Thus, it became necessary to adress them in a separate section. Furthermore, the ecological/palaeoecological aspects are intricately linked with the question about the origin of turtles. Central to the ecology/palaeoecology of turtles is how the varying degree of adaptation to the aquatic environment is expressed in the bone histology of the turtle shell. This is of special interest because of the wide range of habitats of living turtles and the unusual situation that the tortoises, a group of exclusively terrestrial turtles, are secondarily terrestrial. The actualistic concept allows the comparison of the modern and fossil bone histological data sets. The sampling comprises a variety of modern and fossil terrestrial, semi-aquatic, to fully marine turtles, including turtles from the Upper Jurassic 'Solothurn turtle limestone' of northern Switzerland. These turtles are regarded as important for the interpretation of marine adaptation among the Testudinata, because the Solothurn turtle assemblage represents the first marine radiation of turtles. The ecological data thus gained from the bone histology of the turtle shell is transferred to existing phylogenetic hypotheses to understand the ecological transitions from terrestrial to aquatic and even fully marine back to terrestrial in the evolutionary history of turtles.

A characterisation of the degree of adaptation to the aquatic environment of a specific turtle group based on the bone histology of its shell is attempted. It will thus be possible to test the palaeoecological results obtained by Joyce and Gauthier (2004) that were based on limb proportions. In addition, the current bone histological approach allows the investigation of many fossil taxa which lack preserved limbs. All fossil turtles can thus provide data, as long as the preservation of the microstructure of the shell is sufficiently good. The bone histological results thus provide an independent way of testing the degree of aquatic adaptation of a specific turtle, and the results will help to elucidate the unique habitat shifts during the evolutionary history of the group. Furthermore, to address the second question, the bone histology of basal Testudinata is compared to that of recent turtles, for which ecology

and life-style is well known. It is hypothesised that similar ecologies would result in similar bone microstructures.

1.4 Previous work

1.4.1 Historical aspects on bone histology

Since the invention of the microscope in the17th century, histological study has developed alternatively to the study of gross morphological/osteological features (e.g., Leeuwenhoek, 1693; Havers, 1691, in Francillon-Vieillot et al., 1990). Research on fossil bone was subsequently carried out by Seitz (1907), Gross (1934) and Amprino (1947), as well as Enlow and Brown (1956, 1957, 1958). Summaries on aspects of skeletal and bone formation can be found for example in Castanet et al. (1993), Francillon-Vieillot et al. (1990), Halstead (1974), Ricqlès et al. (1991) and Schmidt (1967). Since bones and teeth are the most abundant remains in the fossil record of vertebrates, they are the major source for palaeontological data collection. Instead of being restricted to questions of fossilisation, taphonomy and skeletal reconstruction, the histology of the aforementioned hard tissues provides access to data that is usually restricted to biologists that study recent animals. Although the original mineral and soft-tissue content is altered or simply not preserved respectively, fossil bone shows extremely good preservation of the original bone structure down to the bone cell-level (note that while the original bone cells, the osteocytes, are gone, the cell lacunae and even finer structures like their communicating canals, the canaliculi, can be superbly preserved in fossil bone). By examining these microstructures of, e.g., bone cell lacunae, blood vessel canals and bone tissue types, palaeontologists are able to apply aspects of biology and behaviour to fossil animals, which in many cases have no comparable living descendant.

1.4.2 Dermal bone histology and metaplastic bone formation

Since the turtle shell is largely composed of dermal bones, a small overview of dermal bone histology and dermal bone formation is following. Postcranial dermal bones, i.e., postcranial osteoderms, develop intramembraneously or metaplastically within layers of connective tissue

of the integument (e.g., Francillon-Vieillot et al., 1990; Hall, 2005). No cartilage precursor is involved in the process of osteoderm formation. In the process known as metaplastic bone formation (Haines and Mohuiddin, 1968), localised areas of mesenchymal aggregation in the dermis develop that are subsequently ossified, thus a fully differentiated tissue (i.e., connective tissue of the dermis) is transferred into another (i.e., bone tissue).

In living bone, the orientation of the collagenous fibres and fibre bundles also determines the orientation of the hydroxyapatite crystallites, i.e., the associated mineral phase of the bone. In the fossil bone, the original crystallite orientation is retained, thus allowing the reconstruction of the soft-tissue part of the bone that is usually lost during fossilisation (e.g., Francillon-Vieillot et al., 1990). Furthermore, by studying the microstructure of metaplastic osteoderms, the fossil dermal structure in which the bone formed can be reconstructed (see discussions in Scheyer and Sander, 2004; Scheyer et al., 2007). Thus, the study of tissues on the microscopic level allows the acquisition of additional data on gross morphology. This is especially important for the description and classification of specimens with similar outward appearances or specimens that lack classifiable, morphological characters.

1.4.3 Reptile dermal bone histology

Compared to the abundant studies on general fossil bone histology, reptile dermal bone histology received little attention until the 1970s. Hutton (1986), for example, used osteoderms for age estimations in crocodiles. Zylberberg and Castanet (1985) and Levrat-Calviac and Zylberberg (1986) presented data of squamate osteoderms. Research on *Stegosaurus* sp. dermal armour bone histology was mainly carried out by Farlow et al. (1976), Buffrénil et al. (1986), McWhinney et al. (2001) and lately by Hayashi and Carpenter (2006). Blows (1987), was the first to publish on the histology of ankylosaur armour. The last comparative histological works on the dermal bone of thyreophoran dinosaurs were done by Scheyer and Sander (2004) and Main et al. (2005).

1.4.4 Turtle shell bone histology

Work on the histology of turtles began with the analysis of the microstructural aspects of the turtle integument and the internal organs (e.g., Rathke, 1848; Hoffmann, 1878, 1890; Schmidt, 1921; Lange, 1931). However, with the exceptions of the more recent studies by Kälin (1945), Suzuki (1963) and Wallis (1928), the focus of the work still laid only on soft-tissue anatomy and not so much on the bones of the turtle shell as well. As a result, comparative histological data on the shell bones in the literature is scarce with only occasional descriptions of thin-sections (e.g., Kälin, 1945; Meylan, 1987; Suzuki, 1963; Wallis, 1928; Zangerl, 1969). In the last three decades, numerous scientific approaches have been carried out on the bone histology of turtles, elucidating and validating the age and growth of turtles based on skeletochronology (e.g., Castanet and Cheylan, 1979; Peters, 1983; Zug et al., 1986; Castanet, 1987, 1988; Klinger and Musick, 1992, 1995; Zug and Parham, 1996; Zug and Glor, 1998; Coles et al., 2001; Zug et al., 2001; Snover and Hohn, 2004). However, most of these studies focussed mainly on the sampling of long bone material or, in the case of Zug and Parham (1996), the sclerotic ossicle ring, of marine turtles and tortoises. These two taxa harbor the largest living turtles today. Zug and Parham (1996), like most of the other workers did not include samples of the bony shell in their analyses.

The domed turtle shell bone itself is a composite structure and of a similar nature to a human skull diploe (e.g., Bloom and Fawcett, 1994), i.e. a flat bone in which interior cancellous bone is framed by an external and internal compact bone layer. The cancellous bone consists mostly of bone trabeculae, whereas the compact bone tissue typically shows growth marks that can be similar or quite distinct from lines of arrested growth (LAG; e.g., Castanet, 1981) and radial vascular canals (Zangerl, 1969). According to Francillon-Vieillot et al. (1990) and Castanet et al. (1993), secondary reconstruction appears seldom in the turtle shell bone.

1.4.5 Historical introduction to the development of the turtle shell

By the end of the 18th century, Georges Cuvier was among the first that gave comparative anatomical descriptions of animals, including reptiles. In the following decades, the works of

Geoffroy St. Hillaire (1809), Bojanus (1819-1821) and Carus (1828) profoundly improved the knowledge about turtle anatomy and from the histological point of view these works, which are almost two centuries old, are still in many ways strikingly up to date. Since the second half of the 19th century, there was a significant increase of works addressing the development of the peculiar novel bauplan of the turtle shell, (e.g., Rathke, 1848; Hoffmann, 1878, 1890; Goette, 1899; Newman, 1906; Stehli, 1910; Ogushi, 1911; Schmidt, 1921; Hay, 1922, 1928; Ruckes, 1929; Deraniyagala, 1930; Lange, 1931; Zangerl 1939; Vallén, 1942; Kälin, 1945; Williams and McDowell, 1952; Suzuki, 1963; Yntema, 1968, 1970a,b; Mahmoud et al., 1973). This list is by no means exhaustive. I will refrain from listing all works that comprise developmental studies, because extensive bibliographies can be found for example in Vallén (1942), and especially the works of Miller (1985) and Ewert (1985) are general compendia focussing on the embryology and development of turtles.

1.4.6 Current consensus on the development of the turtle shell

In the following paragraph, a short overview of the shell bone formation is given. This overview mainly represents recent developmental works of Burke (1985, 1987, 1989a,b, 1991), Rieppel (1993), Brüllmann (1999, unpubl. MSc-thesis), Gilbert et al. (2001), Loredo et al. (2001), Greenbaum, (2002), Sheil (2003), Cebra-Thomas et al. (2005), Kuraku et al. (2005) and Sheil (2005), as well as some of the classical works stated above (e.g., Goette, 1899; Vallén, 1942; Kälin, 1945; Suzuki, 1963; Zangerl, 1969). These authors show that the nature of the shell of turtles, with its peculiar bauplan, i.e. shoulder girdle and pelvis within the rib cage, develops early in ontogeny. Sectioned embryos revealed the migration of mesenchymal cells into a dorsolateral bulge dorsal to the limb bud. This bulge, the carapacial ridge, consists of dorsal ectoderm and dermal mesoderm and it is hypothesised to entrap the primordial ribs in the carapacial development (Burke 1989b). Although certain parallels exist between the development of limb buds, i.e., in chicks, and the turtle carapace, it largely remains unclear how and by which molecular mechanisms and gene expressions, the turtle shell forms (see Loredo et al., 2001; Vincent et al., 2003; Kuraku et al., 2005). Early in ontogeny, the keratinous shields develop fully prior to hatching, while the bones below the shields still have to form (Suzuki, 1963; Zangerl, 1969). The earliest bones to ossify within the turtle shell are the elements of the plastron (Rieppel, 1993; Sheil, 2003).

In the turtle shell, only the costals and the neurals develop as a mixture of dermal and endoskeletal bone. In addition to the parts of dermal bone, the endoskeletal bone of the ribs is incorporated into the costal plates. The neurals, on the other hand connect dermal bone and endoskeletal bone of the neural arches. All other bony elements of the carapace (nuchal, pygal, suprapygals and peripherals) and the plastron (epi-, ento-, hyo-, hypo- and xiphiplastra) are of purely dermal origin. Kälin (1945), Suzuki (1963) and Cherepanov (1997) give exemplary descriptions of the development of neurals and costals during early ontogeny. A summary of the turtle shell development was recently given by Cebra-Thomas et al. (2005), so only a short summary will be given here. The ossification of the carapace starts along the median neural row above the vertebral column to proceed mediolaterally along the ribs towards the margins of the shell (e.g., Goette, 1899). In studying early ossification in *Chelydra serpentina*, Rieppel (1993) showed that the ossification of the neural arches is decoupled from the ossification of the centra and that the ossification of the neural arches starts ventrally from two separate ossification centres (one anterior and one posterior). Furthermore, as noted by this author, there seems to be no apparent anteroposterior gradient for the ossification sequence of vertebrae in *C. serpentina*. Generally, ossification of the neurals is induced by the periosteum of the vertebral arches, and the ossification of the neurals essentially follows the development described for the costal plates below.

The ossification of the costals starts at the cartilaginous rods of the ribs that are sheathed in a thin periosteum (e.g., Vallén, 1942; Suzuki, 1963; Cherepanov, 1997; Brüllmann, 1999, unpubl. MSc-thesis). Lateral-trending consolidation of mesenchymal parts within the soft tissue of the dermis leads to a preformation of a three-dimensional spongy meshwork in the integument. Concurrently, small bone spiculae grow laterally from the periosteum of the rib into the adjacent dermal layers (e.g., Suzuki, 1963). A periosteum is directly involved in this initial stage in shell bone formation (see Kälin, 1945). The successive ossification then proceeds along the mesenchymal aggregations, forming a primary cancellous bone structure.

The concept of the involvement of metaplastic ossification in turtle shell bone osteogenesis was first noted by Menger (1922) and then further elaborated by Kälin (1945). Concurrently, the internal cortical bone layer develops (e.g., Suzuki, 1963; Zangerl, 1969; Cherepanov, 1997; Brüllmann, 1999, unpubl. MSc-thesis). Second, the internal cortical bone increases in thickness and the external cortical bone layer develops through metaplastic ossification of preformed dermal structures, thus framing the interior area of cancellous bone. Internal and

external bone layers of the sandwich-like shell reflect distinct dermal structures with different collagenous fibre bundle orientations (Zangerl, 1969).

2. Material and Methods

2.1 Sampling Strategy

The study of the microstructure of turtle shell bone is based upon fossil and extant turtle shell material. Therefore, the gross part of the material was obtained from two major sources, the palaeontological collections and the zoological collections of museums and research institutes. This approach holds some general advantages. It allowed the substantial systematic coverage of the turtle taxa, because sufficient material for the study was available. This fact is not to be underestimated if the work involves destructive sampling of the material. It furthermore enabled the close comparison of the microstructure of fossil and recent material. And last, it was thus possible to place the fossil taxa into a phylogenetic framework that is not restricted to focus mainly on morphological data, but that also includes for example physiological, developmental, and molecular data sets. At the same time, several potential outgroup taxa were sampled. Overall, 102 fossil and recent turtle taxa and 18 fossil outgroup taxa have been studied within the scope of the project. The complete list of all the sampled specimens has been compiled into Appendix 1. Additionally, literature data on archosauromorphs osteoderm (Scheyer and Sander, 2004) and on lepidosaur osteoderms was used (e.g., Moss, 1969; Moss, 1972; Zylberberg and Castanet, 1985; Levrat-Calviac and Zylberberg, 1986) for comparison.

The material was surveyed on site in the zoological and palaeontological museums and institutional collections. In collaboration with the respective experts and collections managers, it was then decided which turtle shell material was best suited for studying the bone histology. Based on the fragmentary nature of some of the fossil specimens, an assignment of the material was possible only to the generic level or to even more inclusive taxa (i.e., “family” level). The sampling of the shell was either done by cutting whole shell elements and shell fragments or by core-drilling (usually in the recent specimens preserved in liquid). This technique worked especially well with the extant turtle taxa and proved useful in rare and endangered species where material has to be used sparingly. In several cases, a large amount of time and paperwork was invested to obtain necessary CITES-permits (list of endangered species) for the recent specimens. It is important to know that most if not all recent sampled turtles were so-called “no data specimens”, meaning they lacked the information about the locality or date of the find. Several of these specimens originate from legal or illegal pet-trade.

As a result, they are not very useful to biologists besides being representatives of a certain genus or species in the collections. On the other hand, in the cases of rare and endangered species, it was very helpful to core-drill the shell, because the rest of the turtle (including the inner organs) was not severely harmed.

Macerated and disarticulated or whole articulated turtle specimens were used for gross morphological and osteological comparison (kindly provided by IPB; MTD; N. Klein, private collection). Additionally, soft tissue samples of the integument of extant Trionychidae were used for comparative work on fossil and recent trionychid shell bones (kindly provided by YPM and ZFMK).

2.2 Preparation

2.2.1 Sampling of turtle shell elements

The subsequent preparation of the material was carried out at the Institute of Palaeontology, University of Bonn. Generally, the preparation of fossil bone material for thin-sectioning is difficult and requires quite a few steps of manual labour that cannot be automated. The preparation of recent (fresh) bone that was either frozen, that had been preserved in liquid (alcohol or formalin) or that was already macerated is even more delicate. Overall, 102 turtle taxa were sampled, thus covering the basal turtles, all major fossil turtle clades and all living crown-group turtle clades. Furthermore, 18 outgroup taxa were obtained for the study, providing essential data on the origin of turtles, as well as data about the bone histology of dermal armour and dermal ossifications in general. Usually, several elements of each taxon were sampled, including neurals, costals, peripherals and elements of the plastron.

2.2.2 Sampling by core-drilling

In the case of recent, unmacerated turtle specimens preserved in alcohol or other preservative liquids (standard procedure in zoological collections), the sampling was also realised by core-drilling (Fig. 6). Note that the method works equally well for articulated,

dried and macerated turtle specimens that cannot be disassembled. This method was first invented and used in the field of palaeontology by Sander (2000). Because of the large size of the then studied sauropod long bones, the method was developed to take core samples out of the mid shaft region of the bones. The advantages were that the long bones did not have to be moved far, a feat usually requiring a lot of logistic energy and manpower, and that they remained in the collections. Even more important, the damage done to the fossil material was held at a minimum level, because former techniques to study the microstructure of the bones usually relied on whole bone cross-sections.

In the current study, the whole turtle shell was put under a drill press equipped with a standard power drill with adjustable drilling speed (Fig. 6). To pull the cores, diamond-sintered hollow drill bits of 12 mm and 22 mm in diameter were used. Slowly revolving and cooled with water as lubricant, the cores could be removed without damaging the rest of the shell or the internal organs.

Figure 6: Sampling of the turtle shell by core-drilling. The cores (12 and 22 mm in diameter) are taken with diamond-sintered hollow drill bits and a standard power drill with adjustable drilling speed mounted on a drill press.

The use of oil as lubricant is not necessary for the drilling of alcohol or formalin-soaked turtle specimens. Neither was is feasible to build small dams to contain the cooling water, because then the collagenous matrix of the drilled bone was clogging the drill bit and obscured the drill site (as done by Klein and Sander, 2007). Instead, the drill site was cooled by adding small amounts of water to the drill bit. The position on the shell, the inner and outer surfaces, as well as the orientation compared to the long-axis of the animal was marked on each core. Where possible, the keratinous shield or soft shell cover and connective tissue was left in place on the bony core. The bone cores were then dried before the embedding in synthetic resin and the following steps in preparation (see chapter 2.2.4).

2.2.3 Planes of Sectioning

If possible, each turtle taxon was sampled from different bones of the carapace and the plastron. The samples were generally sectioned in two planes (see Fig. 1). The neurals were sectioned transversely ('X-section'; perpendicular to the anteroposterior axis of the carapace). Because the peripheral row is curved, the planes of sectioning were chosen to be perpendicular to the anteroposterior axis of each peripheral ('X-section'). The peripheral bones of the trionychid turtle *Lissemys punctata* were sampled as described for the peripherals of other taxa. The costals were sectioned either perpendicular to the progression of the rib ('L-section', parallel to the anteroposterior axis of the carapace) or parallel to the rib ('X-section'; perpendicular to the anteroposterior axis of the carapace). The elements of the plastron were sectioned either parallel ('L-section') or perpendicular ('X-section') to the anteroposterior axis of the plastron. Isolated osteoderms of turtles and osteoderms of turtle outgroups were either sectioned parallel or perpendicular to their respective long axis. In a few cases, a third plane of sectioning (e.g., tangential to the external bone surface) was chosen to better elucidate the microstructural composition of the bones. The individual planes of sectioning are marked as 'X-section' and 'L-section' in Appendix 1. The specimens where the plane of sectioning could not clearly be determined (e.g., fragments of uncertain orientation in the shell) are indicated by a question mark.

2.2.4 Preparation of standard petrographic thin-sections

All bone samples were processed into standard petrographic thin-sections. Therefore, the bone samples (whole shell elements, fragments and drilled cores) had to be stabilised by embedding into synthetic resins (Araldite-2020® or Biresin-L84®). In a second step, the specimens were cut and ground successively with SiC powder (220, 500, 800 and 1000) to eradicate saw marks and smooth out the relief. Third, the bone material was subsequently processed into thin-sections of a thickness around 80 µm or less, again using the SiC grounding powders mentioned above. Because of the highly porous nature and inner vascularisation, some specimens had to be impregnated in vacuum several times with synthetic resins (Araldite-2020® or Biresin-L84®).

The thin-sections of fossil specimens had two important advantages over the thin-sections made from recent bone. First, the fossil bone was generally easier to process into thin-sections as the mineral component is almost 100% instead of about 46% in recent bone. Due to its high content of organic tissue, i.e. the collagen matrix, recent bone is still prone to shrink or expand if heat or water is applied while processing the sections. And second, again due to the increased mineral content of the fossil bone, the polarising abilities of the thin-sections are better, resulting in high-contrast microscopic images.

2.2.5 Analysis and documentation

To understand the three-dimensional arrangement of the observed structures of the bone, the study and documentation of the microstructure was carried out with a binocular microscope (magnifications: 16x and 63x; normal transmitted light) and with a LEICA DMLP® compound polarising microscope (magnifications: 40x, 100x, 400x; normal transmitted and polarised light). The latter one was equipped with a special wide-field lens (1.6x) and a Nikon COOLPIX®-LCD-camera (E995) that allowed high-resolution photographs of histological details. Alternatively, the microscope could be equipped with a KAPPA CF15/4 RGB camera (incl. external control box), connected to a computer via a Hauppauge® framegrabber with SVideo-support. Where low magnification was of special import, additional photomicrographs were shot with a digital camera (Nikon® D1 2,7 mega-pixels and macro

lens) or with COOLPIX®-LCD-cameras (E995 or 3100). Drawings, as well as figure compositions were done using Macromedia Freehand® and Adobe Photoshop®.

In the case of trionychid shell bones, scanning electron microscope (SEM) photographs were made to elucidate the characteristics of the structure (micro- and nano-scale) of the collagenous fibre bundles of the bony elements. Therefore, polished planar sections of the turtle shell elements were etched for three to five seconds with hydrochloric acid (10%). After the acid has been neutralised with distilled water, the sections were then fixated, sputter-coated with gold and analysed under the SEM.

2.2.6 Picture credits

The following photographs were taken by G. Oleschinski, Insitute of Palaeontology, University of Bonn: Fig. 2c, d; 8a,b; 9a, b; 10a, b; 11a-d; 12a; 13a; 14a; 15a; 16a-d; 17a, b; 26a; 49a, b; 54e, f; 56a; 64a-d; 65a. All other photographs were taken by me.

2.3 Terminology

The description of the turtle shell elements follows Zangerl (1969), and the histological descriptions are mainly based on Francillon-Vieillot et al. (1990), Scheyer and Sander (2004) and Scheyer et al. (2007). The terms ‘costal’ and ‘pleural’ that both occur extensively in the literature are treated as being synonymous. The terms ‘external’ and ‘internal’ are used throughout the text instead of ‘dorsal’ and ‘ventral’ to prevent confusion among dorsal carapacial and ventral plastral bones of the turtle shell (e.g., the ‘dorsal’ surface of a carapace bone would be the true dorsal bone surface, while the ‘dorsal’ surface of a plastral bone would indicate the visceral side of the shell element). The term ‘interior’ pertains to the core or centre of the shell bone (i.e., cancellous bone) that is usually framed by the external and internal cortex (Fig. 7). A short glossary and a list of common abbreviations is compiled in Appendix 2.

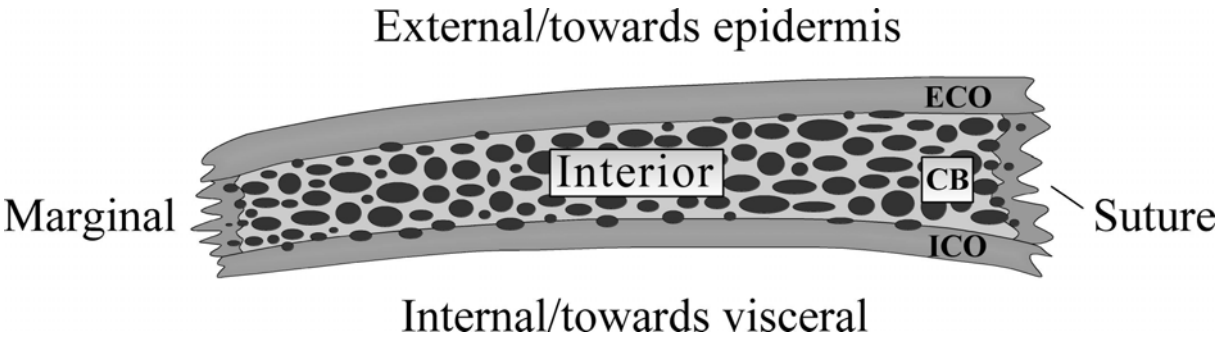

Figure 7: Schematic drawing illustrating topographic terminology of a turtle shell bone in thin-section

In the case of the placodont outgroups, the postcranial armour plates are referred to by the more neutral terms "plate" instead of "osteoderm", because the nature of the placodont armour is to be assessed in the current project as well.

2.4 Institutional abbreviations

Bone material for the study was obtained from the following museums and research institutes: **FM[NH]** The Field Museum, Chicago, Illinois, USA; **GUI-CHE** Testudinate material of Guimarota coal mine currently housed in the collections of the Institut für Geowissenschaften – Fachrichtung Paläontologie, Freie Universität Berlin, Germany (material will be finally deposited in the collections of the Servicio Geológico de Portugal, Lisboa [Geological Survey of Portugal, Lisbon]); **HLMD** Hessisches Landesmuseum Darmstadt, Darmstadt, Germany; **IPB** Goldfuss-Museum, Institute for Palaeontology, University of Bonn, Bonn, Germany; **IPFUB** Institut für Geowissenschaften [formerly Institut für Paläontologie], Freie Universität Berlin, Germany; **NHM** Naturmuseum Solothurn, Solothurn, Switzerland; **NHMM** Natuurhistorisch Museum Maastricht, Maastricht, The Netherlands; **MAGNT** Museum and Art Gallery of the Northern Territory, Darwin, Australia; **MB** Naturhistorisches Forschungsinstitut and Museum für Naturkunde, Zentralinstitut der Humboldt-Universität zu Berlin, Germany; **MHI** Muschelkalkmuseum Hagdorn, Ingelfingen, Germany; **MTD**, Staatliches Museum für Tierkunde Dresden, Germany; **MVZ** Museum of Vertebrate Zoology, University of California at Berkeley, California, USA; **NRM** Swedish

Museum of Natural History, Stockholm, Sweden; **QM** The Queensland Museum, Brisbane, Queensland, Australia; **ROM** Royal Ontario Museum, Toronto, Ontario, Canada; **SAM** Iziko: South African Museum, Cape Town, South Africa; **SGP** Sino-German Project, currently housed at the Institute and Museum of Geology and Palaeontology, University of Tübingen, Germany; **SMNK** Staatliches Museum für Naturkunde Karlsruhe, Karlsruhe, Germany; **SMNS** Staatliches Museum für Naturkunde Stuttgart, Stuttgart, Germany; **TMM** Texas Memorial Museum, University of Texas at Austin, Austin, Texas, USA; **TMP** Royal Tyrrell Museum of Palaeontology, Drumheller, Canada; **UCMP** Museum of Palaeontology, University of California at Berkeley, California, USA; **UNEFM** Centre of Archaeology, Anthropology and Palaeontology, Universidad Nacional Experimental Francisco de Miranda, Coro, Falcon, Venezuela; **UMZC** University Museum of Zoology, Cambridge University, Cambridge, Great Britain; **YPM** Peabody Museum of Natural History at Yale University, New Haven, Connecticut, USA; **ZFMK** Zoologisches Forschungsinstitut und Museum Alexander Koenig, Bonn, Germany; **ZMB** Zoologische Sammlung, Museum für Naturkunde, Humboldt-Universität zu Berlin, Germany.

3. Morphological description of outgroup taxa

To better understand amniote integuments that include ossified dermal armour and for character polarisation of the microstructure of turtle shell bones, dermal ossifications / armour plates of amphibians (Temnospondyli), mammals (Xenarthra), placodonts (Placodontoidea and Cyamodontoidea), pareiasaurs, lepidosaurs (Anguidae, Gekkonidae) and archosauromorphs (Parasuchia, Crocodylia and Dinosauria) were included in this research. The following chapters address the specimens of each sampled taxon, as well as available data on locality and age of the specimens. Furthermore, summaries of the respective outer morphologies and bone surface structures are given. If appropriate, the systematic status of each taxon is also addressed in brief.

3.1 Outgroup 1: Temnospondyl amphibians

The sampling of Temnospondyli included the capitosaur *Mastodonsaurus giganteus* (SMNS 91011), the plagiosaur *Gerrothorax pustuloglomeratus* (SMNS 91012) and the basal temnospondyl *Trimerorhachis* sp. (TMM 40031-59, TMM 40031-60). Due to the fragmentary nature of all samples, it could not be ascertained if the dermal bone elements belong to skulls or shoulder girdles respectively. Detailed morphological descriptions for the taxa, including paragraphs about the dermal sculpturing patterns, can be found for *M. giganteus* in Schoch (1999) and Schoch and Milner (2000), for *G. pustuloglomeratus* in Hellrung (2003) and for *Trimerorhachis* in Colbert (1955) and Holmes (2000).

3.1.1 *Trimerorhachis* sp.

As opposed to most temnospondyl groups, Trimerorhachoidea (both juveniles and adults) remain completely aquatic (Holmes, 2000). Two specimens of *Trimerorhachis* sp. were sampled. Both specimens (TMM 40031-59, TMM 40031-60) are thin bone fragments most probably from the shoulder girdle region of the animal. The genus *Trimerorhachis* (Case, 1935) is restricted to the Sakmarian, Lower Permian (Ruta et al., 2003). The specimens were

recovered from the Tit Mountain locality, Archer County, Texas, USA (Petrolia Formation, Lower Permian). The external surface of the bone shows a sculpturing pattern of reticular ridges in the centre and radially arranged low ridges towards the margins.

3.1.2 *Mastodonsaurus giganteus* (Jaeger, 1828)

The specimen of *M. giganteus* (SMNS 91011) was collected in the Erfurt-Formation ('Lettenkeuper', Ladinian, Upper Triassic) of Kupferzell, southern Germany. Macroscopically, the dermal bone fragment appears massive in cross-section. The internal surface of the bone is smooth, the external surface heavily sculptured with prominent ridges. Some of these ridges anastomose to form a reticular pattern. The margins of the bone fragment are sutured.

3.1.3 *Gerrothorax pustuloglomeratus* (Huene, 1922)

The sampled dermal bone fragment (SMNS 91012) of *G. pustuloglomeratus* is a thick bone fragment of the cranium or the shoulder girdle. It was also found in the Erfurt-Formation ('Lettenkeuper', Ladinian, Upper Triassic) of Kupferzell, southern Germany. The external surface of the bone is sculptured with low ridges, pustules and knobs. The internal surface is smooth with few foramina inserting into the internal cortical bone.

3.2 Outgroup 2: Mammalia

There are few groups among the Mammalia that bear armour plates within the integument. All those groups, fossil and recent, belong to the Xenarthra. Within the Xenarthra, the Folivora (= Phyllophaga) and the Cingulata have osteoderms. While fossil giant ground sloths (Phyllophaga) like *Paramylodon harlani* (Pleistocene, North America) had small, isolated and unfused osteoderms embedded in the skin, the fossil glyptodonts and extant armadillos and their fossil relatives (Cingulata), on the other hand, carry extensive dorsal armoured shells.

While glyptodont dorsal body armour was rigidly fused together, armadillos have movable bands within their armour. The material and the thin-sections of the Xenarthra used in this study were prepared and described by D. Wolf (2006, unpubl. MSc-thesis). While the morphological and bone histological descriptions are essentially based on his results, I had the opportunity to look at his samples and thin-sections myself to verify the given data. Out of this work, material of the taxa *Paramylodon harlani* (Owen, 1840), *Glyptodon clavipes* Owen, 1839 and of the genus *Propalaehoplophorus* Ameghino, 1887 were used for comparison. Similar to the work of D. Wolf, a recent study by Hill (2006), focussed on the bone histology of xenarthran osteoderms. The results given below and those of Hill (2006) essentially agree with each other.

3.2.1 Folivora (Xenarthra)

3.2.1.1 *Paramylodon harlani* (Owen, 1840)

The giant ground sloth *P. harlani* from the Pleistocene of North America had small, isolated and unfused osteoderms embedded in the skin. The gross morphology of these osteoderms can be highly divergent. Some of these osteoderms are irregularly star-shaped, some elongated and some are round and pillow-like. The planes of sectioning followed either the long axis of the osteoderm or cut perpendicularly through conspicuous ridges or protuberances (Wolf, pers. comm.). The largest sampled elongated osteoderm reached 21 mm (TMM 30967-1006) in length while others had diameters ranging between 13 mm and 18 mm (e.g., TMM 30967–2632). All bone surfaces are strongly rugose and are often pitted with foramina that insert into the bone tissue.

3.2.2 Cingulata (Xenarthra)

3.2.2.1 *Propalaehoplophorus* sp.

The studied osteoderms of *Propalaehoplophorus* sp. (Miocene, South America) are of hexagonal shape (e.g., IPB M6151; IPB M6444). The interior part of the bone elements is

usually thinner than the marginal areas. The two longest margins trend parallel to each other, giving the osteoderms a peculiar rectangular appearance. The internal surfaces of the bones are usually slightly concave and smooth, while several scattered foramina insert into the internal bone tissue. The external surface of the bone is flat to slightly convex, with a large central, rounded-polygonal figure. Further ornamental figures may be present towards the margins. Osteoderm lengths ranged between 29 and 32 mm, width between 20 and 25 mm and thicknesses between 6 and 7 mm.

3.2.2.2 *Glyptodon clavipes* Owen, 1839

The material of *G. clavipes* was found in the Pampean Formation (Pleistocene), Santa Cruz Province, Patagonia, Argentina, South America. Two buckler osteoderms of different localities of a fused carapace (YPM 12214) were sampled. Both osteoderms were supposedly sectioned in a sagittal or near-sagittal plane, while one osteoderm half was then also sectioned transversely. Both elements have a hexagonal shape. However, the parallel margins are the longest margins in one osteoderm, while they are the shortest margins in the other. The external surfaces of the two bones are strongly pitted. A central figure surrounded by a groove as well as hair follicles are present. The internal surface of the bones has a fibrous texture and nutrient foramina insert into the internal bone cortex.

3.3 Outgroup 3: non-testudinatan Reptilia

Besides the few armour-bearing mammalian outgroups, Reptilia are the dominant amniote clade that is typically associated with the development of dermal armour. The oldest representatives of Reptilia (i.e. *Hylonomus lyelli*) were discovered in Upper Carboniferous (about 315 Ma; Pennsylvanian) rocks at Joggins, Nova Scotia, Canada. For a discussion about the phylogeny of Reptilia and its terminology see Modesto and Anderson (2004).

3.3.1 Parareptilia (Pareiasauria)

Pareiasaurs are a group of mostly large, herbivorous parareptiles that lived during the Late Permian. Two osteoderms each of the pareiasaur genera *Bradysaurus*, *Pareiasaurus* and *Anthodon* from South Africa were be sampled. While basal pareiasaurs like *Bradysaurus* only had small osteoderms sitting over the median vertebral column, moderately derived forms like *Pareiasaurus* were already extensively covered with larger, if still unfused, osteoderms (e.g., Lee, 1996). According to Lee (1997), the dorsal trunk region was heavily armoured in highly derived dwarf pareiasaurs, e.g., *Anthodon serrarius*, with overlapping osteodermal plates that sometimes are sutured together. The specimens of *A. serrarius* that were sampled in this study, however, lacked sutured margins.

3.3.1.1 *Bradysaurus seeleyi* Haughton and Boonstra, 1929

The specimen SAM-PK-8941 (catalogued as *B. vanderbyli* in the SAM collections) found at the Permian locality of Mynhardtskraal, Beaufort West District, South Africa, had the superficial appearance as a round knoblike osteoderm structure. Thin-sectioning, however, revealed that the only bony matter that could be found in the specimen was restricted to a very tiny sliver at the internal margin of the specimen. The rest of the specimen comprises carbonate rock. While Kuhn (1969) listed *B. vanderbyli* Haughton and Boonstra, 1929 still as a separate species, the taxon is now regarded to be synonymous with *Bradysaurus seeleyi* Haughton and Boonstra, 1929 (see also Lee, 1997; Jalil and Janvier, 2005).

3.3.1.2 *Bradysaurus* sp.

Two specimens (SAM-PK-4348; SAM-PK-12140) of *Bradysaurus* sp. were sampled. Specimen SAM-PK-4348, from Wilgerfontein, Prince Albert District, South Africa, comprises a fragmentary osteoderm fused to an underlying bone, probably from the skull region. The whole specimen is still largely embedded in carbonate matrix, thus little of the external surface of the osteoderm is seen. However, the part of the osteoderm which is free of surrounding rock has irregular ridges extending over the external bone surface. Due to the

fragmentary nature of the specimen and its embedding in carbonate rock, measurements were not possible. Specimen SAM-PK-12140 comprises an isolated osteoderm from Rietfontein, Prince Albert District, South Africa. The margins of the specimen are partly broken. The internal surface of the bone is flat to slightly concave. The external surface of the bone is convex and knoblike, with the apex sitting slightly off-centre. The diameter of the osteoderm varies between 34 and 40 mm, its maximum thickness, measured at the apex, is 19 mm.

3.3.1.3 *Pareiasaurus serridens* Owen, 1876

Specimen SAM-PK-K10036 of P. serridens is an isolated osteoderm that was found in the Late Permian locality Farm127, near Doornplaats, Graaff-Reinet District, South Africa. The osteoderm is still largely covered in carbonate matrix, however, the outer shape of the osteoderm is recognisable. The external surface of the osteoderm is strongly convex, the internal surface similarly strongly concave. The external surface of the bone is ornamented and carries a central boss. The internal bone surface has a rough texture with numerous foramina inserting into the internal cortex. The cross-section of the specimen revealed that the margins of the osteoderm are not sutured.

3.3.1.4 *Pareiasaurus* sp.

Four osteoderms (UMZC R381 T702: one osteoderm; SAM-PK-1058: three osteoderms) of *Pareiasaurus* sp. were sectioned. Specimen UMZC R81 T702 was found in the Tapinocephalus zone (Late Permian), Hottentots River, Prince Albert District, South Africa. The specimens of SAM-PK-1058 were found in Permian strata of Welgevonden, Graaff-Reinet District, South Africa. While the larger slab of SAM-PK-1058 comprises two separate osteoderms still embedded in carbonate matrix, one of which has a broken margin, the smaller slab contains a complete isolated osteoderm. The margins of UMZC R381 T702 are also not preserved. The margins in the well preserved specimens (SAM-PK-1058) are not sutured. All specimens (UMZC R381 T702; SAM-PK-1058) comprise flat to slightly concave internal bone surfaces, while the external bone surfaces are strongly ornamented with irregular ridges.

3.3.1.5 *Anthodon serrarius* Owen, 1876

The two isolated osteoderms (SAM-PK-10074) of *A. serrarius* come from the Late Permian locality of Dunedin, Beaufort West District, South Africa. The osteoderms have oval shapes in externointernal view, a central external boss and an external sculpturing pattern consisting of ridges that extend radially from the centre of the boss to the margin of the osteoderm. The margins were not sutured. The internal surfaces of the osteoderms are rather flat. The smaller but thicker osteoderm is 40 mm long, 30 mm wide and has a maximum thickness of 15 mm (measured at the central boss). The larger but thinner osteoderm is 45 mm long, 36 mm wide and has a maximum thickness of 9 mm (also at the central boss).

3.3.2 Eureptilia (Placodontia)

The Placodontia are an enigmatic group of sauropterygian reptiles restricted to the Triassic. The taxon includes the largely unarmoured Placodontoidea (e.g., Nopcsa, 1923; Rieppel and Zanon, 1997; Rieppel, 2000) and the heavily armoured Cyamodontoidea (Nopcsa, 1923; Peyer and Kuhn-Schnyder, 1955; Westphal, 1975, 1976; Mazin and Pinna, 1993; Rieppel and Zanon, 1997; Rieppel, 2000, 2002). According to Rieppel (2000), the Placodontoidea are presumably paraphyletic with relationships being (*Paraplacodus* (*Placodus*, Cyamodontoidea)). While the basal placodontoid *Placodus gigas* sports only a single row of dermal plates above its spine, derived cyamodontoids superficially resemble turtles in enclosing their body in an armour shell.

3.3.2.1 Placodontoidea

3.3.2.1.1 *Placodus gigas* Agassiz, 1833

A single keeled plate (SMNS 91006) from the dorsal vertebral column was sampled. SMNS 91006 was found in the Trochitenkalk Formation (‘Upper Muschelkalk; Lower Hauptmuschelkalk’, ?m7; Ladinian, Middle Triassic) in Bühlingen near Rottweil, Germany. The plate is roughly triangular in anteroposterior cross-section. The mediolaterally curved

anterior surface and the straight posterior surface form a sharp external keel, slightly off-centre towards the posterior margin of the plate. Both surfaces are sculptured with a fine striation pattern that extends externointernally and medially dips slightly towards the external keel. The internal convex surface of the plate has rounded, blunt edges, instead of distinctly sharp ones. The internal surface also has a rugose texture due to numerous foramina of various sizes. The maximum height as measured from the convex internal surface to the apex of the keel spans 24.5 mm.

3.3.2.2 Cyamodontoidea

3.3.2.2.1 *Psephosaurus suevicus* Fraas, 1896

Four specimens were sampled, including one armour plate (SMNS 91007) from sediments of the Erfurt Formation (Ladinian, Middle Triassic, k1) of Hoheneck near Ludwigsburg, Germany and three plates (MHI 1426/1-3) from the quarry "Hohenloher Steinwerk", Kirchberg/Jagst (Erfurt Formation, Ladinian, Middle Triassic, k1, "Anthrakonit-Bank, Basisbonebed").

The small spiked plate (SMNS 91007) is of circular shape in external view and has a central apex. The maximum as measured between the midpoint of the internal surface and the apex is 11.0 mm. The diameter of the base is 27.0 mm. In externointernal view, concentric growth marks are seen from the apex down to the margin of the plate. Concurrently, the spiked plate shows a very fine radiating striation extending from the apex to the margin of the base of the plate (see Rieppel, 2002). The spiked plate is still embedded in sediment, thus the flat to slightly concave internal surface is only visible in sections. There are no apparent foramina inserting from the internal surface of the bone into the interior of the plate.

The second specimen (MHI 1426/1) resembles a procumbent spike. The external surface of the spike constitutes two pronounced straight edges tapering into an off-centre apex. Opposite to the apical region, the external surface ends a half-circle. At the half-circle end of the plate, the margin is sutured. At the apical side, the margins internal to the external straight edges constitute flat to slightly concave rectangular bone surfaces that meet in a low angle in the

midline of the plate. From the apex and the straight edges, the flat rectangular bone surfaces are also strongly dipping in a 45° angle back towards the internal bone surface. The whole of the external surface of the bone has a pattern of very fine shallow vascular grooves radiating from the apex towards the opposite half-circle margin. Additionally, thin flat ridges radiate from the apex towards the opposite half-circle margin. Being framed by the two angled flat to slightly concave rectangular marginal surfaces, the internal bone surface is a small rugose area of bone of oval shape with a short protrusion at the apical side, thus mirroring the shape of the external surface of the bone. The flat to slightly concave rectangular marginal surfaces of the bone proposedly overlap an adjacent plate in these areas. The largest diameter of the half-circle end of the plate is 13 mm, the distance between the apex and the opposite half-circle margin is 12 mm. While the height of the plate ranges between 5.0 mm at the half-circle margin it measures 11 mm between the internal surface of the bone and the external off-centred apex.

The last two specimens of *P. suevicus* include a larger (MHI 1426/2) and a smaller plate (MHI 1426/3) of hexagonal shape. Both specimens have slightly convex external and slightly concave internal bone surfaces. The margins are sutured in both elements. The external surface of the smaller bony element is rather smooth; the internal one rough due to a shallow reticular pattern. On the external surface of the smaller specimen, a shallow groove is present at the margins, surrounding a central apex. According to Rieppel (2002), similar grooves in part of the holotype of *P. suevicus* (SMNS 7113) indicate a congruence of the plates with overlying keratinous scutes. The distances between margins in the smaller specimen range from 12 to 15 mm, whereas the height measures between 6.0 and 7.0 mm. The larger specimen experienced lateral deformation, thus the marginal sides of the plate are strongly angled. There are no grooves as in the smaller specimen, but the external surface exhibits a very fine superficial vascular pattern radiating outward from the central apex. The internal surface texture of the larger element also appears rough because of shallow reticular bone tissue structures. The diameter of the larger plate (measured at the external surface of the bone) ranges between 23 and 25 mm, while the thickness ranges between 10 mm at the margins and 11 mm in the plate centre. The elements described above may represent the two plate types of the armour of *P. suevicus* observed already by Fraas (1896; see also Rieppel, 2002), where the larger plates are surrounded and separated from each other by the smaller type.

3.3.2.2.2 *Psephosaurus* sp.

Two armour plates (SMNS 91008, 91009) of *Psephosaurus* sp. were sampled. Both plates were found in the Erfurt Formation (Ladinian, Middle Triassic, k1) of Hoheneck near Ludwigsburg, Germany. Similar to *Psephosauriscus sinaiticus* Haas (see Rieppel, 2002:fig. 28), the two samples of *Psephosaurus* sp. from the Erfurt Formation (Ladinian, Middle Triassic) of southern Germany likely represent divergent armour plate morphologies for the carapace and plastron of that taxon. The specimen SMNS 91008 is a flat plate that has a hexagonal contour in external view, while the plate margins are indented, probably representing scute sulci. The plate is hypothesised to be derived from the carapace (see Rieppel, 2002). Its thickness ranges from 4.5 mm in the centre to 6.5 mm at the margins of the plate. The maximum elongation of the plate is 23.0 mm. The bone is still embedded in sediment, thus the slightly concave internal surface of the plate is only observed in cross-section. In the second specimen (SMNS 91009), the base of the plate has a rhomboidal contour in externointernal view, and the external surface is convex with a slightly raised off-centre ridge. This plate is hypothesised to be derived from the plastral region (see Rieppel, 2002). The apical portion of the ridge is broken off, so only a minimum height of 14.0 mm was measured. A maximum distance of 27.0 mm was measured for the subparallel margins of the plate. A small and shallow marginal groove, again interpreted as a scute sulcus, extends all around the raised ridge of the external surface. The internal surface of the armour plate is flat, and the lateral margins show some weak growth lines.

3.3.2.2.3 Cf. *Placochelys* sp.

One dermal armour plate (SMNS 91010) of cf. *Placochelys* sp. was sampled. The specimen was recovered in sediments of the Grabfeld Formation (‘Estherienschichten, Anatinabank’ k2, Lower Carnian, Upper Triassic) of Willsbach near Heilbronn, Germany. Though specimen SMNS 91010 was not found in Hungary, but was recovered from sediments of Carnian age (Upper Triassic) of southern Germany, it strongly resembles some of the plates of the holotype of *Placochelys placodonta* Jaekel from Hungary (compare to Rieppel 2002:12, fig. 12). The triangular armour spike is somewhat unusual in that it is flatly positioned in the armour and not upright as is usually the case with pointed or spiked osteoderms. The spike

has three distinct surfaces. First, one side, the external surface, is broad and convex. Second, the opposite surface, the internal surface, is flat to slightly concave, giving the spike a slightly curved appearance. These two surfaces form two rather blunt marginal edges that taper towards a pointed apex. The third surface opposite the apex represents a marginal surface rather than the "base" of the spike. The long axis of this oval third surface measures 24.0 mm, the short axis 12.0 mm. This latter surface is roughly oval in shape and concave. The spiked plate measures 25.0 mm between apex and midpoint of the concave third surface and a maximum of 27.0 mm between apex and opposite margin. Roughly concentric growth marks are recognisable from the apex down to the concave surface. One of the margins between the external and internal side was broken off and has been reconstructed in plaster prior to the current study.

3.3.2.2.4 *Psephoderma* sp.

Specimen NRM-PZ R.1759a consists of a row of four sutured osteoderms partly embedded in a compact, shell-bearing limestone matrix. The material was found in Wadi Raman (Makhtesh Ramon; 'Muschelkalk', Middle Triassic), Negev, Israel. The armour plates are polygonal in externointernal view, but their exact shapes (?hexagonal) remain hidden by the carbonate matrix. Two of the plates appear smaller in cross-section, but it cannot be deduced if this is an artefact of sectioning irregularly arranged plates or if it is a true size reduction of the armour plates. All plates are well sutured and rectangular in cross-section without a spike or ridge. The bone surfaces have a rough texture. The external bone surface is flat to slightly convex and slightly wavy with shallow pits or grooves (the deeper grooves may represent scute sulci in cross-section). The internal bone surface is flat to slightly concave. The thicknesses of the fused plates range between 8,0 mm and 10,0 mm.

3.3.3 Eureptilia (Lepidosauria)

Osteoderms are generally not viewed as being synapomorphic for Lepidosauria. Morphological and bone histological descriptions of lepidosaur osteoderms are yet quite rare (e.g., Moss, 1969, 1972 for detailed work on osteoderms of *Heloderma horridum*; Zylberberg and Castanet, 1985; Levrat-Calviac and Zylberberg, 1986). For comparative purposes, the histological data of the works of Zylberberg and Castanet (1985) about *Anguis fragilis* and of Levrat-Calviac and Zylberberg (1986) about *Tarentola mauritanica* were used in this study. Please refer to the original literature for data on gross morphology.

3.3.4 Eureptilia (Archosauromorpha)

Because osteoderms are a potential synapomorphy of archosaurs (Benton and Clark, 1988), histological comparison of shell bones of turtles and archosaur osteoderms becomes possible. Several osteoderms of Archosauromorpha were sampled, including basal parasuchians (Phytosauria), fossil and recent crocodiles and thyreophoran dinosaurs. Many of those osteoderm bone histologies were already comparatively described by Scheyer and Sander (2004), thus only new material is described below. The study by Scheyer and Sander (2004) focussed on thyreophoran dinosaurs and included the following taxa: Ankylosauridae indet., Eusuchia indet., *Gastonia* sp., *Goniopholis* sp., Nodosauridae indet., Phytosauria indet., *Pinacosaurus grangeri*, *Polacanthus foxii*, *Saichania chulsanensis*, *Scelidosaurus* sp., *Stegosaurus stenops*, *Stegosaurus* sp. and *Struthiosaurus* sp. In the following, only the new material of the Triassic parasuchian cf. *Mystriosuchus* sp. and the Jurassic thalattosuchid crocodyliform *Steneosaurus* sp. (Teleosauridae) will be described, because they were not part of the earlier bone histological study. Please note that another bone histological study focussing on Thalattosuchia also included two teleosaurid osteoderms, one belonging to *Teleosaurus* and one belonging to *Steneosaurus* (Hua and Buffrénil, 1996).

3.3.4.1 Cf. *Mystriosuchus* sp.

The basal archosaur cf. *Mystriosuchus* sp. (Parasuchia, Pseudopalatinae) exhibits extensive dermal armour, including four dorsal anteroposterior trending rows of unsutured osteoderms (see MacGregor, 1906; Hungerbühler, 2002). The studied osteoderm fragment (SMNS 91013) was found in the Upper Triassic Löwenstein Formation of Heslach near Stuttgart, Germany. The fragment has a strong medial external keel trending anteroposteriorly over the osteoderm. Three quarters of the margins of the osteoderm are broken, thus only the keel and one unbroken margin could be sampled. The external surface of the osteoderm fragment is further ornamented by low ridges that extend mediolaterally from keel to osteoderm margin. The internal surface of the osteoderm fragment is flat to slightly convex. The internal surface of the bone exhibits a superficial pattern of crosshatched collagenous fibre bundles. A few scattered foramina insert into the internal cortical bone. While the length of the osteoderm cannot be reconstructed due to its fragmentary nature, the width of the osteoderm is reconstructed to be 65 mm. The maximum height of 18 mm was measured at the medial keel of the osteoderm fragment.

3.3.4.2 *Steneosaurus* sp.

Thalattosuchia, mostly long slender snouted crocodyliforms (Brochu, 2001; Gasparini et al., 2006), are the only archosaurian lineage that is completely adapted to a marine life-style (Langston, 1973). A recent phylogeny of Thalattosuchia is found for example in Gasparini et al. (2006). In Thalattosuchia, the genus *Steneosaurus* falls into the Teleosauridae. For the current study, one fragmentary osteoderm was sectioned. The specimen was part of a larger collection of armour plates that was found in the Kimmeridgian (Upper Jurassic) 'turtle-limestone' of Solothurn, Switzerland (NMS 7152). The fragment consists of the larger part (about two thirds) of an ovoid osteoderm with a flat internal bone surface, a convex external bone surface, and smooth margins. The external bone surface shows large, deep circular pits.

4. Morphological description of Testudinata

4.1 Basal Testudinata

In addition to *Proganochelys quenstedti* Baur, 1887, several groups seem to belong to the stem group of turtles, the basal Testudinata (Sukhanov, 2001, in Danilov, 2005; Joyce et al., 2004, Joyce, 2007; Sukhanov, 2006). Among the basal forms are also some taxa that have been previously recognised as pleurodires (i.e., *Proterochersis robusta* Fraas, 1913) or cryptodires (i.e., *Kayentachelys aprix, Meiolania s*p.) (e.g., Gaffney et al., 1987; Rougier et al., 1995; Gaffney, 1996). For the current study, these taxa are treated as sister taxa to the more derived Cryptodira and Pleurodira (crown group turtles; Casichelydia Gaffney, 1975c). Of these, only material of *Palaeochersis talampayensis* Rougier et al., 1995, a basal turtle from the upper part of the Triassic Los Colorados Formation, north-western Argentina, South America and *Heckerochelys romani* Sukhanov, 2006 from the Middle Jurassic Peski locality, Moscow Region, Russia, were not available for this study. According to Rougier et al. (1995), *P. talampayensis* belongs to the Australochelyidae, a group that was originally erected to accomodate *Australochelys africanus* Gaffney and Kitching, 1994, a basal turtle from the Early Jurassic Elliot Formation of South Africa. Sukhanov (2006) hypothesised the relationships of basal turtle genera as follows: (*Proganochelys* (*Australochelys*, *Palaeochersis*) (*Proterochersis* (*Heckerochelys* (*Kayentachelys* (Selmacryptodira (*Platychelys*, Eupleurodira))))))).

4.1.1 Proganochelyidae

Proganochelyidae is a monospecific taxon with the Upper Triassic *Proganochelys quenstedti* Baur, 1887 from southern Germany being the type species. *P. quenstedti* is still the basal-most turtle known (e.g., Gaffney, 1990; 1996, Joyce et al., 2004, Sukhanov, 2006) It was first discovered from the middle and upper “Stubensandstein” of the Keuper (Norian, Late Triassic) of Trossingen-Aixheim and Tübingen, Southern Germany (e.g., Gaffney, 1990). Further material was then discovered from Halberstadt, eastern Germany. Today, remains of the genus *Proganochelys* are known from other Late Triassic localities in Thailand

(Broin, 1984) and Greenland (Jenkins et al., 1994). Even though *Proganochelys quenstedti* is younger than *Proterochersis robusta*, it is still the oldest, most completely known turtle.

4.1.1.1 *Proganochelys quenstedti* Baur, 1887

The material of *P. quenstedti* that was obtained for the study included a piece of crushed shell with bits of a plastron fragment and a peripheral of shell fragment SMNS 17203 (see Gaffney, 1990:150-151, fig.99, 100), as well as the smallest of three fused posterior peripherals of SMNS 17203 (see Gaffney, 1990:154, fig.103). Additionally, a costal fragment of shell fragment MB.R. 3449.2 was sectioned. SMNS 17203 derives from the upper Löwenstein-Formation (upper "Stubensandstein", Norian, Late Triassic), *Plateosaurus* quarry in Trossingen, southern Germany (see also Gaffney, 1990:15). MB.R.3449.2 derives from sediments of the same age (Löwenstein-Formation, Norian, Late Triassic) from Halberstadt, eastern Germany. Due to lack of data, it is assumed that, similar to another specimen (MB.1910.45.2), this specimen was recovered from Baerecke and Limpricht Quarry, Halberstadt (see Gaffney, 1990:13). In the first sample, the plastral part is quite thin and flat, while the adjacent peripheral is triangular in cross-section. The second sample, the small posterior peripheral, has an oval base and tapers into an off-centred pointed apex. The peripheral is dorsoventrally flattened, resulting in two lateral ridges that extend from base to apex. The third sample, the costal fragment, has a flat external bone surface. The internal surface of the bone is medially bulged where the rib extends through the costal plate. While the bone material from Trossingen is strongly diagenetically altered, the material from Halberstadt is, although fractured, fairly well preserved. Furthermore, the specimens from Trossingen do show slight marks of preparation, while the bone surfaces of the specimen from Halberstadt are largely undisturbed.

4.1.2 Proterochersidae

Proterochersidae is a monospecific taxon with the Upper Triassic *Proterochersis robusta* Fraas, 1913 from southwestern Germany being the type species. Only postcranial material is

known of this taxon. In Danilov (2005), *Murrhardtia staeschei* Karl and Tichy, 2000 is treated as a junior synonym of *Proterochersis robusta.* The basal turtle *P. robusta* occurs in sediments that are slightly older (lower "Stubensandstein", early Norian, Late Triassic) than the ones where remains of *P. quenstedti* were found in. However, *P. robusta* exhibits some postcranial characters that are more derived compared to *P. quenstedti*.

4.1.2.1 *Proterochersis robusta* Fraas, 1913

The material of specimen SMNS 16442 of *P. robusta* used in this study included a fragmentary peripheral and a small plastron fragment (?hyo- or hypoplastron) from the lower Löwenstein-Formation (lower "Stubensandstein", early Norian, Late Triassic), from a "Fleinswerk" at Murrhardt, southern Germany. The peripheral fragment consists of a straight proximal part and a distal bulging part that tapers into a distal edge. The plastral fragment is a flat plate that locally increases in thickness. This thicker part presumably belongs to a bridge buttress. The external surfaces of the shell elements lack ornamentation. However, the internal and external surfaces of the bones have a slightly rough texture due to a faint and shallow reticular vascularisation pattern.

4.1.3 Kayentachelyidae

Kayentachelyidae is a monospecific taxon, with *Kayentachelys aprix* Gaffney et al., 1987 from the Early Jurassic of Arizona being the type species (Joyce et al., 2004). In Gaffney et al. (1987), *Kayentachelys* was hypothesised to be the oldest cryptodiran turtle. However, according to newer analyses, *Kayentachelys* is now thought to represent one of the basal Testudinata instead (Joyce et al., 2004; Joyce, 2007).

4.1.3.1 *Kayentachelys* sp.

The sample of *Kayentachelys* sp. included a neural (TMM 43669-4.2), the proximal part of a costal (UCMP V85010/150228), another costal fragment (TMM 43669-4.1), two peripherals (UCMP V82319/130079; UCMP V85013/150230) and a plastron fragment (?hyo- or hypoplastron; UCMP V85013/150229). The shell material from the UCMP collections was found in Early Jurassic Kayenta Formation, Coconino Co., Arizona, USA (the type *Kayentachelys aprix* Gaffney et al., 1987 was described from Coconino Co.). The material from TMM collections derives from Early Jurassic Kayenta Formation, Gold Spring Wash locality, Navajo Nation, Arizona, USA. The neural has a slightly curved plate that is roughly square, although one margin is broken off. The neural is roof-shaped in cross-section. The costal fragments are flat bones. A rib head protrudes from the internal bone surface of the proximal costal fragment. Both peripherals are triangular in cross-section. The plastron fragment has a flat external bone surface. The internal surface, however, is flat at one broken margin and gently rises towards the opposite broken margin. Scute sulci were best preserved in the peripheral (UCMP V82319/130079). All elements had a faintly rough external bone surface texture but otherwise lacked a sculpture. The internal surfaces of the bones generally appeared smooth.

4.1.4 Meiolaniidae

The Meiolaniidae are a group of extinct turtles that lived in the southern hemisphere from the Eocene to the Pleistocene, with possible Cretaceous meiolaniid remains occurring in Chubut Province, Argentina (Gaffney, 1996). Meiolaniid turtles share the presence of cranial horns or flanges of bone and a bony tail club. According to Gaffney (1996), the Meiolaniidae are Centrocryptodira, based on cervical vertebral shape and articulation and the morphology of the floor of the *canalis caroticus* within the skull. However, unlike other cryptodires, they were not able to retract their head. Hirayama et al. (2000), followed by Danilov (2005), thought that Meiolaniidae are basal Cryptodira. Based on characters that group the Meiolaniidae with other basal turtles, however, Joyce (2007) argues that the Meiolaniidae do not belong to the Cryptodira at all, instead being basal Testudinata (Joyce et al., 2004).

4.1.4.1 *Meiolania* sp.

The only studied material of *Meiolania* sp. is specimen MB.R. 2426.1. Morphologically, the fragmentary piece of shell bone does not allow an unambiguous identification pertaining to the locality in the bony shell. The shell bone thickness is slightly decreasing from one end of the element to the other. Identifiable sutures or scute sulci are not present. Both the internal and the external surfaces of the fragment show a slight striation. However, based on the poor preservation, it remains unclear if the striation is a primary structure or a preservational/preparatory artefact.

4.2 Pleurodira

Besides the crown-group clades Pelomedusidae, Podocnemidae and Chelidae, the Pleurodira comprises also some purely fossil clades (the basal Dortokidae and Platychelyidae and the more advanced Bothremydidae and Araripemydidae). The Araripemydidae and the Dortokidae were not included in the present study. Taking into account the biogeography of both recent and fossil clades, the Pleurodira have to be considered to represent a cosmopolitan group of turtles. Because *Proterochersis robusta* is not treated as a pleurodire herein, the fossil record of Pleurodira thus commences with the Upper Jurassic.

Podocnemidae, Bothremydidae and Pelomedusidae form the clade Pelomedusoides (Antunes and Broin 1988), one of the two major crown clades of Pleurodira, the other being Chelidae. *Pelomedusa* Wagler, 1830 is monospecific with recent African helmeted turtle *P. subrufa* (Bonnaterre, 1789) being the only representative. *P. subrufa* occurs today in subtropical and tropical regions of Africa (e.g., Ernst and Barbour, 1989). Please note that for example Iverson (1992) or Joyce et al. (2004) give precedence of authority to Bonnaterre (1789) instead of Lacépède (1788) based on unavailability of the latter work as using non-binominal nomenclature. This was recently validated by the ICZN (BZN, Vol. 62, Pt. 1, 2005: opinion 2104 (case 3226)). The same applies to the kinosternid species *Kinosternon subrubrum* Bonnaterre (1789) and the trionychid species *Lissemys punctata* Bonnaterre (1789).

According to Meylan (1996) and Noonan (2000), the Podocnemidae together with the fossil clade Bothremydidae forms the Podocnemoidae. Specimens of *Taphrosphys sulcatus* (Leidy, 1856a), revised by Gaffney, 1975d (see also Gaffney and Zangerl, 1968), *Bothremys barberi* (Schmidt, 1940) and of "*Foxemys* cf. *F. mechinorum*" (see Tong et al., 1998; Tong and Gaffney, 2000; Lapparent de Broin, 2001) were sectioned to sample the Bothremydidae. The first two species are well known from Late Cretaceous marine sediments of North America. The last taxon, "*Foxemys* cf. *F. mechinorum*", derives from Late Cretaceous fluvial sediments of southern France. According to Tong et al. (1998), "*Foxemys*" is tentatively assigned to be a basal bothremydid and is thus treated as sister taxon to the clade (*Taphrosphys* (*Bothremys* + *Rosasia*)). Following Lapparent de Broin (2001), the species is valid, but the generic name "*Foxemys*" has to be considered a junior synonym of *Polysternon*. Notwithstanding the taxonomic and nomenclatural discussions surrounding "*Foxemys* cf. *F. mechinorum*" (Tong and Gaffney, 2000; Lapparent de Broin, 2001), the studied fossil material clearly represents a bothremydid. Adult bothremydid taxa can reach shell lengths of up to 150 cm (e.g., Gaffney 2001). However, shell lengths could not be ascertained with exactitude for the sampled specimens.

4.2.1 Platychelyidae

Platychelyidae comprises only the fossil genus *Platychelys* with *Platychelys oberndorferi* Wagner, 1853 from the Late Jurassic of Europe as type species. According to Joyce et al. (2004), *P. oberndorferi* is one of only three taxa that are currently hypothesised to unambiguously represent the stem-group of Pleurodira. *P. oberndorferi* was first described from lithographic shales (Upper Jurassic) near Kehlheim, southern Germany, but the taxon became much better known from the Upper Jurassic shallow marine limestones that were quarried near Solothurn, Switzerland (Bräm, 1965). Fossil remains of *P. oberndorferi* are relatively scarce, though. The taxon is hypothesised to have been a freshwater turtle that inhabited fluvial systems, swamps and lakes of near-shore environments (Bräm, 1965). Compared to the other turtle taxa from the Solothurn limestone (also known as the Solothurn 'turtle-limestone' or 'Schildkrötenkalk') that most probably lived in the near-shore marine environments, *P. oberndorferi* represents an allochthonous faunal element that was only occasionally brought into the marine limestone series.

4.2.1.1 *Platychelys oberndorferi* Wagner, 1853

The studied material of *P. oberndorferi* includes a complete costal (?left c3) with free distal rib end (NMS 20076), a peripheral (?p5) from the bridge region (NMS 20070) and a left hypoplastron (NMS 20076). The external surface of the hypoplastron is smooth with only a very faint striation pattern, while the costal and the peripheral are strongly sculptured with humps and ridges.

4.2.1.2 Aff. *Platychelys* sp.

Additionally to the material of *P. oberndorferi*, specimens of aff. *Platychelys* sp. from the Kimmeridgian Guimarota coal mine near Leiria, Portugal, (Bräm, 1973; Gassner, 2000; Lapparent de Broin, 2001) were used for studying the microstructure of the shell bones. The material included two small fragments of costal plates (GUI-CHE-50; GUI-CHE-51) and a small fragment of a peripheral (GUI-CHE-52). No sutures were preserved in the fragments. While the bone surface of the peripheral fragment appeared rather smooth, the bone surfaces of the costal fragments were heavily sculptured with humps.

4.2.2 Pelomedusidae

4.2.2.1 *Pelomedusa subrufa* (Bonnaterre, 1789)

A recent *Pelomedusa subrufa* (Bonnaterre, 1789), a small specimen with a SCL of 150 mm, was sampled as a representative for the Pelomedusidae. In the case of specimen MVZ 230517, no complete shell elements, but drilled cores of the shell were sub-sampled. Of the shell, a right costal, a right peripheral and the right hyoplastron were sampled. These samples were of the few that did preserve the interface between the shield cover above, connective tissue in between and bone below in the shell.

4.2.3 Bothremydidae

Bothremydidae comprises a group of widely distributed fossil turtle taxa that, according to Antunes and Broin (1988), used near-shore environments for their dispersal while some taxa like "*Foxemys* cf. *F. mechinorum*" inhabited fluvial or lacustrine environments (Tong et al., 1998).

4.2.3.1 *Bothremys barberi* (Schmidt, 1940)

The sampling of specimen FM P27406 of *B. barberi* included a neural, a costal, a peripheral and a plastron fragment. An ornamentation pattern was not recognised partly due to the weathered condition of the surfaces of the bones. The specimens of *B. barberi* were found in the Campanian Mooreville Chalk (Late Cretaceous), Selma Group, Dallas County, Alabama, USA.

4.2.3.2 *Taphrosphys sulcatus* (Leidy, 1856a)

The sample of specimen YPM 40228 of *T. sulcatus* comprises a neural (figured in Scheyer and Sánchez-Villagra, 2007, figs. 2, 5), a peripheral, a costal fragment and a fragmentary ?hyo- or hypoplastron. The shell material of *T. sulcatus* was found in the Middle Marl Bed (Middle Marl Bed may equal Hornerstown Formation, thus it would indicate a Late Maastrichtian age), Cretaceous, Birmingham, Burlington County, New Jersey, USA. All shell elements were ornamented with a reticular pattern on the external surface.

4.2.3.3 "*Foxemys cf. F. mechinorum*" Tong et al., 1998 = *Polysternon mechinorum* (Tong et al., 1998) fide Lapparent de Broin (2001)

All elements derive from Late Cretaceous (early Maastrichtian) fluvial sediments, Cruzy, Hérault, southern France. The sampling included four specimens: part of a neural (IPB R556),

a fragmentary ?hyo- or hypoplastron (IPB R559), an indeterminate plastron fragment (IPB R558) and a costal fragment (IPB R557). All shell elements were slightly ornamented with a reticular pattern on the external surface. IPB R559 is figured in Scheyer and Sánchez-Villagra (2007, fig. 2F).

4.2.4 Podocnemidae

Podocnemidae comprises South American and African taxa and probably originated in the Late Cretaceous (Gaffney and Forster 2003; see Joyce at al. 2004 for discussion). *Stupendemys geographicus*, for which the complete skull is yet unknown (e.g., Gaffney et al., 1998a), is included in Podocnemidae based on morphological characters of the postcranium, especially on the saddle-shaped central articulations of the cervicals (Wood 1976; Lapparent de Broin et al., 1993). As another representative of Podocnemidae, *Podocnemis erythrocephala* (Spix, 1824), a small living relative of *S. geographicus* from the northern parts of South America (Ernst and Barbour, 1989) that can reach a SCL of about 300 mm, was sampled. *Podocnemis* spp. and *S. geographicus,* among other taxa, may belong to a less inclusive taxon, Podocnemidinae, within Podocnemidae (e.g., Lapparent de Broin et al., 1993; Fuente, 2003). According to Gaffney and Wood (2002) *Bairdemys*, is also a member of Podocnemidae (Podocnemididae *sensu* Gaffney and Wood, 2002) based on skull features.

4.2.4.1 Cf. *Bairdemys* sp.

A single large shell fragment of cf. *Bairdemys* sp. could be sampled. The specimen (UNEFM uncat.) may represent a fragment of a large costal, but because of the weathered and diagenetically altered condition a clear assignment could not be made. Its external surface is curved and appears smooth. Because of the weathered condition of the bone surface as well as due to a thick iron oxide and mineral crust, bone surface textures, sculpturing patterns and scute sulci are obscured. The internal surface has a medial bulge slightly bent towards anterior, that may represent the progression of the rib. However, the structure is broken. The internal surface is also weathered and covered by a thin iron oxide and mineral crust. The

fragment is proximally thickened (thickness about 16 mm) and thins out distally (thickness about 11 mm). The maximum thickness between external surface and internal (?rib) bulge is 42 mm. The margins of the specimen extend mostly subparallel or are slightly curved. The maximum length of the element measures 145 mm, its maximum width 95 mm.

4.2.4.2 *Podocnemis erythrocephala* (Spix, 1824)

A beginning fusion of its individual bony elements was present in the carapacial disk of specimen YPM 11853 of *P. erythrocephala.* The fusion started with the neural elements in the middle of the carapacial disc and continued towards half of the length of the costals. The distal ends of the costals and the peripherals were sutured but still unfused. Samples of *P. erythrocephala* (YPM 11853) include neural2 and right costal3, left costals1-3, a right peripheral and right hypoplastron.

4.2.4.3 *Stupendemys geographicus* Wood, 1976

Two fragmentary costals (A and B) of specimen UNEFM-CIAPP-2002-01 of *S. geographicus* (Aguilera et al., 1994), measuring 3.3 meters in SCL and 2.18 meters in MCW were sampled. The costal fragment A from the mid-region of the carapace has an overall thickness of 3.0 cm, whereas fragment B from the posterior part of the carapace is significantly thinner (about 1 cm). It is assumed that both costal fragments were of similar thickness in the living turtle, thus the cortical bone and broken bone trabeculae of fragment B represent only the lower third part of fragment A. Additionally, articulated pieces of a neural from a smaller fragmentary specimen (UNEFM-101) were also obtained for sectioning. The bone histology of *S. geographicus* was thus observed in two different size categories (Figs. 2A, B, 3). With a calculated SCL of two to three meters, the smaller specimen plots well within other known, certainly adult, complete specimens of *S. geographicus* (Wood 1976; Scheyer and Sánchez-Villagra, 2007), even though the lateral parts of the neural fragment are only a third of the thickness of costal fragment A of UNEFM-CIAPP-2002-01. Compared to the slight stages of erosion found in the neural, both costal fragments express medium to

strong surface damages. It has to be assumed that neither fragment presents the complete histological evidence of undamaged cortices. Likewise measurements of the thicknesses of all fragments give only approximate values that have to be treated with caution. Costal fragment A is figured in Scheyer and Sánchez-Villagra (2007, figs. 2, 3).

4.2.5 Chelidae

The Chelidae are the second major crown clade of Pleurodira, the other being Pelomedusoides. Today, Chelidae represents 52 living species in twelve genera (Joyce et al., 2004), but the fossil record of Chelidae is still considered to be poor. Both modern and fossil Chelidae are restricted to the South American continent and Australasia (Australia and New Guinea, see Georges et al., 1998). Fossil chelids are unambiguously known from the Late Cretaceous of South America (Broin, 1987; Fuente et al., 2001; Lapparent de Broin and Fuente, 2001) and from the Miocene and lately the Eocene/?Palaeocene of Australia (Gaffney et al., 1989; Lapparent de Broin and Molnar, 2001). According to Joyce et al. (2004) turtle remains from the Early Cretaceous of South America may represent stem-group taxa of the Chelidae.

There is still an ongoing controversial discussion about the interrelationships of chelid turtles. In the classical morphological approaches (e.g., Boulenger, 1888a,b; Burbidge et al., 1974; Gaffney, 1977; Gaffney and Meylan, 1988; Shaffer et al., 1997), the long-necked genera of South America (i.e. *Chelus*, *Hydromedusa*) and Australasia (i.e. *Chelodina*) and the South American and Australasian short-necked chelid genera (e.g., *Phrynops*, *Platemys*, *Emydura*) are thought to be closely related. Please note, as Gaffney et al. (1989:7) pointed out, that the "*Emydura* group is characterised almost entirely by features that are plesiomorphic for Chelidae". In contrast, new analyses that rely on molecular and serological data support the idea (even though the support is weak in most cases) that long-necked and short-necked South American chelids on the one hand, and long-necked and short-necked Australasian chelid taxa on the other hand are more closely related to each other respectively (Fujita et al., 2004; Georges et al., 1998; Near et al., 2005; Shaffer et al., 1997). Overall, seven chelid specimens including three long-necked genera and three short-necked genera were sampled.

Short-necked Australasian Chelidae are represented by two turtle specimens (one fossil and one recent) of the genus *Emydura* Bonaparte, 1836. *Emydura* spp. reach carapace lengths of up to about 300 mm. All species are semi-aquatic and restricted to New Guinea and Australia (Iverson, 1992; Ernst and Barbour, 1989). The carapace of this chelid group usually lacks neurals, so the costals meet medially (e.g., Ernst and Barbour, 1989). *E. albertisii* Boulenger (1888b) is considered to be a junior synonym of *Emydura subglobosa* (Krefft, 1876) by Iverson (1992) and Ernst and Barbour (1989).

Chelodina longicollis (Shaw, 1794) represents the long-necked Australasian Chelidae herein. Its thin neck measures about 60 % of the total carapace length (Ernst and Barbour, 1989). *C. longicollis* is known to adapt its skin-colour to the surrounding background by melanophore cell contraction and expansion (Woolley, 1957, in Ernst and Barbour, 1989).

Short-necked Chelidae of South America are represented by *Platemys platycephala* (Schneider, 1791) and by *Phrynops geoffroanus* (Schweigger, 1812). While *P. geoffroanus* reaches CL of about 350 mm, *P. platycephala* is smaller (CL up to 180 mm) and more gracile (e.g., Ernst and Barbour, 1989). While both taxa are similarly distributed in northern South America, *P. platycephala* does not occur as far south and southeast as *P. geoffroanus*, which also inhabits areas of east-central South America (e.g., Pritchard, 1979; Ernst and Barbour, 1989).

Hydromedusa tectifera Cope, 1870a and *Chelus fimbriatus* (Schneider, 1783) were sampled as long-necked South American Chelidae. While *H. tectifera* is a rather inconspicuous turtle that prefers a snail diet (e.g., Pritchard, 1979), *C. fimbriatus* or Matamata from South America is one of the most bizarre turtles alive today. The fringes at the flat triangular head and long neck, together with the brownish colour and the highly humped, keeled and serrated shell effectively help to dissolve the general shape of the turtle. This and a gape-and-suck feeding mechanism make the Matamata an effective ambush predator (e.g., Pritchard, 1979; Ernst and Barbour, 1989).

4.2.5.1 *Emydura subglobosa* (=*Emydura albertisii*) (Krefft, 1876)

A recent specimen of *E. subglobosa* (ZFMK-58215), preserved in alcohol, was sampled. The shell has a CCL of 155 mm, a CCW of 125 mm and a SPL of 130 mm. The specimen derived from New Guinea, but no further data was available. Generally, *E. subglobosa* dwells in rivers, lakes and lagoons (e.g., Ernst and Barbour, 1989). Sampling was done by core-drilling where two cores, each with a diameter of 12 mm, were removed from the proximal part of the left ?costal2 and the left hyoplastron respectively.

4.2.5.2 *Emydura* sp.

Four fossil shell elements of cf. *Emydura* sp. were sampled. A closer identification to species-level was not possible, because of the fragmentary nature of the material. The fossils were collected in the Miocene Etadunna Formation of South Australia (see Gaffney, 1979a; 1981). The material included a thinner (max. 4 mm) and a thicker (max. 9 mm) costal fragment and a peripheral (UCMP V5762/57055) as well as a larger plastron fragment (?hyo- or hypoplastron; max. 12 mm in thickness; UCMP V5774/57270). The plane of sectioning runs craniocaudally for the thicker costal and the plastron fragment and proximodistally for the thinner costal and the peripheral. The costal and plastron fragments showed a characteristic sculpturing consisting of shallow reticular anastomosing grooves on the external bone surfaces. The internal surface of the bones was smooth. The sculpturing patterns as well as two scute sulci (each again in proximodistal orientation) were present on the external surfaces (both dorsal and ventral) of the peripheral. A scute sulcus also extended proximodistally on the external bone surface of the thinner costal. Furthermore, at least five small shallow pits of different depths are present on the external bone surface of the peripheral. It is apparent that these pits are not part of the sculpturing pattern. However, it is unclear if those pits appeared pre-mortem in the living animal, e.g., as the result of some kind of shell disease, or if they represent post-mortem diagenetic or decay structures.

4.2.5.3 *Chelodina longicollis* (Shaw, 1794)

C. longicollis is known from eastern Australia where it inhabits sluggish streams, swamps and lagoons (e.g., Ernst and Barbour, 1989). The sampled specimen (ZMB 27258) of *C. longicollis* has a CCL of 210 mm, a CCW of 173 mm and a CPL of 178 mm. Sampling was done by core drilling. Two cores with 22 mm diameter each were removed from the left ?costal2 and the right hyoplastron. In both cases, the keratinous shields are still attached to the bone cores. The external scute surface of the core from the carapace is rugose, and it shows parts of the sulci of the vertebral2 and of pleural1 and 2. The external scute surface of the core from the hyoplastron is rather smooth, however, due to various degrees of shell necrosis, the keratin layers of the scutes easily flake off.

4.2.5.4 *Platemys platycephala* (Schneider, 1791)

The sampling of *P. platycephala*, the recent twist-necked turtle of South America, included two drilled cores of a small alcohol-preserved specimen (SMNS 10035). The specimen has a SPL of about 135 mm. The keratinous shields were already removed from the specimen in the locations of the drill spots, thus they were not sampled together with the bone core. The first core of the shell bone (22 mm in diameter) covers part of the right costal2 and proximal-most part of the left costal2, as well as the associated vertebra. As stated for example by Ernst and Barbour (1989), neurals are usually not developed and the costals meet at the midline of the shell. The second core (12 mm in diameter) covers the proximal part of the left hypoplastron. The plane of sectioning runs craniocaudally in the hyoplastron, while it runs proximodistally through the sampled costals. The maximum thicknesses of both carapace and plastron samples is 2 mm (excluding the vertebral centrum).

4.2.5.5 *Phrynops geoffroanus* (Schweigger, 1812)

As a second South American short-necked species, *P. geoffroanus* was sampled (YPM 12611). The carnivorous species lives in a wide range of freshwater habitats with slow currents and is basking frequently (e.g., Ernst and Barbour, 1989). Several complete bony

elements of a macerated shell were prepared into thin-sections, including a neural3, a costal3, a peripheral3 and a hyoplastron. Due to the fact that the shell was already disarticulated prior to sampling, its length was not measured. The costal3 has two planes of sectioning, one proximodistally and one craniocaudally. The plane of sectioning trends proximodistally, both in the peripheral3 and the hyoplastron. The neural3 was sampled in cross-section perpendicular to the vertebral column.

4.2.5.6 *Hydromedusa tectifera* Cope, 1870a

The specimen (ZFMK 51656) of *H. tectifera* comes from an area near Montevideo, Uruguay, but no further data was available. It had a CCL of 223 mm, a CCW of 163 mm and a SPL of 155 mm. Sampling of the alcohol-preserved specimen was done by core drilling. Bone cores (each 22 mm diameter) were removed from the proximal part of the left ?costal2 and the left hyoplastron respectively. The keratin shields are still attached to the bone cores. In the case of the carapacial core, sulci of the first and second vertebral and the first pleural are present. In the case of the plastral core, the external scute surface is flat and smooth and carries the sulcus of the pectoral shield.

4.2.5.7 *Chelus fimbriatus* (Schneider, 1783)

C. fimbriatus is found in all major drainage systems of South America where it prefers habitats with slow-moving water (e.g., Ernst and Barbour, 1989). The shell shows three major keels and the flat triangular head and long neck sport fringelike appendages of the skin mimicking dead leaves, while it catches its prey with a gape-suck mechanism. The specimen (FMNH 269459) that was sampled by core-drilling is quite exceptional in another way. Prior to its current storing in the FMNH collections, it was submerged and stored in a preservation liquid of unknown chemistry that stained the shell bone and all other visible bone green. The three core samples (each 22 mm in diameter) of the shell bone are thus homogeneously stained. The locations of the cores were chosen to cover part of a costal and the peripheral region of the carapace, as well as the right hyoplastron respectively. The SPL measures about

338 mm. The thickness of the shell bones ranges from 6 mm in the costal, to a maximum of 10 mm in the peripheral and to 4.5 mm in the hyoplastron. The planes of sectioning run craniocaudally in the hyoplastron and in the costal and proximodistally in the sampled peripheral.

4.3 Cryptodira

The Cryptodira, including the crown-group taxa Chelonioidea (Cheloniidae and Dermochelyidae), Chelydridae, Testudinoidea (*Platysternon megacephalum*, Testudinidae, Bataguridae and Emydidae) and Trionychoidea (Kinosternoidea and Trionychia) are still the most abundant group of turtles. Besides the crown-clades, there exist a large number of fossil clades, from which some could be included in this study (e.g. Solemydidae). The taxonomic status of the recent big-headed turtle *Platysternon megacephalum* Gray, 1831b which was sampled is still under discussion. While morphological analyses grouped *P. megacephalum* as sister taxon to Chelydridae (e.g., Brinkman and Wu, 1999), it was lately hypothesised by Joyce et al. (2004) to represent the sister taxon to Testudinoidea in the clade Cryptoderinea (=Platysternidae and Testudinoidea). Molecular analyses, however, oppose a close relationship of *P. megacephalum* and Chelydridae (e.g., Haiduk and Bickham, 1982; Cervelli et al., 2003; Krenz et al., 2005; Parham et al., 2006). The latest analysis by Parham et al. (2006) retrieved *P. megacephalum* as the sister taxon to Emydidae within Testudinoidea. The Cryptodira include the basal, solely fossil, Paracryptodira and the advanced Eucryptodira (e.g., Gaffney, 1975c; Gaffney and Meylan, 1988; Gaffney, 1996; Hirayama et al., 2000).

The Solemydidae comprise a group of poorly known turtles that lived from the Late Jurassic to the Early Cretaceous in North America and Europe/Asia (Lapparent de Broin and Murelaga, 1996). Referred indeterminate solemydid material is also reported from the Upper Cretaceous of France (Lapparent de Broin, 2001). After Danilov (2005), Solemydidae, Meiolaniidae and three other taxa (Chengyuchelyidae, Kallokibotionidae and Mongolochelyidae) are basal cryptodiran taxa, however, affinities to Pleurosternidae were also proposed (see Milner, 2004 for discussion). Typical for all solemydid taxa is a peculiar ornamentation of single raised knob- or pillar-like structures on the external bone surfaces. All taxa had scutes covering the ornamented shell bones. The fossil North American

solemydid material from the Upper Jurassic of Montana, USA, was described as *Naomichelys* sp. based on plastral bones (Hay, 1908). Hirayama et al. (2000) considered *Naomichelys* Hay, 1908 a junior synonym of *Tretosternon* Owen, 1842. Milner (2004), however, argues that *Tretosternon* is a nomen dubium, and the relevant material should accordingly be reassigned to the senior synonym *Helochelydra* Nopcsa, 1928. There is still an ongoing discussion pertaining to the naming and validity of other solemydid taxa (see Lapparent de Broin, 2001; Milner, 2004; Danilov, 2005). The studied material is referred to as Solemydidae gen. et sp. indet. (aff. *Naomichelys* sp.) in the current study.

The Baenidae, a group of turtles endemic to North America, the more wide-spread Pleurosternidae (e.g., Gaffney, 1975c; Brinkman and Nicholls, 1993; Gaffney, 1996) and the newly described basal paracryptodiran taxon *Arundelemys dardeni* Lipka et al., 2006 are included into the Paracryptodira. The latter taxon is known from Early Cretaceous Potomac Formation, Muirkirk, Maryland, USA, and only includes a single isolated skull. The Baenidae are found in strata from the Early Cretaceous to the late Eocene (e.g., Gaffney, 1972; Gaffney and Meylan, 1988). The Pleurosternidae occur in the Upper Jurassic and the Lower Cretaceous of North America and Europe (e.g., Gaffney, 1996; Brinkman et al., 2000; Milner, 2004). See Danilov (2005) and Lipka et al. (2006) for a summary of synapomorphies of Paracryptodira. If the material that is so far tentatively classified as 'cf. Pleurosternidae' would be positively assigned to that taxon, the fossil record of the taxon would be extended from the Upper Jurassic back into the Bathonian, Middle Jurassic (see Evans and Milner, 1994; Danilov, 2005).

The term Eucryptodira, introduced by Gaffney (1975c), comprises all crown-group cryptodires as well as solely fossil taxa. Basal eucryptodiran taxa are Plesiochelyidae, Eurysternidae, Thalassemydidae and Xinjiangchelyidae. The more derived eucryptodiran taxa, including the fossil Sinemydidae, Adocidae and Nanhsiungchelyidae, are combined within Centrocryptodira (e.g., Gaffney and Meylan, 1988; Gaffney, 1996; Danilov 2005; please note that meiolaniid turtles are not regarded as Centrocryptodira but as basal Testudinata herein). The fossil record of Eucryptodira (e.g., of Plesiochelyidae) reaches at least back into the Upper Jurassic (e.g., Lapparent de Broin, 2001; Danilov, 2005).

While amphicoelous vertebrae with weakly developed central articulations are still found in the basal eucryptodiran taxa Xinjiangchelyidae, Plesiochelyidae, Eurysternidae and

Thalassemydidae (e.g., Danilov, 2005), the derived Centrocryptodira only have procoelous and opisthocoelous vertebrae with well developed articulation surfaces (Gaffney and Meylan, 1988). See Gaffney (1975c, 1996), Gaffney and Meylan (1988) and Danilov (2005), for more detailed characterisations of Eucryptodira and Centrocryptodira.

Described by Lapparent de Broin (2001:162) as "littoral" forms, the Plesiochelyidae, Eurysternidae and Thalassemydidae represent the first marine radiation of turtles, although protostegid turtles also occur already in the Upper Jurassic. All three groups are endemic to Europe. While Thalassemydidae and Eurysternidae are restricted to the Upper Jurassic, the Plesiochelyidae also range up into the Lower Cretaceous (Lapparent de Broin et al., 1996; Hirayama et al, 2000; Lapparent de Broin, 2001).

The material used in this study derives from the Kimmeridgian (Upper Jurassic) limestone quarries of Solothurn, Switzerland, famous for their richness in fossil turtle remains (also referred to 'Solothurner Schildkrötenkalke' in German). Mainly based on divergent shell morphologies, several genera and species have been described from the Solothurn turtle limestone (e.g., Rütimeyer, 1873; Bräm, 1965). Later on, the focus shifted towards newly discovered cranial material and many species were synonymised (e.g., Gaffney, 1975b). However, due to the subsequent discovery and description of associated cranial and postcranial material, the validity and taxonomic status of several taxa from Solothurn is still under discussion.

After Gaffney (1975b), the genus *Craspedochelys* would have to be treated as synonymous with *Plesiochelys*, thus, e.g., the species *Craspedochelys picteti* Rütimeyer, 1873 would have to be renamed to *Plesiochelys picteti* (Rütimeyer, 1873). Lapparent de Broin (2001), however, still lists *C. picteti* Rütimeyer, 1873 as a valid species.

Furthermore, according to Gaffney (1975b), *Plesiochelys etalloni* is the only recognised species of the genus found in Central Europe based on cranial material and the species *P. solodurensis*, *P. jaccardi*, *P. sanctaeverenae*, *Craspedochelys picteti* and *Craspedochelys crassa* are synonymous with *P. etalloni*. After Lapparent de Broin et al. (1996) and Lapparent de Broin (2001), however, the material described by Bräm (1965) as *Plesiochelys etalloni* would in fact represent the lost and rediscovered holotype of *Plesiochelys solodurensis* Rütimeyer, 1873 (see also Joyce, 2000 for further discussion).

Thalassemys hugii Rütimeyer, 1873 and *Tropidemys langi* Rütimeyer, 1873 are considered as valid species by Lapparent de Broin et al. (1996) and Lapparent de Broin (2001), with *Thalassemys hugii* being the only thalassemydid representative from Solothurn limestone. While Bräm (1965) tentatively assigned *Tropidemys langi* to the Thalassemydidae, the taxon is regarded as a plesiochelyid instead by Lapparent de Broin (2001).

Joyce (2000) rejects proposals to synonymise *Eurysternum ignoratum* Bräm, 1965 (the species described from Solothurn) with *Solnhofia parsonsi* Gaffney, 1975a. After Lapparent de Broin (2001), Eurysternidae is, among other taxa, represented by *Solnhofia parsonsi* Gaffney, 1975a, *Idiochelys fitzingeri* Meyer, 1839a and *Eurysternum* spp. To complicate matters, a revision of *Eurysternum wagleri* Meyer, 1839b (the type species of the genus) by Joyce (2003) revealed that the holotype was lost during the Second World War and syntypes and lectotypes were not assigned by Meyer. Furthermore, suitable specimens for neotype designation have not been found yet, thus the only available material of *E. wagleri* and its description is based solely on an illustration (Joyce, 2003).

Taxa that are characterised by procoelous and opisthocoelous vertebrae with well developed articulation surfaces (Gaffney and Meylan, 1988) are included into the Centrocryptodira. Centrocryptodira includes the basal "Sinemydidae" and "Macrobaenidae", as well as the more derived crown group Cryptodira and their close fossil relatives (Polycryptodira Gaffney, 1984 =Cryptodira Cope, 1868 *sensu* Joyce et al., 2004). According to Parham and Hutchison (2003) and Parham (2005), "sinemydid" and "macrobaenid" groups of turtles are still poorly understood and monophyly has not been sufficiently established yet.

The taxon Chelonioidea includes the recent marine turtles, Cheloniidae (hard-shelled sea turtles) and Dermochelyidae (leatherback turtle), as well as the fossil Protostegidae with Cheloniidae being the sister taxon the (Protostegidae, Dermochelyidae) (e.g., Hirayama, 1997, 1998; Danilov, 2005). The well preserved *Santanachelys gaffneyi* Hirayama, 1998 from the Early Cretaceous Santana Formation of Brazil, South America, is hypothesised to be the oldest and basal-most representative of the Protostegidae (e.g., Hirayama, 1998; Joyce et al., 2004; Danilov, 2005). The origin of Chelonioidea as well as their relationship to Plesiochelyidae and Macrobaenidae is still in focus of discussion (e.g., Joyce et al., 2004; Danilov, 2005). While chelonioid taxa flourished during the Cretaceous and Palaeogene (Wood et al., 1996; Hirayama, 1997), the modern marine turtle fauna is greatly reduced in

diversity (Fritz, 2005). A recent review of Cheloniidae and Dermochelyidae is given by Joyce and Bever (2005) and Bever and Joyce (2005) respectively.

The Testudinoidea include the recent families Emydidae, Bataguridae/Geoemydidae, Testudinidae, and the species *Platysternon megacephalum* Gray, 1831b. All three former groups appear in the Northern hemisphere during the Palaeogene (Danilov, 2005). Today, Testudinoidea are known from all continents except Antarctica and Australia (e.g., Pritchard, 1979; Ernst and Barbour, 1989; Lapparent de Broin, 2001; Danilov, 2005). The monophyly of 'Testudinidae' seems reasonably well established, a monophyletic 'Emydidae' is not well supported and the monophyly of 'batagurid/geoemydid' turtles has not been sufficiently tested yet (Joyce and Bell, 2004). Thus, a review of the comparative morphology of extant testudinoid turtles was recently given by Joyce and Bell (2004), in which the authors re-evaluate the characters that are usually taken into account for testudinoid turtle phylogenies. Furthermore, as already pointed out, the taxonomic status of the recent big-headed turtle *Platysternon megacephalum* Gray, 1831b is still under discussion, with the most recent molecular study favouring *P. megacephalum* as sister taxon to Emydidae (Parham et al., 2006).

The Trionychoidea include the Kinosternoidea, Nanhsiungchelyidae, Adocidae and Trionychia. Based on morphological characters, Trionychoidea *sensu* Gaffney and Meylan (1988) are a monophyletic group, however, Shaffer et al. (1997) postulated the distinctiveness of Trionychia based on molecular data. This result was for example recently corroborated by Fujita et al. (2004). As was shown by Meylan and Gaffney (1989), Adocidae is a basal member of Trionychoidea (see also Brinkman, 2003a), as is the monophyletic Nanhsiungchelyidae, which itself is sister group to *Peltochelys* Dollo, 1884 and advanced Trionychia (see Meylan, 1988; Meylan and Gaffney, 1989). Kinosternoidea include the Dermatemydidae and the Kinosternia. Kinosternia further include the genus *Hoplochelys* and Kinosternidae (Gaffney and Meylan, 1988; Joyce et al., 2004).

Trionychia *sensu* Joyce et al., 2004, =Trionychoidae *sensu* Shaffer et al. (1997), include the Carettochelyidae and the Trionychidae. As stated by Engstrom et al. (2004), several molecular studies strengthen this proposed sister relationship of the groups (Shaffer et al., 1997; Fujita et al., 2004; Krenz et al., 2005). However, there is discussion about the systematic position of Trionychia (Gaffney and Meylan, 1988; Meylan and Gaffney, 1989;

Krenz et al., 2005). Following the more traditional approach, Trionychia is here regarded as highly nested in Cryptodira with sister group relationships to Kinosternoidea, Nanhsiungchelyidae and Adocidae.

4.3.1 Cryptodira incertae sedis (Kirtlington turtle sample; Solemydidae)

4.3.1.1 Kirtlington turtle sample

Turtle material was found in the Kirtlington Cement Quarry (Mammal Bed, 3p layer of McKerrow et al., 1969), Bathonian, Middle Jurassic, Kirtlington, Oxfordshire, Great Britain. Gillham (1994) described shell and skull material from the Kirtlington site that carried cryptodiran characteristics, but the material was only tentatively assigned to cf. Pleurosternidae, because clear synapomorphies were not preserved in the material. In the same year, a review of British microvertebrate sites by Evans and Milner (1994) listed the occurrence of cf. Pleurosternidae for two other British sites (Skye and Watton) besides the Kirtlington locality. The sample used in the current study includes six small shell fragments (IPB R583-589) that were, because of their fragmentary condition, difficult to assign to a location on the shell (i.e., carapace or plastron fragment). One of the shell bone fragments has a sculptured external surface (IPB R586), while the other fragments have fairly straight bone surfaces. Due to the broken and weathered nature, not much more can be said about the outer morphology of the shell material.

4.3.1.2 Solemydidae gen. et sp. indet. (aff. *Naomichelys* sp.)

The material that could be obtained for thin-sectioning includes two costals (TMP 90.60.07; FM PR 273), two peripherals (TMP 90.60.07; FM PR 273), one indeterminate plastron fragment (TMP 2000.16.01), two indeterminate shell fragments (TMP 90.60.07) and two osteoderms (FM PR 273). FM PR 273 derives from the Antlers Formation, Trinity Group, Albian, Early Cretaceous, Montague County, Texas, USA. The fragments that are stored in the TMP collections on the other hand, derive from the Foremost Formation, Judith River Group, Milkriver and Pinhorn Ranch, SE Alberta, Canada. Because of the fragmentary nature

of most of the specimens, a secure orientation of the elements was not always possible. Generally, the shell fragments are sculptured with highly characteristic tubercles or columns. The tubercles/columns can be densely packed or can be regularly spaced across the external surface of the bones. Furthermore, the pillar-like tubercles can protrude over several millimetres from the bone surface and where broken off, a circular structure is still seen on the external bone surface. The internal bone surfaces are smooth. The smaller osteoderm has a circular or oval base that is excavated and an external slightly off-centred pointed apex. The larger osteoderm has a circular, slightly excavated internal surface and a convex external surface. A blunt flat lying apex is situated beyond the margin of the internal surface, giving the osteoderm a flat half-moon shape in cross-section. Both osteoderms are sculptured with low tubercles or ridges. Small scattered nutrient foramina insert into the internal bone surface of both elements.

4.3.2 Baenidae

Gaffney (1972) gave a comparative account of the North American Baenidae and presented a first cladogram. The Early Cretaceous genus *Trinitychelys* and the Upper Cretaceous/Early Palaeogene genus *Neurankylus* may represent successive sister taxa of the derived baenid turtles referred to as Baenodd/Baenodda (see Gaffney 1972; Gaffney and Meylan, 1988; Brinkman and Nicholls 1993). *Neurankylus* is the only representative of the "primitive grade" of baeind turtles found in the Late Cretaceous of Alberta, Canada (Brinkman, 2003a:559). The genus *Plesiobaena* is the basal-most member of the more exclusive derived grade, the Baenodda (Brinkman, 2003b). The sampled taxa *Boremys* sp., from the Cretaceous Dinosaur Park Formation of Dinosaur Provincial Park of Alberta, Canada, and *Chisternon* sp., from the Eocene Bridger Formation of Wyoming, USA, represent derived taxa within the Baenodda (Brinkman and Nicholls, 1991, 1993).

4.3.2.1 *Neurankylus* sp.

The specimens of *Neurankylus* sp. derive from Late Cretaceous Dinosaur Park Formation, Judith River Group, near Drumheller, Alberta, Canada. The sectioned specimens include a neural (TMP 86.36.308), a proximal part of a costal (TMP 85.58.26), a peripheral (TMP 91.36.786) and a fragmentary hyoplastron (TMP 94.666.35). The external surface of the bones is flat and has a leathery texture of very fine irregular wrinkles. The spatial orientation of these leathery wrinkles increases somewhat towards the sutured margins of the bone elements. Here, the wrinkles trend more parallel to each other and extend perpendicular towards the bone margins. The internal surface of the bone is smooth or has a fibrous, striated texture. This characteristic is especially pronounced in the hyoplastron, where the internal surface of the bone appears to comprise fibre bundles that trend generally sub-parallel to each other. Scute sulci are present on the external surfaces of the hyoplastron and on the peripheral.

4.3.2.2 *Plesiobaena* sp.

The sampling of *Plesiobaena* sp. includes a neural (TMP 86.78.97), the proximal part of a costal (TMP 93.108.07), a peripheral (TMP 91.36.852) and a right hyoplastron (TMP 84.67.97). The specimens were found in the Late Cretaceous Judith River Group, Dinosaur Provincial Park, Alberta, Canada. Internal surfaces of the bones are generally smooth. The external surfaces are smooth or faintly wrinkled. These faint wrinkles, which are most pronounced on the external surface of the hyoplastron, give the margins of the external bone surfaces a lightly striated texture.

4.3.2.3 *Boremys* sp.

The sampled specimens of *Boremys* sp. from the Late Cretaceous Dinosaur Park Formation, Dinosaur Provincial Park, Alberta, Canada, comprise a neural (TMP 93.108.03), the proximal part of a costal (TMP 1994.12.325), a peripheral (TMP 1986.78.29) and the right hypo- and xiphiplastron (TMP 84.163.70). The external surface of the neural, the costal and the peripheral are strongly sculptured with humps, while the external surfaces of the plastral

elements are smooth. The humps are strongly pronounced in the neural and the costal, but weakly developed in the peripheral. The internal surfaces of all elements are rather smooth or in the plastral elements, faintly striated. The faint striation on the internal surface of the plastral elements seems to be a preparatory artefact; however, the exact nature of the fine striation could not be deduced because of a lacquer coating that covers the surfaces of the bones.

4.3.2.4 *Chisternon* sp.

The material of *Chisternon* sp. derives from the Eocene Bridger Formation, Uinta County (and Sweetwater County?), SW Wyoming, USA. The sample includes a fused neural and costal (UCMP V94071/150182), a peripheral (UCMP V94076/150189), a peripheral fragment from the bridge region of the carapace (UCMP V94076/150189) and a plastron fragment (?hyo- or hypoplastron; UCMP V94078/150190). The external and internal surfaces of the shell elements appear smooth with few scattered pits and grooves. Because of diagenetic compaction and weathering, a more detailed description of the bone surfaces is not possible.

4.3.3 Pleurosternidae

Pleurosternidae *sensu* Gaffney (1979b), Gaffney and Meylan (1988) and Gaffney (1996) include only the two genera *Glyptops* and *Pleurosternon* (=*Mesochelys* Evans and Kemp, 1975). See also discussion in Tong et al. (2002) on basal cryptodiran turtles. A possible relation of *Compsemys* to Pleurosternidae was already proposed by Hutchison (1987), but only recently, skull material of *Compsemys victa* Leidy, 1856b was described (Hutchison and Holroyd, 2003). While Lapparent de Broin (2001:172, 194-195) was unsure if *Desmemys* with type species *D. bertelsmanni* Wegner, 1911 from the Lower Cretaceous of Germany belongs to "?Pleurosternidae (incertae sedis)" or "Chelonii incertae sedis", Milner (2004) confirmed the inclusion of *Desmemys* within Pleurosternidae. Brinkman et al. (2000) proposed relationships of the genera to be (*Pleurosternon* ((*Dinochelys*, *Desmemys*) *Glyptops*)). Material of *Glyptops plicatulus* (the validity of the species was discussed by

Gaffney, 1979b) from the Upper Jurassic Morrison Formation of Wyoming, USA, *Compsemys* sp. from the Hell Creek Formation of Montana, USA, and unidentifiable material of Pleurosternidae of Upper Jurassic of Guimarota coal mine, Portugal, were included in this study.

4.3.3.1 *Glyptops plicatulus* (Cope, 1877)

The studied specimens of *G. plicatulus* were found in Quarry 9, Como Bluff, Wyoming, USA (Morrison Formation, Upper Jurassic). The sample comprises a neural (YPM 57160), the proximal part of a costal (YPM 57161), a costal (YPM 57162), a peripheral (YPM 57163) and a plastron fragment (YPM 57164; ?hyo- or hypoplastron). The external surface of the shell elements are sculptured with small vermiculate low ridges and tubercles, surrounded with a marginal seam of elongate parallel low ridges extending perpendicular towards the sutures of the bone.

4.3.3.2 *Compsemys* sp.

The material of *Compsemys* sp. derives from the early Palaeocene part of the Hell Creek Formation, McCone County, Montana, USA. A neural (UCMP V90077/150197), two costals (UCMP V90077/150195; UCMP V90077/150196), a peripheral (UCMP V87192/150199) and a plastron fragment (?hyo- or hypoplastron; UCMP V87192/150198) are included. The external surface of the shell bones is sculptured with low fine tubercles that only occasionally form short low ridges. Especially at the margins isolated tubercles fuse to form parallel short ridges that extend perpendicular to the sutures of the bones. It is noteworthy that the sculpturing pattern of the samples is generally fainter than the sculpturing pattern of *G. plicatulus*.

4.3.3.3 Pleurosternidae gen. et sp. indet.

Several specimens that could be studied come from Kimmeridgian (Upper Jurassic) beds of the Guimarota coal mine near Leiria, Portugal. The sample includes a costal (GUI-CHE-53), the proximal part of a costal (GUI-CHE-54) and a plastron fragment (?hyo- or hypoplastron; GUI-CHE-55). Furthermore, two specimens, a neural (IPFUB P-Barkas-20) and a peripheral (IPFUB P-Barkas-21), from Upper Jurassic (Tithonian-?Berriasian) alluvial fan deposits of Porto das Barcas, Lourinha, Portugal, were sampled. The external surface of the neural appears weathered and strongly pitted. The external surface of the other shell elements is sculptured with vermiculate low short ridges and tubercles framed by a marginal seam of parallel low ridges extending perpendicular towards the sutures of the bones (compare to specimens of *Glyptops plicatulus*). The internal surface of all shell elements appears smooth.

4.3.4 Eurysternidae

4.3.4.1 *Eurysternum* sp. and ?*Eurysternum* sp.

Three shell elements, a costal (NMS 21908), a left hyoplastron (NMS 20981) and a plastral fragment (NMS 21922) of *Eurysternum* sp. from Solothurn were sampled. Further sampling included a costal fragment and a plastron fragment (both SMNS 91005) of ?*Eurysternum* sp. from the Upper Jurassic (Tithonian) of Tönniesberg near Hannover, Germany. All elements have a fragile appearance. The external and internal surfaces of the bones show various degrees of abrasion and weathering so that the interior spongy structure of the bone becomes visible. The external surface of the hyoplastron (NMS 20981) also shows some minor pitting structures and a shallow striation pattern towards the bridge and the sutured margins. It also shows part of the central plastral fontanella. The external surface of the costal is smooth and unsculptured. The internal surfaces of all bones are also smooth or, in case of the plastra, locally faintly striated.

4.3.5 Plesiochelyidae and Thalassemydidae

4.3.5.1 *Plesiochelys* sp.

The material of *Plesiochelys* sp. includes specimens that are stored in the NMS, the SMNS and the IPB collections. Material from Solothurn of *Plesiochelys* sp. included a neural3 (NMS 8730; labelled as *P. sanctaeverenae*), the proximal part of a right costal3 (NMS 8849), a marginal part of a carapace (NMS 9214; distal part of costals, peripherals) and an indeterminate small fragment from a carapace (NMS 8876). The external surfaces of neural3 and costal3 (NMS 8730, NMS 8849) are partly sculptured with wrinkles and low ridges as seen in the proposed holotype of *Plesiochelys sanctaeverenae* Rütimeyer (in Bräm, 1965: fig.27). At first glance, the external surface of the small fragment of the carapace (NMS 8876) appears strongly weathered and pitted. However, it is not the external surface of the bone but the internal surface, because the bone was broken several times and is preserved now with a strongly concave external bone surface. The internal surfaces of all sampled bones are generally smooth.

Specimen IPB R13, a proximal part of a costal, derives from the Kimmeridgian (Upper Jurassic) of Ahlem near Hannover, Germany. The specimen was labelled as *Plesiochelys hannoverana*. However, the taxon might be synonymous with *Plesiochelys* (=*Craspedochelys*) *brodiei* Lydekker, 1889, a form known from the Wealden of England (see Lapparent de Broin, 2001). SMNS 55831 constitutes a fragment of a hypoplastron of ?*Plesiochelys* sp. from the Lower Kimmeridgian (Upper Jurassic) of the Galgenberg (Landeskrankenhaus) locality near Hildesheim, Germany. The internal surfaces of the costal and the hypoplastron (IPB R13, SMNS 55831) appear smooth with occasional small pores opening into the internal cortical bone, while the external bone surfaces have a very light and inconspicuous roughened texture.

4.3.5.2 *Thalassemys* cf *T. hugii* Rütimeyer, 1873 and *Thalassemys* sp.

The material of *Thalassemys* sp. includes a proximal part of a left costal5 (NMS 8859), the posterior part of a carapace (NMS 9201; neural7; suprapygal1+2; left costal7+8), an oblong

neural (NMS 9159) and a plastron fragment (NMS 9168; possibly a right hyoplastron). NMS 8859 and NMS 9201 are tentatively assigned to *Thalassemys* cf. *T. hugii* based on the shape of both, the costal and the posterior part of the carapace and the scute sulci on the external surface of the bones (compare to Bräm, 1965: fig. 29). Internal surfaces of the bones are smooth. The external surfaces are slightly weathered, and in the case of the neural and the partial carapace (NMS 9159 and NMS 9201), pitted to various degrees. It remains unclear if the occasional hatched lines on the external surfaces of the shell fragments are a preparatory artefact, chemical weathering or shallow biological feeding structures.

4.3.5.3 *Tropidemys* sp.

The studied material consists of the posterior part and left margin of a carapace (NMS 8991) including the posterior neural row, as well as peripherals and distal parts of costal plates. *Tropidemys* has a high-domed keeled carapace, thus the neurals like in NMS 8991 are strongly arched like a roof. The partial left margin is crushed, resulting in internal collapse of the bone interior and shattered external bone surfaces. The internal and external surfaces of the carapace fragment appear smooth and unsculptured.

4.3.6 Xinjiangchelyidae

Xinjiangchelyidae are mainly known from the Middle and Upper Jurassic of Asia. There is no solid bridge of bone connecting the dorsal carapace and the ventral plastron, instead, the connection of both shell elements is ligamentous (Danilov, 2005). According to the phylogenetic analysis of Hirayama et al. (2000), *Brodiechelys brodiei* (Lydekker, 1889) from the Early Cretaceous of England is a close relative of (or even within) Xinjiangchelyidae (see also Danilov, 2005). Lapparent de Broin (2001:176) classifies *B. brodiei* as "? Plesiochelyidae or new family *aff*. Plesiochelyidae". The Xinjiangchelyidae are seen now as direct sister group to Centrocryptodira (Gaffney, 1996; Gaffney et al., 1998b; Brinkman and Wu, 1999; Hirayama et al., 2000). See Tong et al. (2002), Matzke et al. (2004a) and Danilov (2005) for further description and discussion on Xinjiangchelyidae.

4.3.6.1 *Xinjiangchelys chowi* Matzke et al., 2005

Three elements of this recently described taxon (Matzke et al., 2005) could be sampled, including a peripheral (SGP 2001/34a) and two unidentified shell fragments (SGP 2001/34b, c). The material comes from the Upper Middle Jurassic Toutunhe Formation, Liuhonggou locality, near the Toutunhe River, southern Junggar Basin, 50km SW of Urumchi, Xinjiang, China. All bone fragments are small (20-23 mm in length; thicknesses ranging between 4 and 6 mm). The external surface of the peripheral is slightly convex and smooth. The surfaces of the two other bone elements are fractured and weathered, thus a more detailed description is not possible. Matzke et al. (2005) described a slight surface ornamentation with grooves and ridges that increase anteroposteriorly over the carapace. According to the authors' description (Matzke et al., 2005:67), the grooves and ridges "always start in the anterior regions of the vertebrals [scutes], run posteromedially, and vanish in the posterior parts".

4.3.6.2 *Xinjiangchelys* sp.

The material of *Xinjiangchelys* sp. included a costal (SGP 2002/4a), two peripherals (SGP 2002/4b, c) and a plastral fragment (?hyo- or hypoplastron; SGP 2002/4d). The specimens were found in the Upper Middle Jurassic Toutunhe Formation, near Toutunhe River, southern Junggar Basin, 50km SW of Urumchi, Xinjiang, China. Although of similar dimensions as the fragments of *X. chowi*, these specimens show a better preservation with the surfaces of the bones still largely intact. The progression of the rib is partly seen on the internal surface of the costal fragment, while a small ridge flanked by grooves extends along the external surface of the bone. One peripheral is triangular in shape. The other one is more robust and has a rounded apex. The dorsal external surfaces are flat to slightly convex and the ventral external surfaces are slightly concave in both peripherals, thus resulting in a slightly upturned apical region. The external surface of the plastral fragment is flat, while the internal surface is convex towards the plastral pillar. The external surfaces of the bones are generally smooth or with a very faint vascular pattern imprinted into the bone surface.

4.3.7 "Sinemydidae" and "Macrobaenidae"

"Macrobaenid" turtles, first believed to be restricted to the Cretaceous and Palaeocene of Asia are now also recognised in North America (e.g., Parham and Hutchison, 2003), and the fossil record now reaches back into the Upper Jurassic (Danilov, 2005). "Sinemydid" turtles, on the other hand, are only known from the Cretaceous of Asia (e.g., Parham and Hutchison, 2003; Danilov and Sukhanov, 2006).

In their revision of "*Sinemys*" *efremovi* Khosatzky, 1996, Danilov and Sukhanov (2006) restudied several "sinemydid/macrobaenid" taxa. As results of their work, "*Sinemys*" *efremovi* was presented as a senior synonym of the taxon *Dracochelys wimani* Maisch et al., 2003 and "*S.*" *efremovi* was assigned to the genus *Wuguia* Matzke et al., 2004b. The sectioned material is here referred to *Wuguia efremovi* (=*Dracochelys wimani*) accordingly.

According to Parham (2005), the postcranium and the skull of the type specimen of *Osteopygis emarginatus* Cope, 1869 belong to different turtles, the skull being a cheloniid now referred to *Euclastes wielandi* (Hay, 1908) and the postcranium resembling a "macrobaenid". Following Parham (2005), the postcranial material of *Osteopygis emarginatus* is here referred to Eucryptodira incertae sedis (cf. "Macrobaenidae").

4.3.7.1 *Wuguia efremovi* (Khosatzky 1996) (=*Dracochelys wimani*)

The material (SGP 2001/35) derives from the Lianmuxin Formation (Uppermost Lower Cretaceous) of the Tugulu Group, Liuhonggou, west of the Toutunhe River, Junggar Basin, Xinjiang, China. Included in the sample are two fragmentary neurals (SGP 2001/35a, b), two costal fragments (SGP 2001/35c, d), two peripherals (SGP 2001/35e, f) and two plastral fragments (?hyo- or hypoplastra; SGP 2001/35g, h). The larger neural fragment measures about 10 mm in width, while the smaller specimen measures max. 5 mm. The first costal fragment comprises the proximal part of the costal. The other fragment derives from a more distal mid-part of a costal. The peripherals also represent two locations on the carapace. The peripheral from the anterior or posterior part of the shell is flat and triangular. Its apex is not upturned. The second peripheral is a thicker bony element with a blunt margin and a slightly

upturned apex. In the latter specimen, the external bone surfaces, one flat to convex and one slightly concave, extend in a high angle to each other. Preservation of all elements is generally good. External surfaces of the specimens show a very faint vascularisation pattern or additional light striations (i.e., neurals, plastral fragments). The internal surfaces are generally smooth.

4.3.7.2 Eucryptodira incertae sedis (cf. "Macrobaenidae")

The material (YPM 1585) labelled '*Osteopygis emarginatus'* includes a neural, a costal, a peripheral and a plastral fragment (?hyo- of hypoplastron). The specimens were found in the Late Cretaceous ?Hornerstown Formation, Mullica Hill, New Jersey, USA. The exact aging of fossils is sometimes difficult in these sediments, because both the lower Palaeocene Hornerstown Formation and the Uppermost Cretaceous Tinton Formation are lithologically nearly identical in comprising glauconitic sands (see also Miller, 1955; Parham, 2005). The shell elements are quite large and thick (neural: max. anteroposterior length 60 mm, max. width 42 mm; thickness10 mm; costal fragment: min. length 65 mm; width about 50 mm, marginal thickness 6 mm, medial thickness 10 mm; peripheral: mediolateral width 64 mm; anteroposterior length max. 80 mm, proximal thickness about 10 mm, maximum diameter of distal bulge 22 mm; plastral fragment (broken margins!): mediolateral width min. 88 mm, anteroposterior length min.66 mm, thickness between 12 and 17 mm). The shell elements carry a shallow superficial reticular vascularisation pattern on their external bone surface. Internal surfaces of the bones are smooth or have a slightly striated texture.

4.3.8 Cheloniidae *"sensu lato"*

Several genera with problematic taxonomic status are combined within the Cheloniidae "*sensu lato*" (after Parham and Fastovsky, 1997; see also Lapparent de Broin, 2001; Karl, 2002; Lynch and Parham, 2003; Danilov, 2005). Representatives in this study include *Rupelchelys breitkreutzi* Karl and Tichy, 1999 from the Oligocene of Germany, *Ctenochelys* cf. *C. stenoporus* (Hay, 1905) (=*Ctenochelys* cf. *C. acris* Zangerl, 1953) from Upper

Cretaceous strata of USA and UK and *Allopleuron hofmanni* (Gray, 1831a) from the Upper Maastrichtian (Late Cretaceous) of The Netherlands.

R. breitkreutzi was hypothesised by Karl and Tichy (1999) to be a member of the taxon Cheloniinae within Cheloniidae. According to Danilov (2005), however, the relationship of the genus *Rupelchelys* Karl and Tichy, 1999 to crown group Cheloniidae remains unclear, thus listing the taxon in Cheloniidae "*sensu lato*".

The genus *Ctenochelys* is either considered to be a.) a close relative to Cheloniidae (e.g., Gaffney and Meylan, 1988) within Chelonioidea, b.) nested within Cheloniidae (Hirayama, 1998; Lehman and Tomlinson, 2004) or hypothesised to represent one of the oldest pancheloniids (Joyce et al., 2004) and c.) "transitional (intermediate stem-taxa [together with sister taxon *Toxochelys*]) between continental testudines and derived, pelagic chelonioids" (Kear and Lee, 2006:116). Specimens were labelled as *Ctenochelys* cf. *C. acris* in the FM collections. Although, according to Hirayama (1997), the species is synonymous with *Ctenochelys stenoporus* (Hay, 1905).

The taxon *Allopleuron hofmanni* (Gray, 1831a) is proposed to be one of the largest Cretaceous turtles that seems well adapted to a life in pelagic environments (e.g., Moody, 1997). Gaffney and Meylan (1988) proposed that *Allopleuron* is basal to Dermochelyoidea Baur, 1888 (Protostegidae and Dermochelyidae). Hirayama (1997) described *A. hofmanni* as a cheloniid turtle (close to modern cheloniids) that constitutes a starkly reduced shell and lacks keratinous scutes, thus resembling dermochelyid turtles in this respect. Danilov (2005) stressed that, because of the mixture of typical dermochelyid and cheloniid characters the phylogenetic position of *A. hofmanni* is still under discussion. However, as was shown by Mulder (2003), several specimens of *A. hofmanni* do have faint impressions interpreted as scute sulci, thus further debilitating proposed dermochelyid affinities. By adding *A. hofmanni* to the character state matrix of Parham and Fastovsky (1997), Mulder (2003) recovered *A. hofmanni* together with the Miocene genus *Syllomus* Cope, 1896 as unresolved sister group to Cheloniidae "*sensu stricto*".

4.3.8.1 *Rupelchelys breitkreutzi* Karl and Tichy, 1999

Two costals, a peripheral, a fragment that is either a free distal rib end of a costal or the distal part of a plastral element and an unidentified shell fragment (fragmentary ?costal), all accessioned as SMNS 87218, were sampled. The elements were found in the Lower Oligocene (Rupelian, 'Unterer Meeressand'), Neumühle near Weinheim, Germany. The surfaces of the bones show various stages of weathering thus the external surfaces of the bones and also some of the internal surfaces have a porous, rough texture. The surfaces of the peripheral are convex and concave respectively, resulting in a half-moon shape. All shell elements are highly fragmentary with few genuine margins. The thicknesses of the shell elements range between 5 and 9 mm.

4.3.8.2 *Ctenochelys* cf. *C. stenoporus* (Hay, 1905) (=*Ctenochelys* cf. *C. acris* Zangerl, 1953)

The sample (FM PR 442) of the taxon included a neural, a costal, a fragmentary peripheral and a plastral fragment. The material derived from the Campanian Mooreville Chalk (Late Cretaceous), Selma Group, Dallas County, Alabama, USA. The shell elements appear thin and fragile, and especially the costal and neural experienced increased crushing and weathering. The neural is roof-shaped with a central anteroposterior keel and sloping sides. The costal is crushed, thus the exact form is difficult to reconstruct. The sutured lateral margins of the costal extend parallel to each other and the progression of the incorporated rib is observable on the internal surface of the element. The peripheral fragment consists of two sutured parts of adjacent peripherals, whose two flat external bone walls form a distinct distal edge. Most of the interior bone of the peripherals is not preserved. A closer determination of the plastral fragment was not possible. The fragment consists of a flat area of bone with one arcuated margin. Where the external surfaces of the shell elements are better preserved, they appear unsculptured with a faint vascularisation imprinted into the bone surfaces. The internal surfaces are also weathered, but in the area of the incorporated rib of the costal, it appears to be rather smooth.

4.3.8.3 *Allopleuron hofmanni* (Gray, 1831a)

A. hofmanni is well known from the Maastrichtian (latest Cretaceous) of The Netherlands. The material for study from the Maastrichtian type area, Maastricht, The Netherlands, included a larger (NHMM uncat.) and a smaller costal fragment (NHMM uncat.), a peripheral (NHMM uncat.) and several fragmentary plastral rods (NHMM uncat.; distal ends of, e.g., hyo- or hypoplastron). The costal fragments have smooth, unsculptured external surfaces that show little erosion or weathering. A light striation pattern is observed towards the sutured margin of the larger costal element. Broken margins of both bone fragments reveal only spongy bone internal to a compact external layer. The peripheral is roughly triangular in anteroposterior view, with a lateral edge and strongly concave internal surface. The peripheral tapers anteroposteriorly from a broad, well and deeply sutured margin to the opposite, weakly sutured margin. With its curved marginal keel and the trace of a weakly developed rim (see Mulder, 2003: plate 28), the specimen (NHMM uncat.) resembles one of the lateral-most peripherals (?peripheral7). Towards the sutured margins, the external surface of the peripheral is striated. The internal surface is smooth with few smaller (0.5 to 1.5 mm in diameter) and one larger (3 mm in diameter) foramen. Anteroposterior length of the peripheral is 100 mm, its maximum proximodistal width 62 mm. The free rib ends together with the dorsomedial protrusions of the costals (compare to Mulder, 2003: plate 28) do not enter in distinct grooves or pits in the peripheral (Mulder, 2003). This feature was, among others (e.g., very large fontanelles in carapace; extremely short costal plates), interpreted as neoten by Mulder (2003). The plastral elements resemble the finger-like distal ends of the hyo- and hypoplastra (compare to Mulder, 2003; plate 33). The elements are proximally thickened, have a straight shaft and a tapering distal point. Flange-like protrusions of the plastral rods are common. Surfaces of the plastral rods are crushed and weathered to various degrees and sometimes show sharp edges. The sampled plastral rod has a minimum length of about 90 mm. The plane of section cuts through the rod and its lateral flange-like protrusion.

4.3.9 Cheloniidae *"sensu stricto"*

Crown group sea turtles and their close relatives are combined in Cheloniidae "*sensu stricto*" (after Parham and Fastovsky, 1997; see also Lynch and Parham, 2003; Joyce et al.,

2004; Joyce and Bever, 2005; Danilov, 2005). In contrast to the only other extant marine turtle species *Dermochelys coriacea*, the modern cheloniid turtle taxa (*Caretta caretta* (Linnaeus, 1758); *Chelonia mydas* (Linnaeus, 1758); *Eretmochelys imbricata* (Linnaeus, 1766); *Natator depressus* (Garman, 1880); *Lepidochelys kempii* (Garman, 1880), *L. olivacea* (Eschscholtz, 1829)) have a hard shell consisting of internal set of bones covered by epidermal keratinous scutes. In *N. depressus*, the keratin shields wear away with time so that shield contours can fade in old individuals (Zangerl et al., 1988).

4.3.9.1 *Caretta caretta* (Linnaeus, 1758)

The sampling (FMNH 98963) of *C. caretta* ('no data' specimen) was done by core drilling of the left costal2 and the left hyoplastron. This individual had a SPL of about 425 mm. Drilled cores had a diameter of 22 mm and range between 9 and 10 mm in thickness. The keratinous shields were still attached to the bone and are thus also present in the thin-sections.

4.3.9.2 *Chelonia mydas* (Linnaeus, 1758)

An isolated costal fragment (MB.R. 2857) of *C. mydas* was sampled. The specimen had no accompanying data besides the note 'Zehlendorf (Berlin)'. One margin of the costal fragment is still present where a slim part of an adjacent costal is still in sutural contact with the specimen. The external surface of the bone is rugose with numerous fine porous spaces and larger vascular grooves inserting into the external cortical bone. While one end of the grooves ends in a foramen that extends into the cortical bone, the opposite end gets increasingly shallow before it tapers off on the bone surface. The internal surface of the bone is smooth with a light striation pattern that extends sub-parallel to the sutured margin of the costal plate. Three of the apparent striations are slightly elevated compared to the surrounding bone surface. Small holes in the elevations reveal that the structures are a kind of sub-surface hollow tubes (vascular canals?) that extend proximodistally through the costal.

4.3.9.3 *Eretmochelys imbricata* (Linnaeus, 1766)

The neural2, the right costal2 and the right ?peripheral1 of a carapace of *E. imbricata* (SMNS 12604) were sub-sampled by core drilling. The keratin shield covering the neural2 and costal2 was already missing thus ?peripheral1 is the only element that shows the keratinous shield in connection with the underlying bone. The specimen (isolated carapace) was illegally brought to Germany and was confiscated by customs. The species is known to occur in tropical waters of the Atlantic and Indo-Pacific Ocean (e.g., Bass, 1999). The cores all had a diameter of 12 mm. Thicknesses range between 4 and 5 mm for the neural2, between 4 and 7 mm for the costal2 and between 4 and 6 mm for the ?peripheral1.

4.3.10 Protostegidae

During the Lower and Middle Cretaceous, protostegid turtles were a diverse group of chelonioid turtles. As a possible protostegid representative (e.g., Hirayama, 1997; Hooks, 1998), material of *Archelon ischyros* Wieland, 1896 was sampled. However, after a recent study by Joyce (2007, pers. comm.), *A. ischyros* might not be a chelonioid at all, but is a basal eucryptodiran turtle that shows affinities to Plesiochelyidae, Eurysternidae and Thalassemydidae. Impartial from its phylogenetic status, giant *A. ischyros* is well known from the Upper Campanian (Late Cretaceous) of North America where it inhabited open marine environments of the Western Interior Seaway (Wieland, 1896; Hirayama, 1997; Danilov, 2005). As suggested by Karl (2002), the genus *Archelon* may also be present in Upper Cretaceous strata of Europe.

4.3.10.1 *Archelon ischyros* Wieland, 1896

The material (YPM 1783) of *A. ischyros* included a peripheral, a shell fragment that may be a part of the peg-like protrusions of a star-shaped plastron element (i.e., hyo- or hypoplastron) and another indeterminate shell fragment. The exact locality is not known for the material. However, it may have been found in the Niobrara Formation of South Dakota, USA, as Wieland was excavating there in 1899. The peripheral has a tapered proximal part and a

flattened bulged distal end. Sutures are not preserved and the bone surfaces are weathered. Maximum length from tapered apex to distal bulge is 96 mm. The diameter of the distal bulge varies approximately between 50 and 60 mm. The peg-like shell fragment has a general oval or lentil shape with the lateral parts tapering into defined edges. One of the lateral margins is eroded or broken. The bone surface shows a mixture of light and strong stages or weathering. The short axis of the shell fragment measures 25 mm, the long axis was reconstructed to be around 47 mm. The indeterminate shell fragment is a massive cube of bone with well developed external and internal surfaces, but all margins are broken. The internal surface is flat with a rugose texture. The external surface of the bone is lightly convex and the whole surface of the bone is gently dipping on one side towards internal. The external surface of the bone further shows a strong striation pattern with deep furrows extending mostly parallel over the whole surface of the fragment. The plane of sectioning of this specimen was arranged to cut perpendicular to the striation pattern. Minimum height of the cube-like fragment is 32 mm, maximum height is 41 mm.

4.3.11 Dermochelyidae

Dermochelyid turtles appeared in the Upper Cretaceous (Hirayama and Chitoku, 1996). It becomes now increasingly evident that the extensive fossil record of Dermochelyidae mirrors a complex evolution towards the single modern species *Dermochelys coriacea* (Vandellius, 1761). Basal members of Dermochelyidae (i.e., *Mesodermochelys undulates* Hirayama and Chitoku, 1996 from Japan; *Corsochelys haliniches* Zangerl, 1960 from North America) still lack epithecal armour, while still retaining neurals, costals, peripherals and keratinous shields (Hirayama and Chitoku, 1996; Hirayama, 1997; Wood et al., 1996; Bever and Joyce, 2005).

The only living representative of Dermochelyidae is *D. coriacea*. It is the largest and most cosmopolitan turtle species ranging throughout the Pacific, Atlantic and Indian oceans (e.g., Pritchard, 1980). It also occurs in cool waters up to 69° North and down to 47° South (Frazier et al., 2005). The carapace is characterised by a thick leathery hide and lack of keratinous scutes, seven longitudinal keels along the carapace and the unique secondary carapace of thousands of epithecal polygonal platelets (e.g., Wood et al., 1996). The primary thecal armour is greatly reduced or absent (exception: nuchal (proneural); Bever and Joyce, 2005).

The thecal elements of the plastron are still present, but only as thin bony rod-like elements. After Brongersma (1969), the plastron is also covered by isolated rows of small epithecal platelets that coincide with six plastral keels (see also Bever and Joyce, 2005).

The genus *Psephophorus* Meyer, 1846 is known from the Miocene to Pliocene (also possibly Oligocene) of Europe (Moody, 1997; Lapparent de Broin, 2001; Danilov 2005). Over a long period of time many dermochelyid fossils were combined in the 'waste-bucket' genus *Psephophorus*. Taxonomic revisions later elucidated the situation a little, but many forms, currently still assigned to the genus *Psephophorus*, may actually represent other genera (see Joyce and Bever, 2005). The carapace of *Psephophorus polygonus* Meyer, 1847a closely resembles that of the recent *D. coriacea*. Whether it is a direct descendant is still under debate.

4.3.11.1 *Dermochelys coriacea* (Vandellius, 1761)

The sampling of three specimens (hatchling, subadult, adult) of *D. coriacea* was carried out as part of a lab project by Tamara Fletcher under supervision of Dr. Steven Salisbury at the School of Integrative Biology, University of Queensland, Brisbane, Australia. The finished thin-sections were then sent over to serve as comparison to other marine turtles in this study. The following description of the material is mainly based on the report of Tamara Fletcher.

The sampling included the carapace of a hatchling (specimen QMJ 58751; previously fixed in formalin and stored in 70% alcohol). "The section was from above a rib on the left side of the hatchling, cranial to the left hind flipper, to approximately three millimetres past the centre of the carapace to include the osteoderms above the vertebrae".

The subadult specimen (QMJ 581592) was first kept in ice for few days before it was preserved in 90 percent ethanol preventing desiccation. "The location of the preserved section on the original carapace was not recorded; however, it appears to be from the caudal left, as the rib that runs through it gets thinner and ends running from right to left if so aligned. The carapace then thickens towards the left, which is interpreted as thickening towards the fusion

of the plastron and carapace. The cranial orientation of the section was interpreted from the shape of the rib".

Remains of the adult leatherback turtle (QMJ 73979; UQVPI) were left ashore in the mangroves for several months (during which it partially desiccated), before the carapace was collected for the Winton Dinosaur Project Laboratory (WDPL) of the University of Queensland. Due to the desiccation process the carapace locally separated from the ribs.

4.3.11.2 *Psephophorus* sp.

A single polygonal bony platelet (MB. R. 2532.1) of *Psephophorus* sp. was sampled. The specimen was found at Boom near Antwerp, Belgium. The smooth external surface is flat to slightly concave towards the sutured margins. The flat to slightly convex internal surface of the platelet appears rugose and spongy. A shallow trench surrounds the slightly raised centre on the internal surface of the plate. The diameter of the platelet ranges between 28 and 33 mm with a maximum thickness of 8 mm (measured between external and internal surface at centre of the plate).

4.3.12 Chelydridae

The origin of Chelydridae is still under discussion, but it is assumed that they are related to macrobaenid turtles (Sukhanov, 2000; Hutchison, 2000, in Danilov, 2005; Parham and Hutchison, 2003; see Danilov, 2005 for further discussion). The Chelydridae first appear in the fossil record of North America in the Late Cretaceous (Turonian) from where they spread to Eurasia during the Palaeocene/Eocene. Today, the taxon comprises two living species, the common snapping turtle *Chelydra serpentina* (Linnaeus, 1758) and the alligator snapping turtle *Macrochelys temminckii* (Troost, in Harlan, 1835). Although *Macrochelys* and *Macroclemys* are both used widely in the literature for the alligator snapper, according to Webb (1995), *Macrochelys* has precedence over *Macroclemys* (see also Crother, 2000). *C. serpentina* is more widespread (Canada down to Mexico and northern South America) than *M. temminckii,* which occurs in south-central USA (e.g., Ernst and Barbour, 1989).

Representing fossil taxa of Chelydridae, *Chelydropsis murchisoni* (Bell, 1832) and *Chelydropsis* sp. from the middle Miocene of Germany could be sampled. The original description of *C. murchisoni* as "*Chelydra Murchisonii*" (Bell, 1832:380) indicates a close relation of the outer morphology of the fossil specimen with modern snapping turtles. Besides differences in cranial morphology, variations in the shell (e.g., wider bridge, a stronger serrated posterior margin of the carapace and larger epiplastra; see Danilov, 2005), however, led to the assignment of the material to the new fossil genus *Chelydropsis* Peters, 1868.

4.3.12.1 *Chelydropsis murchisoni* (Bell, 1832)

The specimens of *C. murchisoni* that could be sampled for this study include a costal (SMNS 88994), two peripherals (SMNS 88995, 88996), as well as a plastron fragment (SMNS 88997; ?hyo- or hypoplastron). All elements were found in the middle Miocene (MN7) of Steinheim am Albuch, southern Germany. The costal is a flat bone that broadens distally. The distal margin of the costal is curved, and the tip of the rib end protrudes 17 mm over the margin. The peripheral is half-moon shaped and medially carries a triangular groove, where the free rib end of the costal fits in. External surfaces of the bones are unsculptured but have a fine reticular or polygonal vascularisation pattern. Internal surfaces are generally smooth or in the case of the plastral element slightly striated.

4.3.12.2 *Chelydropsis* sp.

The material of *Chelydropsis* sp. derives from the middle Miocene (MN5) lignite strip mining pit Hambach of the company 'Rheinbraun AG', Germany. The turtle fauna of this locality has been recently described by Klein and Mörs (2003). Two elements of *Chelydropsis* sp. from the fauna, one fragmentary peripheral (IPB HaH-3266) and a free distal end of a rib (IPB HaH-3486), were sampled. IPB HaH-3266 is a massive element with a thin tapering proximal part and a thickened distal bulge. The margin tapers to an edge where the dorsal and ventral external surfaces of the bone meet. The ventral external surface of the bone further shows a small area with a narrow depression for the attachment of the integument. The

external surface of the bone has a fine reticular vascularisation pattern. IPB HaH-3486, the broken part of a free rib end, resembles a flattened oval in section with margins tapering into well defined edges. The external surface of the bone carries long thin ridges that extend parallel to the margins. The internal surface of the specimen is smooth.

4.3.12.3 *Chelydra serpentina* (Linnaeus, 1758)

Material (YPM 10857) of the recent *C. serpentina* included a neural3, costal3, peripheral3 and an articulated hyo- and hypoplastron. The neural3 has a flat external plate and extremely long internal neural spine. The plate of neural3 is not symmetrical, because of a lateral convexity of the bone. The costal3 is thin and almost flat. The distal free rib end is triangular in shape with a distal pointed tip that lightly curves towards internal. The progression of the incorporated rib is seen over the full length of the internal surface of the shell element. On the proximal end of the costal3, the proximal part of the rib is well elevated from the internal surface of the bone, and the rib head surmounts the proximal margin of the plate. The peripheral3 carries a distinct triangular groove on its internal side to accommodate the free rib end of the costal. The lateral parts of the hyo-and hypoplastron are flared and end in striated bony protrusions. The marginal rim at these protrusions appears porous. The internal surfaces of all elements are generally smooth, while the external surfaces locally carry a reticular to polygonal pattern of shallow vascular grooves. The complete plastron length of *C. serpentina* was not directly measurable, because only the right hyo- and hypoplastron were obtained for sectioning. The medial anteroposterior extension of hyo- and hypoplastron was measured to span 170 mm. In comparison, the medial anteroposterior extension of the hyo- and hypoplastron in a smaller macerated specimen (N. Klein, private collection) with a complete SPL of about 140 mm is 85 mm. If a linear growth of the two plastral elements (and the anteroposterior extension) is assumed, the reconstructed plastron length would measure about 280 mm.

4.3.13 Testudinoidea indet.

4.3.13.1 *Platysternon megacephalum* Gray, 1831b

P. megacephalum occurs in mountainous areas of southern China and adjacent countries down to northern Thailand and southern Burma, where it inhabits cool rocky streams (Ernst and Barbour, 1989). The carapace is flat with a slight vertebral keel. The head with the hooked beak cannot be retracted into the shell. One specimen of *P. megacephalum* (SMNS 3757; preserved in alcohol) was sampled by core drilling. One drilling site (22 mm diameter) sub-sampled a neural and the adjacent right costal. The second core (12 mm diameter) included two adjacent costals. The third site (12 mm diameter) sub-sampled the left hypoplastron. All three cores still have the keratinous shields still attached to the bone. Sampling of the second specimen (YPM 12615) was done by processing whole macerated shell elements (neural3, costal3, peripheral3 and hypoplastron). No chemicals were used during the maceration process. This juvenile *P. megacephalum* was a pet trade specimen that died due to disease and exhaustion (W.G. Joyce, pers. comm.).

4.3.14 Emydidae

The classification of Emydidae is based on the morphological analysis of Gaffney and Meylan (1988) and the combined morphological-molecular data of Stephens and Wiens (2003). The Emydidae are sub-divided into the more basal Deirochelyinae (e.g., well developed bony bridge and plastral buttresses; no plastral kinesis) and the more derived Emydinae (e.g., bony bridge reduced; often kinetic plastron) (see McDowell, 1964; Gaffney and Meylan, 1988; Danilov, 2005). Emydid turtles are present in North America since the early Eocence, in Central Asia since the upper Eocene and in Europe since the upper Miocene (e.g., Estes and Hutchison, 1980; Lapparent de Broin, 2001; Fritz, 2003; Danilov, 2005).

The sampling of Emydidae included three extant species (*E. orbicularis*, *T. c. triunguis* and *P. peninsularis*), one fossil species from the Pleistocene (*T. scripta*) and fossil material of Emydidae indet. from the Eocene. The latter is unofficially termed ?Platysternoid “C” (J. H. Hutchison, pers. comm.), because the sample might not belong to an emydid turtle at all.

Emys orbicularis (Linnaeus, 1758) is the only living representative of the Old World Emydinae and the only turtle that is distributed over most of Europe and the Middle East, i.e. Iran (e.g., Pritchard, 1979; Ernst and Barbour, 1989; Tortoise & Freshwater Turtle Specialist Group, 1996). It occurs in a wide variety of habitats with slow moving water. The species is recognised in the fossil record since the Pleistocene (Fritz, 2003, in Danilov, 2005).

Terrapene carolina triunguis (Agassiz, 1857) is one of six currently recognised sub-species of *T. carolina* Linnaeus, 1758 (Ernst and Barbour, 1989). *T. carolina triunguis* occurs in southern USA, where it inhabits mostly dry open woodlands (Ernst and Barbour, 1989).

Although the material was labelled as *Pseudemys floridana peninsularis*, Seidel (1994) argued for the elevation of *P. peninsularis* Carr, 1938 into the rank of a valid species. The species ranges throughout peninsular Florida where it dwells in almost all low-current aquatic environments (Ernst and Barbour, 1989).

Trachemys scripta (Schoepff, 1792) ranges through most of the southern States of the USA, Central America and north-western South America (Ernst and Barbour, 1989). Although the species now has a cosmopolitan distribution due to the pet trade, wild populations are increasingly threatened. A re-evaluation of fossil *Trachemys* sp. was given by Jackson (1988).

4.3.14.1 Emydidae indet. (?Platysternoid “C”)

The sample comprised a neural (UCMP V81092/126372), the proximal part of a costal, another costal, a peripheral UCMP V81092/126432 and a plastron fragment (?hyo- or hypoplastron). The latter specimens share the same accession number (UCMP V81092/126432). All shell bones were found in the Eocene Willwood Formation (Wasatchian), Washakie County, Wyoming, USA. The neural is a small bone of hexagonal shape with a curved shield sulcus impressed on the external bone surface. Posterior and anterior margins are curved (one concave, the other convex). The larger costal fragment has a rectangular straight shape. The smaller costal fragment comprises the proximal part of the plate with a broken off rib head on the internal bone surface. Scute sulci of a central and two pleurals meet in a triradiate pint on its external bone surface. The peripheral has a proximal

thin part and a distal bulging part that tapers in an upturned distal edge. There is a distinct kink or bend between the proximal and distal parts of the element. Furthermore scute sulci of a pleural and two marginals are visible. The plastron fragment comprises only the buttress part, while the flatter plate part is almost completely missing.

4.3.14.2 *Emys orbicularis* (Linnaeus, 1758)

The sampled shell of *E. orbicularis* (SMNS 6880; "no data" specimen) has a SPL of 117 mm, a SCL of 121 mm and a SCW of 96 mm. The sampling of the shell included the neural6, the left costal6, the left peripheral8 and the right hyoplastron. The neural6 is of hexagonal shape with a concave anterior margin and a convex posterior margin. The costal6 is straight to slightly curved and broadens distally. Shield impressions of the central4 and the pleurals3 and 4 are visible on the external surface of the bone. The peripheral8 has a thin proximal part and a thickened distal bulge that tapers into a sharp edge. Shield impressions of the pleural3 and the marginals8 and 9 are found on the external bone surface. The right hyoplastron articulates with the right hypoplastron and the left hyoplastron in straight lines. Anterior and lateral to the suture of the hyoplastra, the element articulates with the rectangular-shaped entoplastron and the epiplastron. The bridge part of the hyoplastron, i.e. the axillary buttress, is low and broad. Shield sulci of the humeral, pectoral and abdominal are found extending generally mediolaterally. The shell elements, with the exception of the peripheral bulge, are thin (generally about 2 mm in thickness). The external bone surfaces of all shell elements are flat with few scute growth impressions (especially in the plastron). Otherwise, the external bone surfaces have a slightly rough texture that is often increased due to shell necrotic pitting. The internal bone surfaces are smooth instead.

4.3.14.3 *Terrapene carolina triunguis* (Agassiz, 1857)

A complete shell of *T. c. triunguis* (FMNH 211806) from ?Kentucky, USA, was sampled. Although the carapace of the specimen was fairly crushed (car accident?) prior to sampling, the plastron was still intact. The latter had a SPL of 126 mm. A neural and a right costal were

sampled in a combined section. Additionally, a peripheral was sectioned, and the left hyo- and hypoplastron were sub-sampled by core drilling (about 12 mm in diameter). The keratin shields were still attached to the bone samples. Due to the crushed nature of the shell and the shield coverage, a description of the gross morphology of the bones is not given here.

4.3.14.4 *Pseudemys peninsularis* Carr, 1938

Four shell bone elements, the neural3, the right costal3, the right peripheral4 and the left hypoplastron of an adult specimen of *P. peninsularis* (YPM 13878) were sampled. The animal was found dead in the wild at Lakeland, Polk County, Florida, USA. The neural is elongated and of hexagonal shape, with an anterior concave margin and a posterior slightly convex margin. The irregular scute sulcus of the vertebral3 and 4 extends over the posterior third of the neural. The element is about 32 to 34 mm long, has a maximum width of 30 mm and a plate thickness of about 9 mm. The overall rectangular costal3 has a broader proximal part (width 38 mm) and distal part (width 45 mm) and a narrow shaft (width 35 mm). The anterior margin is concave, the posterior margin straight. Scute sulci of the vertebral2 and 3 and the pleural2 are present. The distal margin of the plate forms three processes. The middle one is overlying the rib, while the anterior and posterior processes are just formed by the costal plate. The costal plate has an overall thickness of 7 to 8 mm. The peripheral4 is a thin, distal ridged u-shaped bridge peripheral. The dorsal part of the peripheral is slightly longer than the ventral part. Shield impressions of pleurals1 and 2 and marginals3 and 4 are present. The external bone surface is unsculptured. The internal bone surface is smooth at the margins, but carries a reticular vascularisation pattern and small foramina towards the centre of the plate. The hypoplastron is a large element of gross quadrangular shape with a prominent inguinal buttress. The external bone surface has a rough texture. Shield impressions of the abdominal, the pectoral, the inguinal and posterior inframarginals are well imprinted. The internal surface of the bone is smooth.

4.3.14.5 *Trachemys scripta* (Schoepff, 1792)

For this study, fossil specimens of *Trachemys scripta* were sectioned, including a neural (ROM 34387), a costal fragment (ROM 34289), a peripheral (ROM 33693) and a fairly complete left hypoplastron (ROM 33978). The neural and the costal were found in the Pleistocene of Englewood, Charlotte County, Florida, USA. The peripheral comes from the Pleistocene strata of Sarasota County, Florida, USA, while the hypoplastron was recovered from the Pleistocene of Port Charlotte, Charlotte County, Florida, USA. The neural is of hexagonal shape. A slightly curved scute sulcus and a low medial keel is present on the external bone surface. Its length measures 33 to 35 mm, the maximum width is about 30 mm and the thickness of the plate ranges between 12 and 15 mm. The costal roughly resembles a rectangle, but the distal part of the plate is not preserved. Its external surface is ornamented with straight ridges or with curved and wavy ridges and tubercles. Scute sulci of a vertebral and two pleurals meet in a triradiate point. Arrangement and style of ornamentation seems to change among the three sectors of external surface that are divided by the scute sulci. The internal surface of the bone is smooth. The peripheral is triangular in section with a slightly concave dorsal part of the external surface and a strongly convex ventral part. The resulting bulge tapers into an upturned edge. Scute sulci of a pleural and two marginals are present and the distal margin of the element is lobed. The proximal margin of the peripheral also shows a circular striated socket to receive a free rib end of a costal. The fragmentary hypoplastron constitutes most of the hypoplastral plate and part of the buttress. The fragment has a square shape although its lateral margin is broken. The external surface of the bone appears mostly smooth, but it is also locally pitted (?pathology) and abraded. A transverse scute sulcus (abdominal and femoral shield) is present. The internal surface of the bone is smooth, and few foramina insert into the bone.

4.3.15 Bataguridae/Geoemydidae

Both taxon names are very common in the literature and the discussion about which term has precedence over the other seems far from over (see Joyce et al., 2004 for discussion). For the purpose of this study, Bataguridae Gray, 1870 and Geoemydidae Theobald, 1868 are used synonymous. Furthermore, there is a lively debate about the taxonomy and relationships of

the taxa included into the Bataguridae/Geoemydidae (e.g., Lapparent de Broin, 2001; Honda et al., 2002; Hervet, 2004a,b; Claude and Tong, 2004; Feldman and Parham, 2004; Spinks et al., 2004; Danilov, 2005).

Though often referred to as 'Old World pond turtle', *Rhinoclemmys pulcherrima* (Gray, 1855) is a species from South America. In their phylogenetic approach, Spinks et al. (2004) recovered a monophyletic *Rhinoclemmys* group as the basal sister-group to all other derived Bataguridae/Geoemydidae.

The genus *Echmatemys* Hay, 1906 is found in North America and Asia (Hirayama, 1984) during the Eocene. Bartels (1993, in Zonneveld et al., 2000) notes that *E. wyomingensis* (Leidy, 1869) was mostly restricted to fluvial environments (note that *E. wyomingensis* was not explicitly named in the original abstract of Bartels, 1993). Claude and Tong (2004:40) recovered *Echmatemys* in a basal polytomy: (*Echmatemys*, *Rhinoclemmys* ("three-keeled Geoemydidae")). See also McCord et al. (2000) and Spinks et al. (2004) for a more detailed phylogenetic analysis of the more derived geoemydid/batagurid taxa.

Cyclemys dentata (Gray, 1831a) is known from East India in the West to Southeast China and south to Malaysia, the Philippines and ?Indonesia where it lives in mountainous and lowland rivers (e.g., Ernst and Barbour, 1989)

Based on morphological characters and the terrestrial habitat preference, some authors reassigned *Cuora flavomarginata* (Gray, 1863) and *Cuora galbinifrons* (Bourret, 1939) to the distinct genus *Cistoclemmys* Gray, 1863 (e.g., Bour, 1980; Hirayama, 1984; Gaffney and Meylan, 1988; Yasukawa et al., 2001). Mostly based on results of DNA analyses, however, other authors (Honda et al., 2002; Spinks et al., 2004; Stuart and Parham, 2004), argued for the synonymy of *Cuora* and *Cistoclemmys*. *Cuora galbinifrons* (Bourret, 1939) is known from Taiwan and southern China (Ernst and Barbour, 1989) where it prefers a woodland and forest habitat.

While Ernst and Barbour (1989) synonymised *Mauremys mutica* (Cantor, 1842) with *M. nigricans* (Gray, 1834), Joyce et al. (2004) list both *M. mutica* and *M.* (=*Chinemys*) *nigricans* as separate valid species. *M. mutica* is known from southern China, Vietnam, Taiwan and Japan, where it prefers aquatic habitats with slow currents (Ernst and Barbour, 1989).

The material that was included in this study was previously identified as belonging to '*Ocadia*' *sophiae* (Ammon, 1911) by Klein and Mörs (2003), based on the vast literature that states that *Ocadia* is present in the Tertiary of Europe. At that time, the authors noted that a more thorough revision of the '*Ocadia-Palaeochelys-Mauremys* group' is strongly needed. Because of the current changes in fossil and recent batagurid/geoemydid taxonomy as discussed above, the material is now referred to as *Mauremys* (= '*Ocadia*') *sophiae* (Ammon, 1911) *sensu* Hervet (2004a).

The small sized taxa of the genus *Ptychogaster* Pomel, 1847 appear in Europe at the Eocene-Oligocene boundary (Lapparent de Broin, 2001; Danilov, 2005). Hervet (2004a,b) includes *Ptychogaster* Pomel, 1847, *Geiselemys* Khosatzky and Młynarski, 1966, *Clemmydopsis* Boda, 1927 and other, yet unidentified and recently described material (*sensu* Hervet, 2003; Hervet, 2004b) into a 'Ptychogasteridae' group. According to Danilov (2005), *Ptychogaster* spp. developed a hinge between hyo- and hypoplastron similar to recent *Terrapene* spp. and *Emys* spp. However, because the bridge has not been reduced as in the recent forms, the anterior plastral lobe of *Ptychogaster* was still well attached to the carapace.

There is still discussion whether material is assigned to *Kachuga* (*Pangshura*) *tentoria* (Gray, 1834) or, if *Pangshura* is a valid genus, to *Pangshura tentoria* (Gray, 1834) instead. Following more recent studies of Spinks et al. (2004) and Joyce et al. (2004), the material is here referred to *Pangshura tentoria* (Gray, 1834).

A revision of the genus *Clemmydopsis* Boda, 1927 by Młynarski and Schleich (1980) led to the revaluation of *Clemmydopsis steinheimensis* as a valid species, after Williams (1954) synonymised the taxon with *C. turnauensis* (Meyer, 1847b). The most recent analysis by Gross (2004), however, again supported the synonymy with *C. turnauensis*. Interestingly, *Clemmydopsis* spp. have a very aberrant shield configuration (e.g., loss of first three vertebrals; therefore very prominent and laterally expanded centrals). Other genera with peculiar shield configurations are *Sakya* Bogačev, 1960 and *Sarmatemys* Chkhikvadze, 1983. Due to this similarity, the three genera are grouped together in the clade (former tribe) Sakyini by some authors (e.g., Młynarski, 1976; Chkhikvadze, 1983). Please note that *Clemmydopsis* Boda, 1927 is included into a 'Ptychogasteridae' group *sensu* Hervet (2004a).

4.3.15.1 *Rhinoclemmys pulcherrima* (Gray, 1855)

A specimen of *R. pulcherrima* (MVZ 230924), which was preserved in alcohol, was sampled by core-drilling. Though the exact locality of this specimen is unknown, the species is known to occur in the lowlands of Mexico and Costa Rica, Guatemala and Honduras in Central America (Ernst and Barbour, 1989). Two bone cores, each with a diameter of 12 mm, were removed from the proximal part of a right costal and from the right hyoplastron. The keratin shields were still attached to each of the two bone cores. The surface of the keratin scutes covering the costal is sculptured externally due to the scute sulci and growth marks of the vertebral pleural shields. The internal bone surface is smooth and shows the medial rib bulge. The core of the hyoplastron is rather flat instead, although a few growth marks of the pectoral can be deeply impressed.

4.3.15.2 *Echmatemys wyomingensis* (Leidy, 1869)

The sample of *E. wyomingensis* includes a neural7 (UCMP V81110/150186), a proximal part of costal4 (UCMP V81110/150184), a proximal part of costal8 (UCMP V81110/150183), a peripheral4 (UCMP V81110/150188) and a plastron fragment (hyo- or hypoplastron, UCMP V81110/150225). All specimens were recovered from the Eocene Bridger Formation, Sweetwater County, Wyoming, USA. External bone surfaces are flat with a faint rugose texture. Scute sulci are impressed on the external bone surfaces of the costal fragments and the peripheral4. Internal surfaces of all shell elements are generally smooth. The shell material can be quite thick, e.g., the thickness of the plate of neural7 is max. 11 mm.

4.3.15.3 *Cyclemys dentata* (Gray, 1831a)

Sampling of *C. dentata* was carried out on a macerated and disarticulated shell (YPM 13290). The shield cover was already removed during preparation. A neural, a costal3, a peripheral3 and the right hyoplastron of the shell were sectioned. The neural is rectangular with a maximum width of 19 mm and a maximum length of 14 mm. The neural is roof-like in cross-section. A medial low keel is present. The costal3 is also rectangular. Scute sulci are

found proximally and in the mid-region of the costal. The peripheral3 consists of a thin proximal part and a irregularly formed distal bulge that tapers into a pointed edge. Scute sulci and growth marks of the shield cover (vertebral and marginals) are deeply impressed onto the external bone surface of the peripheral. The hyoplastron consists of a flat plate and the protruding axillary buttress. The buttress is situated marginally, thus the distal suture with the bridge peripherals extends to the apex of the axillary buttress. A curved scute sulcus (convex towards anterior) is found in the posterior part of the hyoplastron. Small pits and grooves were observed posterior to the curved scute sulcus. A rather straight sulcus extends proximodistally over the anterior part of the bone surface. The external surfaces of the shell bones are faintly rugose, while the internal bone surfaces are smooth.

4.3.15.4 *Cuora picturata* Lehr et al., 1998

A macerated articulated shell (YPM 13877) of *C. picturata*, formerly known as *C. galbinifrons picturata* Lehr et al., 1998 was sampled. The specimen has a SPL of 151 mm. The neural6, left costal6, left peripheral8 and the right hyoplastron were chosen for sectioning. The neural6 is hexagonal, wider (mediolaterally) than long (anteroposteriorly) and lacks a keel. The costal6 is narrow proximally and broadens distally. The anterior sutured margin is slightly convex while the posterior sutured margin is slightly concave, giving the costal a bend appearance. The peripheral8 consists of a thin proximal part and a distal bulging part. The bulge forms through an internal thickening of the bone. The external bone surface is flat, tapering into a distal upturned edge. The internal surface is convex in the bulge region. The posterior margin of the hyoplastron is straight and the suturing to the hypoplastron is reduced to allow the kinetic hinge. Instead, the sutures to the entoplastron and epiplastron are well developed with long bony protrusions. The anterior and medial sutured margins of the hyoplastron are half-circle shaped. The axillary buttress is short and weak (the same is true for the hypoplastron, thus the closure of the shell by lifting the anterior and posterior plastral lobes is possible). Scute sulci are generally not deeply impressed onto the external bone surfaces and shield growth marks are only faintly present. Otherwise, the external and internal bone surfaces of the shell elements are smooth.

4.3.15.5 *Mauremys cf. M. mutica* (Cantor, 1842)

A macerated and disarticulated shell of the semiaquatic turtle *Mauremys cf. M. mutica* (SMNS 6876) was sampled. The distribution of the taxon is restricted to southern China, Vietnam, Taiwan and Japan (e.g., Ernst and Barbour, 1989; Asian Turtle Trade Working Group, 2000), where it inhabits aquatic milieus with slow moving water. The sampling included a neural3, a left costal3, a left peripheral2 and the right hyoplastron. The neural3 is of hexagonal shape with a low medial keel. The costal3 is of rectangular shape with a proximodistal flexure. The free rib head protrudes from the very proximal margin of the internal surface of the costal plate. The progression of the rib is barely traceable. The peripheral is triangular in cross-section tapering in a sharp distal edge. The base of the hyoplastron is flat. The well developed axillary buttress is long and protrudes at a high angle from the base of the hyoplastron. The external surfaces of all bones have a faintly rough texture and lack ornamentation. The internal surfaces of the shell elements are generally smooth.

4.3.15.6 *Mauremys* (= *'Ocadia'*) *sophiae* (Ammon, 1911)

The sample of this taxon from the middle Miocene lignite strip mining pit of the company 'Rheinbraun AG', Hambach, Germany, included the proximal part of a left costal3 (IPB HaH-3348) and a left peripheral8 (IPB HaH-3225) (see Klein and Mörs, 2003). The costal plate shows a small ventral rib bulge and both the external and the internal surfaces of the bone are slightly rough. Shield impressions are not seen. The peripheral has a thin proximal and a bulging distal part. A shield sulcus extends proximodistally over the dorsal and ventral side of the external surface of the bone. The bone surface texture is smooth to slightly rugose.

4.3.15.7 *Mauremys* (= *'Ocadia'*) sp.

Material of *Mauremys* (='*Ocadia*') sp. is a single specimen (SMNK Me 295) from the Middle Eocene Messel pit near Darmstadt, Germany. The specimen is a small carapace fragment that constitutes the sutured proximal parts of two costals. The specimen is slightly

curved with a convex external and a concave internal bone surface. The proximal ends of the incorporated ribs are visible in the respective costal plates. Both bone surfaces are smooth with the external one showing slight shield impressions.

4.3.15.8 *Ptychogaster* sp.

Several shell elements of *Ptychogaster* sp. from the Lower Miocene (MN1) of Tomerdingen, Germany, were sampled. The sample included two costals (SMNS 88988, 88989), two peripherals (SMNS 88990, 88991) and two plastron fragments (?hyo- or hypoplastron: SMNS 88992; ?xiphiplastron: SMNS 88993). The costal fragments are rather flat elements with a low proximodistal curvature. In SMNS 88988, the broken-off rib head protrudes from the plate near the proximal sutural margin. The peripherals are triangular in cross-section. SMNS 88990 is a small and flat peripheral with a distally upturned tapering sharp edge. SMNS 88991 is a larger, thicker peripheral with a more rounded distal ridge. Much of the interior cancellous part of the bone and the internal cortices are not preserved. SMNS 88992 mainly comprises the swelling buttress part of the plastral element, while the flat plate part was broken off prior to sampling. The external surface of the bone element is slightly convex. SMNS 88993 is flat and triangular in cross-section, tapering to a sharp, slightly convex edge. The external bone surface texture of the elements is slightly rugose while the internal surface texture of the bones is smooth.

4.3.15.9 *Pangshura* (=*Kachuga*) *tentoria* (Gray, 1834)

Several shell elements (FMNH 259431) from a female specimen (SPL about 185 mm; note that plastron was disarticulated) of the Indian tent turtle (labelled as *Kachuga tentoria*) from ?Bangladesh (no further data) were sampled, including a neural (?neural4), a costal, a peripheral and a xiphiplastron. The sampled neural has a characteristic anterior medial keel that ends in a posterior-pointed apex. The apex protrudes about 6 mm over the external surface of the neural. The costal and the xiphiplastron are flat elements. The peripheral is hook-shaped with a straight proximal part and a thickened and angled distal part. The internal

surface of the peripheral is smoothly curved, while the external surface has a distinct edge between the proximal and distal part.

4.3.15.10 *Clemmydopsis turnauensis* (Meyer, 1847b)

The sampling of *C. turnauensis* included a costal (SMNS 88998), a peripheral (SMNS 88999) and a plastral fragment (hyo- or hypoplastron; SMNS 89000). The costal is a straight element with little proximodistal curvature. The peripheral divides into a proximal thin part and a distally thickened tapering part. The distal bulge occurs due to an increased convexity of the ventral bone surface. The plastral fragment has a flat plate part and a raised buttress part. The external bone surface of the elements is slightly rugose, while the internal bone surfaces are generally smooth. The costal and the flat plate part of the plastral fragment have a thickness of about 2 mm. Only the bridge part of the plastral fragment and the bulging distal part of the peripheral have higher thicknesses (5 to 7 mm).

4.3.16 Testudinidae

The Testudinidae, commonly known as tortoises, are the only group of purely terrestrial turtles. The oldest known representative of Testudinidae may come from the upper Palaeocene of Mongolia (V. B. Sukhanov, pers. comm., in Danilov, 2005). Based on an extensive fossil record, tortoises are today a highly diverse, wide ranging group of turtles (Ernst and Barbour, 1989). There is still ongoing discussion about exact relationships among Testudinidae (for discussion see Claude and Tong, 2004; Danilov, 2005).

Both the extant genus *Manouria* Gray, 1852 and the fossil genus *Hadrianus* Cope, 1872a from the Eocene of Asia, North America and Europe are basal representatives of Testudinidae (e.g., Claude and Tong, 2004). Because of similar morphologies, it was first proposed that *Hadrianus* was synonymous to *Manouria* (Auffenberg, 1974; Crumly, 1984). However, other authors argued for the validity of *Hadrianus* Cope, 1872a as a separate genus (e.g., Broin, 1977; Takahashi et al., 2003, in Danilov, 2005; Claude and Tong, 2004). As stated by Meylan and Sterrer (2000), skull material is still not known for the genus *Hadrianus* Cope, 1872a.

According to Hutchison (1980), specimens of *Hadrianus* can have carapace lengths of over 61 cm.

Several size categories of Testudinidae are covered with the samples herein. *Hesperotestudo crassiscutata* is a giant tortoise (>1000 mm CL) from the Pleistocene of Florida, USA (Meylan, l995). The Asian *Manouria emys* (to 600 mm CL), the African *Geochelone pardalis* (up to 680 mm CL) and the South American *Geochelone carbonaria* (to 510 mm CL) represent an intermediate size class. The West African *Kinixys homeana* (up to 210 mm CL) and the Indian *Geochelone elegans* (to 280 mm CL) represent the smaller species (Ernst and Barbour, 1989).

Kinixys spp. are the only turtles that have a movable hinge in the carapace, by which the posterior part of the carapace can be raised and lowered.

4.3.16.1 *Hadrianus majusculus* Hay, 1904

The specimens of *H. majusculus* were found in the 'Main Body' unit of the Eocene Wasatch Formation (Wasatchian), Sweetwater County, Wyoming, USA. The sample comprises a neural (UCMP V74024/150212), two costal fragments (UCMP V74024/150213; UCMP V74024/150214), a plastron fragment (UCMP V74024/150215) and a thick shell fragment (UCMP V74024/150216). The neural has a convex external bone surface and a single medial protrusion (=neural spine) on its concave internal bone surface. Costal fragment (UCMP V74024/150213) is strongly curved anteroposteriorly with a prominent rib bulge on the internal surface of the bone. Costal fragment (UCMP V74024/150214), on the other hand, is flat and the internal rib bulge is not as pronounced. The plastron fragment consists of a flat tabular plate and two original unbroken margins. The external surface of the element shows a straight scute sulcus, while the internal bone surface is locally bulged. The external surfaces of the shell elements are rough with a fine vermicular striation pattern. Hutchison (1980) already noted a distinct surface texture present in the genus, without giving a more detailed description. Laterally, a marginal seam is recognisable on the external bone surface where the striation extends more perpendicular towards the margins of the shell elements. With the

exception of the thick shell fragment which has a thickness between 17 and 19 mm, the thicknesses of the other elements is significantly lower (5 to 10 mm).

4.3.16.2 *Hadrianus corsoni* (Leidy, 1871a)

A single peripheral (UCMP V98009/150191) of *H. corsoni* was sampled. The element derives from the Eocene Bridger Formation, Uinta County, Wyoming, USA (see also Lapparent de Broin, 2001). With the dorsal part of the external surface of the bone being flat to slightly wavy and the ventral part of the external surface being convex, the peripheral is lentil-shaped tapering to a pointed distal edge. Only a small, ventrally situated proximal part of the peripheral comprises internal bone surface

4.3.16.3 *Manouria emys* (Schlegel and Müller, 1844)

With up to max. 60 cm CL (?CCL), *M. emys* is the largest tortoise of Asia (e.g., Ernst and Barbour, 1989). The sampled specimen (FMNH 260395; 470 mm SPL) derives from ?northern Malaysia (no further data available), where it lives in tropical highland monsoon woodlands (Ernst and Barbour, 1989). The carapace and plastron both lack hinges. Sampling occurred through core drilling of the macerated shell where two cores were removed. One core sub-sampled the distal part of the right costal2 and the second core sub-sampled the right hyoplastron. The bone surfaces of the costal appeared smooth with the sulcus of the first vertebral extending along the external surface of the core. Pitting of the external surface of the shell increased in the vicinity of the scute sulci. The external surface of the right hyoplastron was also smooth, but a striation pattern was present towards the sutures.

4.3.16.4 *Hesperotestudo* (*Caudochelys*) *crassiscutata* (Leidy, 1889)

The specimens of *H. crassiscutata* derive from Pleistocene sediments of Florida, USA (compare to Meylan, 1995). The sample included a neural (ROM 51460), a ?peripheral fragment (ROM 55400), a costal fragment (ROM 55400) and a xiphiplastron (ROM 55400). Only for the neural is more precise locality known (Pleistocene [Irvingtonian], Port Charlotte, Charlotte County, Florida, USA). Furthermore, a separate osteoderm of unknown position on the body (ROM 34014) could be sampled. The osteoderm was found in the Pleistocene locality of Grassy Point, Charlotte County, Florida, USA. The neural has a hexagonal shape. It was measure to have an anteroposterior length of 90 to 100 mm, a maximum width of 147 mm and a thickness that ranges between 24 mm and 34 mm. The external surface of the neural is irregular and humped. The costal fragment is a large rectangular block of bone where the proximal and distal regions of the costal are broken off, but the lateral sutures are still preserved. The ?peripheral fragment is a thick bulging bone fragment with a straight dorsal and a convex ventral surface. The bulge part tapers into a distal upturned edge. The xiphiplastron is a large and fairly complete element with a maximum anteroposterior length of 130 mm, a maximum width of 120 mm (please note that the medial margin of the xiphiplastron is damaged, therefore the value is too low) and a thickness that ranges between 20 and 32 mm. All shell bone elements have a very rough and rugose (almost spongy) external surface texture, while the internal surface of the bone is rather smooth with slightly striation. The bone histology of specimens ROM 51460 and ROM 55400 of *H. crassiscutata* was best preserved in the xiphiplastron, the peripheral and the costal fragment, whereas the bone of the neural shows strong diagenetic alteration.

4.3.16.5 *Kinixys homeana* Bell, 1827

A macerated and disarticulated juvenile pet trade specimen (W. G. Joyce, pers. comm.) of *K. homeana* was sampled. The species occurs in forests of West Africa, from Liberia eastward to Zaire (Ernst and Barbour, 1989). The studied material (YPM 13876) included the neural series 6-8, costals7 and 8, peripheral series 6-9 and a hyoplastron. All external bone surfaces of the sampled bones have a faintly rough and pitted texture. Scute growth marks and scute sulci are well impressed on the external bone surfaces. The internal surfaces are rather

smooth and small scattered foramina can occur. During ontogeny, the sutured bone margins that will be involved in the peculiar hinge system are gradually resorbed, leading to corrugated and rounded margins. In the sampled elements, the hinge costals and neurals are still weakly sutured, while the hinge peripherals are already detached from each other.

4.3.16.6 *Geochelone pardalis* (Bell, 1828)

G. pardalis occurs only in northeast to southwest Africa (Sudan to South Africa) where it lives in savannah, plain, dry woodland, thorn scrub and grassland habitats (Ernst and Barbour, 1989). The specimen, a shell with strongly domed carapace and sawed off flat plastron, was confiscated by German customs and was then stored at the zoological collections in Stuttgart (SMNS 12605). The plastron has a SPL of 245 mm. While the second vertebral was already removed from the carapace, only the underlying bone was sampled. The sub-sampling of the neural2 and the right costal2 was done by core drilling (12 mm core diameter). Likewise, the right hypoplastron was sub-sampled with the 12 mm core bit. Even though the abdominal shield was still attached to the plastral bone, only the bone itself was sampled in this case.

4.3.16.7 *Geochelone carbonaria* (Spix, 1824)

G. carbonaria ranges from the Caribbean down to east-central South America, where it dwells in humid forests and moist savannahs, plains, dry woodlands, thorn scrub and grasslands (Ernst and Barbour, 1989). The sampled specimen, formerly part of the collections of the Insitute of Zoology, University of Bonn, had a CCL of 310 mm, a CCW of 285 mm and a SPL of 235 mm. Sampling was done by core drilling, which resulted in three bone cores (IPB R560a-c) with keratinous shields still attached. Each core has a diameter of 22 mm. The first and second core sub-sampled the proximal part of a left costal and the distal part of a left costal (bridge region) respectively. The third core sub-sampled mainly the left hypoplastron and the suture to the left hyoplastron. The core through the proximal costal was difficult to remove, because the carapace was strongly humped, with vertebral and pleural shields having an elevated central aureole (=apex) with steep dropping flanks towards the sulci. While the

bone was expanded below the humps, the thickness of the bone reduced to a minimum internal to the scute sulci. Furthermore, connective tissue, i.e. muscle tissue, was still firmly attached to the internal bone surface and had to be carefully removed. The core through the distal part of the costal and through the plastral elements were easily removed instead from the visceral tissue.

4.3.16.8 *Geochelone elegans* (Schoepff, 1795)

A specimen of *G. elegans* with 185 mm CCL, 175 mm CCW and 127 mm SPL was sampled. The exact locality is not known, however, the species occurs today in tropical deciduous forest and dry savannahs of peninsular India and Sri Lanka where it is still dependent on sufficient water supply (Ernst and Barbour, 1989). Sampling of the alcohol-preserved specimen (formerly part of the collections of the Institute of Zoology; University of Bonn) was done by core drilling, resulting in two cores (IPB R561a,b). The right side of the carapace and the left side of the plastron was drilled, thus two bone cores (22 mm diameter) with keratinous shields still attached have been removed from the shell. The first core (IPB R561a) includes the proximal part of a costal and the margin of the adjacent neural. The second core (IPB R561b) includes the posterior part of the left hyoplastron and anterior part of the hypoplastron. Both cores were easily removed from the internal visceral tissue (lung tissue almost immediately internal to the costal; ?muscle fascia internal to the plastron).

4.3.17 Eucryptodira incertae sedis (aff. ?Trionychoidea)

According to Hutchison (1998) and Holroyd et al. (2001), phylogenetic relationships of the early Eocene turtle *Planetochelys* remain unclear, however it may be related to Trionychoidea. Morphologic traits of the genus indicate partly terrestrial habits (Hutchison, 1998). Furthermore, *Planetochelys* is the only early Eocene turtle genus that has a specialised plastral hinge where the hyo- and hypoplastra are not fused together (Holroyd et al., 2001).

4.3.17.1 *Planetochelys* sp.

The sample of *Planetochelys* sp. included a neural (UCMP V81203/130914) as well as five additional associated shell fragments (UCMP V81071/159356). The five fragments comprise a small proximal part of a costal, a larger, more distal part of another costal fragment, a peripheral and two plastron elements (?hyo- or hypoplastron) with one margin belonging to a hinge system. All elements were recovered from the Eocene Willwood Formation (Wasatchian), Washakie County, Wyoming, USA. The external surfaces of the bone fragments are slightly rugose, while the internal surfaces are generally smooth. Of special interest in this taxon are the margins of the hinge elements of the plastron, because they do not show interlocking sutures. Instead, the bone surfaces are smooth with a shallow oblong groove extending over the length of the margin. In both plastral elements, the external surface of the bone narrowly surmounts the internal bone surface, thus the hinge groove is slightly angled.

4.3.18 Dermatemydidae

Dermatemydidae currently encompasses the only living species *Dermatemys mawii* Gray, 1847 and the fossil genus *Baptemys* from the Eocene of North America (Gaffney and Meylan, 1988; Joyce et al., 2004). Other genera like *Adocus* Cope, 1868, *Nanhsiungchelys* Yeh, 1966, *Basilemys* Hay, 1902, *Agomphus* Cope, 1871, were once included in Dermatemydidae, but the genera are now recognised as belonging to the Adocidae (*Adocus*), Nanhsiungchelyidae (*Basilemys*, *Nanhsiungchelys*) and Kinosternia (*Agomphus*) respectively (Yeh, 1966; Hutchison and Bramble, 1981; Meylan and Gaffney, 1989; Joyce et al., 2004). Danilov and Parham (2006) most recently defined the new clade 'Adocusia' to include the fossil adocid and nanhsiungchelyid taxa. Because *Trachyaspis* Meyer, 1843 is most probably a Cheloniidae "*sensu stricto*" instead of a dermatemydid turtle (e.g., Weems, 1974), there are no Dermatemydidae known from Europe (Lapparent de Broin, 2001). After Gaffney (1975c), *D. mawii* is closely related with carettochelyid, trionychid and kinosternid turtles, comprising the Trionychoidea. For this study shell material of *B. garmanii* and *D. mawii* was sampled.

4.3.18.1 *Baptemys garmanii* (Cope, 1872b)

The sampling of *B. garmanii* included a neural (UCMP V74024/150224), two costal fragments (UCMP V74024/150219; UCMP V74024/150220), a peripheral (UCMP V74024/150222) and a plastral fragment (?hyo- or hypoplastron, UCMP V74024/150221). All elements derive from the 'Main Body' unit of the Eocene Wasatch Formation (Wasatchian), Sweetwater County, Wyoming, USA. The neural carries a low, anteroposteriorly extending medial ridge. The costal are rather flat to slightly flexed elements. The peripheral is straight to slightly externally curved with a round distal edge. The plastral bone has a slightly convex external surface and a gently raising part towards the bridge. All sampled elements have scute sulci on their external bone surfaces. These shield impressions are most prominent in the peripheral, resulting in a deeply grooved bone surface. Besides the scute sulci, the external surfaces of the shell elements are unsculptured.

4.3.18.2 *Dermatemys mawii* Gray, 1847

The almost fully aquatic Central American river turtle (also known as Tabasco turtle) is restricted to a small areal between Central Mexico and north-western Honduras, where it inhabits larger rivers, lakes and lagoons and even brackish waters of deltas and estuaries (e.g., Pritchard, 1979; Ernst and Barbour, 1989). The strong adaptation of *D. mawii* to the buoyant aquatic medium expresses itself for example in the weak development of its extremities that are almost too weak to carry it on land over long periods of time (e.g., Pritchard, 1979; Ernst and Barbour, 1989). The sampled specimen (ZMB 9558) of *D. mawii* is relatively small with a CCL of 215 mm, a CPL of 172 mm and a CCW of 200 mm. The proximal part of the left costal2 and the right hyoplastron were sub-sampled by core drilling (22 mm core diameter). In both cases, the extremely thin (skin-like) keratinous shield coverage mostly came apart in small flakes and is thus only partly attached to the bone core (see also Pritchard, 1979).

4.3.19 Kinosternia

Kinosternia, as introduced by Gaffney and Meylan (1988), includes the genus *Hoplochelys* and Kinosternidae. The Palaeocene genus *Hoplochelys* Hay, 1908 from North America, together with Late Cretaceous *Agomphus* Cope, 1871 also from North America, may represent the phylogenetic stem of Kinosternidae (Hutchison and Bramble, 1981; Meylan and Gaffney, 1989; Joyce et al., 2004). Please note, that, as stated by Meylan and Gaffney (1989), the taxon *Agomphus* Cope, 1871 may not be monophyletic. After Meylan et al. (2000) and Holroyd and Hutchison (2002), the genera *Hoplochelys* and *Agomphus* are known only from shell material, while cranial material and non-shell postcranial material has not been found yet.

4.3.19.1 *Hoplochelys* sp.

The sample of *Hoplochelys* sp. included a neural (UCMP V2811/150210), a proximal part of a costal (UCMP V2811/150204), a more distal costal fragment (UCMP V2811/150203), a right peripheral3 (UCMP V2811/150207), a left peripheral8 (UCMP V2811/150206) and a plastron fragment (?hyo- or hypoplastron, UCMP V2811/150208). All shell elements derive from the Palaeocene Nacimiento Formation (Puercan), San Juan County, New Mexico, USA. The neural has a low medial keel flanked by two lateral shallow and wide grooves. A curved scute sulcus crosses perpendicular over the keel. The costal fragments have a slightly humped external bone surface. Costal fragment UCMP V2811/150204 carries a scute sulcus. The rib head does not protrude far over the internal bone surface of this specimen. The progression of the rib can be observed as an internal bulge of the internal surface of costal fragment UCMP V2811/150203. Peripheral3 is bulged and roughly triangular in cross-section with a distally tapering blunt edge. Peripheral8 has a proximal slender straight part and terminating in a distal circular bulge. The plastron fragment has a flat rough external surface with scattered pits. The internal surface of the element is convex with a smooth to faintly striated texture.

4.3.20 Kinosternidae

Following Hutchison (1991), the exclusively New Wold group Kinosternidae is subdivided into the Staurotypinae and the Kinosterninae. In the fossil record, Kinosterninae appear since the Eocene, while Staurotypinae do not occur until the Pleistocene (Hutchison, 1991). Turtles of the Staurotypinae were not sampled in this study. A basal representative of the Kinosternidae might be the Upper Cretaceous *Emarginachelys* Whetstone, 1978 from North America (Gaffney and Meylan, 1989). Originally, the skull of *Emarginachelys* was considered to belong to a chelydrid turtle instead of a kinosternid turtle (Whetstone, 1978).

The Eocene *Baltemys* Hutchison, 1991 with its type species *B. staurogastros* Hutchison, 1991 is a small turtle with a maximum carapace length of 100 mm (Holroyd et al., 2001). Phylogenetically, *Baltemys* might be basal to all other Kinosterninae (Hutchison, 1991).

The species *Sternotherus minor* (Agassiz, 1857) is known from southeastern North America where it inhabits all kinds of freshwater habitats (e.g., Ernst and Barbour, 1989; please note that the species is listed herein as *Kinosternon minor*).

K. subrubrum (Bonnaterre, 1789) is already known from the Pleistocene of Wisconsin, USA (Ernst and Barbour, 1989). Today, it ranges through eastern, central and southern states of the USA, where it mostly dwells in soft-bottomed slow moving water bodies (Ernst and Barbour, 1989).

The plastron of *Kinosternon* spp. either has a single transverse hinge between the pectoral and abdominal shield or two transverse hinges, one anterior and one posterior of the abdominal shield. Furthermore, the plastron lacks an entoplastron (e.g., Ernst and Barbour, 1989).

4.3.20.1 *Baltemys* sp.

The specimens of *Baltemys* sp. were collected in the Eocene Willwood Formation (Wasatchian), Big Horn County, Wyoming, USA. The sample included a neural and two costal fragments (UCMP V78106/122542) and a peripheral and plastron fragment (UCMP

V78106/122545) respectively. All elements and bone fragments were of small size (<20 mm). The neural has two low parasagittal keels that extend anteroposteriorly over the external bone surface. One costal fragment is rectangular with a free distal rib end protruding over the plate margin. The second costal fragment includes a more proximal part of the costal plate. The peripheral consists of a slender proximal part and a distal lentil-shaped bulge that tapers into a distinct edge. The small plastral fragment is flat and one sutured margin is still preserved. The other margins are broken.

4.3.20.2 *Sternotherus minor* (Agassiz, 1857)

A macerated and disarticulated specimen (SMNS 6879) of *S. minor* was sampled. A neural, a costal, a peripheral and the right hyoplastron were taken for analysis. The neural is a small, oblong and of hexagonal shape. The costal and the peripheral are associated, thus the long pointed free rib end fits into the groove of the peripheral. The costal plate is curved, and the progression of the rib is not recognised as a distinct bulge on the internal bone surface. The rib head protrudes over the costal plate only a few millimetres short of the proximal margin of the costal plate. The hyoplastron consists of a rectangular laterally broadening flat plate and a thick elevated laterally flaring buttress part. The medial suture to the adjacent left hyoplastron as well as the anterior suture to the epiplastron (entoplastron is absent) are well developed. The posterior margin is weakly sutured to the hypoplastron over the full width of the element including the lateral buttress part (anterior lobe kinesis, see also Hutchison, 1991). All shell elements have a faintly rough external bone surface and rather smooth internal bone surfaces.

4.3.20.3 *Kinosternon subrubrum* (Bonnaterre, 1789)

The sampling of *K. subrubrum* (YPM 13875), a macerated and disarticulated specimen, included a neural3, a costal3, a peripheral3 and the left hyoplastron. The specimen was caught in the wild by a breeder near ?New Orleans, Louisiana, USA. The neural3 has a hexagonal shape and carries no external keel. The costal3 is moderately flexed. The progression of the rib in the costal is faintly traceable as a proximodistally orientated bulge of the internal

surface of the costal bone plate. The peripheral3 consists of a proximal narrow part and a distal rounded bulge. The hyoplastron has a rectangular flat plate and a broad distally flaring buttress part. The external surfaces of the shell elements had a faintly roughened texture, while the internal bone surfaces were smooth.

4.3.20.4 *Kinosternon* sp.

A specimen of *Kinosternon* sp. (SMNS 7440), which was preserved in alcohol, was sampled by core-drilling. The specimen has a SPL of about 105 mm. Three bone cores, each with a diameter of 22 mm, were removed from the right costal2, the anterior hinge system (right epi- and hyoplastron) and the posterior hinge system (right hypo- and xiphiplastron) of the shell, respectively. The keratin shields were still attached to each of the three bone cores. The core of costal2 is slightly curved with a maximum thickness of 2.5 mm. The progression of the rib is faintly visible as a bulge of the internal surface of the costal plate. The two cores of the plastron range in thickness between 2.5 and 4.5 mm. The elements that are involved in the hinge systems show a slight swelling or bulge adjacent to the hinge line. The keratin shields (pectoral, abdominal and femoral) covering the plastron elements have a wrinkled surface texture. Besides the shield sulci, the shields (vertebral1 and pleural1 and 2) covering the costal2 were smooth and flat.

4.3.21 Adocidae

According to Brinkman (2003a), Adocidae Cope, 1870b comprises a group of large aquatic turtles from the Late Cretaceous of Asia and North America. Only specimens of the genus *Adocus* Cope, 1868 were sampled in this study. Detailed osteological description of the taxon is found in Meylan and Gaffney (1989). According to Meylan and Gaffney (1989:24), “the entire surface [of the carapace] is finely sculptured with a very regular arrangement of minute tubercles lying close enough together that the pattern could also be described as rows of small depressions”.

4.3.21.1 *Adocus* sp.

The sample of *Adocus* sp. included a neural (UCMP V73096/150202), a proximal part of a costal (UCMP V87101150200), a distal peripheral fragment (UCMP V87101/150201) and a plastral element (?hyo- or hypoplastron; UCMP V87071/150192). All shell elements derived from lower Palaeocene (Puercan) rocks (Hell Creek Formation and overlying Tullock Formation) of Montana, USA. The neural is of oblong hexagonal shape. Both, the neural and the costal fragment have flat finely sculptured external surfaces. In the costal fragment, the rib bulge is asymmetrical with a steep flank and a flank that is rising more gently. The peripheral is triangular in cross-section with a blunt rounded edge. The plastral fragment is flat and most of the internal surface of the bone is not preserved. Although the sculpturing pattern of the external surfaces of the shell elements is regular and well observable in most fragment (see description above), it becomes not as distinct in size and elevation as in *Basilemys* sp. (see below).

4.3.22 Nanhsiungchelyidae

Nanhsiungchelyidae comprise the genera *Zangerlia*, *Hanbogdemys*, *Anomalochelys*, *Nanhsiungchelys* and *Basilemys* (Brinkman and Nicholls, 1993; Brinkman and Peng, 1996; Hirayama et al., 2000, 2001; Joyce and Norell, 2005). The different phylogenetic hypotheses among Nanhsiungchelyidae are discussed in Joyce and Norell (2005). Only material of *Basilemys* Hay, 1902 from the Cretaceous of Asia and North America (Hirayama et al., 2000) could be sampled. The assignment of *Basilemys* to Nanhsiungchelyidae seems valid (Nessov, 1986; Meylan and Gaffney, 1989). The external surfaces of the shell bones of *Basilemys*, *Zangerlia* and *Nanhsiungchelys* share a regular "pock-marked" sculpturing pattern (Młynarski, 1972:86, 1976; see also Meylan and Gaffney, 1989). In *Basilemys*, the sculpturing pattern can extend fairly wide into the interior of the shell openings, so that the internal surfaces of bones adjacent to these openings are also heavily sculptured (pers. obs.). Several morphological features (i.e., triturating surfaces of maxilla; robust elephantine limbs, well ossified limb armour, strong epiplastral projections) characterise *Basilemys* as an ecological pendant of tortoises in being terrestrial and herbivorous (Sukhanov and Narmandakh, 1977; Hutchison and Archibald, 1986; Brinkman, 2003a).

4.3.22.1 *Basilemys* sp.

The studied material of FM P27371 of *Basilemys* sp. included a neural fragment, a costal fragment, a pair of sutured peripherals, a plastral fragment (?hyo- or hypoplastron), as well as a marginal shell fragment which could not be unambiguously assigned to either the carapace or the plastron. All material of FM P27371 was found in the Late Cretaceous Kirtland Shale, McKinley County, New Mexico, USA. Further shell material included a large isolated peripheral (YPM 9703) from the Cretaceous Laramie Beds, Schneider Cn., Converse County, Wyoming, USA and two osteoderms (TMP 2003.12.278; TMP 80.08.296) from the ?Oldman Fm. or Dinosaur Park Fm., Judith River Group, Dinosaur Provincial Park, Alberta, Canada. The exact location of the osteoderms on the body is unknown. The costal fragment and the neural fragment of FM P27379 are of similar thickness but the external surfaces of both bones are weathered. The peripherals, the plastral fragment, the shell fragment and the osteoderms show the very regular 'pock-mark' sculpturing pattern with rhomboidal to honeycomb shaped pits that often align in rows. The internal surface of the plastral fragment is smooth with a faint striation pattern. In the case of the smaller osteoderm, a striation of the internal and lateral margin is visible. The larger osteoderm on the other hand shows numerous small foramina inserting both into the internal and external cortices.

4.3.23 Carettochelyidae

The fossil record of Carettochelyidae reaches back into the middle Cretaceous with the Asian *Kizylkumemys schultzi* (Joyce et al., 2004). Hirayama et al. (2000) reported even older fossil Carettochelyidae from the Lower Cretaceous (Hauterivian) of Japan, which may represent the phylogenetic stem of Carettochelyidae (Joyce et al., 2004). According to Danilov (2005), the oldest well known representative of the genus *Kizylkumemys* Nessov, 1977 is known from the Upper Cretaceous (Cenomanian) of Karakalpakia, western Uzbekistan. During the Eocene, Carettochelyidae had its greatest diversity in Asia, Europe and North America. Today, Carettochelyidae is monospecific with the recent *Carettochelys insculpta* Ramsay, 1887. A detailed anatomical description of the shell of a specimen of *C. insculpta* can be found in Walther (1922). The Carettochelyidae can be divided into the more basal Anosteirinae, with *Kizylkumemys* Nessov, 1977, *Anosteira* Leidy, 1871b and

Pseudanosteira Clark, 1932, and the more advanced Carettochelyinae including *Carettochelys* Ramsay, 1887, *Allaeochelys* Noulet, 1867, *Burmemys* Hutchison et al., 2004 and *Chorlakkichelys* Broin, 1987 (e.g., Meylan, 1988; Meylan and Gaffney, 1989; Hutchison et al., 2004; Danilov (2005). While the former group is characterised by smaller body size, a medial keel with bony protrusions of the neurals and the retention of scute sulci, the latter group reaches larger body size and, in adults, lack the shield cover and scute sulci (Meylan, 1988; Hutchison et al., 2004; Danilov, 2005). *Anosteira* Leidy, 1871b is known from the Eocene of Asia and North America, while the closely related *Pseudanosteira* Clark, 1932 is known only from the Eocene of western North America (e.g., Hutchison et al., 2004). Only few characters in carapace morphology (i.e. neural sequence) separate both taxa from each other (Meylan and Gaffney, 1989; Hutchison et al., 2004). Broin (1977) viewed *Pseudanosteira* as being synonymous with *Anosteira*. The genus *Allaeochelys* Noulet, 1867 is the only representative found in Europe (Lapparent der Broin, 2001). Following Meylan (1988), *Allaeochelys* Noulet, 1867 further represents the sister taxon to *Carettochelys* Ramsay, 1887.

4.3.23.1 *Anosteira* sp.

The samples of *Anosteira* sp. (FM PR 819) were found in the Uinta Formation (horizon C, lower part), late Eocene, Uintah County, Utah, USA. The shell material included a neural and adjacent proximal part of a costal, another costal, a peripheral and a left hypoplastron. The neural has a prominent dorsal bony protuberance with a distinct medial apex. The proximal part of the still attached costal as well as the separate costal plate is flat to proximodistally flexed, with slightly concave internal and slightly convex external bone surfaces. The peripheral appears triangular in proximodistal section. The distal edge is blunt and the external surfaces of the peripheral enclose a rather large angle of 70 to 80 degrees. The peripheral also has a characteristic circular groove to accommodate the free rib end of a costal. The hypoplastron has an anteroposterior length of 27 mm and a maximum width of 31 mm. The sculpturing pattern of radiating tubercles and low ridges is best seen on the peripheral, while it is not so distinct on the external surfaces of the other shell elements. Scute sulci are seen on the external surfaces of the neural and of both costal fragments.

4.3.23.2 *Pseudanosteira pulchra* Clark, 1932

A neural, a proximal part of a costal, another costal fragment, a peripheral and a fragmentary plastral element (all UCMP V78031/131731) of *P. pulchra* were sampled. The neural is of rectangular shape, with a maximum length of 14 mm, a maximum width of 6 mm and a height of the plate of about 4 mm. The costal fragments are flat with a light proximodistal flexure. The peripheral is triangular in cross-section with a distinct distal pointed edge and a concave internal surface. The angle between the external surfaces of the peripheral was measured between 45 to 50 degrees. The plastral fragment is strongly striated towards the lateral margin and the striation gets most pronounced at the sutural pegs at the margin. The sculpturing pattern of mainly radiating knobs and tubercles is best observed on the external surface of the peripheral. The external bone surfaces of the neural, the costal fragments and the plastral fragment are weathered and the sculpturing pattern is weak here.

4.3.23.3 *Allaeochelys* cf. *A. crassesculpta* (Harrassowitz, 1922)

The material (HLMD-Me 10468) of cf. *A. crassesculpta* from the Eocene Messel pit near Darmstadt, Germany, includes a costal and two peripheral fragments. The costal is a thin straight bone which slightly broadens distally. The free rib end extends beyond the distal margin of the costal. One peripheral derives from near the bridge region, the other one is situated either at the anterior or the posterior margin of the shell. The first peripheral has a strongly concave internal surface and a distinct edge in its external surface. The external sides of the bone include an angle of about 90 to 100 degrees. The second peripheral is highly flattened with a distal tapering edge that slightly bends towards dorsal. The internal surfaces of the bones are smooth while the external surfaces are faintly wrinkled with low ridges and tubercles.

4.3.23.4 *Carettochelys insculpta* Ramsay, 1887

The Fly River or pig-nosed turtle *C. insculpta*, which can reach a CL of over 55 cm, occurs in rivers and lacustrine habitats with slow currents and it may also enter brackish waters (e.g., Ernst and Barbour, 1989). The species is restricted to New Guinea and Northern Territory of Australia (e.g., Ernst and Barbour, 1989). The shell is highly domed in adults and well ossified. Compared to Trionychidae, the peripherals are well developed. Several elements of a larger specimen (MAGNT R12640) could be acquired for this study, including a neural, a costal, a peripheral and the left hyoplastron. The material was already macerated and disarticulated, thus the skin cover of the shell was not included in the sample. The neural is a diminutive oblong and slender bone compared to the size of the rest of the shell elements. The sampled costal has a narrow proximal shaft that broadened distally. The distal margin of the costal is slightly curved, with the free distal rib end protruding a little further over the margin of the plate. The peripheral tapers distally into a dorsally upturned edge, while the internal surface of the bone is strongly concave. The hyoplastron is of general rectangular shape with a long sutured posterior margin. The posterior margin is slightly wavy to suture with the epi- and entoplastron. All shell elements show the typical wrinkled external sculpturing pattern with radiating or parallel tubercles and low ridges. Generally the sculpturing of the external bone surfaces is not as pronounced as in trionychid turtles. The internal surfaces of all bones are very smooth, and no foramina were observed to insert the internal bone surfaces. The marginal sutures of the shell elements were further composed of rather short and uniform bony interdigitating round pegs or flat bone sheets.

4.3.24 Trionychidae (Plastomeninae, Cyclanorbinae and Trionychinae)

Confirmed Trionychidae first occur in the Lower Cretaceous of North America and Asia (Meylan and Gaffney, 1992; Nessov, 1995; Hirayama et al., 2000; Danilov, 2005). Trionychidae can be subdivided into three taxa, the Cyclanorbinae, the Trionychinae and the exclusively fossil Plastomeninae (e.g., Meylan, 1987). The morphology-based monophyly of both Cyclanorbinae and Trionychinae (e.g., Meylan, 1987; Gaffney and Meylan, 1988) was supported by recent molecular study (Engstrom et al., 2004). The value of trionychid carapacial features for taxonomic and phylogenetic analyses is discussed in Gardner and

Russell (1994) and Gardner et al. (1995). In this respect, the ornamentation pattern of trionychid shells has to be treated with caution.

The Plastomeninae are restricted to the Upper Cretaceous and Palaeocene of North America, but there may be additional 'plastomenine' turtles from Kazakhstan (Chkhikvadze, 1990, in Danilov, 2005; Holroyd and Hutchison, 2002; Hutchison and Holroyd, 2003). The group has a well ossified plastron and the central fontanella of the plastron is small or even absent (see Holroyd and Hutchison, 2002; Hutchison and Holroyd, 2003). *Helopanoplia* Hay, 1908, that died out at the K/T boundary, shows plastomenine affinities in the development of a distinctive "punctate sculpture on the plastron" (Holroyd and Hutchison, 2002:184).

In the fossil record, Cyclanorbinae are known from the Miocene of Saudi Arabia and the Pliocene of Africa and India (Danilov, 2005). Among other characteristics, representatives of the group have a massively ossified shell and fused hyo- and hypoplastra (e.g., Meylan, 1984, 1987; Gaffney and Meylan, 1988; Danilov, 2005). As pointed out by Meylan (1987), the group includes three recent genera with the following species: *Cyclanorbis elegans* (Gray, 1869), *C. senegalensis* (Duméril and Bibron, 1835); *Cycloderma aubryi* (Duméril, 1856), *C. frenatum* Peters, 1854; *Lissemys punctata* (Bonnaterre, 1789), *L. scutata* (Peters, 1868). While Ernst and Barbour (1989) list only five species in three genera, Joyce et al. (2004) recognise *L. scutata* (Peters, 1868) as a valid species instead of sub-species. There is general agreement, that *Lissemys* spp. are today the most basal representatives of the Trionychidae. Furthermore, *Lissemys* spp. still retain small bone elements in the periphery of the soft dermal part of the shell. Even though the V-shaped bone elements strongly resemble peripherals of hard-shelled turtle genera, there is still discussion if they are truly homologous structures (see Meylan 1987). Based on the V-shape and diploe-structure of the peripheral bones of *Lissemys punctata* in cross-section, Meylan (1987) argued for the homology of the elements with peripherals of other turtle taxa.

Trionychinae comprises all soft-shelled turtles whose plastral bones are not firmly fused together but are loosely bonded by connective dermal tissue (e.g., Meylan, 1987; Gaffney and Meylan, 1988). Based on Meylan (1984), the Trionychinae is supposedly monophyletic. *Sensu* Joyce et al. (2004), the group includes eleven recent genera, of which the two species *Apalone ferox* (Schneider, 1783) and *Trionyx triunguis* (Forskål, 1775) were sampled. In the fossil record, trionychine turtles are known from the Lower Cretaceous of North America

(Meylan and Gaffney, 1992; Nessov, 1995, in Danilov, 2005). Trionychid taxa from the Upper Cretaceous of North America were revised by Gardner et al. (1995). In this study, three taxa of *Aspideretoides* (*A. foveatus* (Leidy, 1856c), *A. splendidus* (Hay, 1908) and *A. alleni* (Gilmore, 1923)) and one taxon of *Apalone* (*A. latus* (Gilmore, 1919) were recognised as valid species. If these four taxa are indeed crown trionychids as proposed by Gardner et al. (1995), this would expand the age of the crown clade into the Late Cretaceous (Joyce et al., 2004). A fifth taxon (Trionychidae gen. et sp. indet.) was further recognised by Gardner et al. (1995) based on the characteristic fusion of hyo- and hypoplastron (see also Brinkman, 2003a).

The carapace of *Apalone ferox* (Schneider, 1783) has a reduced pair of costals8. In the plastron, only four callosities appear: two on the fused hyo-hypoplastra; and two on the xiphiplastra (see also Meylan, 1987).

4.3.24.1 *Plastomenus* sp.

The sample of *Plastomenus* sp. includes a neural (UCMP V81108/150227), a proximal part of a costal (UCMP V81108/150227), a distal part of a costal (UCMP V81110/150231), two other costal fragments (UCMP V81108/150227; UCMP V81110/150231) and a plastron fragment (UCMP V81108/150227). All specimens were recovered from the Eocene Bridger Formation, Sweetwater County, Wyoming, USA. The external surfaces of the shell elements show an even sculpture with low ridges and fine pits (see also Hay, 1907). The ornamentation changes in appearance towards the margins. Here, the low ridges are aligned in a parallel fashion and extend perpendicular towards the margins. Where the preservation is adequate, the internal surfaces of the specimens appeared generally smooth.

4.3.24.2 Helopanoplia sp.

Only a single specimen, a costal (UCMP V87051/150193) of this taxon was sampled. The specimen was found in the Puercan (Uppermost Cretaceous?), Hell Creek Formation, McCone County, Montana, USA. Only a single margin of the fragment shows the original

suture, the other margins of the fragment are broken off. The external surface of the bone shows a raised 'punctate' sculpturing pattern of low tubercles and short meandering ridges. The smooth internal surface of the bone fragment is medially elevated where the rib progresses through the costal plate. Few scattered tiny foramina insert into the internal surface of the bone. The bone itself has a high mass, because inner spaces of the bone are filled with pyrite.

4.3.24.3 *Lissemys punctata* (Bonnaterre, 1789)

L. punctata occurs in India and adjacent countries (e.g., Pakistan, Nepal, Bangladesh, Sri Lanka) where it dwells in shallow and quiet riverine, lake and pond habitats (Ernst and Barbour, 1989). Two specimens were sampled for the study. The sampling of SMNS 3705, a small alcohol-preserved specimen, was carried out by core-drilling. One core (12 mm in diameter) was removed from the carapace, sub-sampling ?neural3, together with its skin cover and vertebra. The sampling of YPM 11645, a larger macerated specimen, included whole shell elements, a neural, a costal3, a plastral fragment (?hyo- or hypoplastron) and a 'peripheral' element. All shell elements showed the typical external pustulate ornamentation with ridges, pits and knobs (see Meylan, 1987).

4.3.24.4 *Cyclanorbis senegalensis* (Duméril and Bibron, 1835)

The Central African *C. senegalensis* occurs in Sudan, Cameroon, Gabon, Senegal and Ghana (e.g., Ernst and Barbour, 1989). A single costal of *C. senegalensis* (ZFMK-83284) was sampled. The specimen derives from a dried carapace where the skin was still attached to the bony carapacial disc. The prominent sculpturing pattern is easily traceable through the overlying skin cover in this specimen. The rib extends proximodistally through the whole costal, while the rib head protrudes significantly from the internal surface of the costal.

4.3.24.5 *Aspideretoides foveatus* (Leidy, 1856c)

Only a single neural (TMP 81.20.30) of *A. foveatus* was sampled. The specimen (part of larger associated sample of neurals) was recovered either from the ?Oldman Formation or the Dinosaur Park Formation, Judith River Group, Dinosaur Provincial Park, Alberta, Canada. The neural has a hexagonal shape. Due to weathering, the typical sculpturing pattern is seen only in the centre of the external bone surface while the margins are almost smooth. The element has maximum length of 22 mm. Its plate thickness spans about 4 mm.

4.3.24.6 *Aspideretoides splendidus* (Hay, 1908)

The fossils of *A. splendidus*, a fairly large trionychid species, were found either in the ?Oldman Formation or the Dinosaur Park Formation, Judith River Group, Onefour Area, SE Alberta, Canada. The sample (TMP 89.116.61) included a fragmentary neural, the distal parts of two sutured costals, a small plastron fragment and the distal tip (bony peg) of a plastron element. The neural is a fairly high, reaching a maximum thickness of about 10 mm for the flat plate part. Internal to the plate part, the massive neural arch spans another 11 mm. The anteroposterior length of the neural fragment is 35 mm. The distal margin is preserved in the well sutured costal fragments. The margin itself is sloped, thus first the external ornamentation disappears, followed by a zone of unornamented external bone surface, followed by a broad margin of vascularised, spongy bone. The internal surface of the costal fragments shows a light proximodistal striation. The thickness of the costals spans about 14 to 16 mm (measured at the ornamented part of the costals). The small plastron fragment mostly consists of the external sculptured bone surface and a round margin that lacks a suture. The piece has a maximum thickness of 13 mm. The peg-like distal tip of the plastron fragment is oval in cross-section with numerous circumferential grooves covering the bone surface. The peg-like fragment was a about 18 to 20 mm long, while its maximum diameter was measured to be 9 and 14 mm for its axes respectively.

4.3.24.7 cf. *Aspideretoides* sp.

The sample of cf. *Aspideretoides* sp. included a neural (IPB R533d) and two costal fragments (IPB R533a-c, IPB R533e). IPB R533a and IPB R533b are figured in Scheyer et al. (2007, figs. 3, 4). All shell bones were found in the Late Cretaceous Judith River Group, Kennedy Coulee, North of Goldstone, Montana, USA. The neural has a hexagonal shape. The plate part of the neural is 5 mm thick. The length of the neural is 23 mm. The margins of the costal fragments were mostly broken off, thus length and width could not be measured. Thicknesses ranged between 7 and 8 mm for the costal plates. All external surfaces of the shell bones are typically sculptured with grooves and ridges. A faint striation pattern was locally spotted at the broken margins of the costals directly internal to the extensive external sculpturing pattern.

4.3.24.8 *Apalone ferox* (Schneider, 1783)

A. ferox occurs today in freshwater bodies of Florida and parts of adjacent states (South Carolina, Georgia and Alabama) of south-eastern USA (Ernst and Barbour, 1989). An adult macerated specimen (YPM 13874) was sampled. The material for sectioning included the neural5, the left costal5 and the right xiphiplastron. The quadrangular oblong plate of the neural5 is symmetrical with convex anterior and posterior margins. The slender proximal part of the costal5 broadens distally. The distal margin of the costal is convex with a protruding free rib end. The progression of the rib through the costal is clearly observable on the internal bone surface. Foramina insert on the internal surface of the costal plate on both sides of the rib bulge. The xiphiplastron has a kidney-shaped flat plate from which two anterior and two posterior pointed processes protrude. All sampled elements carried the typical sculpture of grooves, pits and ridges on their external bone surfaces. The internal bone surface of the element is smooth.

4.3.24.9 *Trionyx triunguis* (Forskål, 1775)

T. triunguis, a large species (overall carapace length of over 1000 mm), occurs at the coasts of the eastern Mediterranean countries (from Turkey southwards) to East- and West Africa (e.g., Pritchard, 1979; Iverson, 1992; Ernst and Barbour, 1989). It prefers low-currency freshwater bodies but is sometimes also found in brackish waters and occasionally in ocean waters (Ernst and Barbour, 1989). A single right costal2 from a dried juvenile specimen (IPB R260) was sampled. Details of IPB R260 are figured in Scheyer et al. (2007, fig. 2). The shell had an overall carapace length of ca. 200 mm, whereas the bony carapacial disc had a CCL of 147 mm. The costal2 had a proximodistal plate length of 51 mm. The costal plate itself is almost flat. The free rib end protruded another 20 mm over the distal plate margin. The external bone surface is sculptured with ridges and grooves. The internal bone surface is smooth and the progression of the rib is visible as a massive bulge of the internal bone surface. Medially, the free massive rib head meets the articulation facet between two vertebrae and articulates with both. Scattered foramina insert on the internal bone surface on both sides of the rib bulge.

4.3.24.10 *Trionyx* sp.

Additional material of *Trionyx* sp. included three costal fragments (HLMD-Me 8084; IPB HaH-3120; IPB HaH-3164) and a plastron fragment (SMNS 86264). HLMD-Me 8084, the distal part of a costal, derives from the Eocene Messel pit, near Darmstadt, Germany. A gentle rib bulge is seen on the internal bone surface of this element, but the free rib end is broken off. IPB HaH-3120 and IPB HaH-3164 were recovered from the middle Miocene lignite strip mining pit of the company ‘Rheinbraun AG’ at Hambach, Germany (see also Klein and Mörs, 2003). The costal fragments from Hambach are of similar thickness (7 to 9 mm) but lack distinctive morphological features besides the sculpture. One sutured original margin is present in IPB HaH-3164. SMNS 86264 was found during road building work in the Lower Miocene (MN4b), Langenau 2, (development of highway A2; “Einschnitt Lettenberg”), Germany. All margins of the plastron fragment are broken off, making an orientation difficult. The element increases in thickness towards one of the broken margins. All external bone surfaces of the shell elements show the typical sculpture pattern of grooves, pits and ridges.

5. Bone histological results of outgroup taxa

To quickly assess the nature of the sampled bones, fossil outgroup taxa are marked by a cross in parentheses (†) behind the names in the respective headings. Descriptions of the abbreviations used in the text and figures are compiled in Appendix 2.

5.1 Outgroup 1: Temnospondyl amphibians

5.1.1 *Trimerorachis* sp. (†)

The two samples of *Trimerorhachis* sp. show a diploe with distinct external cortex, cancellous bone and internal cortex (Fig. 8a, b). The external and internal cortices that frame the interior cancellous bone are of similar thickness and are similarly well vascularised (Fig. 8c). The primary osteons and secondary osteons share a similar orientation in the bone.

External cortex—The external cortex consists of parallel-fibred bone with a scattered arrangement of primary osteons, primary vascular canals and few secondary osteons (Fig. 8c). Growth of the parallel-fibred bone is following the wavy ornamentation pattern consisting of ridges and troughs, but distinctive cyclical growth marks are not observable. Fibre bundles that are extending diagonally to the external bone surface in the parallel-fibred bone are dominating the bone tissue. Few fibre bundles insert perpendicular to the bone surface. These fibre bundles are best seen in the areas internal to the ridges of the ornamentation pattern.

Cancellous bone—The trabecular bone of the cancellous bone appears stout, and the vascularisation is characterised by few larger cavities (Fig. 8a-c). Interstitial primary bone tissue that consists of interwoven structural collagenous fibre bundles (ISF) and scattered primary osteons are still found within the centres of larger trabeculae, while the trabecular walls are lined with secondary lamellar bone. Towards external and internal, newly formed erosion cavities lack a complete lamellar bone lining and instead show irregular erosion fronts.

Internal cortex—Towards internal, the ISF of the cancellous bone is grading into parallel-fibred bone of the internal cortex proper (Fig. 8d, e). The nature of the parallel-fibred bone is

best studied in longitudinal sections cut parallel to the ridges of the ornamentation and the long axis of the bone elements. Vascularisation occurs mostly through primary vascular canals that resemble elongated tubes in longitudinal sections and few scattered secondary osteons.

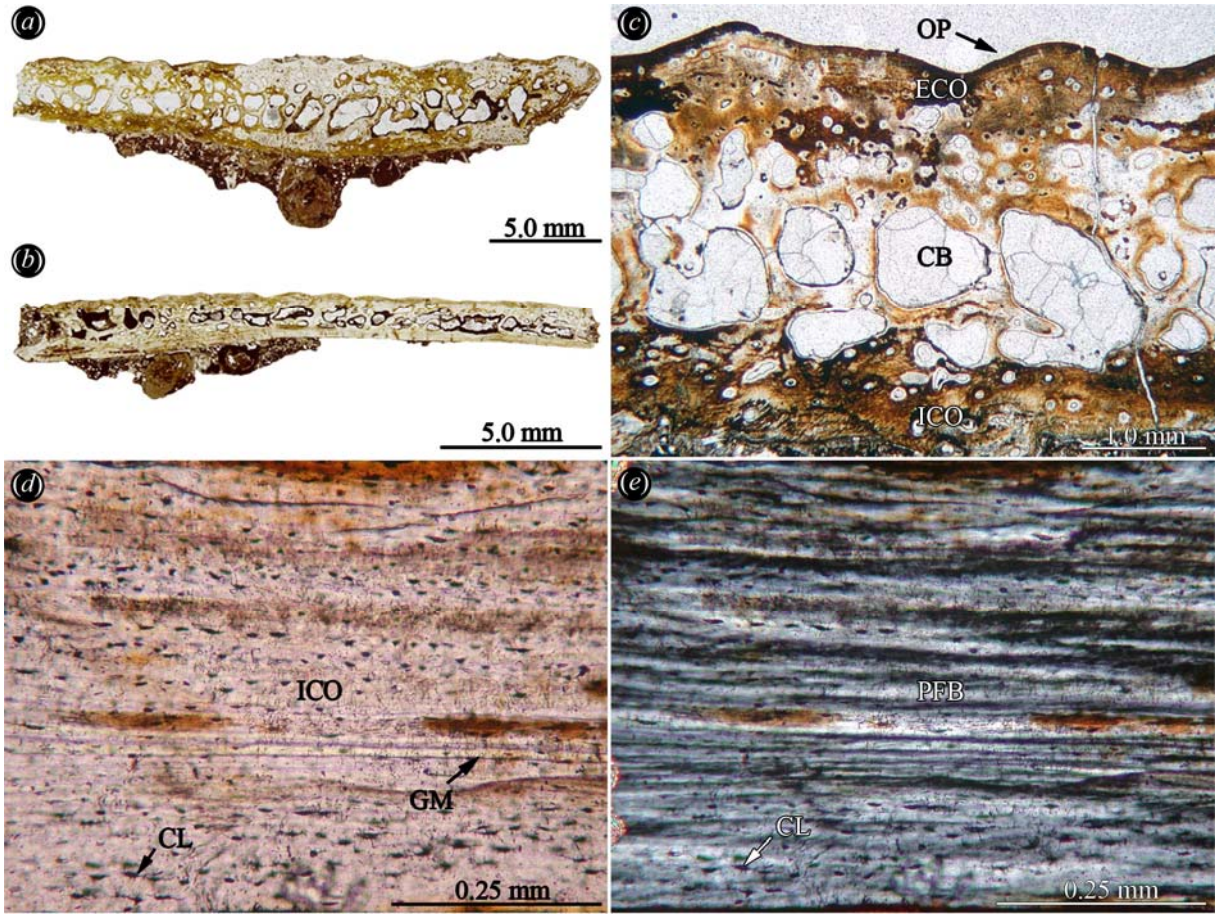

Figure 8: Bone histology of dermal bones of *Trimerorhachis* sp. (*a*) specimen TMM 40031-59 and (*b*) specimen TMM 40031-60 in normal light. (*c*) Close-up of specimen TMM 40031-60 that shows the diploe structure of the sculptured bone. Detail of the parallel-fibred bone of the internal cortex of TMM 40031-60 in (*d*) normal light and (*e*) polarised light.

5.1.2 *Mastodonsaurus giganteus* (Jaeger, 1828) (†)

Macroscopically, the heavily sculptured bone elements of *M. giganteus* appear quite massive (Fig. 9a, b). The microstructure of the sampled bone, however, reveals a diploe with clear distinction between external cortex, internal cortex and interior cancellous bone. The cortices share a similar thickness.

External cortex—The most external layers of the external cortex consist of parallel-fibred bone that towards internal changes to primary ISF (Fig. 9c, d). Weakly developed growth marks are present in the parallel-fibred bone, though their course through the external cortex is difficult to follow. The external cortex is vascularised by primary osteons and primary vascular canals. The primary vascular canals locally reach plexiform organisation. Especially in the troughs between the ornamental ridges, the primary osteons usually follow the progression of the layers of the parallel-fibred bone. In the centre of each ridge, the fibre bundles of the parallel-fibred bone cross each other at moderate angles. At the areas of overlap, Sharpey's fibres, i.e. conspicuously angled connective fibre bundles, insert perpendicular into the bone tissue of the external cortex. Sharpey's fibres are restricted to the ridges of the ornamentation pattern, while they are absent in the troughs in between the ridges.

Cancellous bone—The external front of the cancellous bone is slightly wavy because it parallels the progression of the troughs and ridges of the ornamentation pattern. The cancellous bone consists of primary ISF with numerous vascular cavities of small to medium size. The bone trabeculae that extend parallel to the external and internal bone surfaces are more prominent. However, extensive remodelling affects the whole of the cancellous bone, leading to the formation of larger secondary erosion cavities and numerous secondary osteons. In some of the larger bone trabeculae, the secondary osteons form clusters of Haversian bone (Fig. 9e, f). Interstitial primary ISF and primary osteons are also present within the larger trabeculae, while the walls of the trabeculae usually consist of lamellar bone. The bone elements show sutured margins with short interdigitating bony pegs. Towards the centre of the cancellous bone, remnants of the former growth stages of the bony pegs are observed, although these sutural pegs are subject to increased remodelling.

Internal cortex—The internal cortex (Fig. 9g) consists of parallel-fibred bone in which only the internal-most layers (deposited last) are avascular. Subsequent vascularisation of the bone tissue begins at the transition to the interior cancellous bone. Smaller scattered vascular cavities fuse through further erosion to form larger vascular cavities. Some of the resulting elongated and flat erosion cavities are still without secondary lining with lamellar bone. Some layers of the parallel-fibred bone are not parallel but slightly angled towards the bone surface, thus gradually thinning out along the surface of the bone.

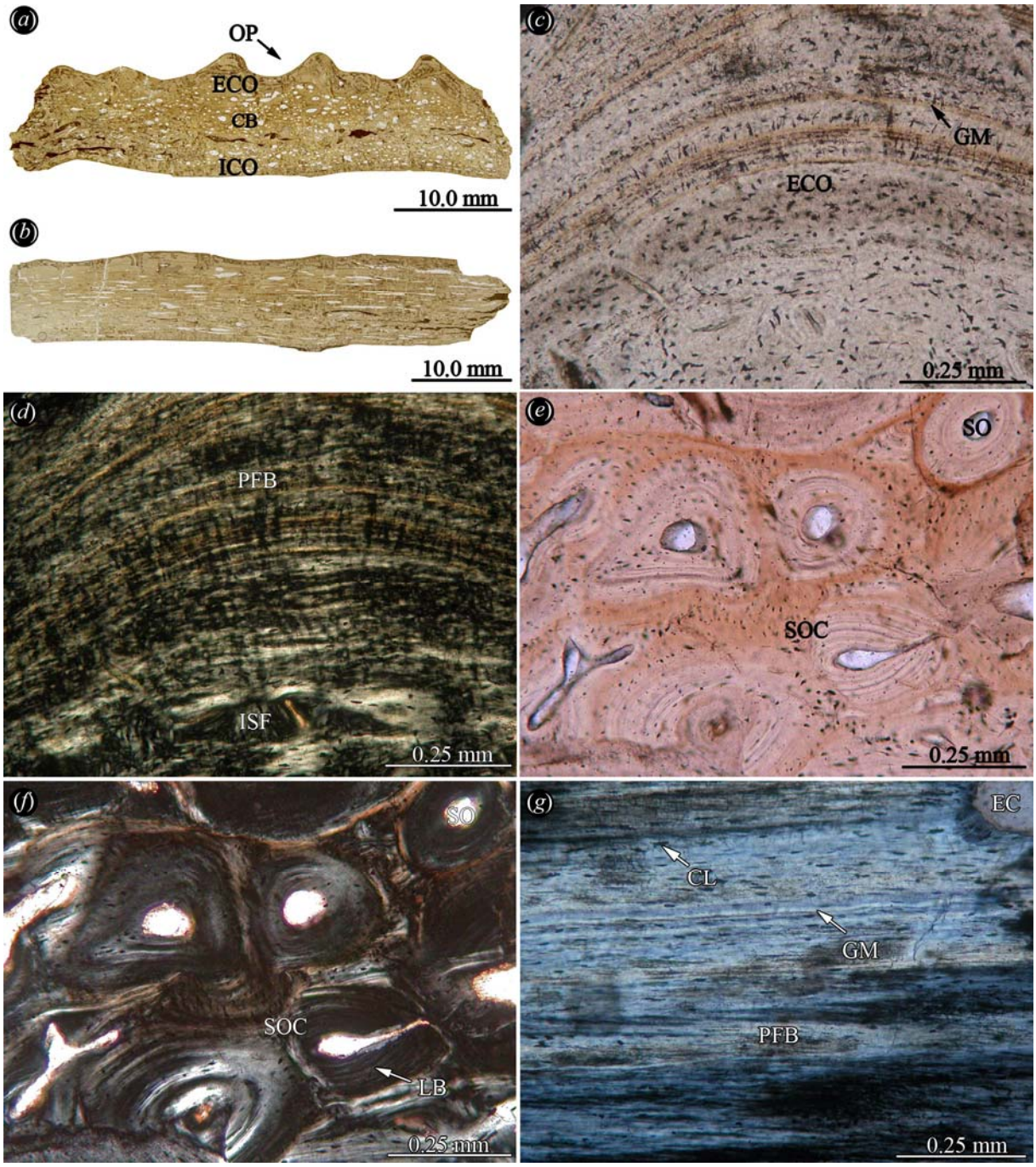

Figure 9: Bone histology of dermal bone of *Mastodonsaurus giganteus*. Specimen SMNS 91011 sectioned (*a*) perpendicular and (*b*) parallel to the ornamental ridges in normal light. Close-up of the parallel-fibred bone of the external cortex and ornamentation of SMNS 91011 (perpendicular section) in (*c*) normal and (*d*) polarised light. Detail of extensive secondary osteon clusters forming Haversian bone of the interior cancellous bone of the same specimen (perpendicular section) in (*e*) normal and (*f*) polarised light. (*g*) Close-up of the internal cortex of the same specimen (perpendicular section) in polarised light.

5.1.3 *Gerrothorax pustuloglomeratus* (Huene, 1922) (†)

The specimen of *G. pustuloglomeratus* shows a diploe with distinct external cortex, internal cortex and interior cancellous bone (Fig. 10a, b). The external and internal cortices are of similar thickness.

External cortex—The eponymous ornamentation pattern consisting of fine isolated pustules and short ridges has a slightly wavy appearance in cross-section (Fig. 10c). The ornamentation pattern constitutes parallel-fibred bone best observed in the intermediate shallow troughs with fibre bundles overlapping at moderate angles in the pustules and ridges. Internal to the ornamentation pattern, a second compact layer of parallel-fibred bone is situated. The transition between ornamentation pattern and this second layer of parallel-fibred bone that extends horizontally is rather distinct (Fig. 10c). The parallel-fibred bone of the internal layer does not reach into the ridges or pustules of the ornamentation pattern. The ornamentation pattern is mainly vascularised by isolated and anastomosing primary vascular canals that mainly extend perpendicular into the ornamentation pattern of the external cortex. The internal, horizontal layer of parallel-fibred bone does exhibit large erosion cavities and scattered secondary osteons.

Cancellous bone—The cancellous bone consists of strongly vascularised primary ISF. The resulting bone trabeculae are slender and gracile. The trabeculae that extend internal-externally are short, while the horizontally arranged trabeculae that extend towards the margins of the bone are elongated. Accordingly, the vascular spaces between the bone trabeculae are flattened and elongated. Growth marks are visible in the tissue of the cancellous bone as less vascularised sheets of bone between thicker zones of well vascularised tissue (Fig. 10d). The bone trabeculae have a lining of secondary lamellar bone.

Internal cortex—The internal cortex consists of parallel-fibred bone (Fig. 10e). The majority of the parallel-fibred bone is well vascularised with scattered primary osteons, secondary osteons and larger erosion cavities. Interstratified layers of bone, which are less vascular or avascular, appear also within the internal cortex. While the orientation of the primary osteons and secondary osteons follows the organisation of the bone, the erosion cavities also cross the boundaries of the layers in the parallel-fibred bone and fuse to form

larger vascular spaces. The degree of vascularisation is higher than in the vascularisation of the external cortex.

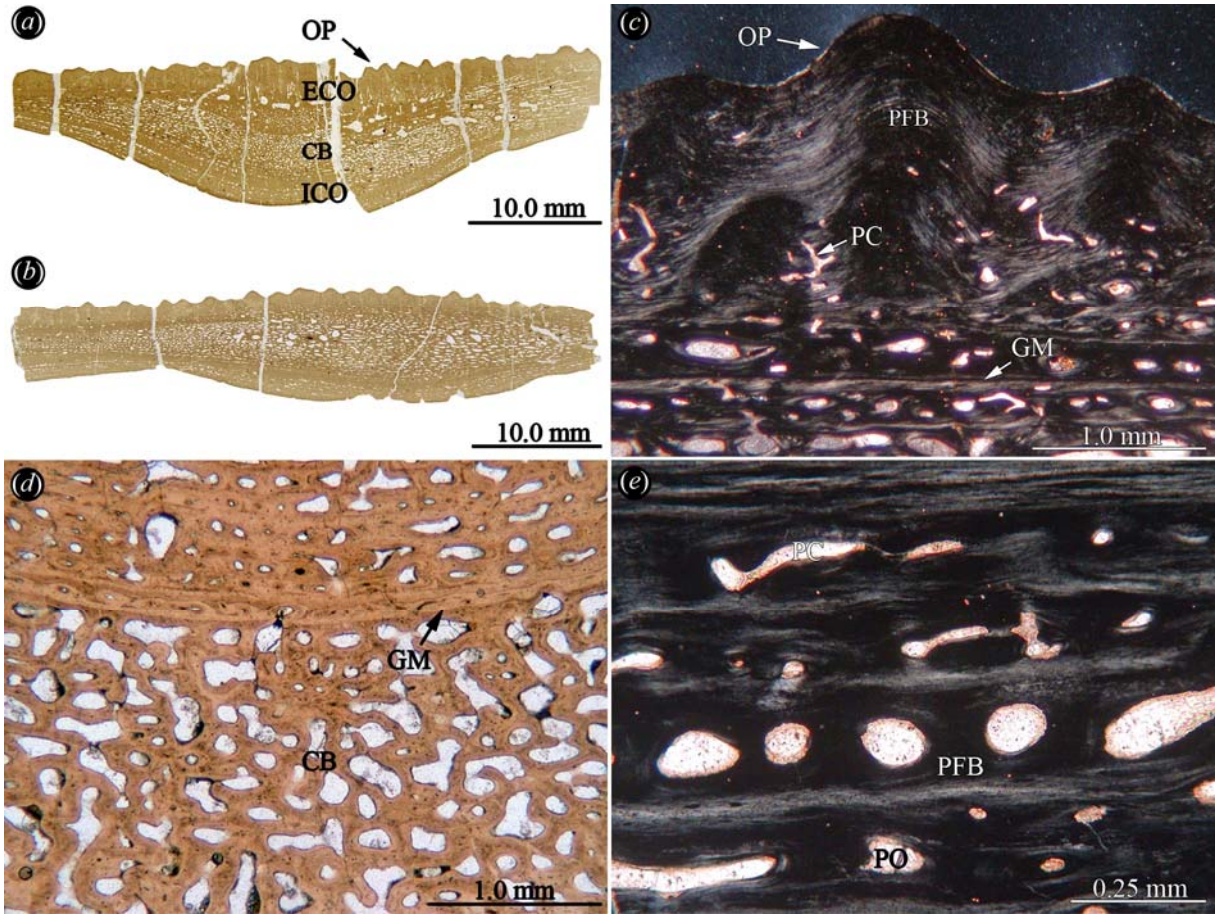

Figure 10: Bone histology of dermal bone of *Gerrothorax pustuloglomeratus*. Specimen SMNS 91012 sectioned (*a*) perpendicular and (*b*) parallel to the long axis of the element in normal light. (*c*) Close-up of the parallel-fibred bone and growth marks of the external cortex and ornamentation of SMNS 91012 (parallel section) in polarised light. (*d*) Detail of interior cancellous bone and growth mark of the same specimen (perpendicular section) in normal light. (*e*) Close-up of the highly vascular internal cortex of the same specimen (parallel section) in polarised light.

5.2 Outgroup 2: Mammalia

5.2.1 Folivora (Xenarthra)

The osteoderm bone histology of xenarthrans (Mammalia) was recently studied by Wolf (2006, unpubl. MSc-thesis). According to his work, xenarthran osteoderms are diverse not only in gross morphology but also in their bone histology. The following paragraphs comprise only a small excerpt of the studied taxa and a synopsis of their respective bone microstructures. For a detailed comparative description please refer to the original work.

5.2.1.1 Osteoderms of *Paramylodon harlani* (Owen, 1840) (†)

The bones generally consist of primary compact bone, well vascularised by primary canals and primary osteons. Vascular canals often extend radially and emerge as foramina on the bone surface. Bone remodelling (e.g., erosion cavities and secondary osteons) can occur in the centre of the osteoderm and occasionally, a small area of interior cancellous bone is developed. The compact bone is dominated by long, coarse interwoven fibre bundles, and sometimes growth marks are observable. The overall organisation of the fibre bundles is random, although in some cases, the fibre bundles extend radially or perpendicular to the osteoderm surface. In some samples, the centre is not remodelled or cancellous but consists also of fibre bundles. The fibre bundles are usually shorter and more densely arranged here.

5.2.2 Cingulata (Xenarthra)

With few exceptions, the glyptodont osteoderms can be assigned to either one of two types. Type I is here represented by *Propalaehoplophorus* sp. and type II by *Glyptodon clavipes*. Osteoderms of type II generally show a higher degree of secondary remodelling, thus most parts of the bone tissue is cancellous.

5.2.2.1 Osteoderm type I - *Propalaehoplophorus* sp. (†)

External cortex—The external cortex consists of parallel-fibred bone (pers. obs.) or lamellar bone tissue. Additionally, fibre bundles that extend perpendicular to the external surface of the bone, are incorporated into the bone tissue. Growth marks and Sharpey's fibres are observable. The transition between external cortex and interior cancellous bone is gradual. Patches of Haversian bone can be developed and towards internal, the compact bone is increasingly remodelled.

Cancellous bone—The interior part of the cancellous bone is well developed and largely secondarily remodelled. It consists of long and slender trabeculae and large vascular spaces. The bone trabeculae generally consist of secondary lamellar bone. The cavities in the cancellous bone are of circular to irregular shape where the vascular spaces interconnect with each other.

Internal cortex—Although variable in thickness, the internal cortex consists of distinctive ISF. The arrangement of the fibre bundles is usually sub-parallel to the internal surface of the bone or slightly radial towards the osteoderm margins. Vascularisation is moderate with scattered round to irregularly anastomosing primary vascular canals, usually ending in foramina in the internal bone surface. At the transition to the interior cancellous bone, scattered secondary osteons are present.

Sutures—In contrast to type II osteoderms, the bone tissue observed at the sutured margins of the osteoderms is largely similar to the tissue of the internal cortex. However, towards internal, the primary bone of the marginal regions is often completely remodelled into secondary cancellous bone.

5.2.2.2 Osteoderm type II - *Glyptodon clavipes* Owen, 1839 (†)

External cortex—Internal to an almost compact external bone layer, the external cortex is heavily vascularised. The external cortex thus hardly exhibits structural differences to the interior cancellous bone. Anastomosing secondary vascular canals form an extensive meshwork throughout the external cortex. The more compact external bone layer consists of

parallel-fibred (pers. obs.) to lamellar bone tissue that is often remodelled into secondary osteons. Growth marks, fibre bundles that extend perpendicular to the external surface of the bone and short Sharpey's fibres are observed in the external cortex.

Cancellous bone—At the transitional zones to the cortical bone layers, the cancellous bone is mainly comprised of secondary osteons and larger erosion cavities, secondarily filled by lamellar bone. Towards the interior part of the cancellous bone consists of long and slender trabeculae and circular to irregularly formed vascular cavities. The trabeculae are largely remodelled and consist of secondary lamellar bone.

Internal cortex—The internal cortex is rather thin or even absent. Where present, the internal cortex consists of thick, coarse and irregularly arranged ISF. The bone tissue is well vascularised with primary vascular canals and primary osteons. Towards external, the cortical tissue is largely replaced by secondary osteons.

Sutures—The sutures are well developed. Towards the margins, primary bone tissue is sometimes observed that largely shares microstructural details with the bone tissue of the external cortical bone.

5.3 Outgroup 3: Reptilia

5.3.1 Parareptilia (Pareiasauria)

5.3.1.1 Pareiasaur osteoderms: *Bradysaurus seeleyi* Haughton and Boonstra, 1929 (†), *Bradysaurus* sp. (†), *Pareiasaurus serridens* Owen, 1876 (†), *Pareiasaurus* sp. (†) and *Anthodon serrarius* Owen, 1876 (†)

While outer shapes differ strongly in pareiasaur osteoderms (Fig. 11a-d), their bone histology is surprisingly homogeneous. The bone microstructure will be presented exemplarily for *A. serrarius* in the following paragraph, and differences to the other taxa will be explicitly stated in the text.

Sampled pareiasaur osteoderms, e.g., of *A. serrarius*, lack well sutured margins and have a flat ventral base and a dorsally convex surface sculptured with radial ridges. A boss is present in osteoderms of *Pareiasaurus* spp. and *A. serrarius* (Fig. 11b-d). External ornamental radial ridges are also known from these taxa. External and internal cortices may be of similar thickness in *A. serrarius* (up to 5 mm or more at margins), although thicknesses of the external cortices can be greatly reduced by extensive vascularisation that can reach up to the external osteoderm surface. The internal cortices are thicker than the external cortices in samples of *Pareiasaurus* spp. and *Bradysaurus* spp. Vascular striation on external bone surfaces is unordered in *Pareiasaurus* spp., ordered and radial in *A. serrarius*. Bone cell lacunae are well developed both in the external cortex and the internal cortex. The external cortex consists of parallel-fibred bone with additional fibre bundles, i.e., presumably Sharpey's fibres, trending perpendicular or at high angles to the dorsal surface (Fig. 11e-g). The marginal compact bone tissue of the osteoderm is indistinct from the external cortex. External cortex vascularisation is quite extensive with small primary osteons, erosion cavities and radially directed primary vascular canals that reach up to the surface of the bone, creating a roughened texture on the bone surface. Towards the interior of the osteoderm, primary vascular canals anastomose frequently, while in the external layers of the external cortex, primary vascular canals are generally single, radial tubes. Few scattered secondary osteons appear towards the cancellous bone. They are absent in the external-most and internal-most layers of the external and internal cortices, respectively. The interior cancellous bone is mostly remodelled (Fig. 11h). Trabeculae are thicker in diameter in flat osteoderms and increase in length and gracility with additional osteoderm height. The internal cortex consists of layers of parallel-fibred bone, but perpendicular extending fibre bundles are absent. Growth marks are usually well developed. In sampled osteoderm SAM-PK-10074, a minimum number of 17 prominent cyclical growth marks are present (see also Fig. 11i, twelve growth marks visible). Coarse Sharpey's fibres insert at moderate to high angles into the compact bone (Fig. 11j). Few scattered primary osteons, primary vascular canals and single larger foramina pervade the internal cortex.

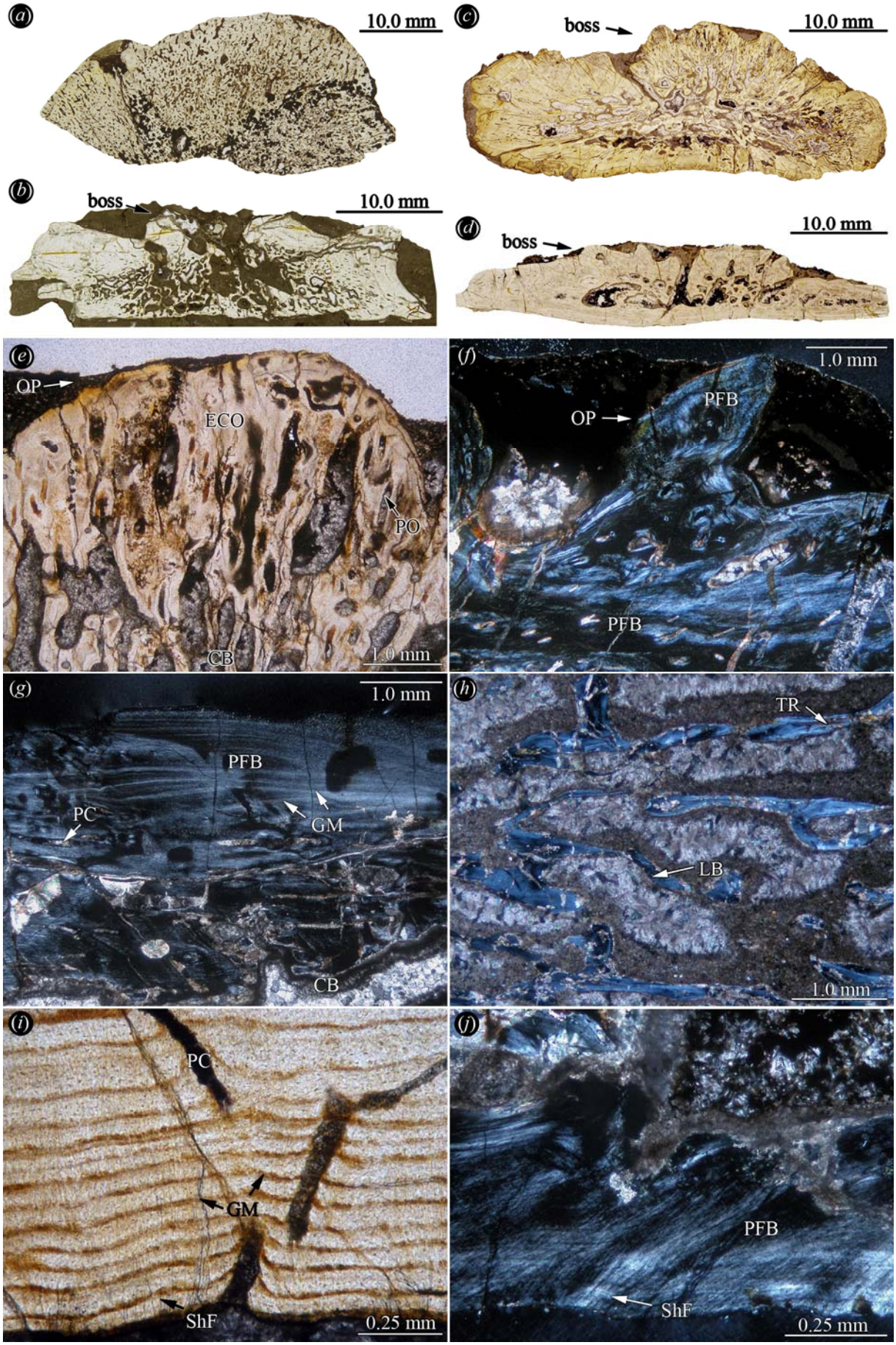
(a)
10.0 mm
(c)
boss
10.0 mm
(b)
boss
10.0 mm
(d)
boss
10.0 mm
(e)
OP
ECO
PO
CB
1.0 mm
(f)
1.0 mm
OP
PFB
PFB
(g)
1.0 mm
PFB
PC
GM
CB
(h)
TR
LB
1.0 mm
(i)
PC
GM
ShF
0.25 mm
(j)
PFB
ShF
0.25 mm

Figure 11: Bone histology of pareiasaur osteoderms. (*a*) Thick osteoderm fragment SAM-PK-12140 of *Bradysaurus* sp., (*b*) small flat osteoderm SAM-PK-1058 of *Pareisasaurus* sp. and (*c*) massive osteoderm and (*d*) flat osteoderm (both SAM-PK-10074) of *Anthodon serrarius* in normal light. (*e*) Close-up of the external cortical bone and radial vascularisation pattern of SAM-PK-10074 (massive osteoderm) in normal light. (*f*) Detail of external cortex and ornamentation of SAM-PK-10074 (flat osteoderm) in polarised light. (*g*) Detail of the parallel-fibred bone and growth marks of the external cortex of SAM-PK-1058 (small flat osteoderm) in polarised light. (*h*) Detail of the cancellous bone of UMZC R 381 T702 of *Pareiasaurus* sp. (*i*) Detail of the internal cortex of SAM-PK-10074 (massive osteoderm) in normal light. Note regular growth marks. (*j*) Detail of the parallel-fibred bone and Sharpey's fibres of the internal cortex of the thick massive osteoderm SAM-PK10036 of *Pareiasaurus serridens* in polarised light.

5.3.2 Eureptilia (Placodontia)

5.3.2.1 Placodontoid armour

5.3.2.1.1 *Placodus gigas* Agassiz, 1833 (†)

The thin-section of the plate shows a differentiation into a compact bone layer surrounding a weakly vascularised interior bone core (Fig. 12a). A true spongy cancellous bone is not developed, thus the core still appears compact. The external areas, including the sharp keel of the plate, consist of well developed external cortical bone. The bone tissues of the interior core and the weakly developed internal cortex of the base of the plate appear superficially similar.

Primary parallel-fibred bone tissue that locally grades into lamellar bone builds up the external cortical bone that covers both sides of the external keel (Fig. 12b). Cyclical growth marks that appear throughout the external cortex extend parallel to the external bone surfaces. The growth marks are mostly diffuse and are thus not as conspicuous as well defined lines of arrested growth. Numerous thin collagenous fibre bundles extend perpendicular to the parallel-fibred bone and lamellar bone of the external cortex. The wavy character of the external bone surfaces in thin-section results from foramina that insert perpendicular into the

external cortex. The foramina continue as vascular canals in the bone tissue of the external cortex. Besides these few vascular canals that seldom anastomose, the primary bone tissue of the external cortex is avascular.

The interior core of the plate is lightly vascularised by scattered primary vascular canals and primary osteons. In general, the primary vascular canals are radially arranged. Because of the absence of larger primary cavities or secondary remodelling (i.e., larger erosion cavities), the interior of the bone has a compact appearance. The interior core is distinct from the similarly compact external and internal cortices in that it lacks parallel-fibred bone and lamellar bone. Instead, it contains a meshwork of randomly arranged structural fibre bundles (Fig. 12c, d). Only a few prominent fibre bundles extend from the margins of the interior bone core in the direction of the apex of the external keel.

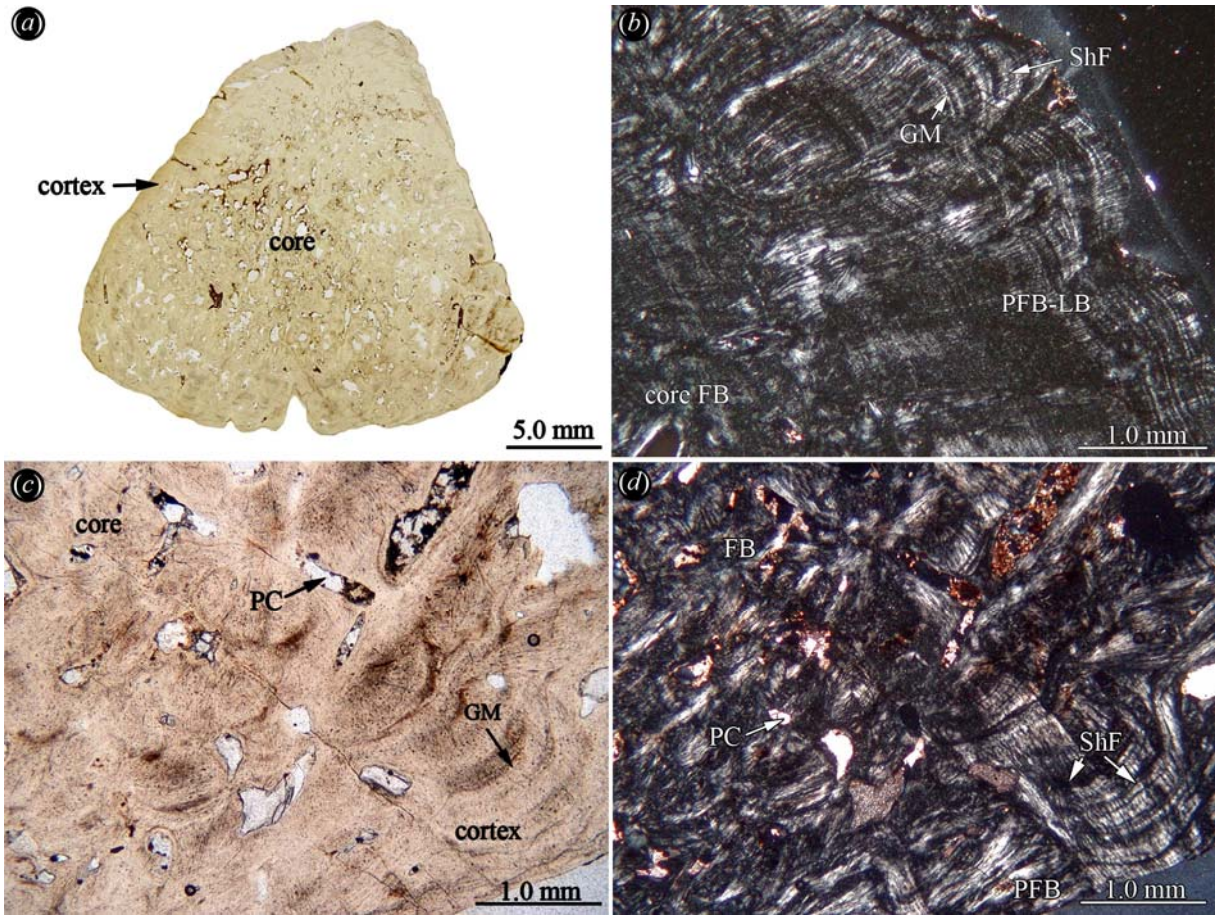

Figure 12: Bone histology of dermal plate of *Placodus gigas*. (*a*) Specimen SMNS 91006 sectioned perpendicular to the keel of the element in normal light. The dorsal tip of the keel is

broken off. (*b*) Close-up of the cortical bone and the interior bone tissue of the flank of the ridge in polarised light. Note Sharpey's fibres inserting into the cortical bone. Close-up of the parallel-fibred bone and growth marks of the cortex and the fibre bundles of the core in (*c*) normal and (*d*) polarised light.

The thin internal cortex at the base and the margins of the plate consists of parallel-fibred bone with growth marks extending subparallel to the internal surface of the bone (Fig. 12d). However, compared to the external cortex, the layers of the parallel-fibred bone are less distinct in the internal cortex, because coarse and thick fibre bundles, i.e., Sharpey's fibres, extend into the parallel-fibred bone. The Sharpey's fibres are responsible for the superficial congruence (an interwoven pattern of fibre bundles) of the interior core and the internal cortex, further obscuring the transition of the two neighbouring bone tissues. The arrangement of the Sharpey's fibres depends on their exact location within the plate. Laterally, on both sides of the external keel, the Sharpey's fibres insert at steep to moderate angles into the internal cortex and generally point towards the medial bone core. The vascularisation of the internal cortex is low, with only a few scattered primary vascular canals that emerge as the foramina seen on the internal bone surface.

5.3.2.2 Cyamodontoid armour

5.3.2.2.1 *Psephosaurus suevicus* (SMNS 91007) (†)

The thin-section of SMNS 91007 reveals a rather homogeneous type of bone tissue throughout the recumbent spike, with only the blunt apex being set off from the rest of the bone (Fig. 13a-c). A distinction into external / internal cortical bone and interior cancellous bone is not recognised. Furthermore, there is almost no secondary remodelling of the primary bone tissue. With the exception of the apex of the plate, the whole bone down to the internal surface of the bone shows parallel growth marks (Fig. 13d). The growth marks are best observed at the margins while they get more diffuse towards the interior centre of the bone. Thirteen cyclical growth marks extend parallel through the spiked plate from the apex to internal surface of the bone. Further sub-cycles are present within some of the thirteen well

developed growth marks, but they are not sufficiently clear to be counted properly. A single large vascular canal extends centrally from the internal bone surface towards the medial area of the apex (not visible in gross morphology because of the sedimentary cover attached to the bone).

The tissue at the very top of the apex does not show any cyclical growth marks but consists of a loose meshwork of a few coarse subparallel bony struts that seldom branch. The almost vertically arranged struts extend from the external surface of the bone towards the first growth mark (Fig. 13b, c). The struts consist of mostly acellular parallel-fibred bone, although few flattened and elongated bone cell lacunae are present. The apical tissue is poorly vascularised by a few primary vascular canals that are associated with and follow the bony struts. A calcified cartilaginous tissue with a distinct fibrous texture completely fills in the spaces between the bony struts. In this tissue, large cells are arranged in diffuse rows. Many of the large cells are completely dark in normal transmitted and polarised light while others appear more translucent. In the majority of the translucent cells, small round black spherical structures are recognised. The calcified cartilaginous tissue in the apex occupies more space than the bony struts.

From the onset of the first growth marks towards the internal bone surface, the bony struts are less coarse and become reduced in thickness and length compared to the apical struts (Fig. 13e, f). Furthermore a differentiation in the arrangement of the struts between the interior bone tissue and the marginal bone tissue becomes obvious. The interior area of the spiked plate is composed of two sets of shorter bony struts being arranged in steep angles to each other and pointing towards the internal bone surface. In the marginal areas, however, the tissue is dominated by somewhat longer, fine bone struts that extend subparallel to the external bone surface. Similarly, the arrangement of the interstitial calcified cartilaginous matrix is less ordered in the medial areas and gets more ordered towards the margins of the plate. Medially, the fibrous calcified cartilaginous tissue forms an almost amorphous mass because of the shifting orientation between the two sets of bony struts. Towards the margins, the cartilage is arranged in rows or stringers parallel to the dominant direction of the bony struts and thus also subparallel to the marginal surface of the bone. The cells in the calcified cartilaginous tissue are of the same type already observed in the apical tissue. Using a lambda compensator in polarised light, fine delineations that are differently coloured due to changes in fibrous arrangement become apparent around the individual cartilage cells. Each of the two

opposite delineations of the cells has similar colourations, thus creating a distinct colour grid within the cartilage tissue. The amount of primary vascular canals and scattered primary osteons increases slightly from the apex towards the internal bone surface, resulting in an overall radial vascularisation pattern that has its focus in the apex of the spiked plate.

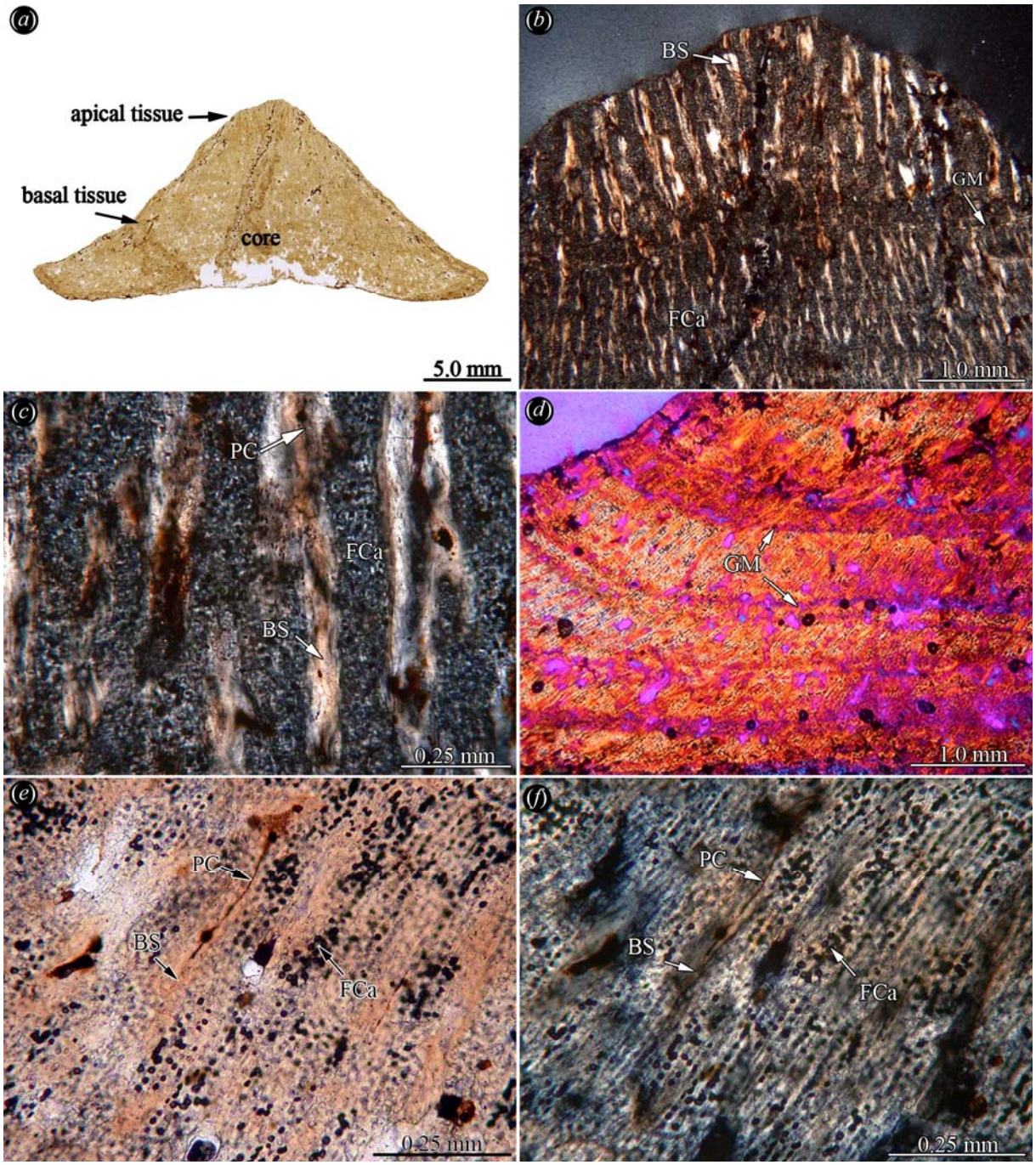

Figure 13: Bone histology of small recumbent spike SMNS 91007 of *Psephosaurus suevicus*. (*a*) Complete thin-section of the specimen in normal light. (*b*) Close-up of the coarse apical calcified cartilaginous bone tissue and the more internal fine calcified cartilaginous bone

tissue of the core of the plate. Note the growth mark separating both tissues. (*c*) Detail of the apical tissue showing the calcified cartilaginous matrix and the vertically arranged bone spiculae in polarised light. (*d*) Margin and interior part of recumbent spike showing several growth marks in polarised light (with lambda compensator). Detail of the fine calcified cartilaginous bone tissue of the core and the margins showing layers of fibrocartilage interspersed with thin bone spiculae in (*d*) normal and (*e*) in polarised light.

5.3.2.2.2 *Psephosaurus* sp. (SMNS 91009) (†)

The thin-section of the rhomboidal plastral plate (SMNS 91009) exhibits three areas of different tissue types: a) parallel-fibred bone with radial vascularisation, b) ordered calcified fibrocartilaginous tissue with spatially ordered bony struts and vascularisation and c) loose calcified fibrocartilaginous tissue with irregular short bony struts (Fig. 14a).

The first tissue type comprises the margins as well as one flank and the apex of the off-centred ridge of the plate, thus representing the majority of the external cortex that rests on the interior core of the plate (Fig. 14b). This tissue is characterised by parallel-fibred bone and cyclical growth marks that parallel the external bone surface. Fibre bundles that extend perpendicular to the external bone surface cross the parallel-fibred bone. Vascularisation of the parallel-fibred bone is achieved by anastomosing, radially arranged primary vascular canals and scattered primary osteons. The radial primary vascular canals extend roughly parallel to the perpendicular fibre bundles. The bone lamellae that directly surround the primary vascular canals often consist of lamellar bone that exhibits a slightly deviating fibre orientation from the interstitial parallel-fibred bone. Areas of secondary bone resorption and secondary osteons are not observed in the tissue.

The second tissue type is found as a broad wedge in between the surrounding first tissue type described above (Fig. 14c). This tissue exhibits a calcified fibrocartilaginous matrix and a distinct radial orientation of bony struts and vascularisation, respectively. The fibrous cartilage cells show a slightly increased spatial organisation in being aligned parallel to the radially arranged primary vascular canals and the associated bony struts. While the struts are shorter and randomly arranged at the transition to the calcified cartilaginous tissue of the core

of the plate, their arrangement in the external cortex increasingly resembles the arrangement described for the first tissue type.

The third tissue type is found in the interior center of the plate, and it extends to the internal surface of the plate, thus forming a low domed core (Fig. 14d). Few isolated large vascular cavities, all surrounded by lamellar bone, occur throughout the plate. The interior domed structure consists of calcified fibrocartilaginous matrix similar to the one described above for the specimen of *P. suevicus*. However, the cartilage cells are arranged to form a loose tissue without a dominant spatial arrangement. Within the calcified cartilaginous matrix, short thin bony struts are randomly arranged. The struts usually do not connect with each other and do not form a trabecular meshwork. Only in the more lateral areas of the core tissue, a few of the struts are more radially aligned. The bony struts are associated with short primary vascular canals and scattered primary osteons. Longer primary vascular canals are not observed in the tissue.

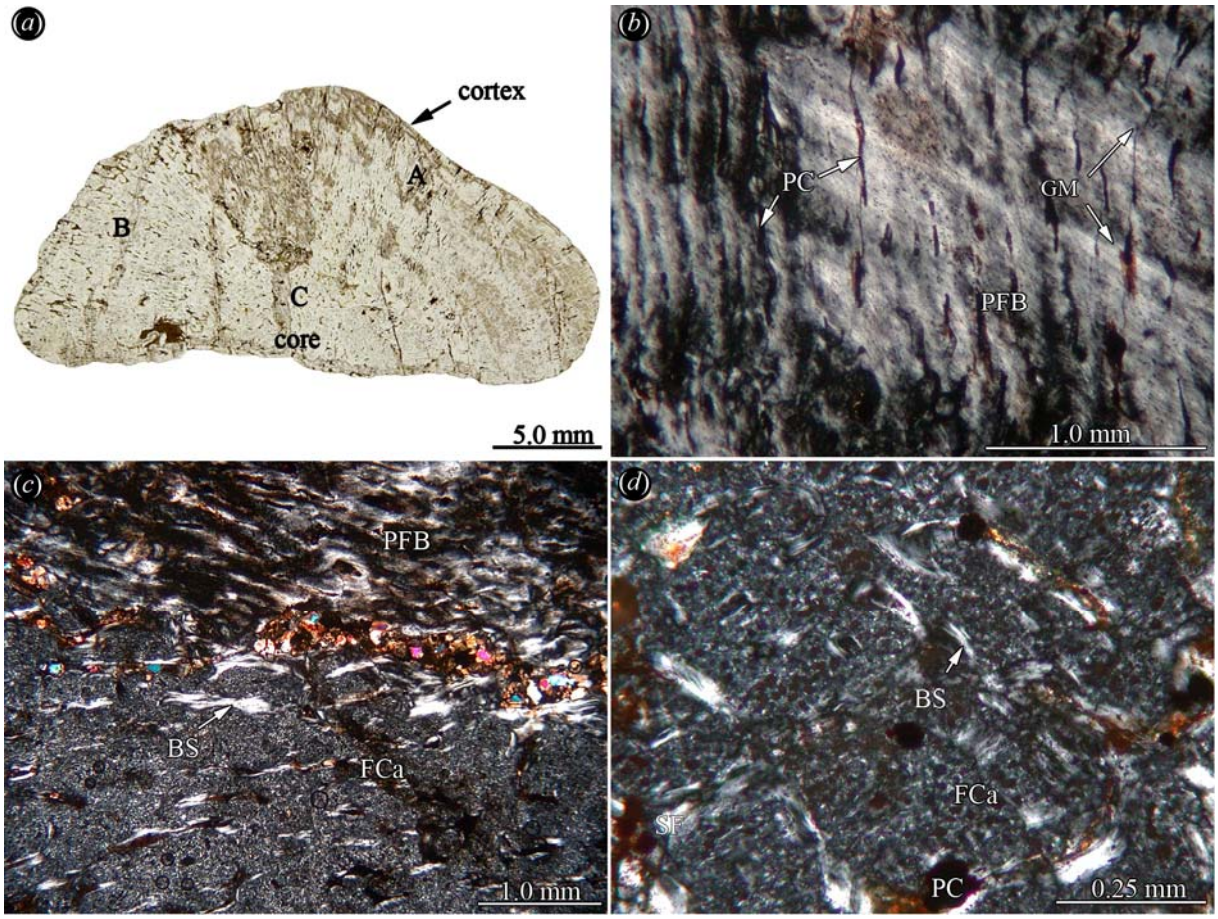

Figure 14: Bone histology of the rhomboidal plastral armour plate SMNS 91009 of

Psephosaurus sp. (*a*) Complete thin-section of the specimen in normal light. (*b*) Close-up of the parallel-fibred bone and radial vascularisation pattern in region A of the external cortex in polarised light. (*c*) Transition between the parallel-fibred bone of region A and the ordered calcified fibrocartilaginous tissue and bone spiculae of region B in polarised light. (*d*) Detail of the calcified fibrocartilaginous tissue and loosely arranged bone spiculae of region C of the core of the plate in polarised light.

5.3.2.2.3 Cf. *Placochelys* sp. (SMNS 91010) (†)

The spiked plate consists of two areas with different tissue types (Fig. 15a). The first is a triangular area that extends from the apex to about one third of the external surface and about half of the length of the internal surface and consists of parallel-fibred bone with three major cyclical growth marks (Fig. 15b). The transition to the second area, that encompasses the rest of the plate to the oval excavated marginal side opposite of the apex, is slightly concave in the thin-section. The growth marks resemble thick, mainly avascular bone layers pervading the parallel-fibred bone. The vascularisation of the parallel-fibred bone, consisting of fine reticular anastomosing primary vascular canals, is thus restricted to the interstitial bone layers. The primary vascular canals that are arranged subparallel to the growth marks dominate the reticular pattern. The growth marks in the parallel-fibred bone parallel the internal surface of the spike in the apical part but deviate slightly towards internal in the median part of the spike, thus extending almost parallel to the transition line to the second tissue type.

The second area, which comprises the rest of the spike, consists of a tissue type that is a mixture of calcified fibrous cartilage and bone. The tissue has a random matrix of large cartilage cells and isolated thin bony struts or trabeculae (Fig. 15c, d). The calcified cartilaginous matrix dominates in volume towards the apex, while the cartilage to bony struts ratio becomes somewhat more even towards the excavated surface opposite the apex. Apically, the struts gain a little in spatial orientation by increasingly extending subparallel to the external and internal bone surface. Towards the excavated surface opposite of the apex, the struts appear in a more random arrangement. The bony struts are associated again with primary vascular canals. Some of the primary vascular canals are still incompletely surrounded by lamellar bone, thus direct transitions between the cartilage matrix and primary vascular canals can occur (Fig. 15 d). The reticular vascularisation pattern of fine

anastomosing primary vascular canals observed in the area of bone tissue near the apex is not encountered in the cartilage tissue. However, the primary vascular canals anastomose and branch more frequently towards the excavated surface opposite of the apical region.

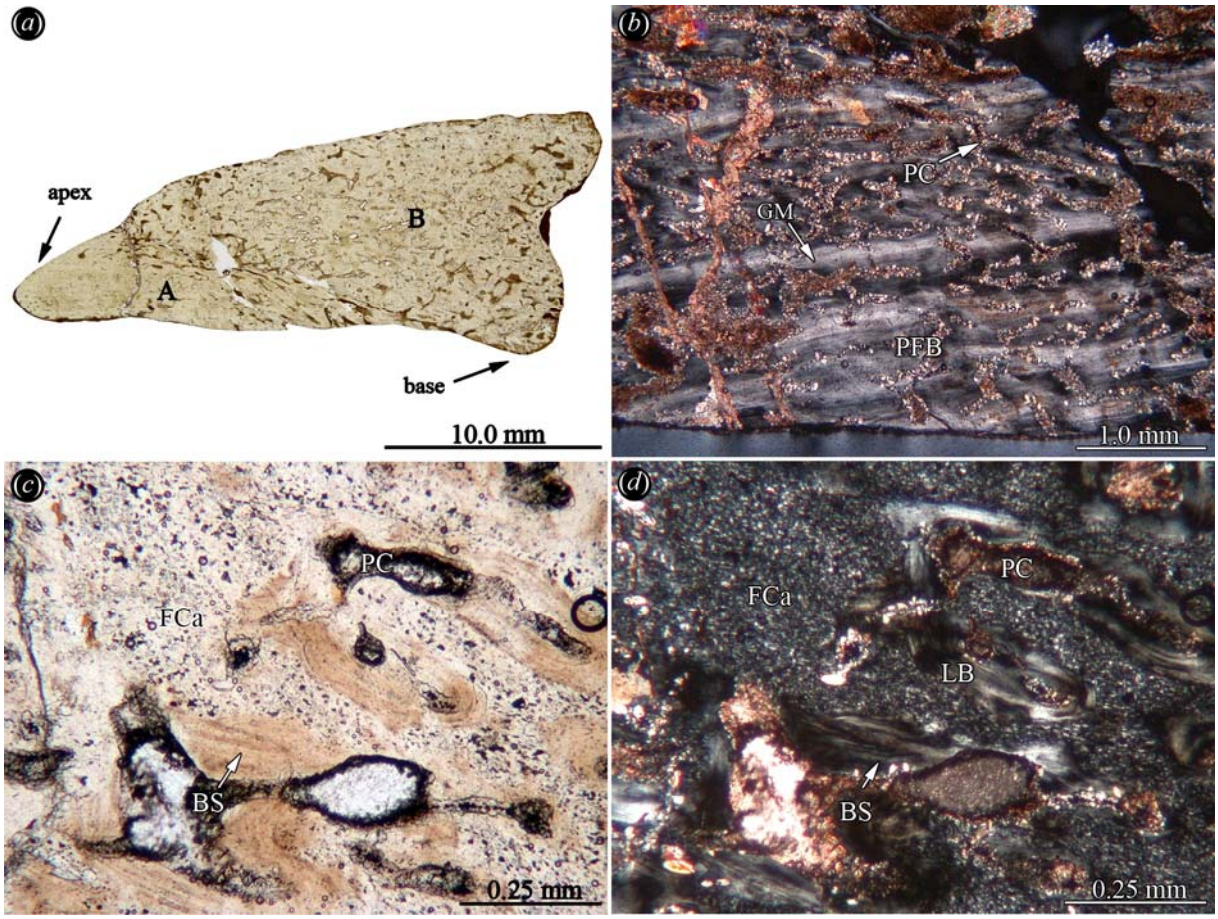

Figure 15: Bone histology of the isolated procumbent spiked plate SMNS 91010 of cf. *Placochelys* sp. (*a*) Complete thin-section of the specimen in normal light. (*b*) Close-up of the parallel-fibred bone and growth marks of the region A in polarised light. Detail of the calcified fibrocartilaginous tissue of region B (near the base of the specimen) in (*c*) normal and (*d*) in polarised light. Note that bone spiculae and the primary vascular canals do not show only a minimum of spatial arrangement here.

5.3.2.2.4 Hexagonal/polygonal armour plates—*Psephoderma* sp. (NRM-PZ R.1759a) (†), *Psephosaurus suevicus* (MHI 1426/1-3) (†) and *Psephosaurus* sp. (SMNS 91008) (†)

The plates of *Psephoderma* sp. (NRM-PZ R.1759a), *Psephosaurus suevicus* (MHI 1426/1-3) and *Psephosaurus* sp. (SMNS 91008) all share bone histological characteristics (Fig. 16a-d), thus they are described in one paragraph. Variation among the taxa is pointed out where appropriate. Although it differs slightly in its outer shape, the procumbent spiked plate of *P. suevicus* (MHI 1426/1) is included here too, because it still retains a roughly hexagonal internal bone surface (Fig. 16d). The hexagonal/polygonal plates consist of external cortical bone, distinct marginal areas, and an internal bone tissue including the central core of the plate and the bone towards the internal surface of the plate. A clear distinction into interior bone and a separate internal cortex is not possible. A well defined cancellous bone, extensive secondary remodelling and calcified fibrous cartilaginous tissue were not encountered in the bony plates.

External cortex and lateral margins—The bone tissue of the external cortical bone and the lateral margins consists of intergradations of parallel-fibred bone and lamellar bone with some weakly developed growth marks (Fig. 16e, f). Where the external surface of the bony plates meets the plate margins, the growth marks of the external cortex deviate towards the internal bone surface and continue parallel to the sutures into the margins of the plate. Shortly after the deviation, however, it becomes increasingly difficult to follow the trend of the growth marks. Thin fibre bundles that are arranged perpendicular or at steep angles to the external bone surface cross the external cortical bone. Towards the margins, the fibre bundles insert more diagonally into the bone tissue and curve slightly towards the interior core of the plate. The vascularisation consists mainly of primary vascular canals and, to a limited extend, scattered primary osteons and small erosion cavities.

Interior core and internal cortex—From the more strongly vascularised core, numerous primary vascular canals radiate outwards towards the surfaces of the bone (Fig. 16a, c, g, h). Those radiating canals that extend towards the external and internal cortical bone dominate the vascularisation pattern. The vascularisation pattern appears as an hour-glass structure of two vascularised conical areas surrounded by less vascularised areas that extend towards the plate margins. The less vascularised marginal areas thus resemble a “ring” around the more vascularised conical areas. The interior core and the internal part of the bony plate consist of a

tissue of randomly arranged fibre bundles. However, fibre bundles that extend from slightly external of the centre of the armour plate (see vascularisation pattern above) towards the external and internal corners of the plate dominate the hourglass-shaped areas that show the strong radial vascularisation. The coarse fibre bundles of the interior core thus generally mirror the arrangement of the primary vascular canals. These coarser fibre bundles normally do not extend into the external cortex and the cortical bone of the margins. Cross-sections through the fibre bundles reveal that the fibre bundles are about 0.35-0.4 mm in diameter and that they are composed of single collagen fibre strands (0.02-0.025 mm in diameter).

Centres of growth—The centre of the radiating vascularisation pattern is not always in the very centre of the plate. Instead, the focus of the radiating pattern is slightly shifted towards the external cortical bone in NRM-PZ R.1759a of *Psephoderma* sp. (Fig. 16a), while it is shifted towards internal in SMNS 91008 of *Psephosaurus sp*. (Fig. 16b). In MHI 1426/1 of *P. suevicus*, the focus is shifted laterally towards the margin internal to the off-center apex of the plate (Fig. 16d). These configurations result in disparate distributions of vascular spaces, in that the conical areas extending towards the external and internal bone surface vary in size. The vascularisation pattern does not change from the interior core towards the internal bone surface, apart from a minor overall reduction in the amount of primary vascular canals.

Sutures—The sutured plate margins comprise numerous sockets and bone pegs of various lengths into which the fibre bundles protrude. The sutural relief is generally low, although occasionally bony pegs interdigitate more strongly with adjacent armour plates (Fig. 16a-d). Fibre bundles are found that extend perpendicular into the sutural bone tissue.

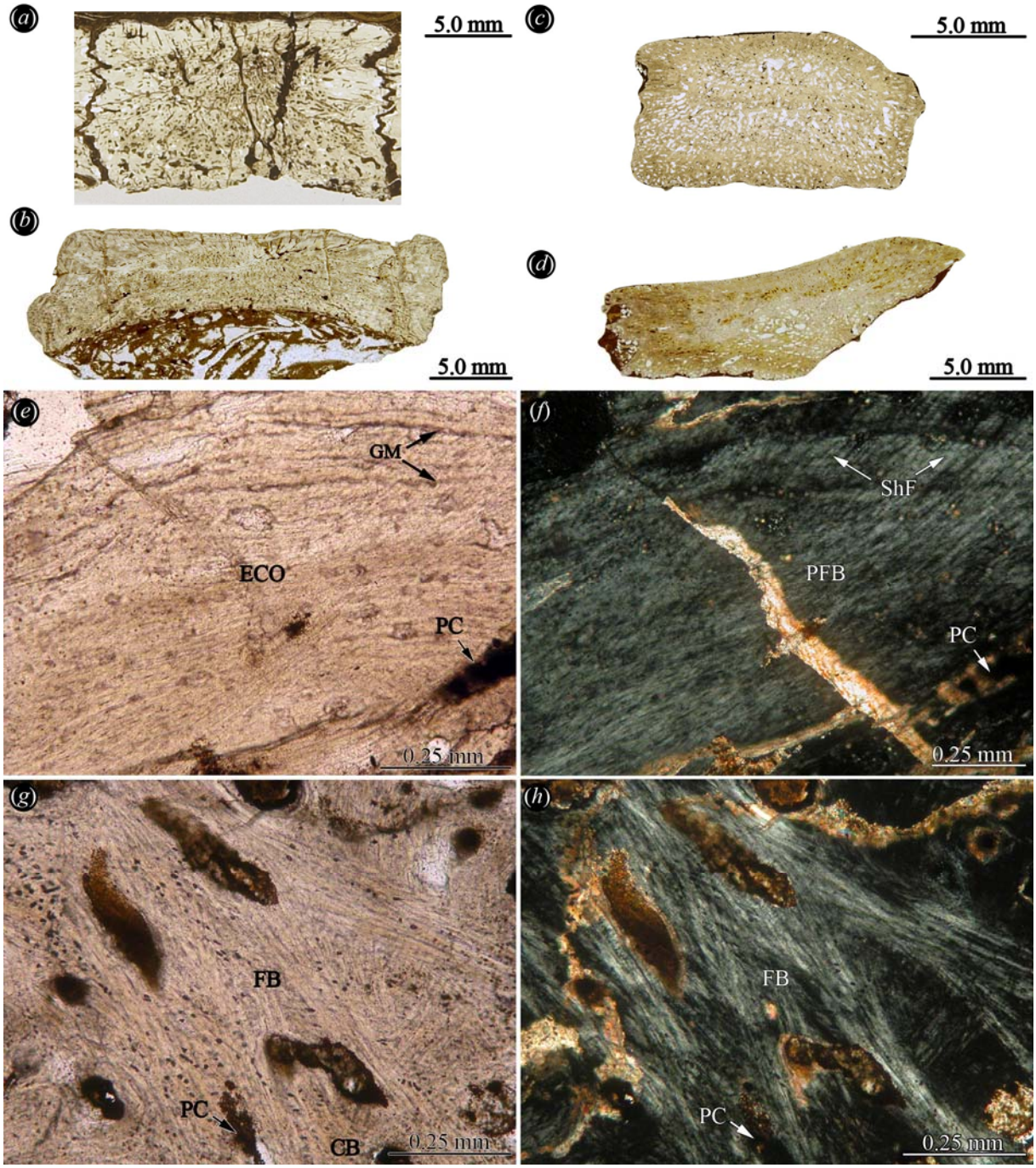

Figure 16: Bone histology of hexagonal/polygonal armour plates of cyamodontoid placodonts. (*a*) Section of sutured polygonal plate NRM-PZ R.1759a of *Psephoderma* sp., (*b*) isolated hexagonal flat plate SMNS 91008 of *Psephosaurus* sp., (*c*) isolated small hexagonal plate MHI 1426/3 and (*d*) procument spiked plate MHI 1426/1 of *Psephosaurus suevicus* in normal light. Close-up of the parallel-fibred bone of the external cortex and Sharpey's fibres of NRM-PZ R.1759a in (*e*) normal and (*f*) polarised light. Detail of fibre bundles and radially arranged primary vascular canals of the interior core of the same specimen in (*g*) normal and (*h*) polarised light.

5.3.3 Eureptilia (Lepidosauria)

5.3.3.1 Literature data on osteoderm bone histology of *Anguis fragilis* and *Tarentola mauritanica*

Description of bone histological data of lepidosaur osteoderms is yet quite rare (e.g., Moss, 1969; Moss, 1972; Zylberberg and Castanet, 1985; Levrat-Calviac and Zylberberg, 1986). The osteoderms are mostly diminutive dermal structures, thus size effects alone can introduce uncertainties in histological comparison (e.g., absence of cancellous bone). *Anguis fragilis* and *Tarentola mauritanica* trunk osteoderms are divided into an internal layer and an partially sculptured external layer (Zylberberg and Castanet, 1985; Levrat-Calviac and Zylberberg, 1986). As preformed soft connective tissue is metaplastically ossified, the basal dense layer denser retains the structure of the deep dermis, while the external layer constitutes the structure of loose superficial dermis (Maderson, 1964; Zylberberg and Castanet, 1985). Both layers retain a lamellar structure in the bone.

5.3.4 Eureptilia (Archosauromorpha)

Only the osteoderm bone histology of the basal archosaur cf. *Mystriosuchus* sp. (Parasuchia), the thalattosuchian *Steneosaurus* sp. and the derived eucrocodilian *Diplocynodon* sp. is described and discussed below. For a detailed morphological and bone histological description of osteoderms of other archosaur taxa, please refer to Scheyer and Sander (2004).

5.3.4.1 Osteoderms of *Mystriosuchus* sp. (†), *Diplocynodon* sp. (†) and *Steneosaurus* sp. (†)

The osteoderms of cf. *Mystriosuchus* sp., *Diplocynodon* sp. and *Steneosaurus* sp. consist of well developed cortices and a small vascular interior core reminiscent of a flat diploe structure (Fig. 17 a-c) see also Hua and Buffrénil, 1996). The unbroken margins of the sampled

osteoderms are smoothly rounded and not sutured. The bone microstructures seen in *Steneosaurus* sp. (Fig. 17b) generally validate the results of Hua and Buffrénil (1996).

External cortex—The external cortex consists of parallel-fibred bone that can locally grade into lamellar bone (Fig. 17d). Towards the cancellous bone, a transition to ISF is observable (Fig. 17d, e). The cortices completely surround an area of interior metaplastic cancellous bone. Growth marks are well visible throughout the cortex. The external bone surface is convex and strongly sculptured. In *Steneosaurus* sp. and *Diplocynodon* sp., the external surface sculpture consists of circular to ovoid pits. In *Steneosaurus* sp., the pits are arranged in a lightly radiating pattern. Bone erosion occurs at the lateral margins of the pits while new bone is laid down at the medial margins (see also Buffrénil, 1982; Scheyer and Sander, 2004). In cf. *Mystriosuchus* sp., the external surface sculpture consists of mediolateral low ridges that are elevated structures because of increased bone deposition compared to the adjacent bone tissue. Vascular striation on the external bone surface is faint in *Diplocynodon* sp., and clearer but unordered in cf. *Mystriosuchus* sp. Sharpey's fibres occur all over the cortical bone but they are most frequent in the internal cortex. Sharpey's fibres appear less ordered in parasuchians compared to those in the crocodilian osteoderms.

Cancellous bone—The cancellous bone is composed of few unordered, primary short and stout trabeculae and scattered secondary osteons (Fig. 17a-d). The osteoderms appear massive with medium interior vascularisation. In *Steneosaurus* sp., interior vascularisation is low, consisting of small vascular spaces, while larger trabeculae are absent. The vascularisation in cf. *Mystriosuchus* sp. is dominated by reticular primary vascular canals that anastomose frequently and extend sub-perpendicular and sub-parallel to the bone surface. In *Diplocynodon* sp., the arrangement of primary vascular canals is more scattered.

Internal cortex—The internal cortex is mostly a flat to convex layer of parallel-fibred bone (Fig. 17f, g). In the parasuchian and in *Diplocynodon* sp., the internal cortex is well developed and numerous Sharpey's fibres insert into the internal cortical bone in oblique angles. In *Steneosaurus* sp., the cortical bone is even thicker, spanning about half of the osteoderm thickness. However, Sharpey's fibres are not as obvious in this taxon (Fig. 17f). Vascularisation of the internal cortex is achieved by primary vascular canals and few scattered primary osteons. Growth marks are clearly visible throughout the cortex (Fig. 17g).

Variation—The osteoderm of *Steneosaurus* sp. has the least amount of interior bone vascularisation and the thickest cortical bone of the three taxa. The osteoderm sampled for the current study is even more compact (due to the very thick internal cortex) than the osteoderm sampled by Hua and Buffrénil (1996), which measured an overall bone volume of 61% for their osteoderm.

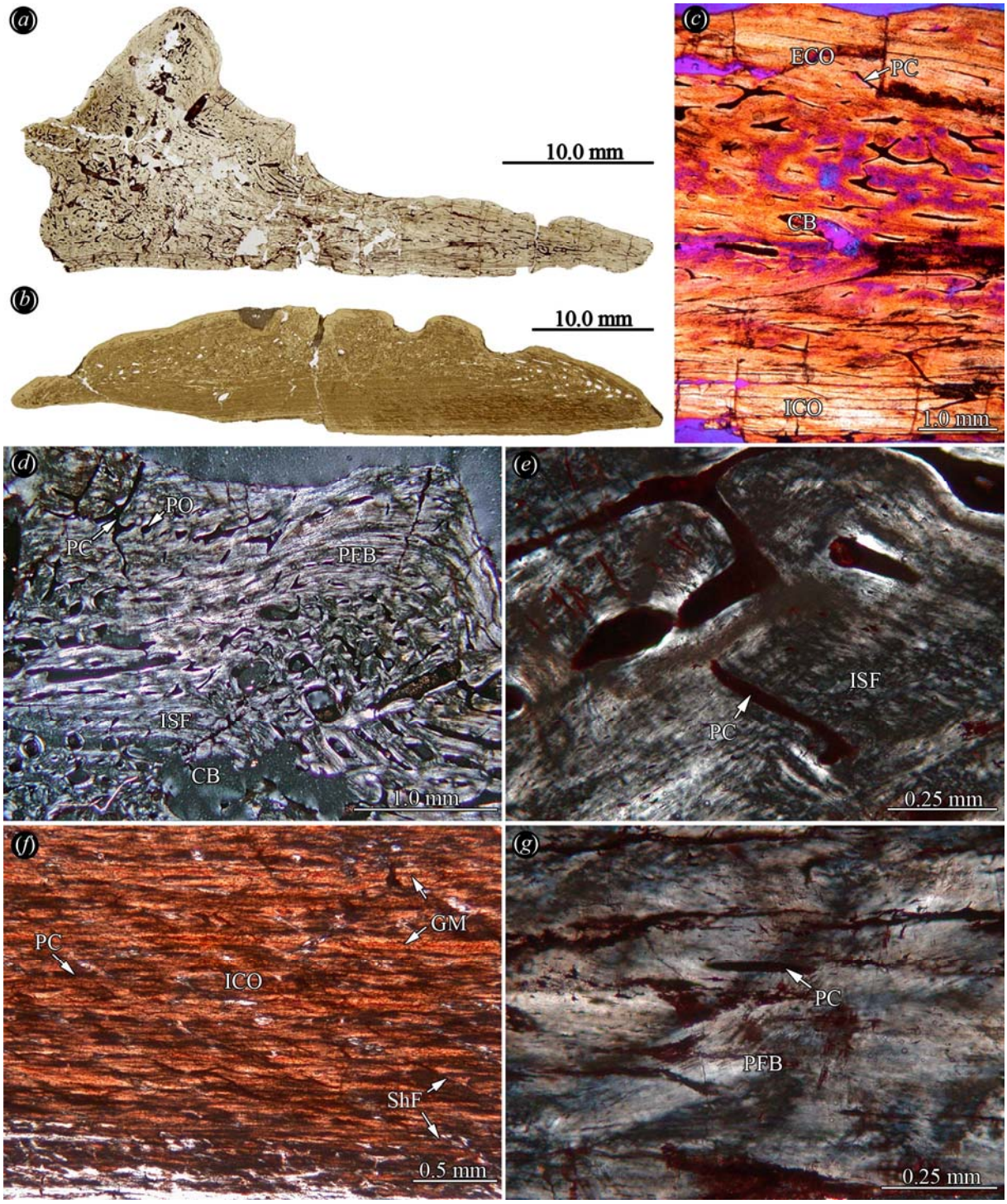

Figure 17: Bone histology of archosaur osteoderms (cf. *Mystriosuchus* sp., *Diplocynodon* sp.

and *Steneosaurus* sp.) (*a*) Keeled osteoderm fragment SMNS 91013 of cf. *Mystriosuchus* sp. and (*b*) flat pitted osteoderm NMS 7152 of *Steneosaurus* sp. (*c*) Close-up of the lateral part of SMNS 91013, with weakly vascularised cortices framing a more strongly vascularised intertior bone tissue in polarised light (with lambda compensator). (*d*) Detail of external cortex and interior cancellous bone parasagittal to the keel of the former specimen in polarised light. Note transition between more external parallel-fibred bone and the more internal ISF. (*e*) Detail of the ISF of the interior part of the external cortex of the former specimen in polarised light. (*f*) Detail of the internal cortex of NMS 7152. Note insertion of Sharpey's fibres. (*g*) Detail of the internal cortex of SMNS 91013 showing parallel-fibred bone and primary vascular canals.

6. Bone histological results of Testudinata

To quickly assess the nature of the sampled bones, fossil turtle taxa are marked by a cross in parentheses (†) behind the names in the respective headings. Descriptions of the abbreviations used in the text and figures are compiled in Appendix 2.

6.1 Basal Testudinata

6.1.1 Proganochelyidae

6.1.1.1 *Proganochelys quenstedti* Baur, 1887 (†)

All sampled shell bones of *P. quenstedti* show similar bone histologies. However, because the material of Halberstadt presented the best bone preservation, the histological data strongly relied on observations from the Halberstadt material instead of the Trossingen material. All elements have a diploe structure, where external cortices and internal cortices frame interior cancellous bone (Fig. 18a). The shell bones appear quite robust with external and internal cortices having similar thicknesses.

External cortex—The external cortex consists of ISF, the metaplastically ossified parts of the integument, which are strongly dominated by fibre bundles that extend perpendicular or in high angles to the surface of the bone (Fig. 18b, c). The bone tissue is vascularised with few scattered primary osteons and primary vascular canals. Sharpey's fibres inserting into the external cortex are present and, due to higher mineralisation, separable from the surrounding fibre bundles of the ISF. Cyclical growth marks are present but too poorly developed in the external cortex to be countable. Few secondary osteons appear at the transition between external cortex and cancellous bone.

Cancellous bone—The cancellous bone is characterised by short secondarily remodelled trabeculae and moderate vascularisation with small marrow cavities (Fig. 18d). Primary interstitial bone is still present within the trabeculae. The secondary lining of the trabeculae consists of lamellar bone. The bone cell lacunae are plumper and of circular shape in the interstitial bone, while they are flattened and elongated in the lamellar bone of the trabeculae.

The flattening and elongation of the bone cell lacunae is usually attributed to slower bone deposition rates, i.e., in lamellar bone.

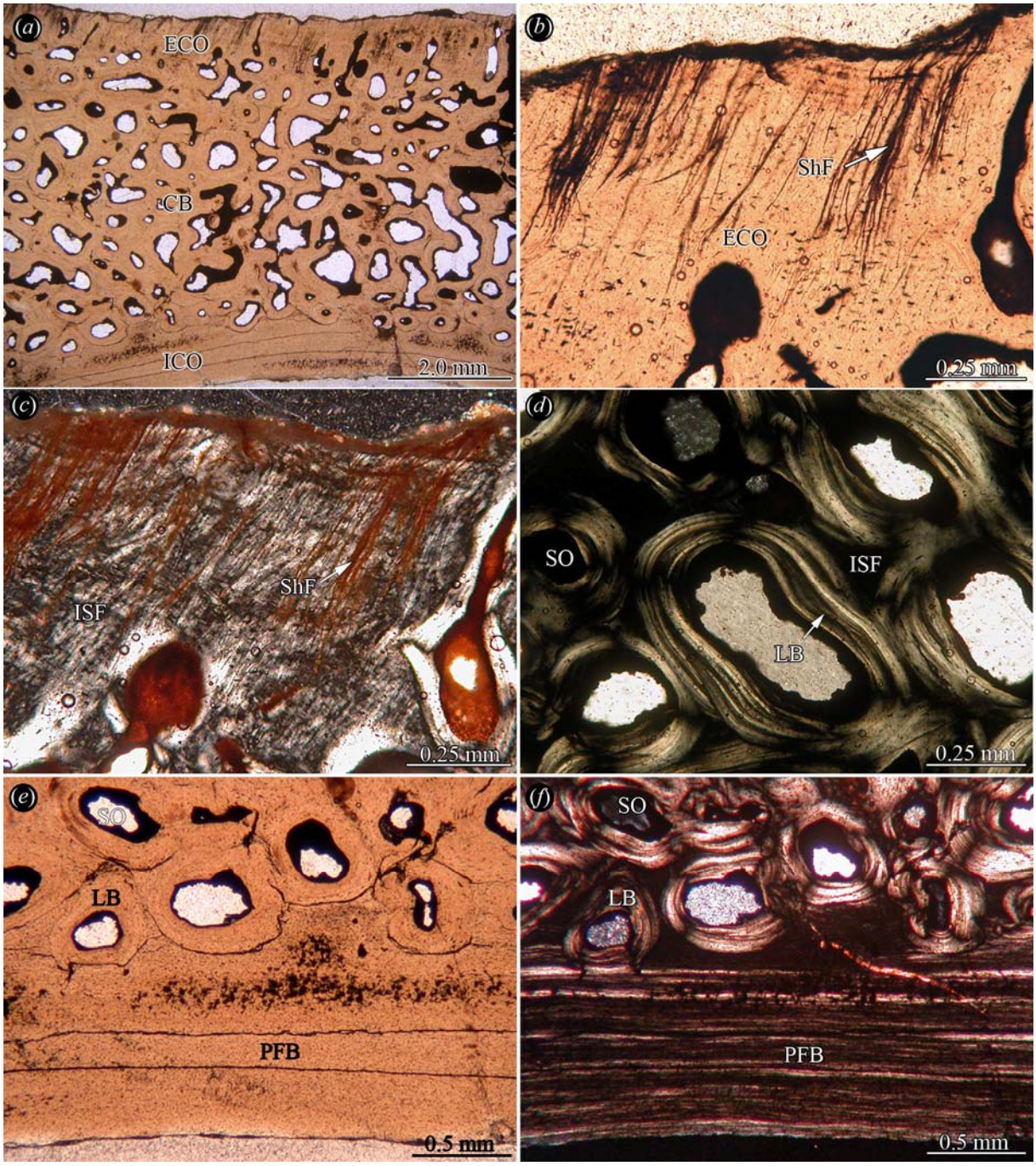

Figure 18: Shell bone histology of Upper Triassic basal turtle *Proganochelys quenstedti*. (*a*) Section of costal MB.R. 3449.2 showing the compact diploe structure of the bone in normal light. Close-up of external cortex of in (*b*) normal transmitted and in (*c*) polarised light. Note differences between Sharpey's fibres and interwoven structural fibre bundles. (*d*) Magnification of the interior cancellous bone of former specimen. Close-up of transition of

interior cancellous bone to compact internal cortex of the former specimen in (*e*) normal and (*f*) polarised light. Note the avascular parallel-fibred bone of the internal cortex.

Internal cortex—The internal cortex comprises parallel-fibred bone (Fig. 18e, f) that locally grades into lamellar bone. Fibre bundles are rather fine and of similar length and thickness. Coarser fibre bundles that may represent Sharpey's fibres are only found directly adjacent to the incorporated rib of the costal plate. The bone tissue is mainly avascular.

Sutures—Sutures were not preserved in the samples from Halberstadt and Trossingen. In the following chapters, sutures will only be described if they are suitably preserved in the specimens.

6.1.2 Proterochersidae

6.1.2.1 *Proterochersis robusta* Fraas, 1913 (†)

A well developed diploe is present in both samples of *P. robusta*. The external and internal cortices that frame the interior cancellous bone are of similar thickness. Because of the fragmentary nature of the samples, the plate margins and sutures could not be studied.

External cortex—The external surfaces of the shell elements are slightly rugose. The external cortex consists of metaplastic ISF. Directions of the fibre bundles within the ISF are either perpendicular and sub-parallel to the external surface of the bone or diagonally angled. None of the differently spatially arranged fibre bundles is dominant within the ISF, thus the bone matrix of the external cortex is rather homogeneously built. Vascularisation occurs through scattered primary osteons and irregularly extending primary vascular canals. In the plastral fragment, the primary vascular canals that are angled towards the external surface of the bone dominate the vascularisation. The primary vascular canals can reach the external bone surface in a pore-like foramen. Few scattered large secondary osteons appear in the transition to the interior cancellous bone. Sharpey's fibres are found only in the internal part of the external surface of the peripheral where the straight proximal shaft starts to thicken into

the distal bulge. Here the homogeneous pattern of the ISF is overlain by sub-parallel coarse fibre bundles, i.e., the Sharpey's fibres that insert into the external cortex at high angles. Bone cell lacunae appear mostly irregularly arranged or clustered within the ISF.

Cancellous bone—The interior cancellous bone consists of irregular bone trabeculae and vascular spaces with generally uniform size. Occasionally, adjacent vascular spaces fuse to form larger, oblong spaces. The trabeculae are rather short if slender. Primary interstitial bone is still present in many trabecular branching areas. The trabeculae themselves usually constitute lamellar bone and occasionally parallel-fibred bone. Bone cell lacunae are more scattered and of circular shape in the primary bone, while they are more elongated and flattened in the lamellar bone of the trabeculae.

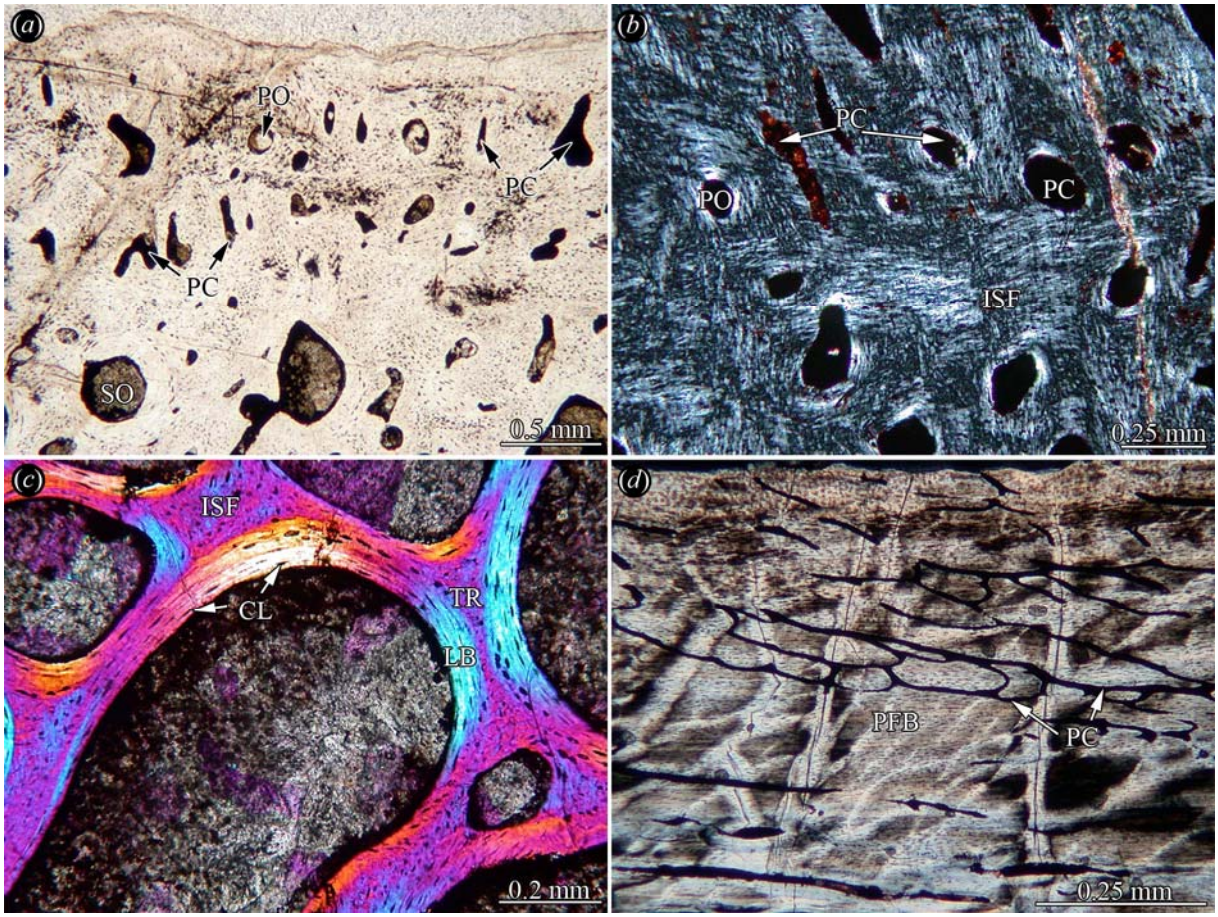

Figure 19: Shell bone histology of Upper Triassic basal turtle *Proterochersis robusta*. (*a*) Magnification of the external cortex of sampled peripheral (SMNS 16442) in normal light. (*b*) Close-up of the interwoven structural fibre bundles of the external cortex of the former specimen in polarised light. The bone tissue is vascularised by scattered primary osteons and primary vascular canals. (*c*) Close-up of the interior cancellous bone in polarised light (with

lambda compensator). Bone trabeculae are primary but lined with secondary lamellar bone. (*d*) Magnification of the internal cortex of the plastron fragment (SMNS 16442; ?hyo- or hypoplastron) in polarised light. Note the thin reticular vascularisation pattern with an opaque mineral infill (pyrite).

Internal cortex—The thick internal cortex of the plastral fragment consists of parallel-fibred bone. The bone tissue is vascularised by a reticular primary vascular canal pattern. This pattern is well observable because the primary vascular canals have an opaque mineral infill, i.e., pyrite. Primary and secondary osteons are absent. Flattened and elongated bone cell lacunae are found throughout the internal cortex. Communicating canaliculi between the cell lacunae are often found. The internal cortex was not observable in the peripheral fragment.

6.1.3 Kayentachelyidae

6.1.3.1 *Kayentachelys* sp. (†)

All shell elements of *Kayentachelys* sp. show a diploe structure with external and internal cortices framing interior cancellous bone (Fig. 20a). Both cortices are of similar thickness. The proximal costal fragment (UCMP V85010/150228) is strongly altered by diagenesis and histological details are almost completely obscured in the thin-section. The description of the following histology is thus based largely on the remainder of the sample.

External cortex—The external cortex consists of metaplastic ISF (Fig. 20b). Fibre bundles that extend perpendicular and sub-parallel to the external surface of the bone dominate the ISF, however fibre bundles that are diagonally angled are also present. Vascularisation of the tissue is achieved by few primary vascular canals and scattered primary osteons. The latter are arranged predominantly perpendicular towards the external surface of the bones. Many of the primary vascular canals open up to the bone surface as small foramina, thus further enhancing the rugose texture of the shell bones. The primary vascular canals seldom branch. Bone cell lacunae are either round or oblong, but little flattened in the ISF.

Cancellous bone—The bone trabeculae of the cancellous bone are primary, although successive remodelling occurs. The arrangement of the bone trabeculae and vascular spaces is irregular. The trabeculae are mostly short and thick; the vascular spaces rather small. Only in the centre of the cancellous bone, larger vascular spaces are developed through trabecular remodelling (Fig. 20c). Interstitial trabecular branching areas and, sometimes, part of the trabeculae themselves still exhibit primary interwoven bone tissue, i.e., ISF. Most of the trabeculae however, have a wall of secondary lamellar bone.

Internal cortex—The internal cortex consists of parallel-fibred bone (Fig. 20d). The bone tissue is less vascularised than the external cortex. Locally, few scattered primary vascular canals are present in the otherwise avascular tissue. Bone cell lacunae can be, as observed in the plastral fragment (UCMP V85013/150229), extremely flat and elongated where they occur sheet-like within the parallel-fibred bone. In the neural (TMM 43669-4.2), directly lateral to the incorporated neural spine, the internal cortex thickens to a semicircular patch of parallel-fibred bone. Here, Sharpey's fibres insert at high angles into the bone tissue.

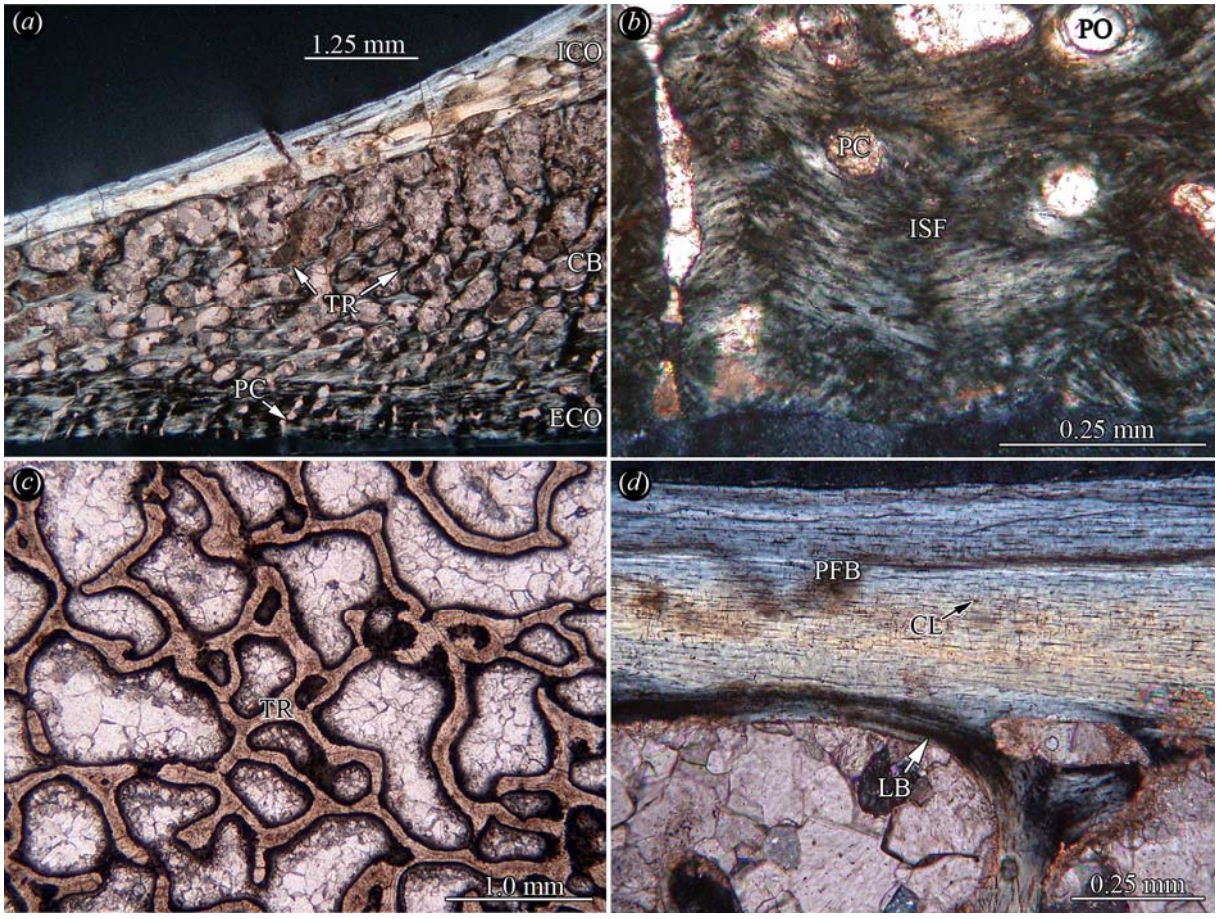

Figure 20: Shell bone histology of Lower Jurassic basal turtle *Kayentachelys* sp. (*a*) Thin-

section of plastron fragment UCMP V85013/150229 in polarised light. (*b*) Close-up of the interwoven structural fibre bundles of the external cortex of the former specimen in polarised light. (*c*) Close-up of the more slender trabeculae of the centre of the interior cancellous bone of peripheral UCMP V82319/130079 in normal transmitted light. (*d*) Magnification of the weakly vascularised parallel-fibred bone of the internal cortex of plastron fragment UCMP V85013/150229 in polarised light.

6.1.4 Meiolaniidae

6.1.4.1 *Meiolania* sp. (†)

The shell element shows a diploe structure with well developed cortical bone layers framing interior cancellous bone. Based on the histological congruence of the cortical bone layers, the shell element is identified as a peripheral fragment. Only the external cortex and the cancellous bone can be described from the specimen, whereas the internal cortex was not preserved in the specimen.

External cortex—The external cortex consists of metaplastic ISF (Fig. 21a, b). The fibre bundles that extend perpendicular, sub-parallel and angled to the bone surfaces are of equal length and diameter, giving the ISF a homogeneous constitution. Orientation of the collagenous fibres within the fibre bundles, and thus the bone apatite crystallites, is parallel. Growth marks are found throughout both (dorsal and ventral) external cortical layers. At least ten major growth cycles are counted and several of these major ones also show fainter subdivisions. Vascularisation is low to moderate with primary osteons and primary vascular canals. Most of the primary osteons and primary vascular canals occur sheet-like within growth cycles (they appear as if they were strung on a chain in cross-section), while some of the primary vascular canals do extend across growth marks. Sharpey's fibres were not observed within the interwoven bone tissue of the external cortex.

Cancellous bone—Trabeculae are short and thick at the transition to the external cortex. They become longer and more gracile towards the centre of the cancellous bone. The arrangement of the trabeculae is irregular (Fig. 21c, d). Vascular spaces are small and circular shaped and increase in size towards the centre of the cancellous bone. Here the form and

shape of the vascular spaces also becomes increasingly irregular. The trabeculae are composed of lamellar bone. Only in branching areas, primary ISF is still present.

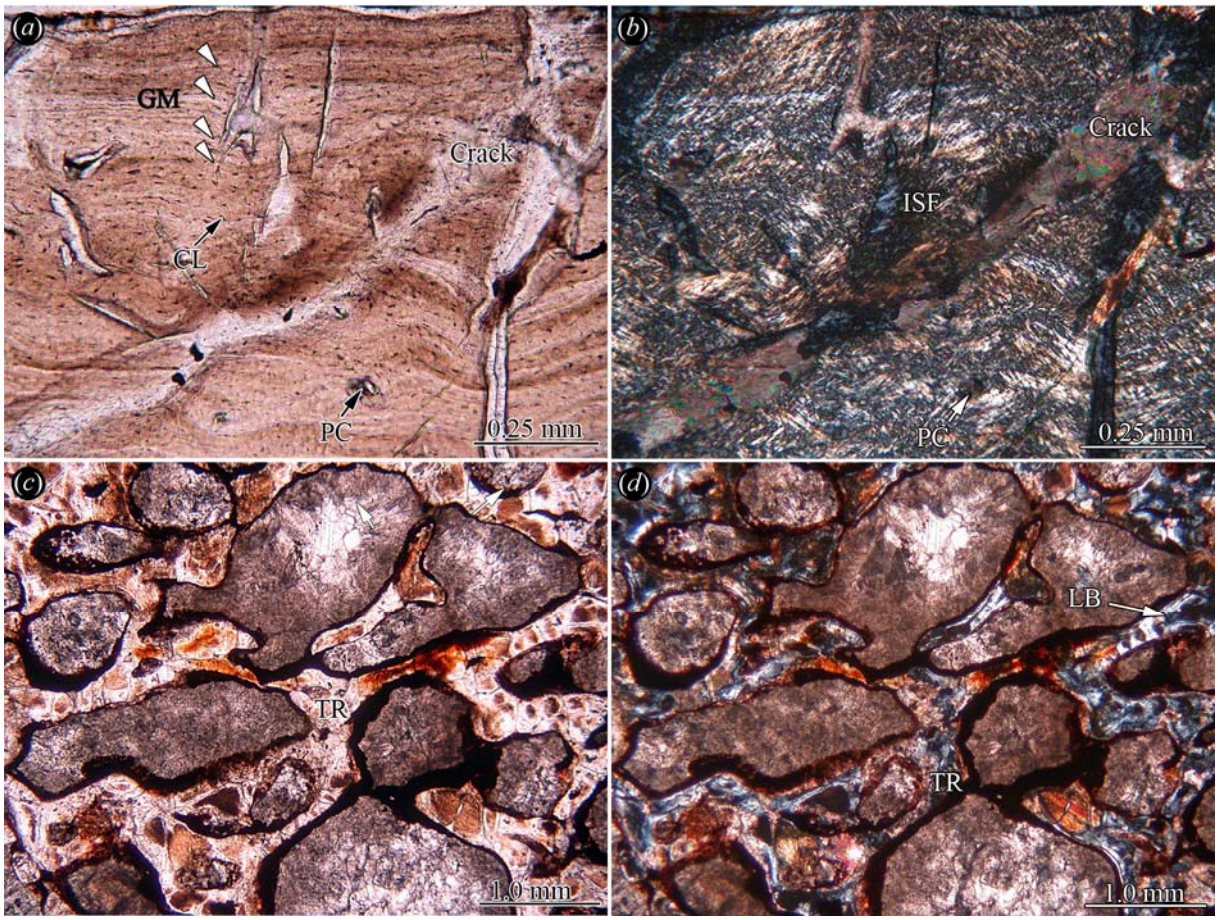

Figure 21: Shell bone histology of *Meiolania* sp. Close-up of the external cortex of peripheral fragment MB.R. 2426.1 in (*a*) normal and (*b*) in polarised light. Note the growth marks of the interwoven bone tissue. Close-up of the bone trabeculae of the interior cancellous bone in (*c*) normal transmitted light and (*d*) in polarised light.

6.2 Pleurodira

6.2.1 Platychelyidae

The sampled material represents two morphotypes. The smaller morph is represented by the material of aff. *Platychelys* sp. from Portugal (histomorph A). The larger one includes the material of *P. oberndorferi* from Switzerland (histomorph B). Besides the differences in shell element size and bone thickness, major distinctions between the two morphs are found in the vascularisation of the bone tissues and in the expression of different bone tissues in the external cortex.

6.2.1.1 Histomorph A: aff. *Platychelys* sp. (†)

The fragments generally show thicker external cortices and thinner internal cortices framing an interior cancellous bone.

External cortex—The external cortex of all elements ranges between 0.6-1.0 mm and the internal cortex of the costals ranges between 0.2-0.3 mm. The external cortex consists of a more external and a more interior zone. The external zone constitutes a finely fibred bone matrix where vertical fibre bundles that stand perpendicular to the bone surface predominate (Fig. 22a, b). Superficially, the matrix itself resembles typical parallel-fibred bone. On closer inspection, however, it is identified as a metaplastic tissue of ISF. The fibre bundles extend not only sub-parallel and perpendicular but also at high angles to the external bone surface, thus creating a interwoven meshwork of fibre bundles. Bone cell lacunae are small and of circular to oval shape here. Growth marks usually occur in this more external zone (Fig. 22b) and at the sutured margins of the shell elements. The more interior zone of the external cortex exhibits coarser and thicker fibre bundles while the perpendicular fibre bundles that dominated the more external zone are not recognised anymore. The coarser fibre bundles trend diagonally, as well as perpendicular and parallel to the external bone surface (Fig. 22b). However, the whole arrangement of fibre bundles is not as ordered as in the more external, fine fibred zone. The bone cell lacunae are thicker and of ovoid to circular shape in the interior zone. The vascularisation is dominated by primary vascular canals that are orientated

dorsoventrally and seldom branch. Primary osteons are scattered between these primary vascular canals. Towards the lateral sutures of the bones, the horizontal growth marks of the external cortex deviate and continue in vertical orientation, subparallel to the bone suture. The bone tissue of fine fibre bundles is similar to the external zone in the external cortex, but no fibre bundles that trend perpendicular to the bone surface are present. Sharpey's fibres are also absent.

Cancellous bone—The primary cancellous bone, framed by the thicker external cortex and the thinner internal cortex, is locally completely remodelled. However, primary bone tissue, sometimes vascularised by primary osteons, is still visible in interstitial areas of many trabeculae (Fig. 22c). The bone trabeculae appear slender and are lined with lamellar bone. Elongated and flattened bone cell lacunae follow the direction of these lining bone lamellae, while the cell lacunae are plump and of circular shape in the interstitial areas. Patches of ISF can be present at the transition to the internal cortex.

Internal cortex—The internal cortex of the costal fragments consists of parallel-fibred bone, where areas of coarse fibre bundles, i.e., ISF, interdigitate with areas of finer fibre bundles (Fig. 22d). The direction of the fibre bundles is subparallel or moderately angled to the interior bone surface. Bone cell lacunae are sparsely distributed, flattened, elongated and devoid of canaliculi.

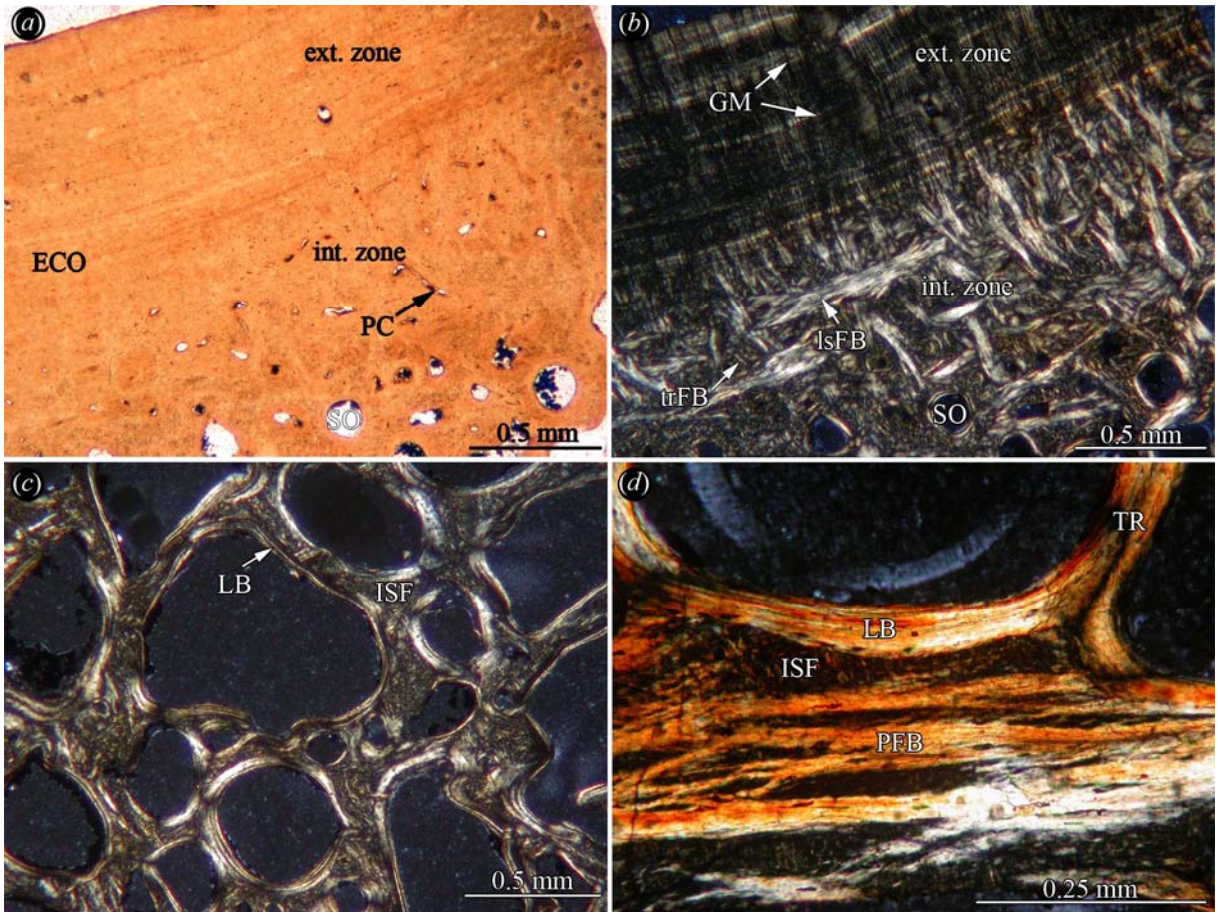

Figure 22: Shell bone histology of aff. *Platychelys* sp. Section of the external cortex of peripheral fragment GUI-CHE-52 in (*a*) normal transmitted and (*b*) in polarised light. Note the clear distinction between the more external zone with growth marks and the more internal coarse-fibred zone. (*c*) Close-up of the irregular primary bone trabeculae of the cancellous bone of GUI-CHE-52 in polarised light where primary trabeculae are lined with secondary lamellar bone. (*d*) Section of the internal cortex of costal fragment GUI-CHE-51 seen in polarised light. Note interwoven structural fibre bundles interdigitating with layers of parallel-fibred bone.

6.2.1.2 Histomorph B: *Platychelys oberndorferi* Wagner, 1853 (†)

The carapacial fragments generally show thicker external cortices and thinner internal cortices framing an interior part of cancellous bone. In the sampled hypoplastron however the

external cortex and the internal cortex are of similar thickness. Typical for the shell of *Platychelys* are the humps and ridges that are also very clearly recognised in the thin-sections.

External cortex—Histomorph B lacks the distinction of the external cortex in a more external and a more internal zone. Instead, the more external zone of histomorph A is missing completely. The external cortex thus resembles only the more internal zone of histomorph A, but the fibre bundles are more evenly distributed and not as coarse (Fig. 23a, b). Vascularisation of the external cortex with scattered primary osteons and primary vascular canals is higher than in histomorph A. Especially the primary osteons can occur as orderly aligned rows through the successive layers of the external cortex.

Cancellous bone—The cancellous bone is almost completely remodelled with only few areas where primary bone tissue is still preserved. The cancellous bone thus superficially resembles that of histomorph A. However, the trabeculae in histomorph B can be more evenly distributed to form regular, similar sized cavities (Fig. 23c). Towards the internal zone of the external cortex, the cancellous bone grades into scattered secondary osteons.

Internal cortex—The internal cortex ofhistomorph B consists of parallel-fibred bone (Fig. 23d). Similar to histomorph A, coarser fibre bundles interdigitate with areas of finer fibre bundles, and the direction of the fibre bundles is largely subparallel to the interior bone surface.

Variation—In this morphotype, light variation in the bone microstructure is present but restricted to the external cortex. The thickness of the external cortex varies in thickness. In the costals and peripherals, the thickness of the external cortex is influenced by the occurrence of the characteristic humps of the shell bones. The interior cancellous bone can also be locally thickened in the region of the humps.

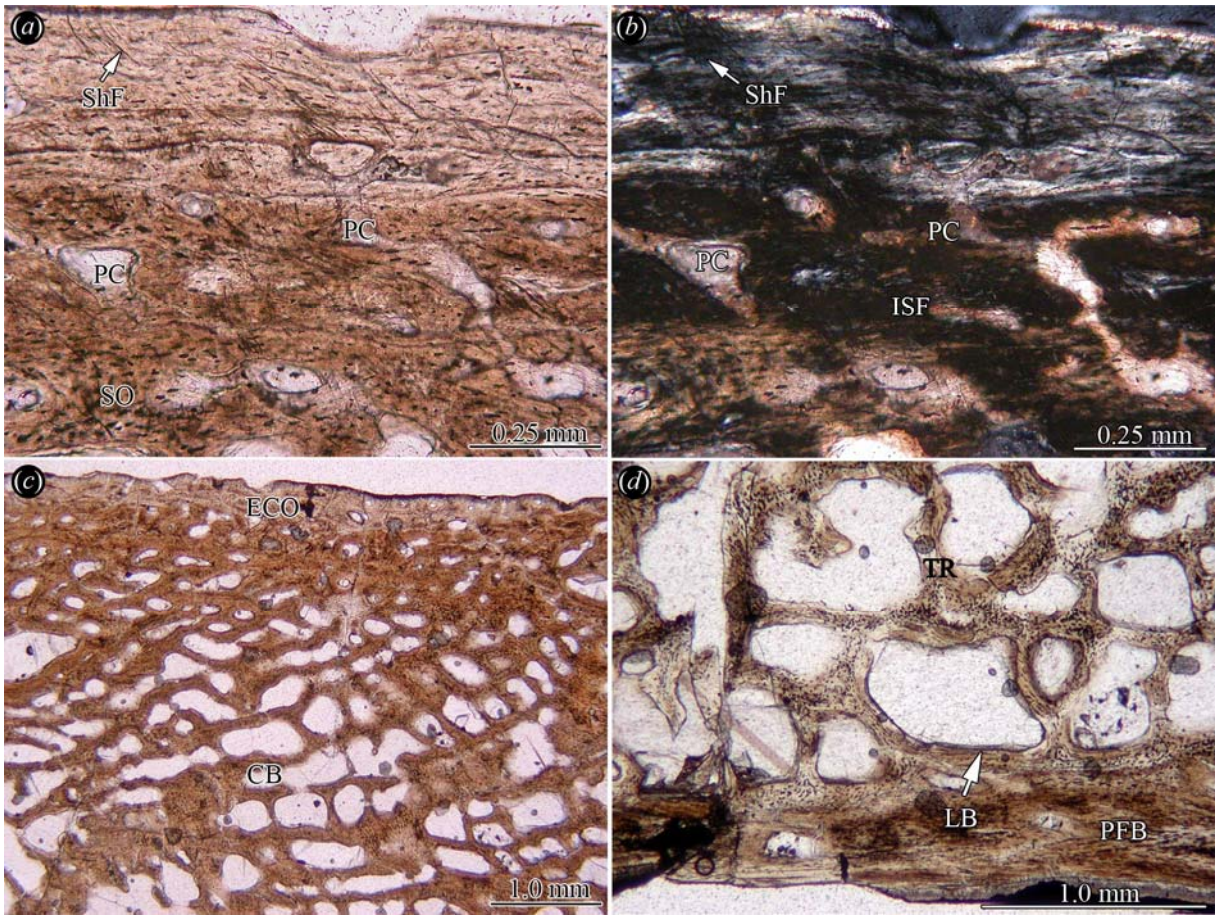

Figure 23: Shell bone histology of Upper Jurassic *Platychelys oberndorferi*. Section of the well vascularised external cortex of the costal NMS 20076 in (*a*) normal transmitted and (*b*) in polarised light. (*c*) Section of the former specimen showing the transition from the external cortex to the interior cancellous bone in normal light. Note the ordered arrangement of bone trabeculae and vascular cavities of the cancellous bone. (*d*) Close-up of transition from cancellous bone to internal cortical bone in polarised light.

6.2.2 Pelomedusidae

6.2.2.1 *Pelomedusa subrufa* (Bonnaterre, 1789)

The samples of *P. subrufa* have a diploe build with well-developed cortices and interior cancellous bone (Fig. 24a, b). Below thin layers of keratin that compose the shield cover and a very thin layer of unossified tissue, the surface of the underlying bone is slightly pitted. Cyclic growth is also present in the keratinous shield. Instead of following the pitted course of the bone, the unossified tissue expands into the pits and fills them.

External cortex—The external cortex expresses a few weakly developed growth marks. It is composed of interwoven collagenous fibre bundles regularly interspersed with primary osteons (Fig. 24c). Scattered secondary osteons are seldom found. Fibre bundles perpendicular to the bone surface can be found throughout the external cortex. They are most clearly visible right below the border where bone meets connective tissue. The orientation of the fibre bundles is predominantly subparallel or diagonal to the external surface of the bone. Bone cell lacunae are mostly round to slightly elongated and they usually do not bear any canaliculi.

Cancellous bone—The interior cancellous bone consists of bone trabeculae and patches of interstitial primary bone that are still quite large. The trabeculae are lined with thin secondary lamellar bone (Fig. 24b). Bone cell lacunae are plump and round in shape in the interstitial areas and slightly elongated within the bone lamellae.

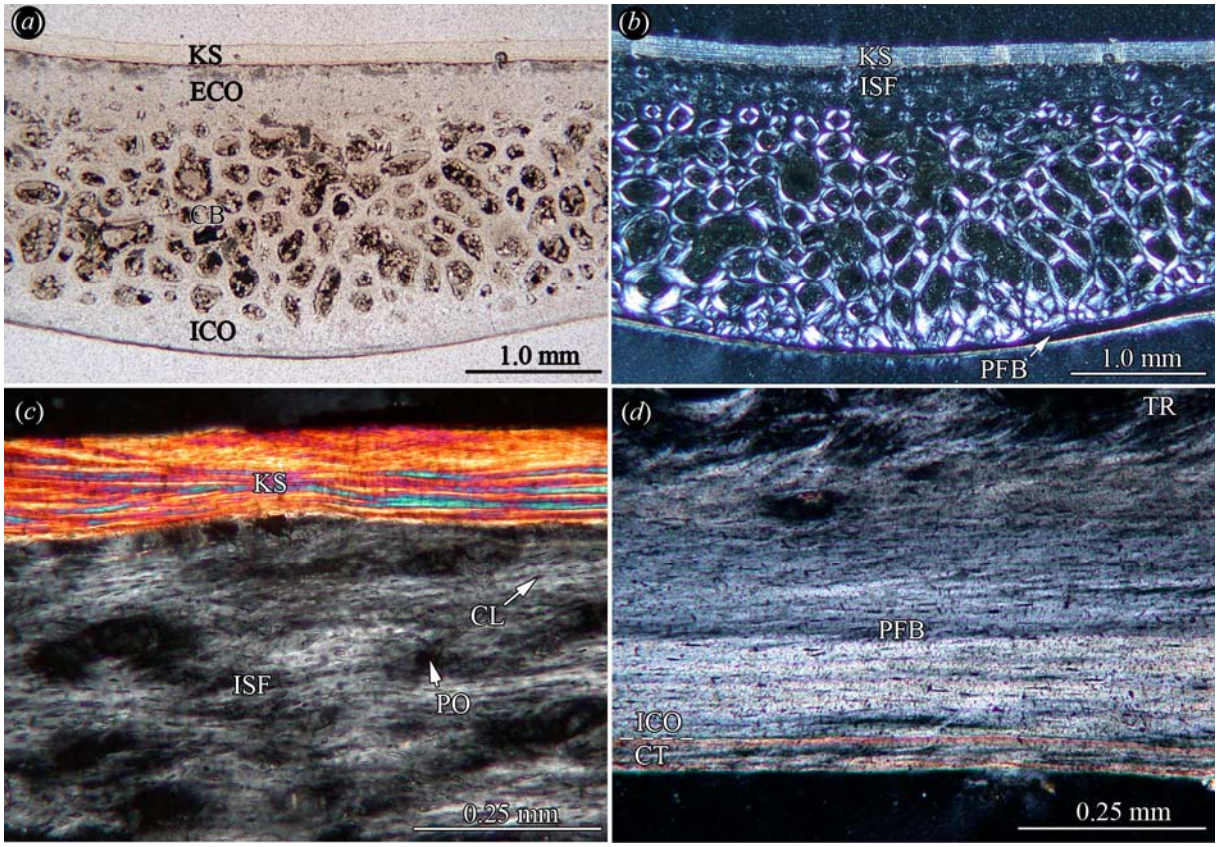

Figure 24: Shell bone histology of *Pelomedusa subrufa*. Thin-section of a sampled costal (MVZ 230517, drilled core) and associated keratinous shield in (*a*) normal light and (*b*) in polarised light. The diploe build of the shell is apparent below the keratinous shield. Note thin layer of connective tissue in between the shield tissue and the bone tissue. The plane of

sectioning lies perpendicular to the incorporated rib in the costal. The former rib is only seen as a dorsoventrally thickened amount of cancellous bone and the slight curvature of the internal cortex. (*c*) Detail of the external cortex of the costal in polarised light where the interwoven fibre bundles are interspersed with primary osteons. Bone cell lacunae that appear within the whole of the cortical bone have round shapes. (*d*) Detail of the parallel-fibred bone of the internal cortex of the same specimen. Below the surface of the bone, a thin layer of fibrous connective tissue is still present.

Internal cortex—The internal surface of the bone is covered with a thin layer of soft connective tissue. The internal compact bone itself is mostly avascular and constitutes parallel-fibred bone tissue (Fig. 24d). Bone cell lacunae in the interior cortical bone are rather flat and elongated and mostly follow the layering of the bone.

6.2.3 Bothremydidae

6.2.3.1 *Bothremys barberi* (Schmidt, 1940) (†), *Taphrosphys sulcatus* (Leidy, 1856a) (†) and of "*Foxemys* cf. *F. mechinorum*" Tong et al., 1998 = *Polysternon mechinorum* (Tong et al., 1998) fide Lapparent de Broin (2001) (†)

The bone histology of these three taxa is rather similar which is why they are described together. In all samples of *B. barberi*, *T. sulcatus* and "*Foxemys* cf. *F. mechinorum*", the internal cortices are significantly thinner than the external cortices (Fig. 25a, b). A symmetrical diploe build of the bony shells in which the cortices have rather similar thicknesses, is not developed.

External cortex—The massive external cortex of all sampled elements is composed of ISF (Fig. 25c, d). Cyclical growth marks are best preserved in the neurals. In the neural of *T. sulcatus,* about 20 growth marks were counted (Fig. 25c). The neural of *B. barberi* has a minimum number of nine growth marks (Fig. 25d) and the neural of "*Foxemys*" has six growth marks. Several shell elements of *T. sulcatus* further show a peculiar bone tissue within the external cortices where, locally, the growth marks of the primary bone tissue of the

cortices were substituted by secondary bone tissue. Here, the secondary bone appears in an inverted triangular-shaped or hemispherical area with a reticular vascularisation pattern. The bone surface directly above the peculiar bone tissue often has a pitted or rugose texture. The fibrous tissue of the external cortices is dominated by diagonally arranged collagen fibre bundles. Irregularly arranged primary osteons are commonly found throughout the external cortex. Additionally, collagenous fibre bundles that trend perpendicular to the bone surface are incorporated in all layers of the external cortices. Scattered secondary osteons are also present, but they are restricted to the interior-most layer of the external cortex. No secondary osteon clusters were found. Primary canals comprise either single or branching tubules that often point towards the external surface of the bone. Bone cell lacunae are slightly elongated in the external-most layers of the external cortex and more round towards the cancellous bone.

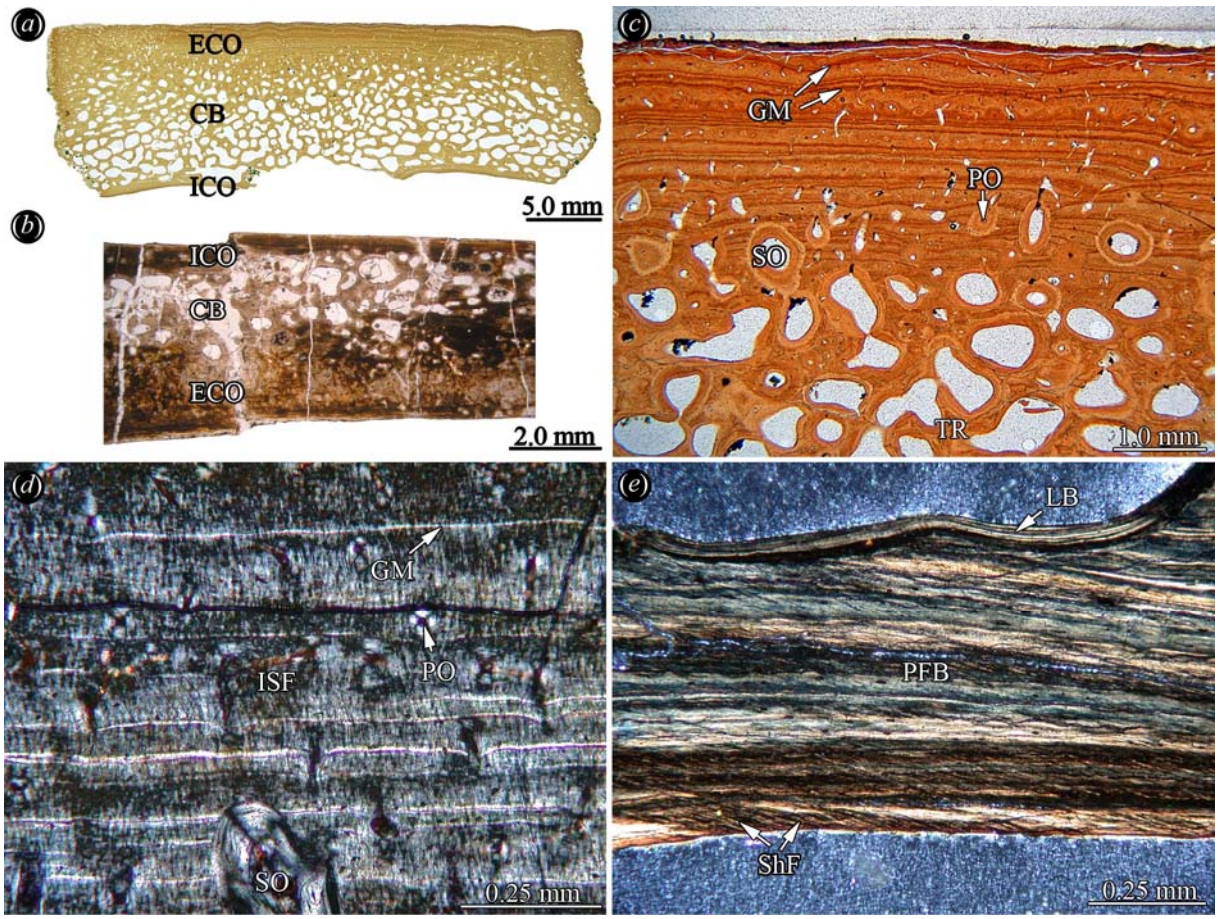

Figure 25: Shell bone histology of bothremydid taxa. (*a*) Complete section of the neural YPM 40288 of *Taphrosphys sulcatus* in normal transmitted light. (*b*) Part of thin-section of the plastron fragment (?hyo- or hypoplastron; IPB R559a) of "*Foxemys* cf. *F. mechinorum*" in

normal transmitted light. In both cases, the internal cortex is reduced compared to the external cortex. (*c*) Close-up of the external cortex and the more external part of the cancellous bone of the neural YPM 40288 in normal light. Note the clear growth marks of the cortical bone tissue. (*d*) Close-up of the interwoven structural fibres of the external cortex of the costal FM P 27406 of *Bothremys barberi* in polarised light. (*e*) Close-up of the parallel-fibred bone of the internal cortex of neural YPM 40288. Note Sharpey's fibres inserting into the parallel-fibred bone.

Cancellous bone—The trabeculae of the interior cancellous bone are composed of secondary lamellar bone with remnants of primary fibrous tissue restricted to interstitial areas of the trabeculae (Fig. 25c, e). Bone cell lacunae are common in the interstitial areas and rather sparsely distributed in the secondary lamellar bone of the trabeculae.

Internal cortex—The internal cortices are usually composed of a thin zone of parallel-fibred bone (Fig. 25e). Secondary osteon clusters are not developed in the internal cortices. Sharpey's fibres extend obliquely towards the surface of the bone in the internal cortices of both neurals and costals of *T. sulcatus* and *B. barberi*.

6.2.4 Podocnemidae

6.2.4.1 cf. *Bairdemys* sp. (†)

The mineral crust covering the bone of the single studied specimen of cf. *Bairdemys* sp. has also strongly affected the bone histology. The thin-section reveals that the bone is well preserved only in the interior part of the shell bone element. The external and internal surfaces of the shell element consist almost exclusively of gypsum and, to a small degree, iron oxide minerals. A diploe is not observed, because a clear internal cortical bone is not preserved due to weathering and erosion.

External cortex—The external cortex is only locally unaltered internal to the mineral crust (Fig. 26a). Parts of the original cortical bone were delaminated by the gypsum minerals and

now seem to “float” in the mineral crust. The external surface of the bone appears thus scalloped. However, where the preservation of bone tissue is better, the cortex constitutes ISF. The arrangement of the fibre bundles in the ISF is homogeneous, with fibre bundles being of similar diameter and length. The fibre bundles extend perpendicular, parallel and oblique to the external surface of the bone. The bone tissue is vascularised by few scattered primary osteons and short primary vascular canals. Few larger erosion cavities open up into the cortical bone, again indicating that part of the external bone cortex is missing (bone fragments that now “float” in the mineral crust). Bone cell lacunae are irregularly spaced in the bone tissue. Their shape ranges from circular to ellipsoid and slightly flattened.

Cancellous bone—The interior cancellous bone consists of irregularly arranged bone trabeculae and vascular cavities (Fig. 26b). The trabeculae are short and primary interstitial bone, i.e., ISF, is present in trabecular branching areas. The trabeculae themselves consist of lamellar bone. The cavities are mostly homogeneous in shape. Most are of round to elongate ellipsoidal shape. A small increasing gradient in size of the cavities is observed from external to internal. At the internal surface of the bone, the trabecular structure is partly fractured and collapsed. However, the gross part of the trabeculae is not collapsed and thus shows the original irregular orientation within the bone. True compact bone is not preserved internal to the interior cancellous bone.

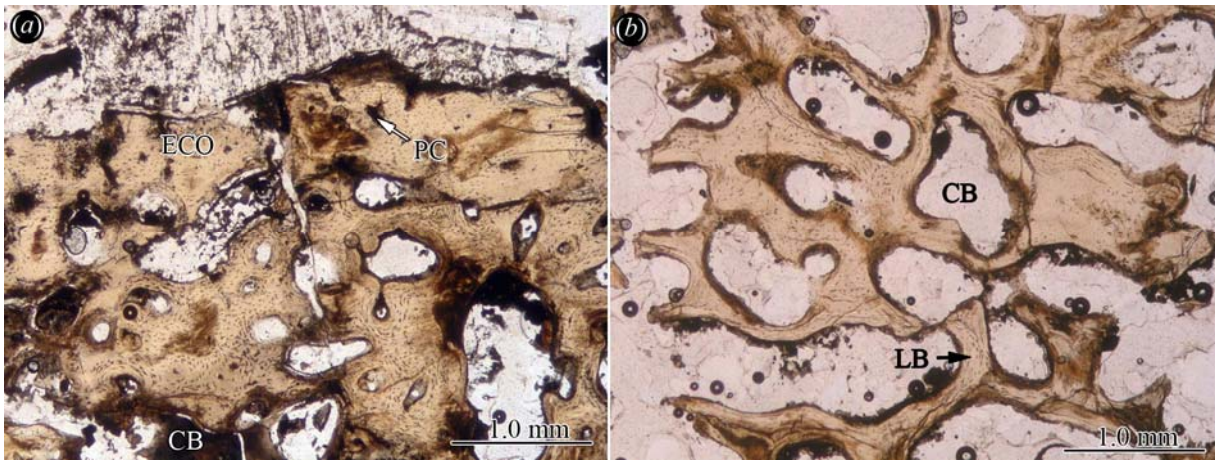

Figure 26: Shell bone histology of cf. *Bairdemys* sp. (*a*) Close-up of the strongly encrusted and eroded external cortex of shell fragment (?costal; UNEFM uncat.) in normal light. Note the clear growth marks of the cortical bone tissue. (*b*) Close-up of the irregularly arranged bone trabeculae of the cancellous bone of the former specimen.

6.2.4.2 *Podocnemis erythrocephala* (Spix, 1824)

All sampled shell elements of *P. erythrocephala* have a clear diploe with internal and external compact bone layers of similar thickness enclosing a cancellous interior (Fig. 27a).

External cortex—The external cortices of the elements are composed of ISF with numerous growth marks (Fig. 27b). Primary and scattered secondary osteons range throughout the whole of the external cortex, but the overall amount of both osteon types decreases towards the external surface of the bone. The arrangement of the fibre bundles within the external-most part of the external cortex is not well structured. The fibre bundles trend in an irregular fashion, with the majority being orientated diagonally towards the surface of the bone. Throughout the whole of the external cortex, extensive fibre bundles that extend perpendicular to the bone surface can be observed. The external part of the cortex is avascular. Bone cell lacunae are elongated and flattened and most have long canaliculi. The external cortex of the sampled costal further exhibits an inverted semicircular patch of secondary remodelled bone (Fig. 27b, c, d). Here, no growth marks within the external cortical bone are observed and the surface of the bone is indented and rugose.

Cancellous bone—The cancellous bone is dominated by short secondary trabeculae, lined with centripetally deposited lamellar bone (Fig. 27a). Elongated and flattened bone cell lacunae that lack canaliculi are abundant within the trabecular bone lamellae. The cancellous bone is replaced by scattered secondary osteons.

Internal cortex—The internal cortex of the shell elements of *P. erythrocephala* consist of lamellar bone with growth marks that, under polarised light, show a very distinct light and dark layering (Fig. 27e, f). Towards the interior cancellous bone, the light and dark layers increase in thickness, and the layering coincides with the growth marks. The congruence between layers and growth marks is not that clear in the internal-most part of the internal cortex. Here, bone lamellae that have predominantly small round-shaped bone cell lacunae alternate with bone lamellae, in which the bone cell lacunae are flat and elongated, thus indicating that the lamellar bone tissue has an orthogonal plywood structure. Canaliculi are seldom found. Sharpey's fibres are present throughout the whole of the internal cortex in the thin-section of the sampled hypoplastron. In the costals, Sharpey's fibres are restricted to

areas next to the incorporated ribs. Sharpey's fibres were not found in the thin-sections of the sampled peripheral and the neural.

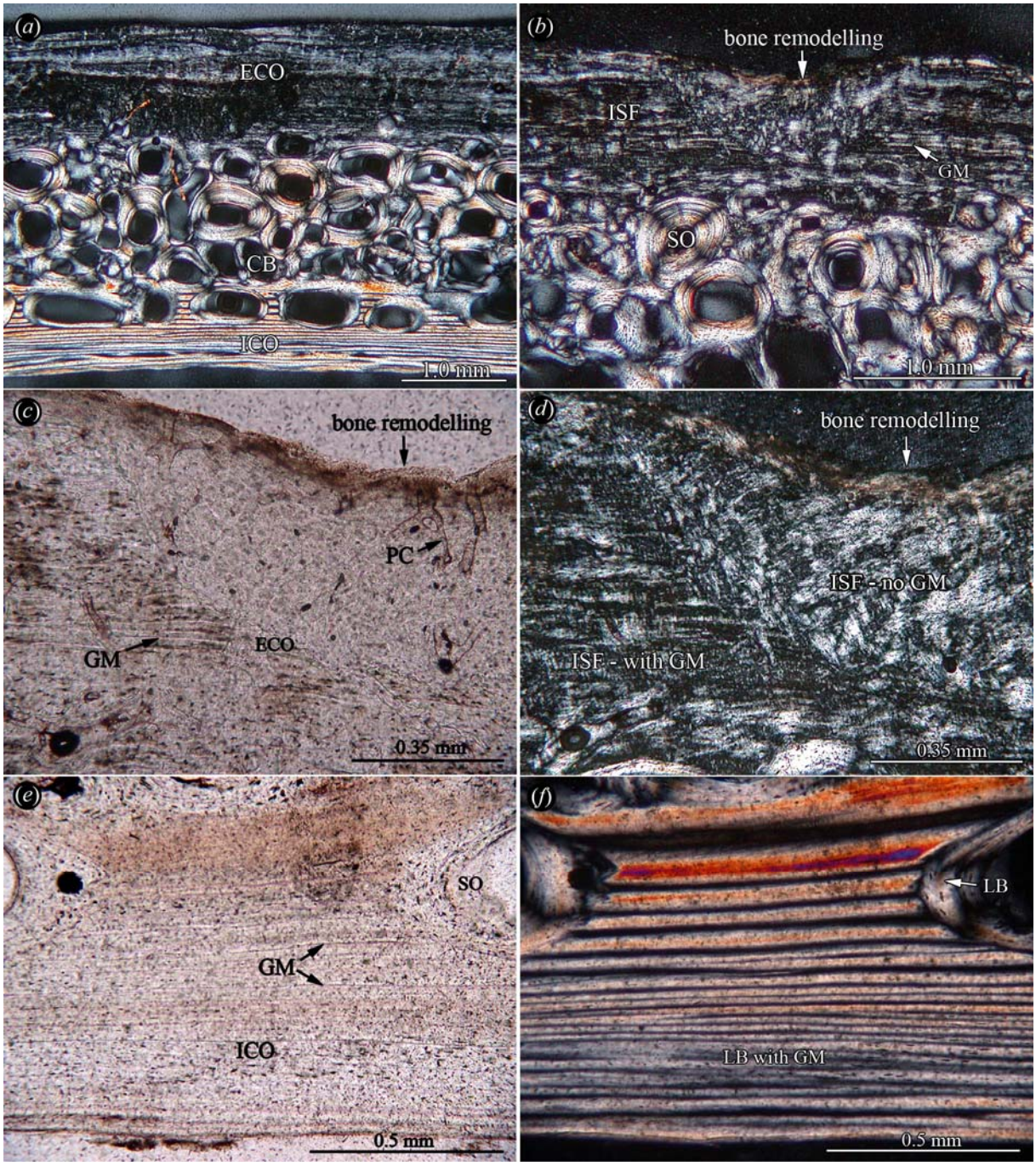

Figure 27: Shell bone histology of *Podocnemis erythrocephala*. (*a*) Thin-section of sampled costal YPM 11853 in polarised light. The diploe structure of the shell is clearly visible. Cortices are of similar size and show growth marks. The interior cancellous bone is largely remodelled by secondary osteons. (*b*) Detail of external cortex in polarised light showing a succession of growth marks in the interwoven fibrous bone tissue disturbed by a semicircular

area of secondary bone remodelling. Close-up of the margin of remodelled area in (*c*) normal transmitted light and (*d*) in polarised light. Note the scalloped line and adjacent bone cell lacunae between the primary tissue with growth marks and the secondary bone. The remodelled area of bone also constitutes interwoven structural fibres, but growth marks are not present. Detail of internal cortex in (*d*) normal and in (*e*) polarised light. Note the growth marks in the lamellar bone tissue and the clearly distinguished light and dark layering of the cortical bone. Light and dark layers in the internal part of the cortex do not always coincide with the growth marks, but constitute lamellae of the lamellar bone tissue.

6.2.4.3 *Stupendemys geographicus* Wood, 1976 (†)

Both costal fragments and the neural fragment have a diploe structure, typical for turtle shell bones, in which well developed internal and external compact bone layers frame an area of cancellous bone. In all three specimens, some of the compact bone layers together with scattered secondary osteons observed in the external and internal cortices are partly eroded.

External cortex—The external cortex of the costals and the neural is a compact bone layer with moderate vascularisation. Right at the bone surfaces, the cortex is mainly composed of fibrous bone tissue interspersed with few primary osteons and large scattered secondary osteons (Fig. 28a, b). Secondary osteon clusters are not developed in the external cortex. The loosely packed interwoven collagen fibre bundles in the cortical bone extend predominantly diagonally through the bone matrix towards the surface of the bone (Fig. 28b). Fibre bundles that extend perpendicular to the external surface of the bone are also present in the interwoven matrix of structural fibre bundles. Cyclical incremental growth marks within the fibrous bone tissue, distinct from lines of arrested growth of periosteal lamellar-zonal bone endoskeletal bones, can be recognised in most areas of the cortex of the neural, while the few growth marks in the costal fragments are mostly discontinuous and not as easily discerned. Towards the midline of the neural, growth marks are also difficult to follow, because the mid-region of the cortex of the neural is slightly crushed. A gradual increase in the amount and in size of the secondary osteons is recognised towards the internal cancellous parts of the bony plates. In the costals, vascular spaces have flattened shapes with long-axes subparallel to the external surface of the bone. In the neural though, Haversian canals of the secondary osteons are mostly round in shape with secondary osteons trending anteroposteriorly through the neural.

Bone cell lacunae within the cortex are mostly of a flattened and elongated shape. In general, the cortical bone cell lacunae bear longer canaliculi than the bone cell lacunae found in the interior cancellous bone tissue. In the neural, Sharpey's fibres insert into the ISF of the bone tissue at moderate angles. They point towards medial on both sides of the midline. The fibre orientation could not be reconstructed in the regions right at the midline of the neural where the bone is slightly crushed. Due to the poor preservation of the bone, it cannot be stated with certainty whether Sharpey's fibres are also present within the external cortices of the costal fragments.

Cancellous bone—The cancellous bone of the costals is composed of thick trabeculae of rather uniform appearance (Fig. 28c). Overall, the bone trabeculae and vascular spaces are evenly distributed in the cancellous bone. Only in a few cases do the spaces between the trabeculae coalesce to form larger vascular cavities. The trabeculae themselves are composed of centripetally deposited secondary bone lamellae. Towards the external and internal cortices, the vascular spaces are dorsoventrally flattened. They are rounder towards the interior of the bone. Flattened and elongated bone cell lacunae and ISF are restricted to interstitial areas of the trabeculae where remnants of primary fibrous bone tissue are preserved. The cancellous interior of the neural fragment is similarly composed of short and rather thick bone trabeculae. This gives the neural a massive and moderately vascularised appearance in cross-section. The trabeculae become thinner and more fragile towards the internal surface of the bone. In the lower part of the neural, along the midline, the trabecular system has collapsed. The largest vascular spaces within the whole of the neural fragment are found in the centre of the cancellous bone.

Internal cortex—Similar to the external cortex, the internal cortex of all fragments is composed of two zones of different bone tissue. Towards the interior of the shell, the compact layer of bone is composed of scattered secondary osteons or secondary osteon clusters (Fig. 28c, d). Towards the internal surface of the bone elements, the cortical bone constitutes fibrous bone tissue. The transition between the two zones is rather sharply defined. Small pockets of primary fibrous bone tissue are also seen in spaces in between the secondary osteons (Fig. 28d). The fibrous bone tissue of the internal cortex is characterised by loosely packed structural collagenous fibre bundles that are orientated either subparallel or obliquely to the internal surface of the bone fragment. Few collagenous structural fibre bundles, which insert perpendicular to the internal surface of the bone, cross the fibrous tissue thus creating

an interwoven appearance. Due to erosion of the cortices of the costal fragments, the thickness of this internal tissue type varies strongly. Besides few scattered primary osteons and erosion cavities, the fibrous bone is mainly avascular.

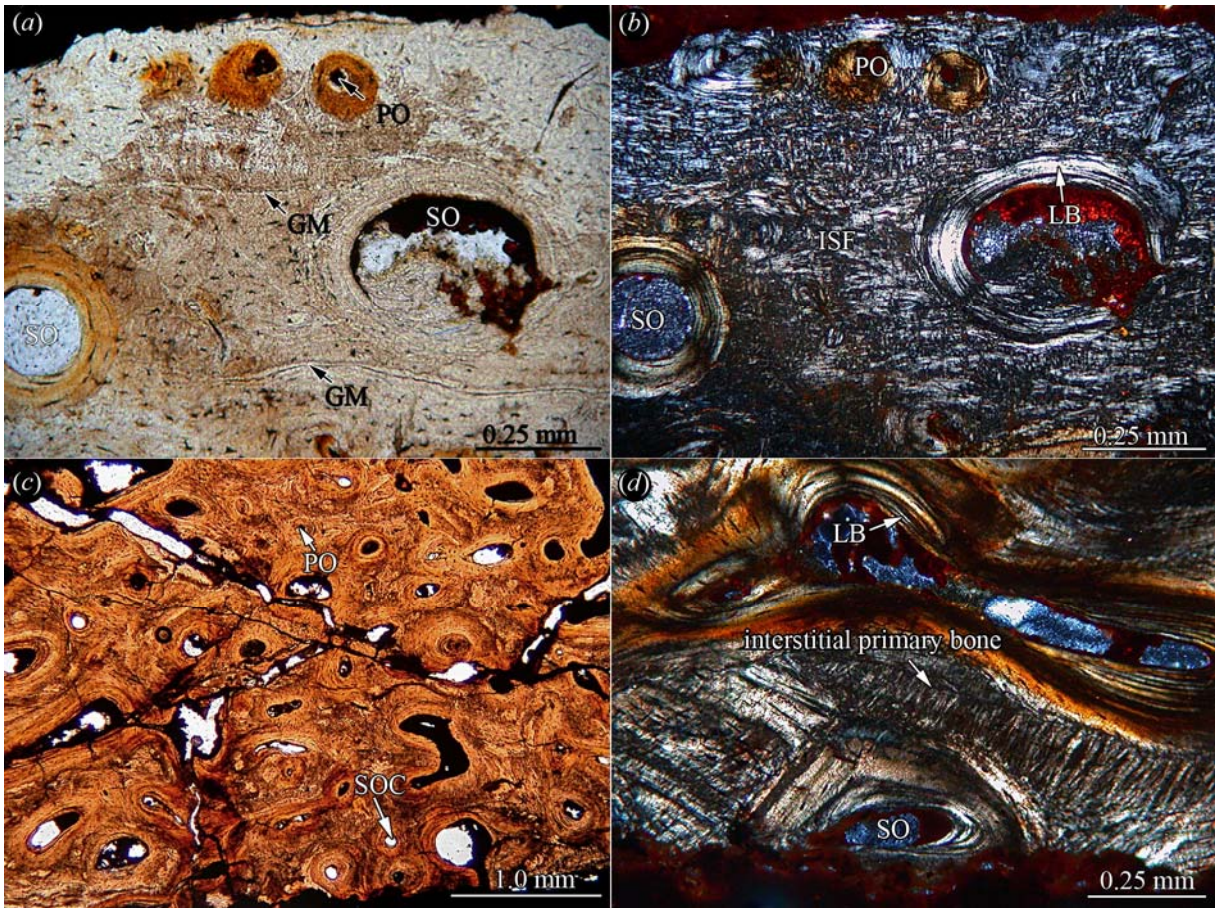

Figure 28: Shell bone histology of *Stupendemys geographicus*. (*a*) Close-up of external cortex of the sampled neural fragment (UNEFM−101) in normal transmitted light. The cortical bone is vascularised by primary and secondary osteons. Growth marks occur throughout the external cortex. (*b*) Another section of the external cortex of the former specimen in polarised light. The external cortex consists of a bone matrix of interwoven structural fibre bundles with scattered primary and secondary osteons. (*c*) Internal cortex and part of the interior cancellous bone of costal fragment A (UNEFM−CIAPP−2002−01) in normal light. Note areas of strong remodelling in the internal cortex where the cortical bone is dominated by secondary osteon clusters. (*d*) Another section of the internal cortex of the former specimen in polarised light. Note that interstitial areas of primary bone tissue in between the osteon clusters are also composed of interwoven structural fibre bundles.

It could not be discerned if Sharpey's fibres *sensu stricto* are present within the interwoven fibrous tissue of the internal cortex of the costals. In the neural fragment, the internal cortex is composed of scattered secondary osteons that become dense towards the midline of the fragment. The cortex appears quite massive in the areas in which they are vascularised by Haversian canals. Medially in the neural fragment, remnants of the incorporated neural arch can be observed. The bone of the incorporated neural arch is composed of tightly clustered secondary osteons. Here, the cell lacunae have a flattened and elongated shape. The roof of the vertebral canal is not seen in the thin-section because the bone is damaged and eroded in this area. Sharpey's fibres crossing the structural collagenous fibres seem to be present in the areas around the incorporated neural arch, but their presence is not as conspicuous as in the external cortex. Remnants of compact bone layers slightly internal to the internal cortex are still traceable through the whole width of the neural fragment. These horizontally trending bone layers remain visible even though they have been extensively interrupted by newly formed bone trabeculae and large scattered secondary osteons.

6.2.5 Chelidae

6.2.5.1 *Emydura subglobosa* (=*Emydura albertisii*) (Krefft, 1876) and *Emydura* sp. (†)

The sampled shell bones show all the same diploe structure with external cortical bone and internal cortical bone framing an interior area of cancellous bone. The internal cortical bone may be reduced in thickness compared to the external cortical bone. While the surface of the internal cortical bone is smooth, the surface of the external cortical bone has small humps and shallow grooves related to the ornamentation pattern described above in the 'Material and Methods' section.

External cortex—The external cortical bone comprises a compact bone tissue of interwoven structural ISF (Fig. 29a, b). Vascularisation is realised by a mixture of primary and secondary osteons and primary vascular canals. The primary vascular canals are reticular and anastomosing with no apparent dominant orientation (Fig. 29c). The primary vascular canals also extend to the surface of the bone. Only the external-most part of the external cortex shows cyclical incremental growth marks and fibre bundles that trend perpendicular to the

bone surface. In the interior-most parts of the external cortex, perpendicular fibres are unobtrusive within the ISF. Bone cell lacunae are abundant in the external cortex. They are mostly round and plump in shape without canaliculi, but they get more compressed and elongated towards the external-most layer showing the growth marks. The cell lacunae are usually following the orientation of the fibre bundles.

Cancellous bone—The cancellous bone is mostly remodelled with remnants of interstitial primary bone tissue (Fig. 29d). The trabeculae are lined with lamellar bone towards the bone cavities. Slightly flattened and elongated bone cell lacunae follow the centripetally deposited lamellar bone linings, but rounder bone cell lacunae are clustered in the interstitial areas of primary bone. As the cancellous bone area increases in thicker shell elements, the size and length of the bone trabeculae remain thick and short and cavities are rather homogeneous. Only in the thicker elements of *Emydura* sp., the ventral part of the cancellous bone and the interior parts of the sampled peripheral show larger cavities through fusion of smaller vascular spaces. Here, the trabeculae may be longer and are thinner in diameter. A remnant of the progression of the former rib was not found in thin-section. Changes in the thicknesses of the trabeculae were encountered in the peripheral. While the trabeculae were thinner in the proximal part, they increased in thickness towards the distal tip.

Internal cortex—The internal cortex consists of parallel-fibred bone (Fig. 29e, f) that interdigitates with lamellar bone tissue. Erosion cavities lined with lamellar bone sometimes reach well into the internal cortex, otherwise the bone tissue is vascularised with scattered primary vascular canals. In *E. subglobosa*, the internal cortex can additionally be vascularised by regularly scattered primary osteons. Elongated and flattened bone cell lacunae occur sheet-like following the fibrous orientation of the bone. The internal cortical bone was devoid of Sharpey's fibres.

Variation—Variation from the bone microstructure described above is seen in the axillary/inguinal buttress part of the plastron fragment (bridge region of the ?hyo- or hypoplastron). Due to a shift in growth direction, the pillar-like bridge region develops above the level of the rest of the plastral level. Compared to other regions of the cancellous bone, the cavities are larger towards the internal cortex here. Furthermore, remnants of former internal cortex indicate earlier growth stages of this shell element. While the current stage of the internal cortex exhibits only a few scattered primary osteons, the interior earlier stages of the

internal cortex are now heavily remodelled by single scattered secondary osteons and the development of trabecular bone.

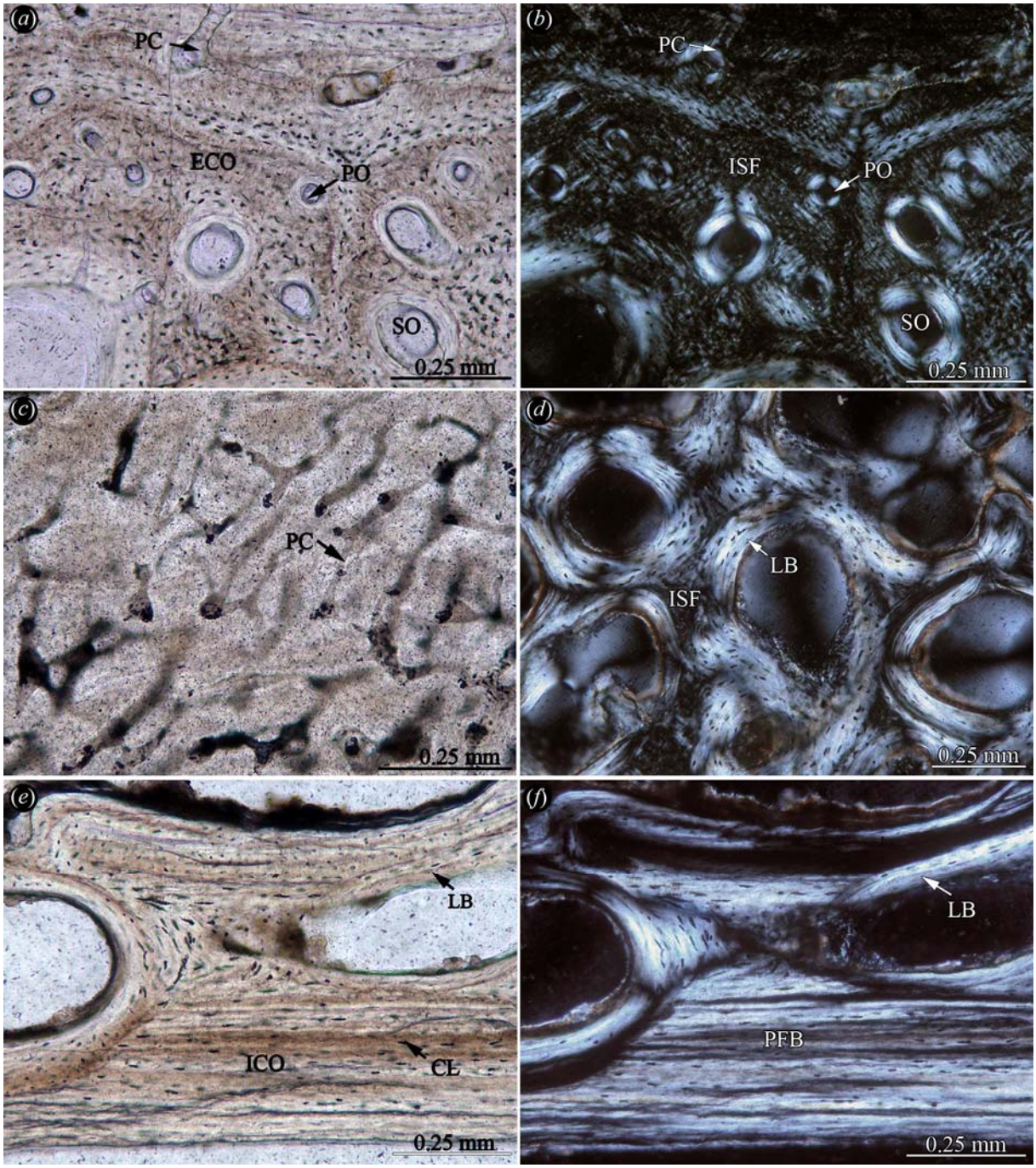

Figure 29: Shell bone histology of *Emydura* spp. Detail of the external cortex of costal UCMP V5762/57055 (x-section) of *Emydura* sp. in (*a*) normal light and (*b*) in polarised light. The bone tissue is vascularised by primary and secondary osteons and primary vascular canals. (*c*) Close-up of the external cortex of the sub-sampled costal ZFMK58215 (drilled core) of *Emydura subglobosa* in normal transmitted light. Note reticular vascularisation of the bone

tissue. (*d*) Close-up of the strongly remodelled cancellous bone of costal UCMP V5762/57055 (L-section) of *Emydura* sp. in polarised light. Detail of internal cortex in (*e*) normal and in (*f*) polarised light.

6.2.5.2 *Chelodina longicollis* (Shaw, 1794)

The bone core samples show a diploe built of the shell in *C. longicollis*. The internal cortex is thinner than the external cortex. In the carapacial core, the sutured margins of the costal to the adjacent costals are visible. The costals are thinnest at the sutures and gain in thickness towards the centre of the plate, where the progression of the rib is seen as an internal bulge of the internal cortex. The thin epidermal keratin shield follows the general sculpture of the external bone surfaces. A thin layer of unossified connective tissue fills the space between the shield and the underlying bone, and smaller rugosities of the bone surface are thus also compensated.

External cortex—The external cortex constitutes a bone tissue consisting of ISF (Fig. 30a, b). Vascularisation is moderate with primary osteons and reticular primary vascular canals. Fibre bundles that insert perpendicular into the external cortex are not observed. Only at the sutured margins of the plates, long parallel fibre bundles, inserting perpendicular to the sutures, are incorporated into the bone tissue.

Cancellous bone—The trabeculae in the cancellous bone are irregular. They are mostly short and thick in diameter (Fig. 30c, d). The walls of the trabeculae consist of lamellar bone. The largest vascular spaces occur towards the internal cortex, while the more externally situated spaces are of smaller size. Roughly in the centres of the vascular spaces, clumped and dried yellow-brown adipose tissue is present.

Internal cortex—The internal cortex comprises parallel-fibred bone (Fig. 30c, d). The tissue is mainly avascular. Flattened and elongated bone cell lacunae follow the bone layers, thus they appear in a sheet-like arrangement in the parallel-fibred bone.

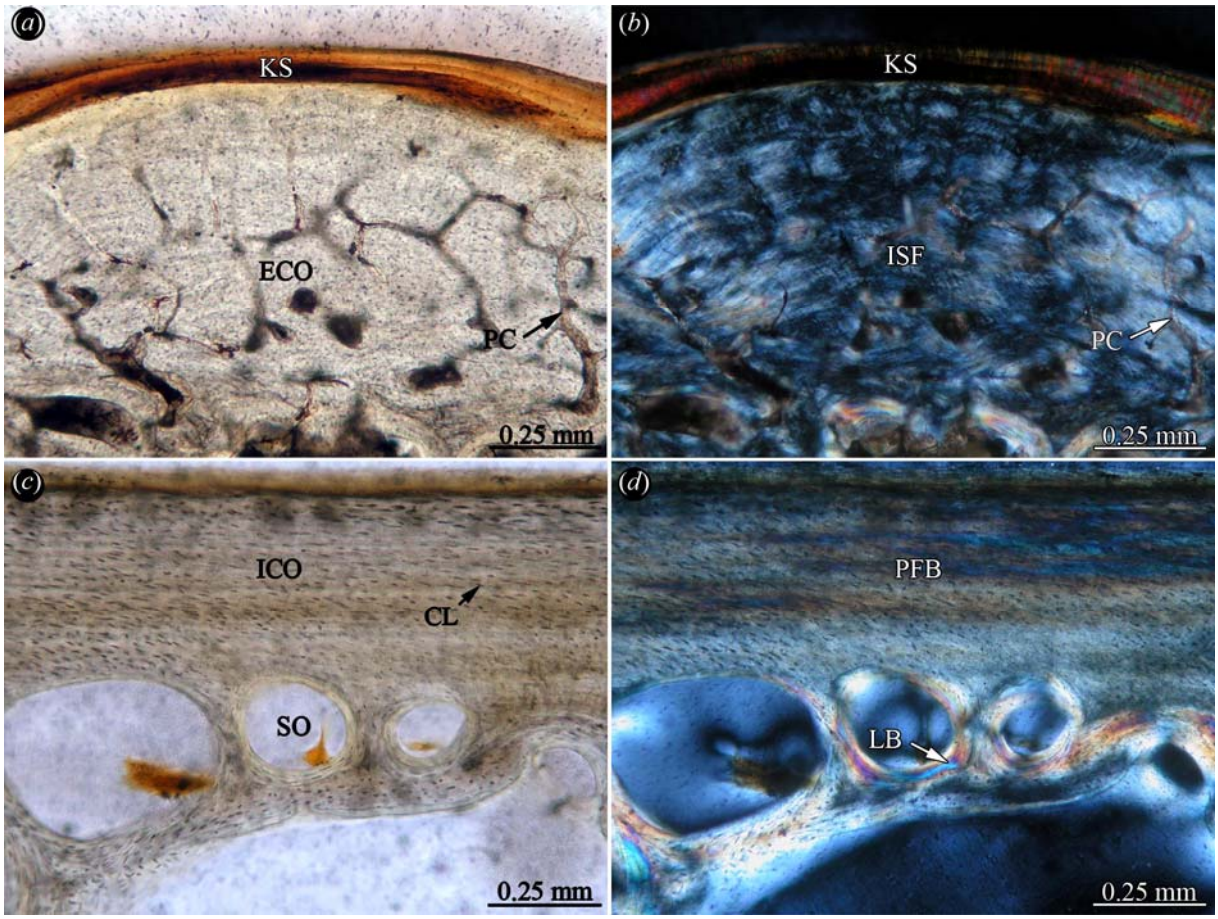

Figure 30: Shell bone histology of *Chelodina longicollis*. Detail of the external cortex of left ?costal2 (ZMB 27258, drilled core) and associated kerationous shield in (*a*) normal light and (*b*) in polarised light. Note reticular vascularisation pattern (*c*) Close-up of the internal cortex and adjacent cancellous bone of the sub-sampled right hyoplastron (ZMB 27258, drilled core) in (*c*) normal and in (*d*) polarised light. The internal cortex consists of parallel-fibred bone, while the predominantly remodelled bone trabeculae consist of lamellar bone.

6.2.5.3 *Platemys platycephala* (Schneider, 1791)

In the case of the core intersecting the costals and the vertebral centrum, the part of the right costal2 is strongly curved due to the coring site being located on one of the two prominent carapacial ridges. The core from the hypoplastron is located in the proximal flat part of the shell element and does not include the inguinal buttress of the bridge region. The cored bone shows a sandwich-like build with similarly thick external cortex (0.3-0.45 mm) and internal cortex (0.25-0.35 mm) framing an interior area of cancellous bone. Generally, the bone cell lacunae density is very low throughout the whole of the sampled bones.

External cortex—The bone surface of the external cortex is covered with small raised humps (<0.1mm in height). The bone tissue consists of ISF. The fibre bundles of the ISF are of similar length and size. The fibre bundles in the ISF trend diagonally and perpendicular to the dorsal bone surface. Vascularisation is achieved mainly by primary osteons. Especially the diagonally arranged fibre bundles of the ISF seem to surround and frame the primary osteons.

Cancellous bone—The cancellous bone consists of primary trabeculae that are secondarily remodelled. The vascular spaces are lined with secondary lamellar bone. In areas of increased shell bone thickness, the trabeculae with dorsoventral orientation slightly dominate the cancellous bone, thus leading to dorsoventrally elongated vascular cavities. The bone cell lacunae seem to be restricted to the primary bone tissue of interstitial areas within the bone trabeculae.

Internal cortex—The internal cortex constitutes parallel-fibred bone. Fibre bundles are arranged diagonally to the surface of the bone in a few areas. Few primary vascular canals pervade the bone tissue horizontally, subparallel to the internal surface of the bones.

Transition between costals and vertebral centrum—Variation in the histology is observed in the transition between the costals and the associated vertebral centrum. Here the bone tissue is substituted by a very fibrous non-ossified connective tissue between the internal cortex of the costal and the remaining bone of the transverse process of the vertebra. The bone of the vertebral centrum itself is reduced to a thin bony rim. Two horizontally arranged kidney-shaped cavities open up between the transverse processes of the vertebral arch, the free rib head of the costal plates and the internal cortex of the costal plates. A thin layer of non-ossified connective tissue trends dorsally from one kidney-shaped cavity to the other, thus dividing the internal cortex of the costals from the vertebral arch. The suture between the right and left costal2 lies sagittal above the vertebral column. Its sutural space is filled with connective tissue and numerous ovoid cell-like structures with circular central depressions, presumably blood cells. Due to the reduction of the centrum to a thin bony rim, the vertebral canal increases significantly in diameter, thus comprising a third large cavity of oval to circular shape (tube-like in lateral view) dorsal and sagittal to the reduced centrum.

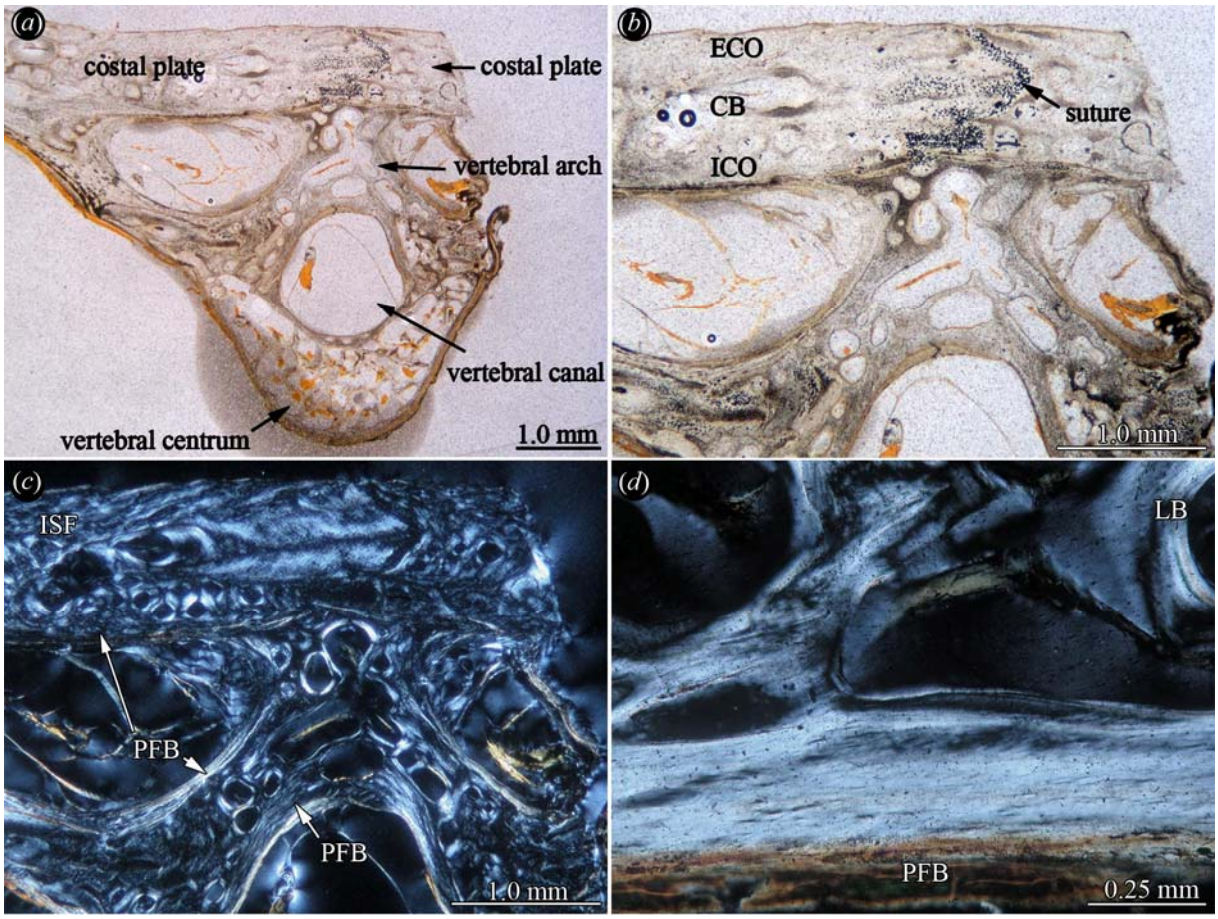

Figure 31: Shell bone histology of *Platemys platycephala*. (*a*) Section of the sampled neural2 (including the vertebral centrum) and proximal part of left costal2 (SMNS 10035) in normal light. Note that the costals meet in the midline over the centrum. A neural is absent. Close-up of the suture zone between the costals and the associated neural arch.in (*b*) normal and in (*c*) polarised light. (*d*) Detail of the parallel-fibred bone of the internal cortex of the costal of the former specimen.

6.2.5.4 *Phrynops geoffroanus* (Schweigger, 1812)

The external and internal cortices of the sampled shell elements of *P. geoffroanus* were of similar thickness and they are framing interior cancellous bone. A slight decrease in thickness of the cortices is observed from the proximal to the distal part of the costal. In cross-section (anteroposterior orientation), the internal cortex of the costal is thickest in the mid-part of the section (former progression of the rib) and gets reduced towards the lateral sutures.

External cortex—The bone surface of the external cortex is rough, resulting from primary vascular canals that open up to the surface of the bone as small foramina. The primary vascular canals have reticular and anastomosing patterns throughout the whole cortical tissue, with horizontally arranged primary vascular canals being more abundant compared to vertically arranged canals (Fig. 32a). The bone tissue is composed of ISF. The matrix of fibre bundles in the ISF is pervaded by primary osteons. Perpendicular fibres are present but inconspicuous among the ISF. Clusters of round and plump bone cell lacunae interdigitate with sheets of poorly elongated cell lacunae. Canaliculi are absent in both round and elongated cell lacunae.

Cancellous bone—The bone trabeculae are predominantly secondary in nature, but interstitial areas within the trabeculae are still composed of primary bone (Fig. 32b, c). Bone cell lacunae are plump and round in shape in the primary bone. Vascular cavities are lined with centripetally deposited secondary lamellar bone, in which flattened cell lacunae follow the direction of the bone lamellae. Vascular spaces and bone trabeculae are proximodistally elongated in the longitudinal section of the costal.

Internal cortex—The internal cortex consists of a mixture of parallel-fibred and lamellar fibred bone (Fig. 32d). The growth marks present are not as distinct as lines of arrested growth. While the internal-most layer of the internal cortex is almost free of bone cell lacunae, they get more frequent towards the interior parts of the internal cortex. Bone cell lacunae that occur in sheets in the bone tissue of the costal are elongated and strongly flattened in anteroposterior section and of slightly flattened to circular shape in proximodistal section.

Sutural areas—The sutural areas of all elements are composed of a bone tissue similar to that found in the external cortex (Fig. 32b, c). However, the bone tissue is dominated by fairly long, horizontal fibre bundles. These fibre bundles form in the external-most and internal-most zones of the cancellous bone and run horizontally into the sutures, thus trending perpendicular to the lateral bone surface of the shell elements. Horizontally arranged compact bone tables also reach from the interior of the bone into the sutural regions. The stacks of these compact bone tables are often vascularised by secondary osteons.

Neural—The bone histology of the neural of strongly influenced by the outer shape of the bone. While the lateral part of the neural (the flat plate part) consists of external cortex, cancellous bone, internal cortex and the sutural areas described above, the medial parts of the internal cortex deviate towards ventral to the lateral surfaces of the incorporated neural arch. A large central cavity opens up right between the cortical bone layers of the shaft of the neural arch. Dorsal and ventral to the cavity lies cancellous bone. A thickened, domed pad of compact bone, pervaded by dorsoventrally trending fibre bundles, below the ventral area of cancellous bone forms the roof of the vertebral canal. Secondary remodelling is spreading within the compact bone layer, with vascularisation following the trend of the compact bone layers. The ventral-most part of the neural consists of the lateral bases of the neural arch. A thin layer of cartilage still caps these bases, thus the neural arch was not fused to the centrum.

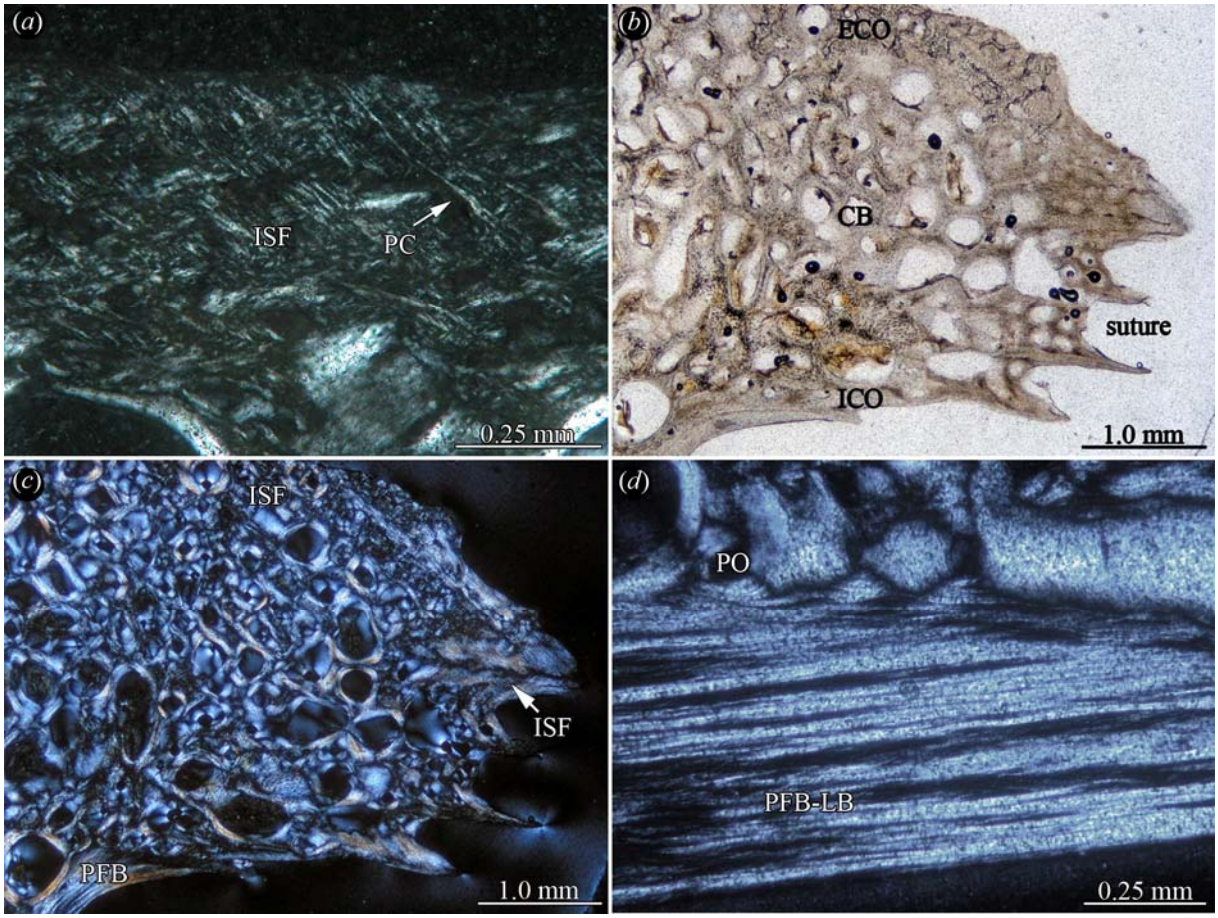

Figure 32: Shell bone histology of *Phrynops geoffroanus*. (*a*) Section of the interwoven structural fibre bundles of the external cortex of the sampled peripheral3 (YPM 12611) in polarised light. (*b*) Close-up of the interior cancellous part and the suture zone of the neural (YPM 12611) in normal and in (*c*) polarised light. (*d*) Detail of the internal cortex of the

costal (YPM 12611, L-section) in polarised light. Note parallel-fibred bone interdigitating with lamellar bone.

6.2.5.5 *Hydromedusa tectifera* Cope, 1870a

The core samples of *H. tectifera* show the diploe structure with external and internal cortices having similar thicknesses. Below the thin epidermal keratin shields, the external sculpturing of the sub-sampled costal has a low relief.

External cortex—The external cortex consists of ISF (Fig. 33a, b). Diagonally arranged fibre bundles dominate the ISF. Small to moderate amounts of fibre bundles that extend perpendicular or in high angles towards the external bone surface are present. The bone tissue is vascularised by scattered primary osteons and primary vascular canals. The primary vascular canals can anastomose and locally, a reticular pattern can be developed. Growth marks occur, but they are mostly too obscure to be counted (partly because of the high collagen content of these recent samples).

Cancellous bone—The cancellous bone is not well developed in the samples. Irregularly arranged trabeculae are short and thick, dividing small vascular spaces (Fig. 33c). Slightly larger vascular spaces are found towards the internal cortex. Most of the vascular spaces show remnants of clumped dried brown adipose tissue. The walls of the trabeculae consist of lamellar bone. Interstitial primary bone tissue is found in larger branching areas of the trabeculae. Bone cell lacunae in the lamellar bone are flattened and elongated, while they are more plump and of circular shape in the interstitial bone.

Internal cortex—In the sub-sampled costal, the internal cortex is thickest in the region of the rib bulge and decreases slightly in thickness towards the lateral sutures of the costal plate. The internal cortex constitutes parallel-fibred bone (Fig. 33d). In both areas lateral to the progression of the rib, Sharpey's fibres insert in the avascular cortical bone tissue at moderate to high angles.

Variation—The only variation between the samples is the decrease of the thickness of the internal cortex in the costal. However, this seems closely tied to the outer morphology (i.e., incorporated rib) of the shell element.

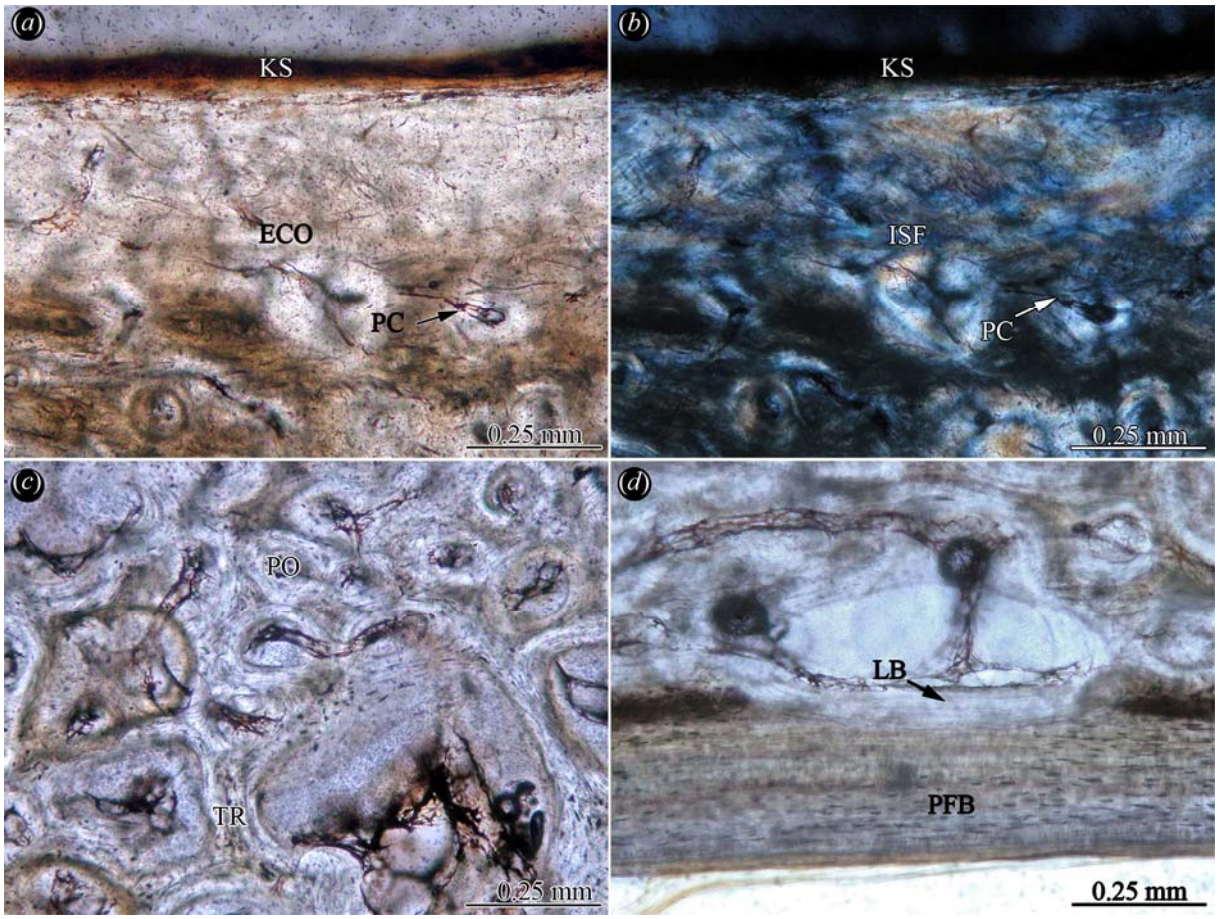

Figure 33: Shell bone histology of *Hydromedusa tectifera*. Close-up of the external cortex and the external part of the cancellous bone of the sub-sampled left ?costal2 (ZFMK-51656, L-section) in (*a*) normal and in (*b*) polarised light. The keratinous shield is still attached to the costal bone. The bone tissue is mainly vascularised by primary vascular canals. (*c*) Close-up of the interior cancellous bone of the former specimen in normal light. (*d*) Detail of the internal part of the cancellous bone and the parallel-fibred matrix of the internal cortical bone of the former specimen in polarised light.

6.2.5.6 *Chelus fimbriatus* (Schneider, 1783)

C. fimbriatus shows among the strongest histological variation between the carapacial and plastral samples of all turtles studied (Fig. 34a, b, e, f). But, again, this variation is strongly

connected to the outer morphology of the elements. No bone sutures were sampled by the drilling process. While the dorsal, external bone surface of the peripheral is covered with a very rough and irregular and often flaky keratin shield, the ventral external surface of the bone is covered with a rather smooth and regular keratin shield instead. The ventral compact bone of the peripheral has the same surface texture as the dorsal compact bone. The internal (towards visceral) cortex of the peripheral was not sampled by the core-drilling. In both the costal and the peripheral, the interface between the keratinous shields and the underlying bone is quite strong, whereas the keratinous shield covering the hyoplastron was easily removable from the bone core. The layer of connective tissue between the keratin shield and the bone of hyoplastron is remarkably thin.

External cortex—The dorsal external bone surfaces of the costal and the peripheral shows a strong topology with humps and ridges (Fig. 34a, b). The connective tissue between bone and keratinous shield either fills in topological differences or it amplifies existing undulations in the topology leading to small humps in the shield cover. The larger humps/ridges of the costal and peripheral are based on variations in thickness of the external cortex. The rough texture of the bone of the hyoplastron is based on the presence of primary vascular canals opening up to the surface of the bone. These primary vascular canals are not as frequent in the costal and the peripheral. The bone tissue itself of all elements is composed of ISF. Within the ISF, the fibre bundles are of similar length and thickness, leading to a uniform spatial arrangement that is vascularised by large amounts of primary osteons and primary vascular canals. The fibre bundles equally trend perpendicular, subparallel and diagonal to the surface of the bone. The anastomosing and branching primary vascular canals form a kind of reticular vascularisation pattern. Sharpey's fibres are present only in some of the humps and ridges of the external cortex. The arrangement of bone cell lacunae that lack canaliculi is irregular with a mixture of clusters and sheets that strongly depend on the fibre bundles arrangement in the external cortex.

Cancellous bone—The transition between the external and internal cortical layer and the interior cancellous bone is rather distinct instead of having interlaced intermediate zones. The trabecular bone is still largely primary with little secondary reconstruction. The larger cavities between the trabeculae are secondarily lined with lamellar bone (Fig. 34b), and secondary osteons are found in more compact areas. Bone cell lacunae are usually restricted to the internal areas of the bone trabeculae and areas of anastomosing trabeculae. Many cavities of

the cancellous bone show remnants of adipose tissue that is now shrunken due to preparative processes.

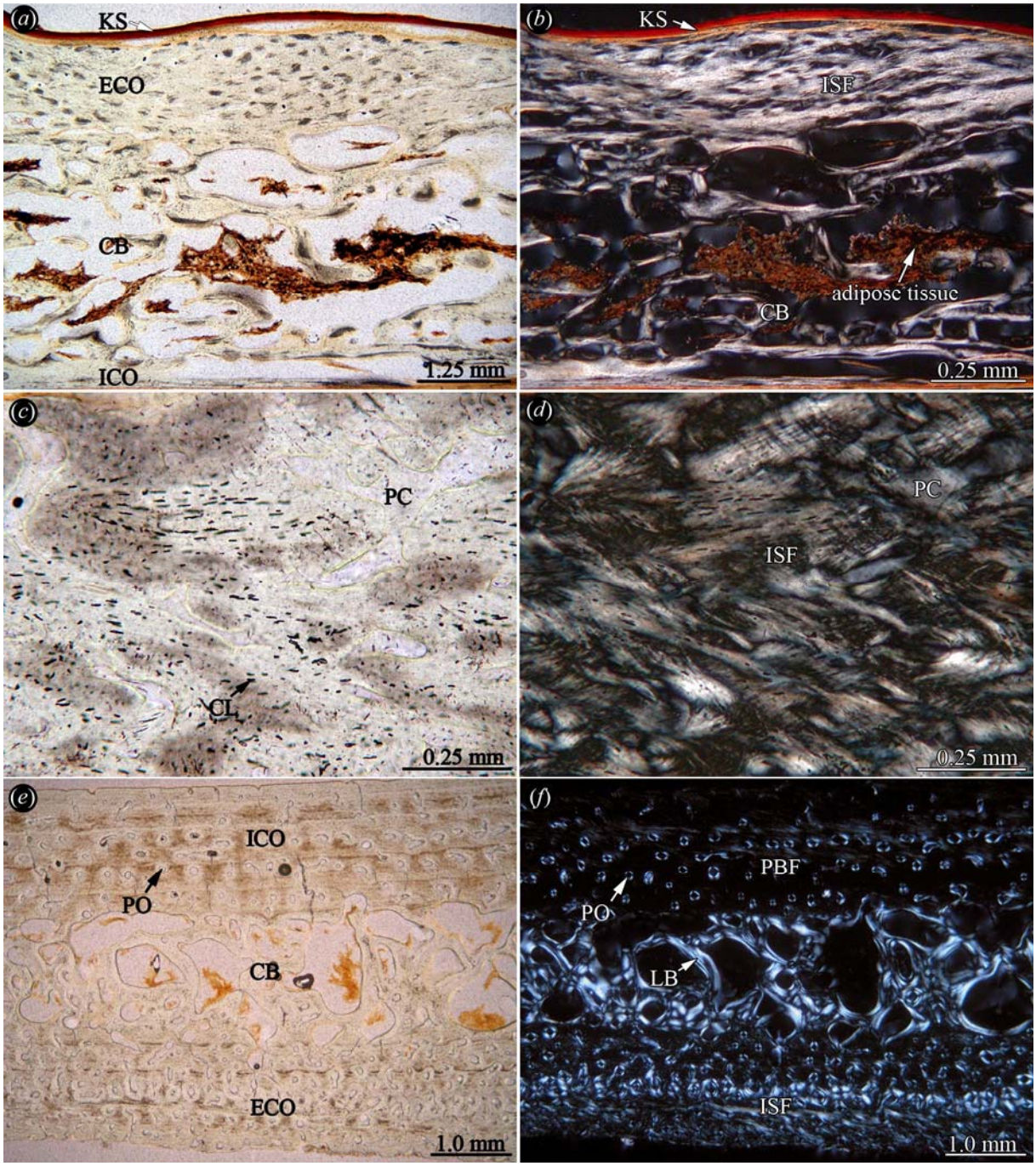

Figure 34: Shell bone histology of *Chelus fimbriatus*. Section of the diploe structure of the sub-sampled costal (FMNH 269459, drilled core) in (*a*) normal and in (*b*) polarised light. The epidermal keratinous shield is still attached to the bone. Note strong fluctuation in external cortical bone thickness and the strongly reduced internal cortex. Close-up of the interwoven structural fibre bundles of the external cortex in (*c*) normal and in (*d*) polarised light. Section

of the sub-sampled right hyoplastron (FMNH 269459, drilled core) in (*e*) normal and in (*f*) polarised light. Note differences in cortical thickness compared to the costal sections of (*a*) and (*b*).

Internal cortex—The surface of the internal cortex of the costal and the hyoplastron is smooth. The internal cortical bone of the costal is composed of parallel-fibred bone. The internal cortex of the hyoplastron has parallel-fibred bone interlaced with areas similar to ISF found in the external cortex. However, the fibre bundle arrangement is dominated by fibre bundles that trend obliquely to the internal bone surface towards the axillary buttress of the hyoplastron, whereas horizontally arranged fibre bundles and fibre bundles that trend perpendicular to the surface of the bone are rare. The vascularisation in the internal cortex is high. In the costal, the bone tissue is mainly vascularised by primary canals and few primary osteons. In the hyoplastron, primary osteons are much more common (Fig. 34e, f). The primary osteons are of similar diameter and stringer-like. They are evenly spaced throughout the successive parallel-fibred layers of the internal bone tissue. Secondary osteons are not found within the bone tissue of both costal and hyoplastron. Bone cell lacunae are more evenly distributed in the internal cortex compared to the external cortex, and they are aligned subparallel to the surface of the bone. The bone cell lacunae are flattened and elongated and lack canaliculi.

6.3 Cryptodira

6.3.1 Cryptodira incertae sedis (Kirtlington turtle sample, Solemydidae)

6.3.1.1 Cryptodira incertae sedis (Kirtlington turtle sample) (†)

Two histomorphs are present in the sample of the Kirtlington turtles. Histomorph I is represented by six specimens (IPB R583-588), while histomorph II is represented only by a single specimen (IPB R589). Histomorph I has essentially the same bone histology as that described for pleurosternid turtles (see chapter 6.3.3 below), therefore I refrain from giving a repetition at this point. Histomorph II, on the other hand, shows fundamental differences to

the pleurosternid taxa and thus will be described in this section. The external and internal cortex in the diploe structure of histomorph II are well developed and of equal thickness (Fig. 35a).

Histomorph II: External cortex—The external cortex is composed of ISF (Fig. 35b). The ISF has a homogeneous distribution of fibre bundles that extend perpendicular, sub-parallel and oblique to the external surface of the bone. The bone tissue is mainly vascularised by primary osteons and primary vascular canals. Many of the canals open up to the external surface of the bone. Growth marks are weakly developed and difficult to follow in the bone tissue. The transition to the cancellous bone is not clearly defined because of the amount of scattered secondary osteons and erosion cavities.

Histomorph II: Cancellous bone—The interior cancellous bone consists of short but overall slender bone trabeculae and cavities of small to moderate size (Fig. 35c). The vascular cavities are round to irregular shaped. Many of the trabeculae still retain primary bone tissue, i.e., ISF, but they are mostly lined with secondary lamellar bone.

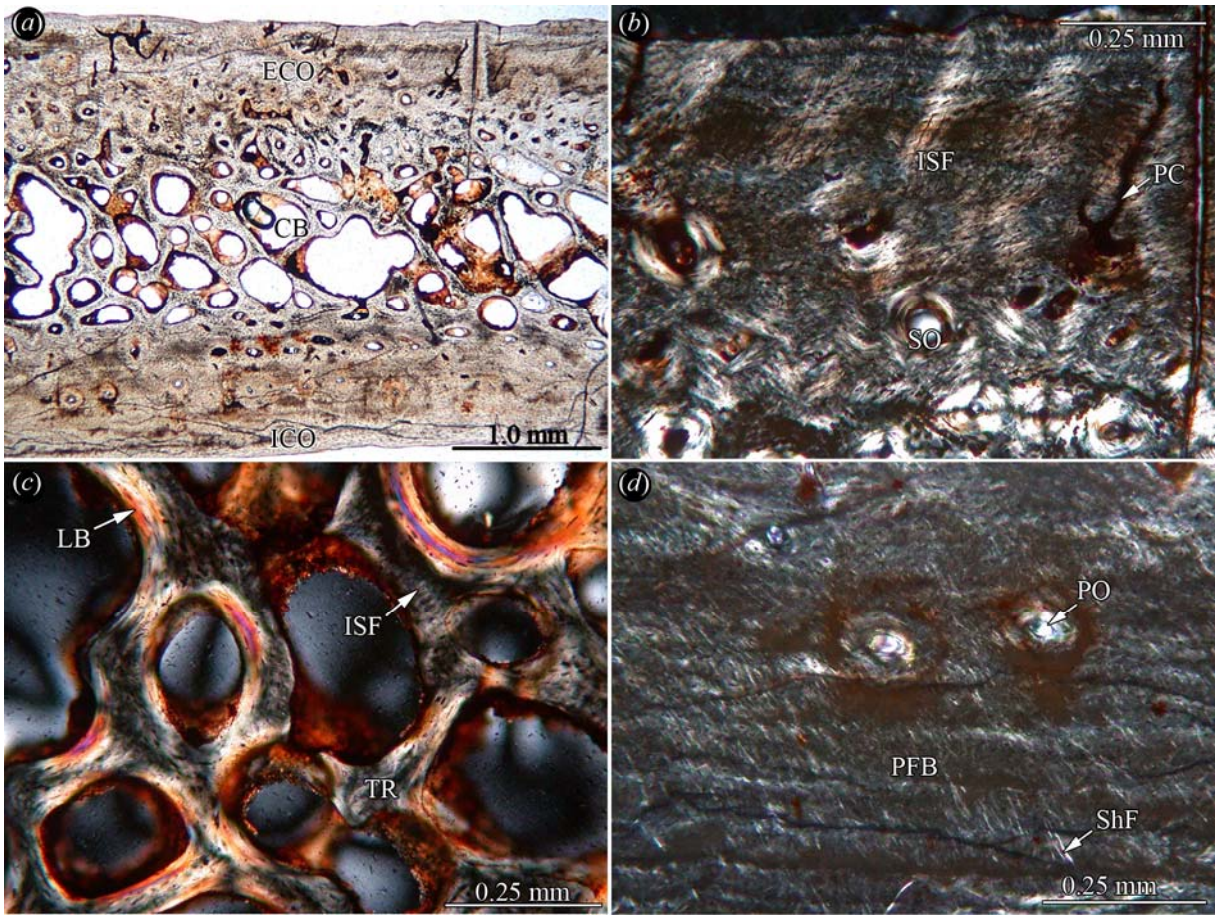

Figure 35: Shell bone histology of Kirtlington turtle sample histomorph II. (*a*) Section of a plastron fragment (IPB R589; ?hyo- or hypoplastron) in normal light. Note well developed diploe structure. (*b*) Close-up of the external cortex of the bone showing interwoven structural fibre bundles in polarised light. (*c*) Close-up of the interior cancellous bone of the former specimen in polarised light. Note the short but overall slender bone trabeculae. (*d*) Detail of the parallel-fibred matrix and Sharpey's fibres of the internal cortical bone in polarised light.

Histomorph II: Internal cortex—The internal cortex consists of parallel-fibred bone (Fig. 35d). Fibre bundles that extend at oblique angles into the parallel-fibred bone, i.e., Sharpey's fibres, are observed. The bone tissue is weakly vascularised by scattered primary osteons and few primary vascular canals. The most internal layers of the cortical bone are avascular.

6.3.1.2 Solemydidae gen. et sp. indet. (aff. *Naomichelys* sp.) (†)

Several shell elements could be sampled; however, the material was generally fragmentary and in various preservational states. Sutures were not preserved in any of the samples. Only the two isolated osteoderms still had original margins. A diploe with external and internal cortices framing interior cancellous bone is developed. The distinct ornamentation on the external bone surfaces is not only the most characteristic osteological feature of the shell elements, but it also has unique bone histology (Fig. 36a, b).

External cortex—The external cortex constitutes two zones (Fig. 36b). Thickness varies for both zones. In most cases, the external zone and the internal zone seem equally strongly developed. However, in badly weathered shell fragments, the external zone can be highly reduced in thickness. In other cases, i.e., the distal apical region of the peripheral, the interior zone appears only as a thin remnant, while in adjacent parts of the bone the thickness of the interior zone again increases. The more internal zone is composed of thick coarse metaplastic ISF. The ISF matrix is vascularised with scattered short primary vascular canals and primary osteons. The more external, second zone is highly distinctive in comprising a thick layer of parallel-fibred bone matrix and the characteristic external tubercular/columnar ornamentation, also of parallel-fibred bone. Fibre bundles that insert perpendicular to the bone surface are

present in both the parallel-fibred bone matrix and the columns. These fibre bundles are most prominent in the columns and in the areas right next to them, while they are more inconspicuous farther away from the columns. Besides scattered primary vascular canals that mostly extend towards the external surface of the bone, the parallel-fibred bone of the external zone is avascular (Fig. 36a, b). The transition between the two zones is mostly well defined with little transgression. At this transition zone, the ornamental columns originate. Starting as small pillow-like and pustule-like protrusions, they have at first a concentric external growth. Adjacent and in between the columns the first layers of parallel-fibred bone are deposited. With continuing growth of the shell plates, the interstitial areas of parallel-fibred bone and the columns grow in external direction until a maximum diameter of the columns is reached. At the margins of the columns, a tight flexure zone develops where the parallel-fibred bone tissue of the columns and the tissue of the adjacent areas meet. The layers of the latter appear to be dragged towards external though the columnar growth. The growth of the external zone of the external cortex is generally well observable due to cyclical growth marks that are present within the parallel-fibred bone of both the columns and the interstitial areas. While the growth marks are widely spaced at first, the space decreases with continued growth. In the samples of presumably old individuals, the growth marks are tightly spaced adjacent to the external surface of the bone. After the external-most layers of interstitial parallel-fibred bone are deposited, the columns can grow further still, until they protrude from the external bone surface for several millimetres. The growth marks and other histological details are best visible where the plane of sectioning cuts medially through an ornamental column. Bone cell lacunae are generally round in the parallel-fibred bone of the columns, while they are slightly flattened in the parallel-fibred bone of the adjacent areas.

Cancellous bone—The cancellous bone consists of an irregular meshwork of short thick and longer, more slender trabeculae (Fig. 36c). The largest vascular spaces are found in the centre of the interior cancellous bone, while the volume of the vascular spaces is reduced externally and internally. Larger secondary osteons are also developed in the more external and more internal regions of the cancellous bone. The trabecular meshwork is primary, however many trabeculae have been secondarily remodelled. The gross of the bone trabeculae constitutes lamellar bone with generally few flattened and elongated bone cell lacunae.

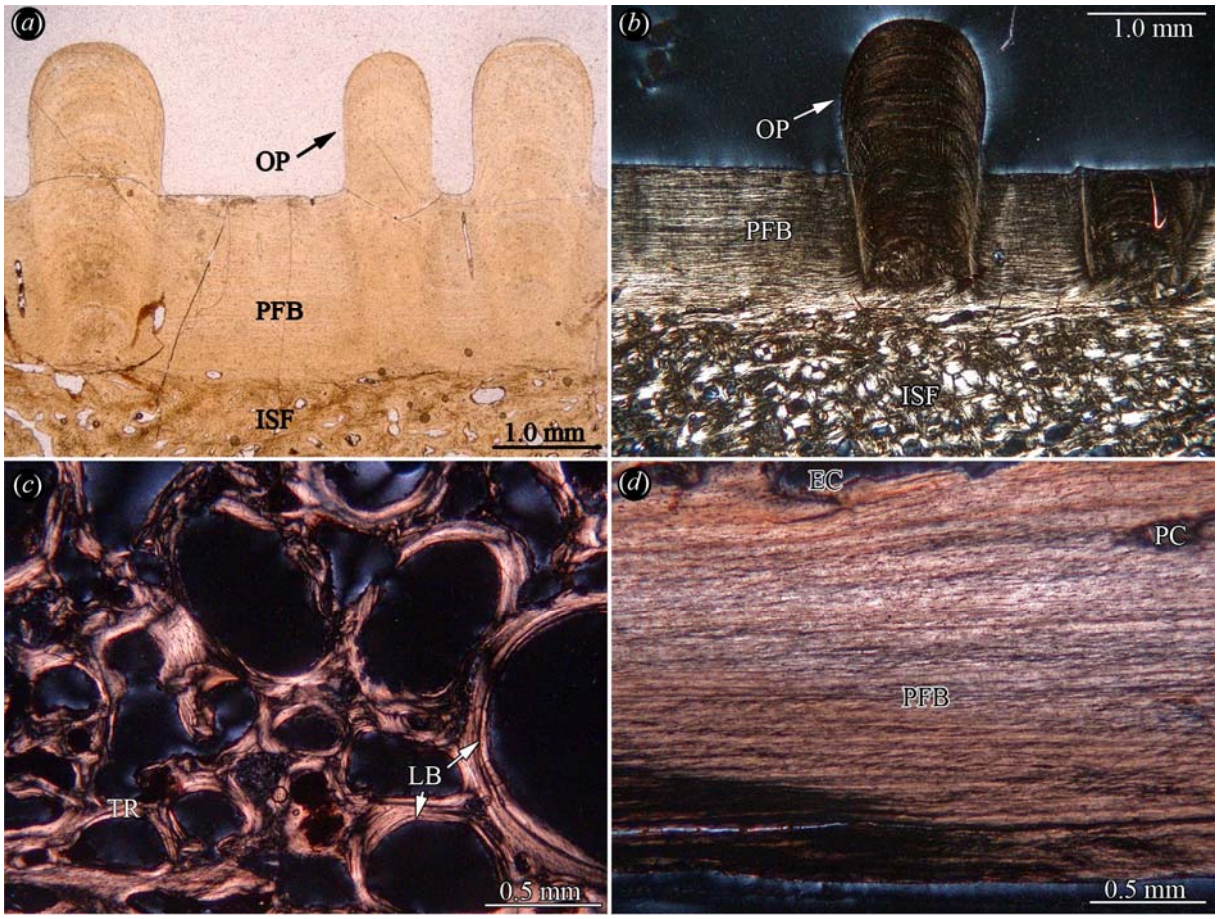

Figure 36: Shell bone histology of Solemydidae gen. et sp. indet. (aff. *Naomichelys* sp.). (*a*) Section of the external cortex of shell fragment TMP 90.60.07 in normal transmitted light, focussing on the peculiar ornamentation pattern. (*b*) Section of external cortex in polarised light, showing both the more internal and the more external zone. (*c*) Close-up of the irregular meshwork of bone trabeculae of the cancellous bone in polarised light. (*d*) Section of the internal cortex in polarised light, showing weakly vascularised parallel-fibred bone tissue.

Internal cortex—The internal cortex consists of parallel-fibred bone (Fig. 36d) that may locally grade into lamellar bone. Distinct growth marks are not observed. Bone cell lacunae are slightly flattened and elongated. Sharpey's fibres are present in some fragments, and they appear extensively adjacent to the rib bulge in the internal cortex of the costal fragment (TMP 90.60.07). Vascularisation is generally low, with an occasional scattered secondary osteon or a primary vascular canal.

Osteoderms—The osteoderms differ from the general structure of the bony shell elements in that they lack the thick external 'ornamental zone'. The external cortex thus is a single bone

tissue unit consisting of ISF. The internal cortex is quite thin in the spiked osteoderm, but better developed in the flat osteoderm.

6.3.2 Baenidae

6.3.2.1 *Neurankylus* sp. (†), *Plesiobaena* sp. (†), *Boremys* sp. (†) and *Chisternon* sp. (†)

The bone histology of the sampled baenid turtles is rather similar. Therefore the bone histology will be described together for all four taxa and variations will be noted where appropriate. All sampled shell bones have a diploe structure, with internal and external compact bone layers framing interior cancellous bone. In thin-section, the shell bones of *Neurankylus* sp. and *Plesiobaena* sp. have a compact appearance. The shell bones of *Boremys* sp. and *Chisternon* sp., on the other hand, are less compact, with a well developed cancellous interior. Similarly, the external and internal compact bone layers are thick and well developed in *Neurankylus* sp. and *Plesiobaena* sp. and thinner and less developed in *Boremys* sp. and *Chisternon* sp.

External cortex—The external cortex consists of ISF (Fig. 37a, b). The fibre bundles in the more internal region of the ISF are quite homogeneous in length, diameter and spatial distribution. Here, the fibre bundles extend perpendicular, sub-parallel and diagonally to the external surface of the bone. Sharpey's fibres are also present, but difficult to discern from the fibre bundles of the ISF matrix. In some cases, the Sharpey's fibres appear in normal transmitted light as coarser, more strongly mineralised fibre bundles. In all sampled neurals, the ISF of the external cortex can be divided into a thin, external and a thick internal region. In the more internal region the structure of the ISF is as described above. In the thin, more external region, however, fibre bundles that extend perpendicular and sub-parallel to the external bone surface dominate the ISF. Here, the structure of the bone tissue resembles parallel-fibred bone (the sub-parallel extending component) that is crossed by an abundance of parallel fibre bundles, i.e., Sharpey's fibres (the perpendicular extending component). Growth marks are very distinctive in the more external region. In *Plesiobaena* sp. and *Neurankylus* sp., vascularisation of the external cortex is low with only few scattered primary osteons and primary vascular canals (Fig. 37a). In *Boremys* sp. and *Chisternon* sp.,

vascularisation is higher with abundant scattered primary osteons and primary vascular canals (Fig. 37b). In all samples, the vascularisation increases at a transition zone to the interior cancellous bone. Here, the amount of primary osteons and primary vascular canals increases and small scattered secondary osteons appear in the bone tissue.

Cancellous bone—In *Neurankylus* sp. and *Plesiobaena* sp., the cancellous bone consists of short and thick irregular bone trabeculae and small vascular spaces (Fig. 37c). In the sampled costals and neurals, the cancellous bone appears thus mostly compact, while the peripheral and plastron elements have slightly larger vascular spaces in the interior-most zone of the cancellous bone. Especially in the sampled neural of *Plesiobaena* sp., the amount of primary compact bone and bone trabeculae are almost not developed at all. Instead, vascularisation of the cancellous bone occurs through large secondary osteons and erosion cavities. The vascular cavities increase in size in the interior-most and internal parts of the cancellous bone. The walls of the trabeculae constitute lamellar bone. In the lamellar bone, bone cell lacunae are flattened and elongated and follow the arrangement of the bone lamellae respectively. However, in the centres of the trabeculae and in branching areas, primary bone tissue is still largely present. The primary bone tissue consists of ISF. Here, the cell lacunae are more circular in shape and arranged in clusters. In contrast, the cancellous bone of *Boremys* sp. and *Chisternon* sp. generally has larger marrow cavities. The bone trabeculae are slender and more gracile, although most are still rather short (Fig. 37d). Primary interstitial bone is less abundant, or in case of *Chisternon* sp., almost completely absent. In *Neurankylus* sp., a gradual transition between the interior primary ISF and the bone tissue of the internal cortex is observable.

Internal cortex—The internal cortex consists of parallel-fibred bone. The bone tissue texture ranges between fine fibred and coarse fibred (Fig. 37 e, f). Occasionally, fibre bundles can change in direction so that they appear in cross-section instead of longitudinal section. In the costals, the fibrous orientation of the bone tissue at the rib bulge differs from that of the adjacent parts of the internal cortex of the costal plates. In the rib bulge, the fibrous arrangement extends in proximodistal fashion, following the progression of the incorporated rib in the costal plate. In the lateral parts, the fibrous orientation is perpendicular (anteroposterior) to that of the rib bulge, although the transition between the two parts is gradual and interdigitating. In the thickened parts of the sampled hyoplastra of *Neurankylus* sp. and *Boremys* sp., a similar strong shift in fibre orientation is observed. The lateral parts

and the internal most layers of the internal cortex have an anteroposterior orientation, while the central and more external part has a proximodistal orientation. In *Plesiobaena* sp., the shift is not as pronounced as in the former two samples. Vascularisation of the internal cortex is generally low to moderate in all sampled baenids. Locally, the vascularisation further increases however, due to strongly vascularised layers constituting small scattered primary osteons or primary vascular canals (Fig. 37g). These layers intercalate with the less vascularised layers of the internal cortex. This feature is more strongly developed in the proximal fragment of the costal of *Boremys* sp. and in the shell elements of *Chisternon* sp. (Fig. 37h). Sharpey's fibres in the internal cortex were found lateral to the rib bulge in the sampled costals of *Neurankylus* sp., *Plesiobaena* sp. and *Boremys* sp. and in the fragmentary hyoplastra of *Neurankylus* sp. and *Boremys* sp.

Sutures—Sutures consisting of bony protrusions and sockets are generally well developed. In the sample of *Chisternon* sp., the carapace elements are not sutured but fused together. The sutural zone between the neural and the costal for example is no longer visible in thin-section. In the other samples, the growth marks in the external cortex, especially those of the neurals, deviate parallel to the sutures, thus revealing that the initial sutural relief was low and became more pronounced during ontogeny. Fibre bundles, i.e., Sharpey's fibres that insert perpendicular to the plate margins are prominent throughout all sutures.

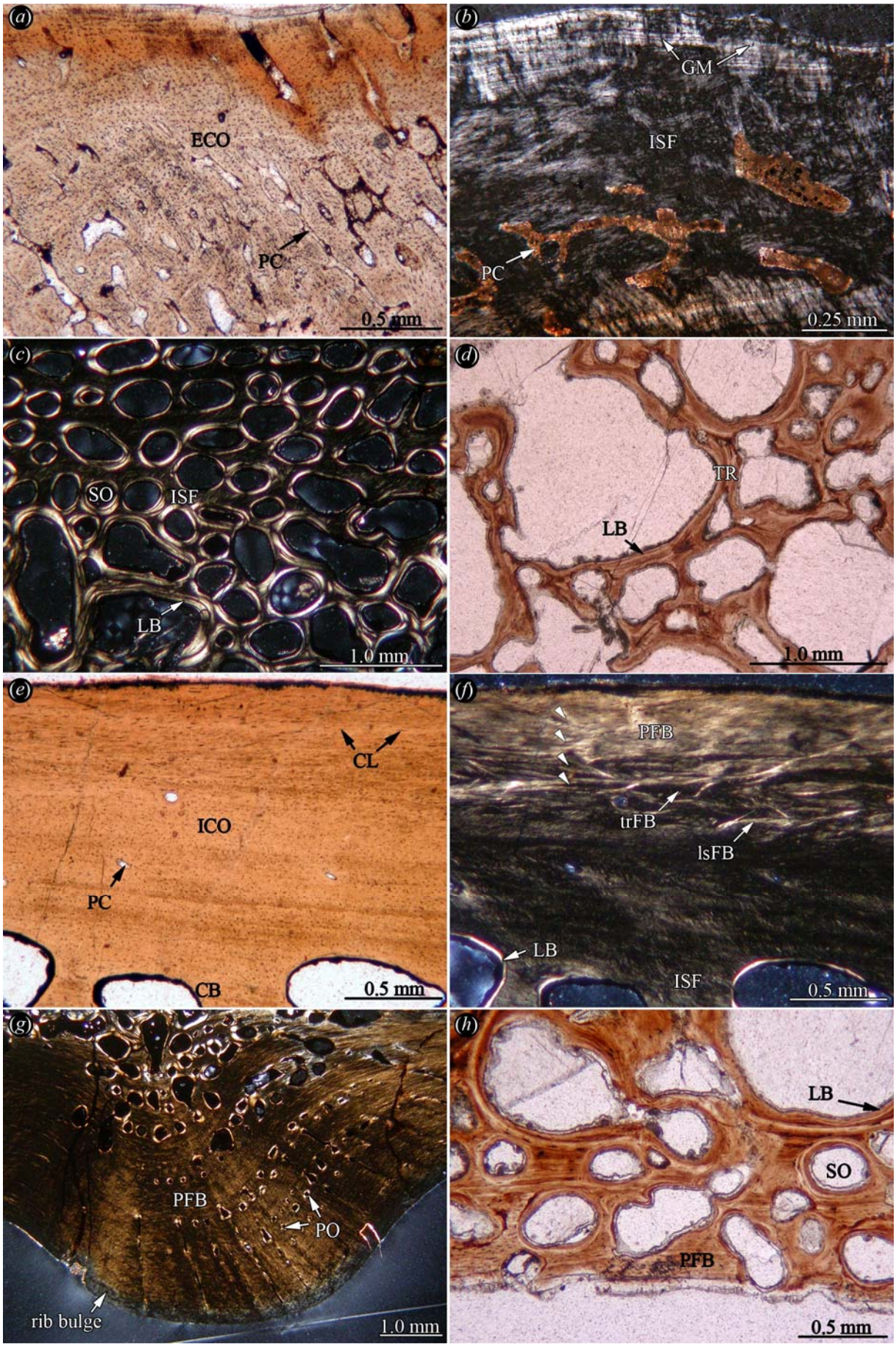
(a)
ECO
PC
0.5 mm
(b)
GM
ISF
PC
0.25 mm
(c)
SO
ISF
LB
1.0 mm
(d)
TR
LB
1.0 mm
(e)
CL
ICO
PC
CB
0.5 mm
(f)
PFB
trFB
lsFB
LB
ISF
0.5 mm
(g)
PFB
PO
rib bulge
1.0 mm
(h)
LB
SO
PFB
0.5 mm

Figure 37: Shell bone histology of baenid turtle taxa. (*a*) Close-up of the external cortex of neural TMP 93.108.03 of *Boremys* sp. in normal light. (*b*) Close-up of the external cortex of peripheral fragment of carapace UCMP V94076/150189 of *Chisternon* sp. in polarised light. (*c*) Close-up of the interior cancellous bone of hyoplastron TMP 94.666.35 of *Neurankylus* sp.in polarised light. Note the short and thick bone trabeculae. (*d*) Close-up of the interior cancellous bone of fused neural and costal UCMP V94071/150182 of *Chisternon* sp. in normal transmitted light. Bone trabeculae are long and slender. Detail of the transition zone between internal cortex and adjacent cancellous bone of hyoplastron TMP 94.666.35 of *Neurankylus* sp. in (*e*) normal and in (*f*) polarised light. (*g*) Close-up of the internal rib bulge of costal TMP 93.108.07 (L-section) of *Plesiobaena* sp in polarised light. Note layered vascular pattern of the parallel-fibred bone tissue. (*h*) Close-up of the highly vascularised and remodelled internal cortex of fused neural and costal UCMP V94071/150182 of *Chisternon* sp. in normal transmitted light.

Variation—Slight variations are present in the external cortices of the sampled peripherals. Here, the fibre bundles of the ISF can vary in diameter, such that coarser fibre bundles seem to be woven into the more homogeneous ISF matrix. Furthermore, due to their morphology, the peripherals trend to have smaller vascular spaces in the distal parts of the cancellous bone, while the larger vascular spaces are usually found in the more proximal parts near the internal cortex if preserved. Although, the carapace bones of *Boremys* sp. were strongly humped, their bone histology was not significantly influenced apart from local variations in bone tissue thicknesses internal and adjacent to these humps.

6.3.3 Pleurosternidae

6.3.3.1 *Glyptops plicatulus* (Cope, 1877) (†), *Compsemys* sp. (†), Pleurosternidae gen. et sp. indet. (†)

The bone histology of the pleurosternid taxa (including Kirtlington histomorph I, see chapter 6.3.1) is very similar and it is described in the same section. Variations among the

taxa will be noted where appropriate. All pleurosternid taxa share a diploe makeup of the shell, with well developed external and internal cortices framing interior cancellous bone.

External cortex—The external cortex of the shell elements of all taxa is a thick layer of compact bone. The cortical bone has a regular wavy external surface due to the section of the regular external ornamentation pattern of the bones (Fig. 38a, b). Few foramina insert into the bone tissue at the interstitial areas adjacent to the vermiculate low ridges and tubercles. The bone tissue consists of ISF. Furthermore, the tissue can be divided into two zones (Fig. 38a-e). The more external zone is less vascularised and it is dominated by fine fibred ISF. The second, more internal zone, has higher levels of vascularisation and is characterised by coarse, irregularly interwoven fibre bundles. These fibre bundles can differ significantly in length and in diameter. The thickness ratio of the more external zone to the more internal zone varies among the taxa, and it is strongly dependent on surface damage by, for example, diagenesis and weathering. Growth marks are present throughout the external cortex; however, they get increasingly more diffuse and difficult to follow in the more internal zone. Growth marks are seen as highly birefringent lines in polarised light in *Compsemys* sp. but as dark lines in the material of *G. plicatulus* and Pleurosternidae gen. et sp. indet. Besides the aforementioned foramina, the more external zone of the external cortex is mainly avascular while the more internal zone is characterised by few scattered primary osteons and short and round primary vascular canals. Additionally, reticular primary vascular canal patterns can be developed.

Cancellous bone—The cancellous bone constitutes short and thick bone trabeculae and mostly vascular spaces of small to medium size (Fig. 38f). Towards the sutured margins of the plates, vascular spaces are often slightly externointernally flattened and elongated. Larger vascular spaces of circular or irregular shape where found in the proximal parts of the sampled peripherals and in the costal fragment (YPM 57161) of *G. plicatulus*. While few erosion cavities lack secondary lamellar bone, the gross of the walls of the bone trabeculae consist of lamellar bone. Primary interstitial bone is preserved in most trabecular branching spots, besides the very thin trabeculae of the sampled peripheral of *G. plicatulus*.

Internal cortex—The internal cortex is well developed but generally thinner than the external cortex (Fig. 38g, h). In *G. plicatulus* and *Compsemys* sp. (Fig. 37h), the internal cortex is avascular. However, small scattered primary vascular canals can be present in the rib bulge of the costal elements. In the sample of Pleurosternidae gen. et sp. indet., the internal

cortex can be weakly vascularised with primary vascular canals. In *G. plicatulus*, the internal cortex consists of homogeneous and ordered layers of parallel-fibred bone. In *Compsemys* sp., Pleurosternidae gen. et sp. indet. and the Kirtlington histomorph I (Fig. 37g), the fibre bundles of the parallel-fibred bone are coarser and deviate in extension and orientation, thus the bone tissue appears less ordered.

Sutures—Sutures are generally well developed in the sampled pleurosternid turtles. Growth marks, which are deflected from the external cortex, can be followed in the bone tissue of the sutures, thus showing an increasing sutural relief during ontogeny. Fibre bundles that extend perpendicular to the sutural margin of the plate are common.

Variation—A unique form of bone tissue erosion and bone deposition was observed in the plastron fragment of *G. plicatulus*. First, within the larger erosion cavities, centripetally deposited lamellar bone was deposited. Second, small circular or semi-circular spaces occur in the lamellae of the lamellar bone. Third, at the margins of the larger cavities new bone deposition seems to occur around the small circular or semi-circular spaces. This phenomenon of bone erosion and deposition, which so far has not been found in any other of the sampled turtles needs further study before any interpretation can be attempted. In the plastron fragment of Pleurosternidae gen. et sp. indet., the orientation of the bone cell lacunae locally does not follow the general trend of the parallel-fibred bone. Instead the bone cell lacunae are angled towards the bone surface in the thickened part of the bone fragment. A similar observation can be made, for example, in the costal rib bulge of the baenid turtle *Boremys* sp. Here, the cell lacunae stand almost perpendicular to the surface of the internal cortex. However, this may be an artefact caused by a peculiar spot of the plane of sectioning, because it seems to occur where morphological structures like plastral buttresses and costal rib bulges and rib heads protrude from the planar parts of the shell elements.

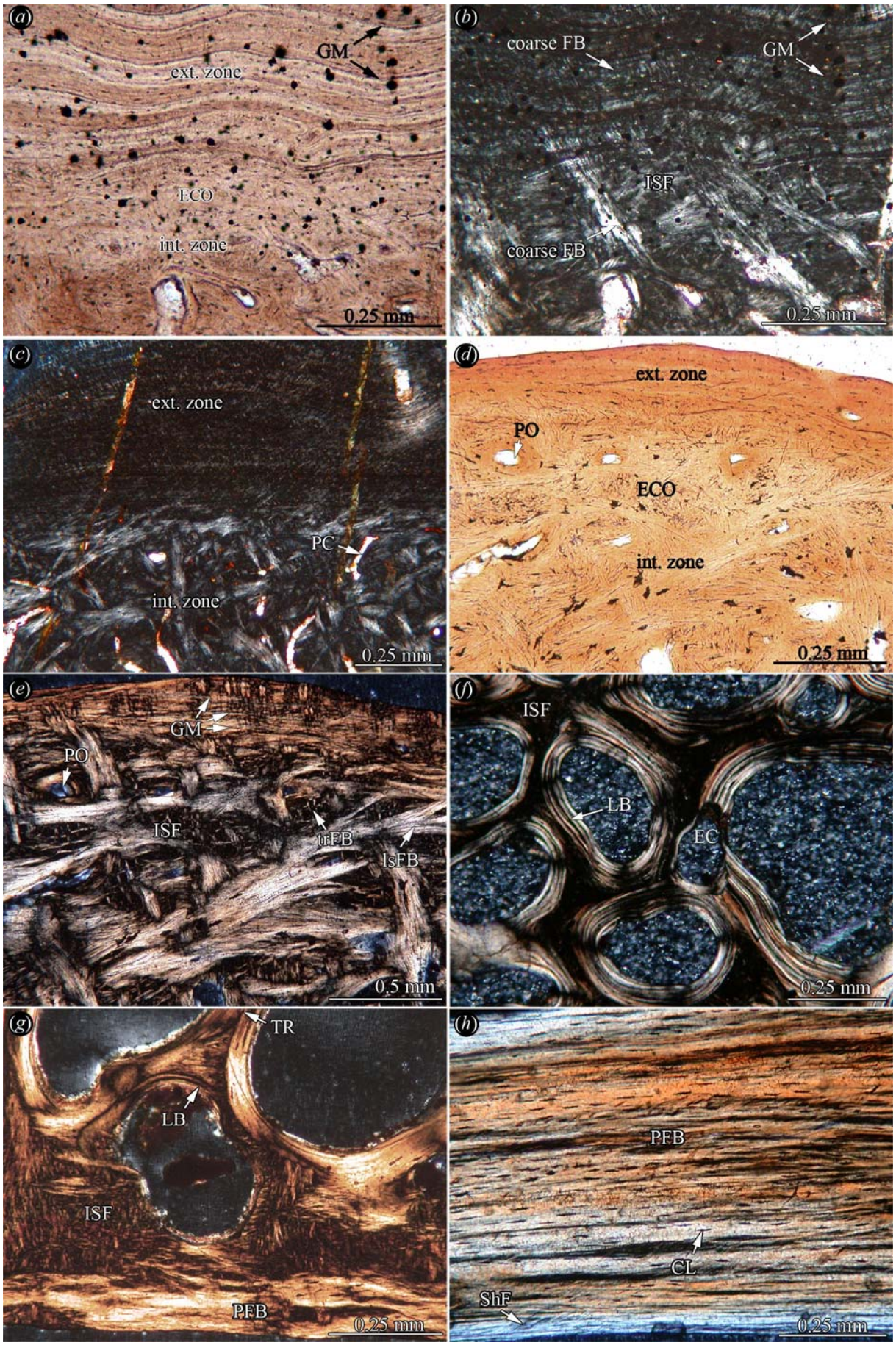
(a)
GM
ext. zone
ECO
int. zone
0.25 mm
(b)
coarse FB
GM
ISF
coarse FB
0.25 mm
(c)
ext. zone
PC
int. zone
0.25 mm
(d)
ext. zone
PO
ECO
int. zone
0.25 mm
(e)
GM
PO
ISF
trFB
lsFB
0.5 mm
(f)
ISF
LB
EC
0.25 mm
(g)
TR
LB
ISF
PFB
0.25 mm
(h)
PFB
CL
ShF
0.25 mm

Figure 38: Shell bone histology of pleurosternid turtle taxa. Close-up of the external cortex of the peripheral (YPM 57163) of *Glyptops plicatulus* in (*a*) normal and in (*b*) polarised light. The more external zone of the external cortex is fine-fibred and growth marks are clearly visible, while the more internal zone consists is coarse-fibred and almost completely lacks growth marks. (*c*) Close-up of the two external cortical zones of peripheral IPFUB P-Barkas 21 of Pleurosternidae gen. et sp. indet. in polarised light. Close-up of the external cortex of the carapace fragment IPB R586 (Kirtlington histomorph I) in (*d*) normal and in (*e*) polarised light. (*f*) Close-up of the interior cancellous bone of the plastron fragment (YPM 57164) of *G. plicatulus* in polarised light. (*g*) Detail of the transition from interwoven structural fibre bundles to parallel-fibred bone in the internal cortex of shell fragment IPB R583 (Kirtlington histomorph I) in polarised light. (h) Detail of the internal cortex of costal UCMP V90077/150195 of *Compsemys* sp. in polarised light. Note Sharpey's fibres inserting into the parallel-fibred bone.

6.3.4 Eurysternidae

6.3.4.1 Eurysternid turtles: *Eurysternum* sp. (†) and ?*Eurysternum* sp. (†)

All shell bones have a diploe structure with external and internal cortices framing interior cancellous bone. The internal cortices are generally slightly reduced in thickness compared to the external cortices (Fig. 39a). An exception is the thin-section of the left hyoplastron (NMS 20981) where the cortical bone is greatly thickened in the region of the axillary buttress.

External cortex—The well developed external cortex consists of ISF. The overall distribution of fibre bundles is homogeneous or slightly dominated by fibre bundles that extend either sub-parallel or obliquely towards the external surface of the bones. Vascularisation of the bone tissue is high because of high amounts of primary vascular canals and primary osteons (Fig. 39a, b). The vascular canals are round to elongated tubes that anastomose frequently. Growth marks are present throughout the cortex. However, the course of the growth marks is often irregular and obscured by secondary remodelling of the bone. Towards internal, a zone rich in scattered secondary osteons marks the transition to the interior cancellous bone.

Cancellous bone—The cancellous bone generally consists of short and thick trabeculae interspersed with round to ovoid vascular cavities. Primary fibrous bone tissue, i.e., ISF, is present within the thicker trabeculae and their branching areas. In the larger branching areas, small primary osteons or vascular canals may be present. The trabecular walls are usually lined with lamellar bone.

Internal cortex—The internal cortex consists of fine parallel-fibred bone layers. The vascularisation of the bone tissue is extensive (Fig. 39c). Circular and short tubular primary vascular canals and primary osteons are aligned in stringers or layers of the bone tissue that interlace with less vascular or even avascular layers. Growth marks, similar to the ones found in the external cortex, pervade the whole internal cortical bone. The growth marks are recognised as dark lines that extend sub-parallel to the internal surface of the bone in polarised light.

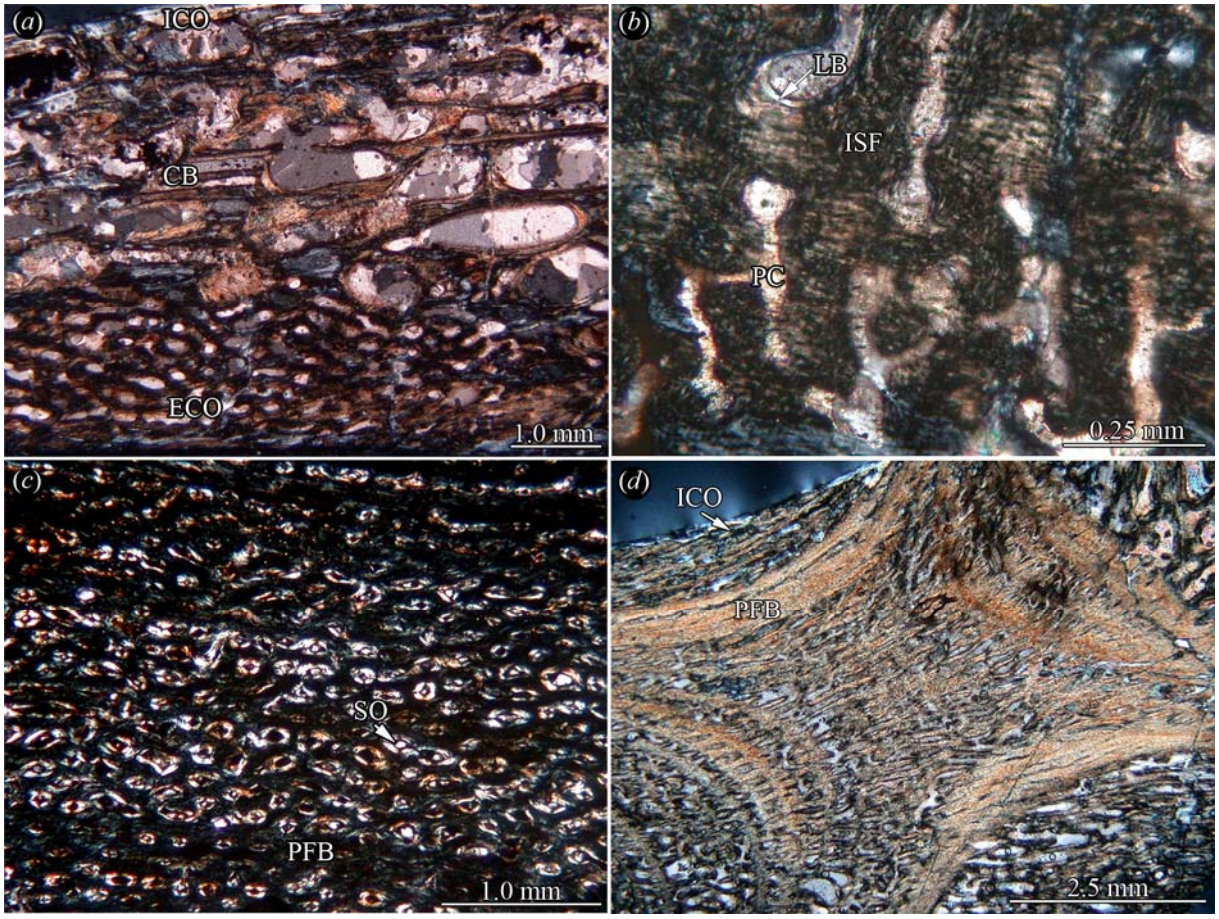

Figure 39: Shell bone histology of *Eurysternum* spp. (*a*) Section of the diploe structure of costal NMS 21908 of *Eurysternum* sp. in polarised light. Note the strong vascularisation of

the external cortical bone and the reduced thickness of the internal cortex. (*b*) Close-up of the interwoven structural fibre bundles and reticular vascular canals of the external cortex of the former specimen in polarised light. (*c*) Close-up of the highly vascular internal cortex of left hyoplastron NMS 20981 in polarised light. (*d*) Close-up of the cruciform pattern of the bone microstrcutre of plastral fragment NMS 21922 of *Eurysternum* sp.

Sutures—Sutures are moderately developed. Fibre bundles that extend perpendicular to the margin of the bone are found in the sutural bony protrusions and sockets.

Variation—A special bone microstructure is observed in the thin-section of the plastral fragment NMS 21922. The microstructure shows patterns that are closely related to the osteogenesis of the fragment. The plate part of the fragment shows planar successive growth marks of the internal cortex and distal margin (towards the buttress). At the buttress of the plate, directed growth towards external forms a cruciform pattern (Fig. 39d) of the microstructure as the buttress develops. The cruciform pattern originates due to successive growth of layers with high vascularisation intercalated with layers that are poorly vascularised or even avascular.

6.3.5 Plesiochelyidae and Thalassemydidae

6.3.5.1 *Plesiochelys* sp. (†), *Thalassemys* cf *T. hugii* Rütimeyer, 1873 (†), *Thalassemys* sp. (†) and *Tropidemys* sp. (†)

The turtle taxa of these groups cannot be distinguished by their bone histology. Variations are subtle and in some cases may be artefacts of diagenetic alteration or of preparing the thin-sections. The external cortices in the diploe structure of the shell bones are thick and well developed. The internal cortex is reduced in thickness compared to the external cortex.

External cortex—The external cortex comprises fine-fibred ISF (Fig. 40a, b). In the ISF, the fibre bundles are of similar size and length. The bone tissue is dominated by fibre bundles that extend perpendicular to the external surface of the bone. The record of growth marks is

extensive. The growth marks are clearly visible throughout the cortical bone, and they appear as dark lines, both in normal transmitted and polarised light. The external cortex is compact, however, an intricate reticular network of primary vascular canals is observed (Fig. 40b). The reticular network is dominated by canals that extend externointernal from the interior cancellous bone to the external bone surface and many of the canals end in small foramina. In *Tropidemys* sp., the reticular pattern appears not as dominant. Instead, the cortical bone is vascularised also by numerous scattered primary osteons in this taxon (Fig. 40c).

Cancellous bone—In all three taxa the cancellous bone is mainly composed of a mixture of short, thick trabeculae (Fig. 40d) and more slender and gracile ones. Larger and smaller vascular cavities are not restricted to certain areas in the cancellous bone. The trabecular system is still largely primary, although bone remodelling, especially in the interior-most parts of the bone is locally extensive. Interstitial primary bone is present in many trabeculae and branching areas. Others are completely composed of secondary lamellar bone.

Internal cortex—The internal cortex comprises layers of parallel-fibred bone. Some of these layers are strongly vascularised by string-like arrangements of primary vascular canals and scattered primary osteons (Fig. 40e, f). The vascularised layers often intercalate with avascular layers. Growth marks are also found in the internal cortex; however, they are not as conspicuous as in the external cortex. The amount of vascularisation was found to be highest in the samples of the *Thalassemys* spp. In the samples of *Tropidemys* sp., vascularisation was lower and the parallel-fibred bone tissue appears to have a slightly more coarse-fibred texture.

Sutures—In the sutures, the growth marks seen in the external cortex are still visible and they extend sub-parallel to the marginal surface of the bone. Former growth stages of the shell bone are thus still visible in the bone tissue, where secondary bone remodelling has not been too extensive. The sutures have a shallow relief with short pegs and sockets. The reticular pattern of primary vascular canals is present in the sutures of the samples of *Plesiochelys* sp. (Fig. 40g, h) and *Thalassemys* spp., but it was not as conspicuous in *Tropidemys* sp.

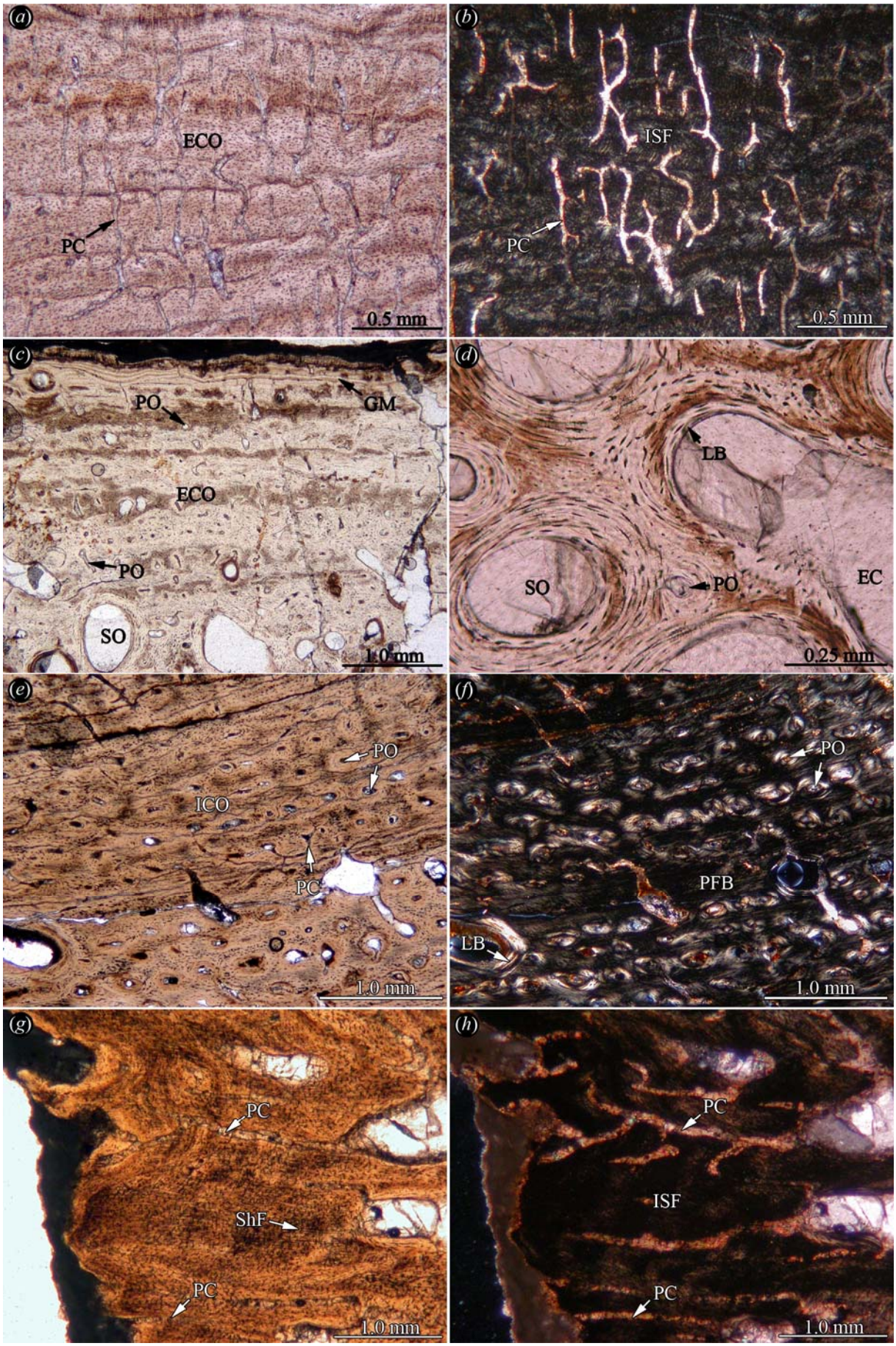
(a)
ECO
PC
0.5 mm
(b)
ISF
PC
0.5 mm
(c)
PO
GM
ECO
PO
SO
1.0 mm
(d)
LB
SO
PO
EC
0.25 mm
(e)
PO
ICO
PC
1.0 mm
(f)
PO
PFB
LB
1.0 mm
(g)
PC
ShF
PC
1.0 mm
(h)
PC
ISF
PC
1.0 mm

Figure 40: Shell bone histology of plesiochelyid and thalassemydid turtles. Close-up of the external cortex of neural3 (NMS 8730) of *Plesiochelys* sp. in (*a*) normal light and in (*b*) polarised light. Note extensive reticular vasculsarisation of the cortical bone tissue. (*c*) Close-up of the less vascular external cortex of peripheral NMS 8991 of *Tropidemys* sp. (*d*) Close-up of the interior cancellous bone of the proximal part of costal5 (NMS 8859) of *Thalassemys* cf. *T. hugii* in normal transmitted light. Note mixture of short and thick and more slender bone trabeculae. Detail of the well vascularised internal cortex of fragmentary hypoplastron SMNS55831 of *Plesiochelys* sp. in (*e*) normal light and in (*f*) polarised light. Note layered vascular pattern of the parallel-fibred bone tissue. Close-up of the sutural zone of neural3 (NMS 8730) of *Plesiochelys* sp. in (*g*) normal and in (*h*) polarised light. Similar to the external cortex, the bone tissue consists also of interwoven structural fibre bundles, and a reticular vascularisation pattern is developed.

6.3.6 Xinjiangchelyidae

6.3.6.1 *Xinjiangchelys chowi* Matzke et al., 2005 (†) and *Xinjiangchelys* sp. (†)

All shell bones have a diploe structure with well developed external and internal cortices and interior cancellous bone. The cortices are generally of similar thickness.

External cortex—The external cortex comprises ISF of finer and predominantly coarser fibre bundles (Fig. 41a, b). The fibre bundles vary in length and diameter, giving the ISF a heterogeneous appearance. Incorporation of fibre bundles that extend perpendicular to the external surface of the bone is extensive. Growth marks are usually seen as bright lines in normal transmitted light and as dark lines in polarised light. Vascularisation of the bone tissue is low with few scattered primary osteons and primary vascular canals.

Cancellous bone—The cancellous bone contains both longer, slender trabeculae and shorter, ticker trabeculae (Fig. 41c). Vascular spaces are of circular to irregular shape. In the peripherals, the larger vascular spaces are situated in the more proximal part of the bone. The trabecular system is largely primary, but towards the interior-most part of the cancellous bone, it is more strongly remodelled. Trabeculae often consist only of lamellar bone here. In

the buttress parts of the plastral bone, the trabeculae and associated vascular cavities are locally elongated and flattened and extend obliquely towards the internal surface of the bone.

Internal cortex—The internal cortex comprises parallel-fibred bone (Fig. 41d). The vascularisation is low to moderate. Primary vascular canals and few primary osteons are found, often occurring in string-like arrangement. The vascularised layers are interlaced with avascular layers of the cortex. The bone cell lacunae have numerous canaliculi. Both, the cell lacunae and the canaliculi appear enlarged, probably through diagenetic processes.

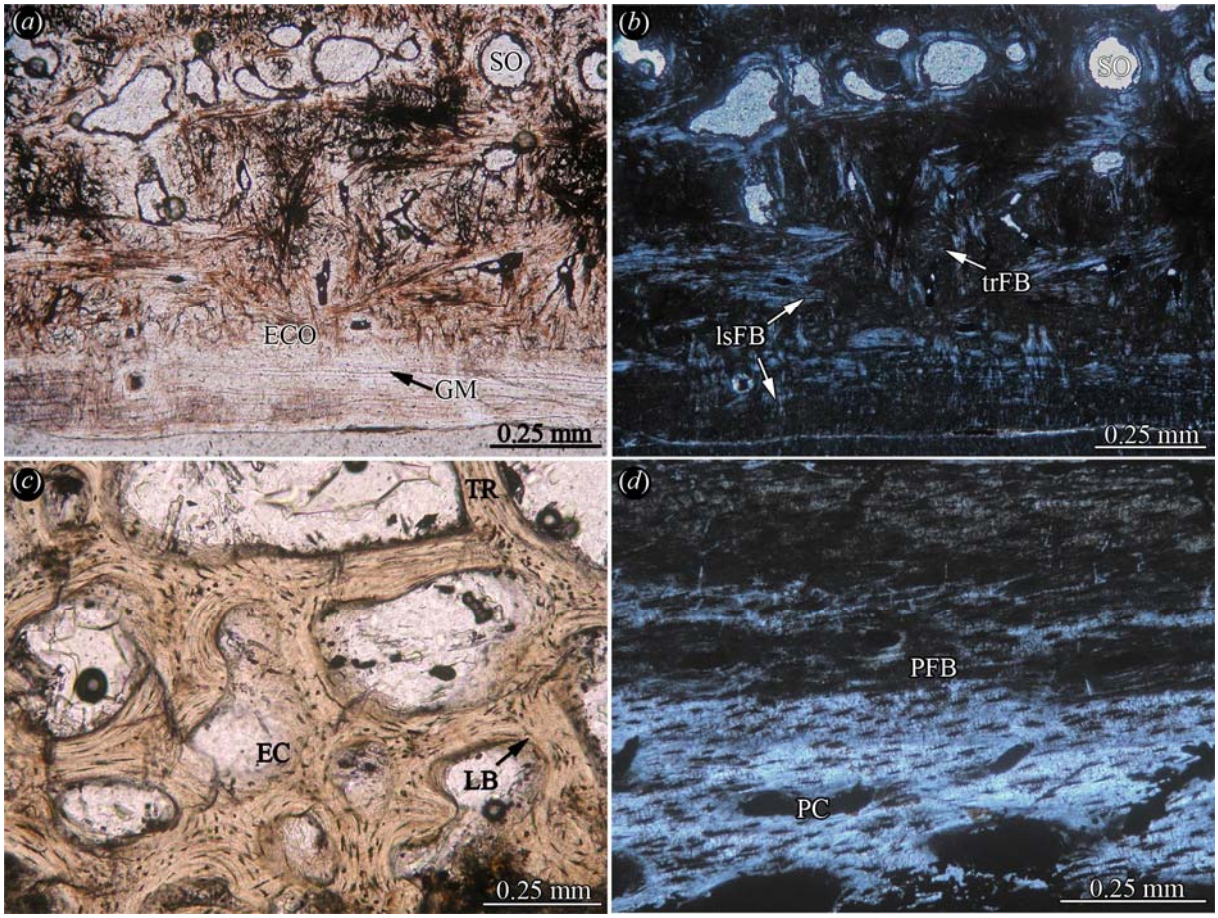

Figure 41: Shell bone histology of xinjiangchelyid turtles. Close-up of the external cortex of peripheral SGP 2002/4b of *Xinjiangchelys* sp. in (*a*) normal and in (*b*) polarised light. Note the predominantly coarse interwoven structural fibre bundles. (*c*) Close-up of the irregular interior cancellous bone of shell fragment SGP 2001/34c of *Xinjiangchelys chowi* in normal transmitted light. (*d*) Detail of the parallel-fibred bone of the internal cortex of plastron fragment SGP 2002/4d of *Xinjiangchelys* sp. in polarised light. Note cell lacunae and network of fine canaliculi.

6.3.7 “Sinemydidae” and “Macrobaenidae”

6.3.7.1 *Wuguia efremovi* (Khosatzky 1996) (=*Dracochelys wimani*) (†)

All shell bones have a diploe structure with well developed external and internal cortices and interior cancellous bone. The cortices are generally of similar thickness. The bones are among the thinnest that were encountered in this study.

External cortex—The external cortex comprises ISF, well vascularised by scattered primary vascular canals. Bone cell lacunae are round and not flattened. The ISF consists of homogeneously distributed fine-fibred fibre bundles (Fig. 42a, b). Growth marks are visible throughout the cortex, but mostly too obscure to be counted.

Cancellous bone—The cancellous bone comprises both short and long, slender trabeculae (Fig. 42c). The trabeculae are still mostly primary with secondary linings of lamellar bone. In the transverse sections of the flat bones, i.e., the costals and plastral bone, the cancellous bone is dominated by trabeculae and vascular spaces that are aligned sub-parallel to the bone surfaces. The cross-sections of the neurals show more circular or irregular vascular cavities. In the peripherals, the largest vascular spaces are not situated in the proximal part of the bones but in a more central and distal position. Instead, the proximal-most area of the peripherals is dominated by small, elongated vascular spaces that often aligned dorsoventrally with their long axes. The transition of the cancellous bone to cortical bone is gradual with a diminishing size of erosion cavities and an overall decrease of vascular spaces.

Internal cortex—The internal cortex constitutes parallel-fibred bone with growth marks (Fig. 42d). Vascularisation of the cortex is medium to high, because of the high amount of scattered primary vascular canals and primary osteons. Elongated and flattened bone cell lacunae follow the successive layering of the bone tissue. Sharpey’s fibres were only observed in the neurals lateral to the incorporated neural arch.

Sutures—Sutural zones are well developed with few but elongated bony peg and socket structures. Additionally, fibre bundles insert perpendicular into the sutural bone tissue.

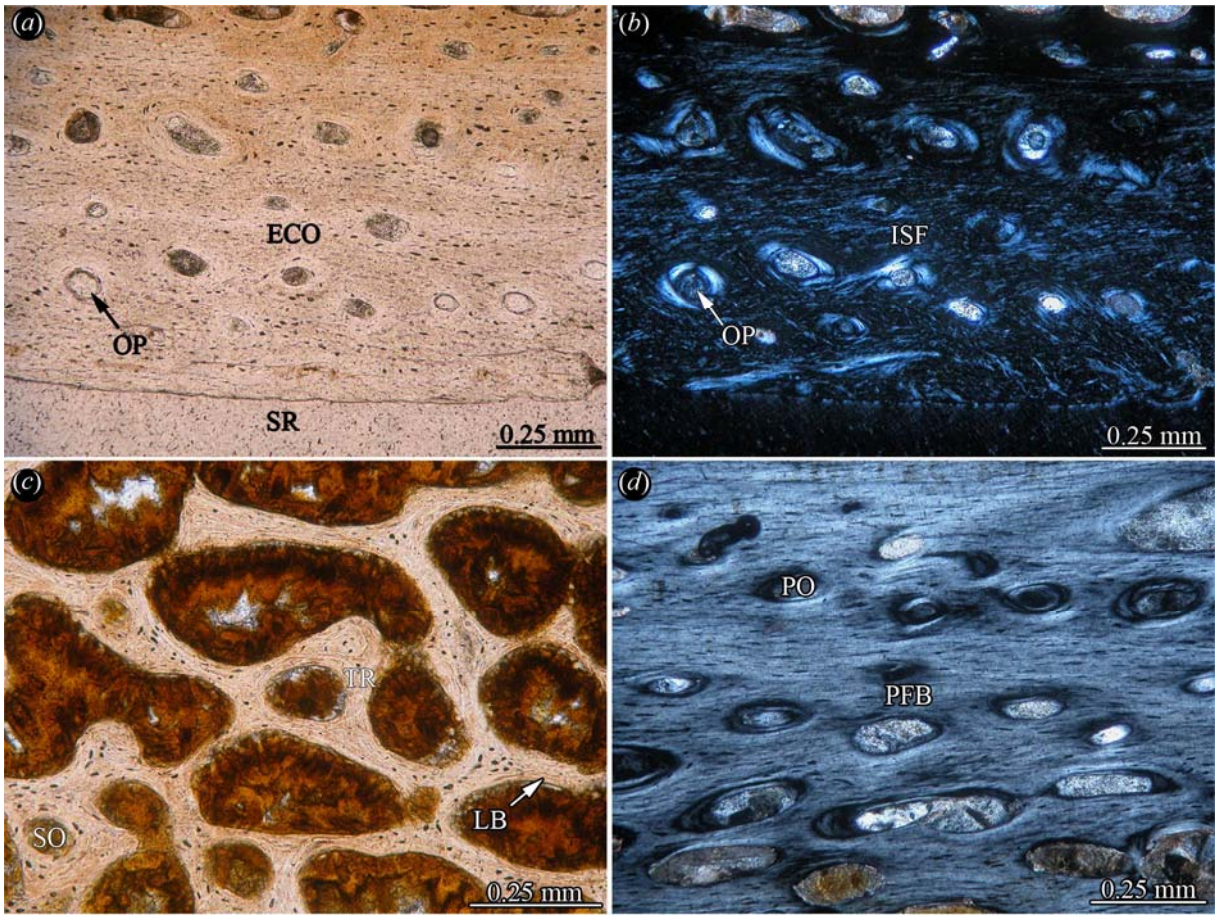

Figure 42: Shell bone histology of *Wuguia efremovi*. Close-up of the external cortex of plastron fragment SGP 2001/35h in (*a*) normal and in (*b*) polarised light. Note homogeneous distribution of the interwoven structural fibre bundles. (*c*) Close-up of the thin gracile bone trabeculae of the cancellous bone of former specimen in normal transmitted light. (*d*) Close-up of the well vascularised parallel-fibred bone of the internal cortex of the former specimen in polarised light.

6.3.7.2 Eucryptodira incertae sedis (cf. “Macrobaenidae”) (†)

All shell bones have a well developed diploe structure with external and internal cortices framing interior cancellous bone. While the external cortex is always a thick layer of compact bone, the thickness of the internal cortex varies between the carapace bones and the bone of the plastron. In the former, the internal cortex is generally reduced in thickness compared to the external cortex. In the latter, the internal cortex ranges from a thin band of bone to a thick layer that equals the thickness of the external bone.

External cortex—The external cortex is a layer of well vascularised fine-fibred ISF. Fibre bundles that extend perpendicular to the external surface of the bone are most common in the ISF (Fig. 43a, b). The bone tissue is vascularised by numerous, often branching primary vascular canals and few primary osteons. Many of the vascular canals extend perpendicular to the bone surface to open up into small foramina. At the transition to the cancellous bone, secondary erosion cavities and scattered secondary osteons are present

Cancellous bone—The cancellous bone is composed of slender trabeculae (Fig. 43c, d). Depending on the plane of sectioning, the trabecular structure is either dominated by short trabeculae and circular to ovoid vascular cavities (e.g., cross-section of the neurals, section perpendicular to the rib in costals) or dominated by long trabeculae and elongate externointernally flattened vascular spaces (e.g., transverse sections of plastral element, sections parallel to the rib in costals). The trabeculae are largely primary. Many erosion cavities still lack secondary lamellar bone.

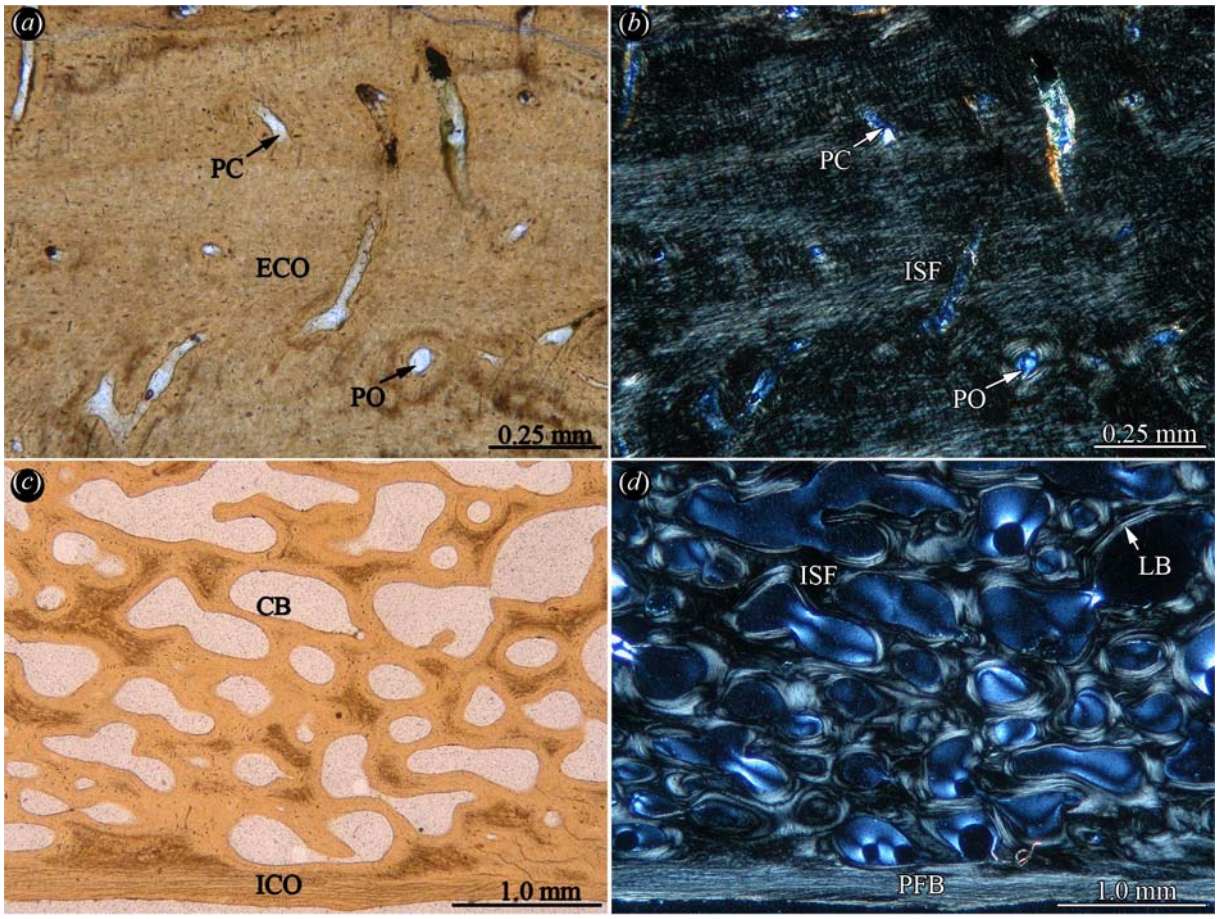

Figure 43: Shell bone histology of Eucryptodira incertae sedis (cf. “Macrobaenidae”). Close-

up of the interwoven structural fibre bundles of the external cortex of neural (YPM 1585) in (*a*) normal and in (*b*) polarised light. Close-up of the cancellous bone and the internal cortex of left hyoplastron (YPM 1585) in (*c*) normal and in (*d*) polarised light. Note primary structure of bone trabeculae and the reduced thickness of the internal cortex.

Internal cortex—The internal cortex is a composed of parallel-fibred bone (Fig. 43d). The bone tissue is vascularised by primary osteons and erosion cavities. The internal-most layer of the cortex is mostly avascular.

Sutures—The sutural zones have a shallow relief, with short protrusions and sockets. In the elements where sutures are observable, i.e., the neural and the costal, the interior cancellous bone reaches far into the sutural zone so that only a very thin sutural compact bone layer is present.

6.3.8 Cheloniidae *"sensu lato"*

The shell bones of these three taxa have in common that a true diploe structure (in which internal and external cortices frame interior cancellous bone) is not developed. Instead, the cortical bone shows various degrees of reduction. In *R. breitkreutzi* and *A. hofmanni*, the internal cortex is only a thin sliver of bone. In cf. *C. stenoporus*, the external and the internal cortices may be reduced in thickness, resulting in an overall fragile shell bone structure. However, the bone microstructures and vascularisation patterns of the shell of these three turtle taxa are distinct enough that they have to be described separately.

6.3.8.1 *Rupelchelys breitkreutzi* Karl and Tichy, 1999 (†)

External cortex—The external cortex is well developed (Fig. 44a, b). The bone matrix comprises ISF. The fibre bundles are coarse and of various lengths and diameters, giving the ISF a heterogeneous appearance (Fig. 44c, d). Furthermore, the fibre bundles trend in two sets

of different spatial directions (one predominantly oblique and one predominantly parallel and perpendicular to the external surface of the bone). Where fibre bundles are observed in cross-sections, the internal structuring of the bundles is visible in polarised light, with black fibre strands delineated by birefringent lines. Locally, the bone tissue is extensively remodelled by successive generations of secondary osteons forming Haversian bone.

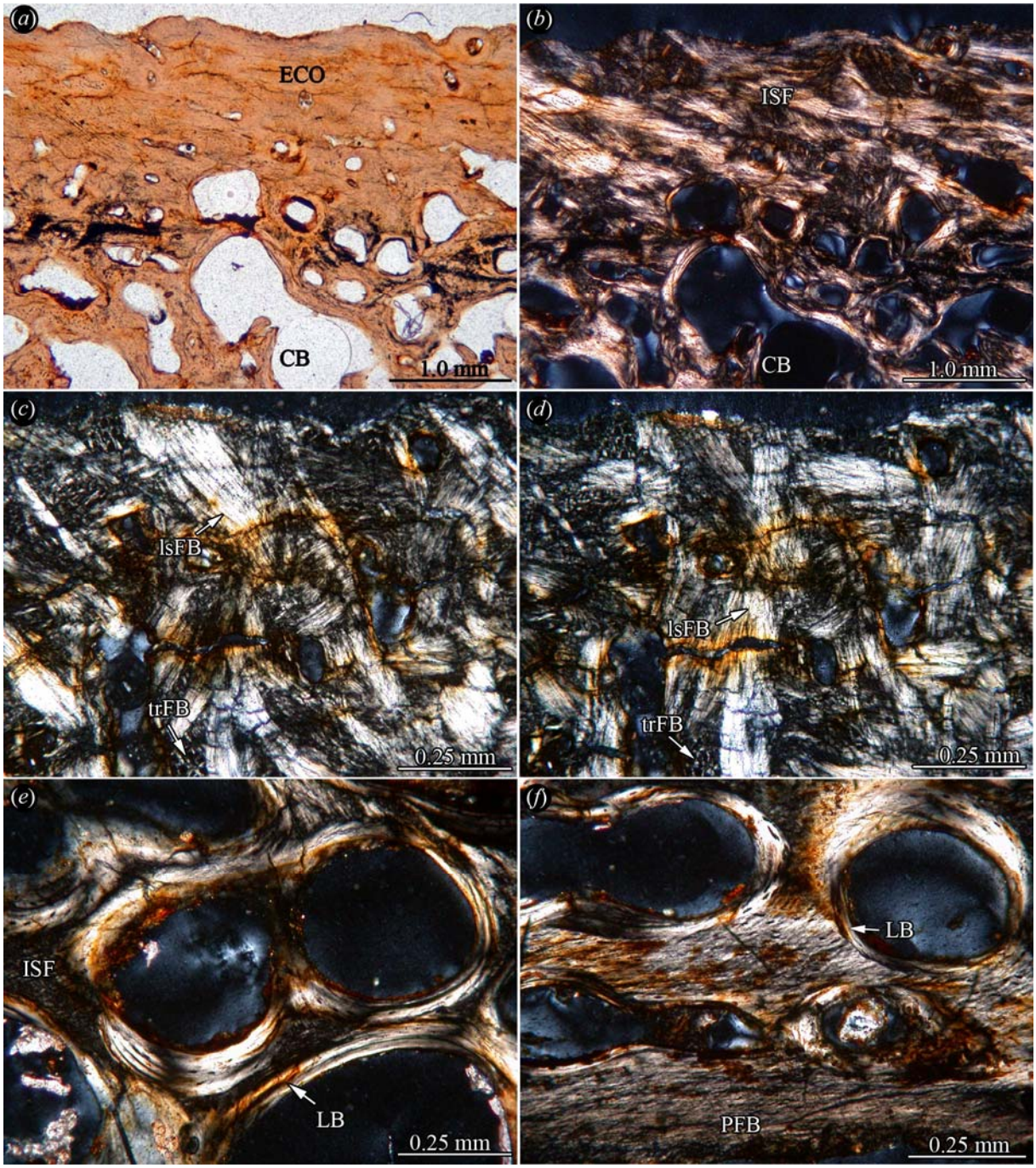

Figure 44: Shell bone histology of *Rupelchelys breitkreutzi*. Close-up of the external cortex and the external part of the cancellous bone of costal fragment (SMNS 87218) in (*a*) normal

and in (*b*) polarised light. (*c*) Close-up of longitudinal and transverse sections of the coarse interwoven fibre bundles of the external cortex of shell fragment (SMNS 87218, ?costal fragment) in polarised light. Note set of structural fibre bundles running obliquely to the external bone surface. (*d*) Same section as in (*c*) rotated about 45°. Note second set of structural fibre bundles extending mainly parallel and perpendicular to the external surface of the bone. (*e*) Detail of the cancellous bone of the former specimen in polarised light. Note the interstitial primary bone in the trabeculae. (*f*) Detail of the thin internal cortex of the former specimen in polarised light. The parallel-fibred bone is strongly remodelled by secondary osteons and erosion cavities.

Cancellous bone—Mostly thick and short bone trabeculae that still retain primary bone tissue, i.e., ISF, are found in the cancellous bone (Fig. 44e, f). The trabecular walls constitute lamellar bone. Towards the interior-most part of the cancellous bone, the trabeculae are more heavily remodelled. The vascular cavities are mostly of ovoid to irregular shapes.

Internal cortex—The internal cortex is a thin layer of bone, that is also heavily vascularised and remodelled by erosion cavities and secondary osteons (Fig. 44g, h). The bone tissue consists of parallel-fibred bone. Sharpey's fibres are observed to insert at high and moderate angles into the internal bone tissue.

Sutures—In the costal plates, the only elements where sutural zones are preserved, the sutures are generally weakly developed. Bone protrusions and sockets are short and interdigitate poorly. The sutural bone tissue differs from the coarse ISF of the external cortex. Instead, the bone tissue comprises finely fibred ISF.

6.3.8.2 *Ctenochelys* cf. *C. stenoporus* (Hay, 1905) (=*Ctenochelys* cf. *C. acris* Zangerl, 1953) (†)

External cortex—The external cortex is generally thin. Locally, the thickness decreases until the cortex is comparable to the trabeculae of the cancellous bone. In the sampled neural, the cortex appears as being an external part of the cancellous bone. The external cortex is a

bone layer of ISF, heavily vascularised by primary osteons and primary vascular canals that often occur arranged in sheets within the cortex (Fig. 45a, b). Growth marks are still visible in the bone tissue. Towards the cancellous bone, bone remodelling is extensive.

Cancellous bone—The structures of the cancellous bone are mostly secondary. The long and slender trabeculae are completely remodelled and consist of secondary lamellar bone (Fig. 45c). The fragile nature of the bone is underscored by extensive collapse structures of the cancellous trabecular system.

Internal cortex—Generally, the internal cortex is a thin layer of parallel-fibred bone with growth marks (Fig. 45d), but in the rib bulge of the costal and the medial regions of the neural, the internal cortex is somewhat thicker still. In both specimens, the bone tissue is also less vascularised with fewer scattered primary vascular canals and primary osteons than in other cortical areas. In the rib bulge, the internal-most layers are even mainly avascular. Sharpey's fibres were observed in the neural parasagittal to the keel and in the costal adjacent to the rib bulge.

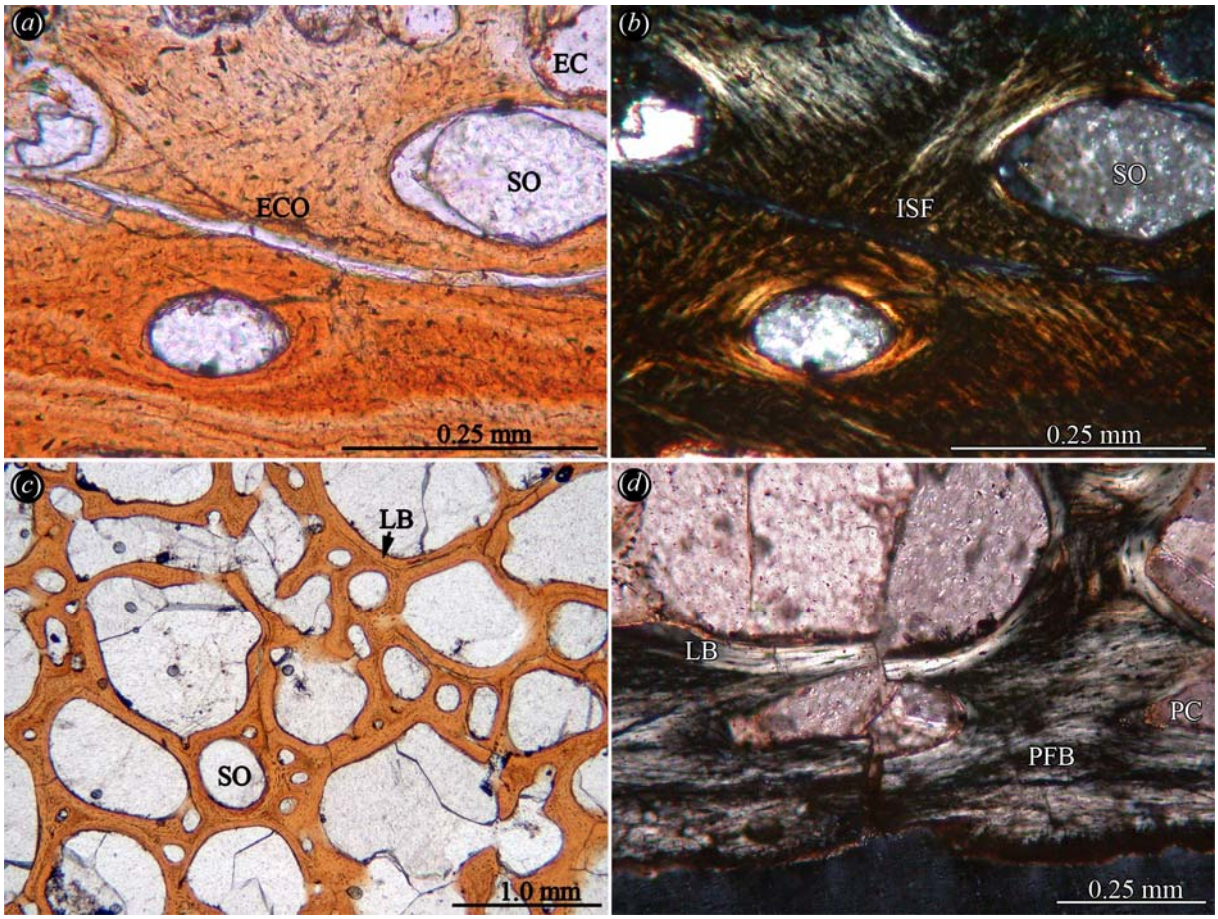

Figure 45: Shell bone histology of *Ctenochelys* cf. *C. stenoporus*. Close-up of the homogeneous interwoven structural fibre bundles of the external cortex of sampled costal (FM PR 442) in (*a*) normal and in (*b*) polarised light. (*c*) Close-up of the remodelled slender trabeculae of the cancellous bone of sampled neural (FM PR 442) in normal transmitted light. (*d*) Close-up of the internal cortex of former specimen in polarised light. Note the remodelling of the thin cortical bone.

6.3.8.3 *Allopleuron hofmanni* (Gray, 1831a) (†)

External cortex—The external cortex is thick and well developed. The bone surface appears smooth and unsculptured in thin-section and only occasionally a foramen inserts into the compact bone tissue. The bone tissue comprises ISF. While the matrix is mainly composed of fibre bundles of homogeneous length and thickness, prominent scattered thick fibrous strands extend through the whole cortex from the interior cancellous bone towards the external surface of the bone. The progression of the parallel fibrous strands (Fig. 46a, b), purportedly Sharpey's fibres, varies between extending almost perpendicular to the external surface of the bone and inserting at oblique angles (lower than 45°). The bone tissue is vascularised by a few scattered large vascular canals and an intricate and extensive reticular network of smaller primary vascular canals (Fig. 46c). The transition from cortical bone to the cancellous interior is distinct. Only a few scattered large secondary osteons and erosion cavities are present in the external cortex.

Cancellous bone—Externally, the cancellous bone constitutes short and thick trabeculae and small vascular cavities of round shapes. Towards internal, the cancellous bone has a more open character with longer and more slender trabeculae and larger vascular spaces (Fig. 46d). The largest cavities are found in the more internal half of the cancellous bone (e.g., Fig. 46e). Here, bone remodelling resulted in fusion of smaller vascular spaces to larger cavities. Bone trabeculae consist of lamellar bone, however primary bone, i.e., ISF, is still present in larger areas of anastomosing trabeculae.

Internal cortex—The internal cortex is represented by a thin layer of compact bone (Fig. 46e). Due to poor preservation, many of the sampled bones lack the internal cortex and the

internal-most parts of the cancellous bone. Where it is still preserved (e.g., in the larger costal fragment), it is observable as a thin layer of parallel-fibred bone.

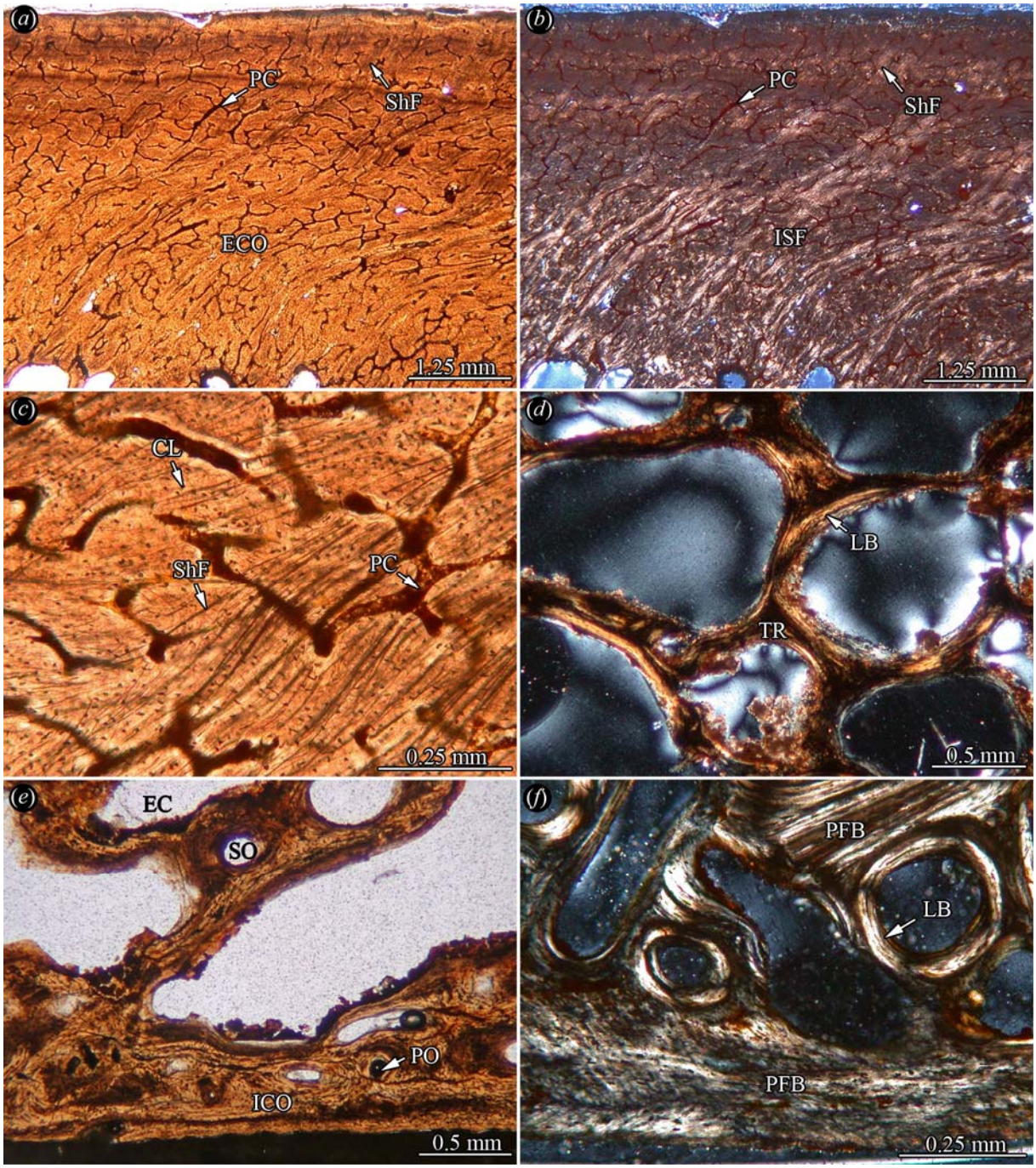

Figure 46: Shell bone histology of *Allopleuron hofmanni*. Close-up of the interwoven structural fibre bundles and the reticular primary canals of the external cortex of costal fragment 2 (NHMM uncat.) in (*a*) normal and in (*b*) polarised light. Sharpey's fibres insert obliquely into the cortical bone tissue. (*c*) Close-up of the external cortex of former specimen in normal transmitted light with focus on the reticular primary canals and the darkly

mineralised Sharpey's fibres. (*d*) Detail of the thin and slender bone trabeculae of the cancellous bone of former specimen in polarised light. Close-up of very thin internal cortices of (*e*) costal fragment 1 (NHMM uncat.) in normal light and of (*f*) plastral fragment (NHMM uncat.) in polarised light.

Plastral rod—Most of the external and interior part of the rod has not been preserved. However, the bone tissues described for the internal and external cortices are still present. While the rod itself comprises cortical ISF externally, interior cancellous bone and parallel-fibred bone internally (Fig. 46f), the flange-like protrusion of the rod is mainly composed of compact parallel-fibred bone surrounding a cancellous interior.

6.3.9 Cheloniidae "*sensu stricto*"

All three taxa have shell bones with a diploe structure, where compact bone layers frame interior cancellous bone. In *C. mydas*, the internal and external cortices are similar in thickness and less vascularised (please note that the description is based on a single shell element). In *C. caretta* and *E. imbricata*, the thickness of the internal cortices is reduced compared to the external cortices. The two taxa share similar bone microstructures and will thus be described in the same section. The amount and ratio of compact bone layers and their respective vascularisation patterns differ to such an extend from *C. mydas* that it is appropriate to describe this taxon in a separate section.

6.3.9.1 *Caretta caretta* (Linnaeus, 1758) and *Eretmochelys imbricata* (Linnaeus, 1766)

External cortex—The external cortex of the bone comprises metaplastic ISF and the external bone surfaces are rough and porous. Within the ISF, the fibre bundles are of similar length and thickness, leading to an even spatial arrangement where fibre bundles equally trend perpendicular, subparallel and diagonal to the surface of the bone. The most obvious characteristic of the cortex is its vascularisation pattern (Fig .47a-c). The bone starts loosing

its compact character due to the very high amount of primary osteons and primary vascular canals, often occurring in successive layers. Towards external, the bone surface is covered by a layer of connective tissue, again followed by a thick epidermal keratinous shield. In *C. caretta*, the keratin layers of the shield have uneven undulating growth marks (Fig. 47b). In *E. imbricata*, the shield has very clear growth marks of the keratin layers, which extend parallel to the shield surface throughout the shield. The layer of intermediate connective tissue comprises loosely arranged fibre bundles that extend sub-parallel to the surface of the bone.

Cancellous bone—The bone trabeculae of the cancellous bone are still largely primary, however, secondary remodelling is extensive in the interior part. ISF is observed in areas where primary bone is still present. The trabeculae are short and homogeneous in *C. caretta* (Fig. 47d), but somewhat thinner and gracile in *E. imbricata* (Fig. 47a). The walls of the trabeculae comprise lamellar bone. Furthermore, the largest vascular cavities are found in this interior-most region of the shell bone. The transition between the cancellous bone and the cortical layers is gradual instead of clearly distinct. The vascular cavities, mostly circular to ovoid in shape, are decreasing in size towards internal and external. In the core sample of the plastron of *C. caretta*, many of the vascular spaces are externointernally flattened. In the core sample of the peripheral of *E. imbricata*, a peculiar erosion pattern is observed in the cancellous bone, where irregularly formed ‘islands’ of primary bone tissue are completely separated from the surrounding bone tissue by erosion canals (please note that the islands are not completely separated three-dimensionally). The other sections of the shell bone of *E. imbricata* lack this peculiar pattern.

Internal cortex—The internal cortex comprises parallel-fibred bone (Fig. 47d-f). The bone tissue of the core samples is strongly vascularised. Similar to the external cortex, the compact nature of the bone is loosened up by primary vascular canals and numerous primary osteons. Many of the primary osteons are arranged string-like in the successive layers of the cortical bone. In the samples of *E. imbricata*, a layer of connective tissue where fibre bundles extend sub-parallel to the internal bone surface is still in contact with the shell bone.

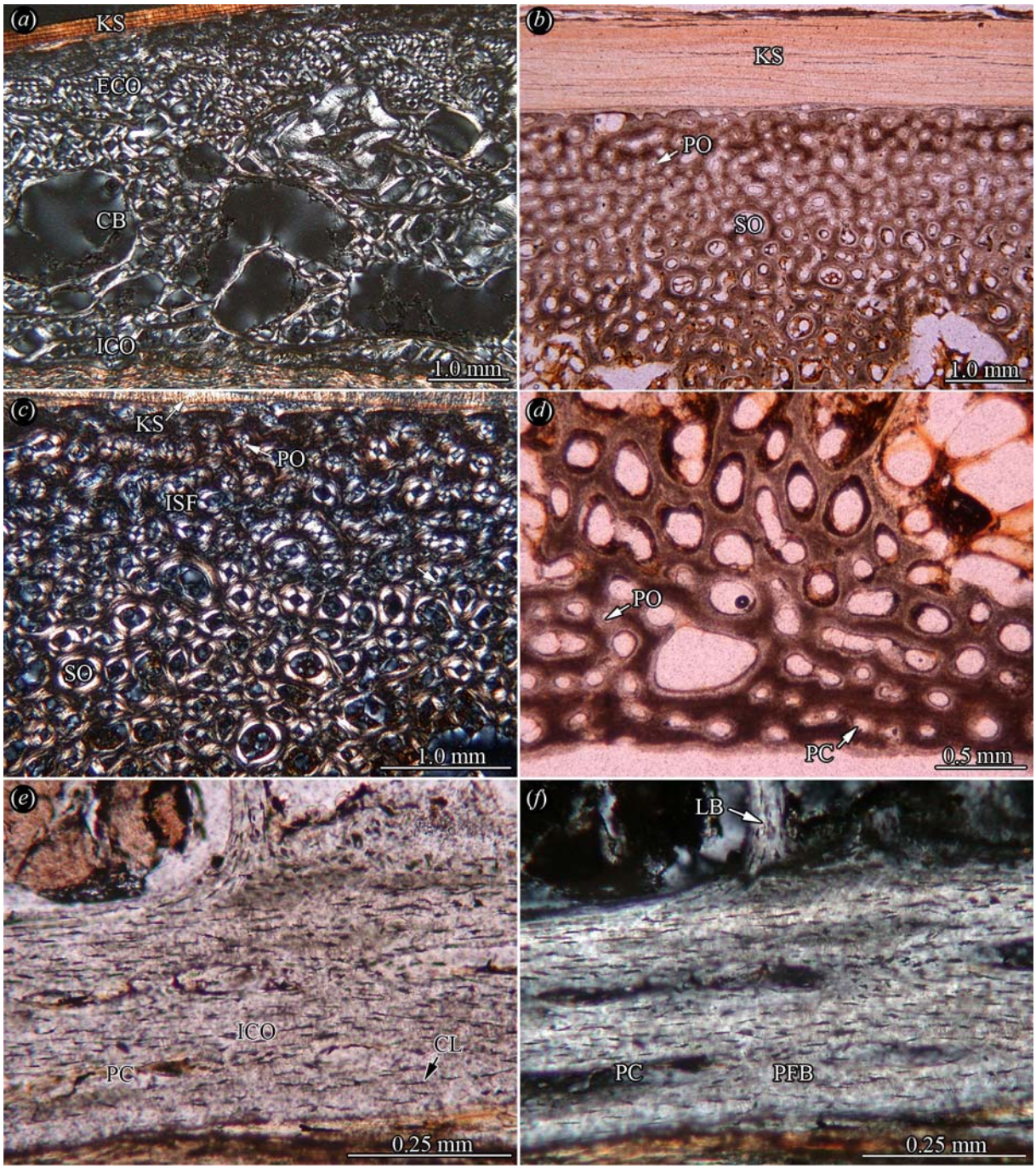

Figure 47: Shell bone histology of *Caretta caretta* and *Eretmochelys imbricata*. (*a*) Section of sub-sampled right peripheral1 (SMNS 12604; drilled core) of *Eretmochelys imbricata* showing the highly vascular diploe structure of the bone in polarised light. (*b*) Close-up of the external cortex and the thick keratinous shield of sub-sampled left costal2 (FMNH 98963; drilled core) of *Caretta caretta* in normal transmitted light. (*c*) Another section of the external cortex of the former specimen in polarised light. Note the loss of the compact nature of the cortical bone tissue based on the high amount of primary and secondary osteons. (*d*) Detail of the cancellous bone and the internal cortex of left costal2 (FMNH 98963; drilled core) of

Caretta caretta in normal transmitted light. Note beginning homogenisation of the cortical and cancellous bone. Close-up of the internal cortex of right costal2 (SMNS 12604) of *Eretmochelys imbricata* in (*e*) normal transmitted and in (*f*) polarised light.

6.3.9.2 *Chelonia mydas* (Linnaeus, 1758)

External cortex—The bone tissue comprises ISF (Fig. 48a, b) similar to that described for *C. caretta*. However, the high amounts of primary osteons found in the cortex of *C. caretta* are not observed in *C. mydas*. The moderate vascularisation is achieved only by anastomosing primary vascular canals. Locally, reticular vascularisation patterns are developed (Fig. 48b). The external surface of the bone is slightly wavy to rugose with shallow irregular troughs and ridges.

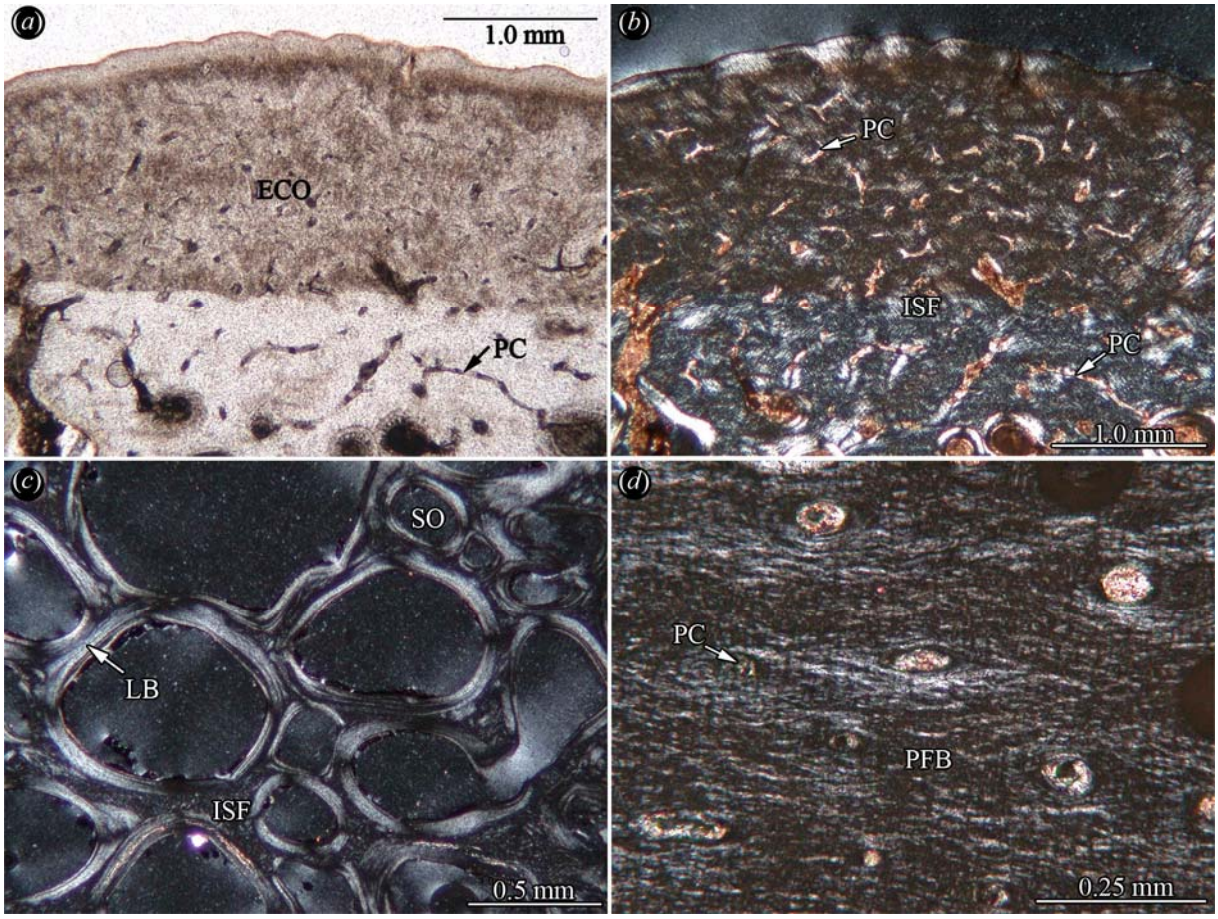

Figure 48: Shell bone histology of *Chelonia mydas*. Close-up of the external cortex of costal MB.R. 2857 in (*a*) normal transmitted and in (*b*) polarised light. Note scalloped surface of the

bone. A reticular vascularisation pattern is moderately developed. (*c*) Detail of the more internally situated bone trabeculae of the interior cancellous bone of former specimen in polarised light. Note that trabeculae are long and slender in this section. (*d*) Close-up of the well vascularised internal cortex of former specimen in polarised light. The fibres of the parallel-fibred bone tissue deviate around the primary vascular canals.

Cancellous bone—The interior cancellous bone is comprised of short and uniform primary trabeculae and vascular spaces of circular to ovoid shape. The largest spaces are found in the internal (lower) third of the cancellous bone (Fig. 48c). A prevalent arrangement of the bone trabeculae is not recognised. Towards external and internal, the transition to the cortical layers shows scattered larger secondary osteons and irregular erosion cavities.

Internal cortex—The internal cortex shows parallel-fibred bone with moderate to high amounts of scattered primary osteons and primary vascular canals. Locally, the parallel-fibred nature of the bone tissue is not easily discernable because of the amount vascular canals (Fig. 48d) and because of Sharpey's fibres inserting at high angles into the parallel-fibred bone.

Sutures—The sutures are well developed with long bony protrusions and sockets. Fibre bundles that insert perpendicular into the sutural bone tissue are short and unobtrusive.

6.3.10 Protostegidae

6.3.10.1 *Archelon ischyros* Wieland, 1896 (†)

The sampled shell bones of *A. ischyros* range among the thickest that were included into the study (Fig. 49a, b). The three specimens show a uniform picture of the bone microstructure. The interior bone structure in the peg-like element has largely collapsed. Therefore, the description is mainly based on the other two shell bones. The rough, spongy surface texture of the bones is connected with numerous primary and secondary osteons opening up to the bone surface. However, this effect may be greatly influenced by the individual preservation of the external-most layers of the bones. A clear histological division between compact bone layers

and interior cancellous bone is not observed (Fig. 49a, b). Instead, the boundaries between cortex and cancellous bone are lost in favor of a single, more homogeneous bone tissue of cancellous appearance. The cortices of the bone are thus not compact but comprise primary cancellous bone tissue with cyclical growth marks (Fig. 49c, d). In the bone tissue directly adjacent to the external and internal surfaces of the shell bones, a general reduction in size is observed in the primary and secondary osteons. The growth marks are recognised as areas of condensed shorter homogeneous trabeculae and small circular vascular spaces arranged roughly sub-parallel to the surface of the bones. Many of the bone trabeculae comprise primary bone within that is walled by secondary lamellar bone. Vascular spaces are smallest in the internal-most and external-most layers of the bones. The spaces are of circular shape here.

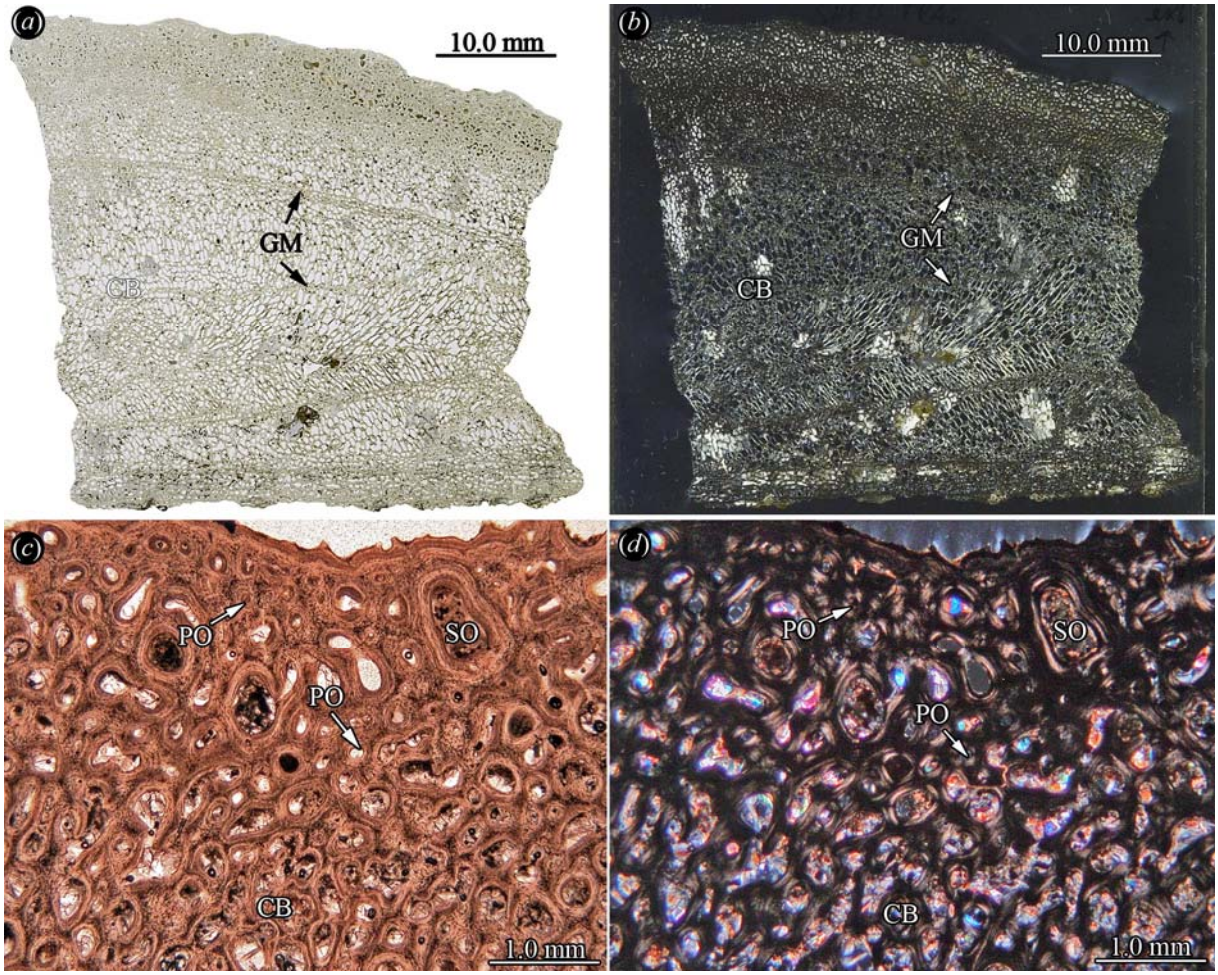

Figure 49: Shell bone histology of *Archelon ischyros*. Complete thin-section of sampled shell fragment (YPM 1783) in (*a*) normal and in (*b*) polarised light. The whole bone tissue is mostly primary and uniformly spongy in appearance. No discrete division into cancellous

bone and cortical bone can be observed. Note primary growth marks thoughout the complete bone tissue. Section of the external part of the shell element in (*c*) normal and in (*d*) polarised light. Towards the external surface of the bone, a general trend in size reduction is seen in the primary and secondary osteons.

Secondary remodelling processes further enlarge the vascular spaces within the cortices and the cancellous bone, but no secondary osteon clusters or Haversian bone was found in *A. ischyros*. Towards the cancellous interior of the bones, the vascular spaces are of ovoid to elongated shape. Many of these vascular spaces are aligned in an externointernal fashion with their respective long-axes. Locally, the arrangement of the trabeculae is reminiscent of the arrangement of trabecular bone aligned along force trajectories in long bones.

6.3.11 Dermochelyidae

6.3.11.1 *Dermochelys coriacea* (Vandellius, 1761)

Three ontogenetic stages in shell bone formation were studied.

Hatchling specimen—The thin-sections of the hatchling (QMJ 58751a, b) show mostly unossified integumentary tissue. In the thin-section comprising a longitudinal cut through the integument (not associated with a rib), mostly unossified integumentary tissue is present (Fig. 50a, b). In the thin-section that shows a transverse cut through the lateral body wall of the hatchling associated with developing rib and vertebra. Beneath the external-most layer, the cuticle follows a layer of fibrous, fatty tissue, with fibre bundles extending mostly sub-parallel to the external surface of the integument. In the longitudinal sections, a thick zone comprising layers of large thick translucent cells intercalated with thin fibrous strands is present, internal to the lipid-rich fibrous tissue (Fig. 50b). This internal zone is hypothesised to belong to the subcutis where adipose tissue (large thick translucent cells) is separated into compartments by connective tissue strands (thin fibrous strands). In the transverse section, thin bony struts (probably belonging to the developing rib) are seen, however, their connection to the surrounding soft-tissue is difficult to interpret. The thin-section is

dominated by the ovoid structure of the vertebra that shows internal cartilage cells surrounded by a thin layer of periosteal bone. Laterally, the ovoid structure has two small protrusions that may comprise parts of the neural arch prior to the incorporation into the flat plate part of the neural. True ossification of epithecal elements, i.e., the mosaic platelets are not observed in the hatchling sections.

Sub-adult specimen—At the sub-adult stage (QMJ 581592), a layer of ossified tissue has developed between the external cuticle and a layer of lipid-rich fibrous tissue, where the fibre bundles trend again sub-parallel to the external surface of the integument (Fig. 50c). In the section, this layer of horizontally arranged fibre bundles is followed internally by a thick, adipose-rich layer of integumentary tissue where fibre bundles are more loosely arranged. The fibre bundles extend in several spatial directions, with a slight dominance of fibre bundles that extend roughly diagonally towards the external surface of the integument. The bony platelet comprises an external cortical bone layer and an internal layer of cancellous bone (Fig. 50c). An internal cortex is not developed. The external cortex constitutes ISF (Fig. 50d, e). The bone tissue is highly vascularised with a reticular network of the primary vascular canals and primary osteons. The external surface of the bone is rough and scalloped with deep foramina inserting into the cortical bone. The internal cancellous bone comprises trabeculae and scattered secondary osteons. The trabeculae are identified as being primary because interstitial primary bone is still present within the lamellar bone walls of many trabecular struts and trabecular branching areas. Other trabeculae are in the process of remodelling. The remodelling results in secondary trabeculae composed solely of lamellar bone. Bone cell lacunae in the lamellar bone are flattened and elongated, while they are more round in interstitial areas.

Adult specimen—The platelet of the adult specimen (QMJ 73979; UQVPI) derives from one of the keels of the carapace therefore the bone is roof-shaped in cross-section (Fig. 50f). The bone was prepared out of the surrounding integumentary tissue which precludes a detailed soft-tissue analysis of the integument here. The mosaic platelet is similar in its bone microstructures to the platelet of the sub-adult specimen. It is marginally thicker than the platelet of the sub-adult stage. The platelet is composed of two layers, a more compact external layer and a more vascular internal layer. The external cortex comprises ISF that are highly vascularised by reticular vascular canals (Fig. 50g).

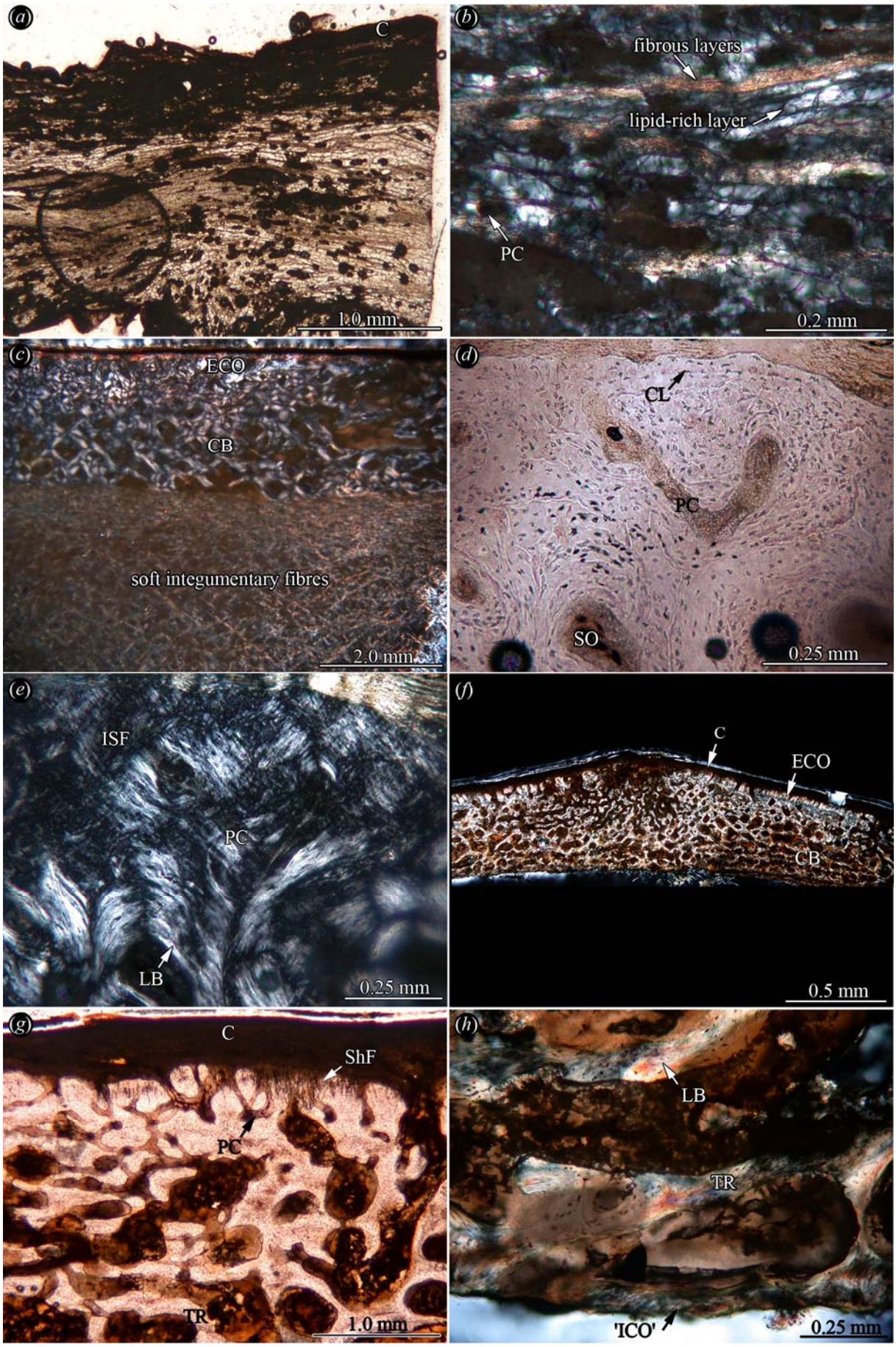
(a)
C
1.0 mm
(b)
fibrous layers
lipid-rich layer
PC
0.2 mm
(c)
ECO
CB
soft integumentary fibres
2.0 mm
(d)
CL
PC
SO
0.25 mm
(e)
ISF
PC
LB
0.25 mm
(f)
C
ECO
CB
0.5 mm
(g)
C
ShF
PC
TR
1.0 mm
(h)
LB
TR
'ICO'
0.25 mm

Figure 50: Shell bone histology of *Dermochelys coriacea*. (*a*) Section of the sampled integument of juvenile specimen (QMJ 58751) in normal transmitted light. The integumentary tissue still lacks ossified secondary armour. (*b*) Detail of the fibrous and lipid-rich layers of the integument. (*c*) Section of the sampled integument of sub-adult specimen (QMJ 581592). The external cortex and the interior cancellous bone of a bony armour platelet are visible, followed internally by a lipid-rich loose meshwork of soft integumentary fibres (of the corium). Close-up of the external cortical bone of the former specimen in (*d*) normal transmitted light and in (*e*) polarised light. The highly vascularised cortical bone tissue consists of interwoven sturctural fibre bundles. (*f*) Section of the roof-shaped platelet of an adult specimen (QMJ 73979; UQVPI). Note that the bone is covered externally by a thick cuticle. (*g*) Close-up of the highly vascularised external cortex of the former specimen in normal light. Note the scalloped surface of the bone, the primary canals opening in foramina and the Sharpey's fibres. (*h*) Close-up of the internal-most part of the platelet where a thin 'internal cortex' seems to be present. Note that this purported cortical bone is no thicker than the slender trabeculae of the interior part of the platelet.

The surface of the bone is scalloped with deep insertions of foramina, partly filled with the tissue that constitutes the external cuticle. Sharpey's fibres are found as thick and dark fibrous strands inserting at high angles into the external-most layers of the cortex. Towards the keel of the platelet, the cortical bone itself resembles only a spongy meshwork of trabecular struts. The large vascular cavities are filled with brown adipose tissue. Towards internal, the trabeculae are longer and more slender, forming an intricate spongy meshwork of bone. Most of the trabeculae comprise only lamellar bone. However, remnants of primary bone are still visible throughout the internal bone layer (i.e., in larger branching areas). The cavities are also filled with brown adipose tissue here. Where the adipose tissue desiccated, small empty vascular spaces are present. Locally, it appears that a very thin internal cortex (no thicker than a gracile trabecular strut) is developed (Fig. 50h). However, this might be an artefact of the plane of sectioning crossing more horizontally aligned trabeculae, because other areas are clearly free of internal cortical bone. On one lateral side of the internal cortex, connective tissue is still attached to the bone. The fibre bundles arrangement in this tissue seems to be sub-parallel to the internal surface of the platelet.

6.3.11.2 *Psephophorus* sp. (†)

Although the outer morphology and size of the polygonal platelet of *Psephophorus* sp. (MB. R. 2532.1) differs from the platelets of *D. coriacea*, the bone microstructure is largely the same. The platelet comprises an external compact layer and an internal zone of cancellous bone. An internal cortex is not developed.

External cortex—In contrast to the platelets of *D. coriacea*, the external surface of the bone is even with a slightly rough texture. The cortex itself is composed of ISF (Fig. 51a, b). The fibre bundles in the ISF are homogeneous in size and diameter with a slight dominance of fibre bundles that extend at high angles to the external bone surface. The bone tissue is moderately to highly vascularised by primary osteons, primary vascular canals and scattered secondary osteons. Few of the vascular canals open up as small foramina to the external bone surface. The amount of secondary osteons increases towards the internal cancellous bone. Bone cell lacunae are round or slightly flattened and elongated and appear irregularly or in clusters. In the lamellar bone of the secondary osteons, the cell lacunae are flattened and elongated and generally align along the secondary bone lamellae.

Cancellous bone—The cancellous bone consists mostly of thick and short trabeculae and large amounts of secondary osteons (Fig. 51c). Locally, the secondary osteons are clustered but no extensive Haversian bone is formed. Most of the interstitial bone is primary, showing ISF. Vascular cavities are irregular and small to medium in size. The internal surface of the bone is strongly scalloped due to extensive remodelling of the cancellous bone trabeculae.

Sutures—The sutural zone is narrow with short bony protrusions and sockets (Fig. 51d). The bone tissue is similar to the ISF described for the external cortex, but more strongly remodelled. The sutural bone tissue is dominated by fibre bundles that extend perpendicular to the margin of the platelet.

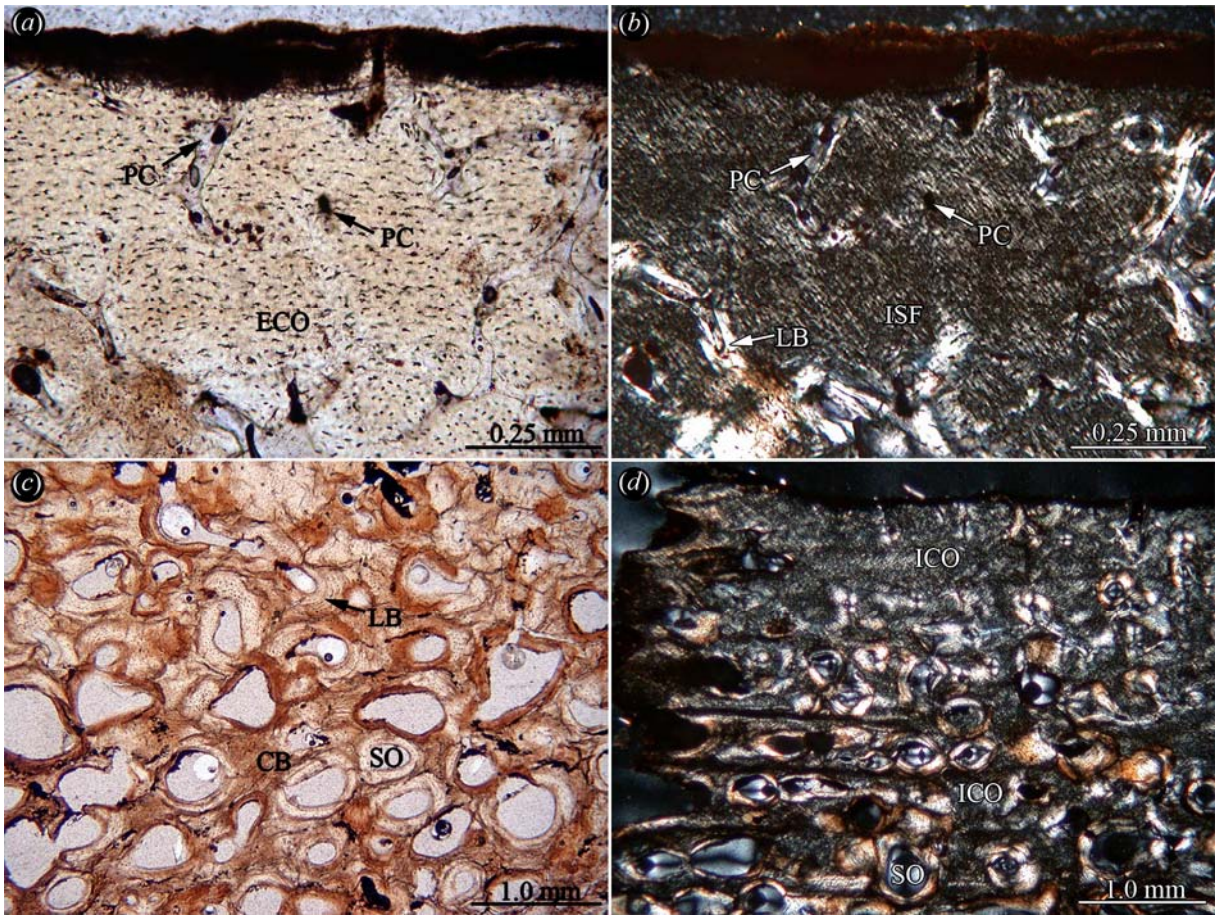

Figure 51: Shell bone histology of *Psephophorus* sp. Close-up of the external cortex of secondary armour platelet MB.R. 25.321 in (*a*) normal transmitted and in (*b*) polarised light. Note the homogeneous texture of the interwoven bone tissue and the branching primary vascular canals. (*c*) Detail of the more internally situated bone trabeculae of the interior cancellous bone in normal transmitted light. Note that trabeculae are predominantly thick and short. (*d*) Close-up of the sutural zone of the specimen in polarised light. The bone tissue of the sutural zone is similar to the bone tissue of the external cortex. However, the sutural bone tissue is more strongly remodelled.

6.3.12 Chelydridae

6.3.12.1 *Chelydra serpentina* (Linnaeus, 1758), *Chelydropsis murchisoni* (Bell, 1832) (†) and *Chelydropsis* sp. (†)

The bone histology of the three taxa is similar, so it will be described in a single section. Variations among the sampled taxa are being pointed out where appropriate. All samples have

a diploe structure where external and internal cortices frame interior cancellous bone. Furthermore, the internal cortex is reduced in thickness compared to the external cortex.

External cortex—The bone tissue of the external cortex constitutes ISF. The external bone surfaces are rough and porous (Fig. 52a). This rough surface texture is linked to vascular canals opening up to the surface of the bone. Within the ISF, the fibre bundles are often of similar length and thickness, leading to an even spatial arrangement where fibre bundles equally trend perpendicular, subparallel and diagonal to the surface of the bone. However, the arrangement of the ISF can be locally dominated by fibre bundles that extend predominantly diagonally from the external bone surface towards the interior cancellous bone (Fig. 52b). This peculiar arrangement of fibre bundles is visible in most samples of *C. serpentina* and *C. murchisoni*, but not in the two specimens of *Chelydropsis* sp. Vascularisation of the bone tissue is high due to the amount of primary vascular canals and primary osteons. However, the bone tissue retains its compact appearance. The primary vascular canals often anastomose and branch, thus forming reticular vascularisation patterns.

Cancellous bone—The bone trabeculae of the cancellous bone are still largely primary, although, especially in the interior-most part of the cancellous bone, secondary remodelling into long and slender secondary trabeculae proceeds (Fig. 52c, d). The larger cavities between the trabeculae show a lining with secondary lamellar bone. The transition between the external and internal cortical layers and the interior cancellous bone in between is characterised by an increasing amount and size of secondary erosion cavities and scattered secondary osteons. Because of the strong progressive remodelling of both specimens of *Chelydropsis* sp., the transition zone is not present between cancellous bone and compact bone.

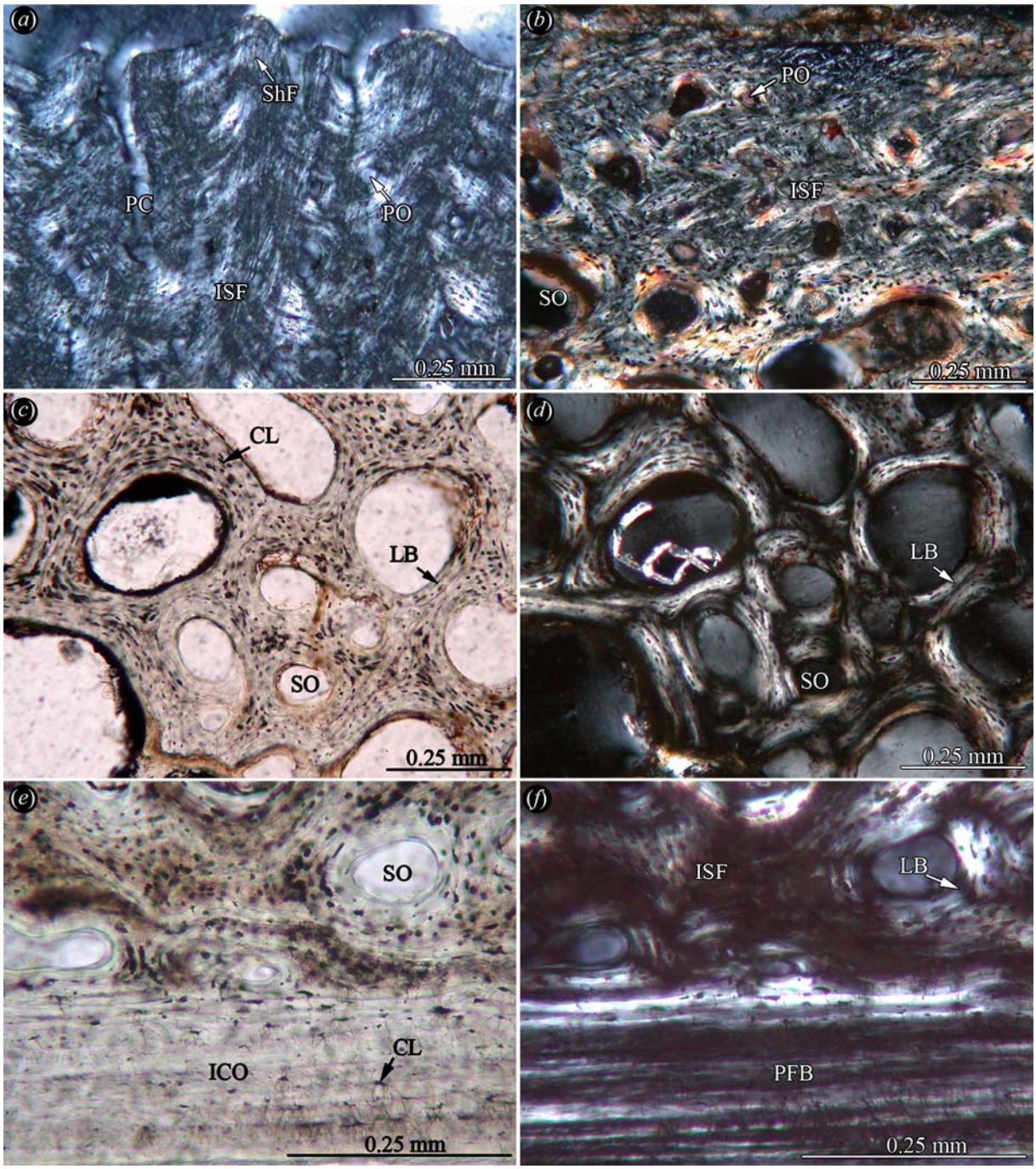

Figure 52: Shell bone histology of chelydrid turtle taxa. (*a*) Close-up of the scalloped external cortex of neural3 (YPM 10857) of *Chelydra serpentina* in polarised light. The bone tissue is highly vascularised by primary vascular canals. Many primary vascular canals end in small foramina on the external bone surface. (*b*) Close-up of the external cortex of sampled costal SMNS 88994 of *Chelydropsis murchisoni* in polarised light. Note predominantly oblique arrangement of interwoven structural fibre bundles. Close-up of the cancellous bone of neural3 (YPM 10857) of *Chelydra serpentina* in (*c*) normal and in (*d*) polarised light. Detail of the parallel-fibred bone tissue of the internal cortex of the former specimen in (*e*) normal

and in (*f*) polarised light.

Internal cortex—The internal cortex constitutes parallel-fibred bone (Fig. 52e, f). The arrangement of the fibres is roughly sub-parallel to the internal bone surface. However, towards and within the costal bulge of the costal of *C. serpentina*, the layers of the bone tissue seem to deviate until they extend perpendicular to the internal bone surface. Here, the bone cell lacunae are of lentil or oval shape and are aligned in an externointernal fashion. However, this peculiar orientation in the bone tissue and its respective bone cell lacunae is an artefact of sectioning the plate right at the location where the rib head (capitulum) protrudes from the costal plate. Instead of extending sub-parallel to the surface of the plate proper, the cell lacunae are aligned sub-parallel to the bone surface of the protruding capitulum. In contrast, the bone cell lacunae in the cortex next to the rib bulge in the costal plate are generally flattened and elongated and extend sub-parallel to the internal bone surface. In the costal of *C. murchisoni*, the plane of sectioning lies distal to the protruding capitulum, thus the arrangement of the bone layers reflects the 'normal' condition found also next to the rib bulge. However, the internal-most tip of the rib bulge has been eroded in the costal of *C. murchisoni*, thus a comparison of this region is not possible. Vascularisation is moderate to high in all bone elements, mainly achieved by scattered primary vascular canals and scattered primary osteons. The primary osteons are of similar diameter and evenly spaced throughout the successive parallel-fibred layers of the internal cortex. Sharpey's fibres were encountered in the sampled plastral elements and adjacent to the rib bulge in the costals.

Sutures—Where preserved, sutures of the shell bones were well developed with long bony protrusions and adjacent sockets. In *C. serpentina*, the bony protrusions and socket structures are elongated, thus reaching far into the bone proper towards its cancellous bone interior. Due to incomplete preservation of the fossil material, fibre bundles that extend perpendicular to the suture into the bone tissue were only found in the recent *C. serpentina*.

6.3.13 Testudinoidea indet.

Because of its divergent shell bone microstructure, as well as the remaining uncertainty of its phylogenetic position, *Platysternon megacephalum* is described separately from the other testudinoid clades.

6.3.13.1 *Platysternon megacephalum* Gray, 1831b

The sampled shell bones show a diploe with well developed cortices framing interior cancellous bone. Neither cortex is reduced in thickness (Fig. 53a, b).

External bone—The external cortex consists of ISF. The arrangement of the fibre bundles in the ISF is mostly obscured by the high amounts of collagenous matter in the samples. Predominantly diagonal directions are discernable in polarised light (Fig. 53c). The bone tissue is well vascularised with primary osteons and primary vascular canals, often extending diagonally and ultimately opening up to the external surfaces of the bones (thus causing the slightly rough external bone surface texture). In the core samples, the bone is overlain externally by a thin layer of connective tissue and the keratinous shield. The shield often has a wavy or scalloped external surface, and the growth marks of the successive keratin layers are also wavy or anastomosing.

Cancellous bone—The cancellous bone comprises thin and long bone trabeculae of secondary lamellar bone (Fig. 53b). Primary bone is found only in interstitial branching areas. The vascular spaces increase in size from external towards internal, and the largest cavities are found in the internal third of the cancellous bone. In the thin shell bones, many of the trabeculae extend externointernally or diagonally towards the cortices. This is often accompanied with a externointernal flattening of the vascular spaces.

Internal cortex—The internal cortex is a thick layer of predominantly avascular parallel-fibred bone (Fig. 53a, d). Only a few scattered primary vascular canals are present. Internal to the bone surface a layer of connective tissue is still present in the core samples.

Sutures—Even though the shell bones are quite thin in the macerated specimen (YPM 12615), the sutures are well developed with elongated bony protrusions and according sockets (Fig. 53d).

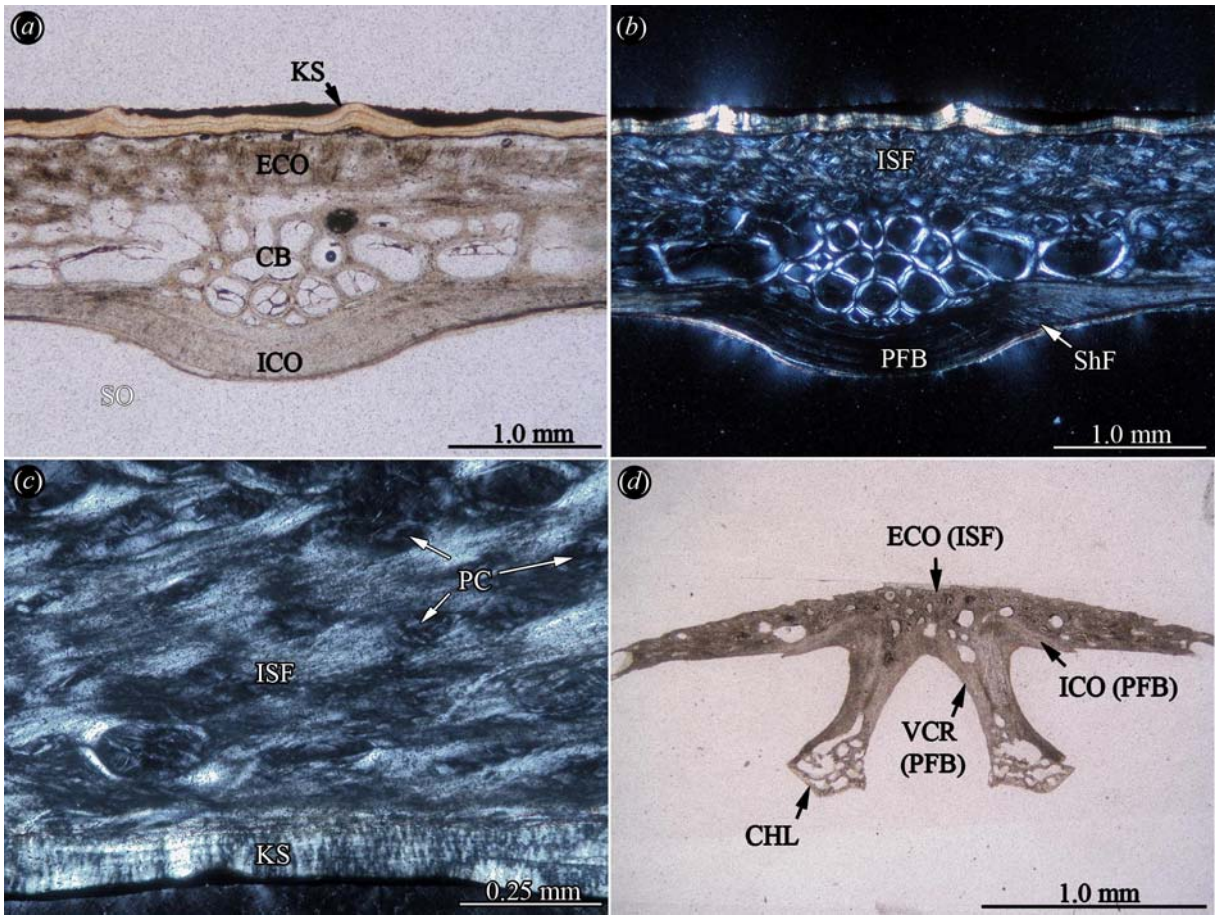

Figure 53: Shell bone histology of *Platysternon megacephalum*. Section of sub-sampled costal and associated keratinous shield (SMNS 3757; drilled core) in (*a*) normal and in (*b*) polarised light. Note the rib bulge of the internal cortex and the cancellous bone. Sharpey's fibres insert into the internal cortex lateral to the rib bulge. (*c*) Close-up of the external cortex of sub-sampled left hypoplastron and associated keratinous shield (SMNS 3757, drilled core) in polarised light. The fibre bundles of the interwoven tissue extend predominantly obliquely towards the external surface of the bone. (*d*) Complete thin-section of neural3 (YPM 12615; juvenile) in normal transmitted light. Note how the internal cortical bone (parallel-fibred bone) deviates towards interal from the flat plate part of the neural to the neural arch. The roof of the vertebral canal consists also of parallel-fibred bone. Chondrocyte lacunae are present at the internal ends of the branches of the neural arch. The sutural zone is well developed with few but long pegs and sockets.

6.3.14 Emydidae, Geoemydidae/Bataguridae and Testudinidae

Variation of the shell bone microstructures among these testudinoid clades is low. Only three histotypes (type I-III) are recognised. While the bone tissue types (e.g., ISF of the external cortex; parallel-fibred bone of the internal cortex) are generally similar for all testudinoid turtles, the histotypes mainly reflect independent levels and patterns of vascularisation of the primary cortical bone tissue as well as the general structure of the cancellous bone.

6.3.14.1 Testudinoid histotype I

Included taxa: Emydid turtles: *Terrapene carolina triunguis* (Agassiz, 1857); geoemydid/batagurid turtles: *Pangshura* (=*Kachuga*) *tentoria* (Gray, 1834); testudinid turtles: *Manouria emys* (Schlegel and Müller, 1844), , *Geochelone pardalis* (Bell, 1828), *Geochelone elegans* (Schoepff, 1795); [intermediates between **histotypes I** and **II**]: Geoemydid/batagurid turtles: *Cuora picturata* Lehr et al. 1998, *Mauremys cf. M. mutica* (Cantor, 1842); testudinid turtles: *Hesperotestudo* (*Caudochelys*) *crassiscutata* (Leidy, 1889) (†)

The bone histology of all included taxa is characterised by the typical diploe build. Internal and external compact bone layers delineate an interior area of cancellous bone. Although overall shell bone thickness differs among the taxa, the cortices are generally well developed. All samples had a micro-rough texture of the external bone surfaces. The internal surfaces of the bones were generally smooth. Growth marks occur in both cortices, but they are often convoluted or discontinuous.

External cortex—The external cortex comprises metaplastic ISF, where the fibre bundles of similar length and diameter are orientated perpendicular, parallel and diagonal to the external bone surface. Depending on the exact plane of sectioning, the fibre bundles seem to resemble a well-ordered close-knit fabric. The vascularisation of the bone tissue is generally low with primary vascular canals and few scattered primary osteons. Many of the primary canals open up towards the surface of the bone, causing the rough texture of the external cortex (see above). Growth marks that extend sub-parallel to the external bone surface are present in the

external cortices of all taxa. The transition to the cancellous bone is usually clearly defined instead of representing a gradual shift. Scattered secondary osteons are generally found at the transition between external cortical and cancellous bone. They increase in size and number in the compact bone layers situated immediately next to the interior cancellous bone, as those cortical layers are first remodelled and vascularised with growth and increasing age of the turtle.

Cancellous bone—The cancellous bone consists of mostly short and thick bone trabeculae and small to medium sized vascular spaces. However, in thicker shell bones, the bone trabeculae can also be longer and more slender, as seen for example in the peripheral of *C. picturata* and in the very thick bones of *H. crassiscutata*. The bone trabeculae are usually lined with secondary lamellar bone towards the vascular spaces, resulting in a well-vascularised meshwork. Some vascular spaces of irregular shape in the trabecular meshwork do not yet have a lining with secondary lamellar bone. Primary bone tissue, i.e., ISF is usually preserved in the interstitial areas of the bone trabeculae. Bone cells and their lacunae are round and numerous in the primary interstitial bone. In the secondary lamellar bone, bone cells and lacunae are flattened and elongated in shape and more sparsely distributed.

Internal cortex—The internal cortex constitutes parallel-fibred bone with local transitions into lamellar bone. The bone tissue is generally weakly vascularised with few scattered primary vascular canals or it is even avascular. Only occasionally, a scattered primary osteon is found in the cortical bone. Lateral to the rib bulge of costals, the incorporated neural arch in neurals and the buttress regions of the hyo- and hypoplastra, many fibre bundles insert obliquely into the internal cortex of the bone, indicating the presence of Sharpey's fibres. In polarised light, the Sharpey's fibres are birefringent. Bone cell lacunae are elongated and irregular in shape in the bone tissue. Similar to the external cortical bone, the transitional zone of the internal cortex to the cancellous bone is clearly marked by scattered secondary osteons.

Sutures—The sutural zones are well developed with moderate to high relief of interdigitating bony pegs and sockets.

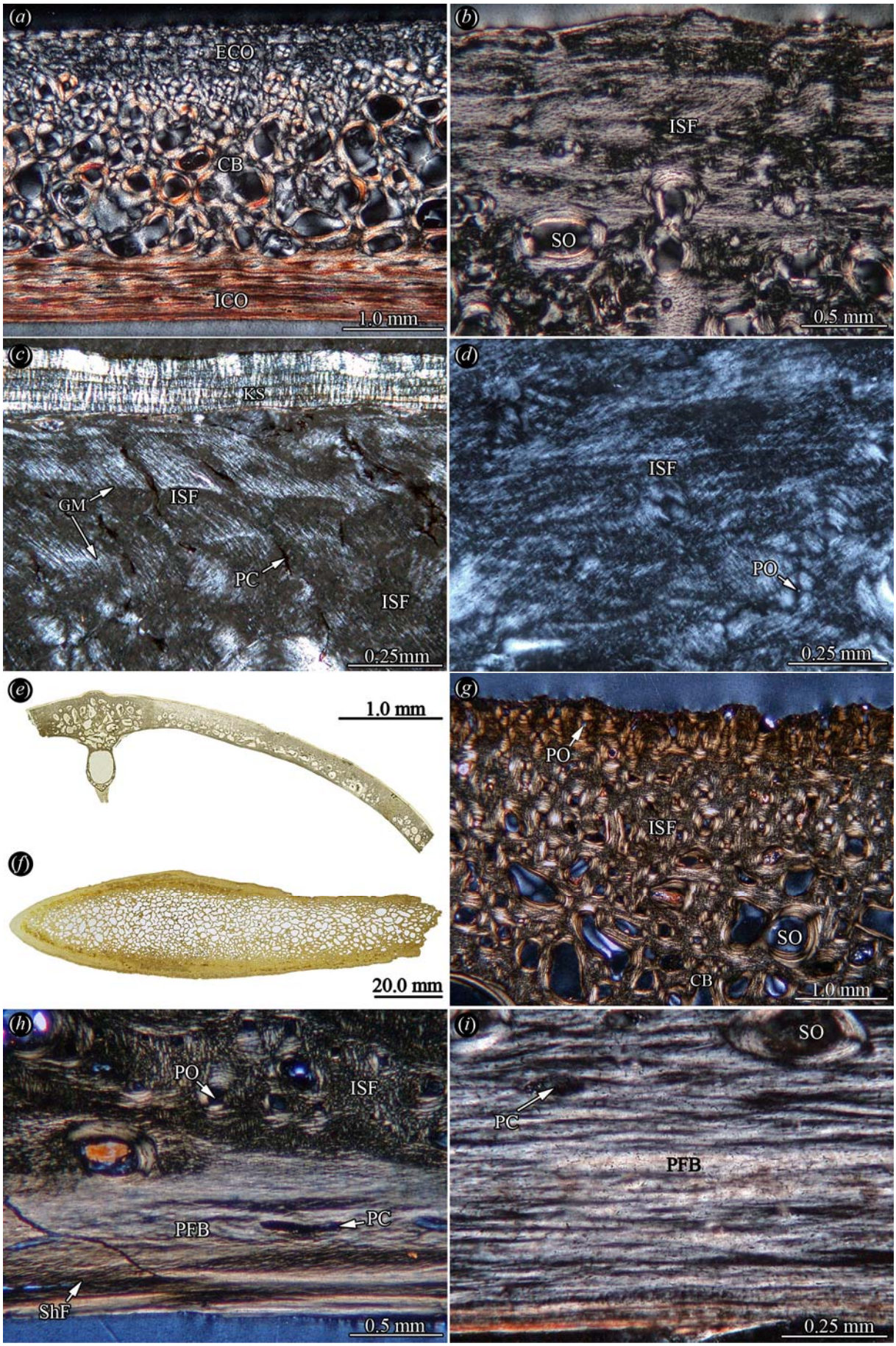
(a)
ECO
CB
ICO
1.0 mm
(b)
ISF
SO
0.5 mm
(c)
KS
GM
ISF
PC
ISF
0.25mm
(d)
ISF
PO
0.25 mm
(e)
1.0 mm
(f)
20.0 mm
(g)
PO
ISF
SO
CB
1.0 mm
(h)
PO
ISF
PFB
PC
ShF
0.5 mm
(i)
SO
PC
PFB
0.25 mm

Figure 54: Testudinoid histotype I. (*a*) Complete thin-section of right hyoplastron (YPM 13877) of *Cuora picturata*. The diploe-structure of the shell bone is well developed. Note typical cross-polarisation of secondary osteons at transition of external cortex and interior cancellous bone. (*b*) Close-up of weakly vascularised interwoven structural fibre bundles of external cortex of right hypoplastron (SMNS 12605) of *Geochelone pardalis*. (*c*) Close-up of interwoven structural fibre bundles of external cortex of costal (FMNH 211806) of *Terrapene carolina triunguis*. The bone is weakly vascularised with few thin primary vascular canals. Note the keratinous shield covering the roughly textured surface of the bone. (*d*) Close-up of interwoven structural fibre bundles of external cortex of left hyoplastron (FMNH 260395) of *Manouria emys* in polarised light. The bone tissue is vascularised by few primary osteons. (*e*) Complete thin-section of neural and costal of *T. c. triunguis* (FMNH 211806) in normal transmitted light. Vascular cavities of the cancellous bone are small, giving the whole bone a compact appearance. (*f*) Complete thin-section of xiphiplastron of *Hesperotestudo crassiscutata* (ROM 55400). The trabeculae in this very thick bone are longer and more slender, building a kind of light-weight interior compared to the cancellous bone seen in *T. c. triunguis*. (*g*) Close-up of external cortex of sampled costal (ROM 55400) of *Hesperotestudo crassiscutata* observed in polarised light. Vascularisation of the cortical bone is observed in form of primary osteons and straight or branching primary canals. Larger scattered secondary osteons are only developed in the direct vicinity of the interior cancellous bone. Interwoven structural fibre bundles appear like a close-knit fabric. Note how some primary osteons trend almost perpendicular to the surface of the bone. (*h*) Internal cortex of former specimen in polarised light. Note that the layers next to the surface of the bone are sparsely vascularised. Large areas of primary interstitial bone of interwoven fibre bundles (again resembling a close-knit fabric), interspersed with primary and secondary osteons, occur in the interior regions of the cortex. (*i*) Close-up of the mainly avascular parallel-fibred bone of the internal cortex of hyoplastron (FMNH 211806) of *T. c. triunguis* in polarised light.

Variation—The vascularisation of the internal cortex is very low in *T. c. triunguis*, *P. tentoria* and *H. crassiscutata*. In these taxa, the bone layers are mostly avascular. In comparison, *C. picturata* and *Mauremys cf. M. mutica* have a slightly increased vascularisation of the internal cortical bone and are thus regarded as being somewhat intermediate between histotypes I and II.

6.3.14.2 Testudinoid histotype II

Included taxa: Emydid turtles: *Pseudemys peninsularis* Carr, 1938, Emydidae indet. (?Platysternoid "C") (†); geoemydid/batagurid turtles: *Mauremys* (= '*Ocadia*') *sophiae* (Ammon, 1911) (†), *Mauremys* (='*Ocadia*') sp. (†), *Cyclemys dentata* (Gray, 1831a), *Rhinoclemmys pulcherrima* (Gray, 1855), testudinid turtles: *Geochelone carbonaria* (Spix, 1824), *Kinixys homeana* Bell, 1827; [Intermediates between **histotypes II** and **III**]: emydid turtle: *Emys orbicularis* (Linnaeus, 1758); geoemydid/batagurid turtle: *Ptychogaster* sp. (†); testudinid turtles: *Hadrianus majusculus* Hay, 1904 (†), *Hadrianus corsoni* (Leidy, 1871a) (†)

All shell bones have a diploe structure, where internal and external cortical bone layers frame interior cancellous bone. Both cortices are well developed, and the whole bone retains a generally compact appearance.

External cortex—The external cortical bone consists of fine-fibred ISF. The fibre bundles in the ISF are mostly similar in length and thickness. Most taxa, e.g., *Pseudemys floridana*, have a homogeneous arrangement of fibre bundles that extend perpendicular, parallel and oblique to the external surface of the bone (Fig. 55a, b). In *E. orbicularis* (fig. 55c) and *K. homeana*, the fibre bundles are somewhat thicker, and the ISF is dominated by surface-parallel and oblique fibre bundles. The vascularisation of the cortical bone is moderate, often with reticular or branching patterns of primary vascular canals. Many of the primary vascular canals reach the surface of the bone as small foramina. Primary osteons appear seldom. Internally, there is a thin transition zone to the interior cancellous bone consisting mostly of scattered small secondary osteons and erosion cavities. Growth marks in the bone tissue are clearly visible. However, they do not always appear as highly birefringent lines in polarised light. In *Hadrianus* spp., the vascularisation of the external bone tissue is moderate to high, because of large amounts of primary osteons (Fig. 55d).

Cancellous bone—The cancellous bone generally consists of short and thick primary bone trabeculae and small vascular spaces. In few cases, e.g., in *P. peninsularis*, the interior of the shell bone is dominated by large secondary osteons and irregular erosion cavities in the primary bone tissue, i.e., ISF. Longer and more slender trabeculae are either absent here, or they are restricted to the most internal parts of the interior cancellous bone. The bone trabeculae are usually lined with a thin sheath of secondary lamellar bone (Fig. 55e). In *G.*

carbonaria, the thickness of the cancellous bone layer is either rather constant (plastron) or highly variable (carapace). This variation is directly connected with the thickness of the cancellous bone in the elements of the carapace (Fig. 55f). While the bone below the centre of a keratinous scute has a well developed cancellous interior, the areas directly internal to the scute sulci appear to consist only of a single fused layer of external and internal compact bone. Still, on close inspection, this fused bone layer is not completely compact and avascular, but small erosion cavities are found.

Internal cortex—The internal cortex consists of parallel-fibred bone (Fig. 55g). The vascularisation is generally low. In most taxa, avascular layers intercalate with layers that are weakly vascularised by primary vascular canals. Depending on the plane of sectioning, the vascular canals appear round to ovoid in shape (e.g., in the cross-section of the costal of *C. dentata*), or they are elongated single or branching tubes (e.g., in transverse section of the costal of *C. dentata*). However, transitions between these two 'terminal' stages are observed. In *Hadrianus* spp. (Fig. 55h), *E. orbicularis* and *Ptychogaster* sp., the vascularisation of the internal bone tissue is raised, due to large amounts of primary osteons and primary vascular canals. Growth marks are present in the internal cortices. Often, the layers of parallel-fibred bone between the growth marks are slightly rotated to each other. In those cases, the internal cortex does not appear as a single zone where fibres all have a similar orientation, but rather as a succession of light and dark bands characteristic of lamellar bone.

Sutures—The sutural zones consist of interdigitating bony pegs and sockets, creating a low to moderate relief. The sutural bone tissue has a similar histology to the external cortical bone. Fibre bundles that insert perpendicular into the marginal bone often dominate the bone tissue here. Because of the unusual presence of a carapacial hinge system, the bone histology of *K. homeana* is somewhat divergent. The hinge sutures show a reduced amount or a complete loss of interdigitating structures. A reduced stage is encountered in the hinge neurals and in the hinge costals. Here, only a few irregular short pegs and sockets are found. The hinge peripherals, on the other hand, lack any interdigitating sutures. Instead, the compact bone of the margins is round and slightly scalloped.

Variation—Because *E. orbicularis*, *Ptychogaster* sp. and *Hadrianus* spp. show a tendency for increased overall vascularisation and a more open cancellous bone structure, they are therefore regarded as intermediate between histotypes II and III.

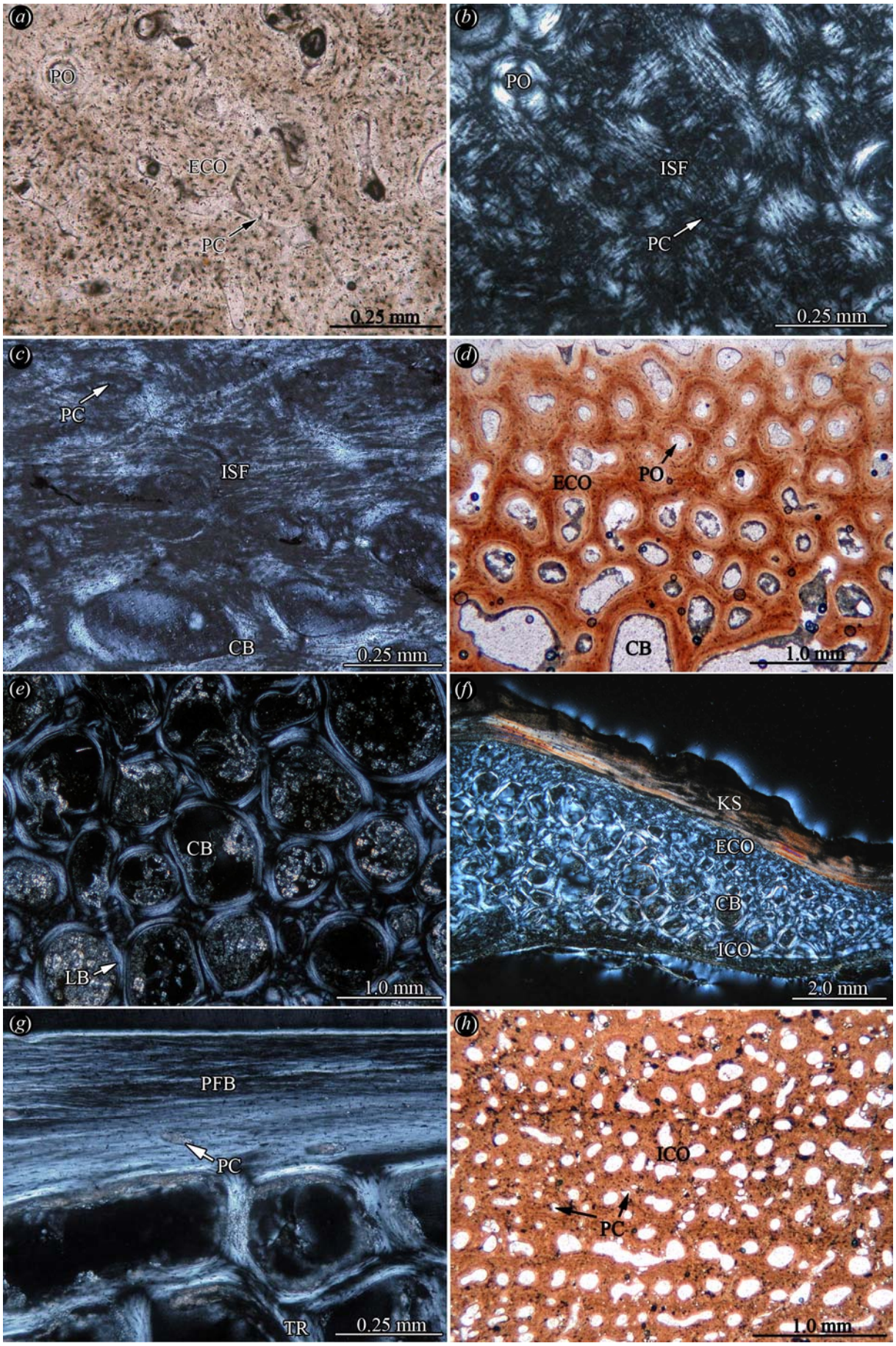
(a)
PO
ECO
PC
0.25 mm
(b)
PO
ISF
PC
0.25 mm
(c)
PC
ISF
CB
0.25 mm
(d)
ECO
PO
CB
1.0 mm
(e)
CB
LB
1.0 mm
(f)
KS
ECO
CB
ICO
2.0 mm
(g)
PFB
PC
TR
0.25 mm
(h)
ICO
PC
1.0 mm

Figure 55: Testudinoid histotype II. Close-up of the external cortex of left hypoplastron of *Pseudemys peninsularis* (YPM 13878) in (*a*) normal and in (*b*) polarised light. The fine-fibred bone tissue is moderately vascularised by branching or reticular primary vascular canals. (*c*) Close-up of the external cortex of sampled costal6 (SMNS 6880) of *Emys orbicularis* in polarised light. Fibre bundles are coarser and extend predominantly parallel or obliquely to the external surface of the bone. (*d*) Close-up of external cortex of the costal UCMP V74024/150213 of *Hadrianus majusculus* in normal transmitted light. The bone tissue is moderately to highly vascularised based on the large amount of primary osteons. Note strongly scalloped external bone surface. (*e*) Detail of the cancellous bone of left hypoplastron (YPM 13878) of *Pseudemys peninsularis* in polarised light. The bone trabeculae are generally thick and short and lined with a thin layer of lamellar bone. (*f*) Section of the sub-sampled proximal part of costal (IPB R560a) of *Geochelone carbonaria* in polarised light. Note the strong variation in bone thickness.The external surface of the bone is covered by a thin layer of connective tissue and a thick scalloped keratinous shield. The keratin layers extend irregularly and often anastomose. The external surface of the shield is highly scalloped. (*g*) Close-up of the internal cortex and internal part of cancellous bone of right hyoplastron (MVZ 230924) of *Rhinoclemmys pulcherrima* in polarised light. The cortical parallel-fibred bone is generally weakly vascularised. (*h*) Close-up of the internal cortex of plastron fragment UCMP V74024/150215 of *Hadrianus majusculus* in normal transmitted light. The cortical bone shows raised vascularisation based on the large amounts of primary osteons and primary vascular canals.

6.3.14.3 Testudinoid histotype III

Included taxa: Emydid turtles: *Trachemys scripta* (Schoepff, 1792) (†); geoemydid/batagurid turtles: *Clemmydopsis turnauensis* (Meyer, 1847b) (†), *Echmatemys wyomingensis* (Leidy, 1869) (†)

All taxa have a diploe structure with external and internal cortices and interior cancellous bone. The thicknesses of the cortical bone layers may vary. Often, the internal cortex is thinner compared to the external cortex.

External cortex—The external cortex comprises ISF with growth marks. The growth marks are more clearly visible and less affected by remodelling in the more external regions of the cortex. Fibre bundles of the ISF are usually homogeneous in distribution, length and diameter. There is also a slight dominance of fibre bundles that extend perpendicular to the external surface of the bone. The grade of vascularisation is medium to high, because of extensive reticular patterns of primary vascular canals, few scattered primary osteons and small secondary osteons. The secondary osteons increase in diameter at the transition to the interior cancellous bone.

Cancellous bone—The cancellous bone is usually well developed. It consists of smaller and larger vascular spaces, with the latter ones occurring mostly in the more internal part of the cancellous bone. Many trabeculae are still primary. Where remodelling processes affected the bone tissue, the trabeculae consist only of lamellar bone. In thicker shell bones, the trabeculae are longer and more gracile. Additionally, larger erosion cavities are observable that still lack a secondary lining of lamellar bone.

Internal cortex—The internal cortex consists of parallel-fibred bone. In *T. scripta* and *C. turnauensis*, the grade of vascularisation is low to medium due to scattered primary vascular canals and secondary osteons. In *E. wyomingensis*, the more external parts of the internal cortex is more extensively remodelled, thus the vascularisation appears generally higher. The transitional zone between the cortical bone layers and the cancellous bone is diffuse instead of a clear boundary.

Sutures—The sutures are moderately developed with short to medium sized interdigitating bony pegs and sockets. Fibre bundles that extend perpendicular to the bone margins are observed. There is almost no compact bone left in the sutural zone, because the interior cancellous bone reaches far laterally towards the bone margin.

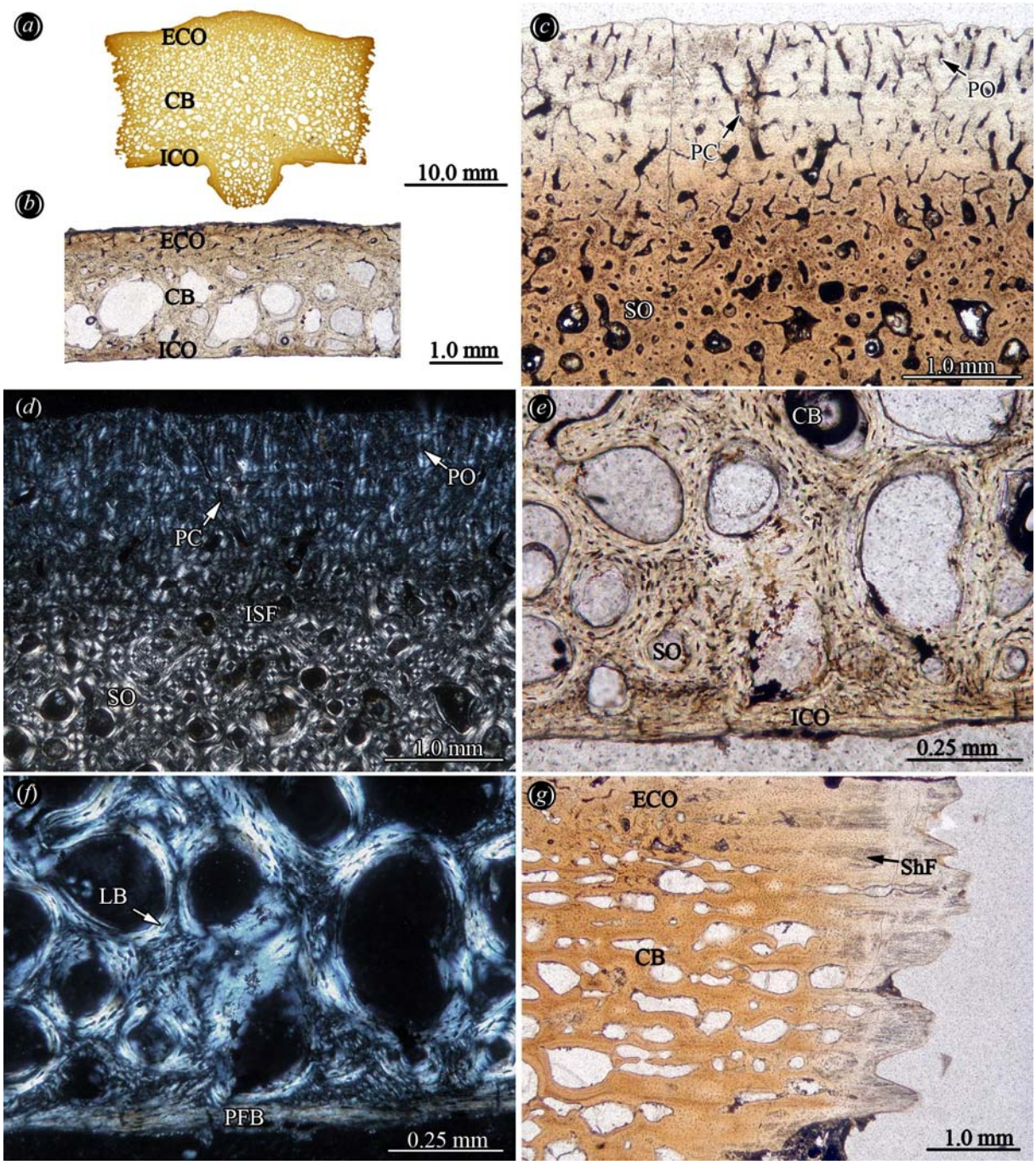

Figure 56: Testudinoid histotype III. (*a*) Complete thin-section of the neural ROM 34287 of *Trachemys scripta* in normal transmitted light. The extensive interior cancellous bone reaches far towards the external and internal surfaces and the lateral margins of the bone. (*b*) Section of the sampled costal SMNS 88998 of *Clemmydopsis turnauensis* in normal transmitted light. Note the reduced internal cortex and the large irregular vascular spaces in the cancellous bone of the diploe-structure. Detail of the extneral cortex of *Echmatemys wyomingensis* in (*c*) normal and in (*d*) polarised light. The bone tissue is strongly vascularised. Close-up of the internal part of the cancellous bone and the internal cortex of costal SMNS 88998 of

Clemmydopsis turnauensis in (*e*) normal and in (*f*) polarised light. The bone trabeculae are mostly remodelled and consist of secondary lamellar bone. The thin internal cortex consists of moderately vascularised parallel-fibred bone. (*g*) Close-up of the sutural zone of the sampled proximal part of costal8 UCMP V81110/150183 of *Echmatemys wyomingensis* in normal transmitted light. The sutural relief is generally low with short to medium sized pegs and sockets. The cancellous bone reaches far towards the lateral bone margins. Sharpey's fibres that insert perpendicular into the marginal bone tissue are common.

6.3.15 Eucryptodira incertae sedis (aff. ?Trionychoidea)

6.3.15.1 *Planetochelys* sp. (†)

In *Planetochelys* sp., the shell elements have a diploe structure. The external cortex is slightly thicker than the internal cortex. The interior cancellous bone has an overall compact appearance. All bones are strongly affected by diagenetic alteration, thus most of the microstructural details are obscured.

External cortex—The cortex consists of fine-fibred ISF, with the fibre bundles having similar lengths and diameters (Fig. 57a). The fibre bundles extend perpendicular, parallel and obliquely towards the external surface of the bone. The bone tissue is vascularised by few scattered primary osteons and short primary vascular canals. There is a narrow transition zone between the external cortex and the interior cancellous bone. This zone is characterised by small scattered secondary osteons and irregularly shaped erosion cavities.

Cancellous bone—The cancellous bone consists of a short and thick primary trabeculae and small to medium sized vascular spaces (Fig. 57b). The shape of the vascular spaces ranges from circular to ovoid or to irregular (Fig. 57b, c). The trabeculae are lined with secondary lamellar bone.

Internal cortex—The internal cortex comprises mainly avascular parallel-fibred bone (Fig. 57d). Only occasionally, scattered primary vascular canals are observed. Remodelling of the compact bone layers is restricted to the more external part of the internal cortex.

Sutures—The sutures generally have a low relief with short bony pegs and sockets. In the two fragments of the plastron that show a hinge margin, however, no interdigitating suture is developed. Instead, the margins of the plastral elements (?hyo- or hypoplastra) are smooth with only a slight transverse groove. The observed bone tissue in the suture zone is similar to the bone tissue of the external cortex.

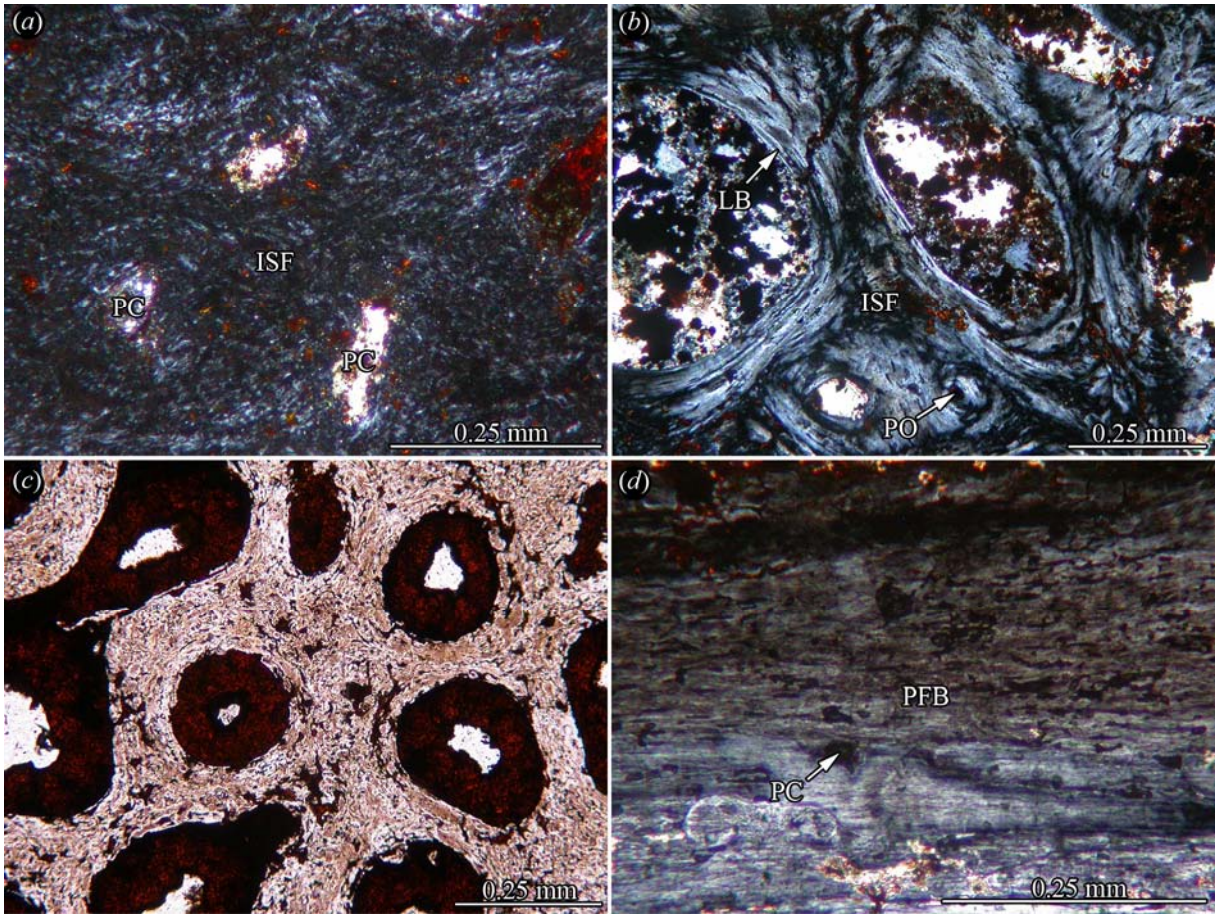

Figure 57: Shell bone histology of *Planetochelys* sp. (*a*) Close-up of the interwoven structural fibre bundles of the external cortex of plastron fragment (UCMP V81071/159356) in polarised light. (*b*) Close-up of the cancellous bone of the proximal part of costal (UCMP V81071/159356, L-section) in polarised light. The primary bone trabeculae are lined with secondary lamellar bone. (*c*) Close-up of the cancellous bone of plastron fragment (UCMP V81071/159356) in normal transmitted light. Note how the bone tissue is diagenetically altered and the histological details are lost. (*d*) Close-up of the internal cortical bone (parallel-fibred bone) of costal (UCMP V81071/159356; X-section) in polarised light. The bone tissue shows little to no vascularisation.

6.3.16 Dermatemydidae

6.3.16.1 *Baptemys garmanii* (Cope, 1872b) (†) and *Dermatemys mawii* Gray, 1847

Both taxa share a highly similar bone microstructure and are thus described in one section. All shell bones have a weakly developed diploe structure with highly vascularised cortices and well developed interior cancellous bone.

External cortex—The external cortex consists of ISF. The fibre bundles of the ISF extend parallel, perpendicular and oblique to the external surface of the bone (Fig. 58a). The bone tissue is dominated by surface-parallel fibre bundles. The vascularisation is moderate to high, because of an extensive reticular patterns of primary vascular canals (fig. 58a, b). Towards internal, there is a broad transition zone between the cortical and cancellous bone with scattered secondary osteons and erosion cavities of different sizes.

Cancellous bone—The cancellous bone is composed of regularly spaced and similarly sized trabeculae and vascular cavities. Most of the trabeculae are remodelled and consist of secondary lamellar bone. Primary bone is restricted to a few interstitial trabecular branching areas. Locally, the trabecular structure is highly ordered into struts that extend perpendicular to each other, thus resulting in rectangular and quadrangular shapes and patterns (Fig. 58c, d) for the vascular spaces (e.g., plastral fragment of *B. garmanii*, UCMP V74024/150221).

Internal cortex—The cortices consist of parallel-fibred bone (Fig. 58e, f). Vascularisation of the tissue is high. In the more external parts, remodelling is extensive and many scattered secondary osteons and erosion cavities are found. Towards internal, the cortical bone is vascularised by numerous primary vascular canals and primary osteons that often appear sheet-like and even spaced in layers. These highly vascularised layers intercalate with layers that are less vascularised or even avascular. Thus a regular pattern of vascular spaces within the cortical bone is developed.

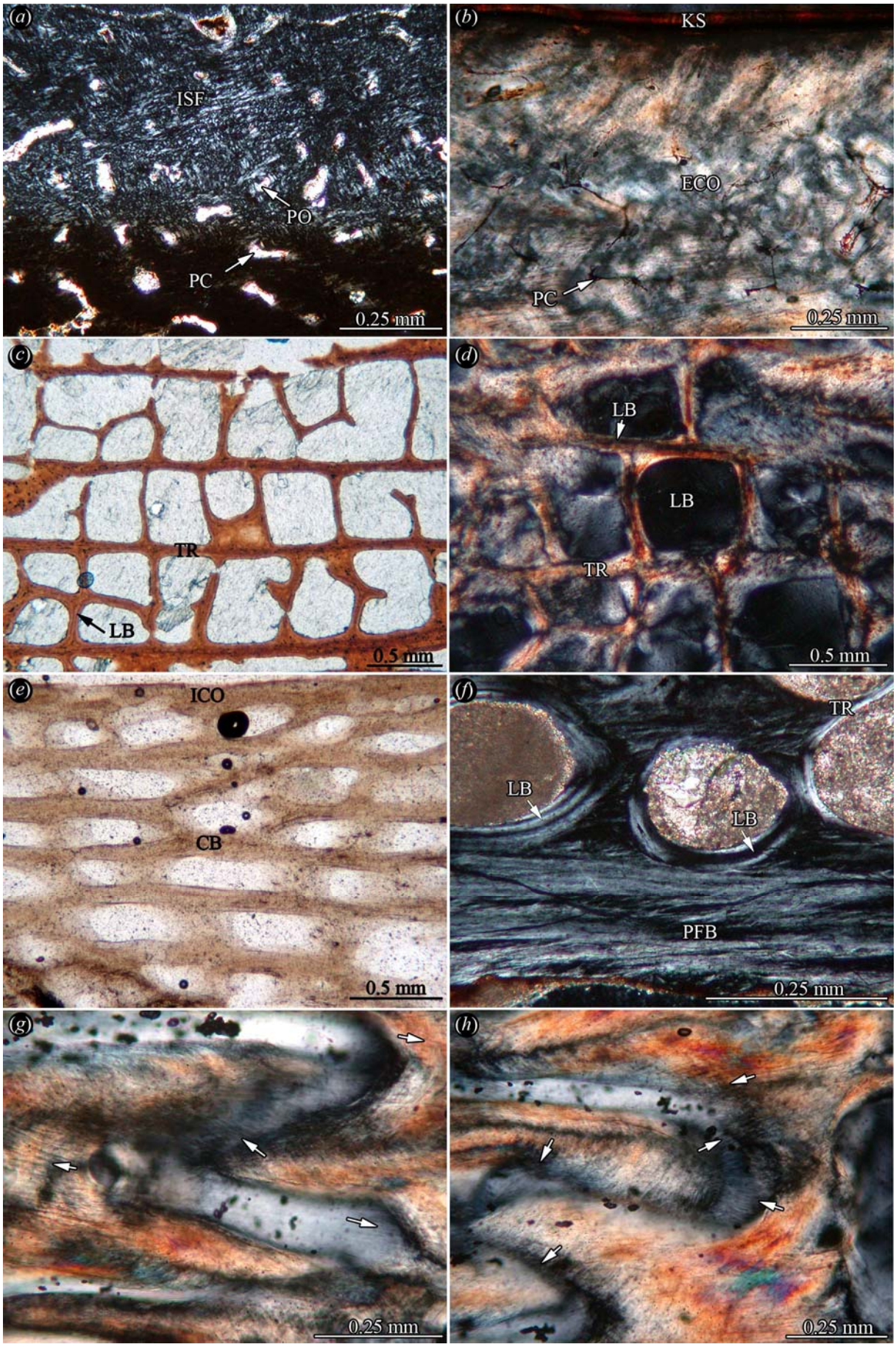
(a)
ISF
PO
PC
0.25 mm
(b)
KS
ECO
PC
0.25 mm
(c)
TR
LB
0.5 mm
(d)
LB
LB
TR
0.5 mm
(e)
ICO
CB
0.5 mm
(f)
TR
LB
LB
PFB
0.25 mm
(g)
0.25 mm
(h)
0.25 mm

Figure 58: Shell bone histology of dermatemydid turtle taxa. (*a*) Close-up of the external cortex of peripheral UCMP V74024/150222 of *Baptemys garmanii* in polarised light. The bone tissue consists of fine interwoven structural fibre bundles. Note the moderate to high vascularisation based on high amount of reticular primary vascualar canals and primary osteons. (*b*) Close-up of the external cortex of sub-sampled left costal2 (ZMB 9558) of *Dermatemys mawii* in polarised light. Note the very thin keratinous shield covering the bone. Similar to *B. garmanii*, vascularisation of the external cortex is moderate to high. (*c*) Close-up of the highly ordered structure of the cancellous bone of plastron fragment UCMP V74024/150221 of *B. garmanii* in normal transmitted light. Locally, the vascular cavities are almost rectangular in thin-section. (*d*) Close-up of similarly ordered structure of the cancellous bone of sub-sampled right hyoplastron (ZMB 9558) of *D. mawii* in polarised light. Note that many of the thin trabeculae consist only of secondary lamellar bone. (*e*) Close-up of internal part of the cancellous bone and the internal cortex of former specimen in normal transmitted light. The internal cortex is greatly reduced in thickness, and the cancellos bone reaches almost up to the surface of the bone. (*f*) Close-up of internal part of the cancellous bone and the internal cortex of neural UCMP V74024/150224 of *B. garmanii*. The internal cortex appears as a more compact layer of parallel-fibred bone. (*g*) and (*h*) Different sections of the sutural zone between sub-sampled costal2 and margin of adjacent costal3 (ZMB 9558, drilled core) of *D. mawii*, both in polarised light. The soft connective tissue between the bones is preserved. Connective fibre bundles, i.e., Sharpey's fibres, are observable that span the suture zone (indicated by white arrows) to insert into the marginal tissue of each bone respectively. Due to the sutural relief, the fibre bundles overlap each other in the apical regions of the bony pegs, while they insert more parallel to each other in the socket regions.

Sutures—The sutures have a high relief with thin elongated bony pegs and sockets. Fibre bundles, i.e., Sharpey's fibres that insert perpendicular to the bone margins are common. Based on the good preservation of the core samples of the recent *D. mawii*, the progression of the fibre bundles is also visible in the soft tissue space between the adjacent bones (Fig. 58g, h). Due to the relief in the suture, the soft fibre bundles overlap in the apical regions of the bony pegs, while they insert parallel to each other in the socket regions.

6.3.17 Kinosternia

6.3.17.1 *Hoplochelys* sp. (†)

The bones of *Hoplochelys* sp. show a barely-developed diploe with compact bone layers framing cancellous bone (Fig. 59a). Due to the reduction of the thickness of cortical bone and heavy vascularisation, the cancellous interior dominates the bone structure.

External cortex—The external cortex consists of ISF. The fibre bundles are homogeneous in size and diameter. The fibre bundles extend perpendicular, parallel and oblique to the external bone surface. The vascularisation of the bone tissue is generally high based on reticular patterns of primary vascular canals and large numbers of primary osteons (Fig. 59b). The reticular patterns are often dominated by vascular canals that extend perpendicular to the external surface of the bone, often opening up to the surface as small foramina. Undulating growth marks are encountered throughout the cortical bone.

Cancellous bone—The interior cancellous bone is composed of homogeneously arranged thick and rather short trabeculae as well as small and closely spaced vascular cavities. The trabeculae are mostly primary bone tissue, i.e., ISF, sheathed in secondary lamellar bone. In the more remodelled central areas of the thicker bones, e.g., the peripherals (Fig. 59c), thin and elongated bone trabeculae are observed that consist mainly of lamellar bone.

Internal cortex—The internal cortex can be separated into two zones. The more external zone shows still the structure of the ISF seen in the external cortex and the interstitial areas of the cancellous bone (Fig. 59d, e). The more internal zone comprises parallel-fibred bone. The whole of the internal cortex is strongly affected by remodelling processes. Overall, the cortex looses its compact nature due to the high amounts of secondary osteons, erosion cavities and primary vascular canals.

Sutures—The sutures have a narrow relief with short and stocky bony pegs and corresponding sockets (Fig. 59f). Generally, the sutural bone tissue appears similar to the ISF that was observed in the rest of the bone. The interior cancellous bone reaches far into the sutural zone, but few layers appear less affected by remodelling processes than the

surrounding tissue. Fibre bundles that extend perpendicular into the marginal bone tissue are not a prominent feature.

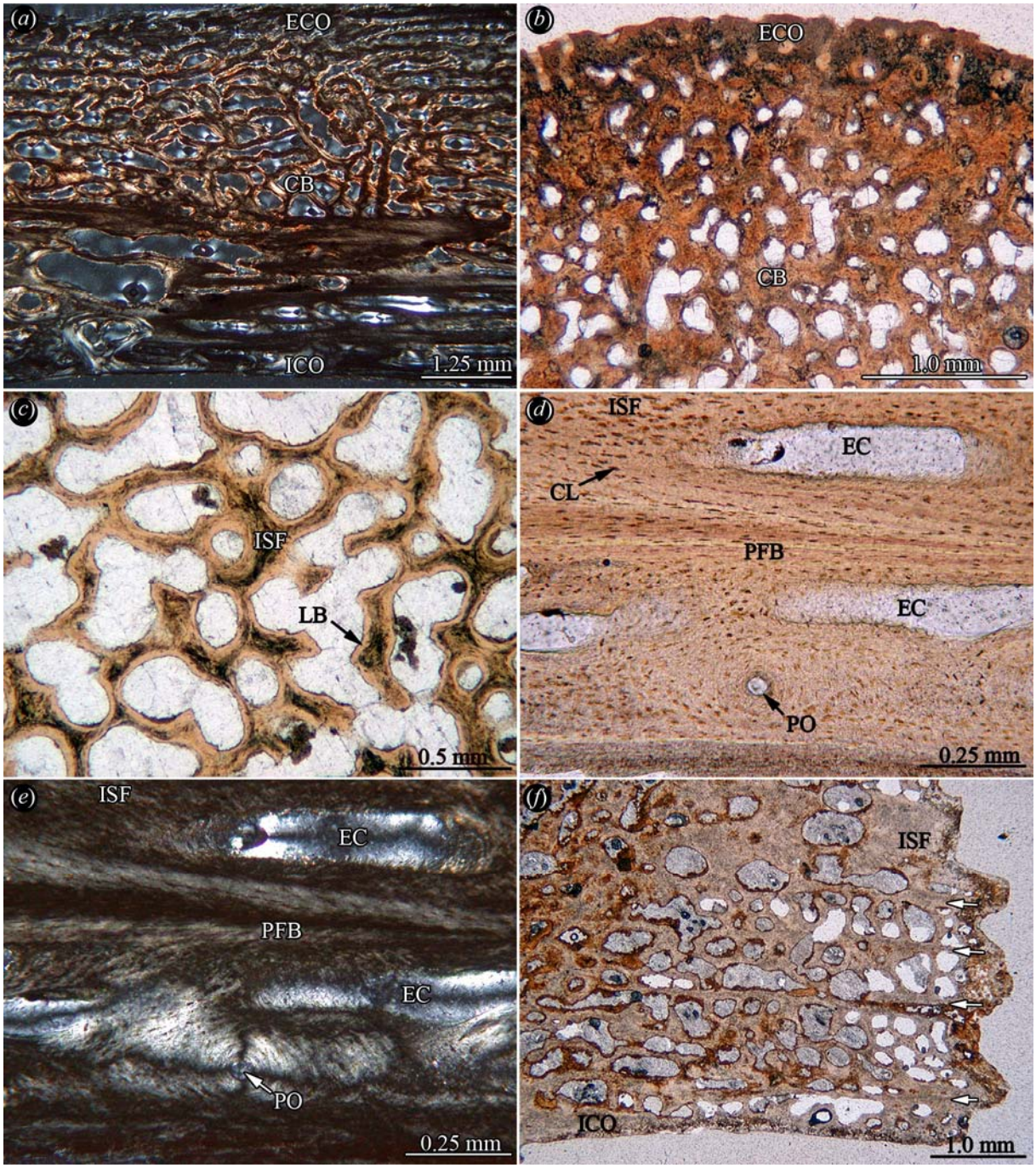

Figure 59: Shell bone histology of *Hoplochelys* sp. (*a*) Section of costal UCMP V2811/150203 in polarised light. Note that the cortical bone is heavily vascularised. (*b*) Close-up of the external cortex of left peripheral8 (UCMP V2811/150206) in normal transmitted light. Based on the high vascularisation, the external cortex looses its compact nature. (*c*) Close-up of the more slender and longer trabeculae of the cancellous bone of the

former specimen in normal transmitted light. Close-up of the internal cortex of costal UCMP V2811/150203 in (*d*) normal and in (e) polarised light. The cortex is strongly remodelled. Internally, the parallel-fibred bone grades into fine interwoven structural fibre bundles. (*f*) Close-up of the suture zone of neural V2811/150210 in normal transmitted light. The sutural zone has a narrow relief with short and blunt pegs and sockets.

6.3.18 Kinosternidae

6.3.18.1 *Baltemys* sp. (†), *Sternotherus minor* (Agassiz, 1857), *Kinosternon subrubrum* (Bonnaterre, 1789) and *Kinosternon* sp.

The four kinosternid taxa show a diploe structures in their shell bones, with well developed cortices framing interior cancellous bone. Both cortices are of similar thickness. Only two shell elements (the peripheral and the plastron fragment) of *Baltemys* sp. are sufficiently unaltered diagenetically that bone histological details are visible. The remainder is so strongly influenced by diagenesis that the bone histology is barely discernable. Two plastral hinge systems were studied in the core samples of *Kinosternon* sp.

External cortex—The bone tissue consists of fine fibred ISF. Fibre bundles in the ISF extend sub-parallel, perpendicular and oblique to the external bone surface. The vascularisation of the tissue is moderate due to anastomosing primary vascular canals and locally, reticular patterns can be developed (Fig. 60a, b). Many of the canals reach the slightly scalloped external bone surface in small foramina (Fig. 60c).

Cancellous bone—The interior cancellous bone is mainly composed of short and thick bone trabeculae (Fig. 60d)and circular to irregularly shaped vascular cavities. The trabeculae are longer and more slender in the interior parts of thicker shell elements, e.g., the peripherals. The trabeculae consist of secondary lamellar bone, but primary bone tissue is still present in interstitial branching areas.

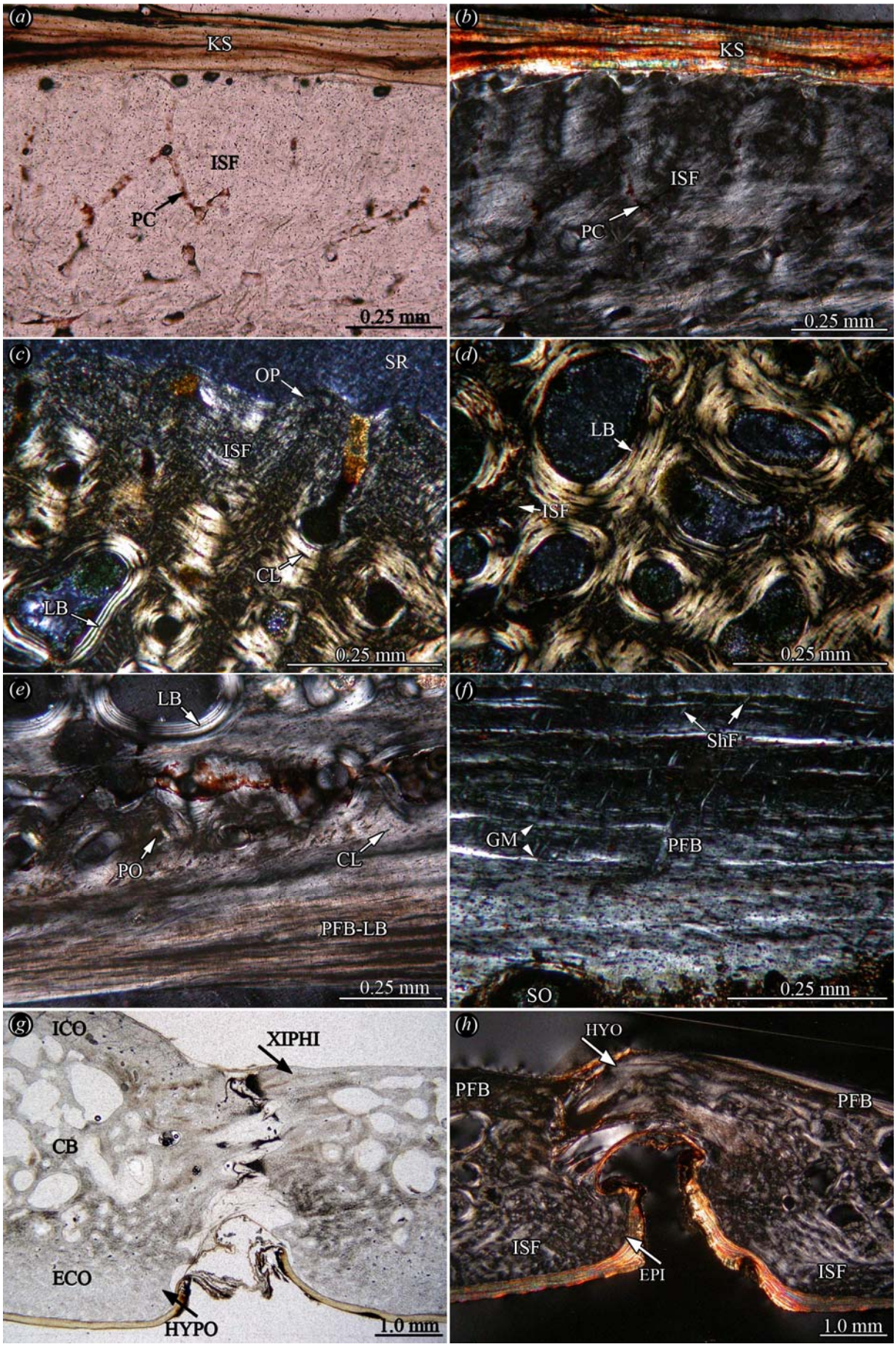
(a)
KS
ISF
PC
0.25 mm
(b)
KS
ISF
PC
0.25 mm
(c)
OP
SR
ISF
CL
LB
0.25 mm
(d)
LB
ISF
0.25 mm
(e)
LB
PO
CL
PFB-LB
0.25 mm
(f)
ShF
GM
PFB
SO
0.25 mm
(g)
ICO
XIPHI
CB
ECO
HYPO
1.0 mm
(h)
HYO
PFB
PFB
ISF
EPI
ISF
1.0 mm

Figure 60: Shell bone histology of kinosternid turtle taxa. Section of sub-sampled costal and associated keratinous shield (SMNS 7440; drilled core) of *Kinosternon* sp. in (*a*) normal and in (*b*) polarised light. Note moderate to high vascularisation of the tissue of interwoven structural fibre bundles. The surface and the growth marks of the keratinous shield appear wavy and irregular. (*c*) Close-up of the external cortex of the peripheral UCMP V78106/122545 of *Baltemys* sp. in polarised light. (*d*) Detail of the short and thick trabeculae of the cancellous bone of former specimen in polarised light. (*e*) Close-up of the internal cortex and internal part of cancellous bone of sub-sampled costal (SMNS 7440; drilled core) of *Kinosternon* sp. in polarised light. Locally, the parallel-fibred bone grades into lamellar bone. (*f*) Close-up of the internal cortex of the sampled plastron fragment (UCMP V78106/122545) of *Baltemys* sp. Growth marks appear as birefringent lines, and Sharpey's fibres insert into the bone tissue. (*g*) Close-up of the posterior hinge system of *Kinsternon* sp. (SMNS 7440). The hinge is situated between hypoplastron and xiphiplastron. A reduced, loose sutural contact is present only between the internal parts of the bones, while a transverse groove is developed between the external parts. (*h*) Close-up of the anterior hinge system of *Kinsternon* sp. (SMNS 7440). The hinge is situated between epiplastron and hyoplastron. The internal half of the hyoplastron and the external half of the epiplastron overlap each other, thus enabling a rotational movement of the epiplastron against the hyoplastron.

Internal cortex—In *K. subrubrum* and *Kinosternon* sp. (Fig. 60e), the parallel-fibred bone tissue grades into and interdigitates locally with lamellar bone. The bone tissue then shows the typical alternation of thin dark and light bone lamellae.In *Baltemys* sp. (Fig. 60f) and *S. minor*, the internal cortex appears as a more homogeneous single zone of parallel-fibred bone. The vascularisation of the bone tissue is low with only few primary vascular canals. Bone cell lacunae are flattened and elongated and follow the layering of the tissue. Growth marks are not observed in the internal cortical bone.

Sutures—Sutural zones are moderately developed. The bony pegs and sockets are not elongated. Fibre bundles that insert perpendicular to the marginal bone surface are strongly present. The interior cancellous bone does not reach far into the marginal compact bone tissue. In both the anterior and posterior hinge systems of *Kinosternon* sp. (SMNS 7440), the sutural contact of the external half of the bone is completely reduced and a transverse groove is developed (Fig. 60g, h). The bone tissue is similar to the bone tissue described for the

external cortex, and the marginal tissue has a flat or slightly scalloped external surface. The external layer of connective tissue and the external shield cover follows the relief of the bone surface into the groove. In the posterior hinge system, a sutural contact of the internal half of the bone still exists, however, the interdigitating elements are reduced in length and in number (Fig. 60g). Both, the hypoplastron and the xiphiplastron are bulging adjacent to the hinge zone. In the anterior hinge system, the internal part of the hyoplastron ends in a single thick marginal bone protrusion that slightly curves towards external. The external half of the epiplastron overlaps the protrusion of the hyoplastron and curves slightly towards internal, thus allowing the epiplastron to rotate against the hyoplastron around the hinge (Fig. 60h). The soft tissue zone between the bones is filled with connective tissue rich in the fibres that insert perpendicular to the margins of the bones.

6.3.19 Adocidae

6.3.19.1 *Adocus* sp. (†)

External and internal cortices that frame the interior cancellous bone are well developed and generally of equal thickness.

External cortex—The external cortex is divided into a more external, surficial zone and a more internal zone bordering the cancellous bone (Fig. 61a, b). The more internal zone is build of ISF, where fine fibre bundles extend equally diagonally, perpendicular and sub-parallel to the external bone surface. In the more external zone, the fibre bundles that extend perpendicular to the external bone surface become increasingly dominant in the ISF. Furthermore, growth marks that are highly birefringent in polarised light are present here. The growth marks have a wavy character throughout the more external zone, thus following the trend of the regular external surface sculpturing of the bones. Vascularisation is low to medium with few primary osteons and primary vascular canals and occasional scattered secondary osteons. The primary vascular canals are predominantly extending towards the external surface of the bone where they insert as small foramina. Based on the variable stages of preservation of the shell elements, the thickness of the more external zone of the cortex

varies greatly. Scattered secondary osteons and secondary osteon cluster are observeable at the transition to the cancellous bone.

Cancellous bone—The cancellous bone is dominated by short and thick trabeculae delimiting mostly circular vascular spaces (Fig. 61c). Primary ISF bone tissue is present in most trabeculae, as well as in trabecular branching areas. In the thick peripheral bone, the bone trabeculae were more slender and longer, but primary bone tissue is still largely retained. The walls of the trabeculae comprise mostly lamellar bone. However, there are also erosion cavities in the trabecular meshwork that still lack the secondary bone deposition.

Internal cortex—The internal cortical bone layers constitute parallel-fibred bone. Adjacent to the cancellous interior, the layer are weakly vascularised with few scattered primary vascular canals and primary osteons (Fig. 61d). Locally, the primary osteons or the primary vascular canals are arranged like strings in single layers of the internal cortex. Towards internal, the bone layers are mostly avascular. Sharpey's fibres were found in the internal cortex of the plastral fragment and the proximal part of the costal fragment, adjacent to the asymmetrical rib bulge. Towards the steep flank of the rib bulge, the cortical bone is thicker, while the cortex thins out on the gently sloping flank. Sharpey's fibres insert obliquely into the cortex on the gently sloping flank of the incorporated rib and they insert at higher angles at the steeper flank.

Sutures—The sutured margins are generally well developed. Long fibre bundles, i.e., Sharpey's fibres that extend perpendicular to the margins of the bone plates are found throughout the bone tissue that constitutes the margins. The bone tissue itself resembles the one described for the more external zone of the external cortex. Indeed, the growth marks often deviate from the external cortex towards the sutured margins, thus extending sub-parallel to the outer bone surface.

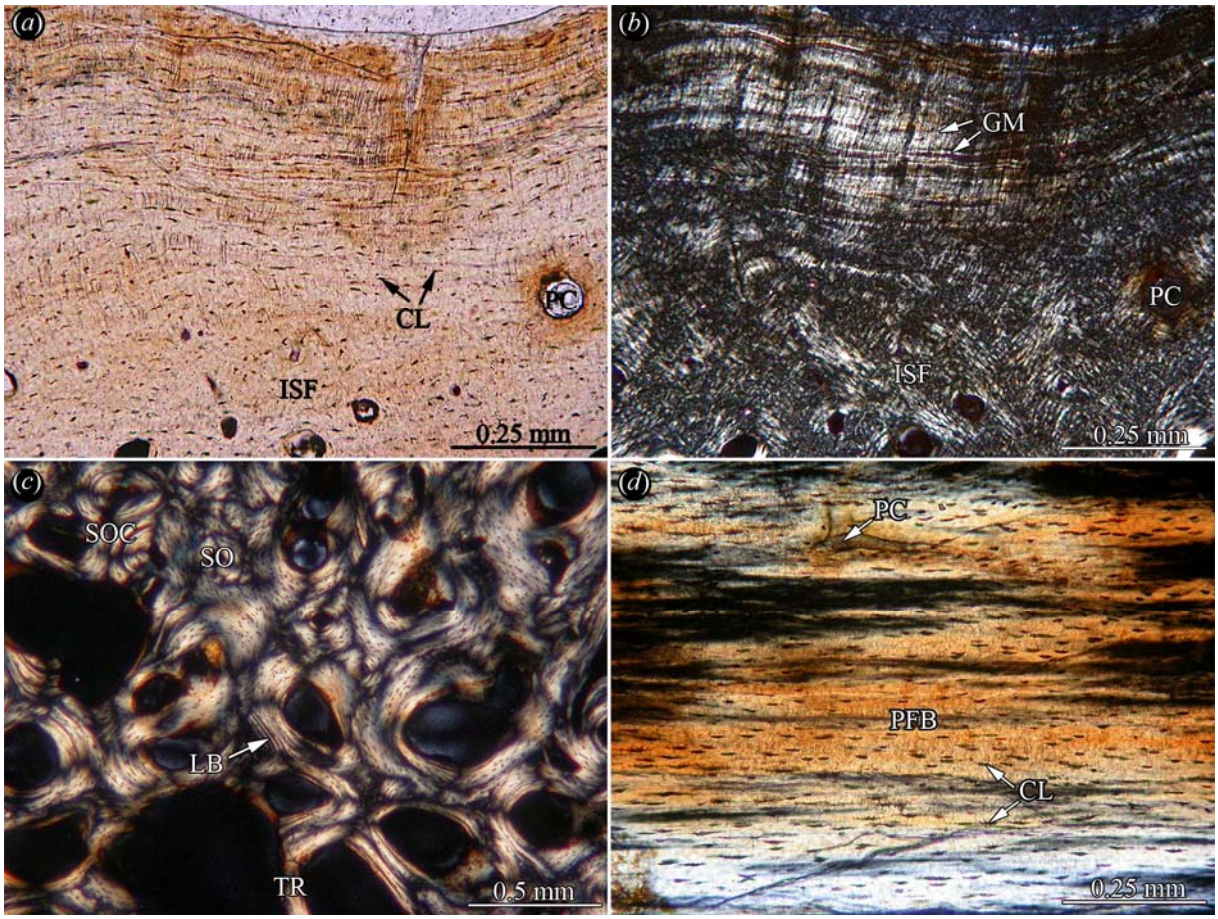

Figure 61: Shell bone histology of *Adocus* sp. Close-up of the external cortex of peripheral UCMP V87101/150201 in (*a*) normal and in (*b*) polarised light. Note the growth marks and perpendicular fibre bundles in the more external zone of the cortex. Towards internal, a zone of fine-fibred homogeneous interwoven structural fibre bundles is seen. (*c*) Close-up of the interior cancellous bone of costal UCMP V87101/150200 (L-section) in polarised light. Short and thick trabeculae dominate the cancellous bone. (*d*) Close-up of internal cortical bone (parallel-fibred bone) of costal UCMP V87101/150200 (X-section) in polarised light. The bone tissue is weakly vascularised, and the internal-most layers are mostly avascular.

6.3.20 Nanhsiungchelyidae

6.3.20.1 *Basilemys* sp. (†)

The shell bones of *Basilemys* sp. have a diploe structure with well developed cortices framing interior cancellous bone. In the two sampled osteoderms, the cortices are of similar thickness. The costal and neural fragment were found to be misassigned to *Basilemys* sp., thus

the only internal cortical bone found in the shell bones derives from the sampled peripheral elements, i.e., the peripheral (YPM 9703) and the fragment from periphery of shell (FM P27371). Here, the internal cortex is somewhat thinner compared to the well developed external cortex.

External cortex—The external cortex can be subdivided in two zones. The thinner, more internal zone comprises ISF with rather homogeneous fibre bundles lengths and diameters. Primary osteons and primary vascular canals are frequently found but growth marks are not visible in this zone. The thicker, more external zone still comprises ISF, however, the bone tissue is characterised by the appearance of growth marks and a slight dominance of structural fibre bundles that extend perpendicular to the external bone surface. The most obvious feature in the more external zone, however, is the orientation of the growth marks (Fig. 62a, b). The growth marks extend sub-parallel at the transition from the more internal to the more external zone. Towards external, the growth marks start with a wavy progression that becomes more pronounced towards the external surface. The wavy character of the growth marks depicts the typical 'pock-mark' surface sculpturing in cross-section and is thus tied to the development of the elaborate ornamentation pattern. Additionally to the successive layering of the bone tissue, there occurs a lateral shift between the layers clearly visible through the growth marks. The wavy 'trough and ridge' arrangement is often phase-delayed, in that the next trough follows external to a ridge and vice versa. The result is often a spindle-like structuring of the more external zone of the external cortex. Vascularisation is decreasing from the more internal zone towards the external surface of the bone. In the more external zone, only scattered primary osteons and primary canals are present. The primary canals locally form a reticular vascularisation pattern. Both zones within the external cortex can vary significantly in thickness. A significant variation from this overall cortical patterning is observed in the neural fragment and the costal fragment. Instead of showing the characteristics described above (which are consistent for all clearly identified shell bone material of *Basilemys* sp.), the two specimens show a highly characteristic plywood-like pattern and ornamentation structures that are synapomorphic for trionychid turtles (see chapter 6.3.22; Fig. 65). The neural and costal fragments are interpreted as having been misidentified as *Basilemys* sp. here.

Cancellous bone—The external and internal parts of the cancellous bone generally consist of short and slender bone trabeculae. In the interior parts of the bones, the trabecular length increases, thus leading to a more open-spaced trabecular meshwork with larger vascular

cavities (Fig. 62c). In the shorter trabeculae and their respective branching areas, large amounts of primary interstitial bone tissue, i.e., ISF, is present and only the trabecular walls consist of lamellar bone. In the more slender trabeculae, the bone tissue is mostly completely remodelled and the trabeculae thus consist of lamellar bone.

Internal cortex—The internal cortical bone is a simple layer of parallel-fibred bone (Fig. 62d, e). The bone tissue is weakly vascularised with scattered primary vascular canals and few primary osteons. The parallel-fibred bone consists mainly of coarse fibres that can deflect to some degrees in their overall orientation. Sharpey's fibres are also inserting into the cortical bone.

Sutures—The shell elements are generally well sutured, however, a strong incorporation of long fibre bundles, i.e., Sharpey's fibres that extend perpendicular to the margins are not observed (Fig. 63f). The fibre bundles in the sutural bone are usually short and unobtrusive and seem to insert into the sutural bone tissue at low angles.

Osteoderms—The osteoderms have the same, sometimes even more pronounced and pointed, elaborate sculpturing pattern as the other sampled bones. Thus, the bone histology of the external cortex is generally similar to that of the shell bones. However, while being present, the spindle-shaped structure (Fig. 62g) of the more external zone is not always as conspicuous as in the shell bones. The cancellous bone is consistent with the one described for the other shell bones. The internal cortex, which is equal in thickness to the external cortex, is not composed of a zone of simple parallel-fibred bone. Instead, the internal cortex constitutes coarsely fibred ISF (Fig. 62h). Especially in the smaller osteoderm, the fibre bundles strands are highly ordered in a lattice (responsible for striations seen in outer morphology). The fibre strands seen in longitudinal section branch and anastomose around fibre strands that are visible in cross-section. Within these cross-sections the compartimentalisation of the fibre bundle strands into single fibre bundles is observable. The fibre bundles are separable from each other in polarised light by thin birefringent lines. Three major orientations of the fibre bundles strands are present, two extending obliquely and at high angles within the cortex (longitudinal sections) and one that extends sub-parallel to the internal surface of the osteoderm (cross-sections).

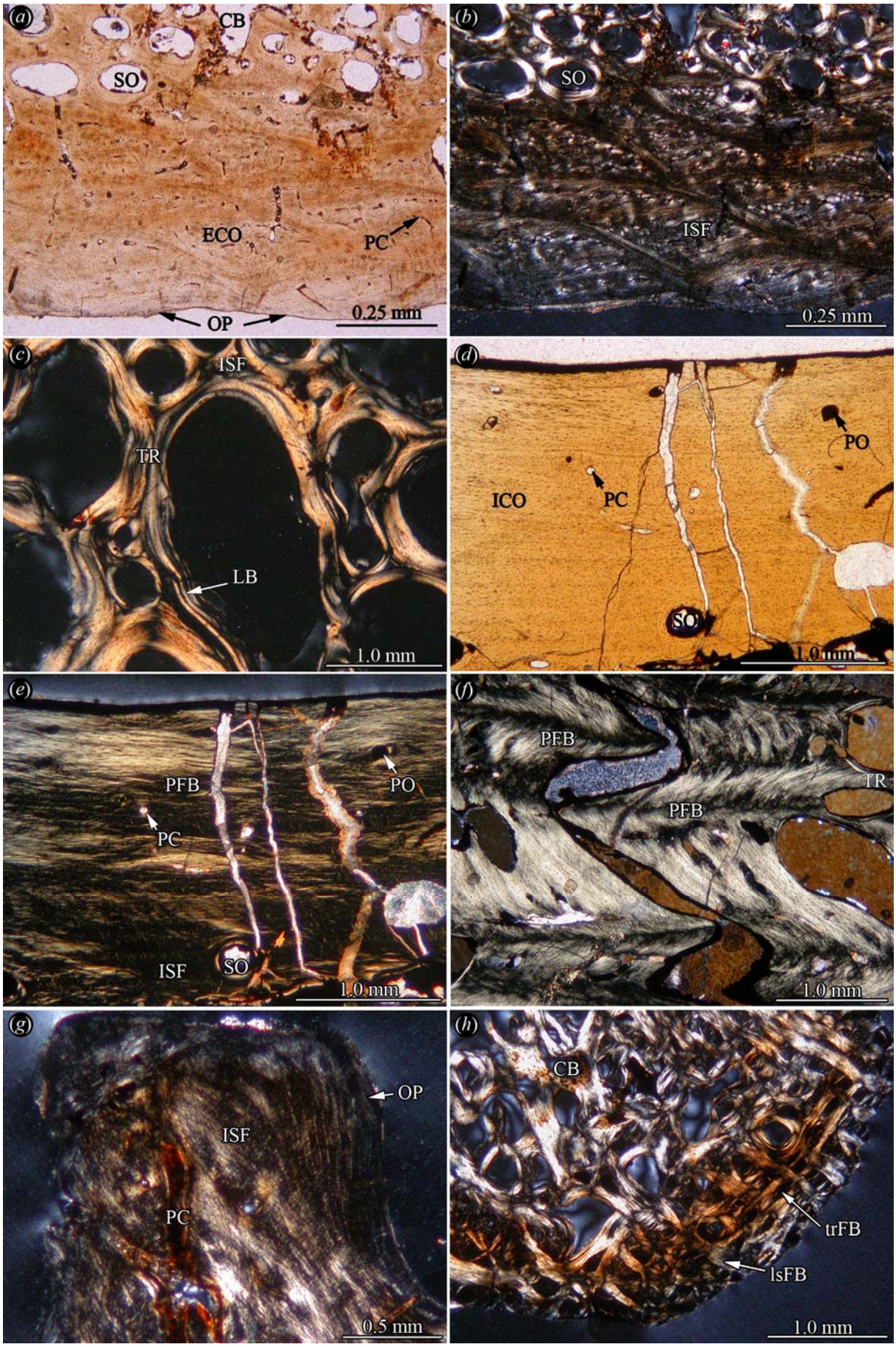
(a)
CB
SO
ECO
PC
OP
0.25 mm
(b)
SO
ISF
0.25 mm
(c)
ISF
TR
LB
1.0 mm
(d)
PO
ICO
PC
SO
1.0 mm
(e)
PFB
PO
PC
ISF
SO
1.0 mm
(f)
PFB
TR
PFB
1.0 mm
(g)
OP
ISF
PC
0.5 mm
(h)
CB
trFB
lsFB
1.0 mm

Figure 62: Shell bone histology of *Basilemys* sp. Section of the external cortex of peripheral YPM 9703 in (*a*) normal and in (*b*) polarised light. Note the wavy character of the growth marks and the 'pock-mark' sculpturing pattern of the bone surface. The wavy growth marks seem to shift laterally between the layers of the cortical bone. The resulting 'trough and ridge' arrangement is often phase-delayed. (*c*) Close-up of the open-spaced trabecular meshwork of the interior cancellous bone of former specimen in polarised light. Close-up of the internal cortex of peripheral shell fragment (FM P27371) in (*d*) normal and in (*e*) polarised light. Towards external, the weakly vascularised parallel-fibred bone is followed by interwoven structural fibre bundles. (*f*) Close-up of the sutural zone between adjacent peripherals (FM P27371). Long fibre bundles that extend perpendicular to the bone margins are not observable. (g) Close-up of the apical external cortex of isolated spiked osteoderm TMP 80.08.296 in polarised light. The characteristic surficial 'pock-mark' sculpturing pattern and the 'trough and ridge' arrangement of the growth marks are present. (*h*) Close-up of internal cortex of the base of former specimen in polarised light. Note regular arrangement of transversely and longitudinally sectioned interwoven structural fibre bundles.

6.3.21 Carettochelyidae

6.3.21.1 *Anosteira* sp. (†), *Pseudanosteira pulchra* Clark, 1932 (†), *Allaeochelys* cf. *A. crassesculpta* (Harrassowitz, 1922) (†) and *Carettochelys insculpta* Ramsay, 1887

All four taxa share similar bone microstructures and thus are described together and characteristic variations will be pointed out in the following text. All sampled shell bones have a diploe structure with internal and external cortices and interior cancellous bone. However, the thicknesses of the cortices can vary. In *Anosteira* sp. and *P. pulchra*, the cortices are of equal thickness. In *Allaeochelys* cf. *A. crassesculpta* and *C. insculpta*, the internal cortices are reduced in thickness compared to the thickness of the external cortical bone. In the thin and slender neural of *C. insculpta*, no real internal cortex is developed. Instead, the internal part of the plate comprises short bony protrusions that belong to the internal neural arch of the respective vertebra. The incorporated rib is seen as an asymmetrical bulge of the internal cortex of the costal of *C. insculpta*.

External cortex—The external cortex of the shell bones consists of ISF (Fig. 63a-c). Locally, as in the peripheral of *Pseudanosteira* sp., distinctive wavy growth marks are visible (Fig. 63c). Each successive layer of ISF bone shows a pronouncement of the wavy growth marks, thus building up the low ridges and tubercles of the ornamentation. In some shell bones, the ISF is not as pronounced, thus the external cortex superficially resembling the more parallel-fibred tssue of the internal cortex. In such cases, e.g., shell bone is the plastron fragment of *P. pulchra*, the wavy growth marks in the external cortex are one characteristic to correctly orientate the thin-sections. Vascularisation of the bone tissue is generally low with few primary osteons and scattered primary vascular canals that extend perpendicular towards the external bone surface. The canals do seldom branch or anastomose. In *Anosteira* sp. and *C. insculpta* (Fig. 63a, b), the vascularisation is increased with anastomosing primary vascular canals and larger amounts of primary osteons that can show string-like arrangements subparallel to the bone surface. Growth marks are present in the cortical bone, but they are visible as dark lines instead of highly birefringent lines in polarised light. ISF is present at the internal-most part of the cortex adjacent to the cancellous bone. In the neural of *C. insculpta*, the thickness of the external cortex differs significantly mediolaterally. Laterally, the cortical bone is well developed. Towards medial the cortex thins out into a slim sliver of cortical bone, as can be observed by the converging growth marks in the compact bone tissue. In *A. crassesculpta*, the poor preservation of the bone tissue does not allow for a clear comparison with the other taxa.

Cancellous bone—The cancellous bone constitutes short and thick trabeculae and small to medium sized cavities (Fig. 63d, e). In *Allaeochelys* cf. *A. crassesculpta*, the bone trabeculae appear more slender throughout the bone. The larger vascular cavities are generally found in the internal (lower) third of the shell bones. Only in the thicker shell elements, i.e., peripherals, the cavities increase proximally in size. Most of the trabeculae are still primary in nature, with primary bone, ISF, being found within the trabeculae and their branching areas (Fig. 63e). The walls of the trabeculae constitute secondary lamellar bone. In the flat shell bone elements, i.e., the costals of *Anosteira* sp. and *P. pulchra*, the vascular spaces show some externointernal flattening.

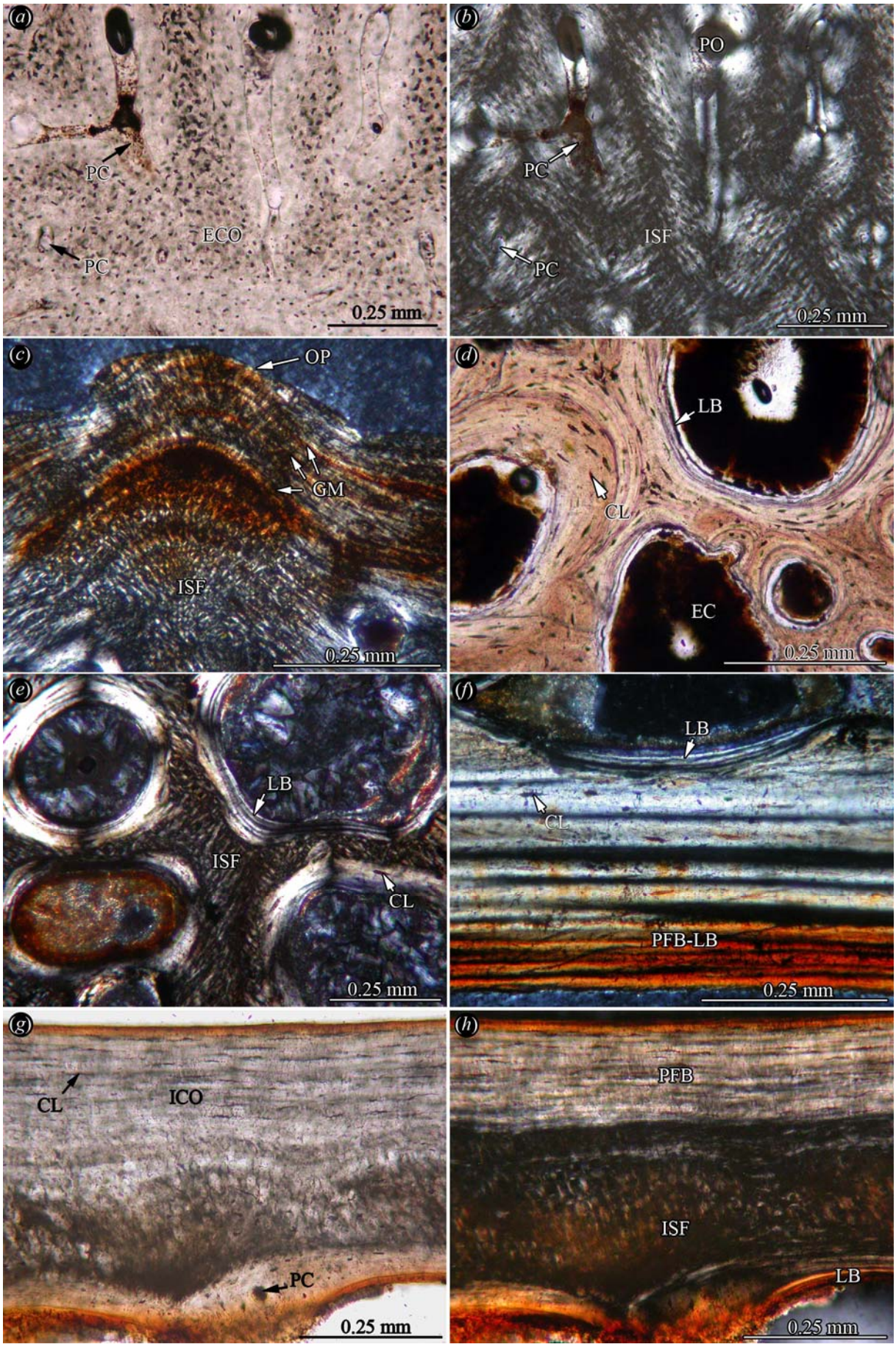
(a)
PC
ECO
PC
0.25 mm
(b)
PO
PC
ISF
PC
0.25 mm
(c)
OP
GM
ISF
0.25 mm
(d)
LB
CL
EC
0.25 mm
(e)
LB
ISF
CL
0.25 mm
(f)
LB
CL
PFB-LB
0.25 mm
(g)
CL
ICO
PC
0.25 mm
(h)
PFB
ISF
LB
0.25 mm

Figure 63: Shell bone histology of carettochelyid turtle taxa. Close-up of the external cortex of left hyoplastron (MAGNT R12640) of *Carettochelys insculpta* in (*a*) normal and in (*b*) polarised light. Note moderate vascularisation of the tissue of interwoven structural fibre bundles. (*c*) Detail of the external cortex and the ornamentation pattern of peripheral (UCMP V78031/131731) of *Pseudanosteira pulchra* in polarised light. Growth marks are clearly visible in the more external part of the cortical bone. (*d*) Close-up of the cancellous bone of sampled costal (FM PR 819) of *Anosteira* sp. The primary trabeculae are thick and short and usually lined with secondary lamellar bone. (*e*) Close-up of the cancellous bone of sampled plastron fragment (UCMP V78031/131731) of *Pseudanosteira pulchra* in polarised light. Note that primary interstitial bone is present in all trabeculae. (*f*) Close-up of the internal cortex of costal (UCMP V78031/131731) of *Pseudanosteira pulchra* in polarised light. The parallel-fibred bone locally grades into lamellar bone. Close-up of the internal cortex of the left hyoplastron (MAGNT R12640) of *Carettochelys insculpta* in (*g*) normal and in (h) polarised light. The parallel-fibred bone is followed externally by interwoven structural fibre bundles.

Internal cortex—In *Anosteira* sp., *P. pulchra* (Fig. 63f) and cf. *A. crassesculpta*, the internal cortex consists of intergrading lamellar bone and parallel-fibred bone. Areas with lamellar bone are visible as a succession of parallel dark and light bands, although the bands do not always extend parallel to each other. In *C. insculpta* (Fig. 63g, h), the internal cortex comprises mainly less ordered parallel-fibred bone. In all sampled bones, the cortex is weakly vascularised adjacent to the cancellous bone, with the more internal parts being avascular. Growth marks are present as birefringent lines in polarised light. Sharpey's fibres were detected in the internal cortex of the hypoplastron of *Anosteira* sp.

Sutures—The sutural zones are thin with rather short bony protrusions and sockets. In thin-section, a strong incorporation of parallel fibre bundles, i.e., Sharpey's fibres that insert perpendicular to the sutures becomes apparent. The long fibre bundles are traceable towards medial well into the cortical bone and towards the margins of the cancellous bone.

6.3.22 Trionychidae

6.3.22.1 *Plastomenus* sp. (†) and *Helopanoplia* sp. (†) (Plastomeninae); *Lissemys punctata* (Bonnaterre, 1789) and *Cyclanorbis senegalensis* (Duméril and Bibron, 1835) (Cyclanorbinae); *Aspideretoides foveatus* (Leidy, 1856c) (†), *Aspideretoides splendidus* (Hay, 1908) (†), cf. *Aspideretoides* sp. (†), *Apalone ferox* (Schneider, 1783), *Trionyx triunguis* (Forskål, 1775) and *Trionyx* sp. (†) (Trionychinae)

Although morphologically and osteologically different, plastomenine, cyclanorbine and trionychine turtles are described together as they share virtually the same bone histological details. Please note that the following paragraph is based on the fossil specimen of cf. *Aspideretoides* sp. (IPB R533a) and other fossil specimens, mainly because of the reasons discussed in the Methods section (i.e., thin-sections of fossil bones are of higher quality and naturally stained). The given values of the angles in the plywood-like pattern described below may well vary among trionychid turtle taxa. However, due to the still small sampling size, a statistical approach of angle variations was not attempted.

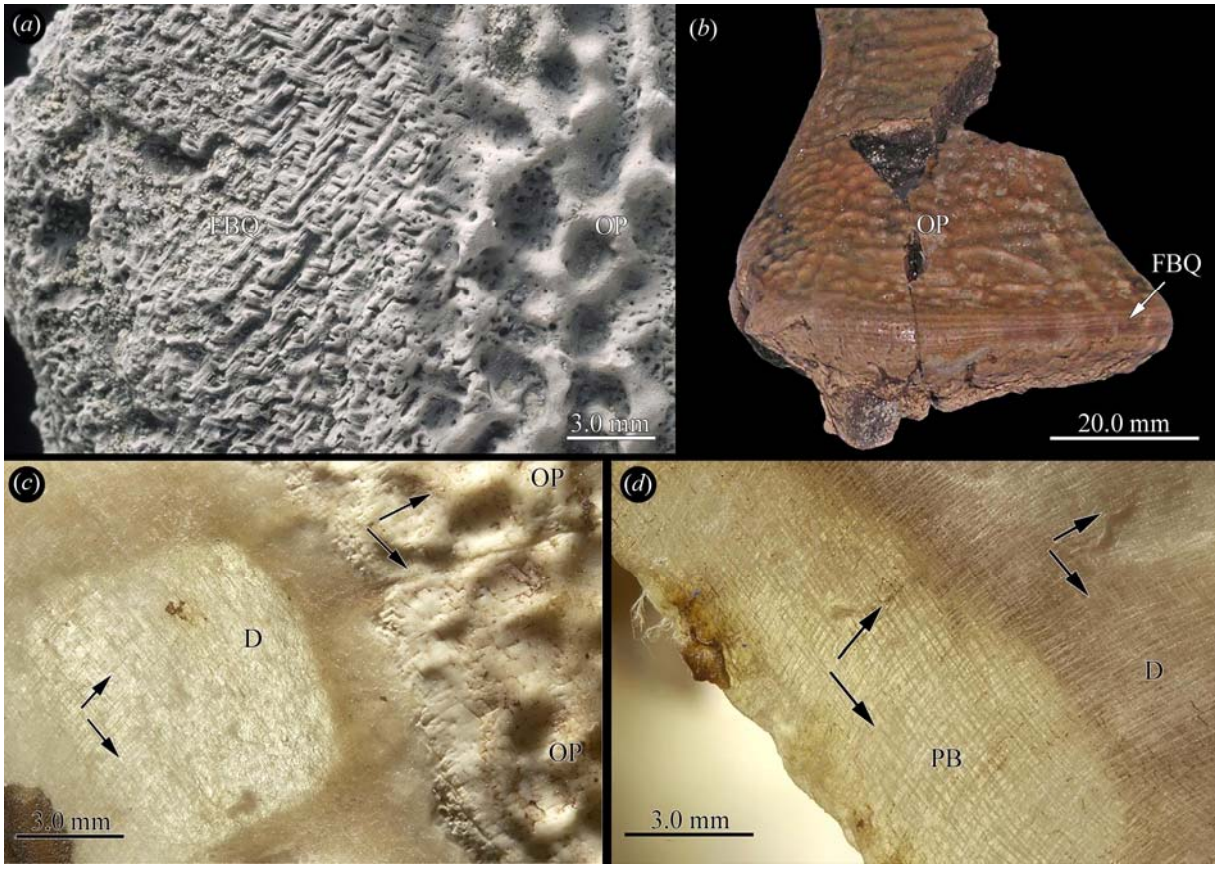

Figure 64: Macroscopic evidence of the plywood-like structure within elements of the

trionychid turtle shell. (*a*) Detail of distal part of costal of fossil *Aspideretoides splendidus* (TMP 85.36.760). The focus lies on the margin of specimen where decussating plies of fibre bundle quadrangles seem to be etched out of the bone matrix. The decussating plies can still be seen in spaces between the ornamentation. (*b*) Incomplete left ?hyoplastron of indeterminate fossil trionychid turtle (TMP 92.94.01) seen in ventrolateral view. The collagen fibre plies are seen as light and dark banding at margin. (*c*) Detail of the carapace of dried specimen of a juvenile *Trionyx triunguis* (IPB R260). Decussating fibre plies (arrows) continue undisturbed from carapacial dermis into the bony margin of the carapace. The ornamentation pattern covers the structural plies and fibre bundle quadrangles of bony shell elements. (*d*) Detail of plastron of former specimen. Dermal tissue showing decussating structural fibre plies (arrows) overlying a plastral bone. In later ontogenetic stages, the fibre plies will be metaplastically incorporated into the bone tissue as the shell parts continue to ossify. D, dermis; FBQ, decussating collagen fibre bundles; OP, ornamentation pattern; PB, plastral bone

The well-ordered arrangement of structural fibres preserved through the mineral phase of the bone is even visible macroscopically at the edge of shell elements as light and dark bands and decussating striations respectively (Fig. 64a, b). In dried specimens (Fig. 64c, d), it becomes apparent that the plywood-like pattern originates through the fibres of the corium being incorporated into the bone matter by metaplastic ossification (Haines and Mohuiddin, 1968).

A diploe-like structure (Fig. 65a), where compact bone layers frame internal cancellous bone, is recognised in all thin-sections of the sampled shell elements. There is also some variation of the sculpturing patterns, especially when plastomenine turtles are compared to cyclanorbine/trionychine turtles.

External cortex—The external compact bone layer can be subdivided into two zones (Fig. 65b-f). The ornamentation pattern of the carapacial elements of the plastomenine, cyclanorbine and trionychine shell represents the outer, more external zone. The more internal zone (external to the inner cancellous bone) comprises the plywood-like structure described below. The ornamentation pattern of the outer zone encompasses reticular raised ridges and knobs. The ornamentation pattern consists of lamellar bone intergrading with parallel-fibred

bone. Sharpey's fibres are observed to insert perpendicular to the surface of the bone into the ridges and knobs, resulting in a fan-shaped pattern.

In the interior zone of the external cortex of cf. *Aspideretoides* sp. (IPB R533a), up to ten distinct plywood-like layers (Humphrey and Delange, 2004) were discernable, with each ply being alternately rotated relative to those above and below (Fig. 65b, c). In this element, the angles in the ply-stack range about 45-50° relatively to those above and below. However, it can be more variable in other trionychid genera. In contrast, the studied shell of *Trionyx triunguis* (IPB R260) showed generally wider angles that range between 70° and almost 90° (see Fig. 64c, d). The plies of the second inner zone below the ornamentation pattern of the carapacial elements are composed of fibre bundle quadrangles (FBQ) that macroscopically appear in the skin as single fibre strands. At the top and bottom of each ply, some FBQ expand slightly to anchor the neighbouring bone layers. In polarised light views of the fossilised bone, the plies are seen as dark and light bands and the FBQ as dark and light patches respectively. The long-axes of the fibre bundles in each quadrangle are perpendicular to those in neighbouring quadrangles. Those FBQ, in which the fibre bundles trend horizontally, usually contain up to three rows of fibre bundles, while the vertically pointing FBQ consist of two parallel fibre bundle rows. The fibre bundles can reach diameters of 10 to 20 µm and are composed of numerous single nano-scale collagen fibres. The layers of FBQ cross each other at approximately 45-55°, e.g., symmetrically to the long axes of costal plates and their incorporated ribs. The FBQ continue without interruption into the unossified part of the lower dermis (Fig. 64c).

Especially in the plastomenine costals (Fig. 65d, e), there is no direct transition between the plywood-like structure and the interior cancellous bone. Instead, a single thick layer of the fibre bundles is present that extend parallel to the rib and sub-parallel to the surface of the bone. Interspersed through the layer, single long fibre bundles extend interoexternally from the external regions of the cancellous bone into the lower layers of the plywood-like pattern of the external cortex.

Cancellous bone—The cancellous bone of the trionychid shell elements is composed of a spongy meshwork of bone trabeculae (Fig. 65a, d). While the interstitial parts of the trabeculae retain some primary bone tissue, i.e., ISF, the rest of the trabeculae mainly show centripetally deposited lamellar bone tissue. Towards the internal and external cortical bone

layers, the vascular cavities of the cancellous bone decreases in amount and size. Towards the external cortex, the fibrous arrangement of the bone tissue changes into the distinct plywood-like pattern described above. Towards the internal cortex, the primary ISF still present in the cancellous bone where it changes into parallel-fibred bone.

Internal cortex—In contrast to the complexity of the external cortex, the internal cortex is a single layer of parallel-fibred bone locally grading into lamellar bone (Fig. 65a, g). Within this zone, the bone lamellae can slightly change angles but it is not distinguishable if they follow a predominant direction in connection to the orientation of the shell element. While the more interior parts of the internal cortex are still weakly vascularised by a few primary vascular canals, the more internal parts are mainly avascular. Throughout the cortex, bone cell lacunae are flattened and elongated and aligned sub-parallel to the internal surface of the bone.

Sutures—Sutures in the carapace of trionychine and cyclanorbine turtles are generally well developed. Still, the sutures between the shell bones themselves and the contacts between the bony elements of the shell and the leathery skin represent potential zones of weakness. However, because the FBQ continue from the bony elements into the dermis, the bones of the carapace and plastron are surrounded by a ring of toughened dermal tissue. Similarly, a bony bridge that would firmly connect the carapace with the plastron is absent in trionychid turtles. Instead the two halves of the shell are held together by the fibre-reinforced skin, resulting in a flexible though tough bridge region.

Variation—Although the surficial sculpturing patterns of the shell bones of plastomenine turtles (e.g., Fig. 65e) are distinct from cyclanorbine and trionychine turtles, the bone histology is not strongly affected. Differences occur in thicknesses of the more external bone tissue, as well as the spatial arrangement of the troughs and ridges that build up the ornamentation. However, the bone tissue types remain unaffected.

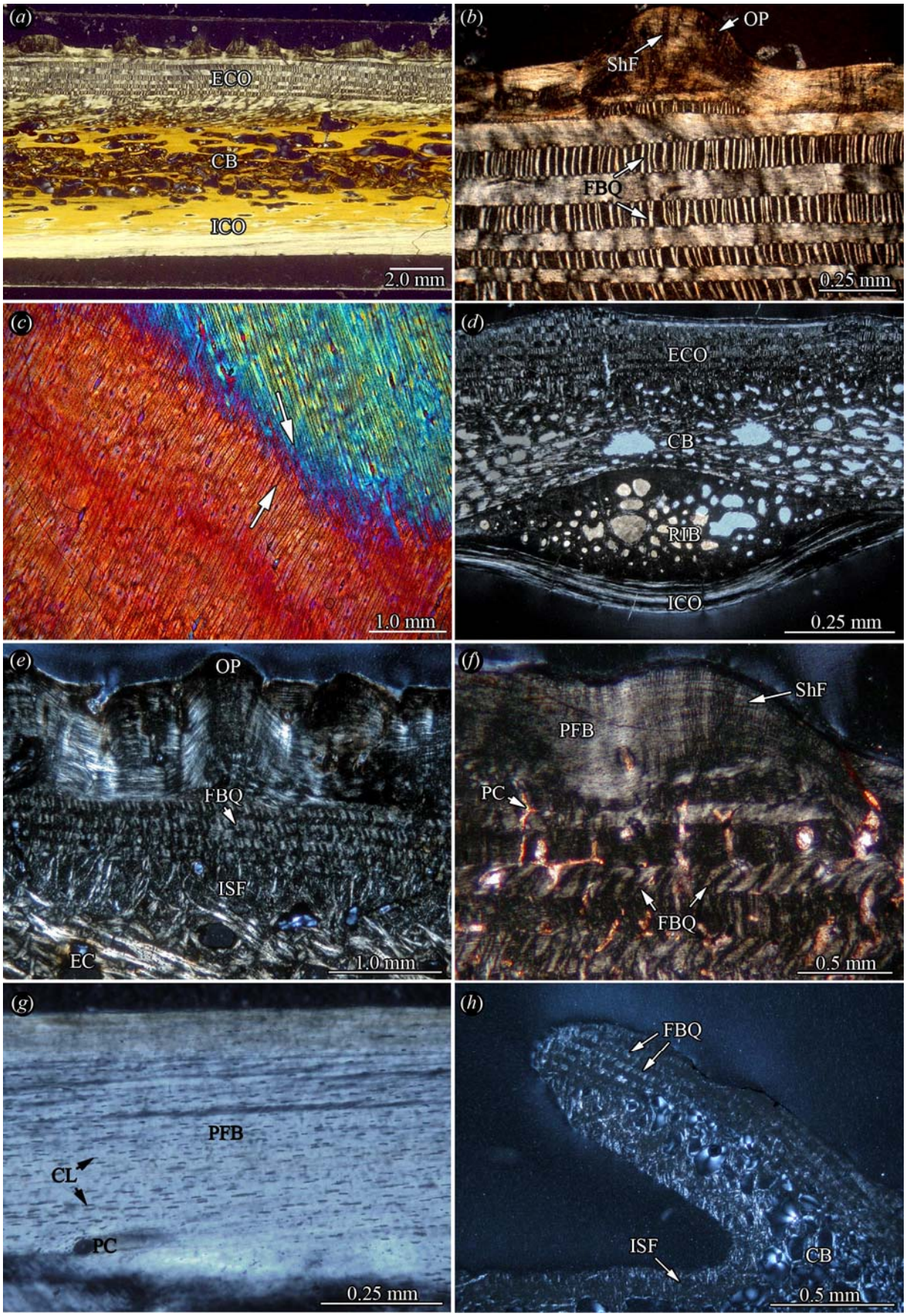

Figure 65: Shell bone histology of trionychid turtle taxa. All pictures are viewed in polarised

light. In (*c*), an additional lambda compensator was used. (*a*) Section of costal (IPB R533a) of cf. *Aspideretoides* sp. A diploe structure is well developed but part of the interior cancellous bone is collapsed. Note the plywood-structure of the external cortex. (*b*) Close-up of the ornamentation pattern and the plywood-structure of the external cortex of former specimen. Note the rotated set of plies composed of dark and light fibre bundle quadrangles. Sharpey's fibres insert into the ornamental ridge. (*c*) Thin-section the former specimen (IPB R 533b). The plane of sectioning crosses tangentially through the external cortex at a low angle. Two sets of rotated plies are seen in external view. The primary orientation of both plies is marked by white arrows. (*d*) Thin-section of distal part of costal (UCMP V81110/150231) of *Plastomenus* sp. The progression of the rib is clearly visible. (*e*) Close-up of the external cortex of distal part of costal UCMP V87051/150193 of *Helopanoplia* sp. Coarse fibre bundles are seen internal to the plywood-structure. (*f*) Close-up of the external cortex of costal fragment FM P27371, formerly assigned to *Basilemys* sp. Based on the plywood-structure found in the fragment, the material is proposed herein to be reassigned to Trionychidae indet. (g) Detail of the mostly avascular internal cortex of right xiphiplastron (YPM 13874) of *Apalone ferox*. (*h*) Section of an isolated peripheral bone (YPM 11645) of *Lissemys punctata*. Similar to other trionychid shell bones, the free peripheral bones of the species also show not only a diploe-structure but also the highly distinctive plywood-structure in the external cortex. Note that the internal cortex of the element, on the other hand, consists rather of interwoven structural fibre bundles instead of parallel-fibred bone.

Isolated posterior peripheral bones—The sampled isolated peripheral bone of *Lissemys punctata* (Fig. 65f) shares very similar bone histological details with that of the sutured shell bones described above. A diploe is developed with internal and external cortical bone framing a cancellous interior. The external cortex of the peripheral bones consists of the external ornamentation pattern and the more internal ply-system described above (Fig. 65f). The internal cortex, however, is composed of ISF instead of a single zone of parallel-fibred bone.

7. Discussion

7.1 Bone histology

It is assumed that the bone histology of basal Testudinata, especially of *Proganochelys quenstedti* and *Proterochersis robusta*, reflect the plesiomorphic microstructure of the turtle shell bones. However, in contrast to Zangerl (1969:313), this study shows that the cortical bone layers of the shell diploe cannot be described simply as "zones of lamellar bone, containing moderately numerous radial vascular canals", but that the cortices are clearly distinct from each other (the external cortical layer is not comprised of lamellar bone). The diploe structure, the ISF of the external cortex, the presence of Sharpey's fibres, the primary cancellous interior that becomes increasingly remodelled into secondary bone trabeculae and the parallel-fibred bone (that can grade into lamellar bone) of the internal cortex are plesiomorphic for all turtle shell bones.

The sampling and comparison of isolated postcranial osteoderms (e.g., limb osteoderms) of different turtle taxa (aff. *Naomichelys* sp., *Basilemys* sp. and *Hesperotestudo crassiscutata*) with the corresponding shell bones revealed generally the same bone microstructures. Thus, it is plausible to assume that the same mechanisms of ossification, i.e., metaplastic ossification of integumentary structures, must have been active in the formation of both hard tissue structures.

Furthermore, the sampled peripheral bone of *Lissemys punctata* shares not only the diploe structure with other sampled trionychid shell bones, but also highly distinctive histological details like the external plywood-system. The situation is thus similar to other turtles where peripheral bone microstructures are generally the same as in the other shell elements respectively. The bone histological analysis therefore does not falsify the morphology-based argument of Meylan (1987) and others that the isolated peripheral bones of *Lissemys* spp. are truly homologous to peripherals of other turtles. The presence of interwoven structural fibres instead of parallel-fibred bone in the internal cortex of the peripheral bone of *Lissemys* is interpreted as a means of anchorage through metaplasia of the isolated element in the pliable skin flap instead of a rigid sutural anchoring to other shell bones.

The following sections of the discussion try to answer the questions that were raised in the introductory chapter (Aims of the study 1.2). What are the results of the general aspects of the shell bone histology? Which functional and systematic characteristics are expressed in the turtle clades, and which aspects of functional morphology influence the microstructures of the shell bone? A chapter on the discussion of the origin of turtles and the quantification of the ecology/paleoecology in light of the newly acquired data is concluding the study. Can the comparison of histological features of turtle and outgroup taxa provide evidence for common ancestors?

7.1.1 Shell bone growth rates, bone remodelling and variation

Growth rates—While true woven-fibred bone (e.g., in long bones of mammals) with its irregular and loosely packed collagen fibre arrangement and general isotropy in polarised light is typically associated with rapid osteogenesis (Francillon-Vieillot et al., 1990), the same cannot be assumed for the metaplastic tissue of interwoven structural fibre bundles recognised in the external cortex of the turtle shell (well ordered fibre bundle arrangement, no general isotropy). For the ISF, detailed bone formation rates are not yet available. The internal cortex on the other hand, usually shows parallel-fibred bone connected with intermediate rates of osteogenesis. In the cases, where the parallel-fibred bone grades into lamellar bone (e.g., internal cortex of podocnemid turtle *P. erythrocephala*: dark and light layering coincides exactly with growth marks), low osteogenetic rates have to be assumed for the cortical bone formation.

Remodelling—Bone remodelling processes were discovered to be present in all turtle shell elements. It is a much more common feature in turtle shell bones than previously hypothesised by Francillon-Vieillot et al. (1990) and Castanet et al. (1993). Bone remodelling is mostly restricted to the interior cancellous bone and directly adjacent to internal and external compact bone areas. The primary trabecular meshwork of the cancellous bone is increasingly remodelled through secondary erosion cavities and secondary osteons. The amount of interstitial primary bone within the bone trabeculae and their branching areas becomes consequently reduced and can, in some cases, be completely remodelled. Growth marks are best observed in primary cortical bone of the neurals and, to some lesser degree, in

costals. Secondary osteon cluster appear seldom in turtles (i.e., in *Stupendemys geographicus Psephophorus* sp., and *Adocus* sp.) and the localised development of Haversian bone is even rarer (i.e., in *Rupelchelys breitkreutzi*). Suzuki (1963) describes the remodelling of interior bone trabeculae into sutural compact bone tissue in hatchling turtles. It might be hypothesised in this respect that the turtle shell bones are used as a mineral reservoir by gravid turtles. However, Suzuki's histological work on *Pseudemys scripta elegans* showed that the shell bone microstructure, in contrast to that of long bones, is not influenced by gravidity and oviposition.

In a few cases (e.g., in *P. erythrocephala* and in *T. sulcatus*), the secondary bone remodelling deviates from what is usually found in the external cortical bone tissue of turtle shells. As observed in a modern turtle taxon (*P. erythrocephala*), a possible reason for such unusual secondary bone deposition could be a reaction to incipient osteomyelitis or 'shell rot' (e.g., Frye, 1991, Sinn, 2004). Often following trauma, microbes enter spaces between the keratinous shields and the underlying bone becomes infected. Similar pathologies, i.e., pitting and other lesions of the turtle shell bone, have already been described in fossil turtles from the Eocene of Wyoming, North America (Hutchison and Frye, 2001). As inferred from modern turtles that are highly aquatic, phenomena like 'shell rot' in fossil turtles can also be related to poor water quality (see also discussion in Hutchison and Frye, 2001).

Although quite variable, secondary bone remodelling is present in all outgroup taxa besides the Placodontia. In the latter group, secondary bone remodelling processes and secondary osteons were not encountered. Extensive Haversian bone, as the extreme opposite, was found for example in *Mastodonsaurus giganteus* and locally in *Propalaehoplophorus* sp.

Variation—Variation in the bone microstructure among the shell bone elements of the same species was uniformly connected to the differences of the outer shapes of the respective elements in that species. *Chelus fimbriatus* and *Geochelone carbonaria* were the taxa with the strongest histological variation between the carapacial and plastral samples of all turtles studied. The strong variation is linked to the extremely humped shell morphology in both taxa (chapter 4.2.5.7; chapter 4.3.16.7). In many other taxa, the bone microstructure of the hyo- and the hypoplastra is further influenced by directed growth because of the change in growth direction for the plastral buttresses (e.g., see 6.3.4.1). Intraspecific variation in bone histology (i.e., ontogenetic variation) and differences due to sexual dimorphism were not encountered,

partly due to the small sample size of each taxon. On the other hand, such variation is not expected either, because major differences in the bone histology of the turtle shell seem to be expressed only on generic or higher taxonomic levels (see chapter 7.2).

7.1.2 Character polarisation of turtle shell microstructures

Although no postcranial osteoderms of the amphibian outgroups were available, it is inferred that the dermal bone samples of *M. giganteus*, *Trimerorhachis* sp. and *G. pustuloglomeratus* are still adequate to polarise the turtle shell bone microstructures. As already indicated in Zylberberg and Castanet (1985), amphibian osteoderms are known to develop through metaplastic ossification. It is here proposed that not only the osteoderms of modern anurans but also the dermal elements of the cranium and the shoulder girdle from fossil temnospondyls originate through metaplastic processes. It remains to be tested, if osteoderms of temnospondyls follow the same osteogenetic processes. The presence of ISF for example in turtles, archosauromorphs and lepidosaurs is presumably plesiomorphic for all tetrapods. Similarly, the development of a diploe structure with equally well developed cortical bone layers is already found in temnospondyls. However, the extensive external surface sculpturing with ridges, grooves and pits and tubercles of temnospondyl dermal bones is not present in the most basal turtles.

The samples of the Xenarthra (Mammalia) are the sister group to all remaining amniotes (Reptilia) in this study. Although Xenarthra themselves are highly derived taxon within the Mammalia, they are the only available taxon that carries extensive bony armour. The small knob-like bones of *P. harlani* are difficult to compare to turtle shells. However, they are also formed through metaplastic ossification. The sectioned carapace bones of the Cingulata superficially resemble the diploe structures found in turtle shell bones, but a closer look reveals striking differences in the respective microstructures. For example, the cortical bone tissues found in turtle shell bones have a completely reversed arrangement in the cingulate armour plates, so that the external cortical bone tissue in turtles resembles that of the internal cortex in cinculates and vice versa.

7.2 Implications for turtle systematics

In several taxa (listed below), bone histology supports previously hypothesised systematic relationships. In other taxa, however, the data of the current study and other studies clearly diverge. New relationships are thus proposed based on the bone histology. A synopsis of the results is shown in Figure 66. In the rest of the taxa, the bone histology is either not informative enough or functional aspects override existing phylogenetic signals.

7.2.1 Systematic value of shell bone microstructures

Basal Testudinata—The phylogenetic position of Meiolaniidae is still largely under discussion. The sample of the taxon consistently falls into ecological category I (chapter 7.6.2). Based on the bone histology, it thus fits well into the group of purportedly terrestrial basal turtles.

Solemydidae (aff. *Naomichelys* sp.)—Additional to a similarly terrestrial palaeoecology, the material of Solemydidae gen. et sp. indet. (aff. *Naomichelys* sp.) shows also highly derived autapomorphic shell bone microstructures (i.e., ornamentation pattern). Future sampling of closely related taxa (i.e., *Solemys*, *Helochelydra* and *Tretosternon*) might indicate these microstructures to be valuable synapomorphies for the more inclusive taxon.

Platychelyidae—The variation in size and bone thickness among the two morphs of *Platychelys* may appear to be attributable to different ontogenetic stages. However, the differences in vascularisation pattern, the trabecular arrangement in the cancellous bone and the complex expression of the bone tissue in the external cortex are so strong that they indicate rather different systematic positions of histomorph A and B instead of ontogenetic stages. The bone histology thus underscores the ambiguity of the sampled fragmentary material from Guimarota. Based on the bone histological results, the assignments of the material to ‘aff. *Platychelys* sp.’ by Lapparent de Broin (2001:168) is to be treated with caution. Furthermore, histomorph A shares bone histological features with pleurosternid turtles. Based on the bone microstructure, the reassignment of the material of ‘aff. *Platychelys* sp.’ to ‘Pleurosternidae gen. et. sp. indet.’ is proposed.

Pleurodira—Among the sampled Pleurodira, the reduction of the internal cortex is synapomorphic for Bothremydidae. Among Testudinata however, the reduction of cortical bone, especially of the internal cortex, appears in several groups and is linked to an increasingly aquatic ecology. The distinct cyclical growth marks in the lamellar bone of the internal cortex of *P. erythrocephala*, perceived as a black and white layering, is not encountered in the other sampled pleurodire turtles and is thus treated as a potential autapomorphy for this taxon.

Pleurosternidae—A separation of the external cortical bone in two distinct zones is common in turtles, e.g., in Pleurosternidae, Trionychidae, aff. *Naomichelys* sp. and *Basilemys* sp. However, the distinct variation in a more external fine-fibred zone and a more internal zone that is composed of irregularly coarse fibre bundles is characteristic only for Pleurosternidae. The other taxa (Trionychidae, aff. *Naomichelys* sp. and *Basilemys* sp.) show unique characteristics of their own in the external cortex that they cannot be mistaken for Pleurosternidae.

Marine turtles from Solothurn—In *Plesiochelys* sp. and the *Thalassemys* spp., the reticular pattern of primary vascular canals observed in the external cortex is also quite dominant in the tissue of the sutured margins of the bones. Such an extensive vascular patterning was not observed in the marginal bone tissue of other turtles, although it is weakly developed in *Tropidemys* sp. The bone histology of *Eurysternum* spp. is divergent from that of the other Solothurn taxa.

Middle Jurassic turtles from Kirtlington—Based on bone histology, there are two different turtles present in the sample from Kirtlington. Histomorph I (IPB R583-588; all dark coloured shell fragments) has a characteristic internal zone of thick, coarse irregular fibre bundles and a more external fine-fibred zone incorporated in the external cortex of the bones. Such an external cortex structure was only found in the material that was assinged to aff. *Platychelys* sp. (herein treated now as Pleurosternidae gen. et. sp. indet.) and in pleurosternid taxa (*Glyptops plicatulus*, *Compsemys* sp. and Pleurosternidae gen. et sp. indet. of Guimarota). *Rupelchelys breitkreutzi and* the *Xinjianchelys* spp., the only other turtles in which coarse fibres dominate the external cortex, lack a more external fine-fibred zone. It is thus plausible that the Kirtlington histomorph I belongs to Pleurosternidae (proposed assignment to

Pleurosternidae gen. et sp. indet.). As such, the fossil record of the group is extended from the Upper Jurassic back into the Middle Jurassic.

Histomorph II (IPB R589; light coloured shell fragment), with its homogeneous arrangement of short and equally fine fibre bundles, resembles bone microstructures found in many taxa of different groups and thus reflects mainly plesiomorphic characters. An assignment beyond 'Cryptodira incertae sedis' is not possible.

P. megacephalum *and Emydidae indet. (Platysternoid "C")*—The bone histology of *P. megacephalum* resembles that of chelydrid turtles in certain aspects, like the dominance of diagonally arranged fibre bundles in the ISF of the external cortex and the overall vascularisation pattern. The bone microstructure of Emydidae indet. (Platysternoid "C") shows several differences to *Platysternon megacephalum*, while it is not greatly distinguishable from the typical testudinoid histotype II. A tentative assingment based on the histological data would indicate a relationship between *P. megacephalum* and Chelydridae on the one hand and Emydidae indet. (Platysternoid "C") and testudinoid turtles on the other. The former relationship would thus follow the morphological hypotheses presented, for example, in Brinkman and Wu (1999) and Danilov and Parham (2005). The latter relationship is already indicated by the formal assignment of the material to Emydidae indet.

Planetochelys *sp.*—In the case of *Planetochelys* sp., the bone tissue is not distinguishable from turtles that fall into the testudinoid histotype I. Otherwise, the bone histology of *Planetochelys* sp.is rather unconspicous and not suited to justify a proposal of reassignment.

Dermatemydidae—The shell bones of both dermatemydid taxa (*D. mawii* and *B. garmanii*) show extreme levels of vascularisation but without the overall homogenisation of the bone tissue seen in *Hoplochelys* sp. and *A. ischyros*. However, the trabecular arrangement in the cancellous bone appears highly organised, reminiscent of the high structural order of thin-sectioned wood or the complex wing venation of insects. This level of organisation was not encountered among other turtles and is autapomorphic for this clade.

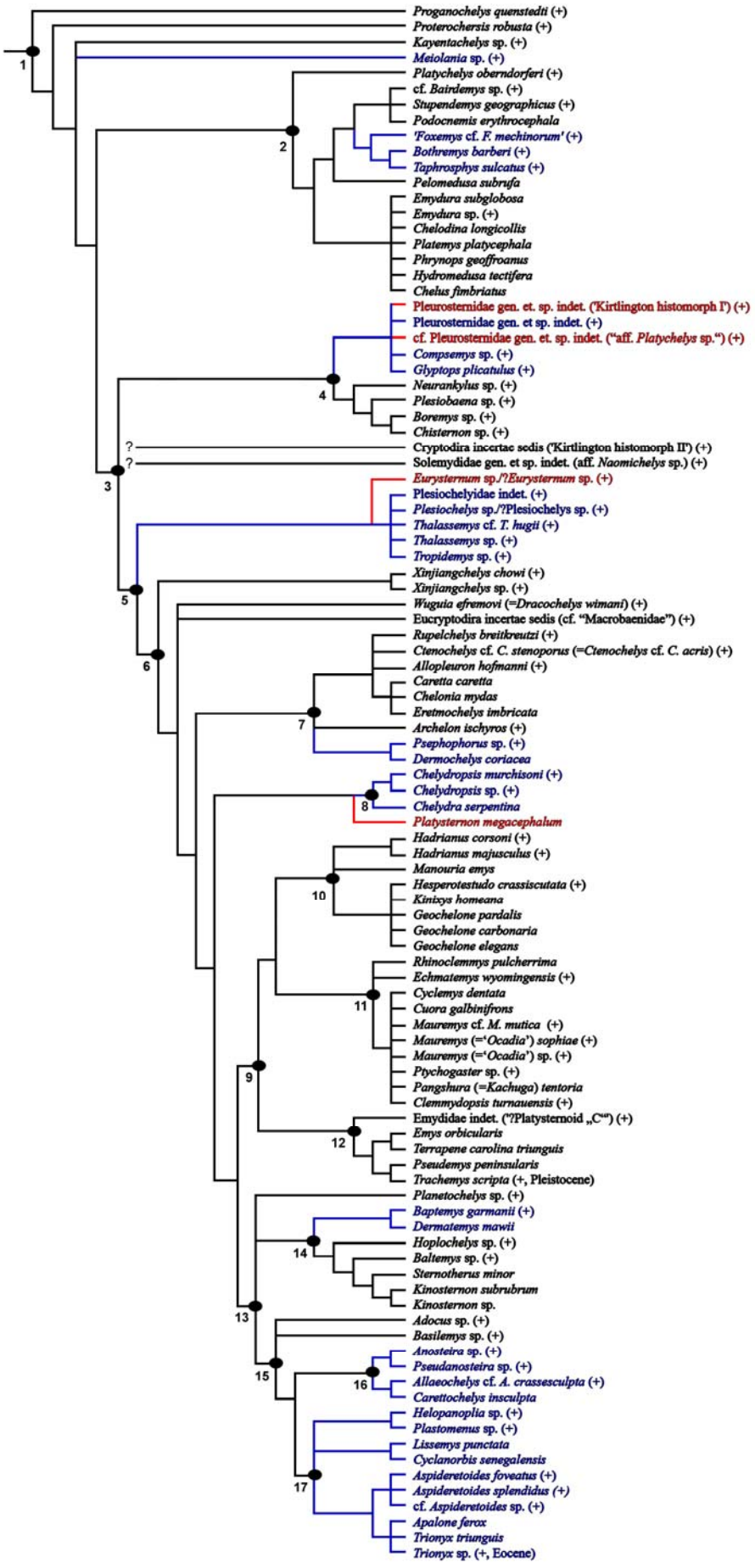
Proganochelys quenstedti (+)
Proterochersis robusta (+)
Kayentachelys sp. (+)
Meiolania sp. (+)
Platychelys oberndorferi (+)
cf. Bairdemys sp. (+)
Stupendemys geographicus (+)
Podocnemis erythrocephala
'Foxemys cf. F. mechinorum' (+)
Bothremys barberi (+)
Taphrosphys sulcatus (+)
Pelomedusa subrufa
Emydura subglobosa
Emydura sp. (+)
Chelodina longicollis
Platemys platycephala
Phrynops geoffroanus
Hydromedusa tectifera
Chelus fimbriatus
Pleurosternidae gen. et. sp. indet. ('Kirtlington histomorph I') (+)
Pleurosternidae gen. et sp. indet. (+)
cf. Pleurosternidae gen. et. sp. indet. ("aff. Platychelys sp.") (+)
Compsemys sp. (+)
Glyptops plicatulus (+)
Neurankylus sp. (+)
Plesiobaena sp. (+)
Boremys sp. (+)
Chisternon sp. (+)
Cryptodira incertae sedis ('Kirtlington histomorph II') (+)
Solemydidae gen. et sp. indet. (aff. Naomichelys sp.) (+)
Eurysternum sp./?Eurysternum sp. (+)
Plesiochelyidae indet. (+)
Plesiochelys sp./?Plesiochelys sp. (+)
Thalassemys cf. T. hugii (+)
Thalassemys sp. (+)
Tropidemys sp. (+)
Xinjiangchelys chowi (+)
Xinjiangchelys sp. (+)
Wuguia efremovi (=Dracochelys wimani) (+)
Eucryptodira incertae sedis (cf. "Macrobaenidae") (+)
Rupelchelys breitkreutzi (+)
Ctenochelys cf. C. stenoporus (=Ctenochelys cf. C. acris) (+)
Allopleuron hofmanni (+)
Caretta caretta
Chelonia mydas
Eretmochelys imbricata
Archelon ischyros (+)
Psephophorus sp. (+)
Dermochelys coriacea
Chelydropsis murchisoni (+)
Chelydropsis sp. (+)
Chelydra serpentina
Platysternon megacephalum
Hadrianus corsoni (+)
Hadrianus majusculus (+)
Manouria emys
Hesperotestudo crassiscutata (+)
Kinixys homeana
Geochelone pardalis
Geochelone carbonaria
Geochelone elegans
Rhinoclemmys pulcherrima
Echmatemys wyomingensis (+)
Cyclemys dentata
Cuora galbinifrons
Mauremys cf. M. mutica (+)
Mauremys (='Ocadia') sophiae (+)
Mauremys (='Ocadia') sp. (+)
Ptychogaster sp. (+)
Pangshura (=Kachuga) tentoria
Clemmydopsis turnauensis (+)
Emydidae indet. ("?Platysternoid „C"") (+)
Emys orbicularis
Terrapene carolina triunguis
Pseudemys peninsularis
Trachemys scripta (+, Pleistocene)
Planetochelys sp. (+)
Baptemys garmanii (+)
Dermatemys mawii
Hoplochelys sp. (+)
Baltemys sp. (+)
Sternotherus minor
Kinosternon subrubrum
Kinosternon sp.
Adocus sp. (+)
Basilemys sp. (+)
Anosteira sp. (+)
Pseudanosteira sp. (+)
Allaeochelys cf. A. crassesculpta (+)
Carettochelys insculpta
Helopanoplia sp. (+)
Plastomenus sp. (+)
Lissemys punctata
Cyclanorbis senegalensis
Aspideretoides foveatus (+)
Aspideretoides splendidus (+)
cf. Aspideretoides sp. (+)
Apalone ferox
Trionyx triunguis
Trionyx sp. (+, Eocene)
1
2
3
4
5
6
7
8
9
10
11
12
13
14
15
16
17
?
?

Figure 66: Revised phylogenetic hypothesis of the sampled turtles of the current study. Taxa and lines in red indicate newly proposed positions, while blue colours indicate strong support of existing phylogenetic hypotheses respectively. For source of data see text.

Basilemys *sp. and* Adocus *sp.*—Two shell elements (i.e. the neural and the costal) that were previously assigned to *Basilemys* sp. were identified to belong to a large trionychid turtle, based on the bone microstructures. A reassignment of the two specimens to "Trionychidae indet." is proposed. Comparing *Basilemys* sp. and *Adocus* sp., there is some indication (i.e., structure and development of external ornamentation) that the Nanhsiungchelyidae and the Adocidae might be closely related, thus supporting the newly introduced taxon Adocusia of Danilov and Parham (2006).

Carettochelyidae—Bone histology is consistent among carettochelyid turtles, while it is separable from that of Trionychidae, their proposed direct sister taxon, as well as from the more basal Nanhsiungchelyidae and Adocidae.

Trionychidae—The plywood-like structures in the external cortical bone of Trionychidae is a true synapomorphy for the group, even though functional purposes might be involved at the same time (see discussion in chapter 7.3) (Scheyer et al., 2007).

7.2.2 Functional adaptation

In those cases, where the microstructures in the shell bones are not very conspicuous, but plesiomorphic for Testudinata, the supple variations can often by attributed to functional adaptations (see chapter 7.6). Such groups are, for example, Chelidae and Testudinoidea. Due to the overall moderate vascularisation of the shell bones, both the South American and the Australasian taxa of Chelidae fitted in an overall pattern of semi-aquatic to mainly aquatic turtles (ecological category II). However, the adaptation to the aquatic environment overrides potential systematic signals. Neither the morphological nor the molecular/serological hypotheses of chelid intrarelationships could be supported by bone histology (see chapter

4.2.5). In Testudinoidea, the shell bone histology is also mainly characterised by the level of adaptation to the aquatic environment (testudinoid histotypes I-III, see chapter 6.3.14).

In taxa like *Archelon ischyros* and *Hoplochelys* sp., the functional aspects, namely the extreme adaptation to the aquatic environment is completely overriding any phylogenetic signals that might have been present. The shell bone tissue is comparable to highly porous endoskeletal bone structures recognised in some tetrapod groups (e.g., ichthyosaurs, dolphins and also the leatherback turtle) secondarily associated with an open marine lifestyle (Buffrénil et al., 1987; Buffrénil and Schoevaert, 1988; Ricqlès, 1989; Buffrénil and Mazin, 1990; Ricqlès and Buffrénil, 2001). For *A. ischyros*, the osteoporoitic trend in the shell is hypothesised to lead to a weight-reduced shell skeleton with lower mass and density (compare to Taylor, 2000), a characteristic further enhanced by the enormous morphological reduction of the shell elements and the presence of large fontanelles (Wieland, 1898).

7.3 Implications for functional morphology of the turtle shell

The diploe structure of the shells, the non-overlapping structure of keratin shields and bone sutures, plywood-patterns of the bone tissue, the sutural connection of the bone and hinge systems are taken into account to survey the functional morphology of the shell. Because the plywood patterns of Trionychidae is one of the most outstanding structures that were encountered in the shell bones, they will be discussed in a separate section.

7.3.1 Microstructural adaptations to strengthen the shell

Diploe structure of the shell bones—Whereas a simple compact domed shell would suffice for a turtle to give its shell enough form stability, especially for larger and ultimately for giant-sized turtles it becomes increasingly important to minimise shell weight during growth due to scaling effects. As seen in the giant *H. crassiscutata* and *S. geographicus*, the diploe structure itself presents such a way of lightweight construction. Form stability and the moment of inertia (in this case, the capacity of the turtle shell to resist bending stresses) of the

domed shell is maintained, because the compact bone layers serve as tension-resistant layers around the meshwork of interior cancellous bone.

Sutural structures—The suture between two adjacent shell bones is usually well developed with long interdigitating bony pegs and equivalent sockets. However, in some taxa the sutural zone has a shallow relief with short and blunt pegs and sockets. Even though the sutures of these bones seem rather weak, this presumed weakness might be compensated through a soft-tissue connection strongly reinforced by Sharpey's fibres. As could be shown by the core-sampling of recent and not yet macerated taxa like *D. mawii* (chapter 6.3.16) and *Kinosternon* sp. (chapter 6.3.18), soft tissue fibres cross the space between the sutures to insert into both shell bones. Due to the relief of the peg and socket structure, the Shapey's fibres overlap each other extensively in the pegs. Similarly, the collagenous fibre bundles that insert perpendicular to the external bone surfaces are interpreted as a means of physically strengthening the interface of the keratinous shield cover and the underlying shell bone, with only a very thin layer of fibrous connective tissue being present in between.

One group with relatively weak bone sutures is the Carettochelyidae. The high domed shells of, e.g., *Allaeochelys* cf. *A. crassesculpta* from the Eocene Messel pit, are mostly flattened and the carapacial bones (and to a lesser degree the bones of the plastron) are rotated out of articulation (pers. obs.). This type of preseration might be explained by the decay of the soft-tissue connection, i.e. the Sharpey's fibres, between the bones, followed by a subsequent loosening of the sutural contact and outward rotation of the elements due to burial compaction of the sediments.

Sharpey's fibres—Sharpey's fibres are not only found in the sutural zones. In the external and internal cortices of the bones, Sharpey's fibres also insert into the ISF or the parallel-fibred bone/lamellar bone respectively. The Sharpey's fibres in the external cortices seem to be uniformly connected with the anchoring of the overlying layers of connective tissue and keratinous shields. Sharpey's fibres that insert into the internal cortices are hypothesised to be associated with carapacial and plastral attachment zones of respiratory, locomotory and kinetic hinge musculature (see below).

Shell kinesis—Hinge systems in the turtle shell were sampled in the fossil *Planetochelys* sp. (whole elements; UCMP 81071/159356), in the recent *Kinosternon* sp. (core-samples; SMNS

7440) and in the recent *Kinixys homeana* (whole elements; YPM 13876). Compared to normal bone sutures, the interdigitating elements (pegs and sockets) of hinge bones are greatly reduced in numbers resulting in only a single bony protrusion and a respective groove serving as a bony connection between adjacent elements. Instead of interdigitating elements, smooth bone margins are formed and the soft tissue connection between the bones remains during shell osteogenesis.

In some cases, the musculature involved into the shell closing mechanisms has been studied. For example, as indicated by the works of Bramble (1974) and Bramble et al. (1984), a diversity of muscles is involved (i.e. *musculus testoscapularis* or *musculus atrahens capitis collique* in anoterior lobe closure; *musculus testoiliacus* or *musculus attrahens pelvim* in posterior lobe closure) in the closing system of emydid and kinosternid turtles. In the pelomedusid genus *Pelusios*, the *musculus levator plastralis*, a derivative of respiratory *musculus diaphragmaticus*, ought to be involved in closing the anterior plastral lobe (Bramble and Hutchison, 1981).

7.3.2 Plywood-like structure in Trionychidae

Although the cancellous bone and the internal cortex of the flat bones of the trionychid shell are rather similar to those recognised in other hard-shelled turtles, the plywood-like arrangement in the external cortex of the bone is unique for the Trionychidae (Scheyer et al., 2007). Figure 67 summarises the trionychid rotated ply-system based on observations of the external cortex of cf. *Aspideretoides* sp. (IPB R533). Because this dermal structure of the shell bone and shell skin is found in all crown group trionychid turtles, it is considered a synapomorphy of this clade. However, based on the uncertain intraspecific variation which correlates with the statistically small amount of studied trionychid individuals, it remains yet unclear if the measured angles between the ply-stacks in the trionychid shell are somehow characteristic on generic- or even species-level. Schmidt (1921) pointed out that the fibre bundles of the so called ‘Bündelschicht’ (plywood-like pattern) are arranged diagonally towards the overall long-axis of the turtle shell. He attributed this arrangement to a biomechanical retention of the shell curvature or as resistance to the flattening of the shell. Structurally, the presence of Sharpey’s fibres in the outer zone, the ornamentation pattern, of

the external cortex of the trionychid shell bones implies a strengthened anchoring of the integument onto the bone. The internal cortex and the inner cancellous bone of the bony shell elements are rather similar to those found in other hard-shelled turtles and are thus considered plesiomorphic.

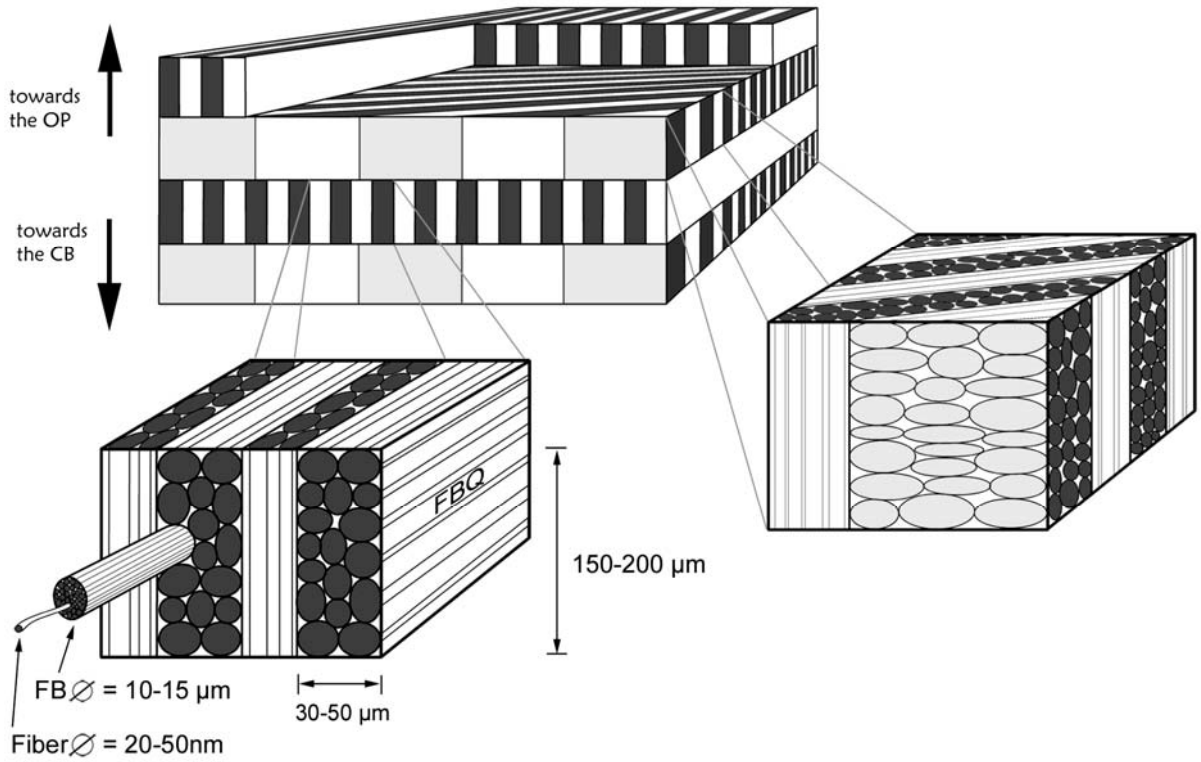

Figure 67: Sketch of bone microstructure of the external cortex based on cf. *Aspideretoides* sp. (IPB R533), illustrating the rotated ply-system. Please note that the actual microstructure (e.g., Fig. 64c, d; dried specimen) is much more variable than the sketch is implying. Each ply consists of numerous fibre bundle quadrangles (FBQ) that again consist of tubular fibre bundles (FB). The magnification of the plywood-like structure highlights the orientation of the FBQ to each other, with neighbouring quadrangles being rotated in 90° angles to each other. Each FB (10-15 µm) in the FBQ consists of multiple single collagen fibre strands (20-50 nm). Vertically trending FBQ that trend from the ornamentation pattern towards the cancellous bone are usually two FB rows thick, while the horizontal ones are usually three FB rows thick (30-50 µm).

At this point, a short comparison to Schmidt's work (1921) seems to be in order to elucidate similarities and discrepancies between his "soft-tissue" analysis and the "hard-tissue" analysis of the current study. All in all, both works complement each other and lead to a clearer understanding of the trionychid turtle shell. Structures similar to those presented herein (see Scheyer et al., 2007) were described in Schmidt's interpretations and drawings of the soft-tissue part. It is hypothesised that the tripartite organisation of the corium into an external '*Bündelschicht*', an interior '*Filzschicht*' and an internal '*Grenzschicht*' as presented by Schmidt (1921:195) corresponds to the metaplastically ossified bone of the trionychid shell with its ply-system in the external cortex, the interior cancellous bone and the internal cortex. Even if, as Kälin (1945) pointed out, the initial ossification of the dermal bone begins below the "*tiefes Stratum compactum*" (Kälin, 1945:160: fig. 11), which is synonymous to Schmidt's '*Grenzschicht*', the subsequent dermal ossification is strongly associated with the "*tiefes Stratum compactum*" justifying the hypothesis of the equivalency of the tissues.

On the other hand, no deviating or anastomosing FBQ, as described by Schmidt, were recognised in the bone of the shell, thus the FBQ appear to be less variable in the bony carapacial disk compared to the peripheral soft tissue part of the shell. Furthermore, Schmidt's assertion that the vertical fibre bundles extend continuously through the whole ply-system could not be corroborated by the bone histology. While occasionally some vertical FBQ do seem to cross the horizontal plies, the majority of them appear to be discontinuous. The vertical FBQ reach into the overlying and underlying plies and expand there to further anchor the ply system, but they do not continue on through the neighbouring plies.

Twisted and orthogonal plywood structures have been decribed in the basal plates of coelacanths and teleosts and the adaptive values of such a highly organised structure in bone has been discussed for example by Giraud et al. (1978), Meunier and Castanet (1982) and Meunier (1988). In Trionychid turtles, several specific adaptive advantages can be hypothesised, including the flattening of the carapace, reduced ossification of the shell and the loss of the keratinous shields (see also Scheyer et al., 2007). First, trionychid turtles have selective advantages in building and maintaining less hard tissues, as the peripheral plates, distal parts of the costal plates and much of the plastral bones are reduced (e.g., Rathke, 1848; Hoffman, 1878; Zangerl, 1969; Meylan, 1987). The decreased demand for minerals and nutrients clearly represents a physiological advantage. Second, the reduced amount of hard tissues leads to an overall lower body mass, a point mentioned already by Schmidt (1921).

The lower body mass facilitates at least fast short-term swimming and higher manoeuvrability, as is seen in many other secondarily aquatic tetrapods (Webb and Buffrénil, 1990). The powerful swimming bursts (Pritchard, 1984; Pace et al., 2001) that can be either used to quickly burrow into soft sediments for hiding (Pritchard, 1984; Bramble, pers. comm. in Meylan, 1987) or to escape from predators, are enabled through the flattened carapace with its movable soft-tissue peripheral flap together with their propelling front feet. Third, since trionychids are ambush predators that hide at the bottom of lakes and rivers, the flattened, easily buried carapace together with the snorkel-like nose increases their hiding abilities and their own success in hunting. Fourth, a flattened shell that is covered with extremely slick and slippery skin is an effective protection against predators both in water and on land because any predator will have difficulties grasping any flat object that tightly hugs the ground. In this instance, a long and agile neck and sharp beak is not only well suited for catching prey like fishes (Pritchard, 1984; see also discussion in Meylan, 1987), but also a dangerous weapon that the trionychid turtle can use to effectively defend itself (pers. obs.). Fifth, based on the striking parallels to man-made fibre-reinforced composite materials, the plywood-like structure may have some kind of biomechanical advantage, be it a heightened resistance against crushing or crack prevention or simply an increase of stability of the flattened carapacial disk. Similar points were already listed by Schmidt (1921) for the soft-tissue part of the shell. These aspects of the plywood-like structure of trionychid shells require further biomechanical studies. Last but not least, the loss of keratinous shields allows for increased cutaneous breathing (Ultsch et al., 1984). Trionychid turtles are presumably unique in their soft carapacial and plastral epidermis acting as an efficient cutaneous breathing organ, allowing a bimodal gas-exchange with ambient water (Girgis, 1961; Bagatto and Henry, 1999). This additional method of respiration, together with buccopharyngeal breathing, allows soft-shelled turtles to remain submerged for a vastly increased period of time compared to turtles lacking this adaptation (Girgis, 1961; Seymour, 1982; Bagatto and Henry, 1999; Gordos et al., 2004). They seldom have to leave their hiding place or extend their long neck and snorkel-like nose to the surface to breathe, which again works in favour of camouflage. However, the reduction of the bony shell poses also a disadvantage by reducing potential storage and buffering of lactic acid, lowering anoxic water tolerance (Jackson et al., 2000). Trionychid turtles prefer normoxic water habitats in which they can fully take advantage of their ability to breathe through their expanded skin surface. Those normoxic habitats are also of great importance for hibernation of trionychids, because they are not able to tolerate raised levels of anoxia for a longer time period (Reese et al., 2003).

Measuring the evolutionary success of a group of organisms is difficult and may often seem speculative. Yet, trionychid turtles experienced certain evolutionary success because the group originated more than 120 million years ago during the Early Cretaceous in Asia and eventually came to be one of the most cosmopolitan and long-lived turtle radiations by spreading to North America, Europe, Africa and Meganesia (e.g., Ernst and Barbour 1989; Iverson 1992; Scheyer et al., 2007). Since their first appearance in the fossil record, though, almost no variation occurred in their overall trionychid shell morphology, and fragments of their shells are among the most obvious and numerous fossil specimens in many Mesozoic or Cenozoic fossil lagerstätten. The current distribution of extant species appears to be limited only by access to suitable river habitat and temperature regions. It is hypothesised that the trionychid shell with its unique composite structure evolved as an alternative lightweight solution to the plesiomorphic domed protection of other turtles, an adaptation that offers additional physiological and biomechanical advantages. However, it is uncertain if the highly unique morphology of trionychids originated and became fixed rapidly, because the record of pre-Early Cretaceous fossil turtles still remains poorly documented and understood.

7.3.3 Functional size/age related differences

A group, where extreme size variation can be observed, is Pelomedusoides (see also Scheyer and Sánchez-Villagra, 2007). The diploe build of the shell, the presence of growth marks and bone tissue that consists of interwoven structural collagenous fibre bundles, found in all taxa from small *Pelomedusa subrufa* to giant *Stupendemys geographicus*, are hypothesised to be plesiomorphic characters. Based on the lack of data available on stress-induced variation of the bone microstructures of different aquatic and terrestrial turtle taxa of varying ontogenetic stages and size classes, it cannot be verified if any of those structures are truly size related. The comparison of the pelomedusoides turtles leads to the conclusion that the truly giant size of *S. geographicus* was not based upon a novel way of shell bone formation that greatly differs to that of other turtles in general (Scheyer and Sánchez-Villagra, 2007).

Heavy remodelling of the bone usually leads to the formation and accumulation of successive generations of secondary osteons, i.e., Haversian bone, with progressive age (e.g.,

Francillon-Vieillot et al., 1990). The higher level of vascularisation linked to the secondary osteon clusters in the compact bone layers in *S. geographicus*, however, appears to be directly influenced not only by the large size but also by the advanced (old) age of the specimens.

According to Rhodin (1985) who studied chondro-osseous growth in endoskeletal bones of fossil and recent turtles, *A. ischyros* showed significant histological similarities (e.g., vascularised cartilage) with the rapidly growing *D. coriacea*. The specimens of *S. geographicus* on the other hand lacked comparable features, instead showing a microstructure similar to recent turtles with a 'normal', slow mode of growth (Rhodin, 1985). In this respect, both the long bone histology (*sensu* Rhodin, 1985) and the shell bone histology (studied herein) show the same pattern for *A. ischyros* and *S. geographicus* (see also Scheyer and Sánchez-Villagra, 2007).

When applying overall growth rates of *D. coriacea* to the presumably slow-growing *S. geographicus*, it would have taken the giant pleurodire turtle a minimum of 30 years to reach a SCL of 3.3 metres. If slower, possibly more realistic, mean growth rates of 3.0-5.3 cm/yr "for most age and size classes" of the cheloniid turtle *C. mydas* are applied (Zug and Glor, 1998:1497), the age estimates would increase to 60 to 110 years. Similar estimates would be obtained using growth rates of the cheloniid *C. caretta* (e.g., Klinger and Musick, 1995: ~5.3 cm/yr to ~2.9 cm/yr for 400-1000 mm SCL). The difference between the visible, measurable histological growth record and real age becomes even more pronounced, considering that all turtles further decrease growth towards maturity and old age (e.g., Peters, 1983; Klinger and Musick, 1995; Zug et al., 2001). None of these given estimates can be constrained further, because the growth record of *S.geographicus* is still insufficiently known.

7.3.4 Primary and secondary turtle armour

Secondary (epithecal) armour was sampled only in the two specimens of Dermochelyidae, the extant *Dermochelys coriacea* and the fossil *Psephophorus* sp. The secondary armour platelets of *D. coriacea* seem to have formed in a connective tissue layer between the cuticle and the lipid-rich fibrous layer where fibre bundles mostly extend horizontally. Initial growth seems to involve metaplastic ossification (see ISF of external cortex and primary trabeculae

structure) while final increase in thickness may be purely attributed to remodelling of the more internal cancellous regions of the platelets. Although morphologically different, the secondary armour platelets of *D. coriacea* and *Psephophorus* sp. share histological structures. Besides the missing connection of the platelets to the endoskeleton (e.g., ribs and vertebral column), there is no indication that the platelets of Dermochelyidae form in any other way different from the dermal parts of the shell of other turtles. Even the locus of osteogenesis seems to be similar in dermochelyid turtles (internal to epidermal cuticle) and other turtles (internal to epidermal keratin shields; except soft-shelled turtles). It is hypothesised that the relative position of bone formation has not changed, but that the external (superficial) position of the secondary platelets is directly linked to the thickening of the integument in dermochelyid turtles.

7.4 Implications for turtle origins

If turtles were to be nested deeply within Pareiasauria (Lee, 1997), strong histological similarities would be expected between turtle shells and derived dwarf pareiasaurs, i.e. *A. serrarius* (chapter 5.3.1). Instead, both bone histologies were consistent throughout each group, thus arguing against the homology of the dermal bone structures. Basal turtle shell bones do not show ornamental bosses, radial ridges and radial vascularisation patterns, while pareiasaur osteoderms lacked diploe structures, scute sulci and a clear distinctiveness of the internal and external cortex (all presumably synapomorphic for turtle shell bones). The strongest argument against this hypothesis, however, is the absence of metaplastic dermal tissue in pareiasaur osteoderms. Because of this lack of metaplastic dermal structures, fundamental differences in osteogenesis are proposed for the turtle shell and for the pareiasaurs osteoderms. The latter bones are hypothesised to represent novel armour structures that displace integumentary tissue instead of incorporating it. Similarly, a partially novel origin was discussed for ossicles of an ankylosaur from Anarctica (*Antarctopelta oliveroi* Salgado and Gasparini, 2006) based on bone histology (Ricqlès et al., 2001). However, as was argued by Scheyer and Sander (2004) and Main et al. (2005), thyreophoran (including ankylosaur) osteoderms truly develop through metaplastic ossification. Because a novel origin is assumed for pareiasaur osteoderms, these osteoderms are not suitable for

reconstructing fossil integumentary structures as was possible in thyreophoran dinosaurs (Scheyer and Sander, 2004) and now is possible in turtles.

Placodontia are the most basal group within Sauropterygia (Rieppel and Reisz, 1999). Furthermore, they are the only sauropterygians with body armour that allow histological comparison to turtle shell bones, although placodonts are not proposed as the potential sistergroup to turtles herein.

Placodont armour is not only morphologically homoplastic to the turtle shell (e.g., Gregory, 1946; Rieppel, 2002); their bone histologies are also very divergent. Placodont dermal armour plates express strong radial growth similar to pareiasaur osteoderms and the plates are compact. Large vascular spaces and extensive secondary bone remodelling are completely absent. However, placodonts are unique among armour-bearing vertebrates in their highly unusual inclusion of calcified fibrocartilaginous tissue, here termed postcranial chondroid bone, in the bone of the dermoskeleton. The cartilage matrix with interspersed bony struts differs from hyaline cartilage of , e.g., the growth plates of long bones in having a distinctive fibrous nature similar to fibrous cartilage, e.g., of the inter-vertebral disks. The presence of calcified cartilaginous tissue separates these bones from true postcranial ‘osteoderms’, because intramembraneous bones/osteoderms strictly form without cartilage precursors (Francillon-Vieillot et al. 1990). Due to the lack of modern homologous structures, the mechanisms to incorporate cartilage in the placodont armour remain yet speculative.

Even though a large number of different dermal bone structures with specific bone histologies developed among archosaurs (e.g., Francillon-Vieillot et al., 1990; Scheyer and Sander, 2004; Main et al., 2005; Hill and Lucas, 2006; present study), the turtle-archosaur sistergroup relationship proposed by molecular studies (Hedges and Poling, 1999; Kumazawa and Nishida, 1999; Janke et al., 2001; Rest et al., 2003; Iwabe et al., 2004) is in accordance with the presented data. Metaplastic ossification as well as diploe-like structures are known from archosaur osteoderms. Indeed, metaplastic ossification of at least parts of the osteoderms is hypothesised as being plesiomorphic for all archosaur groups as well as for the Lepidosauria. Because metaplastic bone formation is also found in anurans, (e.g., Zylberberg and Castanet, 1985), the metaplastic process in dermal osteogenesis might be an even more plesiomorphic, inherited feature in reptiles. In the case of Lepidosauria, osteoderms are not regarded as a synapomorphy for Lepidosauria, as for example, basal lineages lack

osteoderms. They appear only in certain lepidosaur lineages, mostly as diminutive bone structures (see also Hill, 2005).

Evolutionary developmental studies that propose the turtle shell as an evolutionary neomorphic structure are also in accordance with, but not testable by, bone histological data, because the studies obviate armoured ancestors from evolutionary scenarios. The aim of future studies will be a more exact histological classification of the amniote integument and its mineralisations and ossifications, which will result in mappable characters, which can then be plotted on phylogenetic scenarios. This will potentially allow studies of the characters in amniote relationships using parimony and other statistical methods.

7.5 Evolutionary model of osteogenesis of placodont armour

Due to the highly unique nature of the placodont armour, a brief aside on placodont armour development is included in this chapter. Contrary to Westphal's (1975) assessment of growth patterns in placodont plates that were based solely on hexagonal plate forms, quite a few differences in the locations of the centres of growth were found among the studied sample. An evolutionary model of growth together with the correlations of tissues is presented below (see Fig. 68).

Even though placodont dermal plates span a wide variety of gross morphological shapes, a generalised model of histogenesis can be proposed based on the sampled thin-sections. The simplified model of osteogenesis proposed by Westphal (1975) is expanded by including a wider variety of placodont taxa, morphological shapes and bone histological characteristics. The location of the centre of growth, the radial growth pattern including the vascularisation and growth marks and the occurrences of the different histological tissues within the bones are thus taken into account for this study's model. In keeping with its phylogenetic position, the ridged plate (SMNS 91006) of the placodontoid *P. gigas* is hypothesised to represent the plesiomorphic state, while the cyamodontoid plates represent derived states. Reduction in height and subsequent externointernal flattening of specimen SMNS 91006 leads over to the polygonal (?hexagonal) plates of *Psephoderma* sp. (NRM-PZ R.1759a). Through reduction in externointernal thickness, subsequent flattening and suppression of the development internal

to the growth centre, the hexagonal plates of *Psephoderma* sp. (SMNS 91008) and the rhomboidal/hexagonal plates of the *Psephosaurus suevicus* (MHI 1426/2 & 3) and *Psephosaurus* sp. (SMNS 91009) can be derived. A stonger lateral shift leads over to the recumbent spiked plate of *Psephosaurus suevicus* (MHI1426/1). Lateral compression and a rotational component of about 45° around the centre of specimen SMNS 91006 enables a transformation to the procumbent spike of cf. *Placochelys* sp. (SMNS 91009). The spiked specimen of *P. suevicus* (SMNS 91010) can be derived by slight lateral and externointernal compression, as well as a suppression of development lateral and external to the growth centre.

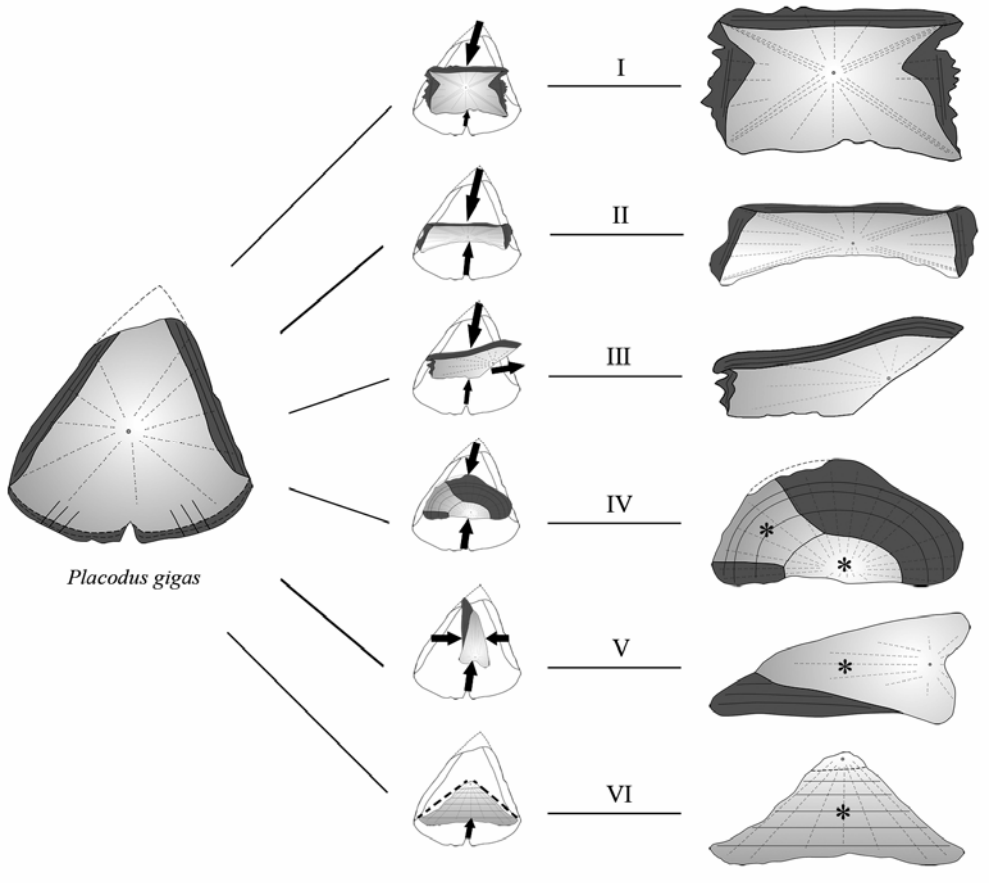

Figure 68: Generalised model of osteogenesis of placodont armour plates. The sectioned armour plates are all scaled to similar size. The cyamodontoid plate forms can be deduced from the basal plate morphology and histology of *Placodus gigas* (SMNS 91006). Please note that in case I, one of the plates of NRM PZ R.1759a was chosen representatively for the hexagonal/polygonal plates. I: *Psephoderma* sp. (NRM PZ R.1759a) *Psephosaurus suevicus* (MHI 1426/2 & 3); II: *Psephosaurus* sp.(SMNS 91008); III: *Psephosaurus suevicus* (MHI 1426/1); IV: *Psephosaurus* sp. (SMNS 91009); V: cf. *Placochelys* sp. (SMNS 91010); VI:

Psephosaurus suevicus (SMNS 91007). Areas where a calcified fibrocartilaginous tissue and bone spiculae, i.e., posterior chondroid bone, was found are marked with an asterisk.

Two different developmental hypotheses can be proposed about placodont armour formation, explaining the presence of cartilage in the plates: 1.) Placodont armour develops as part of the endoskeleton and not as part of the dermal skeleton proper. 2.) The placodont armour is preformed in cartilage that does not belong to the endoskeleton and the formation of the cartilage in the dermis is treated as an evolutionary novelty.

The first case, the retention of cartilage in endoskeletal bone, is widely distributed in endoskeletal elements, e.g., limb bones, ribs and vertebrae, of fossil and recent vertebrate groups that are secondarily adapted to a marine life-style (e.g., Ricqlès, 1989; Ricqlès and Buffrénil, 2001). Morphological data, however, does not provide evidence for a relationship of the placodont armour to the endoskeleton instead of belonging to the dermoskeleton. The second case is not known to occur in the postcranial armour plates of any fossil or recent vertebrate group. This implies that the formation of cartilage in the postcranial dermis of placodonts must have involved some novel developmental mechanisms (e.g., Webster and Zelditch, 2005; Fang and Hall, 1997). On the other hand, as shown for the vertebrate skull, the occurrence of cartilage (e.g., secondary cartilage, chondroid bone and cartilage formation in fracture healing) can be associated with typical dermal or membrane bones that also lack cartilage precursors (Fang and Hall, 1997). Especially chondroid bone, an intermediate tissue that contains both bone and cartilage does show similarities with the tissue recognised in the placodont armour. Chondroid bone is argued to be connected with rapid bone growth during intramembraneous ossification (Lengelé et al., 1990, 1996). It disappears during ontogeny (Fang and Hall, 1997; Hall, 2005). It remains unclear, however, why such a rapid development would occur in placodont armour. The presence of a calcified cartilaginous matrix in part of the placodont samples to the complete absence of cartilage in others, in accordance with cranial chondroid bone, could represent the result of different ontogenetic states of the samples. If the developing chondroid bone of the placodont dermal armour displays a highly reduced potential to fossilise compared to completely ossified tissue, this could explain why the few finds of juvenile placodonts apparently lack postcranial dermal armour plates (see Rieppel, 2002).

The compact nature of the bone associated with the lack of interior cancellous bone in all placodont samples indicates some form of osteosclerosis of the armour plates (compare to Ricqlès and Buffrénil, 2001), a fact that matches well the previously described pachyostotic trends recognised in placodont and other vertebrate long bone histology (e.g., Buffrénil and Mazin, 1992; Hua and Buffrénil, 1996; Ricqlès and Buffrénil, 2001). It is proposed that additional to the pachyostosis found in limb bones, the osteosclerosis of the armour plates in at least the more derived cyamodontoids attributed to some extend to buoyancy control while swimming and browsing for food. Swimming speed, on the other hand, most likely was reduced in the heavily armoured cyamodontoids (compare to Massare, 1988, 1994).

7.6 Implications for the ecology of turtles

Ecology and life-style are hypothesised to have great impact on turtle shell bone microstructures. As a general trend, terrestrial turtles retain a compact diploe with well developed cortical bone layers. With increasing adaptation to an aquatic habitat, the more vascularised the bones become. The most extreme forms of adaptation are found in highly aquatic turtles of the Kinosternia, the Dermatemydidae and the Chelonioidea. In a first step (chapter 7.6.1), the palaeoecology of basal turtles is inferred by comparison to modern turtles, and in a second step (chapter 7.6.2), four categories are introduced and defined to quantify the ecological/palaeoecological signal of all sampled fossil and recent turtles based on their respective bone histologies.

7.6.1 Palaeoecology of basal turtles

The palaeoecology of basal turtles was classically viewed as being semi-aquatic. In the monographic compendium on the osteology of *Proganochelys quenstedti*, Gaffney (1990:25) noted that this basal turtle was probably roughly similar to the American snapper *Macrochelys temminckii* in "size, possible habitat, and some morphologic features", and his resulting reconstruction of the environment (Gaffney, 1990:fig.1) included a swimming *P. quenstedti,* thus underscoring a purportedly semi-aquatic habitat preference. Lately, this view

was questioned based on limb bone proportions, indicating a terrestrial palaeoecology for the turtle stem (Joyce and Gauthier, 2004). In contrast to the study of limb bone proportions by Joyce and Gauthier (2004), the present study is independent to the preservation of axial skeletal elements in fossil turtles, enabling the palaeoecological study of much broader range of incompletely known turtle taxa in the fossil record.

Independent shell bone microstructural evidence for basal Testudinata, especially of the oldest and basal-most turtles *Proterochersis robusta* and *Proganochelys quenstedti*, clearly indicates a terrestrial origin of turtles. Similarity can be observed between the basal turtles and modern turtles with a terrestrial ecology. Shell bones of both groups have a well developed diploe structure with thick external and internal cortices, weak vascularisation of the compact bone layers and a dense nature of the interior cancellous bone with overall short trabeculae. Although *Kayentachelys* aprix was characterised as an aquatic turtle based on various morphological traits, the taxon seems to retain the compact bone histology indicative of terrestrial habits.

On the other hand, modern turtles with aquatic ecologies tend to reduce cortical bone layers, while concurrently increasing overall vascularisation of the bone tissue. This can ultimately lead to an overall homogenisation of cancellous and cortical bone (e.g., in *Archelon ischyros*).

Due to the congruence of basal and modern 'terrestrial' turtles, it is inferred that overall composition of the integument and specific locus of bone development in the integument are comparable in those turtle groups. The strong terrestrial signal in the shells of basal turtles again argues against a proposed marine origin of turtles (see Rieppel and Reisz, 1999).

7.6.2 Quantifying the ecological adaptation in turtles

All turtles are assigned to one of four categories (category I-IV) according to the degree of aquatic adaptation. The categories are mainly based on literature and internet data on the ecology of recent turtles (e.g., Pritchard, 1979; Ernst and Barbour, 1989; Baillie et al., 2004; Ernst et al., 2006) to which bone histological characteristics are then assigned. Comparison with the recent taxa then allows the assignment of fossil taxa to the respective categories. A

definition of the categories follows below, and the complete list of assignment to the categories is compiled in Appendix 3 for each taxon. Note that especially in category II, bone composition and overall vascularisation are subject to gradual changes, often making a clear classification difficult for a taxon (indicated by the tendency to a higher or lower category).

7.6.2.1 Category I (terrestrial)

Two groups of turtles are combined in this category. The first group is composed of the basal Testudinata, the primary terrestrial turtles (see chapter 7.6.1). The second group consists of turtles (e.g., tortoises) that secondarily have returned to a terrestrial ecology. The turtles of this category barely ever enter water bodies and show no adaptations to an aquatic lifestyle. The shell bones appear quite massive in thin-section. The diploe structure of the bone is well developed with thick, weakly vascularised cortices. The cancellous bone is dominated by primary short, thick bone trabeculae and small vascular spaces.

7.6.2.2 Category II (semiaquatic to mainly aquatic)

Turtles that spend much of their live in water fall into category II. However, they more or less often go on land to migrate, forage for food or to bask. Turtles of category II share the following bone microstructural features: all shell bones have a diploe structure, where internal and external cortical bone layers frame interior cancellous bone. Both cortices are well developed, and the whole bone retains a generally compact appearance. However, the vascularisation of the cortical bone is increased compared to category I due to increased amounts of primary vascular canals and secondary osteons. The transition between the cortices and the interior cancellous bone is still conspicuous. In quite a few taxa in category II, a trend to reduce the thickness of cortical bone while increasing overall bone vascularisation is apparent.

7.6.2.3 Category III (fully aquatic)

Turtles of category III rarely leave the aquatic environment to bask or to lay eggs. The shell bones show a reduction of compact bone layers. Especially the internal cortex is strongly reduced in thickness compared to the external cortex. The external cortex itself is strongly vascularised, but seldomly reduced in thickness. Furthermore, in those taxa in which the internal cortex is almost completely reduced, the external cortex is especially well developed (e.g., Dermochelyidae; *Allopleuron*; Plesiochelyidae). The degree of organisation of trabeculae in the cancellous bone is high. It is hypothesised that by retaining a well developed external cortex, the structural stability of these bones is still guaranteed.

7.6.2.4 Category IV (extreme adaptation to aquatic/marine environments)

Similarly to category III, the turtles included in category IV they rarely leave the water. Morphological adaptations to the buoyant medium are apparent (e.g., modification of limbs into flippers; large shell fontanelles retained through adulthood and body shape steamlined, i.e., teardrop-shaped). Taxa of category IV show an extreme stage of adaption to the aquatic environment and, as expected, most of the sea turtles fall into this category. The turtle shell bones show reduction in thickness of the cortices combined with strong vascularisation of the compact bone layers. The cortices loose their compact nature, and the whole bone develops a homogeneous spongy appearance. A clear distinction of the bone tissue in cortical bone and cancellous bone is not possible anymore.

7.6.2.5 Synopsis

Many groups in which more than one turtle taxon was sampled show a consistent picture of aquatic adaptation (e.g., basal Testudinata, Podocnemidae, Pleurosternidae, Carettochelyidae, Cheloniidae "*sensu lato*", Kinosternidae and Trionychidae). In several other groups, however, not all of the genera fall in the same category. These groups are Bothremydidae, Chelidae, Baenidae, Cheloniidae "*sensu stricto*" and Testudinoidea.

In Bothremydidae, the freshwater turtle *Foxemys cf. F. mechinorum* shows less adaptation than the two sampled marine taxa (*Bothremys barberi*, *Taphrosphys sulcatus*). In Baenidae,

the early basal taxa (*Plesiobaena* sp. and *Neurankylus* sp.) fall into category II with tendencies to category I, while the derived taxa (*Boremys* sp. and *Chisternon* sp.) show an increasing vascularity of the bone, thus maybe indicating a trend of increasing aquatic adaptation through time for this group. In Cheloniidae "*sensu stricto*", *Chelonia mydas* falls into category III, while the other two species, *Caretta caretta* and *Eretmochelys imbricata*, are grouped in category IV. Overall, marine turtles (i.e. *B. barberi*, *T. sulcatus*, Eurysternidae, Thalassemydidae, Plesiochelyidae and Chelonioidea) range from category III to IV, with the least adaptations found in the Upper Jurassic marine taxa from Solothurn limestone and the highest adaptations in Chelonioidea. The dermochelyid taxa (fossil *Psephophorus* sp. and recent *Dermochelys coriacea*) both fall into category III. It remains speculative at this point to attribute their less adaptational contition to the reduction of the primary (thecal) shell and the formation of secondary (epithecal) armour.

Trionychid taxa show several shell adaptations (e.g., persisting plastral fontanelles in some taxa, loss of peripherals and free rib ends covered in soft skin flap) that may be attributed to a neoten stage of development compared to other turtles. These adaptations can also be interpreted as advanced adaptations to the aquatic habitats. Trionychid shell bones, on the other hand, are surprisingly compact with well developed and generally weakly vascularised internal and external cortices. They are thus categorised as belonging into category II, with tendencies to category I. I here propose that because of structural reasons of shell stability, the highly unusual trionychid shell bone with its unique plywood-arrangement of the external cortex counteracts or inhibits processes that would otherwise lead to increased vascularisation and further remodelling of the bone. In this case, one functional aspect (maintaining structural stability of the shell) would counteract another (the ecological adaptation to the aquatic medium).

It appears that the turtles of Solothurn, although marine, generally did not reach the level of adaptation as marine turtles from the Cretaceous and latter time periods. On the other hand, there are few non-marine species (Dermatemydidae, *Hoplochelys* sp.) that range among the highest levels of adaptation present in the turtle shells, almost equaling the microstructures of *Archelon ischyros*. A taxon that was expected to show high levels of adaptations similar to marine turtles is *Carettochelys insculpta*. Even though its limbs are modified into flippers like in marine turtles, the bone histology showed comparatively less adaptation.

In the Testudinoidea, there was quite a bit of adaptational variability among the taxa. The purported most basal testudinid genus *Hadrianus* falls within category II (see also chapter 6.3.14). It is hypothesised that the taxon still retains the plesiomorphic bone histology of its direct aquatic ancestors. Strikingly, there are a few other taxa among the tortoises that have raised levels of vascularisation (i.e., in recent *Geochelone carbonaria* and *Kinixys homeana* and in fossil *Hesperotestudo crassiscutata*). In *G. carbonaria* and *K. homeana*, the raised levels of vascularisation are not easily explained. Wether the microstrucures in both taxa are linked to their unique shell morphologis (strongest non-pathological humped carapace in *G. carbonaria*, peculiar carapacial hinge system in *K. homeana*) remains speculative. In the latter taxon, *H. crassiscutata*, a trend to extreme light-weight construction of the shell might play a role (see chapter 7.3.3).

Following Ricqlès and Buffrènil (2001), the strict adherence to the categories of adaptation has to be treated with caution as simplifications might be expressed by the categorisation of the turtles based on microstructural evidence of the shells alone. However, the current study enables and advances comparative works between the shell bone histology (and amniote armour in general) and bone histology of the endoskeleton.

8. Acknowledgements

First of all, I would like to thank my supervisor PD Dr. P. Martin Sander for the possibility to conduct this study and for the great time in the histology study group (Dr. Nicole Klein; Dr. Daniela Kalthoff; Ragna Redelstorff; Dominik Wolf). I also wish to thank Prof. Dr. Thomas Martin, for his acceptance to read and co-referee my "inveterate turtle" work.

I thank the DFG for funding of the project (grant # SA469-15-1/2), the Doris & Samuel P. Welles-Fund, University of California Museum of Palaeontology, Berkeley, California, for covering travel expenses to visit the UCMP collections and all participants of the Graduiertenkolleg 721 "Evolution und Biodiversität in Raum und Zeit", University of Bonn.

I want to sincerely acknowledge all of the following collections managers and their colleagues at the museums and institutions, who agreed to provide turtle material for thin-sectioning purposes. Without their acquiescence, this project could not have been realised: Alan Resetar and Jamie Ladonski (Zoology, FMNH), Olivier Rieppel and William Simpson (Palaeontology, FMNH); Jennifer Clack (UMZC); Rainer Schoch, Ronald Boettcher (Palaeontology, SMNS); Andreas Schlüter and Doris Mörike (Zoology, SMNS); Edith Müller-Merz (NMS); Walter Joyce (Palaeontology, YPM); Gregory Watkins-Colwell (Zoology, YPM), Donald Brinkman and James Gardner (RTMP); Marcello Sánchez-Villagra (NHM, London); Anne Schulp (NHMM); Orangel Aguilera (UNEFM); Patricia Holroyd and Howard Hutchison (UCMP); Chris Conroy (MVZ); Thomas Gassner and David Unwin (MB); Andreas Matzke and Michael Maisch (Institute of Geosciences, University of Tübingen); Steve Perry and Klaus Völker (Zoology, University of Bonn); Gavin Dally (MAGNT); Stephen Salisbury and Andrew Amey (QM); Hans Hagdorn (MHI); Kevin Seymour (ROM); Timothy Rowe (TMM); Thomas Mörs (NRM); Norbert Micklich and Gabriele Gruber (HLMD); Sheena Kaal and Roger Smith (SAM Isiko); Uwe Fritz and Markus Auer (MTD); Eberhard Dino Frey and Wolfgang Munk (SMNK); Wolfgang Böhme (ZFMK); Rainer Günther (ZMB); Susan Evans and Mark Jones (Evolutionary Anatomy Unit; University College London).

I also wish to say thanks to all friends and colleagues and also to the technical, scientific and administrative staff of the Institute of Palaeontology in Bonn, for their various supports. Especially I would like to thank Olaf Dülfer for his great help in preparing the thin-sections, Dorothea Kranz for her technical advice concerning digital imagery, Georg Oleschinski for all things concerning photography and Devran Ekinci for computer and data security.

I dearly thank my wife Elke Goldbeck and my son Norik for their support, patience and endless discussions, as well as the rest of my family in Emmelshausen and Aachen.

Last, I thank all the people and friends that remain unnamed most of the times, but who provide invaluable help and strength every day.

9. References

Agassiz, L. 1833-45. Recherches sur les Poissons Fossiles. Imprimaire de Petitpierre, Neuchâtel.

Agassiz, L. 1857. Contributions to the Natural History of the United States of America Vol. 1, Pts. 1 & 2. 452 pp. Little, Brown, Boston.

Aguilera, O., R. Sánchez, and F. Terrible. 1994. Un nuevo registro de *Stupendemys geographicus* Wood 1976 (Testudinidae: Pelomedusidae) de la Formación Urumaco (Mioceno Tardío) en el Estado Falcón, Venezuela. Convención Anual de ASOVAC, 54, Coro, UNEFM, Acta Científica Venezolana, Resúmenes 45:333.

Ammon, L. von. 1911. Schildkröten aus dem Regensburger Braunkohlenton. Jahresbericht des Naturwissenschaftlichen Vereins zu Regensburg 12 (Separate Beilage):1–35.

Amprino, R. 1947. La structure du tissu osseux envisagee comme l'expression de différences dans la vitesse de l'accroissement. Archives de Biologie 58:315-330.

Antunes, M. T., and F. de Broin. 1988. Le Crétacé terminal de Beira Litoral, Portugal: remarques stratigraphiques et écologiques, étude complémentaire de Rosasia soutoi (Chelonii, Bothremydidae). Ciências da Terra 9:153-200.

Asian Turtle Trade Working Group 2000. *Mauremys mutica*. In: IUCN 2006. 2006 IUCN Red List of Threatened Species. <www.iucnredlist.org>. Downloaded on 14 August 2006.

Auffenberg, W. 1974. Checklist of fossil land tortoises (Testudinidae). Bulletin of the Florida State Museum, Biological Sciences 18:121-251.

Bagatto, B., and R. P. Henry. 1999. Exercise and forced submergence int he pond slider (*Trachemys scripta*) and softshell turtle (*Apalone ferox*): influence on bimodal gas exchange, diving behaviour and blood acid-base status. Journal of Experimental Biology 202:267-278.

Baillie, J. E. M., C. Hilton-Taylor, and S. N. Stuart (Editors) 2004. 2004 IUCN Red List of Threatened Species. A Global Species Assessment. XXIV + 191 pp. IUCN, Gland, Switzerland and Cambridge, UK.

Bartels, W. S. 1993. Niche separation of fluvial and lacustrine reptiles from the Eocene Green River and Bridger Formations of Wyoming. Journal of Vertebrate Paleontology 13 (Supplement to Number 3):25A.

Bass, A. L. 1999. Genetic analysis to elucidate the natural history and behavior of hawksbill turtles (*Eretmochelys imbricata*) in the wider Caribbean: a review and re-analysis. Chelonian Conservation and Biology 3:195-199.

Baur, G. 1887. Ueber den Ursprung der Extremitäten der Ichthyopterygia. Berichte über die Versammlungen des Oberrheinischen Geologischen Vereines 20:17-20.

Bell, T. 1827. On two new genera of land tortoises. Transactions of the Linnean Society of London 15:392-401.

Bell, T. 1828. Characters of the order, families, and genera of the Testudinata. Zoological Journal 3:513-516.

Bell, T. 1832. Zoological observations on a new fossil species of *Chelydra* from Oeningen. Transactions of the Geological Society of London, 2nd Series 5:379-381.

Benton, M. J. 2005. Vertebrate Palaeontology. Third Edition. 455 pp. Blackwell Science Ltd., Oxford.

Benton, M. J., and J. M. Clark. 1988. Archosaur phylogeny and the relationships of the Crocodylia; pp. 295-338 *in* M. J. Benton (ed.), The Phylogeny and Classification of the Tetrapods, Volume 1: Amphibians, Reptiles, Birds. Clarendon Press, Oxford.

Bever, G. S., and W. G. Joyce. 2005. Dermochelyidae - Lederschildkröten; pp. 235-248 *in* U. Fritz (ed.), Handbuch der Reptilien und Amphibien Europas. Band 3/IIIB: Schildkröten (Testudines) II (Cheloniidae, Dermochelyidae, Fossile Schildkröten Europas). Aula-Verlag, Wiebelsheim.

Bloom, W., and D. W. Fawcett. 1994. A Textbook of Histology. 460 pp. Chapman & Hall, New York.

Blows, W. T. 1987. The armoured dinosaur *Polacanthus foxi* from the Lower Cretaceous of the Isle of Wight. Palaeontology 30:557-580.

Boda, A. 1927. *Clemmydopsis sopronensis* n. g. n. sp. aus der unteren pannonischen Stufe von Sopron in Ungarn. Centralblatt für Mineralogie, Geologie und Paläontologie, B 1927:375-383.

Bogačev, V. V. 1960. Nowaja pontičeskaja čerepacha iz Kryma [A new pontic turtle of the Crimea; Eine neue pontische Schildkröte von der Krim]. Voprosy geologii burenija i dobyči nefti 10:88-92. [in Russian]

Bojanus, L. H. 1819-1821. Anatome testudinis europaeae. Zawadzki, Vilna, Lithuania.

Bonnaterre, P. J. 1789. Tableau Encyclopédique et Méthodique des Trois Règnes de la Nature. Erpétologie. 72 pp. Panckoucke, Paris.

Boulenger, G. A. 1888a. On the characters of the chelonian families Pelomedusidae and Chelydidae. Annual Magazine of Natural History, Series 61:346–347.

Boulenger, G. A. 1888b. On the chelydoid chelonians of New Guinea. Annali del Museo Civico di Storia Naturale di Genova. 2 Ser. 6:449-452.

Bour, R. 1980. Position systématique de *Geoclemys palaeannamitica* Bourret, 1941 (Reptilia-Testudines-Emydidae). Amphibia-Reptilia 1:149-159.

Bourret, R. 1939. Notes herpetologiques sur l'Indochine Française, XVIII. Reptiles et batraciens reçus au Laboratoire des Science Naturelles de l'Université au cours de l'année 1939. Descriptions de quatre espèces et d'une variété nouvelles. Bulletin Général de l'Instruction Publique Indochine, Hanoi 1939:539.

Bramble, D. M. 1974. Emydid shell kinesis: biomechanics and evolution. Copeia 1974:707-727.

Bramble, D. M., and J. H. Hutchison. 1981. A reevaluation of plastral kinesis in African turtles of the genus *Pelusios*. Herpetologica 37:205-212.

Bramble, D. M., J. H. Hutchison, and J. M. Legler. 1984. Kinosternid shell kinesis: structure, function and evolution. Copeia 1984:456-475.

Bräm, H. 1965. Die Schildkröten aus dem oberen Jura (Malm) der Gegend von Solothurn. Schweizerische Paläontologische Abhandlungen 83:1-190.

Bräm, H. 1973. Chelonia from the Upper Jurassic of Guimarota mine (Portugal). Contribuição para o conhecimento da Fauna do Kimeridgiano da Mina de Lignito Guimarota (Leiria, Portugal) III. Parte, VII. - Memorias dos Servicos geológicos de Portugal, (nova Série) 22:135-141.

Brinkman, D. B. 2003a. A review of nonmarine turtles from the Late Cretaceous of Alberta. Canadian Journal of Earth Sciences 40:557-571.

Brinkman, D. B. 2003b. Anatomy and systematics of *Plesiobaena antiqua* (Testudines: Baenidae) from the mid-Campanian Judith River Group of Alberta, Canada. Journal of Vertebrate Paleontology 23:146-155.

Brinkman, D. B., and E. L. Nicholls. 1991. Anatomy and relationships of the turtle *Boremys pulchra* (Testudines: Baenidae). Journal of Vertebrate Paleontology 11:302-315.

Brinkman, D. B., and E. L. Nicholls. 1993. New specimen of *Basilemys praeclara* Hay and its bearing on the relationships of the Nanhsiungchelyidae (Reptilia: Testudines). Journal of Paleontology 67:1027-1031.

Brinkman, D. B., and J.-H. Peng. 1996. A new species of *Zangerlia* (Testudines: Nanhsiungchelyidae) from the Upper Cretaceous redbeds at Bayan Mandahu, Inner Mongolia, and the relationships of the genus. Canadian Journal of Earth Sciences 33:526-540.

Brinkman, D. B., and X.-C. Wu. 1999. The skull of *Ordosemys*, an Early Cretaceous turtle from Inner Mongolia, People's Republic of China, and the interrelationships of Eucryptodira (Chelonia, Cryptodira). Paludicola 2:134-147.

Brinkman, D. B., K. Stadtman, and D. Smith. 2000. New material of *Dinochelys whitei* Gaffney, 1979, from the Dry Mesa Quarry (Morrison Formation, Jurassic) of Colorado. Journal of Vertebrate Paleontology 20:269-274.

Brochu, C. A. 2001. Crocodylian snouts in space and time: phylogenetic approaches toward adaptive radiation. American Zoologist 41:564-585.

Broin, F. de 1977. Contribution à l'étude des chéloniens. Chéloniens continentaux du Crétacé et du Tertiaire de France. Mémoires du Muséum Nationale d'Histoire Naturelle C38:1-366.

Broin, F. de 1984. *Proganochelys ruchae* n. sp., chélonien du Trias supérieur de Thaïlande. Studia Geologica Salmanticensia Vol. especial 1 (Studia Palaeocheloniologica I):87-97.

Broin, F. de 1987. Lower vertebrates from the early-middle Eocene Kuldana Formation of Kohat (Pakistan): Chelonia. Contributions from the Museum of Paleontology, University of Michigan 27:169-185.

Brongersma, L. D. 1969. Miscellaneous notes on turtles, II A-B. Proceedings of the Koninklijke Nederlandse Akademie van Wetenschappen Serie C 72:76-102.

Brüllmann, B. 1999. Die Ontogenese der Costalia bei Pleurodira - Ein Beitrag zur Morphologie des Carapax und der Evolution der Schildkröten. Unpublished MSc-thesis, Faculty of Biology, Eberhard-Karls-University, Tübingen. 86 pp.

Buffrénil, V. de 1982. Morphogenesis of bone ornamentation in extant and extinct crocodilians. Zoomorphology 99:155-166.

Buffrénil, V. de, and D. Schoevaert. 1988. On how the periosteal bone of the delphinid humerus becomes cancellous: ontogeny of a histological specialization. Journal of Morphology 198:149-164.

Buffrénil, V. de, and J.-M. Mazin. 1990. Bone histology of the ichthyosaurs: comparative data and functional interpretation. Paleobiology 16:435-447.

Buffrénil, V. de, and J.-M. Mazin. 1992. Contribution de l'histologie osseuse à l'interprétation paléobiologique du genre *Placodus* Agassiz, 1833 (Reptilia, Placodontia). Revue de Paléobiologie 11:397–407.

Buffrénil, V. de, J. O. Farlow, and A. de Ricqlès. 1986. Growth and function of *Stegosaurus* plates: Evidence from bone histology. Paleobiology 12:459-473.

Buffrénil, V. de, J.-M. Mazin, and A. de Ricqlès. 1987. Caractères structuraux et mode de croissance du fémur d'*Omphalosaurus nisseri*, ichthyosaurien du Trias moyen de Spitzberg. Annales de Paléontologie (Vert.-Invert.) 73:195-216.

Burbidge, A. A., J. A. W. Kirsch, and A. R. Main. 1974. Relationships within the Chelidae (Testudines: Pleurodira) of Australia and New Guinea. Copeia 1974:392-409.

Burke, A. C. 1985. Morphogenesis of the chelonian carapace. American Zoologist 25:94A.

Burke, A. C. 1987. Experimental evidence for the embryonic origin of the chelonian plastron. American Zoologist 27:34A.

Burke, A. C. 1989a. Epithelial-mesenchymal interactions in the development of the chelonian bauplan. Fortschritte der Zoologie/Progress in Zoology 35:206-209.

Burke, A. C. 1989b. Development of the turtle carapace: implications for the evolution of a novel bauplan. Journal of Morphology 199:363-378.

Burke, A. C. 1991. The development and evolution of the turtle body plan: inferring intrinsic aspects of the evolutionary process from experimental embryology. American Zoologist 31:616-627.

Caldwell, M. W., and M. S. Y. Lee. 2001. Live birth in Cretaceous marine lizards (mosasaurids). Proceedings of the Royal Society of London, Series B 268:2397-2401.

Cantor, T. 1842. General features of Chusan, with remarks on the flora and fauna of that island. The Annals and Magazine of Natural History, Zoology, Botany and Geology 11:481-493.

Carr, A. F. J. 1938. A new subspecies of *Pseudemys floridana*, with notes on the *floridana* complex. Copeia 1938:105-109.

Carroll, R. L. 1988. Vertebrate Paleontology and Evolution. 698 pp. W. H. Freeman and Company, New York.

Carroll, R. L. 1993. Paläontologie und Evolution der Wirbeltiere. 684 pp. Georg Thieme Verlag, Stuttgart.

Carus, C. G. 1828. Von den Urtheilen des Knochen- und Schalengerüstes, Leipzig.

Case, E. C. 1935. Description of a collection of associated skeletons of *Trimerorhachis*. Contributions of the Museum of Paleontology, University of Michigan 4:227-274.

Castanet, J. 1981. Nouvelles données sur les lignes cimentantes de l'os. Archives Biologiques 92:1-24.

Castanet, J. 1987. La squelettochronologie chez les reptiles III - application. Annales des Sciences Naturelles, Zoologie, Paris [13^{e} Série] 8:157-172.

Castanet, J. 1988. Les méthodes d´estimation de l´age chez les chéloniens. Mésogée 48:21-28.

Castanet, J., and M. Cheylan. 1979. Les marques de croissance de l'age chez *Testudo hermanni* et *Testudo graeca* (Reptilia, Chelonia, Testudinidae). Canadian Journal of Zoology 57:1649-1665.

Castanet, J., H. Francillon-Vieillot, F. J. Meunier, and A. de Ricqlès. 1993. Bone and individual aging; pp. 245-283 *in* B. K. Hall (ed.), Bone Volume 7: Bone Growth - B. CRC Press, Boca Raton.

Castant, J. 1985. La squelettochronologie chez les reptiles II. Resultats experimentaux sur la signification des marques de croissance squelettiques chez les lezards et les tortues. Annales des Sciences Naturelles, Zoologie 13e Serie 7:23-40.

Cebra-Thomas, J., F. Tan, S. Sistla, E. Estes, G. Bender, C. Kim, P. Riccio, and S. F. Gilbert. 2005. How the turtle forms its shell: a paracrine hypothesis of carapace formation. Journal of Experimental Zoology (Mol Dev Evol) 304B:558-569.

Cervelli, M., M. Oliverio, A. Bellini, M. Bologna, F. Cecconi, and P. Mariottini. 2003. Structural and sequence evolution of U17 small nucleolar RNA (snoRNA) and its phylogenetic congruence in chelonians. Journal of Molecular Evolution 57:73-84.

Cherepanov, G. O. 1984. On the nature of the plastron anterior elements in turtles [in Russian]. Zoologichezky Zhurnal 63:1529-1534.

Cherepanov, G. O. 1997. The origin of the bony shell of turtles as a unique evolutionary model in reptiles. Russian Journal of Herpetology 4:155-162.

Chkhikvadze, V. M. 1983. Iskopajemyje čerepachi Kawkaza i Sewernogo Pričernomorja [Fossil turtles from the Caucasus and the northern part of the Black Sea; Fossile Schildkröten aus dem Kaukasus und dem Norden des Schwarzen Meeres]. 149 pp. Tiflis (Meznіereba). [in Russian]

Chkhikvadze, V. M. 1990. Paleogenowyje cerepachi SSSR [Paleogene turtles of the USSR; Neogene Schildkröten der UdSSR]. 96 pp. Tiflis (Meznіereba). [in Russian]

Clark, J. 1932. A new anosteirid from the Uinta Eocene. Annals of the Carnegie Museum 21:161-170.

Claude, J., and H. Tong. 2004. Early Eocene testudinoid turtles from Saint-Papoul, France, with comments on the early evolution of modern Testudinoidea. Oryctos 5:3-45.

Colbert, E. H. 1955. Scales in the Permian amphibian *Trimerorhachis*. American Museum Novitates 1740:1-17.

Coles, W. C., J. A. Musick, and L. A. Williamson. 2001. Skeletochronology validation from a long-term recaptured adult loggerhead (*Caretta caretta*). Copeia 1:240-242.

Cope, E. D. 1868. On some Cretaceous Reptilia. Proceedings of the Academy of Natural Sciences of Philadelphia 1868:233-242.

Cope, E. D. 1869. The fossil reptiles of New Jersey. American Naturalist 3:84-91.

Cope, E. D. 1870a [1869]. Seventh contribution to the herpetology of tropical America. Proceedings of the American Philosophical Society 11:147-169.

Cope, E. D. 1870b. On the Adocidae. Proceedings of the American Philosophical Society 11:547-553.

Cope, E. D. 1871. Supplement to the "Synopsis of the extinct Batrachia and Reptilia of North America." Proceedings of the American Philosophical Society 12:41-52.

Cope, E. D. 1872a. Second account of new vertebrata from the Bridger Eocene of Wyoming Territory. Proceedings of the American Philosophical Society 12:466-468. [*Hadrianus* Cope, 1872]

Cope, E. D. 1872b [1871]. On a new genus of Pleurodira from the Eocene of Wyoming. Proceedings of the American Philosophical Society 12:472-477. [*Notomorpha garmanii*; *Baptemys garmani*: Hutchison, 1998; *Baptemys garmanii*: Holroyd et al., 2001]

Cope, E. D. 1877. On reptilian remains from the Dakota beds of Colorado. Proceedings of the American Philosophical Society 17:193-196. [*Glyptops plicatulus* (Cope)]

Cope, E. D. 1896. Sixth contribution to the knowledge of the marine Miocene fauna of North America. Proceedings of the American Philosophical Society 35:139-146.

Crother, B. I. (ed.). 2000 (2001). Scientific and Standard English Names of Amphibians and Reptiles of North America North of Mexico, with Comments Regarding Confidence in Our Understanding. SSAR Herpetological Circular 29. iii + 82 pp.

Crumly, C. R. 1984. A hypothesis for the relationship of land tortoise genera (family Testudinidae). Studia Geologica Salmanticensia Vol. especial 1 (Studia Palaeocheloniologica I):115-124.

Danilov, I. G. 2005. Die fossilen Schildkröten Europas; pp. 329-441 *in* U. Fritz (ed.), Handbuch der Reptilien und Amphibien Europas. Band 3/IIIB: Schildkröten (Testudines) II. Aula-Verlag, Wiebelsheim.

Danilov, I. G., and V. B. Sukhanov. 2006. A basal eucryptodiran turtle "*Sinemys*" *efremovi* (= *Wuguia efremovi*) from the Early Cretaceous of China. Acta Palaeontologica Polonica 51:105-110.

Danilov, I., and J. F. Parham. 2005. A reassessment of the referral of an isolated skull from the Late Cretaceous of Uzbekistan to the stem-testudinoid turtle genus *Lindholmemys*. Journal of Vertebrate Paleontology 25:784-791.

Danilov, I., and J. F. Parham. 2006. A redescription of '*Plesiochelys*' *tatsuensis* from the Late Jurassic of China, with comments on the antiquity of the crown clade Cryptodira. Journal of Vertebrate Paleontology 26:573-580.

deBraga, M., and O. Rieppel. 1997. Reptile phylogeny and the interrelationships of turtles. Zoological Journal of the Linnean Society 120:281-354.

Deraniyagala, P. E. P. 1930. Testudinate evolution. Proceedings of the Zoological Society 68:1057-1070.

Dollo, L. 1884. Premiere note sur les cheloniens de Bernissart. Bulletin du Musée Royal d'Histoire Naturelle de Belgique / Mededelingen van het Koninklijk Natuurhistorisch Museum van België 3:64-79.

Duméril, A. M. C. 1856. Note sur les reptiles du Gabon. Revue et Magasin de Zoologie Pure et Appliquée (2. Série) 8:369-377.

Duméril, A. M. C., and G. Bibron. 1835. Erpétologie Générale ou Histoire Naturelle Complète des Reptiles. Vol. 2. 680 pp. Librairie Encyclopédique de Roret, Paris.

Engstrom, T. N., B. S. Shaffer, and W. P. McCord. 2004. Multiple data sets, high homoplasy, and the phylogeny of softshell turtles (Testudines: Trionychidae). Systematic Biology 53:693-710.

Enlow, D. H., and S. O. Brown. 1956. A comparative histological study of fossil and recent bone tissues. Part I. The Texas Journal of Science 9:405-443.

Enlow, D. H., and S. O. Brown. 1957. A comparative histological study of fossil and recent bone tissues. Part II. The Texas Journal of Science 9:186-214.

Enlow, D. H., and S. O. Brown. 1958. A comparative histological study of fossil and recent bone tissues. Part III. The Texas Journal of Science 10:187-230.

Ernst, C. H., and R. W. Barbour. 1989. Turtles of the World. 313 pp. Smithonian Institution Press, Washington D. C.

Ernst C. H., R. G. M. Altenburg, and R. W. Barbour. 2006. Turtles of the World. [http://nlbif.eti.uva.nl/bis/turtles.php]

Eschscholtz, J. F. 1829. Zoologischer Atlas enthaltend Abbildungen und Beschreibungen neuer Thierarten, während des Flottcapitains von Kotzebue zweiter Reise um die Welt, auf der Russisch-Kaiserlichen Kriegsschlupp Predpriaetië in den Jahren 1823-1826, Part 1. 16 pp. G. Reimer, Berlin.

Esteban, M. 1990. Environmental influences on the skeletochronological record among recent and fossil frogs. Annales des Sciences Naturelles, Zoologie 11:201-204.

Estes, R., and J. H. Hutchison. 1980. Eocene lower vertebrates from Ellesmere Island, Canadian Arctic Archipelago. Palaeogeography, Palaeoclimatology, Palaeoecology 30:325-347.

Evans, J., and T. S. Kemp. 1975. The cranial morphology of a new Lower Cretaceous turtle from southern England. Palaeontology 18:25-40.

Evans, S. E., and A. R. Milner. 1994. Middle Jurassic microvertebrate assemblages from the British Isles; pp. 303-321 *in* N. C. Fraser, and H.-D. Sues (eds.), In the Shadow of the Dinosaurs: Early Mesozoic Tetrapods. Cambridge University Press, Cambridge.

Ewert, M. A. 1985. Embryology of turtles; pp. 75-268 *in* C. Gans, F. Billet, and P. F. A. Maderson (eds.), Biology of the Reptilia. Volume 14 - Development A. John Wiley & Sons, New York.

Fang, J., and B. K. Hall. 1997. Chondrogenic cell differentiation from membrane bone periostea. Anatomy and Embryology 196:349-362.

Farlow, J. O., C. V. Thomson, and D. E. Rosner. 1976. Plates of the dinosaur *Stegosaurus*: Forced convection heat loss fins? Science 192:1123-1125.

Feldman, C. R., and J. F. Parham. 2004. Molecular systematics of Old World stripe-necked turtles (Testudines: *Mauremys*). Asiatic Herpetological Research 10:28-37.

Forskål, P. 1775. Descriptiones animalium avium, amphibiorum, piscium, insectorum, vermium; quae in itinere orientali observavit. 164 pp. Möllerus, Haunia.

Fraas, E. 1896. Die schwäbischen Trias-Saurier nach dem Matrial der Kgl. Naturalien-Sammlung in Stuttgart zusammengestellt. Mitteilungen aus dem Königlichen Naturalien-Kabinett zu Stuttgart 5:1-18.

Fraas, E. 1913. *Proterochersis*, eine pleurodire Schildkröte aus dem Keuper. Jahreshefte des Vereins für vaterländische Naturkunde in Württemberg 80:1-30.

Francillon-Vieillot, H., V. de Buffrénil, J. Castanet, J. Géraudie, F. J. Meunier, J. Y. Sire, L. Zylberberg, and A. de Ricqlès. 1990. Microstructure and mineralization of vertebrate skeletal tissues; pp. 471-530 *in* J. G. Carter (ed.), Skeletal Biomineralization: Patterns, Processes and Evolutionary Trends. Van Nostrand Reinhold, New York.

Frazier, J., D. Gramerntz, and U. Fritz. 2005. *Dermochelys* Blainville, 1816 - Lederschildkröten; pp. 249-328 *in* U. Fritz (ed.), Handbuch der Reptilien und Amphibien Europas. Band 3/IIIB: Schildkröten (Testudines) II. Aula-Verlag, Wiebelsheim.

Fritz, U. 2003. Die Europäische Sumpfschildkröte (Zeitschrift für Feldherpetologie - Supplement 1). 224 pp. Laurenti, Bielefeld.

Fritz, U. 2005. Handbuch der Reptilien und Amphibien Europas. Band 3/IIIB: Schildkröten (Testudines) II. 448 pp. Aula-Verlag, Wiebelsheim.

Frye, F. L. 1991. Reptile Care, an Atlas of Diseases and Treatments (Vol. 1&2). 637 pp. T.F.H. Publications, Neptune City.

Fuente, M. de la, F. de Lapparent de Broin, and T. Manera de Bianco. 2001. The oldest and first nearly complete skeleton of a chelid, of the *Hydromedusa* sub-group (Chelidae, Pleurodira), from the Upper Cretaceous of Patagonia. Bulletin de la Société Géologique de France 2:237-244.

Fuente, M. de la. 2003. Two new pleurodiran turtles from the Portezuelo Formation (Upper Cretaceous) of Northern Patagonia, Argentina. Journal of Paleontology 77:559-575.

Fujita, M. K., T. N. Engstrom, D. E. Starkey, and B. S. Shaffer. 2004. Turtle phylogeny: insights from a novel nuclear intron. Molecular Phylogenetics and Evolution 31:1031-1040.

Gaffney, E. S. 1972. The systematics of the North American family Baenidae (Reptilia, Cryptodira). Bulletin of the American Museum of Natural History 147:243-312.

Gaffney, E. S. 1975a. *Solnhofia parsonsi*, a new cryptodiran turtle from the late Jurassic of Europe. American Museum Novitates 2576:1-25.

Gaffney, E. S. 1975b. A taxonomic revision of the Jurassic turtles *Portlandemys* and *Plesiochelys*. American Museum Novitates 2574:1-19.

Gaffney, E. S. 1975c. A phylogeny and classification of the higher categories of turtles. Bulletin of the American Museum of Natural History 155:387-436.

Gaffney, E. S. 1975d. A revision of the side-necked turtle *Taphrosphys sulcatus* (Leidy) from the Cretaceous of New Jersey. American Museum Novitates 2571:1-24.

Gaffney, E. S. 1977. The side-necked turtle family Chelidae: a theory of relationships using shared derived characters. American Museum Novitates 2620:1-28.

Gaffney, E. S. 1979a. Fossil chelid turtles of Australia. American Museum Novitates 2681:1-23.

Gaffney, E. S. 1979b. The Jurassic turtles of North America. Bulletin of the American Museum of Natural History 162:93-135.

Gaffney, E. S. 1981. A review of the fossil turtles of Australia. American Museum Novitates 2720:1-38.

Gaffney, E. S. 1990. The comparative osteology of the Triassic turtle *Proganochelys*. Bulletin of the American Museum of Natural History 194:1-263.

Gaffney, E. S. 1996. The postcranial morphology of *Meiolania platyceps* and a review of the Meiolaniidae. Bulletin of the American Museum of Natural History 229:1-166.

Gaffney, E. S., and C. A. Forster. 2003. Side-necked turtle lower jaws (Podocnemididae, Bothremydidae) from the Late Cretaceous Maevarano Formation of Madagascar. American Museum Novitates 3397:1-13.

Gaffney, E. S., and J. W. Kitching. 1995. The morphology and relationships of *Australochelys*, an Early Jurassic turtle from South Africa. American Museum Novitates 3130:1-29.

Gaffney, E. S., and P. A. Meylan. 1988. A phylogeny of turtles; pp. 157-219 *in* M. J. Benton (ed.), The Phylogeny and Classification of the Tetrapods. Volume 1: Amphibians, Reptiles, Birds. Clarendon Press, Oxford.

Gaffney, E. S., and R. C. Wood. 2002. *Bairdemys*, a new side-necked turtle (Pelomedusoides: Podocnemididae) from the Miocene of the Caribbean. American Museum Novitates 3359:1-28.

Gaffney, E. S., and R. Zangerl. 1968. A revision of chelonian genus *Bothremys* (Pleurodira: Pelomedusidae). Fieldiana Geology 16:193-239.

Gaffney, E. S., J. H. Hutchison, F. A. Jenkins Jr., and L. J. Meeker. 1987. Modern turtle origins: the oldest known cryptodire. Science 237:289-291.

Gaffney, E. S., K. E. Campbell, and R. C. Wood. 1998a. Pelomedusoid side-necked turtles from late Miocene sediments in southwestern Amazonia. American Museum Novitates 3245:1-11.

Gaffney, E. S., L. Kool, D. B. Brinkman, T. H. Rich, and P. Vickers-Rich. 1998b. *Otwayemys*, a new cryptodiran turtle from the early Cretaceous of Australia. American Museum Novitates 3233:1-28.

Gaffney, E. S., M. Archer, and A. White. 1989. Chelid turtles from the Miocene freshwater limestones of Riversleigh Station, Northwestern Queensland, Australia. American Museum Novitates 2959:1-10.

Gardner, J. D., A. P. Russell, and D. B. Brinkman. 1995. Systematics and taxonomy of soft-shelled turtles (family Trionychidae) from the Judith River Group (mid-Campanian) of North America. Canadian Journal of Earth Sciences 32:631-643.

Gardner, J. D., and A. P. Russell. 1994. Carapacial variation among soft-shelled turtles (Testudines: Trionychidae) and its relevance to taxonomic and systematic studies of fossil taxa. Neues Jahrbuch der Geologie und Paläontologie, Abhandlungen 193:209-244.

Garman, S. 1880. On certain species of Chelonioidae. Bulletin of the Museum of Comparative Zoology 6:123-126.

Gasparini, Z., D. Pol, and L. A. Spalletti. 2006. An unusual marine crocodyliform from the Jurassic-Cretaceous boundary of Patagonia. Science 311:70-73.

Gassner, T. 2000. The turtles from the Guimarota mine; pp. 55-58 *in* T. Martin, and B. Krebs (eds.), Guimarota - A Jurassic Ecosystem. Verlag Dr. Friedrich Pfeil, München.

Geoffroy-Saint-Hillaire, E. 1809. Mémoire sur les tortues molles, nouveau genre sous le nom de *Trionyx*, et sur la formation des carapaces. Annales du Musée d'Histoire Naturelle de Paris 14:1-20.

Geoffroy-Saint-Hillaire, E. 1809. Mémoire sur les tortues molles, nouveau genre sous le nom de *Trionyx*, et sur la formation des carapaces. Annales du Musée d'Histoire Naturelle de Paris 14:1-20.

Georges, A., J. Birrell, K. M. Saint, W. McCord, and S. C. Donnellan. 1998. A phylogeny for side-necked turtles (Chelonia: Pleurodira) based on mitochondrial and nuclear gene sequence variation. Biological Journal of the Linnean Society 67:213-246.

Gilbert, S. F., G. A. Loredo, A. Brukman, and A. C. Burke. 2001. Morphogenesis of the turtle shell: the development of a novel structure in tetrapod evolution. Evolution & Development 3:47-58.

Gillham, C. 1994. A fossil turtle (Reptilia: Chelonia) from the Middle Jurassic of Oxfordshire, England. Neues Jahrbuch der Geologie und Paläontologie. Monatshefte 10:581-596.

Gilmore, C. W. 1919. New fossil turtles, with notes on two described species. Proceedings of the United States National Museum 56:113-132.

Gilmore, C. W. 1923. A new species of *Aspideretes* from the Belly River Cretaceous of Alberta, Canada. Transactions of the Royal Society of Canada, Section 4, Series 3. 17:1-10.

Giraud, M. M., J. Castanet, F. J. Meunier, and Y. Bouligand. 1978. The fibrous structure of coelacanth scales: a twisted 'plywood'. Tissue & Cell 10:671-686.

Girgis, S. 1961. Aquatic respiration in the common Nile turtle *Trionyx triunguis* (Forskål). Comparative Biochemistry and Physiology C 3:206-217.

Godley, B. J., A. C. Broderick, R. Frauenstein, F. Glen, and G. C. Hays. 2002. Reproductive seasonality and sexual dimorphism in green turtles. Marine Ecology Progress Series 226:125-133.

Goette, A. 1899. Über die Entwicklung des knöchernen Rückenschildes (Carapax) der Schildkröten. Zeitschrift für Wissenschaftliche Zoologie 76:407-434.

Gordos, M. A., C. E. Franklin, C. J. Limpus, and G. Wilson. 2004. Blood-respiratory and acid–base changes during extended diving in the bimodally respiring freshwater turtle *Rheodytes leukops*. Journal of Comparative Physiology B 174:347-354.

Gray, J. E. 1831a. Synopsis Reptilium or Short Descriptions of the Species of Reptiles, Pt. 1, Cataphracta. Tortoises, Crocodiles, Enaliosaurians. 85 pp. Treuttel, Wurtz & Co., London.

Gray, J. E. 1831b. Characters of a new genus of freshwater tortoise from China. Proceedings of the Zoological Society of London 1831:106-107.

Gray, J. E. 1834. Characters of several new species of freshwater tortoises (*Emys*) from India and China. Proceedings of the Zoological Society of London 1834:53-54.

Gray, J. E. 1847. Description of a new genus of Emydidae. Proceedings of the Zoological Society of London 1847:55-56.

Gray, J. E. 1852. Descriptions of a new genus and some new species of tortoises. Proceedings of the Zoological Society of London 1852:133-135.

Gray, J. E. 1855. Catalogue of Shield Reptiles in the Collection of the British Museum, Pt. 1, Testudinata (Tortoises). 79 pp. Taylor and Francis, London.

Gray, J. E. 1863. Observations on the box tortoises, with the descriptions of three new Asiatic species. Proceedings of the Zoological Society of London 1863:173-179.

Gray, J. E. 1869. Notes on the families and genera of tortoises (Testudinata), and on the characters afforded by the study of their skulls. Proceedings of the Zoological Society of London 1869:165-225.

Gray, J. E. 1870. Supplement to the Catalogue Collection of the British Museum, Pt. 1, Testudinata. 120 pp. Taylor and Francis, London.

Greenbaum, E. 2002. A standardized series of embryonic stages for the emydid turtle *Trachemys scripta*. Canadian Journal of Zoology 80:1350-1370.

Gregory, W. K. 1946. Pareiasaurs versus placodonts as near ancestors to the turtles. Bulletin of the American Museum of Natural History 86:275-326.

Gross, M. 2004. Sumpfschildkröten (*Clemmydopsis turnauensis* (MEYER, 1847); Bataguridae) aus der Tongrube Mataschen (Pannonium, Steiermark). Joannea - Geologie und Paläontologie 5:131-147.

Gross, W. 1934. Die Typen des mikroskopischen Knochenbaues bei fossilen Stegocephalen und Reptilien. Zeitschrift für Anatomie und Entwicklungsgeschichte 203:731-764.

Haiduk, M. W., and J. W. Bickham. 1982. Chromosomal homologies and evolution of testudinoid turtles with emphasis on the systematic placement of *Platysternon*. Copeia 1982:60-66.

Hailey, A., and M. R. K. Lambert. 2002. Comparative growth patterns in Afrotropical giant tortoises (Reptilia Testudinidae). Tropical Zoology 15:121-139.

Haines, R. W., and A. Mohuiddin. 1968. Metaplastic bone. Journal of Anatomy 103:527-538.

Hall, B. K. 2005. Bones and Cartilage. Developmental and Evolutionary Skeletal Biology. 760 pp. Elsevier Academic Press, Amsterdam.

Halstaed, L. B. 1974. Vertebrate Hard Tissues. 179 pp. Wykeham Publications Ltd, London.

Harrassowitz, H. L. F. 1922. Die Schildkrötengattung *Anosteira* von Messel bei Darmstadt und ihre stammesgeschichtliche Bedeutung. Abhandlungen der Hessischen Geologischen Landesanstalt zu Darmstadt 6:133-239.

Haughton, S. H., and Boonstra L. D., 1929. Pareiasaurian studies. Part I. An attempt at a classification of the Pareiasauria based on skull features: Annals of the South African Museum 28:79-87.

Havers, C. 1691. Osteologia nova, or, some new observations of the bones and the parts belonging to them, with the manner of their accretion, and nutrition, communicated to the Royal Society in several discourses. 294pp. Samuel Smith, London.

Hay, O. P. 1898. On *Protostega*, the systematic position of *Dermochelys*, and the morphogeny of the chelonian carapace and plastron. American Naturalist 32:929-948.

Hay, O. P. 1902. Description of two species of extinct tortoises, one new. Proceedings of the Academy of Natural Sciences of Philadelphia 54:383-388. [*Basilemys*]

Hay, O. P. 1904. On some fossil turtles belonging to the Marsh collection in Yale University Museum. American Journal of Science, Ser. 4 18:261-276. [*Hadrianus majusculus*]

Hay, O. P. 1905. A revision of the species of the family of fossil turtles called Toxochelyidae, with descriptions of two new species of *Toxochelys* and a new species of *Porthochelys*. Bulletin of the American Museum of Natural History 21:177-185. [*Ctenochelys stenoporus* (Hay)]

Hay, O. P. 1906. Descriptions of two new genera (*Echmatemys* and *Xenochelys*) and two new species (*Xenochelys formosa* and *Terrapene putnami*) of fossil turtles. Bulletin of the American Museum of Natural History 22:27-31.

Hay, O. P. 1907. Descriptions of seven new species of turtles from the Tertiary of the United States. Bulletin of the American Museum of Natural History 23:847-863.

Hay, O. P. 1908. The fossil turtles of North America. Carnegie Institute Publications Washington 75:1-568.

Hay, O. P. 1922. On the phylogeny of the shell of the Testudinata and the relationships of *Dermochelys*. Journal of Morphology 36:421-445.

Hay, O. P. 1928. Further consideration of the shell of *Chelys* and of the constitution of the armor of turtles in general. Proceedings of the United States National Museum 73:1-12.

Hayashi, S., and K. Carpenter. 2006. Osteoderm histology of *Stegosaurus stenops* (Ornithischia: Thyreophora): implications for plate and spike growth. Journal of Vertebrate Paleontology 26 (Supplement to No. 3):73A.

Hays, G. C., S. Akesson, A. C. Broderick, F. Glen, B. J. Godley, F. Papi, and P. Luschi. 2003. Island-finding ability of marine turtles. Proceedings of the Royal Society of London. Series B - Biological Sciences (Supplement) 270:S5-S7.

Hedges, S. B., and L. L. Poling. 1999. A molecular phylogeny of reptiles. Science 283:998-1001.

Hellrung, H. 2003. *Gerrothorax pustuloglomeratus*, ein Temnospondyle (Amphibia) mit knöcherner Branchialkammer aus dem Unteren Keuper von Kupferzell (Süddeutschland). Stuttgarter Beiträge zur Naturkunde, Ser. B 330:1-130.

Hervet, S. 2003. Le groupe "*Palaeochelys sensu lato - Mauremys*" dans le contexte systématique des Testudinoidea aquatiques du Tertiaire d'Europe occidentale. Apports à la biostratigraphie et à la paleobiogeographie: PhD-thesis, Museum National d'Histoire Naturelle, Paris, 406 pp.

Hervet, S. 2004a. Systématique du groupe « *Palaeochelys sensu lato – Mauremys* » (Chelonii, Testudinoidea) du Tertiaire d'Europe occidentale: principaux résultats / Systematic of the "*Palaeochelys sensu lato – Mauremys*" group (Chelonii, Testudinoidea) from the Tertiary of Western Europe: principal results. Annales de Paléontologie 90:13-78.

Hervet, S. 2004b. A new genus of 'Ptychogasteridae' (Chelonii, Testudinoidea) from the Geiseltal (Lutetian of Germany). Comptes Rendues Palevol 3:125-132.

Hill, R. V. 2005. Integration of morphological data sets for phylogenetic analysis of Amniota: the importance of integumentary characters and increased taxonomic sampling. Systematic Biology 54:530-547.

Hill, R. V. 2006. Comparative anatomy and histology of xenarthran osteoderms. Journal of Morphology 267:1441-1460.

Hill, R. V., and S. G. Lucas. 2006. New data on the anatomy and relationships of the Paleocene crocodylian *Akanthosuchus langstoni*. Acta Palaeontologica Polonica 51:455-464.

Hirayama, R. 1984. Cladistic analysis of batagurine turtles (Batagurinae: Emididae: Testudinoidea); preliminary results. Studia Geologica Salmanticensia Vol. especial 1 (Studia Palaeocheloniologica I):140–157.

Hirayama, R. 1997. Distribution and diversity of Cretaceous chelonioids; pp. 225-241 *in* J. M. Callaway, and E. L. Nicholls (eds.), Ancient Marine Reptiles. Academic Press, San Diego, California.

Hirayama, R. 1998. Oldest known sea turtle. Nature 392:705-708.

Hirayama, R., and T. Chitoku. 1996. Family Dermochelyidae (superfamily Chelonioidea) from the Upper Cretaceous of North Japan. Transactions and proceedings of the Palaeontological Society of Japan, New Series 184:597-622.

Hirayama, R., D. B. Brinkman, and I. G. Danilov. 2000. Distribution and biogeography of non-marine Cretaceous turtles. Russian Journal of Herpetology 7:181-198.

Hirayama, R., S. Kazuhiko, C. Tsutomu, K. Gentaro, and K. Norio. 2001. *Anomalochelys angulata*, an unusual land turtle of family Nanhsiungchelyidae (superfamily Trionychoidea; order Testudines) from the Upper Cretaceous of Hokkaido, North Japan. Russian Journal of Herpetology 8:127-138.

Hoffmann, C. K. 1878. Beiträge zur vergleichenden Anatomie der Wirbelthiere. Niederländisches Archiv für Zoologie 4:112-248.

Hoffmann, C. K. 1890. Bronn's Klassen und Ordnungen des Thier-Reichs, wissenschaftlich dargestellt in Wort und Bild. Bd. 6, Abt. III Reptilien. I. Schildkröten. 442 pp. Winter'sche Verlagsbuchhandlung, Leipzig.

Holmes, R. B. 2000. Chapter 7: Palaeozoic temnospondyls; pp. 1081-1120 *in* H. Heatwole, and R. L. Carroll (eds.), Amphibian Biology. Volume 4: Palaeontology – The Evolutionary History of Amphibians. Surrey Beatty & Sons, Chipping Norton.

Holroyd, P. A., and J. H. Hutchison. 2002. Patterns of geographic variation in the latest Cretaceous vertebrates: evidence from the turtle component. Geological Society of America Special Paper 361:177-190.

Holroyd, P. A., J. H. Hutchison, and S. G. Strait. 2001. Turtle diversity and abundance through the lower Eocene Willwood Formation of the southern Bighorn Basin. University of Michigan Papers on Paleontology 33:97-107.

Honda, M., Y. Yasukawa, R. Hirayama, and H. Ota. 2002. Phylogenetic relationships of the Asian box turtles of the genus *Cuora sensu lato* (Reptilia: Bataguridae) inferred from mitochondrial DNA sequences. Zoological Science 19:1305-1312.

Hooks III, G. E. 1998. Systematic revision of the Protostegidae, with a redescription of *Calcarichelys gemma* Zangerl, 1953. Journal of Vertebrate Paleontology 18:85-98.

Hua, S., and V. de Buffrénil. 1996. Bone histology as a clue in the interpretation of functional adaptations in the Thalattosuchia (Reptilia, Crocodylia). Journal of Vertebrate Paleontology 16:703-717.

Huene, F. von. 1922. Beitrage zur Kenntnis der Organisation einiger Stegocephalen der Schwabischen Trias. Acta Zoologica Cracoviensia 3:395-460.

Humphrey, J. D., and S. L. Delange. 2004. An Introduction to Biomechanics: Solids and Fluids, Analysis and Design. 631 pp. Springer Verlag, Heidelberg.

Hungerbühler, A. 2002. The Late Triassic phytosaur *Mystriosuchus westphali*, with a revision of the genus. Palaeontology 45:377-418.

Hutchison, J. H. 1980. Turtle stratigraphy of the Willwood Formation, Wyoming: preliminary results. Papers on Paleontology, the Museum of Paleontology, University of Michigan 24:115-118.

Hutchison, J. H. 1987. New cranial material of *Compsemys* (Testudines) and its systematic implications. Journal of Vertebrate Paleontology 7 (Supplement to No. 3):19A.

Hutchison, J. H. 1991. Early Kinosterninae (Reptilia: Testudines) and their phylogenetic significance. Journal of Vertebrate Paleontology 11:145-167.

Hutchison, J. H. 1998. Turtles across the Paleocene/Eocene epoch boundary in west-central North America; pp. 401-408 *in* M.-P. Aubry, S. G. Lucas, and W. A. Berggren (eds.), Late Paleocene-Early Eocene Climatic and Biotic Events in the Marine and Terrestrial Records. Princeton University Press, Princeton.

Hutchison, J. H. 2000. Diversity of Cretaceous turtle faunas of Eastern Asia and their contribution to the turtle faunas of North America. Paleontological Society of Korea, Special Publication 4:27-38.

Hutchison, J. H., and D. M. Bramble. 1981. Homology of the plastral scales of the Kinosternidae and related turtles. Herpetologica 37:73-85.

Hutchison, J. H., and F. L. Frye. 2001. Evidence of pathology in early Cenozoic turtles. PaleoBios 21:12-19.

Hutchison, J. H., and J. D. Archibald. 1986. Diversity of turtles across the Cretaceous/Tertiary boundary in northeastern Montana. Palaeogeography, Palaeoclimatology, Palaeoecology 55:1-22.

Hutchison, J. H., and P. A. Holroyd. 2003. Late Cretaceous and early Paleocene turtles of the Denver Basin, Colorado. Rocky Mountain Geology 38:121-142.

Hutchison, J. H., P. A. Holroyd, and R. L. Ciochon. 2004. A preliminary report on Southeast Asia's oldest Cenozoic turtle fauna from the late middle Eocene Pondaung Formation, Myanmar. Asiatic Herpetological Research 10:38-52.

Hutton, J. M. 1986. Age determination of living Nile crocodiles from the cortical stratification of bone. Copeia 1986(2):332-341.

Iverson, J. B. 1992. A Revised Checklist with Distribution Maps of the Turtles of the World. 363 pp. Privately published, Richmond, IN.

Iwabe, N., Y. Hara, Y. Kumazawa, K. Shibamoto, Y. Saito, T. Miyata, and K. Katoh. 2004. Sister group relationship of turtles to the bird-crocodilian clade revealed by nuclear DNA–coded proteins. Molecular Biology and Evolution 22:810-813.

Jackson, D. R. 1988. A re-examination of fossil turtles of the genus *Trachemys* (Testudines: Emydidae). Herpetologica 44:317-325.

Jaeger, G. F. 1828. Über die fossile Reptilien, welche in Württemberg aufgefunden worden sind. 48 pp. J. B. Metzler, Stuttgart.

Jalil, N.-E., and P. Janvier. 2005. Les pareiasaures (Amniota, Parareptilia) du Permien supérieur du Bassin d'Argana, Maroc. Geodiversitas 27:35-132.

Janke, A., D. Erpenbeck, M. Nilsson, and U. Arnason. 2001. The mitochondrial genomes of the iguana (*Iguana iguana*) and the caiman (*Caiman crocodylus*): implications for amniote phylogeny. Proceedings of the Royal Society of London. Series B 268:623-631.

Jenkins Jr., F. A., N. H. Shubin, W. W. Amaral, S. M. Gatesy, C. R. Schaff, L. B. Clemmensen, W. R. Downs, A. R. Davidson, N. Bonde, and F. Osbaeck. 1994. Late Triassic continental vertebrates and depositional environments of the Fleming Fjord Formation, Jameson Island, East Greenland. Meddelelser om Grønland, Geoscience 32:1-25.

Joyce, W. G. 2000. The first complete skeleton of *Solnhofia parsonsi* (Cryptodira, Eurysternidae) from the Upper Jurassic of Germany and its taxonomic implications. Journal of Paleontology 74:684-700.

Joyce, W. G. 2003. A new Late Jurassic turtle specimen and the taxonomy of *Pelomedusa testa* and *Eurysternum wagleri*. PaleoBios 23:1-8.

Joyce, W. G. 2004. A phylogeny of turtles and the age of the turtle crown. Journal of Vertebrate Paleontology 24 (Supplement to Number 3):77A.

Joyce, W. G. 2005. Phylogeny and ecology of basal turtles. Journal of Vertebrate Paleontology 25 (Supplement to Number 3):76A.

Joyce, W. G. 2007. Phylogenetic relationships of Mesozoic turtles. Bulletin of the Peabody Museum of Natural History 48:3-102.

Joyce, W. G., and C. J. Bell. 2004. A review of the comparative morphology of extant testudinoid turtles (Reptilia: Testudines). Asiatic Herpetological Research 10:53-109.

Joyce, W. G., and G. S. Bever. 2005. Cheloniidae - Seeschildkröten; pp. 13-24 *in* U. Fritz (ed.), Handbuch der Reptilien und Amphibien Europas. Band 3/IIIB: Schildkröten (Testudines) II (Cheloniidae, Dermochelyidae, Fossile Schildkröten Europas). Aula-Verlag, Wiebelsheim.

Joyce, W. G., and M. A. Norell. 2005. *Zangerlia ukhaachelys*, new species, a nanhsiungchelyid turtle from the late Cretaceous of Ukhaa Tolgod, Mongolia. American Museum Novitates 3481:1-19.

Joyce, W. G., J. F. Parham, and J. A. Gauthier. 2004. Developing a protocol for the conversion of rank-based taxon names to phylogenetically defined clade names, as exemplified by turtles. Journal of Paleontology 78:989-1013.

Kälin, J. 1945. Zur Morphogenese des Panzers bei den Schildkröten. Acta Anatomica 1:144-176.

Kamat, S., R. Ballarini, and A. H. Heuer. 2000. Structural basis for the fracture toughness of the shell of the conch *Strombus gigas*. Nature 405:1036-1040.

Karl, H.-V. 2002. Übersicht über die fossilen Schildkröten Zentraleuropas (Reptilia, Testudines). Mauritiana (Altenburg) 18:171-202.

Karl, H.-V., and G. Tichy. 1999. Zur Taxonomie eines neuen Tribus von Seeschildkröten aus dem Oligozän von Deutschland (Testudines: Chelonioidea). The taxonomy of a new tribe of sea-turtles from the Oligocene of Germany (Testudines: Chelonioidea). Joannea - Geologie und Paläontologie 1:61-77.

Karl, H.-V., and G. Tichy. 2000. *Murrhardtia staeschei* n. gen. n. sp. – eine neue Schildkröte aus der Oberen Trias von Süddeutschland. Joannea - Geologie und Paläontologie 2:57-72.

Kear, B. P., and M. S. Y. Lee. 2006. A primitive protostegid from Australia and early sea turtle evolution. Biology Letters 2:116-119.

Khosatzky, L. I. 1996. New turtle from the Early Cretaceous of Central Asia. Russian Journal of Herpetology 3:89-94.

Khosatzky, L. I., and M. Młynarski. 1966. Fossil tortoises of the genus *Geoemyda* Gray, 1834 (s. lat.) of Europe. Acta Zoologica Cracoviensia 11:397-421.

Klein, N., and P. M. Sander. 2007. Bone histology and growth of the prosauropod dinosaur *Plateosaurus engelhardti* von Meyer, 1837 from the Norian bonebeds of Trossingen (Germany) and Frick (Switzerland). Special Papers in Palaeontology 77:169-206.

Klein, N., and T. Mörs. 2003. Die Schildkröten (Reptilia: Testudines) aus dem Mittel-Miozän von Hambach (Niederrheinische Bucht, NW-Deutschland). Palaeontographica Abt. A 268:1-48.

Klingenberg, C. P. 1998. Heterochrony and allometry: the analysis of evolutionary change in ontogeny. Biological Reviews 73:79-123.

Klinger, R. C., and J. A. Musick. 1992. Annular growth layers in juvenile loggerhead turtles (*Caretta caretta*). Bulletin of Marine Science 51:224-230.

Klinger, R. C., and J. A. Musick. 1995. Age and growth of loggerhead turtles (*Caretta caretta*) from Chesapeake Bay. Copeia 1:204-209.

Kordikova, E. G. 2000. Paedomorphosis in the shell of fossil and living turtles. Neues Jahrbuch der Geologie und Paläontologie, Abhandlungen 218:399-446.

Kordikova, E. G. 2002. Heterochrony in the evolution of the shell of Chelonia. Part 1: Terminology, Cheloniidae, Dermochelyidae, Trionychidae, Cyclanorbidae and Carettochelyidae. Neues Jahrbuch der Geologie und Paläontologie, Abhandlungen 226:343-417.

Krefft, G. 1876. Notes on Australian animals in New Guinea with description of a new species of fresh water tortoise belonging to the genus *Euchelymys* (Gray). Annali del Museo Civico di Storia Naturale di Genova. 8:390-394.

Krenz, J. G., G. J. P. Naylor, B. S. Shaffer, and F. J. Janzen. 2005. Molecular phylogenetics and evolution of turtles. Molecular Phylogenetics and Evolution 37:178-191.

Kuhn, O. 1969. Teil 6: Cotylosauria. Handbuch der Paläoherpetologie [Encyclopedia of Paleoherpetology]. 89 pp. Gustav Fisher Verlag, Stuttgart.

Kumazawa, Y., and M. Nishida. 1999. Complete mitochondrial DNA sequences of the green turtle and blue-tailed mole skink: statistical evidence for archosaurian affinity of turtles. Molecular Biology and Evolution 16:784-792.

Kuraku, S., R. Usuda, and S. Kuratani. 2005. Comprehensive survey of carapacial ridge-specific genes in turtle implies co-option of some regulatory genes in carapace evolution. Evolution & Development 7:3-17.

Lacépède, B. G. E. de 1788. Histoire des quadrupèdes ovipares et des serpens (1788-89, Tome I & II), Paris.

Lange, B. 1931. II. Integument der Sauropsiden; pp. 375-448 *in* L. Bolk, E. Göppert, E. Kallius, and W. Lubosch (eds.), Handbuch der Vergleichenden Anatomie der Wirbeltiere. 1. Band. Urban & Schwarzenberg, Berlin.

Langston, W. 1973. The crocodilian skull in historical perspective; pp. 263-284 *in* C. Gans, and T. S. Parsons (eds.), Biology of the Reptilia. Volume 4: Morphology D. Academic Press, New York.

Lapparent de Broin, F. de, and M. S. de la Fuente. 2001. Oldest world Chelidae (Chelonii, Pleurodira), from the Cretaceous of Patagonia, Argentina. Comptes Rendues de l'Academie des Sciences Paris, Sciences de la Terre et des Planètes / Earth and Planetary Sciences 333:463-470.

Lapparent de Broin, F. de, and R. E. Molnar. 2001. Eocene chelid turtles from Redbank Plains, Southeast Queensland, Australia. Geodiversitas 23:41-79.

Lapparent de Broin, F. de, and X. Murelaga. 1996. Une nouvelle faune de chéloniens dans le Crétacé supérieur européen. Comptes Rendus de l'Academie des Sciences Paris, Sciences de la Terre et des Planètes / Earth and Planetary Sciences [Série II a] 323:729-735.

Lapparent de Broin, F. de, B. Lange-Badré, and M. Dutrieux. 1996. Nouvelles decouvertes de tortues dans le Jurassique Supérieur du Lot (France) et examen du taxon Plesiochelyidae. Revue de Paléobiologie 15:533-570.

Lapparent de Broin, F. de, J. Bocquentin, and F. R. Negri. 1993. Gigantic turtles (Pleurodira, Podocnemididae) from the Late Miocene-Early Pliocene of South Western Amazon. Bulletin de l'Institut Français d'Études Andines 22:657-670.

Lapparent de Broin, F. de. 2000. African chelonians from the Jurassic to the Present: phases of development and preliminary catalogue of the fossil record. Palaeontologica Africana 36:43-82.

Lapparent de Broin, F. de. 2001. The European turtle fauna from the Triassic to the Present. Dumerilia 4:155-217.

Laurin, M., and R. R. Reisz. 1995. A reevaluation of early amniote phylogeny. Zoological Journal of the Linnean Society 113:165-223.

Lee, M. S. Y. 1993. The origin of the turtle body plan: bridging a famous morphological gap. Science 261:1716-1720.

Lee, M. S. Y. 1996. Correlated progression and the origin of turtles. Nature 379:812-815.

Lee, M. S. Y. 1997. Pareiasaur phylogeny and the origin of turtles. Zoological Journal of the Linnean Society 120:197-280.

Lee, M. S. Y. 2001. Molecules, morphology, and the monophyly of diapsid reptiles. Contributions to Zoology 70:1-22.

Leeuwenhoek, A. von. 1678. Microscopical observations on the structure of teeth and other bones. Philosophical Transactions of the Royal Society of London 12:1002-1003.

Lehman, T. M., and S. L. Tomlinson. 2004. *Terlinguachelys fischbecki*, a new genus and species of sea turtle (Chelonioidea: Protostegidae) from the Upper Cretaceous of Texas. Journal of Paleontology 78:1163-1178.

Lehr, E., U. Fritz, and F. J. Obst. 1998. *Cuora galbinifrons picturata* subsp. nov., eine neue Unterart der Hinterindischen Scharnierschildkröte. Herpetofauna, Weinstadt 20:5-11.

Leidy, J. 1856a. Notices of remains of extinct turtles of New Jersey, collected by Prof. Cook, of the State Geological Survey, under the direction of Dr. W. Kitchell. Proceedings of the Academy of Natural Sciences of Philadelphia 8:303-4.

Leidy, J. 1856b. Notices of extinct Vertebrata discovered by Dr. F. V. Hayden, during the expedition to the Sioux country under command of Lieut. G. K. Warren. Proceedings of the Academy of Natural Sciences of Philadelphia 8:311-312.

Leidy, J. 1856c. Notices of the remains of extinct reptiles and fishes discovered by Dr. F.V. Hayden in the bad lands of the Judith River, Nebraska Territory. Proceedings of the Academy of Natural Sciences of Philadelphia 8:72-73.

Leidy, J. 1869. Notice of some extinct vertebrates from Wyoming and Dakota. Proceedings of the Academy of Natural Sciences of Philadelphia 1869:63-67. [*Echmatemys wyomingensis*]

Leidy, J. 1871a. Remarks on a fossil *Testudo* from Wyoming and on supposed fossil turtles eggs. Proceedings of the Academy of Natural Sciences of Philadelphia 1871:154-155. [*Hadrianus corsoni*]

Leidy, J. 1871b. Remarks on extinct turtles from Wyoming Territory, *Anosteira ornata* and *Hybemys arenarius*. Proceedings of the Academy of Natural Sciences of Philadelphia 1871:102-103.

Leidy, J. 1889. Description of vertebrate remains from Peace Creek, Florida. Transactions of the Wagner Free Institute of Science of Philadelphia 2:13-31.

Lengelé, B., A. Dhem, and J. Schowing. 1990. Early development of the primitive cranial vault in the chick embryo. Journal of Cranofacial Genetics and Developmental Biology 10:103-112.

Lengelé, B., J. Schowing, and A. Dhem. 1996. Chondroid tissue in the early facial morphogenesis of the chick embryo. Anatomy and Embryology 193:505-513.

Levrat-Calviac, V., and L. Zylberberg. 1986. The structure of the osteoderms in the gekko: *Tarentola mauritanica*. American Journal of Anatomy 176:437-446.

Liem, K. F., W. E. Bemis, W. F. Walker Jr., and L. Grande. 2001. Functional Anatomy of the Vertebrates - An Evolutionary Perspective. 703 pp. Harcourt College Publishers, Fort Worth.

Linnaeus, C. 1758. Systema naturæ per regna tria naturæ, secundum classes, ordines, genera, species, cum characteribus, differentiis, synonymis, locis. Tomus I. Editio Decima, Reformata. 823 pp. Holmiae.

Linnaeus, C. 1766. Systema naturæ per regna tria naturæ, secundum classes, ordines, genera, species, cum characteribus, differentiis, synonymis, locis. Tomus I. Editio Duodecima, Reformata. 832 pp. Holmiae.

Lipka, T. R., F. Therrien, D. B. Weishampel, H. A. Jamniczky, W. G. Joyce, M. W. Colbert, and D. B. Brinkman. 2006. A new turtle from the Arundel clay facies (Potomac Formation, Early Cretaceous) of Maryland, U.S.A. Journal of Vertebrate Paleontology 26:300-307.

Loredo, G. A., A. Brukman, M. P. Harris, D. Kagle, E. E. Leclair, R. Gutman, E. Denney, E. Henkelman, B. P. Murray, J. F. Fallon, R. S. Tuan, and S. F. Gilbert. 2001. Development of an evolutionarily novel structure: fibroblast growth factor expression in the carapacial ridge of turtle embryos. Journal of Experimental Zoology (Mol Dev Evol) 291:274-281.

Lydekker, R. A. 1889. On remains of Eocene and Mesozoic Chelonia and a tooth of (?) *Ornithopsis*. The Quarterly Journal of the Geological Society of London, 45: 227-246.

Lynch, S. C., and J. F. Parham. 2003. The first report of hard-shelled sea turtles (Cheloniidae *sensu lato*) from the Miocene of California, including a new species (*Euclastes hutchisoni*) with unusually plesiomorphic characters. PaleoBios 23:21-35.

MacGregor, J. H. 1906. The Phytosauria, with especial reference to *Mystriosuchus* and *Rhytidodon*. Memoirs of the American Museum of Natural History 9:27-101.

Maderson, P. F. A. 1964. The skin of snakes and lizards. British Journal of Herpetology 3:151-154.

Mahmoud, I. Y., G. L. Hess, and J. Klicka. 1973. Normal embryonic stages of the western painted turtle, *Chrysemys picta bellii*. Journal of Morphology 141:269-280.

Main, R. P., A. de Ricqlès, J. R. Horner, and K. Padian. 2005. The evolution and function of thyreophoran dinosaur scutes: implications for plate function in stegosaurs. Paleobiology 31:291-314.

Maisch, M. W., A. T. Matzke, and G. Sun. 2003. A new sinemydid turtle (Reptilia: Testudines) from the Lower Cretaceous of the Junggar Basin (NW-China). Neues Jahrbuch der Geologie und Paläontologie, Monatshefte 12:705-722.

Märkel, K., and P. Gorny. 1973. Zur funktionellen Anatomie der Seeigelzähne (Echinodermata, Echinoidea). Zeitschrift für Morphologie der Tiere 75:223-242.

Massare, J. A. 1988. Swimming capabilities of Mesozoic marine reptiles: implications for methods of predation. Paleobiology 14:187-205.

Massare, J. A. 1994. Swimming capabilities of Mesozoic marine reptiles: a review; pp. 133-149 *in* L. Maddock, Q. Bone, and J. M. V. Rayner (eds.), Mechanics and Physiology of Animal Swimming. Cambridge University Press, Cambridge.

Matzke, A. T., M. W. Maisch, G. Sun, H. U. Pfretzschner, and H. Stöhr. 2005. A new Middle Jurassic xinjiangchelyid turtle (Testudines; Eucryptodira) from China (Xinjiang, Junggar Basin). Journal of Vertebrate Paleontology 25:63-70.

Matzke, A. T., M. W. Maisch, G. Sun, H.-U. Pfretzschner, and H. Stöhr. 2004a. A new xinjiangchelyid turtle (Testudines, Eucryptodira) from the Jurassic Qigu Formation of the Southern Junggar Basin, Xinjiang, North-West China. Palaeontology 47:1267-1299.

Matzke, A. T., M. W. Maisch, H.-U. Pfretzschner, G. Sun, and H. Stöhr. 2004b. A new basal sinemydid turtle (Reptilia: Testudines) from the Lower Cretaceous Tugulu Group of the Junggar Basin (NW China). Neues Jahrbuch der Geologie und Paläontologie, Monatshefte 3:151-167.

Mazin, J.-M., and G. Pinna. 1993. Palaeoecology of the armoured placodonts. Paleontologia Lombarda della Società Italiana di Scienze Naturali e del Museo Civico di Storia Naturale di Milano. Nuova serie 2:83-91.

McCord, W. P., J. B. Iverson, P. Q. Spinks, and H. B. Shaffer. 2000. A new genus of geoemydid turtle from Asia. Hamadryad 25:20-24.

McDowell, S. B. 1964. Partition of the genus *Clemmys* and related problems in the taxonomy of the aquatic Testudinidae. Proceedings of the Zoological Society of London 143:239-279.

McKerrow, W. S., R. T. Johnson, and M. E. Jakobson. 1969. Palaeoecological studies in the Great Oolite at Kirtlington, Oxfordshire. Palaeontology 12:56-83.

McWhinney, L. A., B. M. Rotschild, and K. Carpenter. 2001. Posttraumatic chronic osteomyelitis in *Stegosaurus* dermal spikes; pp. 141-156 *in* K. Carpenter (ed.), The Armored Dinosaurs. Indiana University Press, Bloomington.

Menger, W. 1922. Ontogenie und Phylogenie des Schildkrötenpanzers. PhD-thesis, Philosophische Fakultät, Hessische Ludwigs-Universität zu Giessen, Giessen. 102 pp.

Meunier, F. J. 1988. Nouvelles données sur l'organisation spatiale des fibres de collagène de la plaque basale des écailles des téléostéens. Annales des Sciences Naturelles, Zoologie 9:113-121.

Meunier, F. J., and J. Castanet. 1982. Organisation spatiale des fibres de collagène de la plaque basale des écailles des Téléostéens. Zoologica Scripta 11:141-153.

Meyer, H. von. 1839a. *Idiochelys Fitzingeri*, Taf. VII. fig. 1. Eine Schildkröte aus dem Kalkschiefer von Kehlheim. Beiträge zur Petrefacten-Kunde 1:59-74.

Meyer, H. von. 1839b. *Eurysternum Wagleri*, Münster. Eine Schildkröte aus dem Kalkschiefer von Solnhofen. Beiträge zur Petrefacten-Kunde 1:75-82.

Meyer, H. von. 1843. Mittheilungen an Professor Bronn gerichtet. Neues Jahrbuch für Mineralogie, etc. 1843:698-704. [*Trachyaspis*]

Meyer, H. von. 1846. [Without title, letter on several fossil specimens]. Neues Jahrbuch für Mineralogie, Geognosie, Geologie und Petrefaktenkunde 1846:462-476.

Meyer, H. von. 1847a. Mittheilungen an Professor Bronn gerichtet. Neues Jahrbuch für Mineralogie, Geognosie, Geologie und Petrefaktenkunde 1847:572-581. [*Psephophorus polygonus*]

Meyer, H. von. 1847b. Viele tertiäre Knochen aus Steyermark. Neues Jahrbuch für Mineralogie, Geognosie, Geologie und Petrefaktenkunde, II. Briefwechsel, B. Mittheilungen an Prof. Bronn 1847:190. [*Clemmydopsis turnauensis*]

Meylan, P. A. 1984. Evolutionary relationships of recent trionychid turtles: evidence from shell morphology. Studia Geologica Salmanticensia Vol. especial 1 (Studia Palaeocheloniologica I):169-188.

Meylan, P. A. 1987. Phylogenetic relationships of soft-shelled turtles (Family Trionychidae). Bulletin of the American Museum of Natural History 186:1-101.

Meylan, P. A. 1988. *Peltochelys* Dollo and the relationships among the genera of the Carettochelyidae (Testudines: Reptilia). Herpetologica 44:440-450.

Meylan, P. A. 1995. Pleistocene amphibians and reptiles from the Leisey Shell Pit, Hillsborough County, Florida. Bulletin of the Florida Museum of Natural History 37 (Pt. I):273-297.

Meylan, P. A. 1996. Skeletal morphology and relationships of the Early Cretaceous side-necked turtle, *Araripemys barretoi* (Testudines: Pelomedusoides: Araripemydidae), from the Santana Formation of Brazil. Journal of Vertebrate Paleontology 16:20-33.

Meylan, P. A., and E. S. Gaffney. 1989. The skeletal morphology of the Cretaceous cryptodiran turtle, *Adocus*, and the relationships of the Trionychoidea. American Museum Novitates 2941:1-60.

Meylan, P. A., and E. S. Gaffney. 1992. *Sinaspideretes* is not the oldest trionychid turtle. Journal of Vertebrate Paleontology 12:257-259.

Meylan, P. A., and W. Sterrer. 2000. *Hesperotestudo* (Testudines: Testudinidae) from the Pleistocene of Bermuda, with comments on the phylogenetic position of the genus. Zoological Journal of the Linnean Society 128:51-76.

Meylan, P. A., R. T. J. Moody, C. A. Walker, and S. D. Chapman. 2000. *Sandownia harrisi*, a highly derived trionychid turtle (Testudines: Cryptodira) from the Early Cretaceous of the Isle of Wight, England. Journal of Vertebrate Paleontology 20:522-532.

Miller, H. W. Jr. 1955. A check-list of the Cretaceous and Tertiary Vertebrates of New Jersey. Journal of Paleontology 29:903-914.

Miller, J. D. 1985. Embryology of marine turtles; pp. 269-328 *in* C. Gans, F. Billet, and P. F. A. Maderson (eds.), Biology of the Reptilia. Volume 14 - Development A. John Wiley & Sons, New York.

Milner, A. R. 2004. The turtles of the Purbeck Limestone Group of Dorset, southern England. Palaeontology 47:1441-1467.

Młynarski, M. 1969. Fossile Schildkröten. 128 pp. A. Ziemsen Verlag, Wittenberg.

Młynarski, M. 1972. *Zangerlia testudinimorpha* n. gen., n. sp., a primitive land tortoise from the Upper Cretaceous of Mongolia. Palaeontologia Polonica 27:85-92.

Młynarski, M. 1976. Teil 7: Testudines. Handbuch der Paläoherpetologie [Encyclopedia of Paleoherpetology]. 130 pp. Gustav Fischer Verlag, Stuttgart.

Młynarski, M., and H.-H. Schleich. 1980. Die Schildkrötenarten der jungtertiären Gattung *Clemmydopsis* Boda, 1927 (Emydidae - Batagurinae). Amphibia-Reptilia 1:75-84.

Modesto, S. P., and J. S. Anderson. 2004. The phylogenetic definition of Reptilia. Systematic Biology 53:815-821.

Moody, R. T. J. 1997. The paleogeography of marine and coastal turtles of the North Atlantic and trans-saharan regions; pp. 259-278 *in* J. M. Callaway, and E. L. Nicholls (eds.), Ancient Marine Reptiles. Academic Press, San Diego, California.

Moss, M. L. 1969. Comparative histology of dermal sclerifications in reptiles. Acta Anatomica 73:510-533.

Moss, M. L. 1972. The vertebrate dermis and the integumental skeleton. American Zoologist 12:27-34.

Motani, R. 2005. Evolution of fish-shaped reptiles (Reptilia: Ichthyopterygia) in their physical environments and constraints. Annual Review of Earth and Planetary Sciences 33:395-420.

Mulder, E. W. A. 2003. Comparative osteology, palaeoecology and systematics of the Late Cretaceous turtle *Allopleuron hofmanni* (Gray 1831) from the Maastrichtian type area. Publicaties van het Natuurhistorisch Genootschap in Limburg, Reeks XLIV (Aflevering 1): 23-92.

Müller, J. 2003. Early loss and multiple return of the lower temporal arcade in diapsid reptiles. Naturwissenschaften 90:473-476.

Musick, J. A. 1999. Ecology and conservation of long-lived marine animals. American Fisheries Society Symposium 23:1-10.

Near, T. J., P. A. Meylan, and B. S. Shaffer. 2005. Assessing concordance of fossil calibration points in molecular clock studies: an example using turtles. American Naturalist 165:137-146.

Nessov, L. A. 1977. A new genus of pitted-shelled turtle from the Upper Cretaceous of Karakalpakia. Paleontological Journal 11:96–107. [English translation of Paleontologicheskii Zhurnal 1977:103-114]

Nessov, L. A. 1986. Some late Mesozoic and Paleocene turtles of Soviet Middle Asia. Studia Geologica Salmanticensia 2:7-22.

Nessov, L. A. 1995. On some Mesozoic turtles of the Fergana Depression (Kyrgyzstan) and Dzhungur Alatau Ridge (Kazakhstan). Russian Journal of Herpetology 2:134-141.

Newman, H. H. 1906. The significance of scute and plate "abnormalities" in Chelonia. Biological Bulletin 10:68-114.

Noonan, B. P. 2000. Does the phylogeny of pelomedusid turtles reflect vicariance due to continental drift? Journal of Biogeography 27:1245-1249.

Nopcsa, F. 1923. Die Familien der Reptilien. Fortschritte der Geologie und Palaeontologie 2:1-210.

Nopcsa, F. 1928. Palaeontological notes on reptiles. Geologica Hungarica, Palaeontology Series 1:1–84.

Noulet, J. B. 1867. Nouveau genre de tortues fossiles proposé sous le nom d'*Allaeochelys*. Mémoires de l'Académie des Sciences, Toulouse (6me Série) 5:172-177.

Ogushi, K. 1911. Anatomische Studien an der japanischen dreikralligen Lippenschildkröte (*Trionyx japanicus*). I. Mitteilung. Morphologisches Jahrbuch 43:1-106.

Owen, R. 1839. Description of a tooth and part of the skeleton of the *Glyptodon*, a large quadruped of the edentate order, to which belongs the tessellated bony armour figured by

Mr. Clift in his memoir on the remains of the *Megatherium*, brought to England by Sir Woodbine Parish, F.G.S. Proceedings of the Geological Society of London 3:108-113.

Owen, R. 1840. Fossil Mammalia (4); *in* C.R. Darwin (ed.), The Zoology of The Voyage of the Beagle, 1 (13), 81–111. Smith, Elder and Co., London.

Owen, R. 1842. Report on British fossil reptiles, part II. Report for the British Association for the Advancement of Science, Plymouth 1841. 11:60-204.

Owen, R., 1876. Descriptive and illustrated catalogue of the Fossil Reptilia of South Africa in the British Museum. London 1876:1-88.

Pace, C. M., R. W. Blob, and M. W. Westneat. 2001. Comparative kinematics of the forelimb during swimming in red-eared slider (*Trachemys scripta*) and spiny softshell (*Apalone spinifera*) turtles. Journal of Experimental Biology 204:3261-3271.

Parham, J. F. 2005. A reassessment of the referral of the sea turtle skulls to the genus *Osteopygis* (Late Cretaceous, New Jersey, USA). Journal of Vertebrate Paleontology 25:71-77.

Parham, J. F., and D. E. Fastovsky. 1997. The phylogeny of cheloniid sea turtles revisited. Chelonian Conservation and Biology 2:548-554.

Parham, J. F., and J. H. Hutchison. 2003. A new eucryptodiran turtle from the Late Cretaceous of North America (Dinosaur Provincial Park, Alberta, Canada). Journal of Vertebrate Paleontology 23:783-798.

Parham, J. F., C. R. Feldman, and J. L. Boore. 2006. The complete mitochondrial genome of the enigmatic bigheaded turtle (*Platysternon*): description of unusual genomic features and the reconciliation of phylogenetic hypotheses based on mitochondrial and nuclear DNA. BMC Evolutionary Biology 6:1-11.

Peters, R. H. 1983. The Ecological Implications of Body Size. 329 pp. Cambridge University Press, Cambridge.

Peters, W. K. H. 1868. Eine Mitteilung über eine neue Nagergattung, *Chiropodomys penicillatus*, so wie über einige neue oder weniger bekannte Amphibien und Fische. Monatsbericht der Königlich-Preussischen Akademie der Wissenschaften zu Berlin 1868:448-453.

Peters, W. K. H. 1954. Übersicht der auf seiner Reise nach Mossambique beobachteten Schildkröten. Monatsberichte der Königlich Preußischen Akademie der Wissenschaften zu Berlin 1854:215-216.

Peyer, B., and E. Kuhn-Schnyder. 1955. Placodontia; pp. 459-486 *in* J. Piveteau (ed.), Traité de Paléontologie. Masson et Cie, Paris.

Pfretzschner, H.-U. 1986. Structural reinforcement and crack propagation in enamel. Mémoires du Muséum National d'Histoire Naturelle, Paris (Série C) 53:133-143.

Pfretzschner, H.-U. 1994. Biomechanik der Schmelzmikrostruktur in den Backenzähnen von Grossäugern. Palaeontographica Abt. A 234:1-88.

Pomel, A. 1847. Note sur les animaux fossiles decouverts dans le departement de l'Allier. Bulletin de la Société Géologique de France, 2. Série 4. 1847:378-385.

Pritchard, P. C. H. 1979. Encyclopedia of Turtles. 895 pp. T. F. H. Publications, Neptune, New Jersey.

Pritchard, P. C. H. 1980. *Dermochelys*, *D.* coriacea. Catalogue of American Amphibians and Reptiles 238:1-4.

Pritchard, P. C. H. 1984. Piscivory in turtles, and evolution of the long-necked Chelidae; pp. 87-110 *in* M. W. Ferguson (ed.), The Structure, Development and Evolution of Reptiles. Zoological Society of London Symposium, London.

Ramsay, E. P. 1887. On a new genus and species of freshwater tortoise from the Fly River, New Guinea. Proceedings of the Linnaean Society of New South Wales (Second Series) 1 (Pt. 1):158-162.

Rathke, H. 1848. Über die Entwickelung der Schildkröten. 267 pp. Friedrich Vieweg und Sohn, Braunschweig.

Reese, S. A., D. C. Jackson, and G. R. Ultsch. 2003. Hibernation in freshwater turtles: softshell turtles (*Apalone spinifera*) are the most intolerant of anoxia among North American species. Journal of Comparative Physiology B 173:263-268.

Rest, J. S. R., J. C. Ast, C. C. Austin, P. J. Waddell, E. A. Tibbetts, J. M. Hay, and D. P. Mindell. 2003. Molecular systematics of primary reptilian lineages and the tuatara mitochondrial genome. Molecular Phylogenetics and Evolution 29:289-297.

Rhodin, A. G. J. 1985. Comparative chondro-osseous development and growth of marine turtles. Copeia 1985:752-771.

Rhodin, A. G. J., J. A. Ogden, and G. J. Conlogue. 1981. Chondro-osseous morphology of *Dermochelys coriacea*, a marine reptile with mammalian skeletal features. Nature 290:244-246.

Ricqlès, A. de 1989. Les mécanismes hétérochroniques dans le retour des tétrapodes au milieu aquatique. Geobios mémoire spécial n^{o} 12:337-348.

Ricqlès, A. de, and V. de Buffrénil. 2001. Bone histology, heterochronies and the return of tetrapods to life in water: where are we?; pp. 289-310 *in* J.-M. Mazin, and V. de Buffrénil

(eds.), Secondary Adaptations of Tetrapods to Life in Water. Verlag Dr. Friedrich Pfeil, München.

Ricqlès, A. de, F. J. Meunier, J. Castanet, and H. Francillon-Vieillot. 1991. Comparative microstructure of bone; pp. 1-78 *in* K. Hall (ed.), Bone. Volume 3: Bone Matrix and Bone Specific Products. CRC Press, Boca Raton.

Ricqlès, A. de, X. Pereda Suberbiola, Z. Gasparini, and E. Olivero. 2001. Histology of dermal ossifications in an ankylosaurian dinosaur from the Late Cretaceous of Antarctica. Asociación Paleontológica Argentina. Publicación Especial 7:171-174.

Rieppel, O. 1993. Studies on skeleton formation in reptiles: patterns of ossification in the skeleton of *Chelydra serpentina* (Reptilia, Testudines). Journal of Zoology, London 231:487-509.

Rieppel, O. 2000. *Paraplacodus* and the phylogeny of the Placodontia (Reptilia: Sauropterygia). Zoological Journal of the Linnean Society 130:635-659.

Rieppel, O. 2001. Turtles as hopeful monsters. BioEssays 23:987-991.

Rieppel, O. 2002. The dermal armor of the cyamodontoid placodonts (Reptilia, Sauropterygia): morphology and systematic value. Fieldiana: Geology, New Series 46:1-41.

Rieppel, O., and M. deBraga. 1996. Turtles as diapsid reptiles. Nature 384:453-455.

Rieppel, O., and R. R. Reisz. 1999. The origin and early evolution of turtles. Annual Review of Ecology and Systematics 30:1-22.

Rieppel, O., and R. T. Zanon. 1997. The interrelationships of Placodontia. Historical Biology 12:211-227.

Rougier, G. W., M. S. de la Fuente, and A. B. Arcucci. 1995. Late Triassic turtles from South America. Science 268:855-857.

Ruckes, H. 1929. Studies in chelonian osteology. Part II: The morphological relationships between the girdles, ribs and carapace. Annales of the New York Academy of Sciences 31:81-120.

Ruta, M., M. I. Coates, and D. L. J. Quicke. 2003. Early tetrapod relationships revisited. Biological Reviews 78:251-345.

Rütimeyer, L. 1873. Die fossilen Schildkröten von Solothurn und der übrigen Juraformation, mit Beiträgen zur Kenntniss von Bau und Geschichte. Neue Denkschriften der Schweizerischen Naturforschenden Gesellschaft 25:1-192.

Salgado, L., and Z. Gasparini. 2006. Reappraisal of an ankylosaurian dinosaur from the Upper Cretaceous of James Ross Island (Antarctica). Geodiversitas 28:119-135.

Sander, P. M. 2000. Longbone histology of the Tendaguru sauropods: implications for growth and biology. Paleobiology 26:466-488.

Scheyer, T. M., and M. R. Sánchez-Villagra. 2007. Carapace bone histology in the giant turtle *Stupendemys geographicus* (Pleurodira: Podocnemidae): phylogenetic and functional aspects. Acta Palaeontologica Polonica 52:137-154.

Scheyer, T. M., and P. M. Sander. 2004. Histology of ankylosaur osteoderms: implications for systematics and function. Journal of Vertebrate Paleontology 24:874-893.

Scheyer, T. M., P. M. Sander, W. G. Joyce, W. Böhme, and U. Witzel. 2007. A plywood structure in the shell of fossil and living soft-shelled turtles (Trionychidae) and its evolutionary implications. Organisms, Diversity & Evolution 7:136-144.

Schlegel, H., and S. Müller. 1844. Over de Schildpadden van den Indischen Archipel. Beschrijving einer nieuwe soort van Sumatra; pp. 29-36 *in* C. J. Temminck (ed.), Verhandelingen over de Natuurlijke Geschiedenis der Nederlandsche Overzeesche Bezittingen, Part. 3. S. and J. Luchtmans and van der Hoek, Leiden.

Schmidt, H. 1967. Verkalkungsstudien am entmineralisierten Zahn- und Knochengewebe. Nova Acta Leopoldina 32:1-324.

Schmidt, K. P. 1940. New turtle of the genus *Podocnemis* from the Cretaceous of Kansas. Geological series of Field Museum of Natural History 8:1-12.

Schmidt, W. J. 1921. Die Panzerhaut der Weichschildkröte *Emyda granosa* und die funktionelle Bedeutung ihrer Strukturen. Archiv für Mikroskopische Anatomie 95:186-246.

Schneider, J. G. 1783. Allgemeine Naturgeschichte der Schildkröten, nebst einem systematischen Verzeichnisse der einzelnen Arten und zwey Kupfern. 364 pp. Johann Gotfried Müllersche Buchhandlung, Leipzig.

Schneider, J. G. 1791. Beschreibung und Abbildung einer neuen Art von Wasserschildkröte nebst Bestimmungen einiger bisher wenig bekannten fremden Arten. Schriften der Gesellschaft naturforschender Freunde zu Berlin 10:259-284.

Schoch, R. R. 1999. Comparative osteology of *Mastodonsaurus giganteus* (Jaeger, 1828) from the Lettenkeuper (Longobardian) of Germany (Baden-Württemberg, Bayern, Thüringen). Stuttgarter Beiträge zur Naturkunde B 278:1-175.

Schoch, R. R., and A. R. Milner. 2000. Teil 3B: Stereospondyli. Handbuch der Paläoherpetologie [Encyclopedia of Paleoherpetology]. 203 pp. Verlag Dr. Friedrich Pfeil, München.

Schoepff, J. D. 1792-1801. Historia Testudinum iconibus illustrata. 160 pp. Palm, Erlangae.

Schweigger, A. F. 1812. Prodromus monographiae Cheloniorum, Pt. 1. Königsberger Archiv für Naturwissenschaft und Mathematik 1812:271-458.

Seidel, M. E. 1994. Morphometric analysis and taxonomy of cooter and red-bellied turtles in the North American genus *Pseudemys* (Emydidae). Chelonian Conservation and Biology 1:117-130.

Seitz, A. L. L. 1907. Vergleichende Studien über den mikroskopischen Knochenbau fossiler und rezenter Reptilien, und dessen Bedeutung für das Wachstum und Umbildung des Knochengewebes im Allgemeinen. Abhandlungen der kaiserlichen Leopold-Carolingischen deutschen Akademie der Naturforscher, Nova Acta 87:230-370.

Seymour, R. S. 1982. Physiological adaptations to aquatic life; pp. 1-51 *in* C. Gans, and F. H. Pough (eds.), Biology of the Reptilia. Volume 13 - Physiology D (Physiological Ecology). Academic Press, London.

Shaffer, H. B., P. Meylan, and M. L. McKnight. 1997. Tests of turtle phylogeny: Molecular, morphological, and paleontological approaches. Systematic Biology 46:234-268.

Shaw, G. 1794. Zoology of New Holland. 33 pp. Sowerby, London.

Sheil, C. A. 2003. Osteology and skeletal development of *Apalone spinifera* (Reptilia: Testudines: Trionychidae). Journal of Morphology 256:42-78.

Sheil, C. A. 2005. Skeletal development of *Macrochelys temminckii* (Reptilia: Testudines: Chelydridae). Journal of Morphology 263:71-106.

Sheldon, A. 1997. Ecological implications of mosasaur bone microstructure; pp. 333-354 *in* J. M. Callaway, and E. L. Nicholls (eds.), Ancient Marine Reptiles. Academic Press, San Diego, California.

Sinn, A. D. 2004. Pathologie der Reptilien - eine retrospektive Studie. PhD-thesis, Institut für Zoologie, Fischereibiologie und Fischkrankheiten der Tierärztlichen Fakultät, Ludwig-Maximilian-Universität, München. 160 pp.

Snover, M. L., and A. A. Hohn. 2004. Validation and interpretation of annual skeletal marks in loggerhead (*Caretta caretta*) and Kemp's ridley (*Lepidochelys kempii*) sea turtles. Fishery Bulletin 102:682-692.

Spinks, P. Q., H. B. Shaffer, J. B. Iverson, and W. P. McCord. 2004. Phylogenetic hypotheses for the turtle family Geoemydidae. Molecular Phylogenetics and Evolution 32:164-182.

Spix, J. B. de. 1824. Animalia nova sive species novae Testudinum et Ranarum, quas in itinere per Brasiliam annis MDCCCXVII - MDCCCXX jussu et auspiciis Maximiliani Josephi I. Bavariae Regis suscepto collegit et descripsit. 53 pp, Leipzig.

Stehli, G. 1910. Ueber die Beschuppung der Reptilien. Jenaer Zeitschrift für Naturwissenschaften 46:737-800.

Stephens, P. R., and J. J. Wiens. 2003. Ecological diversification and phylogeny of emydid turtles. Biological Journal of the Linnean Society 79:577-610.

Stuart, B. L., and J. F. Parham. 2004. Molecular phylogeny of the critically endangered Indochinese box turtle (*Cuora galbinifrons*). Molecular Phylogenetics and Evolution 31:164-177.

Sukhanov, V. B. 2000. Mesozoic turtles of Middle and Central Asia; pp. 309-367 *in* M. J. Benton, M. A. Shishkin, D. M. Unwin, and E. N. Kurochkin (eds.), The Age of Dinosaurs in Russia and Mongolia. Cambridge University Press, Cambridge.

Sukhanov, V. B. 2001. Archaičnaja čerepacha is srednej Jury Moskowskoj oblasti i ee položenije w basalnoj radiazii otrjada Testudines [An archaic turtle from the Middle Jurassic of Moscow Region and its position in basal radiation of the order Testudines]; pp. 282-284 *in* N. B. Ananjeva, I. S. Darevsky, E. A. Dunaev, N. N. Iordansky, S. L. Kuzmin, and V. F. Orlova (eds.), Woprosy Gerpetologii [The problems of Herpetology. Proceedings of the 1st Meeting of the Nikolsky Herpetological Society, Puščino and Moscow; Russian with English summary].

Sukhanov, V. B. 2006. An archaic turtle, *Heckerochelys romani* gen. et sp. nov., from the Middle Jurassic of Moscow region, Russia. Fossil Turtle Research, Vol. 1, Russian Journal of Herpetology 13 (Suppl.):112-118.

Sukhanov, V. B., and P. Narmandakh. 1977. The shell and limbs of *Basilemys orientalis* (Chelonia,Dermatemyidae): a contribution to the morphology and evolution of the genus. Fauna, flora i biostratgrafiya Mezozoya i Kainozoya Mongolii. Sovmestnaya Sovetsko-Mongol'skaya Nauchneissledovat El'skaya Geologicheskaya Ekspeditsiya, Trudy 4:57-79.

Suzuki, H. K. 1963. Studies on the osseous system of the slider turtle. Annals of the New York Academy of Sciences 109:351-410.

Takahashi, A., H. Otsuka, and R. Hirayama. 2003. A new species of the genus *Manouria* (Testudines; Testudinidae) from the Upper Pleistocene of the Ryukyu Islands, Japan. Paleontological Research 7:195-217.

Taylor, M. A. 2000. Functional significance of bone ballastin in the evolution of buoyancy control strategies by aquatic tetrapods. Historical Biology 14:15-31.

Theobald, W. 1868. Catalogue of Reptiles in the Museum of the Asiatic Society of Bengal. Journal of the Asiatic Society of Bengal 378 (extra no. i-vi):6-88.

Tong, H., and E. S. Gaffney. 2000. Description of the skull of *Polysternon provinciale* (Matheron, 1869), a side-necked turtle (Pelomedusoides: Bothremydidae) from the Late Cretaceous of Villeveyrac, France. Oryctos 3:9-18.

Tong, H., E. Buffetaut, and V. Suteethorn. 2002. Middle Jurassic turtles from southern Thailand. Geological Magazine 139:687-697.

Tong, H., E. S. Gaffney, and E. Buffetaut. 1998. *Foxemys*, a new side-necked turtle (Bothremydidae: Pelomedusoides) from the Late Cretaceous of France. American Museum Novitates 3251:1-19.

Tortoise & Freshwater Turtle Specialist Group 1996. *Emys orbicularis*. In: IUCN 2006. 2006 IUCN Red List of Threatened Species. <www.iucnredlist.org>. Downloaded on 15 August 2006.

Ultsch, G. R., C. V. Herbert, and D. C. Jackson. 1984. The comparative physiology of diving in North American Freshwater turtles. I. Submergence tolerance, gas exchange and acid–base balance. Physiological Zoology 57:620-631.

Vallén, E. 1942. Beiträge zur Kenntnis der Ontogenie und der vergleichenden Anatomie des Schildkrötenpanzers. Acta Zoologica 23:1-127.

Vandellius, D. 1761. Epistola de holothurio, et testudine coriacea ad celeberrimum Carolum Linnaeum equitem naturae curiosorum dioscoridem II. 12 pp. Conzatti, Patavius.

Vincent, C., M. Bontoux, N. M. Le Douarin, C. Pieau, and A.-H. Monsoro-Burq. 2003. Msx genes are expressed in the carapacial ridge of the turtle shell: a study of the European pond turtle, *Emys orbicularis*. Development Genes and Evolution 213:464-469.

Völker, H. 1913. Über das Stamm-, Gliedmassen- und Hautskelet von *Dermochelys coriacea* L. Zoologisches Jahrbuch (Anatomie) 33:432-552.

Wagler, J. G. 1830. Natürliches System der Amphibien, mit vorangehender Classification der Säugtiere und Vögel. 354 pp. J. G. Cotta'sche Buchhandlung, München.

Wagner, A. 1853. Beschreibung einer fossilen Schildkröte und etlicher anderer Reptilien-Überreste aus den lithographischen Schiefern und dem grünen Sandstein von Kehlheim. Abhandlungen der mathematisch-physischen Classe der Königlich-Bayerischen Akademie der Wissenschaften 7:239-264.

Wallis, K. 1928. Zur Knochenhistologie und Kallusbildung beim Reptil (*Clemmys leprosa* Schweigg.). Zeitschrift für Zellforschung und mikroskopische Anatomie 6:1-26.

Walther, W. G. 1922. Die Neu-Guinea-Schildkröte *Carettochelys insculpta* Ramsay. Nova Guinea (Zoologie) 13:607-704.

Webb, R. G. 1995. The date of publication of Gray's *Catalogue of Shield Reptiles*. Chelonian Conservation and Biology 1:322-323.

Webster, M., and M. L. Zelditch. 2005. Evolutionary modifications of ontogeny: heterochrony and beyond. Paleobiology 31:354-372.

Weems, R. E. 1974. Middle Miocene sea turtles (*Syllomus*, *Procolpochelys*, *Psephophorus*) from the Calvert Formation. Journal of Paleontology 48:278-303.

Wegner, T. 1911. *Desmemys Bertelsmanni* n. g. n. sp. Ein Beitrag zur Kenntnis der Thalassemydidae Rütimeyer. Palaeontographica 58:105-132.

Westphal, F. 1975. Bauprinzipien im Panzer der Placodonten (Reptilia triadica) - Principles of structure and growth in the dermal armor of placodonts (Reptilia triadica). Paläontologische Zeitschrift 49:97-125.

Westphal, F. 1976. The dermal armour of some Triassic placodont reptiles; pp. 31-41 *in* A. d'A. Bellairs, and C. B. Cox (eds.), Morphology and Biology of Reptiles. Academic Press, London.

Whetstone, K. N. 1978. A new genus ofcryptodiran turtles (Testudinoidea, Chelydridae) from the upper Cretaceous Hell Creek Formation of Montana. The University of Kansas Science Bulletin 51:539-563.

Wieland, G. R. 1896. *Archelon ischyros*: a new gigantic cryptodire testudinate from the Fort Pierre Cretaceous of South Dakota. American Journal of Science 2:399-413.

Williams, E. 1954. *Clemmydopsis* Boda a valid lineage of Emydine Turtles from the European Tertiary. Breviora 28:1-9.

Williams, E. E., and S. B. McDowell. 1952. The plastron of soft-shelled turtles (Testudinata, Trionychidae): a new interpretation. Journal of Morphology 90:263-280.

Wolf, D. 2006. Osteoderm histology of extinct and recent Cingulata and Phyllophaga (Xenarthra, Mammalia): Implications for biomechanical adaptation and systematics. Unpublished MSc-thesis, Institute of Palaeontology, University of Bonn, Germany. 225 pp.

Wood, R. C. 1976. *Stupendemys geographicus*, the world's largest turtle. Breviora 436:1-31.

Wood, R. C., J. Johnson-Gove, E. S. Gaffney, and K. F. Maley. 1996. Evolution and phylogeny of leatherback turtles (Dermochelyidae), with descriptions of new fossil taxa. Chelonian Conservation and Biology 2:266-286.

Woolley, P. 1957. Colour change in a chelonian. Nature 179:1255-1256.

Wyneken, J. 2001. The anatomy of sea turtles. NOAA Technical Memorandum NMFS-SEFSC-470:1-172.

Yasukawa, Y., R. Hirayama, and T. Hikida. 2001. Phylogenetic relationships of geoemydine turtles (Reptilia: Bataguridae). Current Herpetology 20:105–133.

Yeh, H.-K. 1966. A new Cretaceous turtle of Nanhsiung, Northern Kwangtung. Vertebrata PalAsiatica 10:191-200.

Yntema, C. L. 1968. A series of stages in the embryonic development of *Chelydra serpentina*. Journal of Morphology 125:219-251.

Yntema, C. L. 1970a. Survival of xenogeneic grafts of embryonic pigment and carapace rudiments in embryos of *Chelydra serpentina*. Journal of Morphology 132:353-360.

Yntema, C. L. 1970b. Extirpation experiments on embryonic rudiments of the carapace of *Chelydra serpentina*. Journal of Morphology 132:235-244.

Zangerl, R. 1939. The homology of the shell elements in turtles. Journal of Morphology 65:383-409.

Zangerl, R. 1953. The vertebrate fauna of the Selma Formation of Alabama. Part III: the turtles of the family Protostegidae. Fieldiana: Geology Memoirs 3:57-133.

Zangerl, R. 1960. The vertebrate fauna of the Selma Formation of Alabama. Part V: an advanced cheloniid sea turtle. Fieldiana: Geology Memoirs 3:279-312.

Zangerl, R. 1969. The turtle shell; pp. 311-339 *in* C. Gans, A. d. A. Bellairs, and T. S. Parsons (eds.), Biology of the Reptilia. Vol. 1 Morphology A. Academic Press, London.

Zangerl, R., L. P. Hendrickson, and J. R. Hendrickson. 1988. A redistribution of the Australian flatback sea turtle *Natator depressus*. Bishop Museum Bulletins in Zoology 1:1-69.

Zonneveld, J.-P., G. F. Gunnell, and W. S. Bartels. 2000. Early Eocene fossil vertebrates from the southwestern Green River Basin, Lincoln and Uinta Counties, Wyoming. Journal of Vertebrate Paleontology 20:369-386.

Zug, G. R., A. H. Wynn, and C. Ruckdeschel. 1986. Age determination of loggerhead sea turtles, *Caretta caretta*, by incremental growth marks in the skeleton. Smithonian Contributions to Zoology 427:1-34.

Zug, G. R., and J. F. Parham. 1996. Age and growth in leatherback turtles, *Dermochelys coriacea* (Testudines: Dermochelyidae): a skeletochronological analysis. Chelonian Conservation and Biology 2:244-249.

Zug, G. R., and R. E. Glor. 1998. Estimates of age and growth in a population of green sea turtles (*Chelonia mydas*) from the Indian River lagoon system, Florida: a skeletochronological analysis. Canadian Journal of Zoology 76:1497-1506.

Zug, G. R., G. H. Balazs, J. A. Wetherall, D. M. Parker, and S. K. K. Murakawa. 2001. Age and growth of Hawaiian green seaturtles (*Chelonia mydas*): an analysis based on skeletochronology. Fishery Bulletin 100:117-127.

Zylberberg, L., and J. Castanet. 1985. New data on the structure and the growth of the osteoderms in the reptile *Anguis fragilis* L. (Anguidae, Squamata). Journal of Morphology 186:327-342.

Appendix 1: List of taxa, reference numbers and localities

No.	Taxon name	Origin	Shell element	Plane of sectioning	Reference number	Notes and locality
	Testudinata (n=102 taxa; 66 fossil, 36 recent)					
1	*Proganochelys quenstedti* Baur, 1887	Fossil	Peripheral and plastron fragment	?L-section	SMNS 17203	upper Löwenstein-Formation (upper "Stubensandstein", Norian, Late Triassic),*Plateosaurus* quarry" near Trossingen-Aixheim, SW Germany
			Posterior peripheral	X-section	SMNS 17203	upper Löwenstein-Formation (upper "Stubensandstein", Norian, Late Triassic),*Plateosaurus* quarry" near Trossingen-Aixheim, SW Germany
			Costal (labelled as „Triassochelys")	L-section	MB.R. 3449.2	upper Löwenstein-Formation (upper "Stubensandstein", Norian, Late Triassic), ?Baerecke/Limpricht Quarry; Halberstadt, E Germany
2	*Proterochersis robusta* Fraas, 1913	Fossil	Peripheral	X-section	SMNS 16442	lower Löwenstein-Formation (lower "Stubensandstein", early Norian, Late Triassic), "Fleinswerk" at Murrhardt, Germany
			Plastron fragment (?hyo- or hypoplastron)	L-section	SMNS 16442	lower Löwenstein-Formation (lower "Stubensandstein", early Norian, Late Triassic), "Fleinswerk" at Murrhardt, Germany
3	*Kayentachelys* sp.	Fossil	Neural	X-section	TMM 43669-4.2	Early Jurassic Kayenta Fm., Gold Spring Wash locality, Navajo Nation, Arizona, USA
			Proximal part of costal	L-section	UCMP V85010/150228	Early Jurassic Kayenta Fm., Coconino Co., Arizona, USA
			Costal	X-section	TMM 43669-4.1	Early Jurassic Kayenta Fm., Gold Spring Wash locality, Navajo Nation, Arizona, USA
			Peripheral	X-section	UCMP V82319/130079	Early Jurassic Kayenta Fm., Coconino Co., Arizona, USA
			Peripheral	X-section	UCMP V85013/150230	Early Jurassic Kayenta Fm., Coconino Co., Arizona, USA
			Plastron fragment (?hyo- or hypoplastron)	X-section	UCMP V85013/150229	Early Jurassic Kayenta Fm., Coconino Co., Arizona, USA
4	*Meiolania* sp.	Fossil	Peripheral	X-section	MB.R. 2426.1	Prov. Salta, Argentina, South America
5	Solemydidae gen. et sp. indet. (aff.*Naomichelys* sp.)	Fossil	Costal	L-section	TMP 90.60.07	Foremost Fm., Judith River Group, Pinhorn Ranch, SE Alberta, Canada
			Costal	L-section	FM PR 273	Antlers Fm., Trinity Group, Albian, Early Cretaceous, Montague County, Texas, USA
			Peripheral	X-section	TMP 90.60.07	Foremost Fm., Judith River Group, Pinhorn Ranch, SE Alberta, Canada
			Peripheral	X-section	FM PR 273	Antlers Fm., Trinity Group, Albian, Early Cretaceous, Montague County, Texas, USA
			Plastron fragment	X-section	TMP 2000.16.01	Foremost Fm., Judith River Group, Milkriver, SE Alberta, Canada
			Shell fragment (large, with several protrusions)	?	TMP 90.60.07	Foremost Fm., Judith River Group, Pinhorn Ranch, SE Alberta, Canada
			Shell fragment (smaller fragment with three protrusions)	?	TMP 90.60.07	Foremost Fm., Judith River Group, Pinhorn Ranch, SE Alberta, Canada
			Osteoderm (procumbent)	Short axis	FM PR 273	Antlers Fm., Trinity Group, Albian, Early Cretaceous, Montague County, Texas, USA
			Osteoderm (spike)	Long axis	FM PR 273	Antlers Fm., Trinity Group, Albian, Early Cretaceous, Montague County, Texas, USA
6	*Platychelys oberndorferi* Wagner, 1853	Fossil	Costal	L-section	NMS 20076	Kimmeridge (Malm), Jurassic, Quarry St. Niklaus (Sekt. 4, 193), Rüttenen near Solothurn, Switzerland
			"	X-section	NMS 20076	Kimmeridge (Malm), Jurassic, Quarry St. Niklaus (Sekt. 4, 193), Rüttenen near Solothurn, Switzerland
			Peripheral	X-section	NMS 20070	Kimmeridge (Malm), Jurassic, Quarry St. Niklaus (Sekt. 4, 203d), Rüttenen near Solothurn, Switzerland
			Hypoplastron (left)	X-section	NMS 20076	Kimmeridge (Malm), Jurassic, Quarry St. Niklaus (Sekt. 4, 203a, avec 193), Rüttenen near Solothurn, Switzerland
			"	L-section	NMS 20076	Kimmeridge (Malm), Jurassic, Quarry St. Niklaus (Sekt. 4, 203a, avec 193), Rüttenen near Solothurn, Switzerland
7	Platychelyidae indet. (aff.*Platychelys* sp.)	Fossil	Costal (thick element)	L-section	GUI-CHE-50	Kimmeridge, Jurassic, Guimarota coal mine, near Leiria, Portugal
			Costal (thin element)	?	GUI-CHE-51	Kimmeridge, Jurassic, Guimarota coal mine, near Leiria, Portugal
			Peripheral	X-section	GUI-CHE-52	Kimmeridge, Jurassic, Guimarota coal mine, near Leiria, Portugal
8	*Pelomedusa subrufa* (Bonnaterre, 1789)	Recent	Costal (right)	L-section	MVZ 230517	no data; occurs today in tropical and subtropical regions of Africa; drilled core, about 12 mm diameter
			Peripheral (right)	X-section	MVZ 230517	no data; occurs today in tropical and subtropical regions of Africa; drilled core, about 12 mm diameter
			Hyoplastron (right)	L-section	MVZ 230517	no data; occurs today in tropical and subtropical regions of Africa; drilled core, about 12 mm diameter
9	*Bothremys barberi* (Schmidt, 1940)	Fossil	Neural	X-section	FM P 27406	Campanian Mooreville Chalk (Late Cretaceous), Selma Group, Dallas County, Alabama, USA
			Costal	L-section	FM P 27406	Campanian Mooreville Chalk (Late Cretaceous), Selma Group, Dallas County, Alabama, USA
			Peripheral	X-section	FM P 27406	Campanian Mooreville Chalk (Late Cretaceous), Selma Group, Dallas County, Alabama, USA
			Plastron fragment	?	FM P 27406	Campanian Mooreville Chalk (Late Cretaceous), Selma Group, Dallas County, Alabama, USA
10	*Taphrosphys sulcatus* (Leidy, 1856a)	Fossil	Neural	X-section	YPM 40288	Middle marl bed (may equal Hornerstown Fm., thus Late Maastrichtian?), Cretaceous, Birmingham, Burlington County, New Jersey, USA
			Costal	L-section	YPM 40288	Middle marl bed (may equal Hornerstown Fm., thus Late Maastrichtian?), Cretaceous, Birmingham, Burlington County, New Jersey, USA
			"	X-section	YPM 40288	Middle marl bed (may equal Hornerstown Fm., thus Late Maastrichtian?), Cretaceous, Birmingham, Burlington County, New Jersey, USA
			Peripheral	X-section	YPM 40288	Middle marl bed (may equal Hornerstown Fm., thus Late Maastrichtian?), Cretaceous, Birmingham, Burlington County, New Jersey, USA
			Plastron fragment (?Hyo- or hypoplastron)	L-section	YPM 40288	Middle marl bed (may equal Hornerstown Fm., thus Late Maastrichtian?), Cretaceous, Birmingham, Burlington County, New Jersey, USA
11	*Foxemys* cf. *F. mechinorum*' Tong et al., 1998	Fossil	Neural	X-section	IPB R556a + b	Late Cretaceous (early Maastrichtian) fluvial sediments near Cruzy, Hérault, southern France
	= *Polysternon mechinorum* (Tong et al., 1998)		Costal	L-section	IPB R557a + b	Late Cretaceous (early Maastrichtian) fluvial sediments near Cruzy, Hérault, southern France
	fide Lapparent de Broin (2001)		Plastron fragment	X-section	IPB R558a + b	Late Cretaceous (early Maastrichtian) fluvial sediments near Cruzy, Hérault, southern France
			Plastron fragment (?Hyo- or hypoplastron)	X-section	IPB R559a + b	Late Cretaceous (early Maastrichtian) fluvial sediments near Cruzy, Hérault, southern France
12	Cf. *Bairdemys* sp.	Fossil	Shell fragment (?costal)	?	UNEFM uncat.	late Miocene, upper part of Urumaco Formation, Venezuela, South America
			"	?	UNEFM uncat.	late Miocene, upper part of Urumaco Formation, Venezuela, South America
13	*Podocnemis erythrocephala* (Spix, 1824)	Recent	Neural2 and costal3 (right)	X-section	YPM 11853	recent red-headed Amazon River turtle, South America (provenance unknown)
			Costal1-3 (left)	L-section	YPM 11853	recent red-headed Amazon River turtle, South America (provenance unknown)
			Peripheral (right)	X-section	YPM 11853	recent red-headed Amazon River turtle, South America (provenance unknown)
			Hypoplastron (right)	L-section	YPM 11853	recent red-headed Amazon River turtle, South America (provenance unknown)

No.	Taxon name	Origin	Shell element	Plane of sectioning	Reference number	Notes and locality
14	*Stupendemys geographicus* Wood, 1976	Fossil	Neural	X-section	UNEFM-101	late Miocene Urumaco Formation, Venezuela, South America; smaller carapace: 2-3 meters in length
			Costal fragment A	L-section	UNEFM-CIAPP-2002-01	late Miocene Urumaco Formation, Venezuela, South America; carapace 3.3 m long and 2 m wide
			"	X-section	UNEFM-CIAPP-2002-01	late Miocene Urumaco Formation, Venezuela, South America; carapace 3.3 m long and 2 m wide
			Costal fragment B	L-section	UNEFM-CIAPP-2002-01	late Miocene Urumaco Formation, Venezuela, South America; lower third part of Costal fragment A
15	*Emydura subglobosa* (=*Emydura albertisii*) (Krefft, 1876)	Recent	Proximal part of costal2 (left)	L-section	ZFMK-58215	New Guinea, no further data; labeled as Emydura albertisi; possibly female specimen; drilled core, about 12 mm diameter
			Hyoplastron (left)	L-section	ZFMK-58215	New Guinea, no further data; labeled as Emydura albertisi; possibly female specimen; drilled core, about 12 mm diameter
16	*Emydura* sp.	Fossil	Costal	L-section	UCMP V5762/57055	Etadunna Fm., Miocene, South Australia
			Costal	X-section	UCMP V5762/57055	Etadunna Fm., Miocene, South Australia
			Peripheral	X-section	UCMP V5762/57055	Etadunna Fm., Miocene, South Australia
			Plastron fragment (?Hyo- or hypoplastron)	L-section	UCMP V5774/57270	Etadunna Fm., Miocene, South Australia
17	*Chelodina longicollis* (Shaw, 1794)	Recent	?Costal2 (left)	L-section	ZMB 27258	no data; Aquarium, Berlin; occurs in eastern Australia (northern Queensland to southern South Australia); drilled core, about 22 mm diameter
			Hyoplastron (right)	L-section	ZMB 27258	no data; Aquarium, Berlin; occurs in eastern Australia (northern Queensland to southern South Australia); drilled core, about 22 mm diameter
18	*Platemys platycephala* (Schneider, 1791)	Recent	Neural2 and proximal part of costal2 (left)	X-section	SMNS 10035	Guiana, South America; drilled core, about 22 mm diameter
			Hypoplastron (left)	L-section	SMNS 10035	Guiana, South America; drilled core, about 12 mm diameter
19	*Phrynops geoffroanus* (Schweigger, 1812)	Recent	Neural3	X-section	YPM 12611	no data; species ranges from southwestern Venezuela to eastcentral South America
			Costal3	X-section	YPM 12611	no data; species ranges from southwestern Venezuela to eastcentral South America
			"	L-section	YPM 12611	no data; species ranges from southwestern Venezuela to eastcentral South America
			Peripheral3	X-section	YPM 12611	no data; species ranges from southwestern Venezuela to eastcentral South America
			Hyoplastron	X-section	YPM 12611	no data; species ranges from southwestern Venezuela to eastcentral South America
20	*Hydromedusa tectifera* Cope, 1870a	Recent	?Costal2 (left)	L-section	ZFMK-51656	near Montevideo, Uruguay, South America; possibly male? (deep anal notch, long thick tail, concave plastron); drilled core, about 22 mm diameter
			Hyoplastron (left)	L-section	ZFMK-51656	near Montevideo, Uruguay, South America; possibly male? (deep anal notch, long thick tail, concave plastron); drilled core, about 22 mm diameter
21	*Chelus fimbriatus* (Schneider, 1783)	Recent	Costal	L-section	FMNH 269459	no data; all major drainage systems of South America; drilled core, about 22 mm diameter; bone stained with green color; chemical not known
			Peripheral	X-section	FMNH 269459	no data; all major drainage systems of South America; drilled core, about 22 mm diameter; bone stained with green color; chemical not known
			Hyoplastron (right)	L-section	FMNH 269459	no data; all major drainage systems of South America; drilled core, about 22 mm diameter; bone stained with green color; chemical not known
22	Cryptodira incertae sedis (Kirtlington turtle sample)	Fossil	Shell fragment (1)	?	IPB R583	Kirtlington Cement Quarry (Mammal Bed, 3p layer of McKerrow et al., 1969), Bathonian, Middle Jurassic, Kirtlington , Oxfordshire, UK; Morph I
			Shell fragment (2)	?	IPB R584	Kirtlington Cement Quarry (Mammal Bed, 3p layer of McKerrow et al., 1969), Bathonian, Middle Jurassic, Kirtlington , Oxfordshire, UK; Morph I
			Shell fragment (3)	?	IPB R585	Kirtlington Cement Quarry (Mammal Bed, 3p layer of McKerrow et al., 1969), Bathonian, Middle Jurassic, Kirtlington , Oxfordshire, UK; Morph I
			?Carapace fragment (4)	?	IPB R586	Kirtlington Cement Quarry (Mammal Bed, 3p layer of McKerrow et al., 1969), Bathonian, Middle Jurassic, Kirtlington , Oxfordshire, UK; Morph I
			Plastron fragment (?Hyo- or hypoplastron) (5)	?	IPB R587	Kirtlington Cement Quarry (Mammal Bed, 3p layer of McKerrow et al., 1969), Bathonian, Middle Jurassic, Kirtlington , Oxfordshire, UK; Morph I
			Plastron fragment (?Hyo- or hypoplastron) (6)	?	IPB R588	Kirtlington Cement Quarry (Mammal Bed, 3p layer of McKerrow et al., 1969), Bathonian, Middle Jurassic, Kirtlington , Oxfordshire, UK; Morph I
			Plastron fragment (?Hyo- or hypoplastron) (7)	?	IPB R589	Kirtlington Cement Quarry (Mammal Bed, 3p layer of McKerrow et al., 1969), Bathonian, Middle Jurassic, Kirtlington , Oxfordshire, UK; Morph II
23	Pleurosternidae gen. et sp. indet.	Fossil	Neural	X-section	IPFUB P-Barkas 20	Alluvial fan deposits, Upper Jurassic (Tithonian-?Berriasian), Porto das Barcas, Lourinha, Portugal
			Costal	L-section	GUI-CHE-53	Jurassic (Kimmeridgian), Guimarota coal mine, near Leiria, Portugal
			Costal, proximal part	X-section	GUI-CHE-54	Jurassic (Kimmeridgian), Guimarota coal mine, near Leiria, Portugal; see mineral infill
			Peripheral	X-section	IPFUB P-Barkas 21	Alluvial fan deposits, Upper Jurassic (Tithonian-?Berriasian), Porto das Barcas, Lourinha, Portugal
			Plastron fragment (?Hyo- or hypoplastron)	X-section	GUI-CHE-55	Jurassic (Kimmeridgian), Guimarota coal mine, near Leiria, Portugal
			"	L-section	GUI-CHE-55	Jurassic (Kimmeridgian), Guimarota coal mine, near Leiria, Portugal
24	*Compsemys* sp.	Fossil	Neural	X-section	UCMP V90077/150197	Early Palaeocene (Puercan), Hell Creek Fm., McCone County, Montana, USA
			Costal	L-section	UCMP V90077/150196	Early Palaeocene (Puercan), Hell Creek Fm., McCone County, Montana, USA
			Costal	X-section	UCMP V90077/150195	Early Palaeocene (Puercan), Hell Creek Fm., McCone County, Montana, USA
			Peripheral	X-section	UCMP V87192/150199	Early Palaeocene (Puercan), Hell Creek Fm., McCone County, Montana, USA
			Plastron fragment (?Hyo- or hypoplastron)	X-section	UCMP V90077/150198	Early Palaeocene (Puercan), Hell Creek Fm., McCone County, Montana, USA
25	*Glyptops plicatulus* (Cope, 1877)	Fossil	Neural	X-section	YPM uncat.	Quarry 9, Como, Wyoming, USA (Morrison Fm., Upper Jurassic)
			Costal, proximal part	L-section	YPM uncat.	Quarry 9, Como, Wyoming, USA (Morrison Fm., Upper Jurassic)
			Costal	X-section	YPM uncat.	Quarry 9, Como, Wyoming, USA (Morrison Fm., Upper Jurassic)
			Peripheral	X-section	YPM uncat.	Quarry 9, Como, Wyoming, USA (Morrison Fm., Upper Jurassic)
			Plastron fragment (?Hyo- or hypoplastron)	X-section	YPM uncat.	Quarry 9, Como, Wyoming, USA (Morrison Fm., Upper Jurassic)
			"	L-section	YPM uncat.	Quarry 9, Como, Wyoming, USA (Morrison Fm., Upper Jurassic)
26	*Neurankylus* sp.	Fossil	Neural	X-section	TMP 86.36.308	?Oldman Fm. or Dinosaur Park Fm., Judith River Group, Dinosaur Provincial Park; Alberta, Canada
			Costal	L-section	TMP 85.58.26	Steveville Railroad Grade, Dinosaur Park Fm., Judith River Group, Alberta, Canada
			Peripheral	X-section	TMP 91.36.786	Dinosaur Park Fm., Judith River Group, Dinosaur Provincial Park, Alberta, Canada
			Hyoplastron	L-section	TMP 94.666.35	Dinosaur Park Fm., Judith River Group, Steveville Badlands, Dinosaur Provincial Park, Alberta, Canada

No.	Taxon name	Origin	Shell element	Plane of sectioning	Reference number	Notes and locality
27	*Plesiobaena* sp.	Fossil	Neural	X-section	TMP 86.78.97	Dinosaur Park Fm., Judith River Group, Dinosaur Provincial Park, Alberta, Canada
			Costal	L-section	TMP 93.108.07	?Oldman Fm. or Dinosaur Park Fm., Judith River Group, Dinosaur Provincial Park, Alberta, Canada
			Peripheral	X-section	TMP 91.36.852	?Oldman Fm. or Dinosaur Park Fm., Judith River Group, Dinosaur Provincial Park, Alberta, Canada
			Hyoplastron (right)	L-section	TMP 84.67.97	Dinosaur Park Fm., Judith River Group, Steveville Badlands, Dinosaur Provincial Park, Alberta, Canada
			"	X-section	TMP 84.67.97	Dinosaur Park Fm., Judith River Group, Steveville Badlands, Dinosaur Provincial Park, Alberta, Canada
28	*Boremys* sp.	Fossil	Neural	X-section	TMP 93.108.03	?Oldman Fm. or Dinosaur Park Fm., Judith River Group, Dinosaur Provincial Park, Alberta, Canada
			Costal	L-section	TMP 94.12.325	Dinosaur Park Fm., Judith River Group, Dinosaur Provincial Park, Alberta, Canada
			"	X-section	TMP 94.12.325	Judith River Group, Dinosaur Provincial Park; Alberta, Canada
			Peripheral	X-section	TMP 86.78.29	Dinosaur Park Fm., Judith River Group, Dinosaur Provincial Park; Alberta, Canada
			Hypoplastron and xiphiplastron	L-section	TMP 84.163.70	?Oldman Fm. or Dinosaur Park Fm., Judith River Group, Dinosaur Provincial Park, Alberta, Canada
			"	X-section (hyopl.)	TMP 84.163.70	?Oldman Fm. or Dinosaur Park Fm., Judith River Group, Dinosaur Provincial Park, Alberta, Canada
29	*Chisternon* sp.	Fossil	Neural and costal (fused)	X-section	UCMP V94071/150182	Bridger Fm., Uinta County, SW Wyoming, USA; see mineral infill
			Peripheral	X-section	UCMP V94076/150189	Bridger Fm., Uinta County, SW Wyoming, USA
			Periphery of carapace (brigde region)	?	UCMP V94076/150189	Bridger Fm., Uinta County, SW Wyoming, USA
			Plastron fragment (?Hyo- or hypoplastron)	L-section	UCMP V94078/150190	Bridger Fm., Uinta County, SW Wyoming, USA
30	*Eurysternum* sp.	Fossil	Costal	L-section	NMS 21908	Upper Jurassic (Kimmeridgian) limestone quarries, Solothurn, Switzerland
			"	X-section	NMS 21908	Upper Jurassic (Kimmeridgian) limestone quarries, Solothurn, Switzerland
			Left hyoplastron	X-section	NMS 20981	Upper Jurassic (Kimmeridgian) limestone quarries, Solothurn, Switzerland
			Plastron fragment (?Hyo- or hypoplastron)	L-section	NMS 21922	Upper Jurassic (Kimmeridgian) limestone quarries, Solothurn, Switzerland
31	?*Eurysternum* sp.	Fossil	Costal fragment	L-section	SMNS 91005	Upper Jurassic (Tithonian); Tönniesberg near Hannover; from old inventories; [originally identified as ?Megalurus]
			Plastron fragment	L-section	SMNS 91005	Upper Jurassic (Tithonian); Tönniesberg near Hannover; from old inventories; [originally identified as ?Megalurus]
32	*Plesiochelys* sp.	Fossil	Neural3	X-section	NMS 8730	Upper Jurassic (Kimmeridgian) limestone quarries, Solothurn, Switzerland; labelled as'*Plesiochelys St. Verenae*'
			"	L-section	NMS 8730	Upper Jurassic (Kimmeridgian) limestone quarries, Solothurn, Switzerland; labelled as'*Plesiochelys St. Verenae*'
			Costal3 (proximal part)	L-section	NMS 8849	Upper Jurassic (Kimmeridgian) limestone quarries, Solothurn, Switzerland; wrinkles on external surface
			Costal (proximal part)	L-section	IPB R13	Upper Jurassic (Kimmeridgian); Ahlem near Hannover; labeled as*P. hannoverana*
			fragment with peripheral and distal part of costal	X-section	NMS 9214	Upper Jurassic (Kimmeridgian) limestone quarries, Solothurn, Switzerland
33	?*Plesiochelys* sp.	Fossil	Hypoplastron (fragment)	X-section	SMNS 55831	Lower Kimmeridgian (Upper Jurassic), 'Landeskrankenhaus' at the Galgenberg near Hildesheim, Germany
			"	L-section	SMNS 55831	Lower Kimmeridgian (Upper Jurassic), 'Landeskrankenhaus' at the Galgenberg near Hildesheim, Germany
34	Plesiochelyidae indet.	Fossil	Carapace fragment	X-section	NMS 8876	Upper Jurassic (Kimmeridgian) limestone quarries, Solothurn, Switzerland
35	*Thalassemys* cf. *T. hugii* Rütimeyer, 1873	Fossil	Proximal part of costal5 (left)	L-section	NMS 8859	Upper Jurassic (Kimmeridgian) limestone quarries, Solothurn, Switzerland
			Neural7 and costal7 (left posterior part of carapace)	L-section (for costal)	NMS 9201	Upper Jurassic (Kimmeridgian) limestone quarries, Solothurn, Switzerland
36	*Thalassemys* sp.	Fossil	Plastron fragment (?Hyo- or hypoplastron)	X-section	NMS 9168	Upper Jurassic (Kimmeridgian) limestone quarries, Solothurn, Switzerland
			"	L-section	NMS 9168	Upper Jurassic (Kimmeridgian) limestone quarries, Solothurn, Switzerland
			Neural	X-section	NMS 9159	Upper Jurassic (Kimmeridgian) limestone quarries, Solothurn, Switzerland
37	*Tropidemys* sp.	Fossil	Neural	X-section	NMS 8991	Upper Jurassic (Kimmeridgian) limestone quarries, Solothurn, Switzerland
			Peripheral, ?distal part of costal	L-section (for costal)	NMS 8991	Upper Jurassic (Kimmeridgian) limestone quarries, Solothurn, Switzerland
38	*Xinjiangchelys chowi* Matzke et al., 2005	Fossil	Peripheral	X-section	SGP 2001/34a	upper Middle Jurassic Toutunhe Formation, Liuhonggou locality, near Toutunhe River, S Junggar Basin, 50km SW of Urumchi, Xinjiang, China
			Shell fragment	?	SGP 2001/34b	upper Middle Jurassic Toutunhe Formation, Liuhonggou locality, near Toutunhe River, S Junggar Basin, 50km SW of Urumchi, Xinjiang, China
			Shell fragment	?	SGP 2001/34c	upper Middle Jurassic Toutunhe Formation, Liuhonggou locality, near Toutunhe River, S Junggar Basin, 50km SW of Urumchi, Xinjiang, China
39	*Xinjiangchelys* sp.	Fossil	Costal	L-section	SGP 2002/4a	upper Middle Jurassic Toutunhe Formation (?'bonebed locality'), near Toutunhe River, S Junggar Basin, 50km SW of Urumchi, Xinjiang, China
			Peripheral	X-section	SGP 2002/4b	upper Middle Jurassic Toutunhe Formation (?'bonebed locality'), near Toutunhe River, S Junggar Basin, 50km SW of Urumchi, Xinjiang, China
			Peripheral	X-section	SGP 2002/4c	upper Middle Jurassic Toutunhe Formation (?'bonebed locality'), near Toutunhe River, S Junggar Basin, 50km SW of Urumchi, Xinjiang, China
			Plastron fragment (?Hyo- or hypoplastron)	X-section	SGP 2002/4d	upper Middle Jurassic Toutunhe Formation (?'bonebed locality'), near Toutunhe River, S Junggar Basin, 50km SW of Urumchi, Xinjiang, China
40	*Wuguia efremovi* Khosatzky, 1996	Fossil	Neural (larger element)	X-section	SGP 2001/35a	Lianmuxin Formation (Uppermost Lower Cretaceous) of the Tugulu Group, Liuhonggou, west of Toutunhe River, Junggar Basin, Xinjiang, China
	(=*Dracochelys wimani* Maisch et al., 2003)		Neural (smaller element)	X-section	SGP 2001/35b	Lianmuxin Formation (Uppermost Lower Cretaceous) of the Tugulu Group, Liuhonggou, west of Toutunhe River, Junggar Basin, Xinjiang, China
			Costal	X-section	SGP 2001/35c	Lianmuxin Formation (Uppermost Lower Cretaceous) of the Tugulu Group, Liuhonggou, west of Toutunhe River, Junggar Basin, Xinjiang, China
			Costal	L-section	SGP 2001/35d	Lianmuxin Formation (Uppermost Lower Cretaceous) of the Tugulu Group, Liuhonggou, west of Toutunhe River, Junggar Basin, Xinjiang, China
			Peripheral	X-section	SGP 2001/35e	Lianmuxin Formation (Uppermost Lower Cretaceous) of the Tugulu Group, Liuhonggou, west of Toutunhe River, Junggar Basin, Xinjiang, China
			Peripheral	X-section	SGP 2001/35f	Lianmuxin Formation (Uppermost Lower Cretaceous) of the Tugulu Group, Liuhonggou, west of Toutunhe River, Junggar Basin, Xinjiang, China
			Plastron fragment (?Hyo- or hypoplastron)	X-section	SGP 2001/35g	Lianmuxin Formation (Uppermost Lower Cretaceous) of the Tugulu Group, Liuhonggou, west of Toutunhe River, Junggar Basin, Xinjiang, China
			Plastron fragment (?Hyo- or hypoplastron)	L-section	SGP 2001/35h	Lianmuxin Formation (Uppermost Lower Cretaceous) of the Tugulu Group, Liuhonggou, west of Toutunhe River, Junggar Basin, Xinjiang, China

No.	Taxon name	Origin	Shell element	Plane of sectioning	Reference number	Notes and locality
41	Eucryptodira incertae sedis (cf. "Macrobaenidae")	Fossil	Neural	X-section	YPM 1585	Late Cretaceous sediments, ?Hornerstown Fm., Mullica Hill, New Jersey, USA; was labeled as Osteopygis emarginatus
			Costal	L-section	YPM 1585	Late Cretaceous sediments, ?Hornerstown Fm., Mullica Hill, New Jersey, USA; was labeled as Osteopygis emarginatus
			"	X-section	YPM 1585	Late Cretaceous sediments, ?Hornerstown Fm., Mullica Hill, New Jersey, USA; was labeled as Osteopygis emarginatus
			Peripheral	X-section	YPM 1585	Late Cretaceous sediments, ?Hornerstown Fm., Mullica Hill, New Jersey, USA; was labeled as Osteopygis emarginatus
			Plastron fragment (?Hyo- or hypoplastron)	X-section	YPM 1585	Late Cretaceous sediments, ?Hornerstown Fm., Mullica Hill, New Jersey, USA; was labeled as Osteopygis emarginatus
			"	L-section	YPM 1585	Late Cretaceous sediments, ?Hornerstown Fm., Mullica Hill, New Jersey, USA; was labeled as Osteopygis emarginatus
42	*Rupelchelys breitkreutzi* Karl and Tichy, 1999	Fossil	free distal rib end or distal part of plastron element?	X-section	SMNS 87218	Lower Oligocene (Rupelian, 'Unterer Meeressand'), Neumühle near Weinheim/Alzey, Germany
			Costal	X-section	SMNS 87218	Lower Oligocene (Rupelian, 'Unterer Meeressand'), Neumühle near Weinheim/Alzey, Germany
			Costal	X-section	SMNS 87218	Lower Oligocene (Rupelian, 'Unterer Meeressand'), Neumühle near Weinheim/Alzey, Germany
			Peripheral	X-section	SMNS 87218	Lower Oligocene (Rupelian, 'Unterer Meeressand'), Neumühle near Weinheim/Alzey, Germany
			Shell fragment (?costal fragment)	?	SMNS 87218	Lower Oligocene (Rupelian, 'Unterer Meeressand'), Neumühle near Weinheim/Alzey, Germany
43	*Ctenochelys cf. C. stenoporus* (Hay, 1905)	Fossil	Neural	X-section	FM PR 442	Campanian Mooreville Chalk (Late Cretaceous), Selma Group, Dallas County, Alabama, USA; labelled as Ctenochelys cf. C. acris Zangerl, 1953
	(=*Ctenochelys* cf. *C. acris* Zangerl, 1953)		Costal	L-section	FM PR 442	Campanian Mooreville Chalk (Late Cretaceous), Selma Group, Dallas County, Alabama, USA; labelled as Ctenochelys cf. C. acris Zangerl, 1953
			Peripheral	X-section	FM PR 442	Campanian Mooreville Chalk (Late Cretaceous), Selma Group, Dallas County, Alabama, USA; labelled as Ctenochelys cf. C. acris Zangerl, 1953
			plastron fragment	?	FM PR 442	Campanian Mooreville Chalk (Late Cretaceous), Selma Group, Dallas County, Alabama, USA; labelled as Ctenochelys cf. C. acris Zangerl, 1953
44	*Allopleuron hofmanni* (Gray, 1831a)	Fossil	Neural	X-section	NHMM 1992084	Late Cretaceous (Maastrichtian type area), Maastricht, Netherlands
			Costal fragment 1 (larger element)	?	NHMM uncat.	Late Cretaceous (Maastrichtian type area), Maastricht, Netherlands
			Costal fragment 2 (smaller element)	?	NHMM uncat.	Late Cretaceous (Maastrichtian type area), Maastricht, Netherlands
			Peripheral	X-section	NHMM uncat.	Late Cretaceous (Maastrichtian type area), Maastricht, Netherlands
			Plastron rods	X-section	NHMM uncat.	Late Cretaceous (Maastrichtian type area), Maastricht, Netherlands
45	*Caretta caretta* (Linnaeus, 1758)	Recent	Costal2 (left)	L-section	FMNH 98963	no data; Cosmopolitan marine species ranging from tropical to temperate waters; drilled core, about 22 mm diameter
			Hyoplastron (left)	L-section	FMNH 98963	no data; Cosmopolitan marine species ranging from tropical to temperate waters; drilled core, about 22 mm diameter
46	*Chelonia mydas* (Linnaeus, 1758)	Recent	Costal	L-section	MB.R. 2857	labelled with 'Zehlendorf (Berlin)' ; no further data available
47	*Eretmochelys imbricata* (Linnaeus, 1766)	Recent	Neural2	X-section	SMNS 12604	confiscated by customs (no data); marine species occuring in Atlantic and Indo-Pacific tropical waters; drilled core, about 12 mm diameter
			Costal2 (right)	L-section	SMNS 12604	confiscated by customs (no data); marine species occuring in Atlantic and Indo-Pacific tropical waters; drilled core, about 12 mm diameter
			Peripheral1 (right)	X-section	SMNS 12604	confiscated by customs (no data); marine species occuring in Atlantic and Indo-Pacific tropical waters; drilled core, about 12 mm diameter
48	*Archelon ischyros* Wieland, 1896	Fossil	Peripheral	X-section	YPM 1783	no data (specimen may come from Niobrara Fm., South Dakota, USA, as Wieland was excavating there in 1899)
			Shell fragment	?	YPM 1783	no data (specimen may come from Niobrara Fm., South Dakota, USA, as Wieland was excavating there in 1899)
			Shell fragment (?part of peg-like protrusion of plastron)	X-section	YPM 1783	no data (specimen may come from Niobrara Fm., South Dakota, USA, as Wieland was excavating there in 1899)
49	*Psephophorus* sp.	Fossil	Polygonal armour platelet	L-section	MB.R. 25.321	Boom near Antwerp, Belgium; Genus is known from Miocene of Europe
			"	X-section	MB.R. 25.321	Boom near Antwerp, Belgium; Genus is known from Miocene of Europe
50	*Dermochelys coriacea* (Vandellius, 1761)	Recent	section of integument of juvenile specimen	X- & L-section	QMJ 58751	locality not known
			section of integument & armour plate of subadult specimen	X-section	QMJ 581592	sharks net at the Gold Coast (25th of September 2004)
			isolated armour plate of adult specimen	X-section	QMJ 73979; UQVPI	Moreton Bay, Queensland, Australia
51	*Chelydropsis murchisoni* (Bell, 1832)	Fossil	Costal	X-section	SMNS 88994	middle Miocene (MN7) of Steinheim am Albuch, southern Germany
			"	L-section	SMNS 88994	middle Miocene (MN7) of Steinheim am Albuch, southern Germany
			Peripheral	X-section	SMNS 88995	middle Miocene (MN7) of Steinheim am Albuch, southern Germany
			Peripheral	X-section	SMNS 88996	middle Miocene (MN7) of Steinheim am Albuch, southern Germany
			Plastron fragment (?Hyo- or hypoplastron)	L-section	SMNS 88997	middle Miocene (MN7) of Steinheim am Albuch, southern Germany
52	*Chelydropsis* sp.	Fossil	Peripheral	X-section	IPB HaH-3266	middle Miocene lignite strip mining pit of the company 'Rheinbraun AG', Hambach, Germany
			Free end of rib	L-section	IPB HaH-3486	middle Miocene lignite strip mining pit of the company 'Rheinbraun AG', Hambach, Germany
53	*Chelydra serpentina* (Linnaeus, 1758)	Recent	Neural3	X-section	YPM 10857	Woodbridge, New Haven County, Connecticut, USA. Disarticulated carapax about 40cm; plastron about 25cm long (W. Joyce, pers. commun.)
			Costal3	L-section	YPM 10857	Woodbridge, New Haven County, Connecticut, USA. Disarticulated carapax about 40cm; plastron about 25cm long (W. Joyce, pers. commun.)
			Peripheral3	X-section	YPM 10857	Woodbridge, New Haven County, Connecticut, USA. Disarticulated carapax about 40cm; plastron about 25cm long (W. Joyce, pers. commun.)
			Hyoplastron and hypoplastron	L-section	YPM 10857	Woodbridge, New Haven County, Connecticut, USA. Disarticulated carapax about 40cm; plastron about 25cm long (W. Joyce, pers. commun.)
54	*Platysternon megacephalum* Gray, 1831b	Recent	Neural3	X-section	YPM 12615	locality unknown; pet trade; juvenile specimen; mountainous areas of southern China and adjacent countries down to N Thailand and S Burma
			Costal3	X-section	YPM 12615	locality unknown; pet trade; juvenile specimen; mountainous areas of southern China and adjacent countries down to N Thailand and S Burma
			"	L-section	YPM 12615	locality unknown; pet trade; juvenile specimen; mountainous areas of southern China and adjacent countries down to N Thailand and S Burma
			Peripheral3	X-section	YPM 12615	locality unknown; pet trade; juvenile specimen; mountainous areas of southern China and adjacent countries down to N Thailand and S Burma
			Hypoplastron	L-section	YPM 12615	locality unknown; pet trade; juvenile specimen; mountainous areas of southern China and adjacent countries down to N Thailand and S Burma
			Neural and costal (right)	X-section	SMNS 3757	no data; mountainous areas of southern China and adjacent countries down to N Thailand and S Burma; drilled core, about 22 mm diameter
			Costals	L-section	SMNS 3757	no data; mountainous areas of southern China and adjacent countries down to N Thailand and S Burma; drilled core, about 12 mm diameter
			Hypoplastron (left)	L-section	SMNS 3757	no data; mountainous areas of southern China and adjacent countries down to N Thailand and S Burma; drilled core, about 12 mm diameter

No.	Taxon name	Origin	Shell element	Plane of sectioning	Reference number	Notes and locality
55	Emydidae (?Platysternoid "C")	Fossil	Neural	X-section	UCMP V81092/126372	Eccene Willwood Fm. (Wasatchian), Washakie County, Wyoming, USA; general preservation is poor
			Proximal part of a costal	X-section	UCMP V81092/126432	Eccene Willwood Fm. (Wasatchian), Washakie County, Wyoming, USA; general preservation is poor
			Costal	X-section	UCMP V81092/126432	Eccene Willwood Fm. (Wasatchian), Washakie County, Wyoming, USA; general preservation is poor
			Peripheral	X-section	UCMP V81092/126432	Eccene Willwood Fm. (Wasatchian), Washakie County, Wyoming, USA; general preservation is poor
			Plastron fragment (?Hyo- or hypoplastron)	L-section	UCMP V81092/126432	Eccene Willwood Fm. (Wasatchian), Washakie County, Wyoming, USA; general preservation is poor
56	*Emys orbicularis* (Linnaeus, 1758)	Recent	Neural6, costal6, peripheral8 (left)	X-section	SMNS 6880	no data available; species ranges through most of Europe south to Middle East (i.e., Iran)
			Hyoplastron (right)	X-section	SMNS 6880	no data available; species ranges through most of Europe south to Middle East (i.e., Iran)
57	*Terrapene carolina triunguis* (Agassiz, 1857)	Recent	Neural, costal (right)	X-section	FMNH 211806	no detailed data; ?Kentucky, USA
			Peripheral	X-section	FMNH 211806	no detailed data; ?Kentucky, USA
			Hyo- and hypoplastron (left)	L-section	FMNH 211806	no detailed data; ?Kentucky, USA; drilled core, about 12 mm
58	*Pseudemys peninsularis* Carr, 1938	Recent	Neural3	X-section	YPM 13878	Lakeland, Polk County, Florida, USA (was found dead in the wild)
			Costal3 (right)	L-section	YPM 13878	Lakeland, Polk County, Florida, USA (was found dead in the wild)
			Peripheral4 (right)	X-section	YPM 13878	Lakeland, Polk County, Florida, USA (was found dead in the wild)
			Hypoplastron (left)	X-section	YPM 13878	Lakeland, Polk County, Florida, USA (was found dead in the wild)
59	*Trachemys scripta* (Schoepff, 1792)	Fossil	Neural	X-section	ROM 34287	Pleistocene, Englewood, Charlotte County, Florida, USA
			Costal fragment	X-section	ROM 34289	Pleistocene, Englewood, Charlotte County, Florida, USA
			Peripheral	X-section	ROM 33693	Pleistocene, Sarasota County, Florida, USA
			Hypoplastron (left)	L-section	ROM 33978	Pleistocene, Port Charlotte, Charlotte County, Florida, USA
60	*Rhinoclemmys pulcherrima* (Gray, 1855)	Recent	Costal (right)	L-section	MVZ 230924	locality unknown; Mexico and Central America (Costa Rica, Guatemala, and Honduras); drilled core, about 12 mm diameter, preserved in liquid
			Hyoplastron (right)	L-section	MVZ 230924	locality unknown; Mexico and Central America (Costa Rica, Guatemala, and Honduras); drilled core, about 12 mm diameter, preserved in liquid
61	*Echmatemys wyomingensis* (Leidy, 1869)	Fossil	Neural7	X-section	UCMP V81110/150186	Eccene Bridger Fm., Sweetwater County, Wyoming, USA
			Proximal part of costal8	L-section	UCMP V81110/150183	Eccene Bridger Fm., Sweetwater County, Wyoming, USA
			Proximal part of costal4	X-section	UCMP V81110/150184	Eccene Bridger Fm., Sweetwater County, Wyoming, USA
			Peripheral4	X-section	UCMP V81110/150188	Eccene Bridger Fm., Sweetwater County, Wyoming, USA
			Plastron fragment (?hyo- or hypoplastron)	X-section	UCMP V81110/150225	Eccene Bridger Fm., Sweetwater County, Wyoming, USA
62	*Cyclemys dentata* (Gray, 1831a)	Recent	Neural	X-section	YPM 13290	pet trade specimen, no further data available; East India to Southeast China and south to Malaysia, Phillippines, and ?Indonesia
			Costal3	X-section	YPM 13290	pet trade specimen, no further data available; East India to Southeast China and south to Malaysia, Phillippines, and ?Indonesia
			"	L-section	YPM 13290	pet trade specimen, no further data available; East India to Southeast China and south to Malaysia, Phillippines, and ?Indonesia
			Peripheral3	X-section	YPM 13290	pet trade specimen, no further data available; East India to Southeast China and south to Malaysia, Phillippines, and ?Indonesia
			Hyoplastron (right)	X-section	YPM 13290	pet trade specimen, no further data available; East India to Southeast China and south to Malaysia, Phillippines, and ?Indonesia
63	*Cuora picturata* Lehr et al., 1998	Recent	Neural6	X-section	YPM 13877	pet trade specimen, no further data available; species is restricted to Vietnam and China
			Costal6 (left)	X-section	YPM 13877	pet trade specimen, no further data available; species is restricted to Vietnam and China
			"	L-section	YPM 13877	pet trade specimen, no further data available; species is restricted to Vietnam and China
			Peripheral8	X-section	YPM 13877	pet trade specimen, no further data available; species is restricted to Vietnam and China
			Hyoplastron (right)	X-section	YPM 13877	pet trade specimen, no further data available; species is restricted to Vietnam and China
64	*Mauremys* cf. *M. mutica* (Cantor, 1842)	Recent	Neural3	X-section	SMNS 6876	no data available; species occurs today in southern China, Vietnam, Taiwan, and Japan
			Costal3 (left)	X-section	SMNS 6876	no data available; species occurs today in southern China, Vietnam, Taiwan, and Japan
			Peripheral2 (left)	X-section	SMNS 6876	no data available; species occurs today in southern China, Vietnam, Taiwan, and Japan
			Hyoplastron (right)	X-section	SMNS 6876	no data available; species occurs today in southern China, Vietnam, Taiwan, and Japan
65	*Mauremys* (= '*Ocadia*') *sophiae* (Ammon, 1911)	Fossil	Costal3 (left), proximal part	L-section	IPB HaH-3348	middle Miocene lignite strip mining pit of the company 'Rheinbraun AG', Hambach, Germany [WU 085]
			Peripheral8 (left)	X-section	IPB HaH-3225	middle Miocene lignite strip mining pit of the company 'Rheinbraun AG', Hambach, Germany [WU 1216]
66	*Mauremys* (= *'Ocadia'*) sp.	Fossil	Two sutured costals	L-section	SMNK Me 295	Middle Eocene, Messel pit near Darmstadt, Germany
67	*Ptychogaster* sp.	Fossil	Costal	L-section	SMNS 88988	Lower Miocene (MN1) of Tomerdingen, Germany
			Costal	X-section	SMNS 88989	Lower Miocene (MN1) of Tomerdingen, Germany
			Peripheral	X-section	SMNS 88990	Lower Miocene (MN1) of Tomerdingen, Germany
			Peripheral	X-section	SMNS 88991	Lower Miocene (MN1) of Tomerdingen, Germany
			Plastron fragment (?hyo- or hypoplastron)	X-section	SMNS 88992	Lower Miocene (MN1) of Tomerdingen, Germany
			Plastron fragment (?xiphiplastron)	L-section	SMNS 88993	Lower Miocene (MN1) of Tomerdingen, Germany
68	*Pangshura* (=*Kachuga*) *tentoria* (Gray, 1834)	Recent	Neural4	X-section	FMNH 259431	?Bangladesh, female, no further data
			Costal	X-section	FMNH 259431	?Bangladesh, female, no further data
			"	L-section	FMNH 259431	?Bangladesh, female, no further data
			Peripheral	X-section	FMNH 259431	?Bangladesh, female, no further data
			Xiphiplastron	X-section	FMNH 259431	?Bangladesh, female, no further data

No.	Taxon name	Origin	Shell element	Plane of sectioning	Reference number	Notes and locality
69	*Clemmydopsis turnauensis* (Meyer, 1847b)	Fossil	Costal	X-section	SMNS 88998	Middle Miocene (MN7), Steinheim am Albuch, southern Germany
			Peripheral	X-section	SMNS 88999	Middle Miocene (MN7), Steinheim am Albuch, southern Germany
			Plastron fragment (?hyo- or hypoplastron)	X-section	SMNS 89000	Middle Miocene (MN7), Steinheim am Albuch, southern Germany
			„	L-section	SMNS 89000	Middle Miocene (MN7), Steinheim am Albuch, southern Germany
70	*Hadrianus majusculus* Hay, 1904	Fossil	Neural	X-section	UCMP V74024/150212	Main Body of the Eocene Wasatch Fm. (Wasatchian), Sweetwater County, Wyoming, USA
			Costal	L-section	UCMP V74024/150213	Main Body of the Eocene Wasatch Fm. (Wasatchian), Sweetwater County, Wyoming, USA
			Costal	X-section	UCMP V74024/150214	Main Body of the Eocene Wasatch Fm. (Wasatchian), Sweetwater County, Wyoming, USA
			Plastron fragment	L-section	UCMP V74024/150215	Main Body of the Eocene Wasatch Fm. (Wasatchian), Sweetwater County, Wyoming, USA
			Thick shell fragment	?	UCMP V74024/150216	Main Body of the Eocene Wasatch Fm. (Wasatchian), Sweetwater County, Wyoming, USA
71	*Hadrianus corsoni* (Leidy, 1871a)	Fossil	Peripheral	X-section	UCMP V98009/150191	Eocene Bridger Fm. (Bridgerian), Uinta County, Wyoming, USA
72	*Manouria emys* (Schlegel and Müller, 1844)	Recent	Distal part of costal2 (right)	L-section	FMNH 260395	?Northern Malaysia, no further data; drilled core, about 22 mm diameter
			Hyoplastron (left)	L-section	FMNH 260395	?Northern Malaysia, no further data; drilled core, about 22 mm diameter
73	*Hesperotestudo (Caudochelys) crassiscutata* (Leidy, 1889)	Fossil	Neural	X-section	ROM 51460	Pleistocene (Irvingtonian), Port Charlotte, Charlotte County, Florida, USA
			?Peripheral	X-section	ROM 55400	Pleistocene, Florida, USA
			Costal fragment	L-section	ROM 55400	Pleistocene, Florida, USA
			Xiphiplastron	L-section	ROM 55400	Pleistocene, Florida, USA
74	*Hesperotestudo (Caudochelys) crassiscutata*? (Leidy, 1889)	Fossil	Osteoderm (spiked)	?	ROM 34014	Pleistocene, Grassy Point, Charlotte County, Florida, USA; location on body unknown
75	*Kinixys homeana* Bell, 1827	Recent	Neurals6, 7, hinge, 8	L-section	YPM 13876	juvenile pet trade specimen lacking data; species occurs in forests of West Africa (Liberia to Zaire)
			Costals7, hinge, 8	L-section	YPM 13876	juvenile pet trade specimen lacking data; species occurs in forests of West Africa (Liberia to Zaire)
			Peripherals6, 7, hinge, 8	L-section	YPM 13876	juvenile pet trade specimen lacking data; species occurs in forests of West Africa (Liberia to Zaire)
			Peripheral9	X-section	YPM 13876	juvenile pet trade specimen lacking data; species occurs in forests of West Africa (Liberia to Zaire)
			Hyoplastron	L-section	YPM 13876	juvenile pet trade specimen lacking data; species occurs in forests of West Africa (Liberia to Zaire)
76	*Geochelone pardalis* (Bell, 1828)	Recent	Neural2	X-section	SMNS 12605	confiscated by customs; northeast to southwest Africa (Sudan to South Africa); drilled core, about 12 mm diameter
			Costal2 (right)	L-section	SMNS 12605	confiscated by customs; northeast to southwest Africa (Sudan to South Africa); drilled core, about 12 mm diameter
			Hypoplastron (right)	L-section	SMNS 12605	confiscated by customs; northeast to southwest Africa (Sudan to South Africa); drilled core, about 12 mm diameter
77	*Geochelone carbonaria* (Spix, 1824)	Recent	Proximal part of costal (left)	L-section	IPB R560a	locality unknown (occurs in the Caribbean down to central-east South America); drilled core, about 22 mm diameter, preserved in liquid
			Distal part of costal (left)	L-section	IPB R560b	locality unknown (occurs in the Caribbean down to central-east South America); drilled core, about 22 mm diameter, preserved in liquid
			Hypoplastron (left)	L-section	IPB R560c	locality unknown (occurs in the Caribbean down to central-east South America); drilled core, about 22 mm diameter, preserved in liquid
78	*Geochelone elegans* (Schoepff, 1795)	Recent	Costal (right) and part of neural	X-section	IPB R561a	locality unknown (occurs in peninsular India and Sri Lanka); drilled core, about 22 mm diameter, preserved in liquid
			Hyo- and hypoplastron	L-section	IPB R561b	locality unknown (occurs in peninsular India and Sri Lanka); drilled core, about 22 mm diameter, preserved in liquid
79	*Planetochelys* sp.	Fossil	Neural	X-section	UCMP V81203/130914	Eocene Willwood Fm. (Wasatchian), Washakie County, Wyoming, USA
			Costal, proximal part	L-section	UCMP V81071/159356	Eocene Willwood Fm. (Wasatchian), Washakie County, Wyoming, USA; ?hematite infill
			Costal	X-section	UCMP V81071/159356	Eocene Willwood Fm. (Wasatchian), Washakie County, Wyoming, USA
			Peripheral	X-section	UCMP V81071/159356	Eocene Willwood Fm. (Wasatchian), Washakie County, Wyoming, USA
			Plastron fragment (?hyo- or hypoplastron), hinge	L-section	UCMP V81071/159356	Eocene Willwood Fm. (Wasatchian), Washakie County, Wyoming, USA
			Plastron fragment (?hyo- or hypoplastron), hinge	L-section	UCMP V81071/159356	Eocene Willwood Fm. (Wasatchian), Washakie County, Wyoming, USA
80	*Baptemys garmanii* (Cope, 1872b)	Fossil	Neural	X-section	UCMP V74024/150224	Main Body of the Eocene Wasatch Fm. (Wasatchian), Sweetwater County, Wyoming, USA
			Costal	X-section	UCMP V74024/150219	Main Body of the Eocene Wasatch Fm. (Wasatchian), Sweetwater County, Wyoming, USA
			Costal	L-section	UCMP V74024/150220	Main Body of the Eocene Wasatch Fm. (Wasatchian), Sweetwater County, Wyoming, USA
			Peripheral	X-section	UCMP V74024/150222	Main Body of the Eocene Wasatch Fm. (Wasatchian), Sweetwater County, Wyoming, USA
			Plastron fragment (?Hyo- or hypoplastron)	X-section	UCMP V74024/150221	Main Body of the Eocene Wasatch Fm. (Wasatchian), Sweetwater County, Wyoming, USA
81	*Dermatemys mawii* Gray, 1847	Recent	Costal2 (left) and margin of adjacent costal3	L-section	ZMB 9558	Central America, no further data; specimen from Zoological Garden, Berlin; drilled core, about 22 mm diameter, preserved in liquid
			Hyoplastron (right)	L-section	ZMB 9558	Central America, no further data; specimen from Zoological Garden, Berlin; drilled core, about 22 mm diameter, preserved in liquid
82	*Hoplochelys* sp.	Fossil	Neural	X-section	UCMP V2811/150210	Palaeocene Nacimiento Fm. (Puercan), San Juan County, New Mexico, USA
			Costal	X-section	UCMP V2811/150203	Palaeocene Nacimiento Fm. (Puercan), San Juan County, New Mexico, USA
			Costal	L-section	UCMP V2811/150204	Palaeocene Nacimiento Fm. (Puercan), San Juan County, New Mexico, USA
			Peripheral3 (right)	X-section	UCMP V2811/150207	Palaeocene Nacimiento Fm. (Puercan), San Juan County, New Mexico, USA
			Peripheral8 (left)	X-section	UCMP V2811/150206	Palaeocene Nacimiento Fm. (Puercan), San Juan County, New Mexico, USA
			Plastron fragment (?Hyo- or hypoplastron)	L-section	UCMP V2811/150208	Palaeocene Nacimiento Fm. (Puercan), San Juan County, New Mexico, USA
83	*Baltemys* sp.	Fossil	Neural	X-section	UCMP V78106/122542	Eocene Willwood Fm. (Wasatchian), Big Horn County, Wyoming, USA; strong diagenetic alteration (like an aquarelle)
			Costal	L-section	UCMP V78106/122542	Eocene Willwood Fm. (Wasatchian), Big Horn County, Wyoming, USA; strong diagenetic alteration (like an aquarelle)
			Costal	X-section	UCMP V78106/122542	Eocene Willwood Fm. (Wasatchian), Big Horn County, Wyoming, USA; strong diagenetic alteration (like an aquarelle)
			Peripheral	X-section	UCMP V78106/122545	Eocene Willwood Fm. (Wasatchian), Big Horn County, Wyoming, USA
			Plastron fragment	L-section	UCMP V78106/122545	Eocene Willwood Fm. (Wasatchian), Big Horn County, Wyoming, USA
			„	X-section	UCMP V78106/122545	Eocene Willwood Fm. (Wasatchian), Big Horn County, Wyoming, USA

No.	Taxon name	Origin	Shell element	Plane of sectioning	Reference number	Notes and locality
84	*Sternotherus minor* (Agassiz, 1857)	Recent	Neural	X-section	SMNS 6879	no data available; species occurs in southeastern North America
			Costal	X-section	SMNS 6879	no data available; species occurs in southeastern North America
			Peripheral	X-section	SMNS 6879	no data available; species occurs in southeastern North America
			Hyoplastron (right)	X-section	SMNS 6879	no data available; species occurs in southeastern North America
85	*Kinosternon subrubrum* (Bonnaterre, 1789)	Recent	Neural3	X-section	YPM 13875	?New Orleans, Louisiana, USA (was caught in the wild)
			Costal3	L-section	YPM 13875	?New Orleans, Louisiana, USA (was caught in the wild)
			"	X-section	YPM 13875	?New Orleans, Louisiana, USA (was caught in the wild)
			Peripheral3	X-section	YPM 13875	?New Orleans, Louisiana, USA (was caught in the wild)
			Hyoplastron (left)	L-section	YPM 13875	?New Orleans, Louisiana, USA (was caught in the wild)
86	*Kinosternon* sp.	Recent	Costal2 (right)	L-section	SMNS 7440	no data available; from Eastern North America S/SW to northern South America; drilled core, about 22 mm diameter, preserved in liquid
			Hinge, epi- & hyoplastron (right)	L-section	SMNS 7440	no data available; from Eastern North America S/SW to northern South America; drilled core, about 22 mm diameter, preserved in liquid
			Hinge, hypo- & xiphiplastron (right)	L-section	SMNS 7440	no data available; from Eastern North America S/SW to northern South America; drilled core, about 22 mm diameter, preserved in liquid
87	*Adocus* sp.	Fossil	Neural	X-section	UCMP V73096/150202	Early Palaeocene (Puercan), Tullock Fm., Garfield County, Montana, USA
			Proximal part of a costal	L-section	UCMP V87101/150200	Early Palaeocene (Puercan), Hell Creek Fm., McCone County, Montana, USA
			"	X-section	UCMP V87101/150200	Early Palaeocene (Puercan), Hell Creek Fm., McCone County, Montana, USA
			Distal peripheral fragment	X-section	UCMP V87101/150201	Early Palaeocene (Puercan), Hell Creek Fm., McCone County, Montana, USA
			Plastron fragment (?Hyo- or hypoplastron)	L-section	UCMP V87071/150192	Early Palaeocene (Puercan), Hell Creek Fm., McCone County, Montana, USA
88	*Basilemys* sp.	Fossil	Neural fragment	X-section	FM P27371	Kirtland Shale, Late Cretaceous, McKinley County, New Mexico, USA; proposed reassignment to "Trionychidae indet."
			Costal fragment	L-section	FM P27371	Kirtland Shale, Late Cretaceous, McKinley County, New Mexico, USA; proposed reassignment to "Trionychidae indet."
			Peripherals with suture	L-section	FM P27371	Kirtland Shale, Late Cretaceous, McKinley County, New Mexico, USA
			Fragment from periphery of shell	?	FM P27371	Kirtland Shale, Late Cretaceous, McKinley County, New Mexico, USA
			Shell fragment with suture	?	FM P27371	Kirtland Shale, Late Cretaceous, McKinley County, New Mexico, USA
			Peripheral	X-section	YPM 9703	Cretaceous Laramie Beds, Schneider Cn., Converse County, Wyoming, USA; was assigned to „Adocus vigoratus" in the YPM collections
			Plastron fragment (?Hyo- or hypoplastron)	L-section	FM P27371	Kirtland Shale, Late Cretaceous, McKinley County, New Mexico, USA
			Ostzoderm (ridged form with three spikes)	Long axis	TMP 2003.12.278	Judith River Group, Dinosaur Provincial Park, Alberta, Canada
			Ostzoderm (single spike)	Long axis	TMP 80.08.296	?Oldman Fm. or Dinosaur Park Fm., Judith River Group, Dinosaur Provincial Park, Alberta, Canada
89	*Anosteira* sp.	Fossil	Neural and costal	X- & L-section	FM PR 819	Uinta Fm. (horizon C, lower part), Late Eocene, Uintah County, Utah, USA
			Costal	L-section	FM PR 819	Uinta Fm. (horizon C, lower part), Late Eocene, Uintah County, Utah, USA
			"	X-section	FM PR 819	Uinta Fm. (horizon C, lower part), Late Eocene, Uintah County, Utah, USA
			Peripheral	X-section	FM PR 819	Uinta Fm. (horizon C, lower part), Late Eocene, Uintah County, Utah, USA
			Hypoplastron (left)	L-section	FM PR 819	Uinta Fm. (horizon C, lower part), Late Eocene, Uintah County, Utah, USA
			"	X-section	FM PR 819	Uinta Fm. (horizon C, lower part), Late Eocene, Uintah County, Utah, USA
90	*Pseudanosteira pulchra* Clark, 1932	Fossil	Neural	X-section	UCMP V78031/131731	Turtle Butte Anosteirire Bed, Eocene Washakie Fm. (Uintan), Sweetwater County, Wyoming, USA; see mineral infill
			Costal, proximal part	L-section	UCMP V78031/131731	Turtle Butte Anosteirire Bed, Eocene Washakie Fm. (Uintan), Sweetwater County, Wyoming, USA
			Costal	X-section	UCMP V78031/131731	Turtle Butte Anosteirire Bed, Eocene Washakie Fm. (Uintan), Sweetwater County, Wyoming, USA
			Peripheral	X-section	UCMP V78031/131731	Turtle Butte Anosteirire Bed, Eocene Washakie Fm. (Uintan), Sweetwater County, Wyoming, USA
			Plastron fragment	L-section	UCMP V78031/131731	Turtle Butte Anosteirire Bed, Eocene Washakie Fm. (Uintan), Sweetwater County, Wyoming, USA
			"	X-section	UCMP V78031/131731	Turtle Butte Anosteirire Bed, Eocene Washakie Fm. (Uintan), Sweetwater County, Wyoming, USA
91	*Allaeochelys* cf. *A. crassesculpta* (Harrassowitz, 1922)	Fossil	Costal	X-section	HLMD-Me 10468	Middle Eocene, Messel pit near Darmstadt, Germany
			Peripheral	L-section	HLMD-Me 10468	Middle Eocene, Messel pit near Darmstadt, Germany
			Peripheral	X-section	HLMD-Me 10468	Middle Eocene, Messel pit near Darmstadt, Germany
92	*Carettochelys insculpta* Ramsay, 1887	Recent	Neural	X-section	MAGNT R12640	locality unknown; species is restricted to New Guinea and Northern Territory of Australia
			Costal	L-section	MAGNT R12640	locality unknown; species is restricted to New Guinea and Northern Territory of Australia
			Peripheral	X-section	MAGNT R12640	locality unknown; species is restricted to New Guinea and Northern Territory of Australia
			Hyoplastron (left)	L-section	MAGNT R12640	locality unknown; species is restricted to New Guinea and Northern Territory of Australia
93	*Plastomenus* sp.	Fossil	Neural	X-section	UCMP V81108/150227	Eocene Bridger Fm., Sweetwater County, Wyoming, USA; poor preservation, see mineral infill
			Costal	X-section	UCMP V81110/150231	Eocene Bridger Fm., Sweetwater County, Wyoming, USA; poor preservation, see mineral infill
			Costal, distal part	L-section	UCMP V81110/150231	Eocene Bridger Fm., Sweetwater County, Wyoming, USA; poor preservation, see mineral infill
			Costal, proximal part	L-section	UCMP V81108/150227	Eocene Bridger Fm., Sweetwater County, Wyoming, USA; poor preservation, see mineral infill
			Costal	L-section	UCMP V81108/150227	Eocene Bridger Fm., Sweetwater County, Wyoming, USA; poor preservation, see mineral infill
			Plastron fragment	X-section	UCMP V81108/150227	Eocene Bridger Fm., Sweetwater County, Wyoming, USA; poor preservation, see mineral infill
			"	L-section	UCMP V81108/150227	Eocene Bridger Fm., Sweetwater County, Wyoming, USA; poor preservation, see mineral infill
94	*Helopanoplia* sp.	Fossil	Distal costal fragment	L-section	UCMP V87051/150193	Hell Creek Fm., Puercan (Uppermost Cretaceous?), McCone County, Montana, USA; pyrite infill

No.	Taxon name	Origin	Shell element	Plane of sectioning	Reference number	Notes and locality
95	*Lissemys punctata* (Bonnaterre, 1789)	Recent	?Neural3 and part of costals	X-section	SMNS 3705	occurs today in India and adjacent countries (e.g. Pakistan, Nepal, Bangladesh, Sri Lanka); drilled core, about 12 mm diameter, preserved in liquid
			Neural	X-section	YPM 11645	occurs today in India and adjacent countries (e.g. Pakistan, Nepal, Bangladesh, Sri Lanka)
			Costal3	X-section	YPM 11645	occurs today in India and adjacent countries (e.g. Pakistan, Nepal, Bangladesh, Sri Lanka)
			"	L-section	YPM 11645	occurs today in India and adjacent countries (e.g. Pakistan, Nepal, Bangladesh, Sri Lanka)
			Posterior peripheral bone	X-section	YPM 11645	occurs today in India and adjacent countries (e.g. Pakistan, Nepal, Bangladesh, Sri Lanka)
			Plastron fragment (?Hyo- or hypoplastron)	X-section	YPM 11645	occurs today in India and adjacent countries (e.g. Pakistan, Nepal, Bangladesh, Sri Lanka)
			"	L-section	YPM 11645	occurs today in India and adjacent countries (e.g. Pakistan, Nepal, Bangladesh, Sri Lanka)
96	*Cyclanorbis senegalensis* (Duméril and Bibron, 1835)	Recent	Costal	L-section	ZFMK-83284	occurs today in Central Africa (Sudan, Cameroon, Gabon, Senegal, and Ghana)
97	*Aspideretoides foveatus* (Leidy, 1856c)	Fossil	Neural	X-section	TMP 81.20.30	?Oldman Fm. or Dinosaur Park Fm., Judith River Group, Dinosaur Provincial Park, Alberta, Canada
98	*Aspideretoides splendidus* (Hay, 1908)	Fossil	Neural	X-section	TMP 89.116.61	?Oldman Fm. or Dinosaur Park Fm., Judith River Group, Onefour area, SE Alberta, Canada
			Costals	L-section	TMP 89.116.61	?Oldman Fm. or Dinosaur Park Fm., Judith River Group, Onefour area, SE Alberta, Canada
			Plastron fragment	X-section	TMP 89.116.61	?Oldman Fm. or Dinosaur Park Fm., Judith River Group, Onefour area, SE Alberta, Canada
			Plastron fragment (bony peg)	X-section	TMP 89.116.61	?Oldman Fm. or Dinosaur Park Fm., Judith River Group, Onefour area, SE Alberta, Canada
99	cf. *Aspideretoides* sp.	Fossil	Neural	X-section	IPB R533d	Judith River Group, Kennedy Coulee, N of Goldstone, MT, USA
			Costal	X-section	IPB R533a	Judith River Group, Kennedy Coulee, N of Goldstone, MT, USA
			"	planar	IPB R533b	Judith River Group, Kennedy Coulee, N of Goldstone, MT, USA
			"	L-section	IPB R533c	Judith River Group, Kennedy Coulee, N of Goldstone, MT, USA; perpendicular to IPB R533a
			Costal with suture	planar	IPB R533e	Judith River Group, Kennedy Coulee, N of Goldstone, MT, USA; angled cut through plywood-like structure and sutures
100	*Apalone ferox* (Schneider, 1783)	Recent	Neural5	X-section	YPM 13874	no data; species occurs in Florida and parts of adjacent states (South Carolina, Georgia, and Alabama) of south-eastern USA
			Costal5 (left)	X-section	YPM 13874	no data; species occurs in Florida and parts of adjacent states (South Carolina, Georgia, and Alabama) of south-eastern USA
			"	L-section	YPM 13874	no data; species occurs in Florida and parts of adjacent states (South Carolina, Georgia, and Alabama) of south-eastern USA
			Xiphiplastron (right)	L-section	YPM 13874	no data; species occurs in Florida and parts of adjacent states (South Carolina, Georgia, and Alabama) of south-eastern USA
101	*Trionyx triunguis* (Forskål, 1775)	Recent	Costal2 (right)	L-section	IPB R260	juvenile specimen; no further data; species occurs at the coasts of east Mediterranean states (from Turkey southwards) to East- and West Africa
			"	X-section	IPB R260	juvenile specimen; no further data; species occurs at the coasts of east Mediterranean states (from Turkey southwards) to East- and West Africa
102	*Trionyx* sp.	Fossil	Costal	L-section	HLMD-Me 8084	Middle Eocene, Messel pit near Darmstadt, Germany; poor preservation
			Costal	L-section	IPB Hal-3120	middle Miocene lignite strip mining pit of the company 'Rheinbraun AG', Hambach, Germany
			Costal	L-section	IPB Hal-3164	middle Miocene lignite strip mining pit of the company 'Rheinbraun AG', Hambach, Germany
			Plastron fragment	?	SMNS 86264	Lower Miocene (MN4b), Langenau 2, (roadcut during development of highway A2; insection Lettenberg), Germany
	Additional soft-tissue samples					
1	*Amyda cartilaginea*	Recent	Periphery of carapace	Transverse	ZFMK-14040	Additional soft tissue samples of trionychid integument
2	*Apalone ferox emoryi*	Recent	Periphery of carapace	Transverse	ZFMK-47482	Additional soft tissue samples of trionychid integument
3	*Aspideretes gangeticus*	Recent	Periphery of carapace	Transverse	ZFMK-13563	Additional soft tissue samples of trionychid integument
4	*Cyclanorbis senegalensis*	Recent	Periphery of carapace	Transverse	ZFMK-83284	Additional soft tissue samples of trionychid integument
5	*Dogania subplana*	Recent	Periphery of carapace	Transverse	ZFMK-65847	Additional soft tissue samples of trionychid integument
6	*Lissemys punctata*	Recent	Periphery of carapace	Transverse	YPM 10882	Additional soft tissue samples of trionychid integument
		Recent	Periphery of carapace	Transverse	YPM 11645	Additional soft tissue samples of trionychid integument
		Recent	Periphery of carapace	Transverse	YPM 13153	Additional soft tissue samples of trionychid integument
7	*Palea steindachneri*	Recent	Periphery of carapace	Transverse	ZFMK-81541	Additional soft tissue samples of trionychid integument
8	*Pelodiscus sinensis*	Recent	Periphery of carapace	Transverse	ZFMK-58971	Additional soft tissue samples of trionychid integument
9	*Rafetus euphraticus*	Recent	Periphery of carapace	Transverse	ZFMK-13938	Additional soft tissue samples of trionychid integument

No.	Taxon name	Origin	Shell element	Plane of sectioning	Reference number	Notes and locality
	Outgroup 1: Temnospondyl amphibians (n=3 taxa)					
1	*Mastodonsaurus giganteus* (Jaeger, 1828)	Fossil	Bone fragment (?cranium/shoulder girdle)	Long axis	SMNS 91011	Kupferzell, southern Germany (Erfurt-Formation, Ladinian, Upper Triassic, 'Lettenkeuper')
			"	Short axis	SMNS 91011	Kupferzell, southern Germany (Erfurt-Formation, Ladinian, Upper Triassic, 'Lettenkeuper')
2	*Gerrothorax pustuloglomeratus* (Huene, 1922)	Fossil	Bone fragment (?cranium/shoulder girdle)	Short axis	SMNS 91012	Kupferzell, southern Germany (Erfurt-Formation, Ladinian, Upper Triassic, 'Lettenkeuper')
			"	Long axis	SMNS 91012	Kupferzell, southern Germany (Erfurt-Formation, Ladinian, Upper Triassic, 'Lettenkeuper')
3	*Trimerorhachis* sp.	Fossil	smaller sculptured bone fragment (?shoulder girdle)	Long axis	TMM 40031-59	smaller osteoderm (Temnospondyli); Tit Mountain locality, Archer County, Texas, USA (Petrolia Formation, Lower Permian)
			larger sculptured bone fragment (?shoulder girdle)	Long axis	TMM 40031-60	larger osteoderm (Temnospondyli); Tit Mountain locality, Archer County, Texas, USA (Petrolia Formation, Lower Permian)
	Outgroup 2: Mammalia (n=3 taxa)					
4	*Paramylodon harlani* (Owen, 1840)	Fossil	Osteoderm		TMM 30967-1006	see Wolf (2006; unpubl. MSc-thesis) for further information
			Osteoderm		TMM 30967-2632	see Wolf (2006; unpubl. MSc-thesis) for further information
5	*Propalaehoplophorus* sp.	Fossil	Osteoderm		IPB M6444	see Wolf (2006; unpubl. MSc-thesis) for further information
			Osteoderm		IPB M6151	see Wolf (2006; unpubl. MSc-thesis) for further information
6	*Glyptodon clavipes* Owen, 1839	Fossil	Two osteoderms of fused part of carapace		YPM 12214	see Wolf (2006; unpubl. MSc-thesis) for further information
	Outgroup 3: non-testudinatan Reptilia (n=12 taxa)					
	Pareiasauria (Parareptilia)					
7	*Bradysaurus seeleyi* Haughton and Boonstra, 1929	Fossil	Osteoderm fragment		SAM-PK-8941	mainly a carbonate rock with little cancellous bone preserved at margin; Mynhardtskraal, Beaufort West District, South Africa; Permian
8	*Bradysaurus* sp.	Fossil	Osteoderm		SAM-PK-12140	margins of osteoderm are partly damaged; external bone surface convex and knoblike; Rietfontein, Prince Albert District, South Africa; Permian
			Osteoderm		SAM-PK-4348	osteoderm fragment fused to skull bone?; Wilgerfontein, Prince Albert District, South Africa; Permian
9	*Pareiasaurus serridens* Owen, 1876	Fossil	Osteoderm		SAM-PK-10036	excavated osteoderm; Late Permian locality Farm127, near Doornplaats, Graaff-Reinet District, South Africa
10	*Pareiasaurus* sp.	Fossil	Osteoderm		UMZC R 381 T702	flat osteoderm; Tapinocephalus zone (Late Permian), Hottentots River, Prince Albert District, South Africa [D. M. S. Watson Collection]
			Osteoderm		SAM-PK-1058	flat small osteoderm still in sediment; Welgevonden, Graaff-Reinet District, South Africa; Permian
			Two osteoderms		SAM-PK-1058	two flat osteoderms separated by sediment; Welgevonden, Graaff-Reinet District, South Africa; Permian
11	*Anthodon serrarius* Owen, 1876	Fossil	Osteoderm		SAM-PK-10074	osteoderm mostly free of sediment; Late Permian locality of Dunedin, Beaufort West District, South Africa
			Osteoderm		SAM-PK-10074	osteoderm mostly free of sediment; Late Permian locality of Dunedin, Beaufort West District, South Africa
	Placodontia (Sauropterygia)					
12	*Placodus gigas* Agassiz, 1833	Fossil	Armour plate	Short axis	SMNS 91006	Bühlingen near Rottweil, Germany (?Trochitenkalk Formation, Ladinian, Middle Triassic, 'Upper Muschelkalk; Lower Hauptmuschelkalk', ?m7)
13	*Psephosaurus suevicus* Fraas, 1896	Fossil	Armour plate	Long axis	SMNS 91007	Erfurt Formation (Ladinian, Middle Triassic, k1), Hoheneck near Ludwigsburg, Germany; also used for SEM
			Armour plate (procumbent spiked plate)	Long axis	MHI 1426/1	Erfurt Formation (Ladinian, Middle Triassic, k1, "Anthrakonit-Bank, Basisbonebed"); quarry "Hohenloher Steinwerk", Kirchberg/Jagst, Germany
			Armour plate (large hexagonal plate)	Long axis	MHI 1426/2	Erfurt Formation (Ladinian, Middle Triassic, k1, "Anthrakonit-Bank, Basisbonebed"); quarry "Hohenloher Steinwerk", Kirchberg/Jagst, Germany
			Armour plate (small hexagonal plate)	Long axis	MHI 1426/3	Erfurt Formation (Ladinian, Middle Triassic, k1, "Anthrakonit-Bank, Basisbonebed"); quarry "Hohenloher Steinwerk", Kirchberg/Jagst, Germany
14	*Psephosaurus* sp.	Fossil	Armour plate (hexagonal plate, from carapace?)	Long axis	SMNS 91008	Erfurt Formation (Ladinian, Middle Triassic, k1), Hoheneck near Ludwigsburg, Germany
			Armour plate (rhomboidal plate, from plastron?)	Short axis	SMNS 91009	Erfurt Formation (Ladinian, Middle Triassic, k1), Hoheneck near Ludwigsburg, Germany
15	cf. *Placochelys* sp.	Fossil	Armour plate (procumbent spiked plate)	Long axis	SMNS 91010	Grabfeld Formation (Lower Karnian, Upper Triassic, 'Estherienschichten, Anatinabank' k2), Willsbach near Heilbronn, Germany
16	*Psephoderma* sp.	Fossil	Row of four fused armour plates	Long axis	NRM-PZ R.1759a	Middle Triassic ('Muschelkalk') Wadi Raman (Makhtesh Ramon), Negev, Israel
	Archosauromorpha (Diapsida)					
17	cf. *Mystriosuchus* sp.	Fossil	Osteoderm	Short axis	SMNS 91013	Triassic, Heslach near Stuttgart, Germany
18	*Steneosaurus* sp.	Fossil	Osteoderm	Short axis	NMS 7152	Upper Jurassic (Kimmeridgian) 'turtle-limestone' quarries, Solothurn, Switzerland

Appendix 2: Glossary and general abbreviations

Terms and abbreviations associated with the bony turtle shell (after Zangerl, 1969)

br: bridge – lateral transition between carapace and plastron

carap: carapace – dorsal dome of the shell consisting usually of about fifty bones

co: costal – bony plate associated with ribs

ento: entoplastron – single element framed by epiplastra and hyoplastra often with dorsal bony spur pointing towards posterior

ep: epithecal platelets – small bone plates of the secondary (epithecal) armour of turtles

epi: epiplastron – paired anterior-most elements of the plastron

hyo: hyoplastron – paired elements between anterior epiplastra/entoplastron and posterior hypoplastra; lateral anterior part of bridge in plastron

hypo: hypoplastron – paired elements between anterior hyoplastra and posterior xiphiplastra; lateral posterior part of bridge in plastron

meso: mesoplastron – additional paired elements between hyo- and hypoplastra; two pairs of mesoplastra present only in basal-most genera (e.g., *Proganochelys*, *Proterochersis*); one pair of mesoplastra present only in Mesozoic and early Cenozoic forms (e.g., Paracryptodira); lost in modern forms

n: neural – bony plate associated with neural arches of the vertebrae

nu: nuchal – medial anterior-most plate of the carapace; broad, laterally flaring element in trionychid turtles

p: peripheral – wedge-shaped plates at the lateral margin of the carapace; the ‘bridge peripherals’ constitute the carapacial part of the bridge

pl: plastron – flattened ventral part of the shell usually consisting of nine bones

pyg: pygal – medial posterior-most plate of the carapace

r: rib – ribs can be more or less incorporated in the costal plates of the shell; peripherals often carry a groove to accommodate the free rib end of the respective costal

spyg: suprapygal – 1 or 2 plates anterior to the pygal; posterior to the neurals

xiphi: xiphiplastron – posterior-most paired elements of plastron

Measurements of the turtle shell (after Wyneken, 2001)

BD: body depth – measures the maximum body height with callipers from ventral-most point of plastron to dorsal-most point of carapace

C: cuticule – thick leathery epidermal layer external to the dermis

CCL: curved carapace length; measures the length over the curvature of the carapace between midpoint of nuchal to posterior-most point of carapace

CCW: curved carapace width – widest span of carapace measured over the curvature of the shell

CL: carapace length – measured either as CCL (with flexible measure tape) or SCL (with callipers); CCL is slightly larger than SCL

CPL: curved plastron length – measures the length over the curvature from anterior-most end to posterior-most end

CW: carapace width - measured either as CCW (with flexible measure tape) or SCW (with callipers); CCW is slightly larger than SCW

PL: plastron length –measured either as CPL (with flexible measure tape) or SPL (with callipers); CPL is slightly larger than SPL

SCL: straightline carapace length – measures the straight length of the carapace between midpoint of nuchal to posterior-most point of carapace

SCW: straightline carapace width – widest span of carapace measured in a straight line between the lateral-most peripherals of the shell

SPL: straightline plastron length – measured straight from anterior-most end to posterior-most end

TCL: total caudal length – series of caudal vertebrae; ideally measures the length from the first caudal vertebra to the tip of tail; TCL can only be measured if complete set of caudals is present, otherwise length measurements are given just for the caudals present

TTL: total tail length – in live turtles: length between the posterior-most tip of plastron to tip of tail

Histological terms and abbreviations used in text and figures (after Francillon-Vieillot et al., 1990 and works herein; Scheyer and Sander, 2004; Scheyer et al., 2007)

BS: bone spiculae – small sheet or rod-like protrusions of bone tissue

CB: cancellous bone – area build by meshwork of bone trabeculae between external and internal layers of compact bone

CHL: chondrocyte lacunae – small areas that are occupied by chondrocytes in the living bone

CL: bone cell lacunae – small areas that are occupied by osteocytes in the living bone; can either be empty or filled with minerals in fossil bone

CO: cortical bone – layer of compact bone; usually avascular or with low vascularisation

CT: connective tissue – major tissue in the body used for connection, support, binding or separation of other tissues or organs; in the integument, the CT has high amounts of collagen and elastic fibres

D: dermis (= corium) – layer of the integument between the epidermis and the subcutis

EC: erosion cavities – sometimes vermicular, secondary tube-like erosional spaces within the bone

ECO: external cortex – external layer of compact bone outwardly framing cancellous bone

FB: collagenous fibre bundles – organisation of numerous collagen fibres into tubular bundles; major structural elements of the connective tissue

lsFB: longitudinally sectioned fibre bundle

trFB: longitudinally sectioned fibre bundle

FBQ: collagenous fibre bundle quadrangles – special arrangement of FB into elongated rectangles within the plywood-like structure of the corium of Trionychidae

FCa: calcified fibrocartilaginous tissue, calcified fibrous cartilage

GM: growth marks – all kinds of variation in growth rates recorded in hard tissues, e.g., lines of arrested growth in bone

HC: Haversian canal – canal in the centre of a secondary osteon

ICO: internal cortex – internal layer of compact bone; inwardly framing cancellous bone

ISF: interwoven structural collagenous fibre bundles – texture of metaplastically ossified connective tissue where SF trend in different spatial (horizontal, diagonal and perpendicular) directions

KS: keratinous shield –usually consisting of several layers of keratin; develops by the uppermost layer of the integument, the epidermis, in turtles and other reptiles

LB: lamellar bone – bone matrix with high spatial organisation; thin alternate lamellae with orthogonal plywood or as twisted plywood pattern; usually occur as thin light and dark layering in polarised light; typically found in the centripetally concentric seams of secondary osteons or secondary trabecular bone; usually attributed to slow osteogenesis

OP: ornamentation pattern – all kinds of raised or caved in ornamentation or embossment compared to a general level of outer compact bone

PATH: pathology – area with abnormal bone growth; areas are usually affected by diseases (e.g., bacterial or fungal infection) or malformed through inadequate nutrition

PC: primary vascular canal – vascular canal without surrounding bone lamellae

PFB: Parallel-fibred bone – bone matrix with moderate spatial organisation; FB arranged primarily parallel to each other; usually attributed with moderate osteogenetic rates intermediate between those of lamellar bone and woven bone.

PO: primary osteon – vascular canal surrounded by concentric bone lamellae; no line of resorption

SF: structural collagenous fibre bundles – collagenous fibre bundles responsible for the texture of a respective connective tissue

ShF: Sharpey's fibres – soft connective tissue attachments (e.g., muscle, tendons, ligaments, dermis) within mineralised skeletal tissue

SO: secondary osteon – synonymous to Haversian system; erosional lacunae secondarily filled with centripetally deposited concentric bone lamellae; always delimited by line of resorption; vascular canal in the centre of the SO is called Haversian canal

SOC: secondary osteon cluster – small area of bone remodelling with few subsequent generations of secondary osteons; initial stage of Haversian bone formation

SR: synthetic resin – chemical substance used to glue, saturate and stabilise bone for histological thin-sections; i.e. Araldite 2020®

St. c.: stratum compactum – lower layer of the corium of the reptile integument

St. l.: stratum laxum – upper layer of the corium of the reptile integument

TR: bone trabeculae – spongy meshwork of bony pillars and struts

VCR: roof of vertebral canal– internal cortical bone layer of the neural arch that dorsally and laterally encloses the spinal cord

Terms associated with keratinous shields covering the bony shell (after Zangerl, 1969)

abdominal – paired shield anterior to the femorals and posterior to the pectorals; covers most of the hypoplastron (and mesoplastron if present)

anal – posterior-most pair of shields; covers mostly part of xiphiplastron

axillary – paired shield at the anterior part of bridge region; covers part of the axillary buttress of the hyoplastron

cervical – single medial anterior-most shield, anterior to the vertebrals; covers part of the nuchal

femoral – pair of shields between the posterior anal shields and anterior abdominal shields; covers mostly the posterior part of the hypoplastron and the anterior part of the xiphiplastron

gular – anterior-most pair of shields if intergular shields are not present; covers mostly the epiplastra and the entoplastron

humeral – paired shield posterolateral to the gular shields and anterior to the pectorals; covers most of the anterior part of the hyoplastron

inframarginal – additional row of shields between the axial and inguinal shields

inguinal – paired shield at the posterior part of bridge region; covers part of the inguinal buttress of the hyoplastron

intergular – additional pair of shields that may occur anterior to the gular shields

marginal – lateral rows of usually twelve shields mostly covering the peripherals and the nuchal

pectoral – pair of shields between the posterior abdominals and anterior humerals; mostly covers posterior part of the hyoplastron

pleural – paired row of usually four shields between the vertebrals and the marginal/supramarginals; covering most part of costals

sulcus – impression of the rim of the keratinous shield into the surface of the underlying bone

supramarginal – additional paired rows of lateral shields between marginals and vertebrals; occur only in some taxa (e.g., Baenidae; Pleurosternidae)

vertebral – single median row of usually five shields covering the neurals and proximal part of costals

General terms associated with the reptile integument (after Lange, 1931)

corium (= dermis, = Lederhaut) – intermediate layer of the integument between the epidermal layers and the subcutis; can generally be subdivided into an upper stratum laxum and a lower stratum compactum

epidermis – uppermost keratinous layers of the integument, topping the corium

stratum compactum – lower layer of the corium usually built of horizontally trending, interwoven collagenous fibre bundles; the fibre bundles can either be arranged quite regularly or felt-like

stratum laxum – upper layer of the corium of more loosely interwoven collagenous fibre bundles, with many fibre bundles trending diagonal or perpendicular to the skin surface; elastic fibres may be present

subcutis – lowest layer of the integument separating the corium from the underlying musculature

Appendix 3: Ecological characterisation of turtles

Category I (terrestrial)

*Proganochelys quenstedti B*aur, 1887 (†); *Proterochersis robusta,* Fraas, 1913 (†); *Kayentachelys* sp. (†); *Meiolania* sp. (†); Solemydidae gen. et sp. indet. (aff. *Naomichelys* sp.) (†); *Terrapene carolina triunguis* (Agassiz, 1857); *Pangshura* (=*Kachuga*) *tentoria* (Gray, 1834); *Manouria emys* (Schlegel and Müller, 1844), *Geochelone pardalis* (Bell, 1828), *Geochelone elegans* (Schoepff, 1795); *Basilemys* sp. (†); **tendencies to category II**: *Cuora picturata* Lehr et al., 1998, *Mauremys cf. M. mutica* (Cantor, 1842); *Hesperotestudo* (*Caudochelys*) *crassiscutata* (Leidy, 1889) (†); *Planetochelys* sp. (†)

Category II (semiaquatic to mainly aquatic)

Tendencies to category I: *Pelomedusa subrufa* (Bonnaterre, 1789); cf. *Bairdemys* sp. (†); *Podocnemis erythrocephala*(Spix, 1824); *Stupendemys geographicus*Wood, 1976 (†); *Chelodina longicollis* (Shaw, 1794); *Platemys platycephala* (Schneider, 1791); *Phrynops geoffroanus* (Schweigger, 1812); *Hydromedusa tectifera* Cope, 1870a; *Glyptops plicatulus* (Cope, 1877) (†);*Compsemys* sp. (†); Pleurosternidae gen. et sp. indet. (†); Pleurosternidae gen. et sp. indet. ('Platychelyid histomorph A') (†); Pleurosternidae gen. et sp. indet. ('Kirtlington histomorph I') (†);Cryptodira incertae sedis ('Kirtlington histomorph II') (†); *Neurankylus* sp. (†); *Plesiobaena* sp. (†); *Pseudemys peninsularis* Carr, 1938; Emydidae indet. (?Platysternoid "C") (†); *Mauremys* (= '*Ocadia*') *sophiae* (Ammon, 1911) (†); *Mauremys* (='*Ocadia*') sp. (†); *Cyclemys dentata* (Gray, 1831a); *Rhinoclemmys pulcherrima* (Gray, 1855); *Geochelone carbonaria* (Spix, 1824); *Kinixys homeana* Bell, 1827; *Adocus* sp. (†);*Plastomenus* sp. (†); *Helopanoplia* sp. (†); *Lissemys punctata* (Bonnaterre, 1789); *Cyclanorbis senegalensis* (Duméril and Bibron, 1835); *Aspideretoides foveatus* (Leidy, 1856c) (†); *Aspideretoides splendidus* (Hay, 1908) (†); cf. *Aspideretoides* sp. (†); *Apalone ferox* (Schneider, 1783); *Trionyx triunguis* (Forskål, 1775); *Trionyx* sp. (†) **main bulk of category II**: *Platychelys oberndorferi* Wagner, 1853 (†); *Foxemys* cf. *F. mechinorum'* Tong et al., 1998 (†); *Emydura subglobosa* (=*Emydura albertisii*) (Krefft, 1876); *Emydura* sp. (†); *Chelus fimbriatus* (Schneider, 1783); *Boremys* sp. (†); *Chisternon* sp. (†);*Tropidemys* sp. (†); *Xinjiangchelys chowi* Matzke et al., 2005 (†); *Xinjiangchelys* sp. (†); *Wuguia efremovi*

Khosatzky, 1996 (†); Eucryptodira incertae sedis (cf. "Macrobaenidae") (†); *Chelydra serpentina* (Linnaeus, 1758); *Chelydropsis murchisoni* (Bell, 1832) (†); *Chelydropsis* sp. (†); *Platysternon megacephalum* Gray, 1831b; *Emys orbicularis* (Linnaeus, 1758); *Ptychogaster* sp. (†); *Hadrianus majusculus* Hay, 1904 (†); *Hadrianus corsoni* (Leidy, 1871a) (†);*Trachemys scripta* (Schoepff, 1792) (†); *Clemmydopsis turnauensis* (Meyer, 1847b) (†), *Echmatemys wyomingensis* (Leidy, 1869) (†); *Baltemys* sp. (†); *Sternotherus minor* (Agassiz, 1857); *Kinosternon subrubrum* (Bonnaterre, 1789); *Kinosternon* sp.; *Anosteira* sp. (†); *Pseudanosteira pulchra* Clark, 1932 (†);*Allaeochelys* cf. *A. crassesculpta* (Harrassowitz, 1922) (†); *Carettochelys insculpta* Ramsay, 1887; **tendencies to category III**: *Eurysternum* sp. (†); ?*Eurysternum* sp. (†); *Plesiochelys* sp. (†); *?Plesiochelys* sp. (†); Plesiochelyidae indet. (†); *Thalassemys* cf. *T. hugii* Rütimeyer, 1873 (†); *Thalassemys* sp. (†)

Category III (fully aquatic)

Bothremys barberi (Schmidt, 1940) (†); *Taphrosphys sulcatus* (Leid, 1856a) (†); *Rupelchelys breitkreutzi* Karl and Tichy, 1999 (†); *Ctenochelys cf. C. stenoporus* (Hay, 1905) (†); *Allopleuron hofmanni* (Gray, 1831a) (†); *Chelonia mydas* (Linnaeus, 1758); *Psephophorus* sp. (†); *Dermochelys coriacea* (Vandellius, 1761)

Category IV (extreme adaptation to aquatic/marine environments)

Caretta caretta (Linnaeus, 1758); *Eretmochelys imbricata* (Linnaeus, 1766); *Archelon ischyros* Wieland, 1896 (†); *Baptemys garmanii* (Cope, 1872b) (†); *Dermatemys mawii* Gray, 1847; *Hoplochelys* sp. (†)